NASA Contractor Report 4019

Simulated Flight Acoustic Investigation of Treated Ejector Effectiveness on Advanced Mechanical Suppressors for High Velocity Jet Noise Reduction

J. F. Brausch, R. E. Motsinger,
and D. J. Hoerst

CONTRACT NAS3-23275
NOVEMBER 1986

NASA

NASA Contractor Report 4019

Simulated Flight Acoustic Investigation of Treated Ejector Effectiveness on Advanced Mechanical Suppressors for High Velocity Jet Noise Reduction

J. F. Brausch, R. E. Motsinger,
and D. J. Hoerst
General Electric Company
Cincinnati, Ohio

Prepared for
Lewis Research Center
under Contract NAS3-23275

National Aeronautics
and Space Administration

Scientific and Technical Information Branch

1986

TABLE OF CONTENTS

SECTION	PAGE

1.0 SUMMARY

In pursuit of an acoustically acceptable, high performance exhaust system capable of meeting Federal Aviation Regulation Stage 3 (FAR36 Stage 3) noise goals for an Advanced Supersonic Transport (AST) application, a design study was conducted within NAS3-23038 (Reference 1) to incorporate an acoustically treated ejector shroud into a 20-chute suppressor exhaust system. That contract additionally evaluated the aerodynamic performance of the suppressor/ ejector exhaust design in a scale-model system at various flight mission points including takeoff, subsonic cruise, transonic cruise, and supersonic cruise; results are presented within Reference 1. This reports acoustic performance evaluation contract utilized the NAS3-23038 "takeoff" design point's aero-dynamic flowlines as a starting point around which to evolve a scale-model system for acoustic testing. Ten scale-model nozzles were tested within the General Electric, Evendale Anechoic Free-Jet Facility, obtaining an acoustic data base of 188 static/simulated-flight test points. The test points primarily patterned the operating throttle line of an Advanced Supersonic Transport/Variable Cycle Engine (AST/VCE) utilizing an inverted-velocity-profile coannular propulsion nozzle. Within this report, overview acoustic parameters such as OASPL, PNL and EPNL are presented for the full operating cycle time; more detailed comparisons of spectra and directivity are presented at the primary cycle points of takeoff, intermediate and cutback.

An additional diagnostic measurements data base was acquired on select configurations/test points in the forms of a) laser velocimeter (LV) mean and turbulent velocity plume surveys, b) shadowgraph-photographs, and c) P_S and T_S surface measurements on the suppressor chutes and within the ejector's inner flowpath. The LV measurements are used primarily to compare plume structure and decay rates among various configurations as an aid in understanding acoustic trends. The shadowgraph photography allowed for improved under-standing of shock-cell-noise contributions to total jet noise and its subsequent alternation through application of treatment to the plug surface and through ejector application. The P_S measurements on the suppressor surface allowed for estimating thrust degradation due to chute base drag, a primary thrust loss mechanism for mechanical suppressor nozzles.

The scale model test configurations investigated ejector variables of a) hardwall ejectors application to a coannular nozzle with a 20-chute outer annular suppressor, b) ejector axial positioning, c) ejector length variation, d) extent of treatment application within the ejector system, i.e., treatment application to ejector surface only and treatment application to both ejector and plug surfaces, and e) treatment design through variation of acoustic impedance. Additionally, the baseline unejected coannular-suppressed nozzle was tested to reference its performance level to a previous similar suppressor system. Acoustic treatment was also applied to the plug surface of the base-line unejected coannular-suppressed nozzle to investigate a pseudo-porous plug concept's impact on potential shock noise alleviation.

Salient results from analysis of the measured data include: a) application of hardwall ejectors is significantly beneficial in reduction of both forward and aft quadrant noise, b) application of treatment to plug and ejector surfaces is additionally effective, primarily at forward and broadside acoustic angles and in the cutback to intermediate cycle range, c) the optimum treated ejector system added 5.5 ΔEPNL suppression to the baseline mechanically-suppressed nozzle at takeoff cycle, d) all ejector systems yielded high forward quadrant suppression, not previously experienced with non-ejector systems, e) axial location of the ejector is very significant, further aft location being both aerodynamically and acoustically superior, f) treatment design variation, within limits evaluated, was not critical to suppression, and g) treatment application to the plug surface of a non-ejector system was not effective in further reduction of shock noise.

An existing computations methodology to predict ejector/treatment suppression was refined to handle treatment on both the shroud and plug surfaces and to improve the modal propagation model, including effects of flow on mode cut-on-ratio. Comparisons of predicted and measured suppression levels show a) good agreement in frequency bands dominated by the mid-to-low frequency jet noise, b) the effect of hardwall shroud by itself is predicted very well, c) relative benefits of the long versus short ejectors and of treatment on the outer wall, only, versus on both walls, are predicted reasonably well, and d) at high frequencies a discrepancy occurred that is thought to stem from noise leakage out the gap between nozzle exit and ejector inlet, a flanking path.

2.0 INTRODUCTION

Environmentally acceptable acoustics has been one of the major technical challenges to be met prior to the development of an Advanced Supersonic Transport (AST) by American industry. A dominant problem has been community jet noise associated with the propulsion system and more specifically the propulsion exhaust system. Traditionally, noise abatement schemes have been applied to exhaust systems with some success; however, the performance penalties previously associated with these schemes have been large and thus have not been economically viable for an AST application. Recent Contract NAS3-23038, sponsored by NASA-Lewis as the counterpart aerodynamic performance study to this program's acoustic effort, as well as this contracts work efforts, have offered the potential of accomplishing acoustic suppression with favorable trades on propulsion performance. The results of these works indicate that a superposition of three acoustic suppression schemes in a single exhaust system offers the potential to satisfy stringent noise goals with the potential for performance levels appropriate to the attainment of an economically feasible AST aircraft.

The NAS3-23038 contract's final report, Reference 1, presented the results of design studies to identify important features for a viable aero/acoustic AST/VCE exhaust system plus scale model test results to investigate aerodynamic performance of the fully integrated ejector shroud system at the important flight points including takeoff, subsonic cruise, transonic cruise and supersonic cruise. This acoustic performance evaluation contract utilized the "takeoff" aerodynamic flow-line design of the NAS3-23038 contract to evolve a base scale-model hot flow nozzle system around which important features were evaluated for impact on noise suppression. Acoustic treatment design, areas of treatment application, ejector length and ejector axial location were detail evaluated over an AST/VCE cycle line from subsonic exhaust nozzle operation to beyond takeoff cycle. Primary regions of investigation were the takeoff and community-cutback cycles. Results of this acoustic evaluation study are detail-presented herein.

2.1 BACKGROUND

Under NASA Contract NAS3-23038 (Reference 1), a two part program was conducted, consisting of a design study and a subscale model wind tunnel effort to define an exhaust system for supersonic transport application. In the design study three exhaust systems were evaluated, i.e., coannular, 20-chute suppressor, and suppressor ejector shroud system. Study results were used in a mission analysis scenerio; aircraft takeoff gross weights were determined to perform a nominal design mission, constrained by Federal Aviation Regulation (1969) Part 36, Stage 3 noise requirements. Mission trade study results confirmed that the suppressor/ejector shroud design was the best of the three exhaust systems studied. This Advanced Supersonic Technology (AST) exhaust system, shown schematically in Figure 2-1 in takeoff mode and in Figure 2-2 in supersonic cruise model, is documented in Reference 2. In the subscale model wind tunnel test program, this AST exhaust system was used as the base for model design, developing a .123 scaled version of the full scale study nozzle. In this report's contract effort the AST exhaust system in takeoff mode was modeled in a .135 scaled version of the same full scale study nozzle. It was then subjected to extensive acoustic and diagnostic test efforts within the General Electric, Evendale Anechoic Free-Jet Facility.

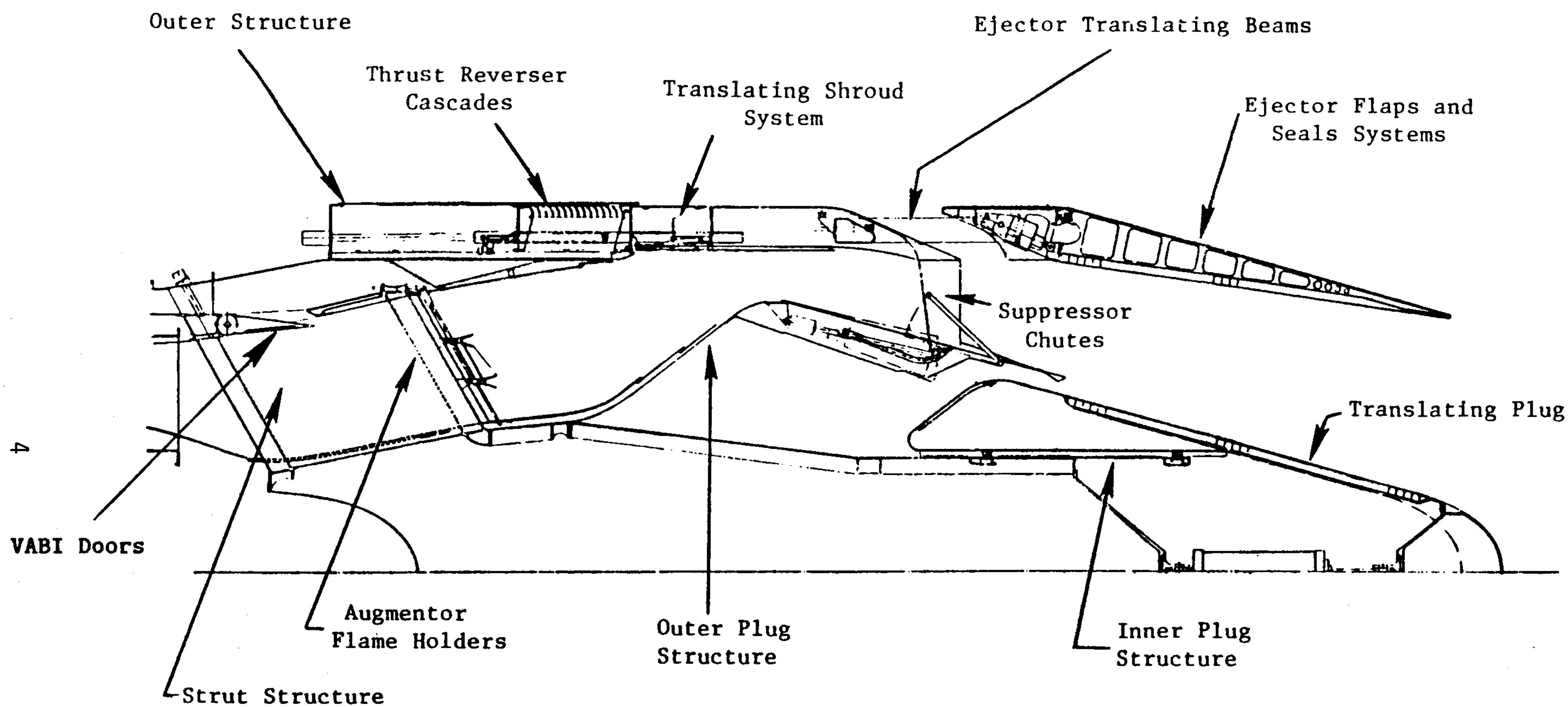

FIGURE 2-1 20-CHUTE SUPPRESSOR EJECTOR SHROUD NOZZLE (TAKEOFF MODE)

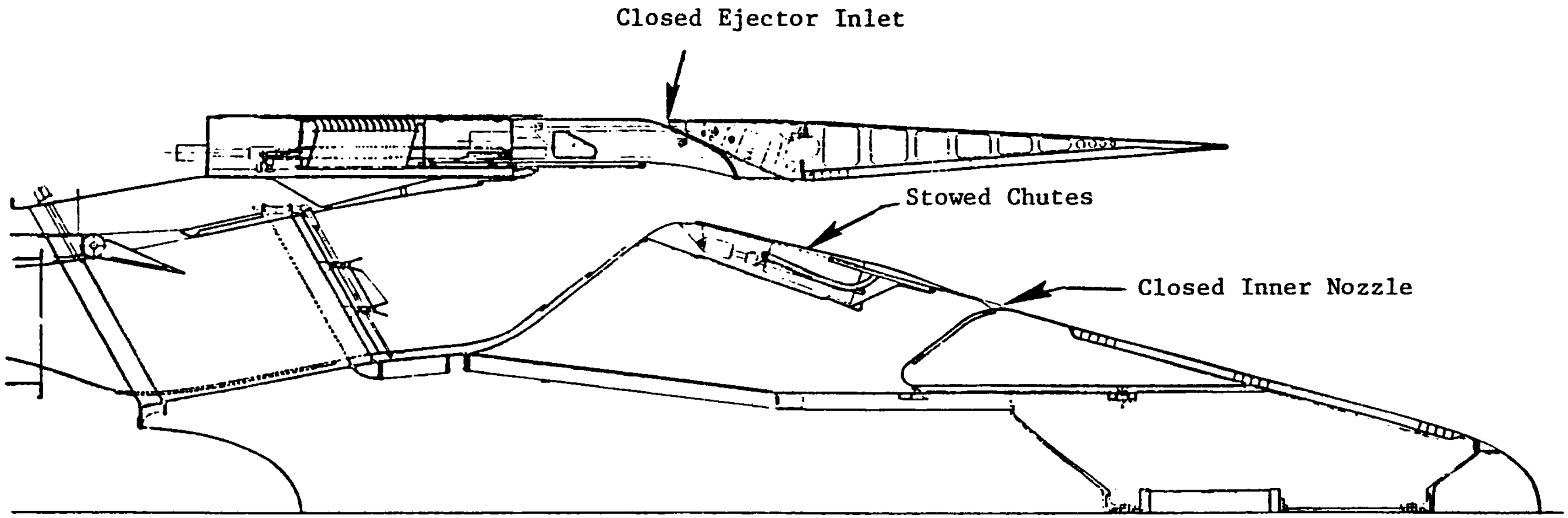

FIGURE 2-2 20-CHUTE SUPPRESSOR EJECTOR SHROUD NOZZLE (SUPERSONIC CRUISE MODE)

The AST exhaust system is a high radius ratio plug nozzle with a fixed primary nozzle cowl and a translating center plug nozzle. A translating outer shroud adjusts the exit area ratio for high performance throughout the pressure ratio range. The outer shroud inner surface is contoured to closely match the primary throat area requirements at the more important operating points. The translating center plug nozzle exhausts the excess bypass airflow that cannot flow through the primary nozzle throat. During noise suppression/ takeoff, bypass flow is ducted from the outer fan passage through eight strut-ducts into the plug beam and then to the center plug nozzle. This arrangement, along with the high radius ratio primary nozzle, provides the characteristic inverted-jet-velocity-profile coannular suppression. Additional suppression is obtained by deploying 20 chutes in the outer stream during suppressed-takeoff operation. Still higher suppression is obtained by shrouding the nozzle discharge with ejected ambient air using a mechanical shroud and lining the shroud and plug surfaces with sound absorbing material. The ejector shroud is attached to the aft end of the translating shroud. For unsuppressed operation, most of the bypass air is mixed with the core stream, the suppressor chutes are stowed in the nozzle plug outer surface, and the ejector inlet is closed for high internal performance. The ejector shroud is made of variable area flaps and seals so that the required expansion ratio for good performance can be met throughout the wide pressure ratio operating range.

The exhaust system includes a cascade type thrust reverser. The thrust reverser cascades are attached to the forward end of the translating outer shroud. When the shroud is fully extended, the cascades are exposed on the outside and inside and a shroud mounted door assembly is expanded to contract the fixed plug crown to block the flow through the primary nozzle. The cascades occupy three quarters of the circumference, but may be positioned in the total circumference if the reverser discharge efflux can be controlled to prevent airframe impingement and engine reingestion. A low temperature rise augmentor is used in the exhaust system to provide augmented thrust during acceleration.

The following sections discuss details of the design study nozzle's individual components plus operational characteristics in the suppressed-takeoff mode.

Translating Outer Shroud

The outer shroud is a cylindrically shaped fabrication made up of matched rings, sheet metal rolled rings and honeycomb. The aft end is shaped to provide a path for ambient airflow ventilation of the backside of the suppressor chutes. Twelve reverser blocker doors are contained in a cavity near the middle of the cylinder. The thrust reverser cascade boxes are located near the forward end of the shroud. They occupy 270° of the circumference and can be arranged in any desired circumferential location to prevent a) exhaust gas impingement on the aircraft and/or b) engine hot gas reingestion. The forward end of the shroud supports the linkage which drives the reverser blocker doors. The inner liner of the shroud provides convective cooling for the shroud inner surface to the end of the liner and film cooling beyond the end of the liner. The aft cavity of the shroud contains the support and positioning system for the ejector shroud.

Ejector Shroud

The ejector shroud is composed of a flap support ring forming the aft surface of the ejector inlet and containing the flap actuators, 20 variable area flaps, 10 support beams and an actuating ring housed in the aft cavity of the translating outer shroud. The forward outer end of the flap support ring contains the seal for the ejector inlet in the inlet closed position. The inner surface of the support ring contains 20 chute-inlet cavity fillers to provide a continuous inner flowpath when the inlet is closed. The flaps are conventional sheet metal fabrication and incorporate sound absorption panels on the inner surface of the flaps. The sound absorption panels are constructed similar to honeycomb with the chambers vented to the inner flowpath.

Outer Cowl

The outer cowl provides the outer flow surface between the aft end for the aircraft nacelle and the translating shroud. It also retains the cowl to shroud seal at the aft end and thus functions as the outer container wall for the bypass cooling air for the shroud liner.

Outer Structure

The outer structure is a cylindrical structure with a bulkhead at the forward end and a stiffening ring at the aft end. The outer forward end of the bulkhead has a step to provide for the nacelle-exhaust nozzle interface. The aft ring contains the inner shroud seal to separate the shroud cooling air from the main stream. Two sets of longitudinal tracks are contained in the cylindrical portion of the outer structure. One set of four tracks support the outer shroud. The other set of twelve tracks provide for positioning of the reverser blocker doors.

Strut Structure

The strut structure is composed of eight pairs of radial beams (slanted 60° to the engine centerline) joined by outer and inner circumferential rings. The forward outer ring is joined through vanes in the bypass stream to the bypass duct outer spacer ring. The supporting loads for the inner nozzle are thus transferred to the engine outer bypass duct through radial beams and strut sidewalls for the bypass air duct. Upper and lower cylindrical surfaces between struts form the boundary for the core engine airflow passage, and the upper surface supports the VABI doors. This strut structure is encased with cooling air liners that blend with the turbine frame liner to form continuous struts from the turbine frame entrance to the bypass strut exit. A portion of the liner is sound absorbing material.

VABI Doors

Twenty-four Variable Area Bypass Injector Doors, in sets of three between each of the eight struts, are hinged to the forward outer part of the strut structure. One power hinge per set of three doors maintains the VABI door position. The doors are conventional sheet metal structure with sound absorbing panels on the core flowpath side.

Outer Plug Structure

The outer plug structure is composed of welded sheet metal and machined rings to form the core flow inner flowpath. It is supported at the forward end by the strut structure aft inner ring. The aft end ring forms the outer flowpath of the inner nozzle. This structure also contains the suppressor chutes and their actuation mechanism.

Inner Plug Structure

The inner plug structure consists of a truss support attached at the forward end of the strut structure aft inner ring, a mid ring that supports an aft stiffened cylinder which in turn supports the four sets of guide rollers, and the actuator for the translating plug.

Translating Plug

The translating inner plug is composed of welded sheet metal and machined rings stiffened at the forward end with honeycomb and containing a honeycomb type sound absorption covering cone. Thus, the inner bypass flowpath contributes to the jet noise suppression. The inner plug is supported by four sets of guide tracks that engage the guide rollers on the plug structure.

Suppressor Chutes

Twenty suppressor chutes are mounted in the outer plug structure. Each chute is supported by a link and a set of two rollers engaging tracks attached to the plug. The chute construction can be sheet metal or cast. The 1.75 nozzle-to-base area ratio suppressor allows a lightweight simple stowed position arrangement that does not require a cover door and a cover door actuation system. The chutes are retracted into cavities on the outer plug surface such that they blend with the plug outer contour to form the inner flowpath of the outer stream.

Suppressor Takeoff Operating Mode

The suppressor chutes are deployed and the translating outer shroud is positioned to mate with the chute outer edges. The translating shroud forms the outer flowpath of the high pressure outer stream, and the outer nozzle throat is formed between chutes at their aft edges. The ejector shroud is translated aft relative to the translating shroud to enable ejector ambient air induction and allow mixing of ambient air and the outer stream discharge from the suppressor chutes. The ejector flaps are positioned to match the full expansion area requirement of the mixed ambient air, outer stream and inner stream. Most of the bypass air flows from the bypass duct through the eight struts to the inner annulus and then exhausts through the open-positioned inner plug nozzle. Some of the bypass flow passes through the twenty-four Variable Area Bypass Injector (VABI) doors and is mixed with core flow. This feature allows the engine to be operated efficiently with the limited variation in the outer nozzle throat area.

For use within this test program, the above described design study nozzle was developed into a basic model exhaust system. Variations of the full scale ejector positioning and length, as well as treatment design and areas of application, were exercised. Details of this scale model hardware system are discussed in Section 3.2, "Scale Model Test Hardware".

3.0 EXPERIMENTAL PROGRAM

All of the acoustic and diagnostic tests of this program were conducted in the General Electric Anechoic Free-Jet Facility located in Evendale, Ohio. Brief descriptions of the facility, data acquisition and data reduction procedures are presented in Section 3.1. Detailed descriptions of the facility plus acoustic data acquisition, reduction and flight transformation procedures are provided in this contracts comprehensive data report, Reference 3. Section 3.2 detail defines the ten model test configurations, method of acoustic treatment application and aerodynamic Ps and Ts instrumentation. It also presents the methodology adopted to systematically evaluate parameters which impact acoustic performance, describing the chronology of test configurations needed to "on-line" select optimum design parameters. Further details of treatment development can be found in Reference 4, also included as part of this reports comprehensive data report.

Tabulations that summarize the aerodynamic flow conditions and extent of tests conducted for the acoustic, laser velocimeter, shadowgraph-photograph and aerodynamic Ps/Ts investigations are provided in Section 3.3. Measured acoustic and diagnostic data are reported in detail in the comprehensive data report.

3.1 TEST FACILITY, DATA ACQUISITION AND REDUCTION SYSTEMS, DIAGNOSTIC TEST APPARATUS

3.1.1 Anechoic Free-Jet Facility

The General Electric, Evendale, Anechoic Free-Jet Facility, schematically shown in Figure 3-1, is a cylindrical chamber 13.1 meters (43 feet) in diameter and 21.95 meters (72 feet) high. The inner surfaces of the chamber are lined with anechoic wedges made of fiberglass wool to yield a low frequency cutoff below 220 Hz and an absorption coefficient of 0.99 above 220 Hz. Descriptions and results of the tests conducted in order to determine the acoustic characteristics of the anechoic chamber (such as inverse square law tests) and the mean velocity and turbulence intensity distributions in the free jet are presented in Reference 5.

The facilitity can accommodate model configurations up to a size of 17.3 cm (6.8 inch) in equivalent flow diameter. The required streams of heated air for a dual-flow arrangement, produced by two separate burners, flow through silencers and plenum chambers before entering the test nozzle.

The tertiary air system consists of a 250,000 scfm (50 inches water column static pressure) fan and a 3,500-hp electric motor. The transition duct work and silencer route the air from the fan discharge to the tertiary silencer plenum chamber. The air is then discharged through the 1.2-m (48 inch) free-jet exhaust. Tertiary flow at its maximum permits simulation up to a Mach number of 0.41. Mach number variation is obtained by changing the tertiary airflow rate achieved by adjusting the fan inlet vanes. The combined airflow is exhausted through a "T" stack directly over the nozzles in the ceiling of the chamber.

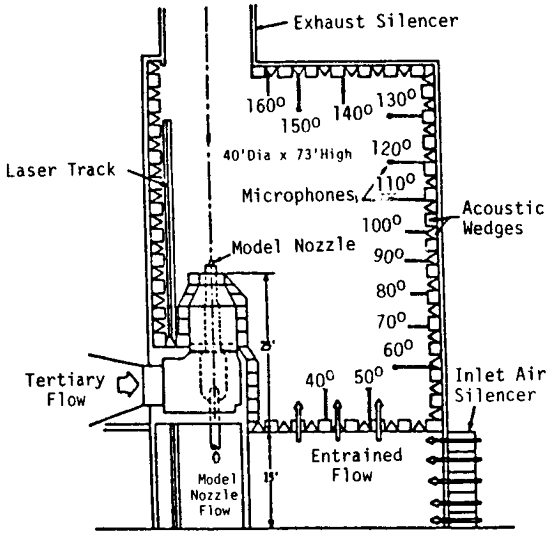

Angle (Degrees)	Radial Distance m	ft
40	7.92	26.0
50	9.48	31.1
60	9.50	31.18
70	8.76	28.73
80	8.36	27.42
90	8.23	27.00
100	8.36	27.42
110	8.76	28.73
120	9.5	31.18
130	10.74	35.25
140	9.17	30.17
150	8.33	27.0
160	7.92	26.0

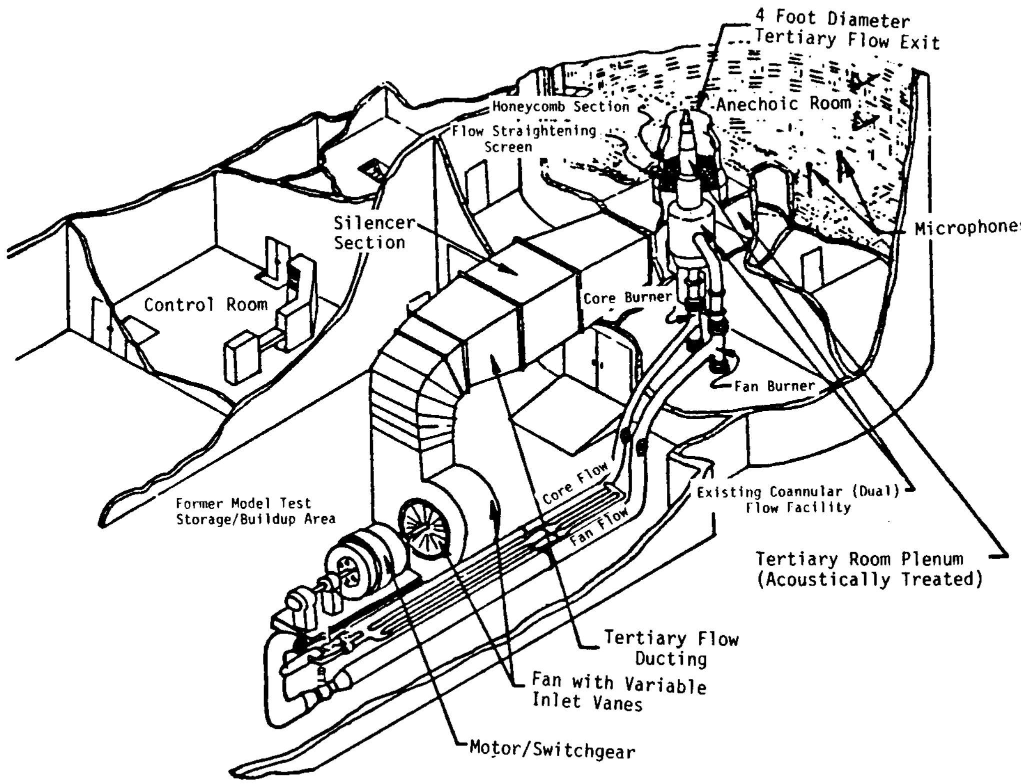

FIGURE 3-1. ANECHOIC FREE-JET/JET NOISE FACILITY SCHEMATIC.

3.1.2 Aerodynamic Data Acquisition and Reduction Procedures

Facility Operational Method

The facility operating parameters are monitored during testing at the control console to a) ensure that prescribed facility limits are not exceeded, and b) set the test-point conditions.

The core and fan discharge pressures are measured on rakes at the metering station and are used for setting the desired nozzle pressure ratios. These parameters also are routed through the Dymec scanning system and recorded along with nozzle performance data by the aerodynamic data management (DMS) system.

Facility temperatures are monitored at the control console using a Doric multichannel temperature indicator. The unit has a 24-channel capability and is designed for use with Type K thermocouples (chromel-alumel). It is used for safety monitoring and setting test-point temperatures for the dual-flow system. A system schematic is shown in Figure 3-2.

Nozzle Pressure and Temperature Measurement

A critical parameter used in evaluating acoustic test results is nozzle exhaust velocity. Determination of this velocity depends on an accurate measurement of the exhaust temperature and pressure which, in turn, depends on adequate sampling across the stream to account for profile effects. Special multi-element rakes have been designed for use on the dual flow systems. The system uses four rakes, two on each stream, each having three pressure and three temperature elements with spacing of the elements corresponding to centers of six equal area annular segments of the flow stream. These rakes use shielded Type K thermocouples (chromel-alumel) which have a recovery factor very close to unity.

Pressure measurement accuracy is controlled by the accuracy of the transducer used for the measurement. The scanivalve transducers that are used are rated 0.1% of full-scale range.

Performance Data Processing

Aerodynamic parameters are calculated based on the acquired temperature and pressure information. The input information for nozzle performance consists of ambient pressure (P_{amb}), nozzle discharge total temperature (T_T), and nozzle total pressure (P_T). For the case of dual flow and tertiary flow, similar parameters are required for each stream.

Output of the processing program consists of tabulations of the individual input parameters with their identification, averages of similar parameters (e.g., P_T rake average), and calculated parameters such as flow rates, Mach number, ideal velocity, and ideal thrust.

3.1.3 Acoustic Data Acquisition and Reduction Procedures

A flow chart of the acoustic data acquisition and reduction system is shown in Figure 3-3. This system has been optimized for obtaining the acoustic data up to the 80 kHz 1/3-octave-band center frequency. The

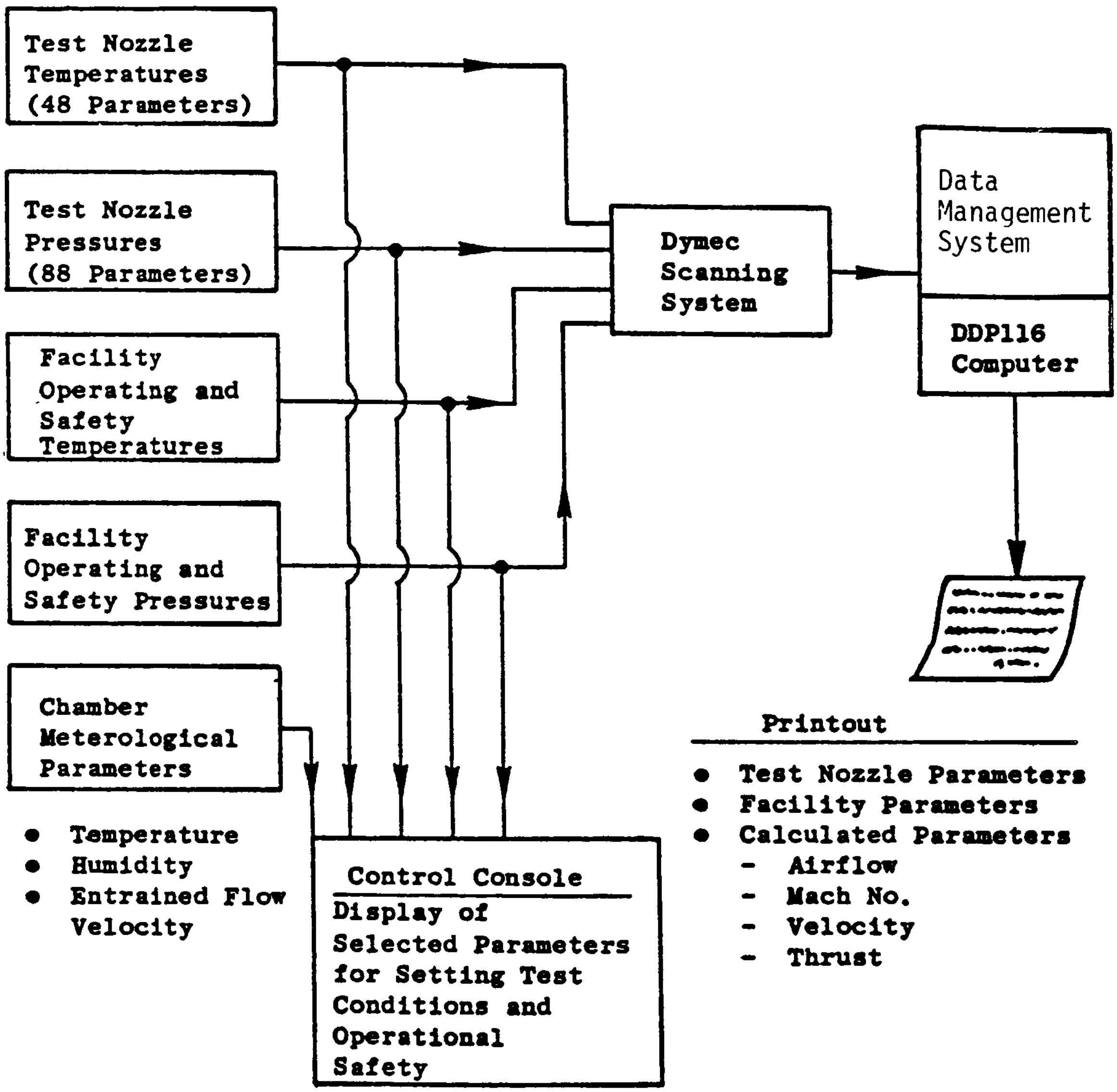

FIGURE 3-2. GENERAL ELECTRIC ANECHOIC CHAMBER AERODYNAMIC DATA PROCESSING SYSTEM.

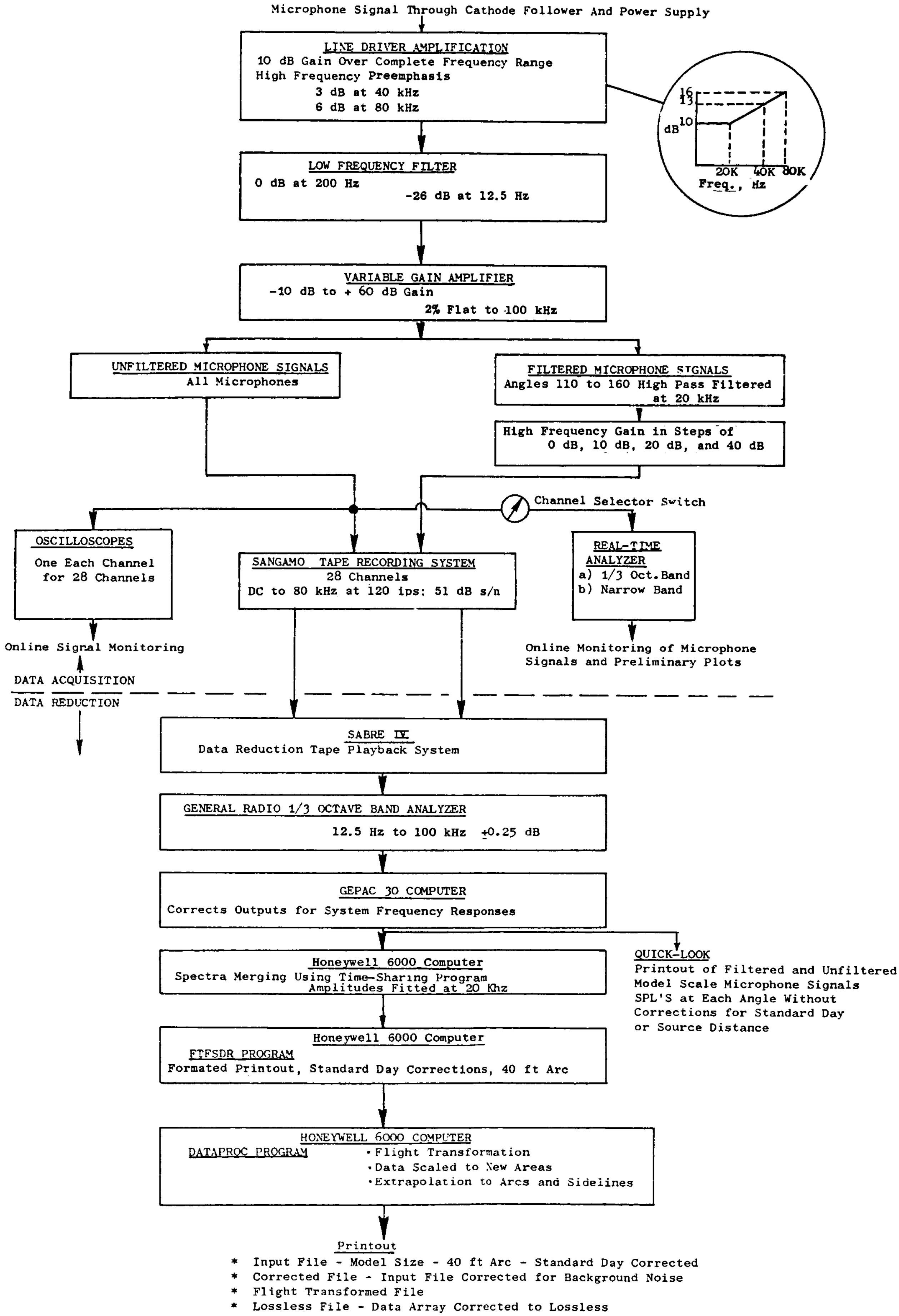

FIGURE 3-3. ACOUSTIC DATA ACQUISITION AND REDUCTION SYSTEM.

microphones used to obtain 80 kHz data are the B&K 4135, 0.64 cm (1/4 inch), condenser microphones with the microphone grid caps removed to obtain the best frequency response. The cathode followers used in the chamber are transistorized B&K 2619 for optimum frequency response and lower inherent system noise characteristics. All systems utilize the B&K 2801 power supply operated in the direct mode.

The output of the power supply is connected to a line driver adding 10 dB of amplification to the signal as well as adding "preemphasis" to the high frequency portion of the spectrum. The net effect of this amplifier is a 10 dB gain at all frequencies, plus an addition 3 dB at 40 kHz and 6 dB at 80 kHz due to pre-emphasis. This increases the ability to measure low amplitude, high frequency data. In order to remove low frequency noise, high pass filters with attenuations of approximately 26 dB at 12.5 Hz, decreasing to 0 dB at 200 Hz, are installed in the system.

The tape recorder amplifiers have a variable gain from -10 dB to +60 dB in 10 dB steps and a gain trim capability for normalizing incoming signals. High pass filters are incorporated in the acoustic data acquisition systems for microphones from 110° to 160° to enhance high frequency data otherwise potentially lost in the tape recorder electronic noise floor. The microphone signal below the 20-Hz 1/3-octave band is filtered out, and the gain is increased to boost the "signal-to-noise" ratio of the remaining high frequency signal. For microphones from 110° to 160°, both the filtered and unfiltered signals are recorded on tape. The sound pressure levels for frequencies below 20 kHz are obtained using the unfiltered signal; above 20 kHz the filtered and de-emphasized signal is used. The final jet noise spectra at a given angle is obtained by computationally merging these two spectra.

The prime system used for recording acoustic data is a Sangamo/Sabre IV, 28-track FM recorder. The system is set up for wide band Group I (intermediate band double extended) at 120-ips tape speed. Operating at 120-ips tape speed provides the improved dynamic range necessary for obtaining the high frequency/low amplitude portion of the acoustic signal. The tape recorder is set up for ± 40% carrier deviation with a recording level of 8 volts peak-to-peak. During recording, the signal gain is adjusted to maximum without exceeding the 8 volt peak-to-peak level.

Individual monitor scopes are used for observing signal characteristics during operation. On-line data monitoring is available through a Rockland narrowband analyzer or a General Radio 1921 1/3-octave analyzer with their outputs on display scopes or hard copy through a Tektronic plotter.

Standard data reduction is conducted in the General Electric AEBG Instrumentation Data Room (IDR). The analog data tapes are played back on a CDC3700B tape deck with electronics capable of reproducing signal characteristics within the specifications indicated for wide band Groups I and II. An automatic shuttling control is incorporated in the system. In normal operation, a tone is inserted on the recorder in the time slot designed for data analysis. Tape control automatically shuttles the tape, initiating an integration start signal to the analyzer at the tone as the tape moves in its forward motion. This motion continues until an "integration complete" is received from the analyzer at which time the tape direction is reversed and the tape restarts at the tone in the forward direction, advancing to the next channel to be analyzed until all the channels have been processed. A time code generator is also utilized to signal the tape position of the readings as directed by the computer program control. After each total reading is completed, the tape is advanced to the next reading.

All 1/3-octave analyses are performed on a General Radio 1921 analyzer. Normal integration time is set for 32 seconds to ensure good integration for the low frequency content. The analyzer has 1/3-octave filter sets from 12.5 Hz to 100 kHz with a rated accuracy of $\pm$ 1/4 dB in each band. Each data channel is passed through an interface to the GEPAC 30 computer where the data are corrected for microphone frequency response. Also, the data are corrected to standard day (59° F, 70% RH) atmospheric attenuation conditions using the Shields and Bass model (Reference 6) and then processed to calculate the perceived noise level and overall sound pressure level from the spectra. For calculation of the acoustic power, or scaling to other nozzle sizes, or extrapolation to different farfield distances, the data are sent to the Honeywell 6000 computer for data processing. This step is accomplished by transmitting the SPL's through a direct time-share link to the 6000 computer through a 1200 Band Modem. In the 6000 computer, the data are processed through the Flight-Transformed Full-Scale Data Reduction (FTFSDR) program where the appropriate calculations are performed. The data printout is accomplished on a high-speed "remote" terminal.

The detailed FTFSDR program flow chart is shown in Figure 3-4. The as-measured data are first extrapolated from the measured distance to a common 40 foot arc. This is accomplished by subtracting both the distance correction that is, 20 log (40-foot distance/measured distance) and the atmospheric attenuation correction over the measured distance R_{obs}, where R_{obs} is measured in feet. The Shields and Bass Pure Tone Method (Reference 6) is used for all atmospheric attenuation corrections. The data are then coverted to standard day at the 40-foot arc location by adding in the standard day correction. The data are printed in tabulated form for SPL, OASPL, and PWL (for full sphere and based on the lossless data). For this program, scale model data below the chamber cutoff frequency are ignored, data are presented for 250 Hz and above, model size.

The scale model simulated-flight data are corrected next for background noise using the background noise spectra obtained with the tertiary jet at the required simulated flight velocity. The corrected scale model data are processed next through a flight transformation procedure to obtain results that are representative of the noise produced in actual flight. In addition, the FTFSDR program writes a magnetic tape for computer plotting of the data used in the course of data analyses of the test results.

3.1.4 Laser Velocimeter System

The laser velocimeter (LV) available for use during this program is a system developed under a USAF/DOT-sponsored program and reported in detail in Reference 7. The basic optics system is a differential doppler, backscatter, single-package arrangement that has the proven feature of ruggedness for the severe environments encountered in close proximity to high velocity, high temperature jets. Figure 3-5 shows a photograph of the LV system in the General Electric Anechoic Test Facility. The dimensions of the control volume are 0.636 cm (0.25 inch) for the major axis and 0.518 cm (0.020 inch) for the minor axis. The range of the LV control volume from the laser hardware is 2.16 m (85.0 inches). The three steering mirrors and the beam splitter are mounted on adjustable supports, all of the same aluminum alloy, which minimizes temperature-alignment problems.

Details of the LV system are included in Appendix B of this report.

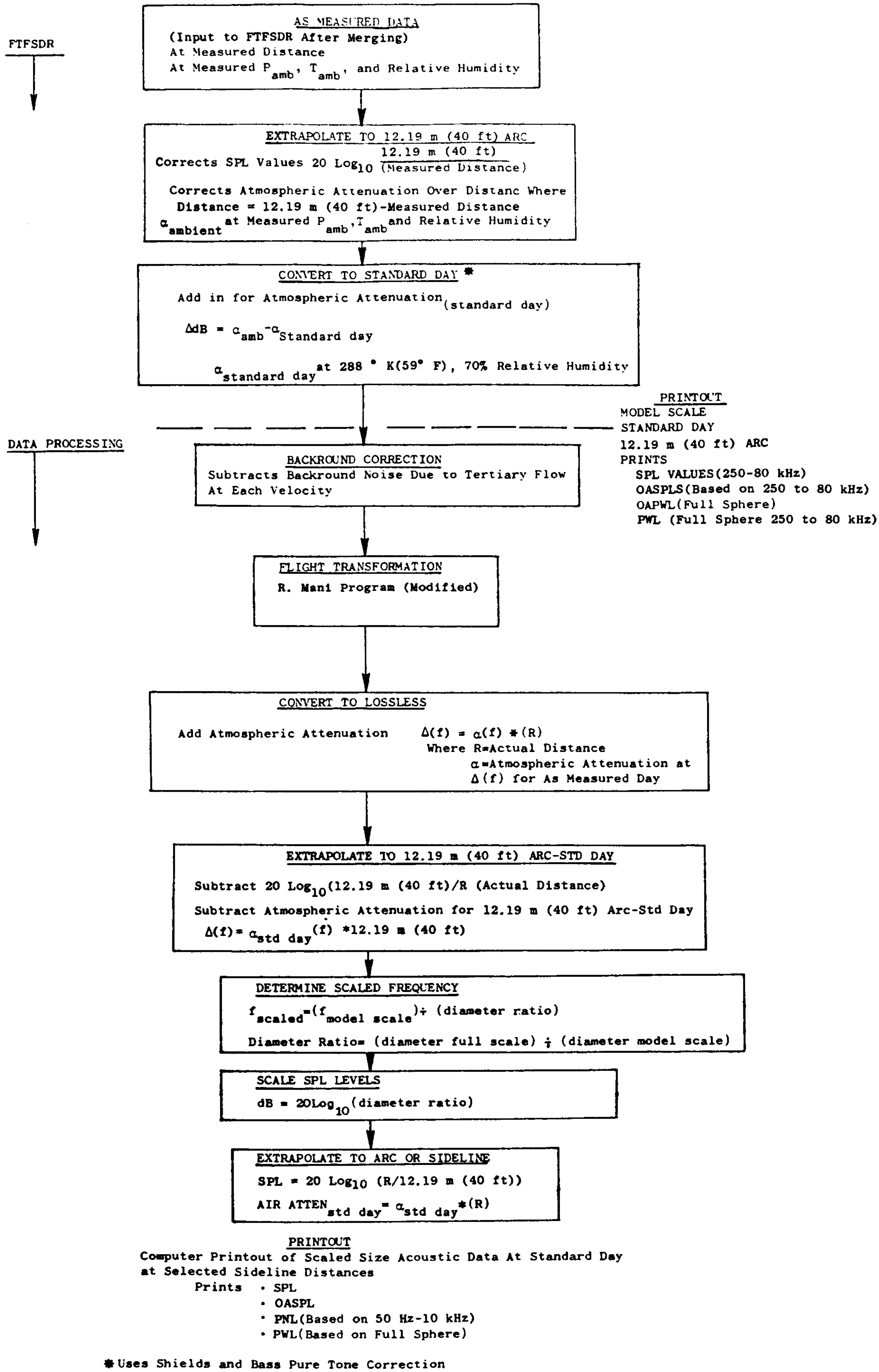

FIGURE 3-4. ACOUSTIC DATA PROCESSING FLOW CHART.

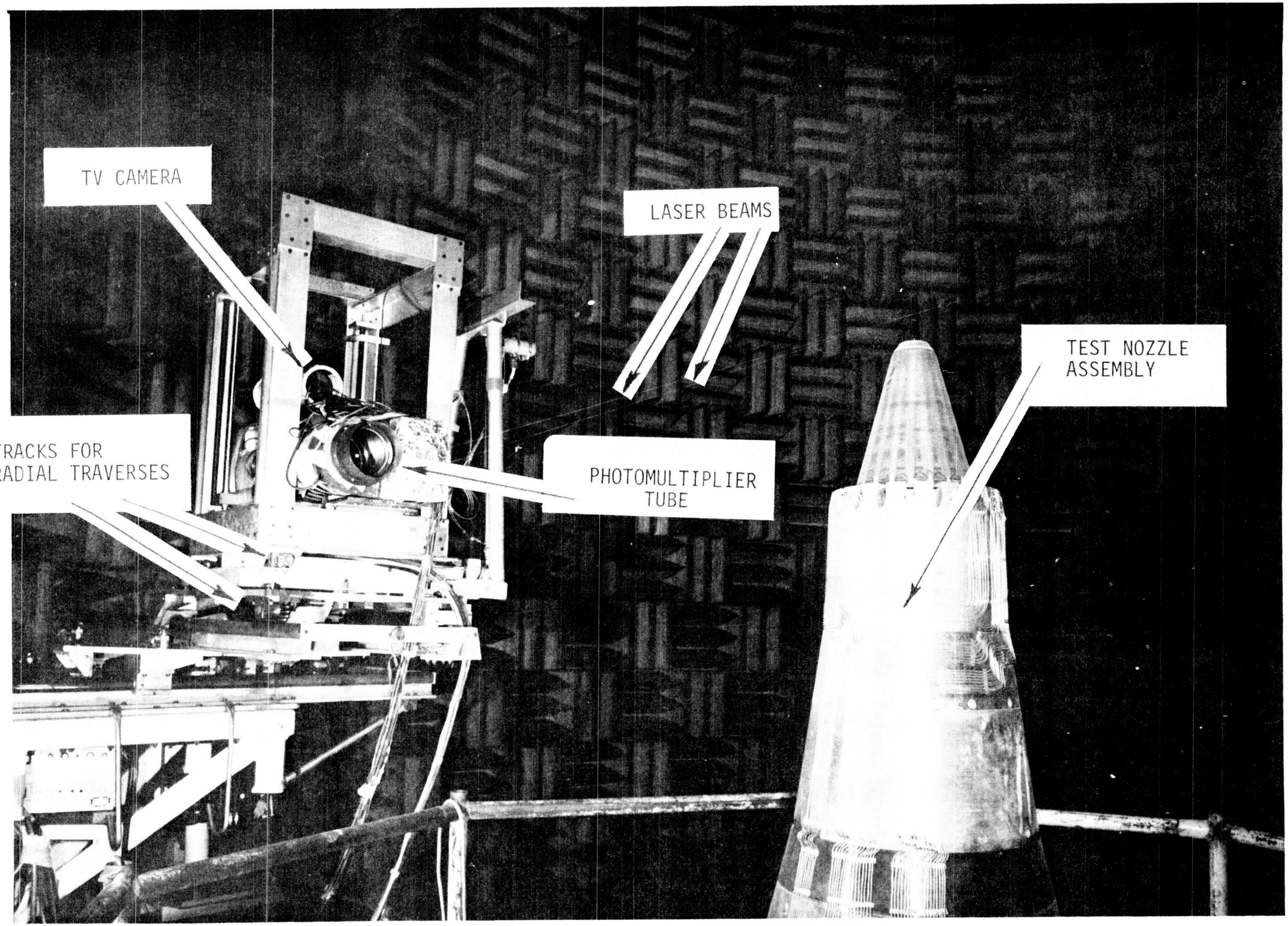

FIGURE 3-5. A PHOTOGRAPH SHOWING THE LASER VELOCIMETER SYSTEM AND A TEST NOZZLE ASSEMBLY FOR PLUME SURVEY IN THE ANECHOIC FACILITY.

3.1.5 Diagnostic Shadowgraph System

A shadowgraph system, illustrated in Figure 3-6, has been employed in the anechoic free-jet facility to accomplish flow visualization and documentation. The system includes:

- o A mounting in close proximity to the free jet nozzle for good resolution
- o A steady-state light system
- o A 10-inch-diameter mirror system to collimate the light through the test volume
- o A backdrop screen of sufficient size to encompass the total test section
- o A mounting platform for the light source, mirror, and camera system so as to control remotely and record the position of the shadowgraph system for an approximate 3-foot vertical plume definition.

3.2 SCALE MODEL TEST HARDWARE

3.2.1 Suppressor-Ejector Model Definition: Configurations TE-1 to TE-10

The AST exhaust system of Figures 2-1 and 2-2 was modeled (.123 scale factor) within Contract NAS3-23038 (Reference 1) for wind tunnel aerodynamic performance testing. Within this program's effort, the Figure 2-1 takeoff mode system was modeled (.135 scale factor) for evaluation of acoustic peformance. The basic acoustic model suppressor-ejector system layout is shown in Figure 3-7. It essentially duplicates the full scale study nozzle, is a 1.093 scaled version of the aerodynamic model, and consists of a) a coannular inverted-velocity-profile plug nozzle with 20-shallow chute outer stream suppressor, b) an acoustically treated center plug, and c) an acoustically treated ejector system. Geometric variables identified to potentially influence acoustic performance were:

- o Ejector length
- o Ejector axial location
- o Treatment design
- o Extent of treatment application

To study these variables within the model hardware system, variations were introduced in the hardware geometry, per Figure 3-8. Specific variables and extent of variation allowed for acoustic study were:

- o Ejector axial location: S1 = nominal, S2 = extended
- o Treatment design: T1 = high density, T2 = low density
- o Ejector length: L1 = nominal, L2 = extended
- o Treatment application extent:
  - Fully treated on ejector and plug surfaces
  - Treated ejector surface only
  - Hardwalls, no treatment

Details of these design variables will be discussed in later text.

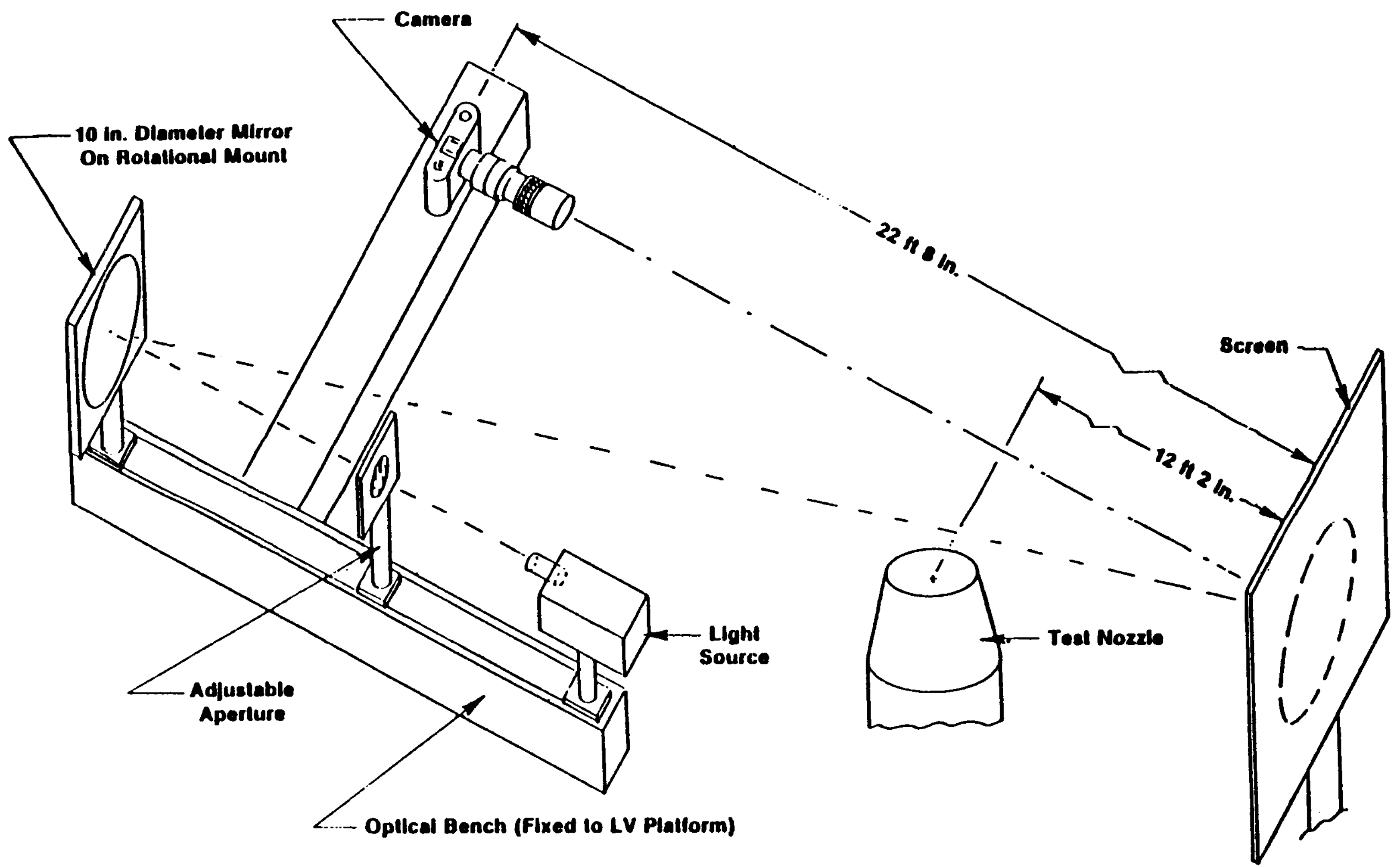

FIGURE 3-6. SCHEMATIC ARRANGEMENT OF THE SHADOWGRAPH SYSTEM IN THE ANECHOIC JET FACILITY.

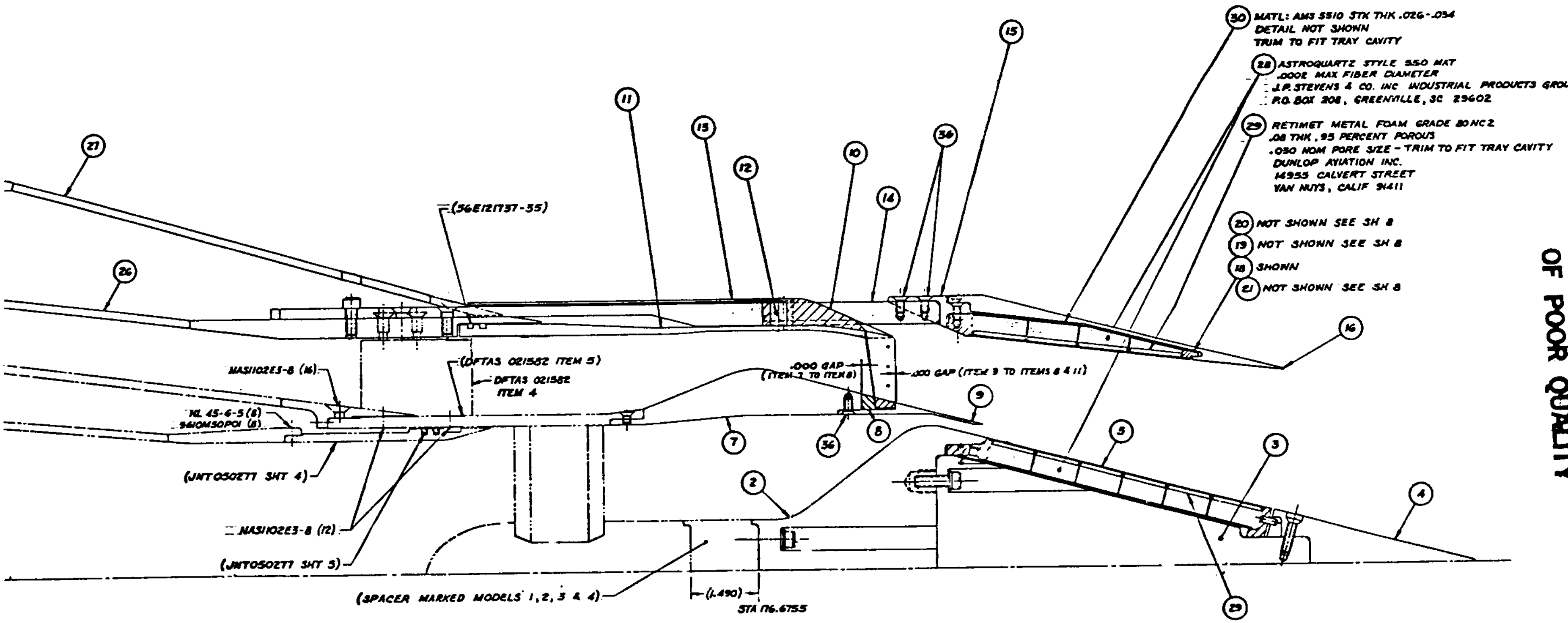

FIGURE 3-7 BASIC SUPPRESSOR/EJECTOR SYSTEM LAYOUT SHOWING NOMINAL LENGTH TREATED EJECTOR AND TREATED PLUG

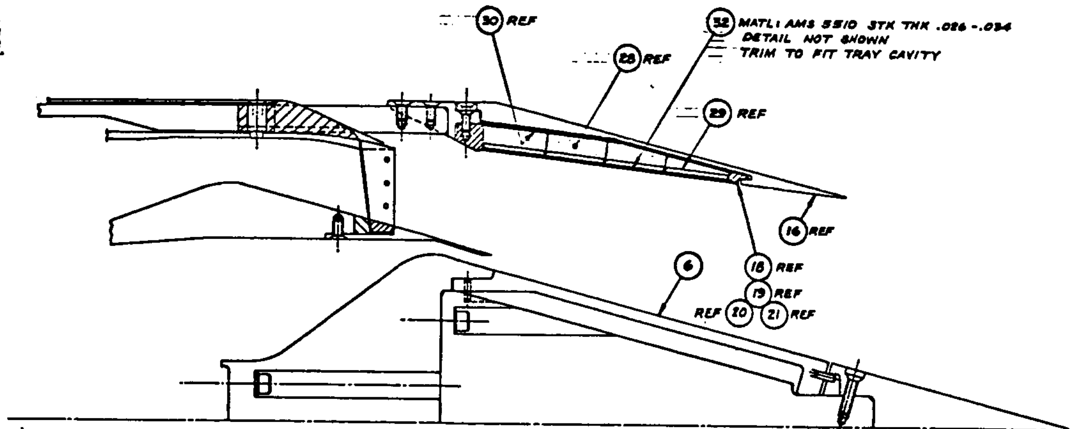

a) Supplemental Assembly, Nominal Length Treated Ejector, Hardwall Plug

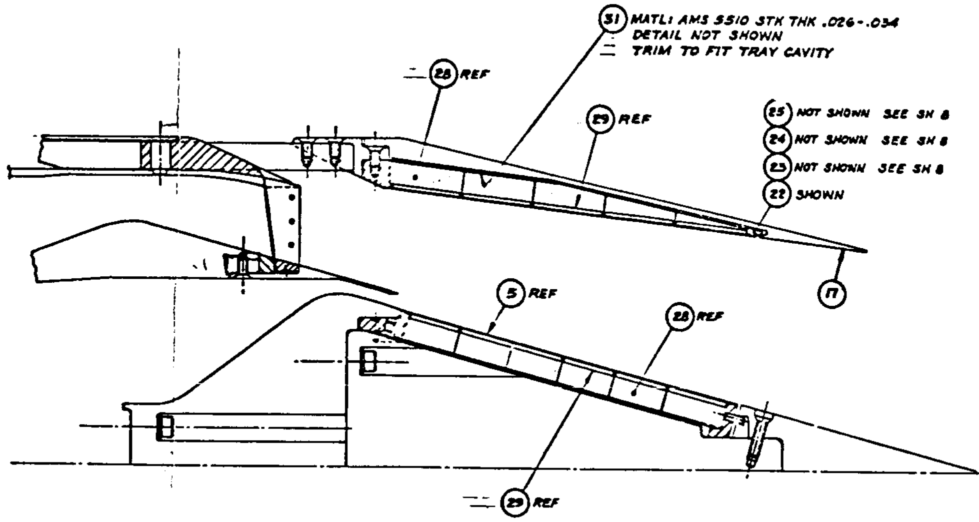

b) Supplemental Assembly, Extended Length Treated Ejector, Treated Plug

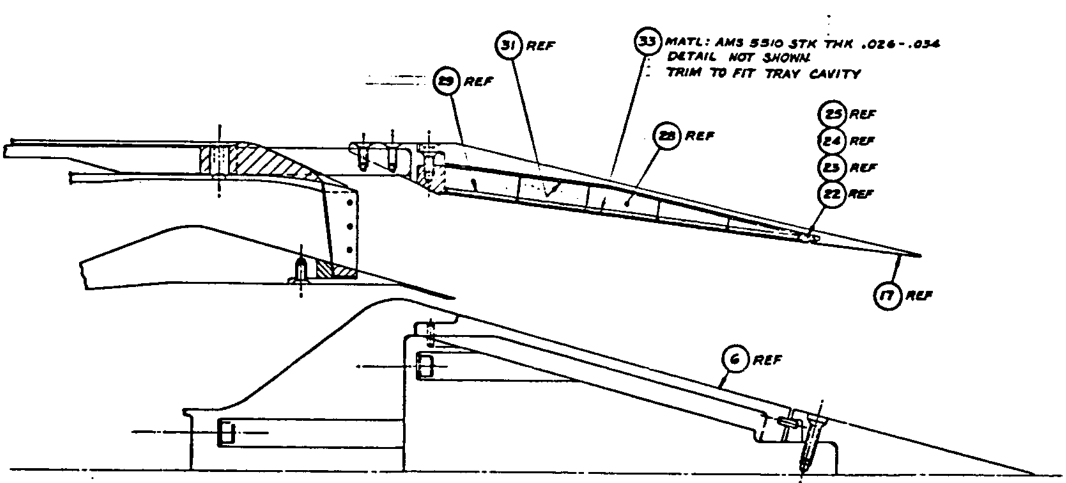

c) Supplemental Assembly, Extended Length Treated Ejector, Hardwall Plug

FIGURE 3-8 SUPPLEMENTAL SUPPRESSOR/EJECTOR SYSTEM LAYOUTS SHOWING EJECTOR AND PLUG VARIATIONS

To systematically study the influence of these variations, ten test models were selected, defined as follows:

Configuration TE-1: Baseline Coannular Inverted-Velocity - Profile Plug Nozzle with 20-Shallow Chute Outer Stream Suppressor, Hardwall Plug and No Ejector; Figure 3-9.

Configuration TE-2: Baseline Nozzle with Hardwall Plug and with Hardwall Ejector of Nominal Length, L1, at Extended Spacing, S2; Figure 3-10.

Configuration TE-3: Baseline Nozzle with Hardwall Plug and with Treated Ejector, T2, of Nominal Length, L1, at Extended Spacing, S2; Figure 3-11.

Configuration TE-4: Baseline Nozzle with Treated Plug, T2, and Treated Ejector, T2, of Nominal Length, L1, at Extended Spacing, S2; Figure 3-12.

Configuration TE-5: Baseline Nozzle with Treated Plug, T1, and Treated Ejector, T1, of Nominal Length, L1, at Nominal Spacing, S1; Figure 3-13.

Configuration TE-6: Baseline Nozzle with Treated Plug, T2, No Ejector; Figure 3-14.

Configuration TE-7: Baseline Nozzle with Hardwall Plug and with Treated Ejector, T2, of Extended Length, L2, at Extended Spacing, S2; Figure 3-15.

Configuration TE-8: Baseline Nozzle with Treated Plug, T2, and with Treated Ejector, T2, of Extended Length, L2, at Extended Spacing, S2; Figure 3-16.

Configuration TE-9: Baseline Nozzle with Treated Plug, T1, and with Treated Ejector, T1, of Nominal Length, L1, at Extended Spacing, S2; Figure 3-17.

Configuration TE-10: Baseline Nozzle with Hardwall Plug and with Hardwall Ejector of Extended Length, L2, at Extended Spacing, S2; Figure 3-18.

Figures 3-19 and 3-20 photos show the baseline Configuration TE-1 details and as-mounted in the Anechoic Test Facility, respectively. Figure 3-21 photo shows the details of Configuration TE-6 with application of treatment to the plug surface. Photos of the full suppressor-ejector system assembly, as mounted in the Anechoic Test Facility, are shown in Figures 3-22 through 3-24.

In order to systematically evaluate parameters which impact acoustic peformance, a chronology of test configurations was developed, per Figure 3-25. The methodology of comparisons evolved as follows:

	OUTER	INNER	TOTAL
AREA, IN2	22.750	4.747	27.497
Deq., IN	5.382	2.458	5.917

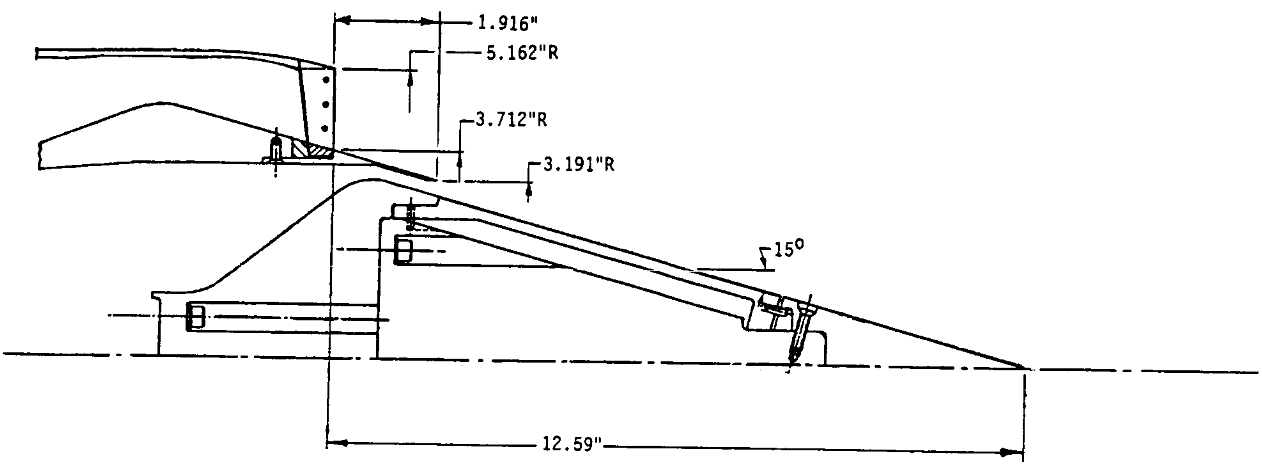

FIGURE 3-9 CONFIGURATION TE-1; BASELINE COANNULAR INVERTED-VELOCITY-PROFILE PLUG NOZZLE WITH 20-SHALLOW CHUTE OUTER STREAM SUPPRESSOR, HARDWALL PLUG AND NO EJECTOR

	OUTER	INNER	TOTAL
AREA, IN^2	22.750	4.747	27.497
Deq., IN	5.382	2.458	5.917

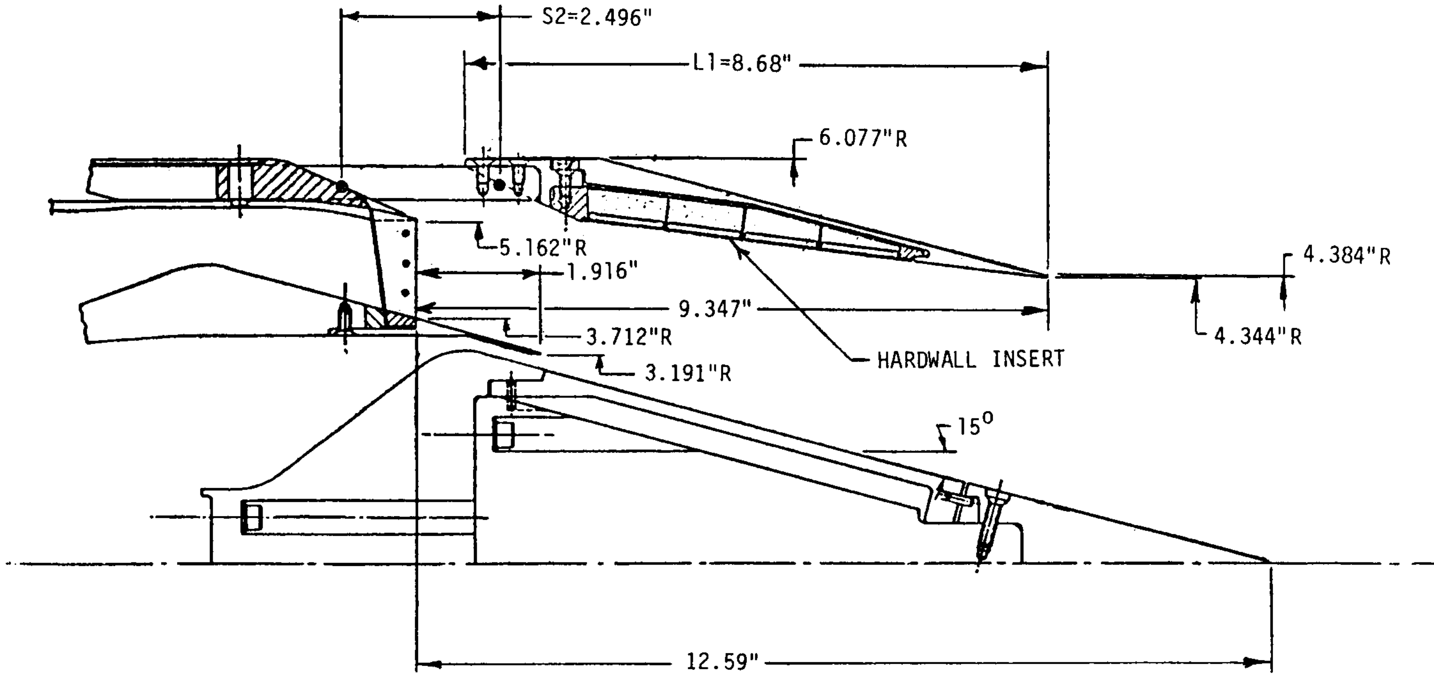

FIGURE 3-10 CONFIGURATION TE-2; BASELINE NOZZLE WITH HARDWALL PLUG AND WITH HARDWALL EJECTOR OF NOMINAL LENGTH, L1, AT EXTENDED SPACING, S2

"T2" TREATMENT DESIGN

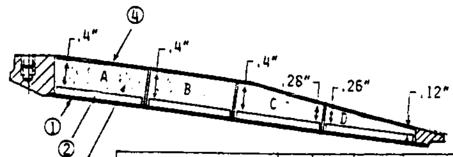

COMPARTMENT	A	B	C	D
LAYERS OF .2" THICK ASTROQUARTZ BLANKET	2	2	1.5	1

① PERFORATED SHEET 37% POROSITY, .045"Ø HOLES ON STRAIGHT LINE PATTERN WITH .067" SPACING ON CENTERS, 225 HOLES PER SQUARE INCH, 24 GA.(.025" THICK, INCONEL 625

② .08" THICK RETIMET METAL FOAM GRADE 80NC2, 95% POROUS, TRIMMED TO FIT INDIVIDUAL TRAY CAVITIES

③ ASTROQUARTZ STYLE 550 MAT, PACKED AS SHOWN

④ COVER PLATE, .030" THICK

	OUTER	INNER	TOTAL
AREA, IN^2	22.750	4.747	27.497
Deq., IN	5.382	2.458	5.917

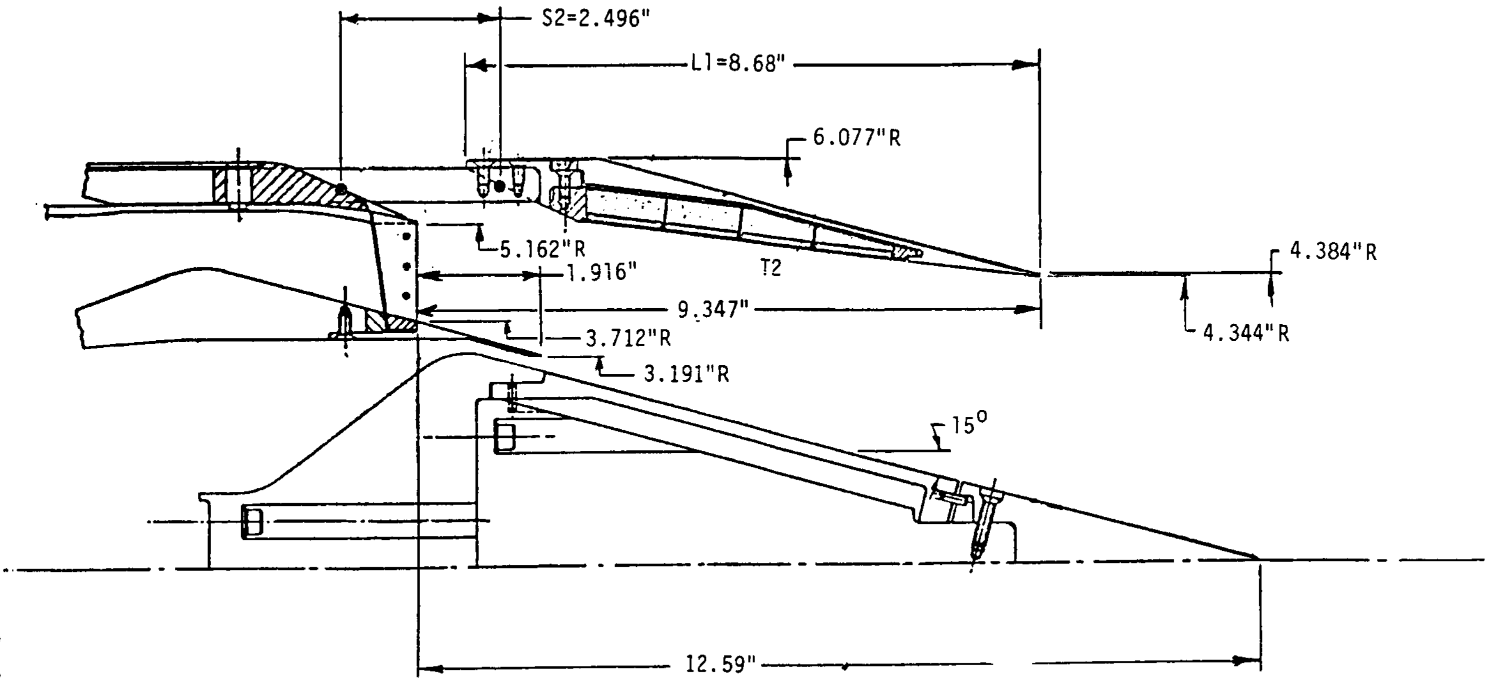

FIGURE 3-11 CONFIGURATION TE-3; BASELINE NOZZLE WITH HARDWALL PLUG AND WITH TREATED EJECTOR, T2, OF NOMINAL LENGTH, L1, AT EXTENDED SPACING, S2

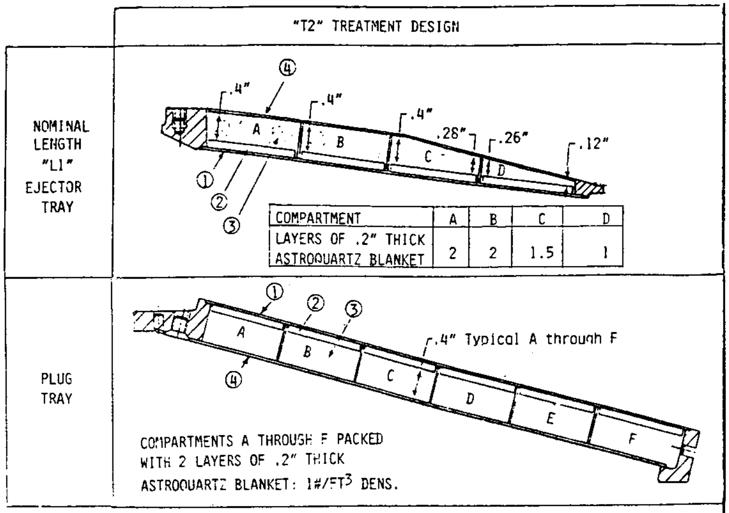

COMPARTMENT	A	B	C	D
LAYERS OF .2" THICK ASTROQUARTZ BLANKET	2	2	1.5	1

① PERFORATED SHEET 37% POROSITY, .045"Ø HOLES ON STRAIGHT LINE PATTERN WITH .067" SPACING ON CENTERS, 225 HOLES PER SQUARE INCH, 24 GA.(.025") THICK, INCONEL 625

② .08" THICK RETIMET METAL FOAM GRADE 80NC2, 95% POROUS, TRIMMED TO FIT INDIVIDUAL TRAY CAVITIES

③ ASTROQUARTZ STYLE 550 MAT, PACKED AS SHOWN

④ COVER PLATE, .030" THICK

	OUTER	INNER	TOTAL
AREA, IN^2	22.750	4.747	27.497
Deq., IN	5.382	2.458	5.917

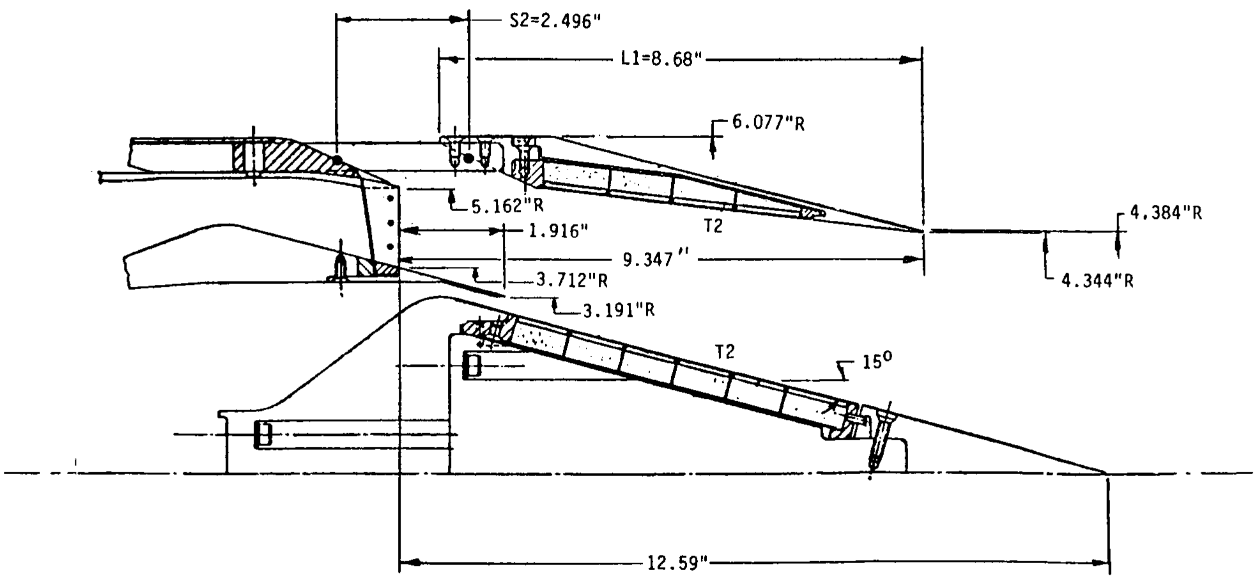

FIGURE 3-12 CONFIGURATION TE-4; BASELINE NOZZLE WITH TREATED PLUG, T2, AND TREATED EJECTOR, T2, OF NOMINAL LENGTH, L1, AT EXTENDED SPACING, S2

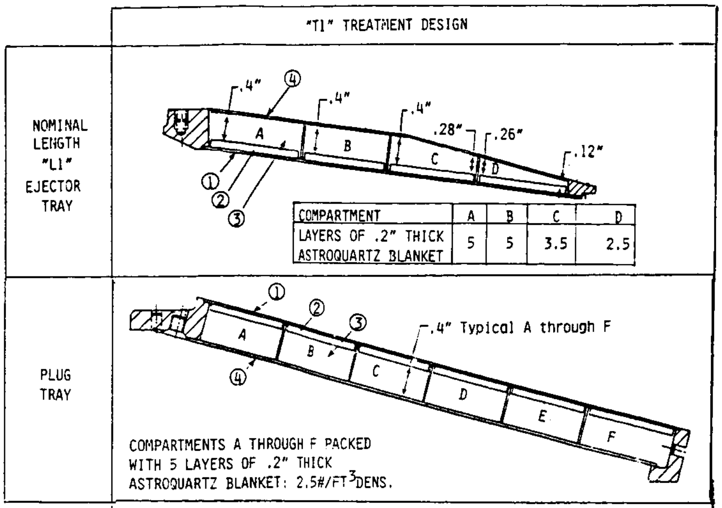

① PERFORATED SHEET 37% POROSITY, .045"Ø HOLES ON STRAIGHT LINE PATTERN WITH .067" SPACING ON CENTERS, 225 HOLES PER SQUARE INCH, 24 GA.(.025") THICK, INCONEL 625

② .08" THICK RETIMET METAL FOAM GRADE 80NC2, 95% POROUS, TRIMMED TO FIT INDIVIDUAL TRAY CAVITIES

③ ASTROQUARTZ STYLE 550 MAT, PACKED AS SHOWN

④ COVER PLATE, .030" THICK

	OUTER	INNER	TOTAL
AREA, IN^2	22.750	4.747	27.497
Deq., IN	5.382	2.458	5.917

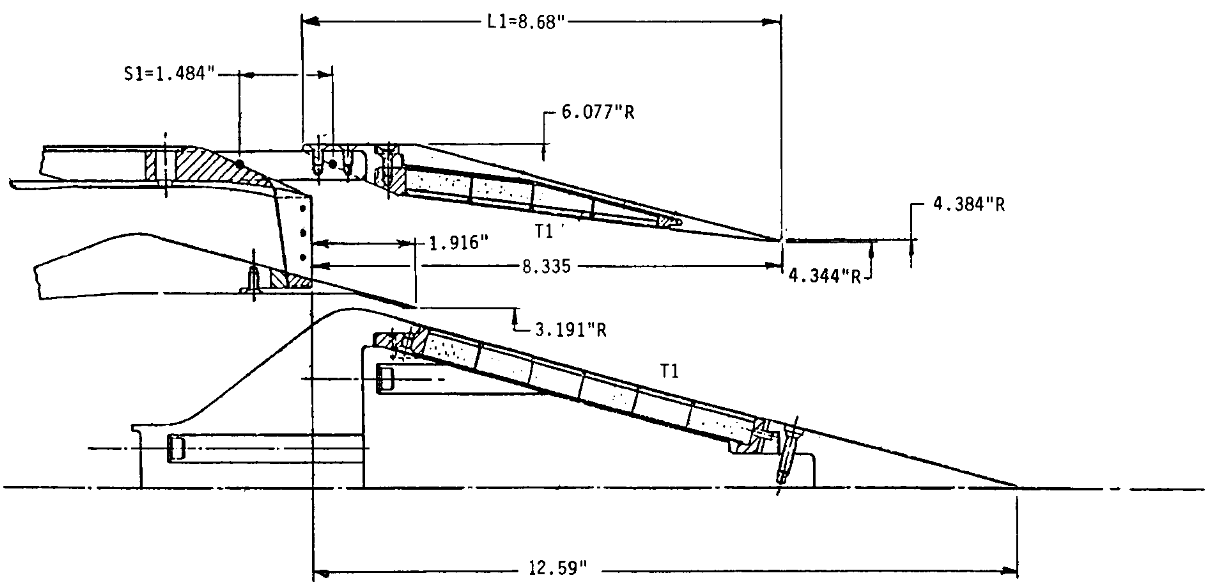

FIGURE 3-13 CONFIGURATION TE-5; BASELINE NOZZLE WITH TREATED PLUG, T1, AND TREATED EJECTOR, T1, OF NOMINAL LENGTH, L1, AT NOMINAL SPACING, S1

"T2" TREATMENT DESIGN

① PERFORATED SHEET 37% POROSITY, .045"Ø HOLES ON STRAIGHT LINE PATTERN WITH .067" SPACING ON CENTERS, 225 HOLES PER SQUARE INCH, 24 GA.(.025") THICK, INCONEL 625

② .08" THICK RETIMET METAL FOAM GRADE 80NC2, 95% POROUS, TRIMMED TO FIT INDIVIDUAL TRAY CAVITIES

③ ASTROQUARTZ STYLE 550 MAT, PACKED AS SHOWN

④ COVER PLATE, .030" THICK

PLUG TRAY

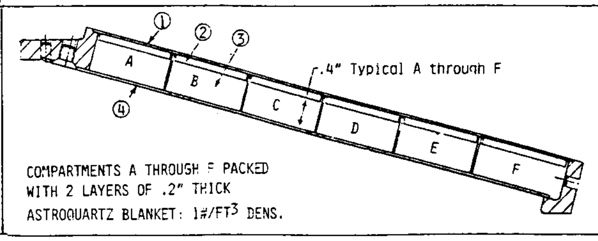

	OUTER	INNER	TOTAL
AREA, IN^2	22.750	4.747	27.497
Deq., IN	5.382	2.458	5.917

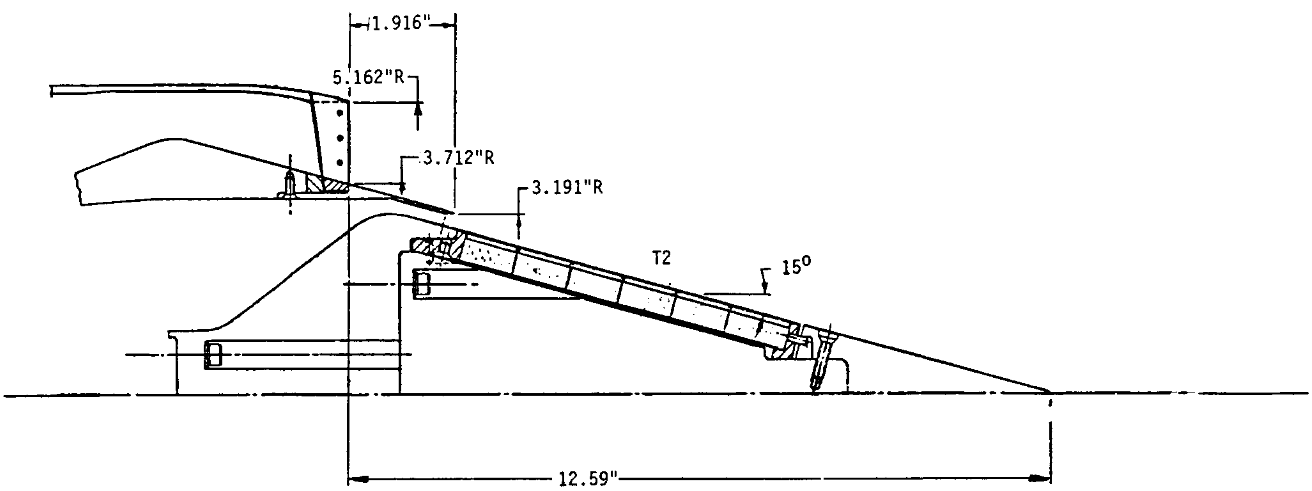

FIGURE 3-14 CONFIGURATION TE-6; BASELINE NOZZLE WITH TREATED PLUG, T2; NO EJECTOR

"T2" TREATMENT DESIGN

EXTENDED LENGTH "L2" EJECTOR TRAY

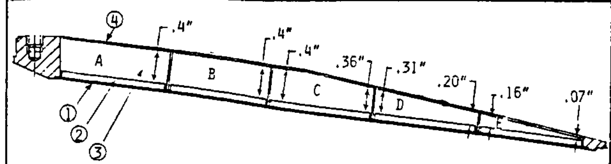

COMPARTMENT	A	B	C	D	E*
LAYERS OF .2" THICK ASTROQUARTZ BLANKET	2	2	2	1.5	1 to.5

* 1 LAYER FWD HALF
.5 LAYER AFT HALF

① PERFORATED SHEET 37% POROSITY, .045"Ø HOLES ON STRAIGHT LINE PATTERN WITH .067" SPACING ON CENTERS, 225 HOLES PER SQUARE INCH, 24 GA.(.025") THICK, INCONEL 625

② .08" THICK RETIMET METAL FOAM GRADE 80NC2, 95% POROUS, TRIMMED TO FIT INDIVIDUAL TRAY CAVITIES

③ ASTROQUARTZ STYLE 550 MAT, PACKED AS SHOWN

④ COVER PLATE, .030" THICK

	OUTER	INNER	TOTAL
AREA, IN^2	22.750	4.747	27.497
Deq., IN	5.382	2.458	5.917

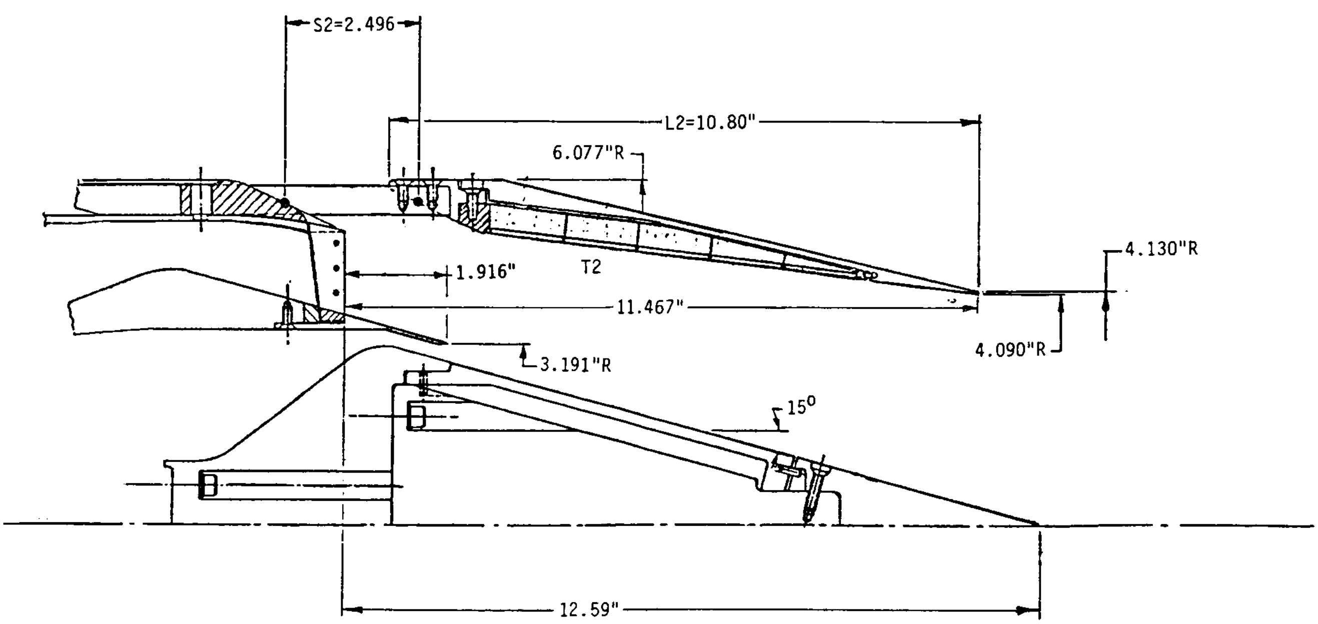

FIGURE 3-15 CONFIGURATION TE-7; BASELINE NOZZLE WITH HARDWALL PLUG AND WITH TREATED EJECTOR, T2, OF EXTENDED LENGTH, L2, AT EXTENDED SPACING, S2

"T2" TREATMENT DESIGN

EXTENDED LENGTH "L2" EJECTOR TRAY

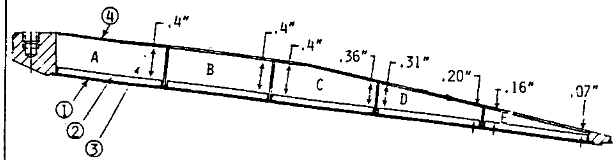

COMPARTMENT	A	B	C	D	E*
LAYERS OF .2" THICK ASTROQUARTZ BLANKET	2	2	2	1.5	1 to .5

* 1 LAYER FWD HALF
.5 LAYER AFT HALF

PLUG TRAY

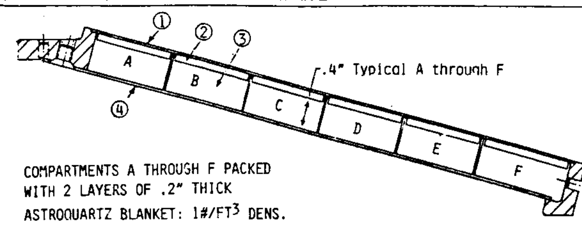

COMPARTMENTS A THROUGH F PACKED WITH 2 LAYERS OF .2" THICK ASTROQUARTZ BLANKET: 1#/FT^3 DENS.

① PERFORATED SHEET 37% POROSITY, .045"Ø HOLES ON STRAIGHT LINE PATTERN WITH .067" SPACING ON CENTERS, 225 HOLES PER SQUARE INCH, 24 GA.(.025") THICK, INCONEL 625

② .08" THICK RETIMET METAL FOAM GRADE 80NC2, 95% POROUS, TRIMMED TO FIT INDIVIDUAL TRAY CAVITIES

③ ASTROQUARTZ STYLE 550 MAT, PACKED AS SHOWN

④ COVER PLATE, .030" THICK

	OUTER	INNER	TOTAL
AREA, IN^2	22.750	4.747	27.497
Deq., IN	5.382	2.458	5.917

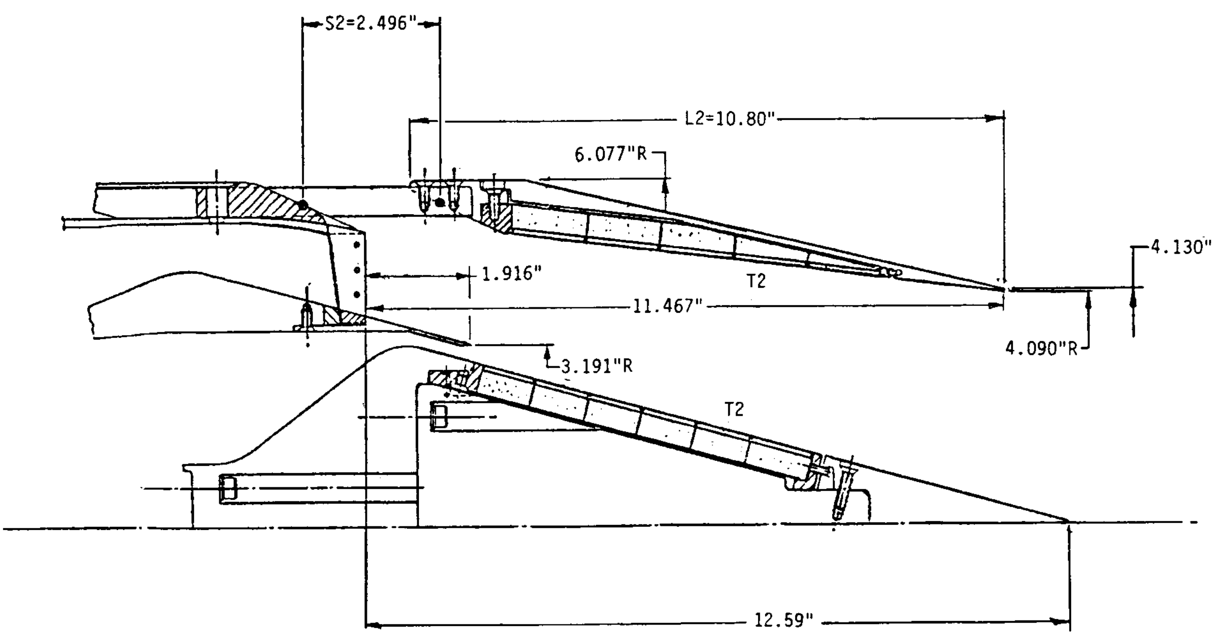

FIGURE 3-16 CONFIGURATION TE-8; BASELINE NOZZLE WITH TREATED PLUG, T2, AND WITH TREATED EJECTOR, T2, OF EXTENDED LENGTH, L2, AT EXTENDED SPACING, S2

"T1" TREATMENT DESIGN

NOMINAL LENGTH "L1" EJECTOR TRAY

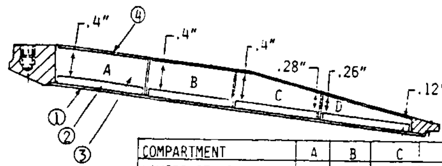

COMPARTMENT	A	B	C	D
LAYERS OF .2" THICK ASTROQUARTZ BLANKET	5	5	3.5	2.5

PLUG TRAY

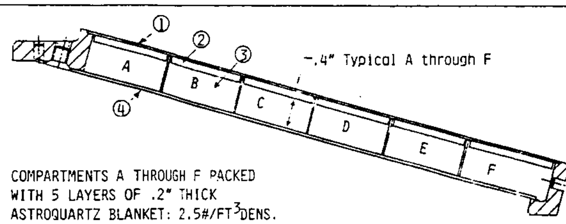

COMPARTMENTS A THROUGH F PACKED WITH 5 LAYERS OF .2" THICK ASTROQUARTZ BLANKET: 2.5#/FT^{3}DENS.

① PERFORATED SHEET 37% POROSITY, .045"Ø HOLES ON STRAIGHT LINE PATTERN WITH .067" SPACING ON CENTERS, 225 HOLES PER SQUARE INCH, 24 GA.(.025") THICK, INCONEL 625

② .08" THICK RETIMET METAL FOAM GRADE 80NC2, 95% POROUS, TRIMMED TO FIT INDIVIDUAL TRAY CAVITIES

③ ASTROQUARTZ STYLE 550 MAT, PACKED AS SHOWN

④ COVER PLATE, .030" THICK

	OUTER	INNER	TOTAL
AREA, IN^2	22.750	4.747	27.497
Deq., IN	5.382	2.458	5.917

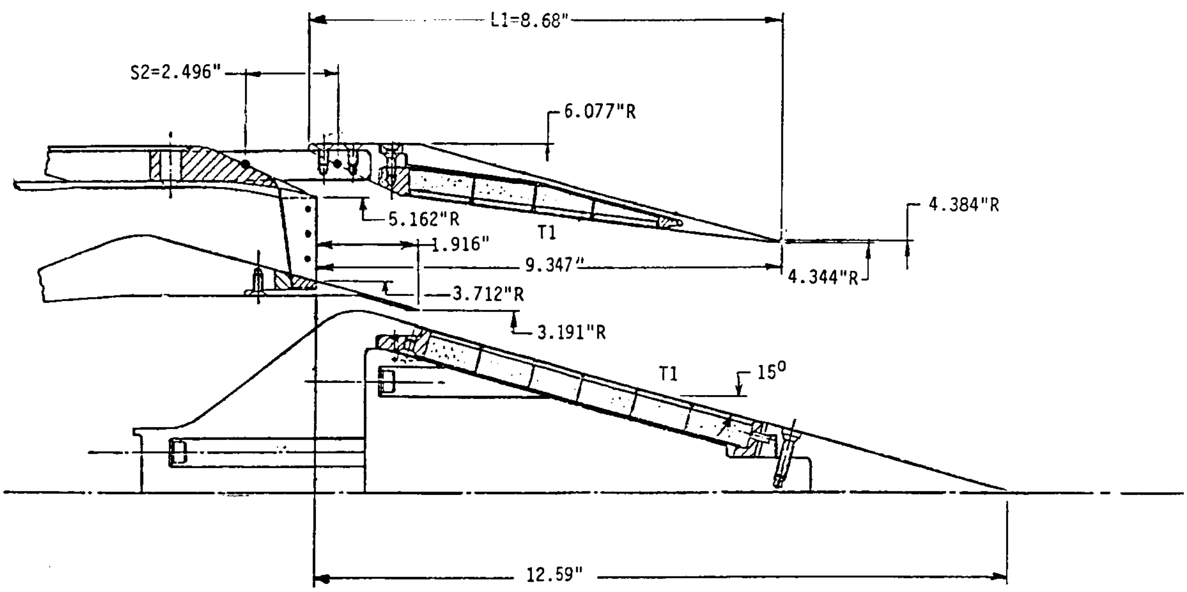

FIGURE 3-17 CONFIGURATION TE-9; BASELINE NOZZLE WITH TREATED PLUG, T1, AND WITH TREATED EJECTOR, T1, OF NOMINAL LENGTH, L1, AT EXTENDED SPACING, S2

	OUTER	INNER	TOTAL
AREA, IN^2	22.750	4.747	27.497
Deq., IN	5.382	2.458	5.917

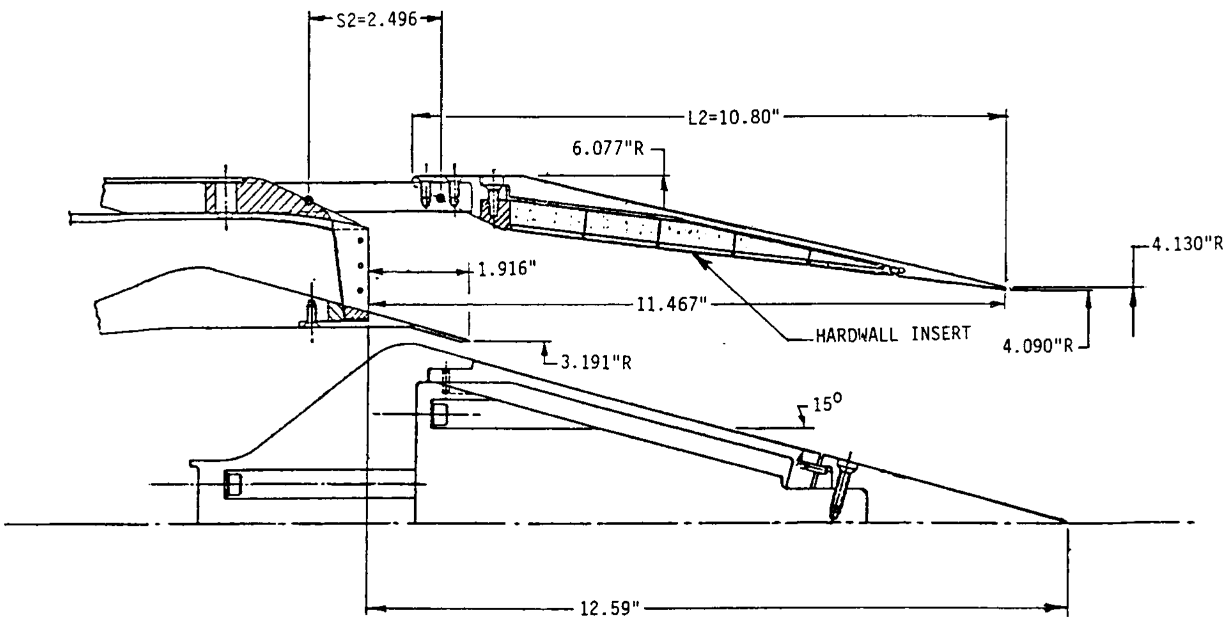

FIGURE 3-18 CONFIGURATION TE-10; BASELINE NOZZLE WITH HARDWALL PLUG AND WITH HARDWALL EJECTOR OF EXTENDED LENGTH, L2, AT EXTENDED SPACING, S2

"AS BUILT" PARAMETERS

Parameter	Outer Nozzle	Inner Nozzle
Type	20-Chute	Annular
A_{flow}, in.^{2}	22.75	4.747
$D_{flow,eq}$, in.	5.382	2.458
$A_{blocked}$, in.^{2}	17.634	-
Area Ratio	1.775	-
Throat Plane Angle Re Vert., Degrees	0	15
R_{tip}, in.	5.162	3.190
R_{hub}, in.	3.713	2.952
Radius Ratio	.719	.926
A_{inner}/A_{outer}	.21	

• All Items Dwg No. 4013312-428

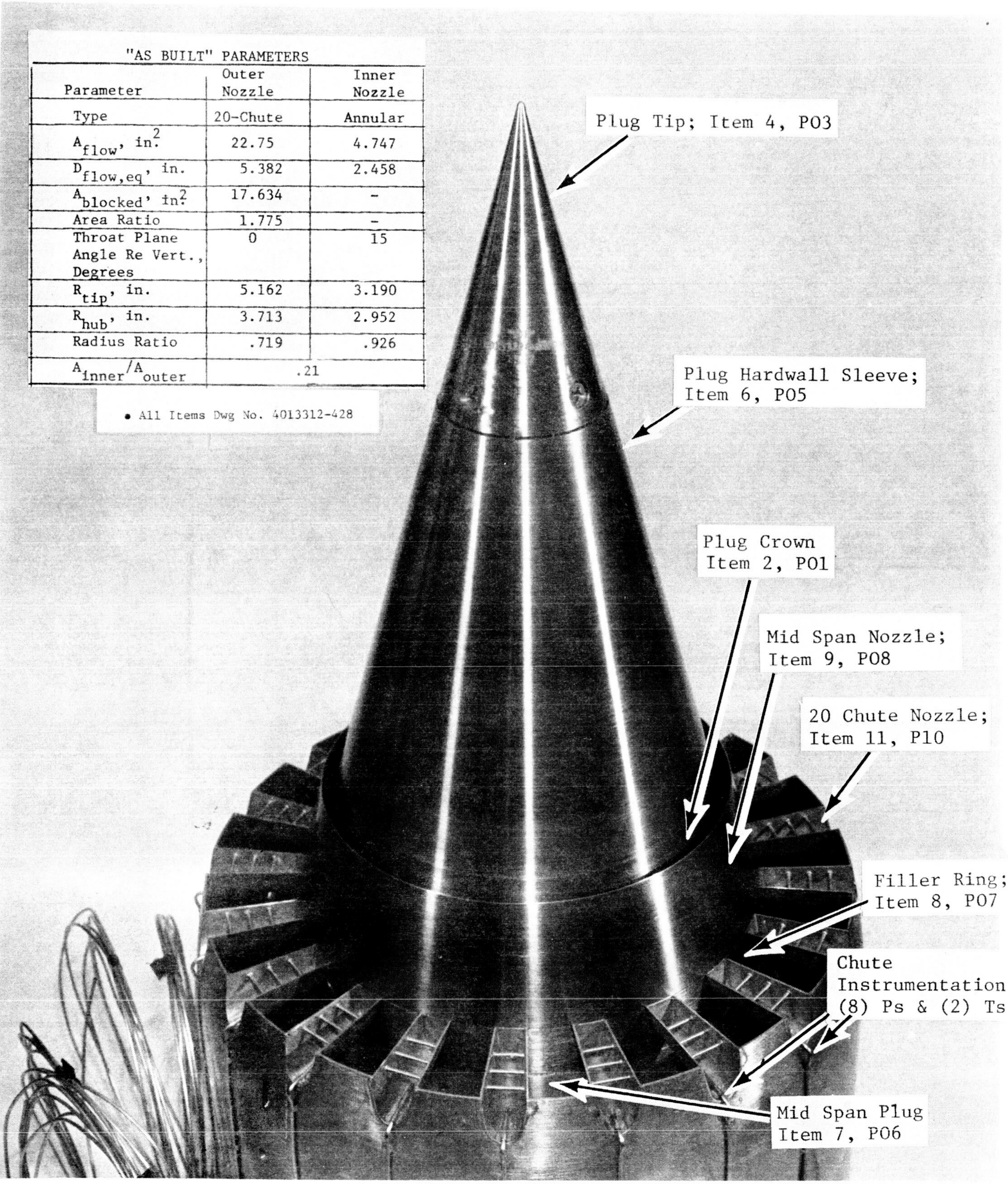

FIGURE 3-19. CONFIGURATION TE-1 ASSEMBLY DETAILS

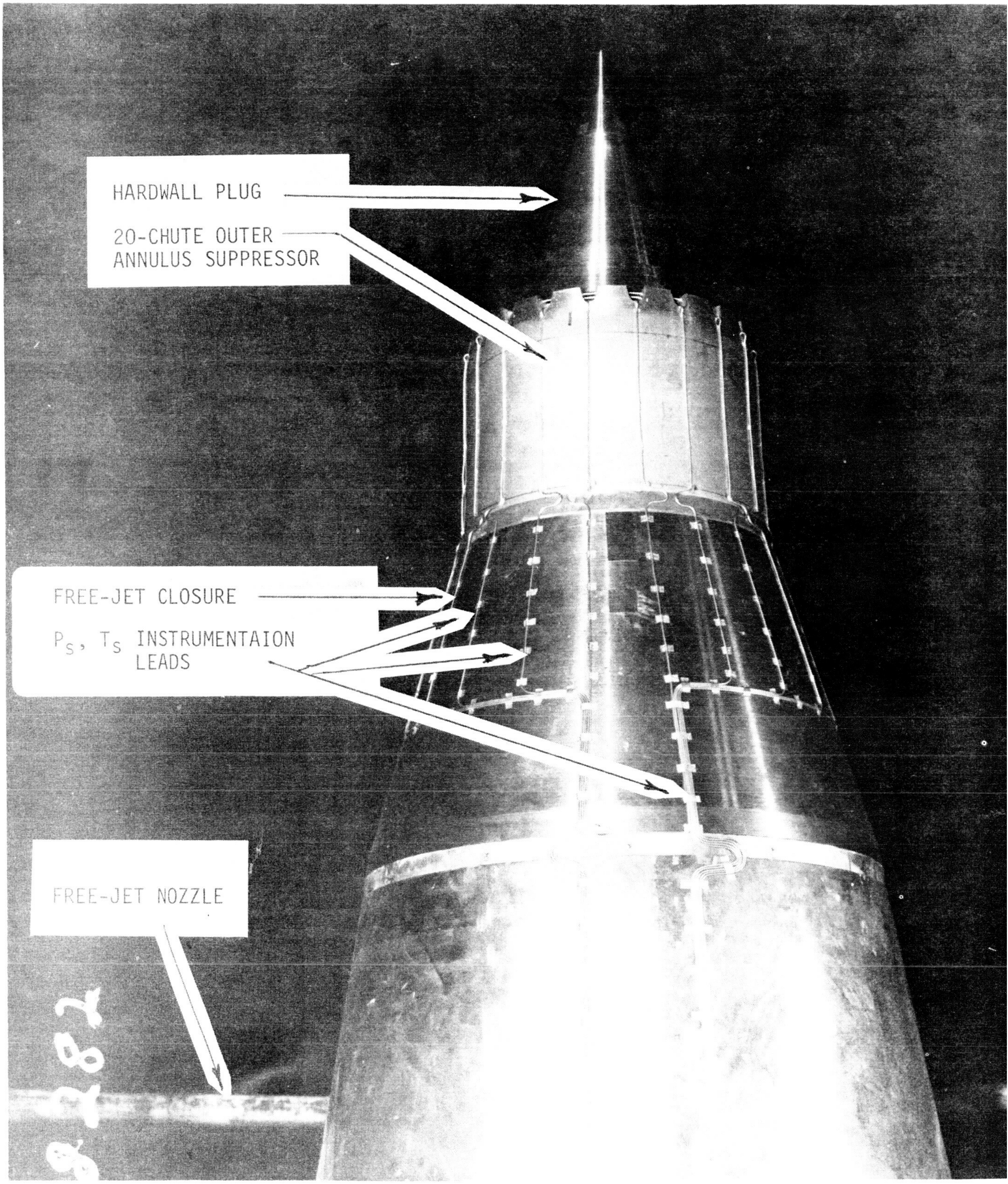

FIGURE 3-20. CONFIGURATION TE-1 ASSEMBLY AS-MOUNTED IN THE ANECHOIC FREE JET FACILITY

"AS BUILT" PARAMETERS

Parameter	Outer Nozzle	Inner Nozzle
Type	20-Chute	Annular
A_{flow}, $in.^2$	22.75	4.747
$D_{flow,eq}$, in.	5.382	2.458
$A_{blocked}$, $in.^2$	17.634	-
Area Ratio	1.775	-
Throat Plane Angle Re Vert., Degrees	0	15
R_{tip}, in.	5.162	3.190
R_{hub}, in.	3.713	2.952
Radius Ratio	.719	.926
A_{inner}/A_{outer}	.21	

• All Items Dwg No. 4013312-428

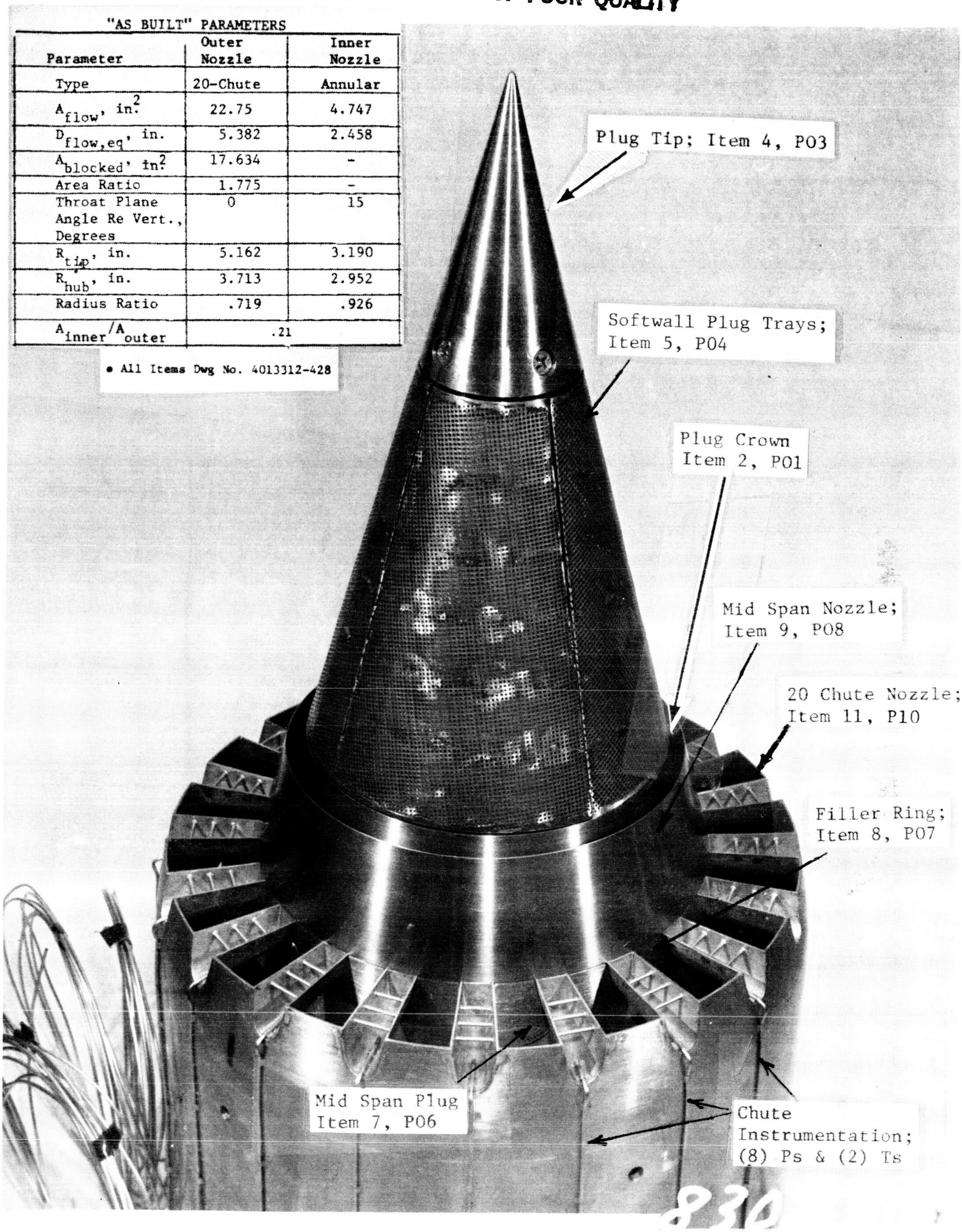

FIGURE 3-21. CONFIGURATION TE-6 ASSEMBLY DETAILS

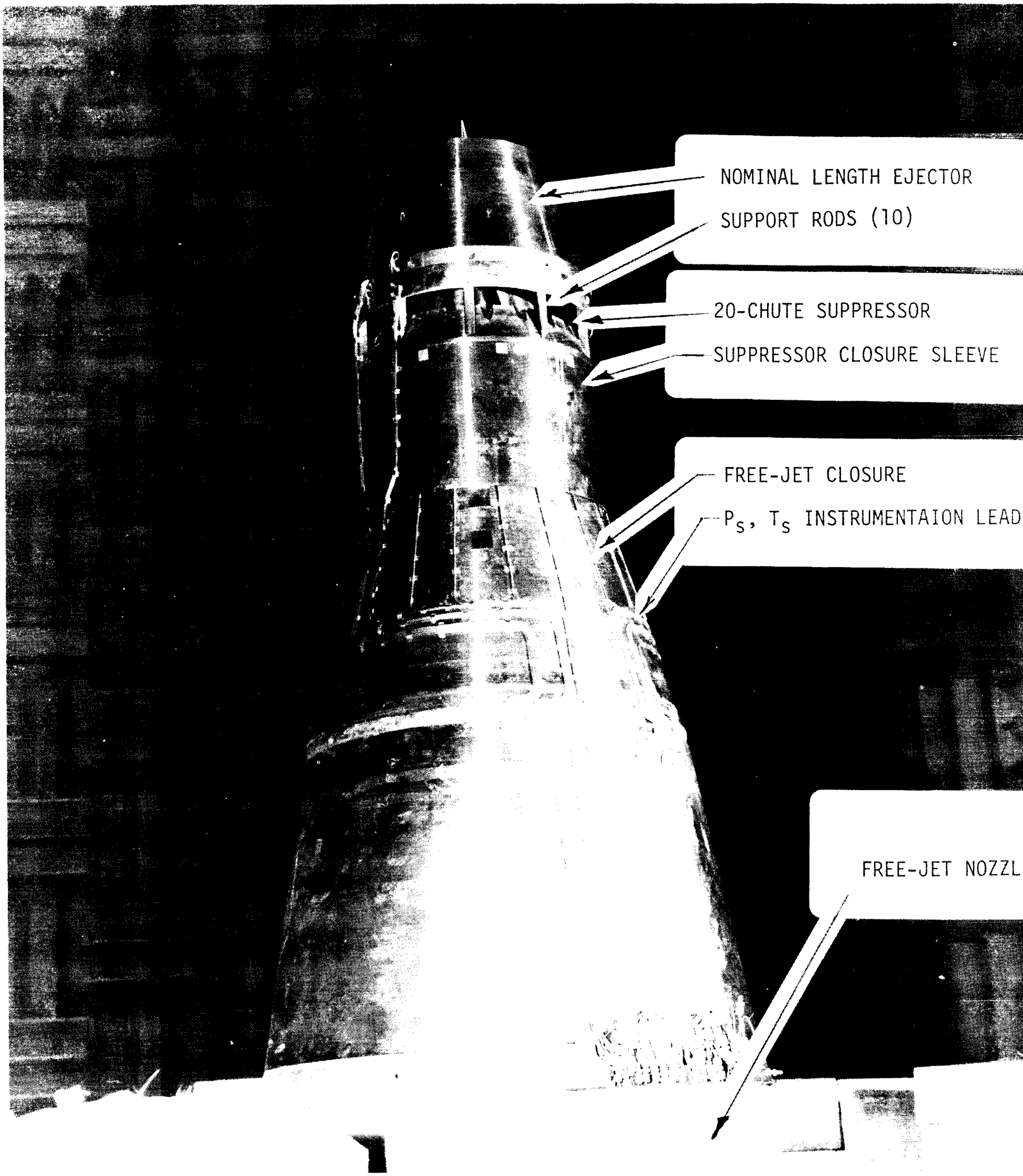

FIGURE 3-22. TYPICAL SUPPRESSOR-EJECTOR MODEL INSTALLATION WITHIN THE ANECHOIC FREE-JET FACILITY

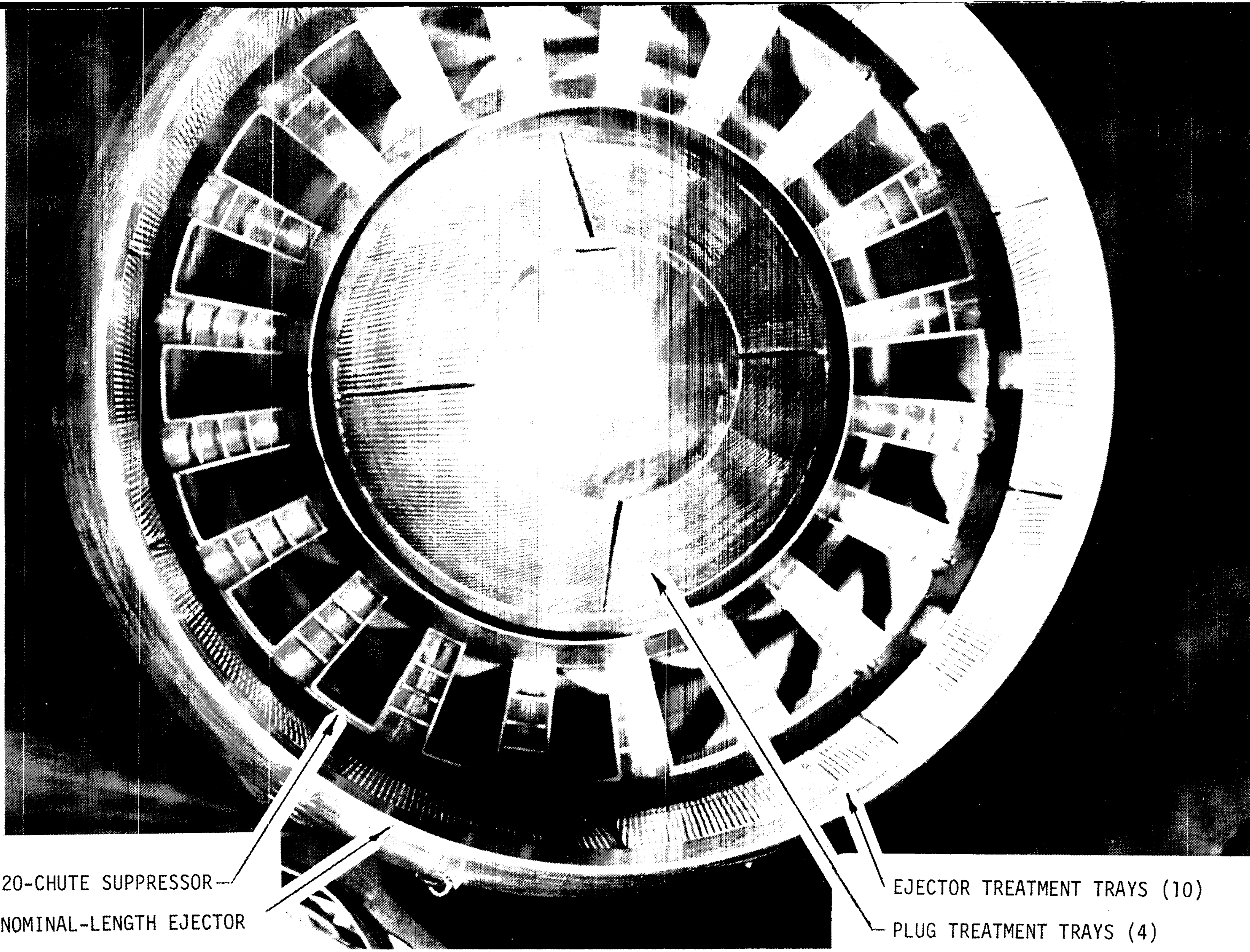

FIGURE 3-23. TYPICAL SUPPRESSOR-EJECTOR MODEL INSTALLATION WITHIN THE ANECHOIC FREE-JET FACILITY

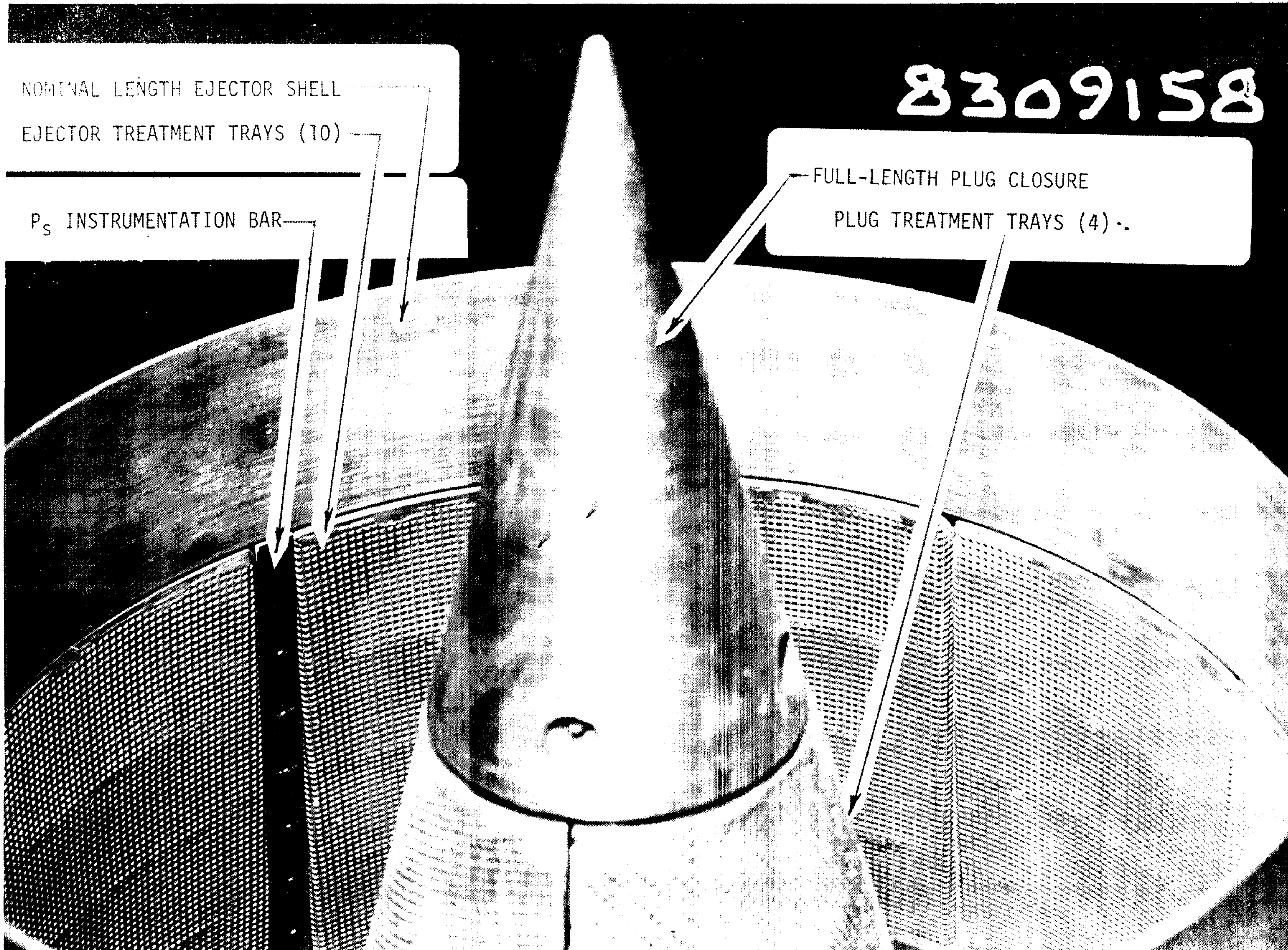

FIGURE 3-24. TYPICAL SUPPRESSOR-EJECTOR MODEL INSTALLATION WITHIN THE ANECHOIC FREE-JET FACILITY

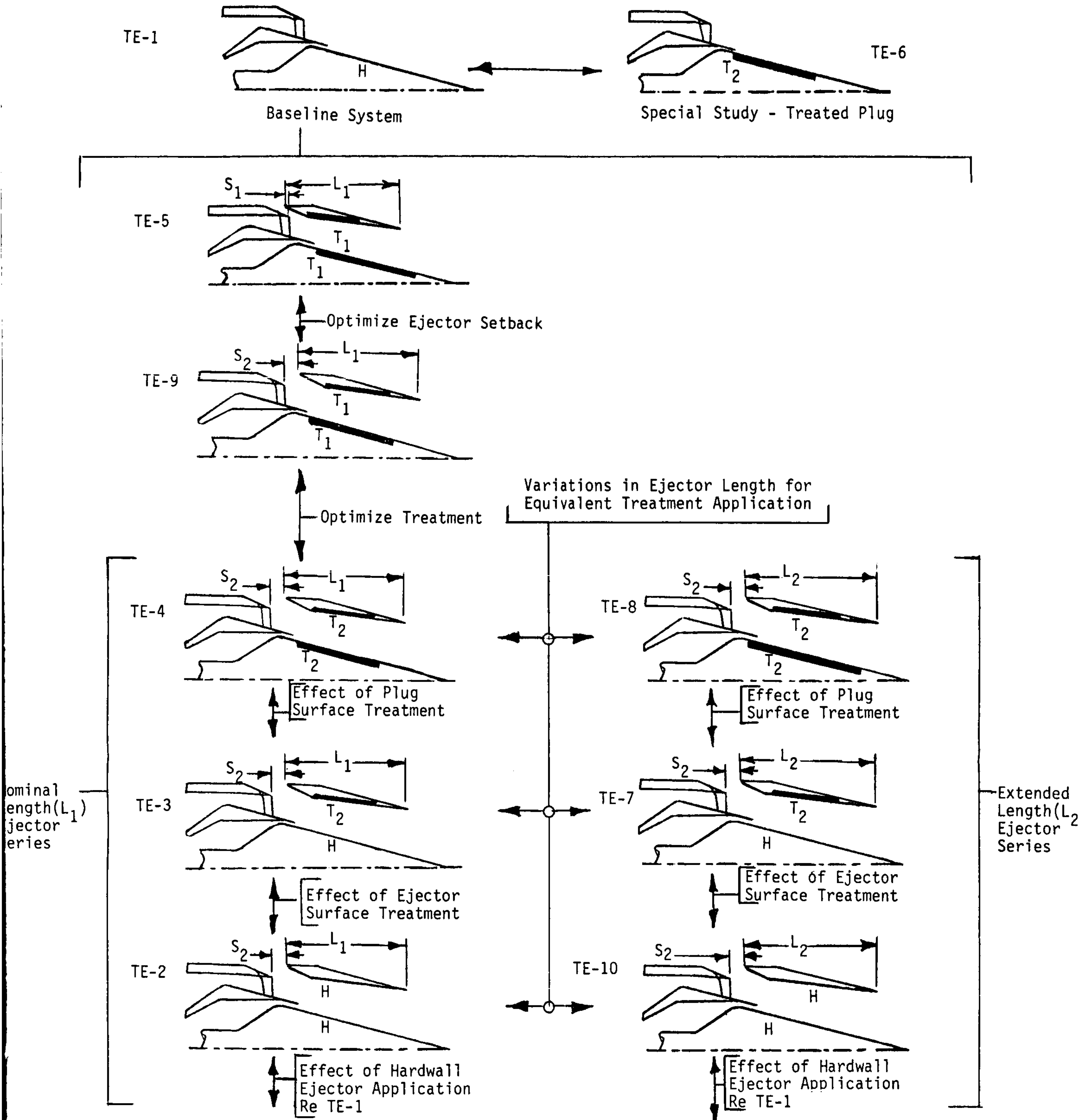

FIGURE 3-25 FLOW SCHEMATIC OF TEST CONFIGURATIONS RELATIVE TO EVALUATION OF ACOUSTIC PERFORMANCE

- o Configuration TE-1, Baseline nozzle system to which all ejector/treatment systems would be referenced. This configuration is somewhat similar to previous Configuration 10.1 of NASA-GE study Contract NAS3-21608 (Reference 8).

- o Configuration TE-6, in comparison to Configuration TE-1 would study the potential influence of a softwall plug on alleviation of shock-cell strength and subsequent shock related noise.

- o Configurations TE-5 and TE-9 would optimize ejector axial positioning between S1 and S2. The S1 ejector setback distance is compatible with the full scale design value of 11.0" (1.484" model scale). The S2 position (18.5" full scale and 2.496" model scale) was that found optimum among the positions tested for aerodynamic performance while at takeoff cycle pressure ratio (Reference 1). The S2 position was judged acoustically more favorable from on-line acoustic data during test, and, therefore, maintained for all subsequent test configurations.

- o Configurations TE-9 and TE-4 would optimize treatment performance between T1 and T2 designs. The treatment designs are documented in detail within Reference 4, appended within Volume II of this program's comprehensive data report. The T2 design was judged acoustically more favorable from on-line acoustic data during test, and, therefore, maintained for all subsequent test configurations.

- o Series TE-4, TE-3 and TE-2 would allow systematic evaluation of treatment extent-of-application, from fully treated to no treatment hardwall surfaces, within the nominal length, L1, ejector system. The nominal length ejector was scaled directly from the full-scale design of Reference 2 and allowed for acoustic treatment application over approximately 70% of the ejector flap length.

- o Series TE-8, TE-7 and TE-10 would allow similar evaluation within he extended length, L2, ejector system. This ejector applies treatment to a length equivalent to that of the full flap length of the nominal length ejector system. The additional untreated closure length is similar to that of the nominal length ejector.

- o Configurations TE-2 and TE-10 relative to TE-1 would allow evaluation of hardwall ejector system to the baseline suppressor/coannular nozzle system.

3.2.1.1 Baseline Nozzle System

The baseline nozzle system, per Figure 3-19 schematic and photo, was a coannular inverted-velocity-profile plug nozzle with 20-shallow-chute outer stream suppressor (hardwall plug and no ejector). The nozzle "as-built" geometric parameters are as per Figure 3-19. Previous model studies on shock noise alleviation (References 9 and 10) indicated a sharp-tipped plug was beneficial in reducing shock strength and associated shock-cell noise. This plug-tip design was adopted in this study program's models, and, therefore, deviated from the full scale study nozzle of Figure 2-1. The model system, with A^{o}_{flow} = 22.75 in^2 and A^{i}_{flow} = 4.747 in^2, was a .135 scaled version of the full scale study exhaust system.

3.2.1.2 Ejector Systems

Two ejector systems, designated nominal length, L1, and extended length, L2, were designed and fabricated. The nominal length system, shown schematically as influencing test configuration variations, in Figures 3-10, 3-11, 3-12, 3-13 and 3-17 and photographically in Figures 3-26 and 3-27, was scaled directly from the full scale and aerodynamic scale-model systems (Reference 1 and 2 and Figure 2-1). The nominal length ejector is 8.68" long model-scale and allows for acoustic treatment application over approximately 70% of its flap length. The extended length ejector system is shown schematically as influencing test configuration variations in Figures 3-15, 3-16 and 3-18 and photographically in Figure 3-28. This ejector is 10.80" long model-scale and applies treatment to a length equivalent to that of the full flap length of the nominal length ejector system. The additional untreated closure length is similar to that of the nominal length ejector.

The two ejector systems used a common ejector inlet ring (Figures 3-26 and 3-28) and common (10) support rods (Figure 3-27) to mount the systems to the primary nozzle. The ejector rods had two fixed-location mounting points to accommodate the S1 and S2 axial positions. Each ejector assembly had (10) treatment trays; (8) regular width (36^o angular sector) and (2) narrower width (31.5^o angular sector). The narrow trays allowed accommodation of P_S and T_S instrumentation bars within the ejector shells. Note that full defintion of all test hardware is available within the comprehensive data report, Volume II, Appendix B, "Model Hardware Design Documentation". All hardware manufacturing drawings are presented within that appendix.

3.2.2 Acoustic Treatment Definition

Acoustic treatment application within the ejector systems was accomplished through use of "packed" compartmentalized treatment trays, shown photographically in Figure 3-29 for the nominal length ejector and in Figure 3-30 for the extended length ejector. The nominal length trays each had (4) compartments of approximately 1.1" length; the extended length trays each had (5) compartments of approximately 1.3" length. Compartmentalized trays, per Figure 3-31, were also used for acoustic treatment application to the plug surface. As defined in individual configuration sketches (Figures 3-10 through 3-18) and as summarized in Figure 3-32, the tray construction/treatment packing consisted of:

- Perforated sheet faceplate of 37% porosity
- .08" thick Retimet metal foam, 95% porous, trimmed to fit individual tray cavities; applied to protect the treatment from degradation due to flow turbulence
- Astroquartz style 550 mat, packed to specifications of Figure 3-32.
- Solid cover plates over each compartment

Layers of the .2" thick Astroquartz blanket were applied and compressed within the cavities to attain the desired treatment density. Treatment design procedure and final selections are documented within Reference 4, TM 84-395; included within this program's CDR Volume II as Appendix C.

ORIGINAL PAGE IS
OF POOR QUALITY

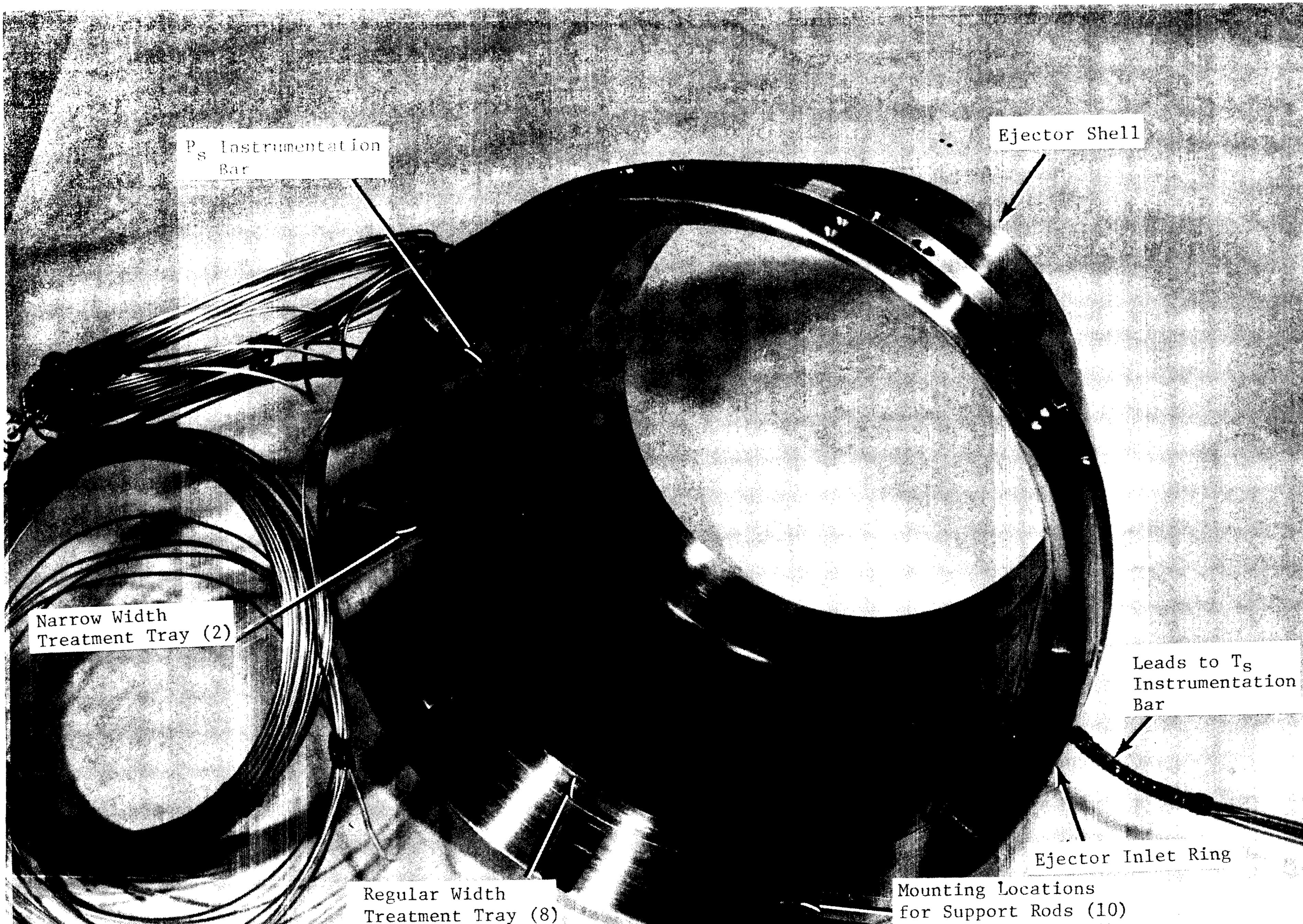

FIGURE 3-26. NOMINAL LENGTH EJECTOR ASSEMBLY, FWD-LOOKING-AFT

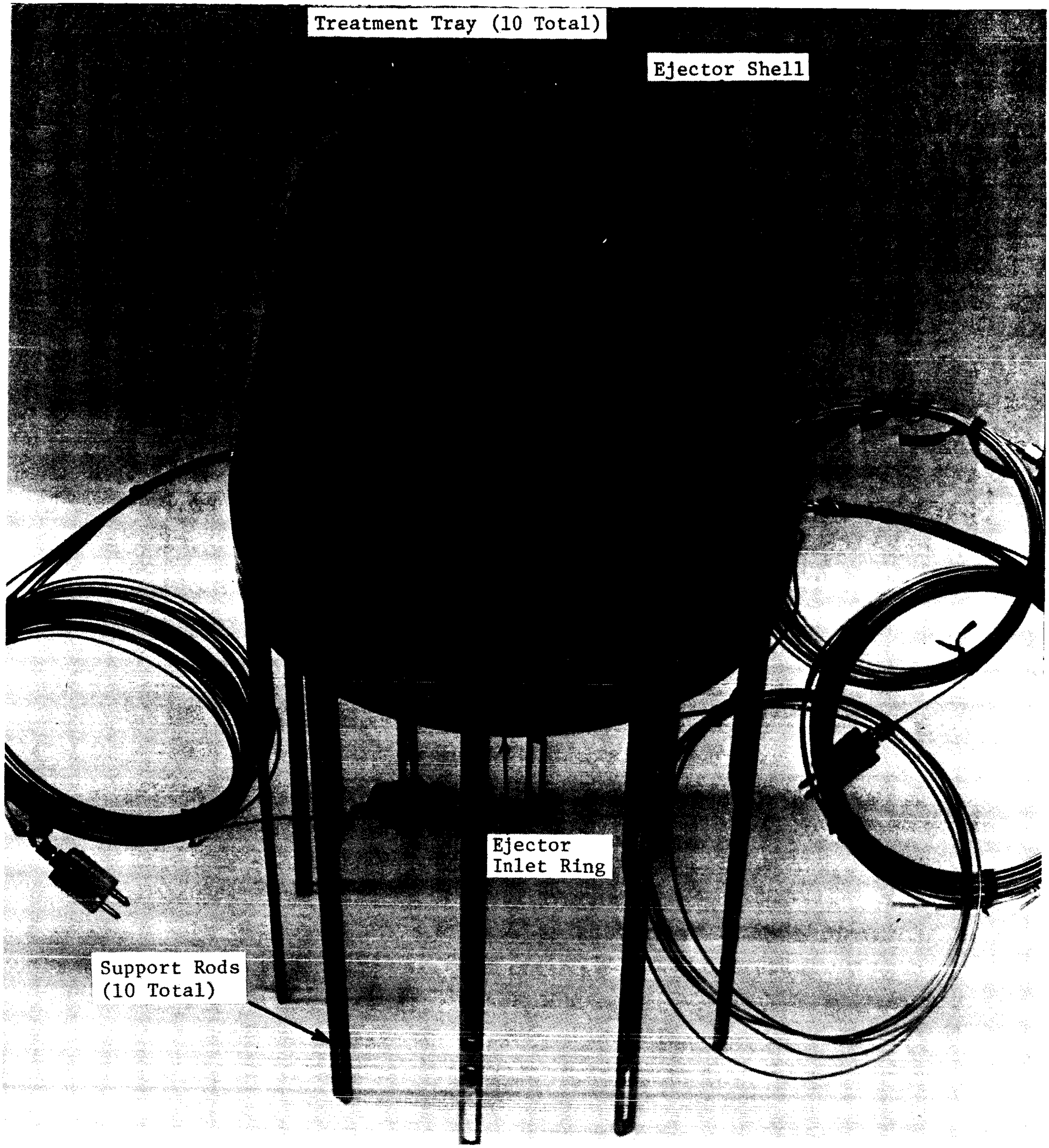

FIGURE 3-27. NOMINAL LENGTH EJECTOR/SUPPORT ROD ASSEMBLY, SIDE VIEW

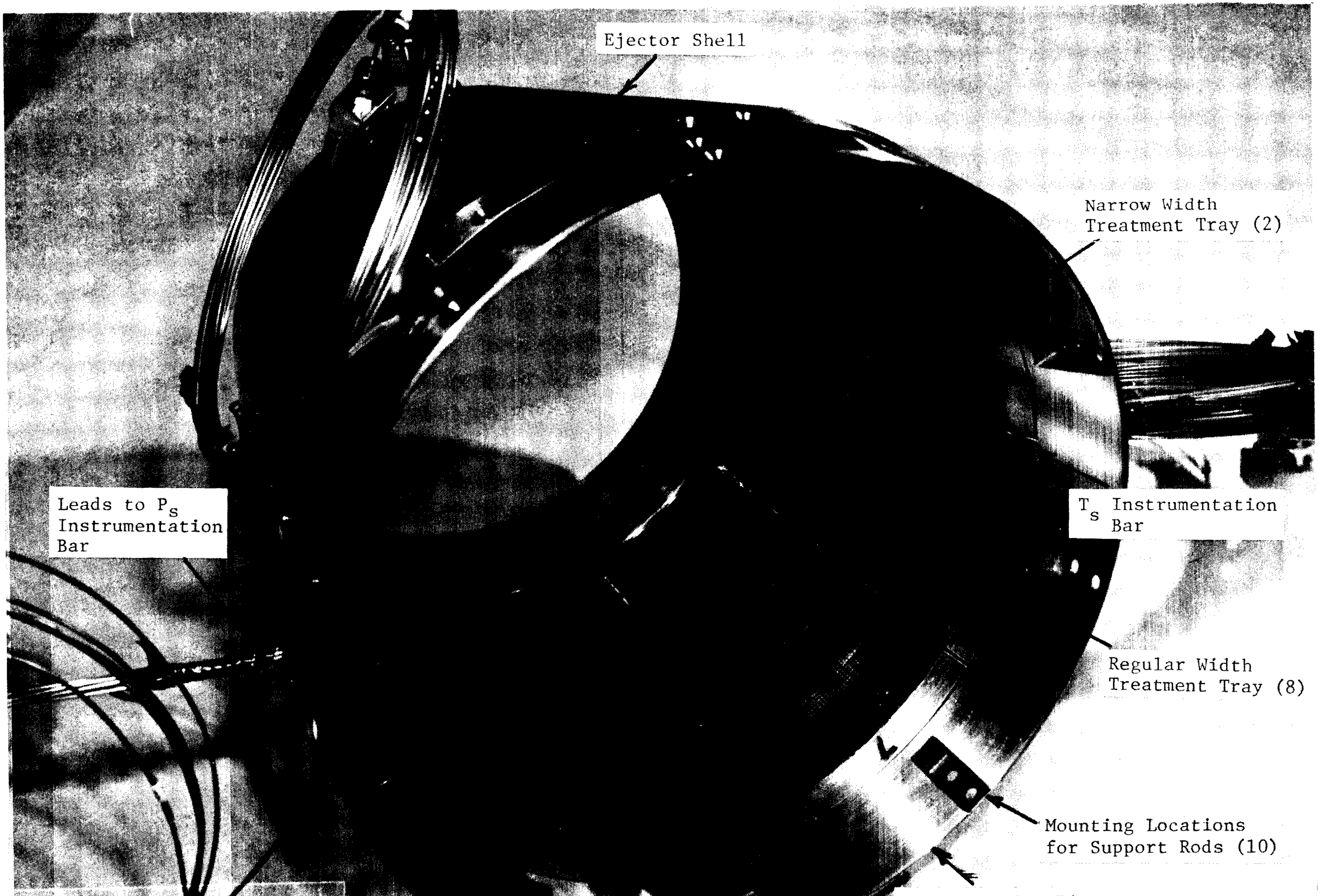

FIGURE 3-28. EXTENDED LENGTH EJECTOR ASSEMBLY, FWD-LOOKING-AFT

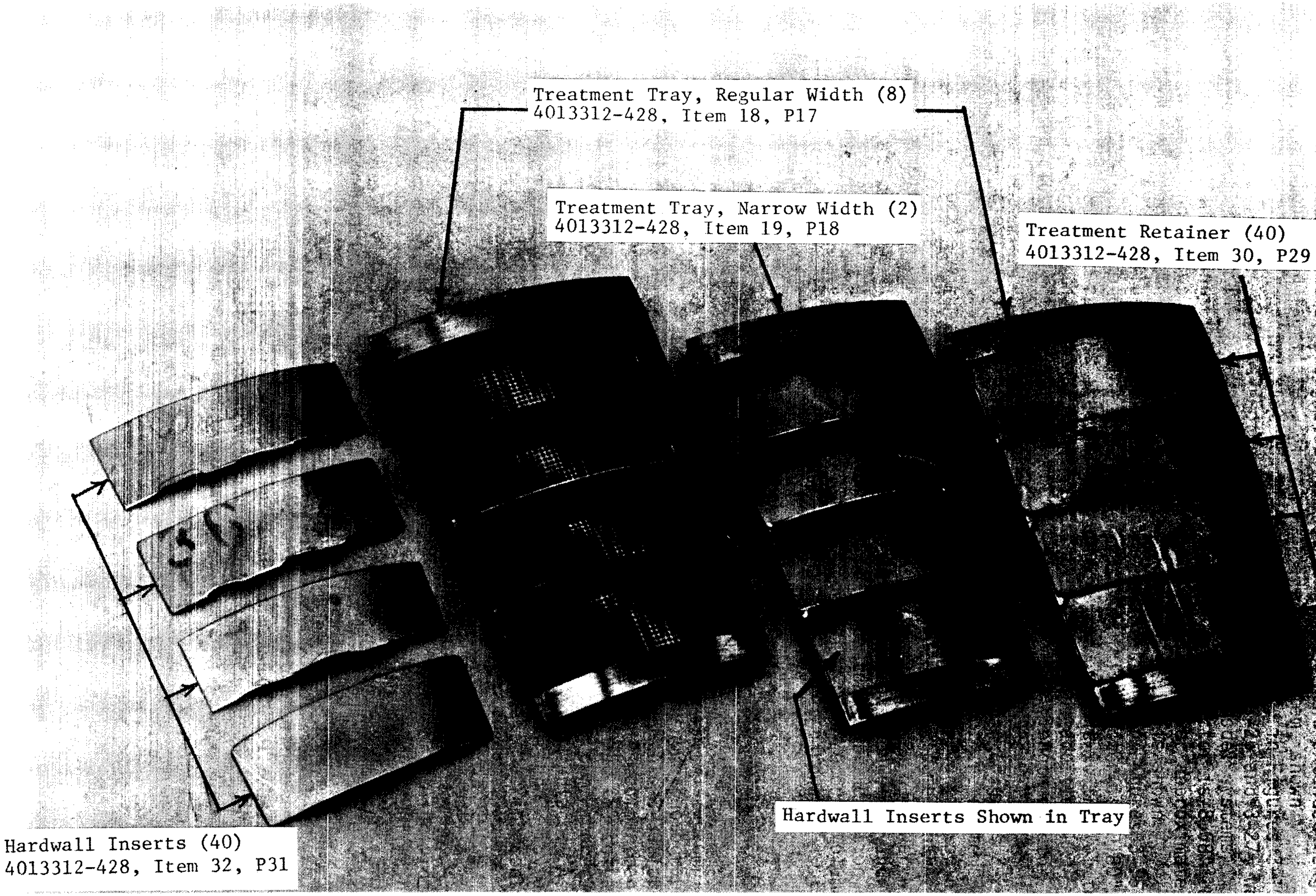

FIGURE 3-29. ACOUSTIC TREATMENT TRAYS FOR NOMINAL LENGTH EJECTOR, REGULAR AND NARROW WIDTH

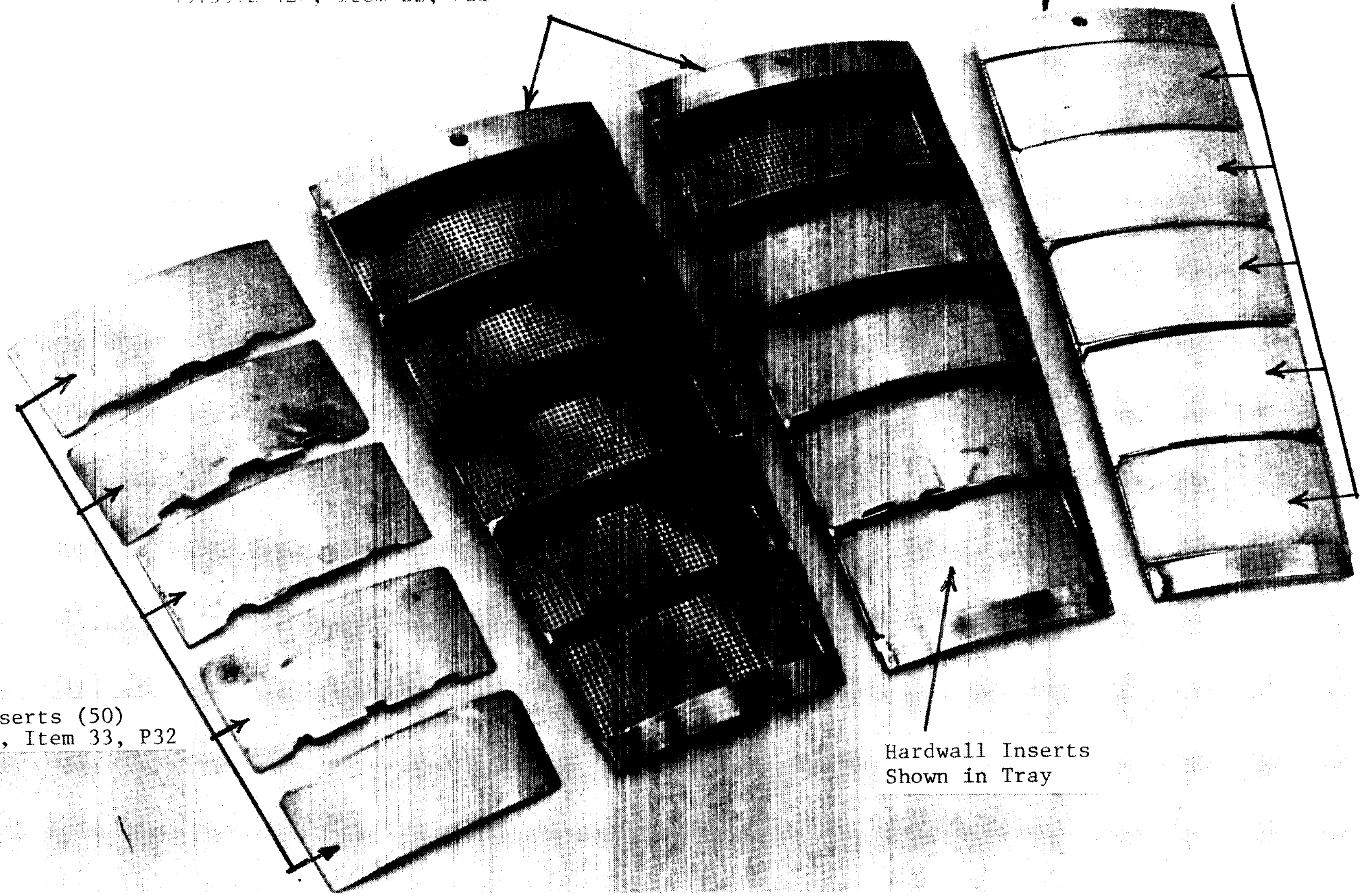

FIGURE 3-30. ACOUSTIC TREATMENT TRAYS FOR EXTENDED LENGTH EJECTOR, REGULAR AND NARROW WIDTH

ORIGINAL PAGE IS
OF POOR QUALITY

ORIGINAL PAGE IS
OF POOR QUALITY

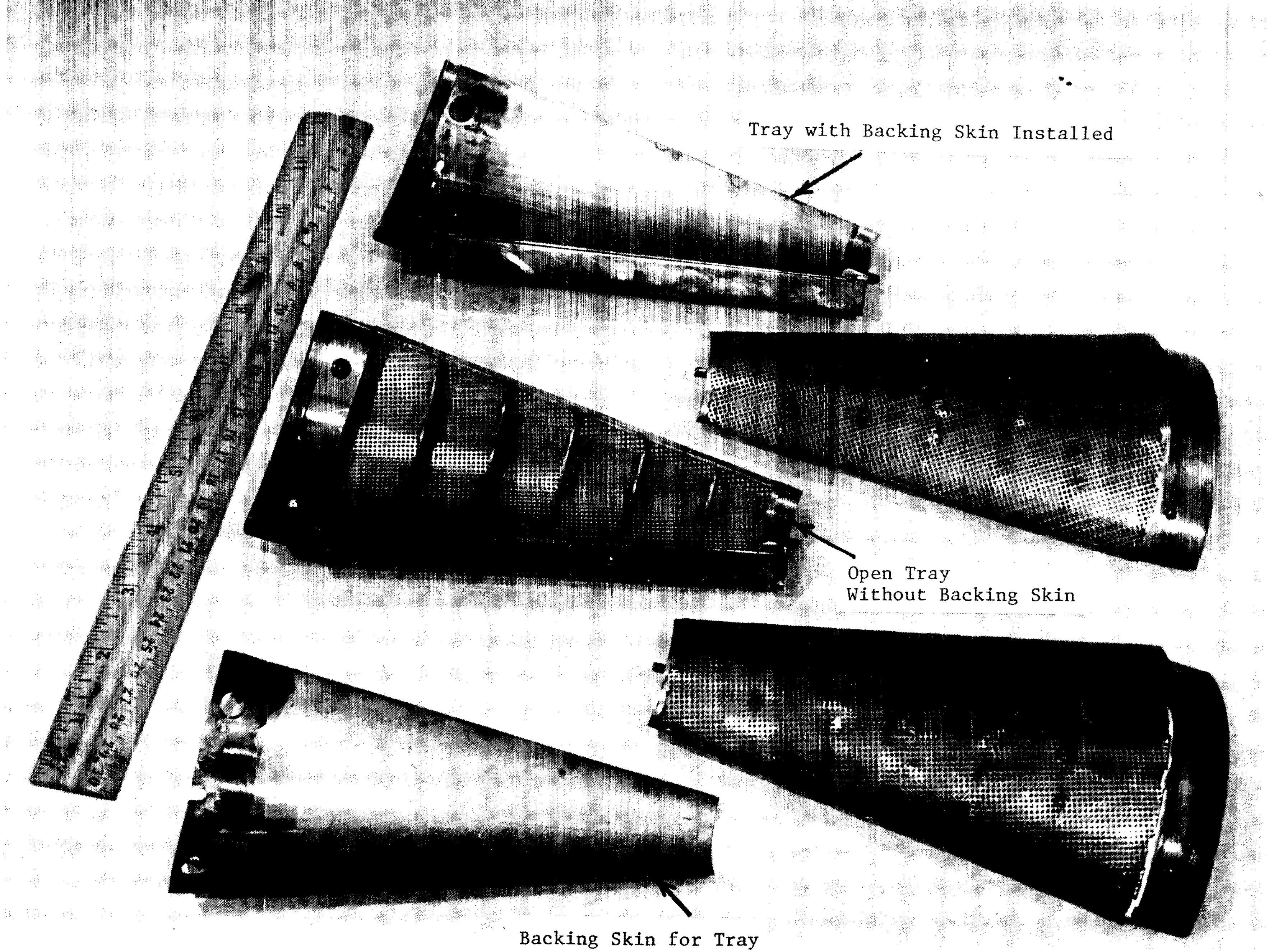

FIGURE 3-31. ACOUSTIC TREATMENT TRAYS FOR PLUG SURFACE APPLICATION

NOMINAL LENGTH "L1" EJECTOR TRAY

"T1" TREATMENT DESIGN

• CONFIGURATIONS TE-5 & TE-9

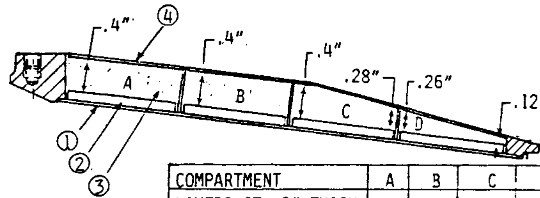

COMPARTMENT	A	B	C	D
LAYERS OF .2" THICK ASTROQUARTZ BLANKET	5	5	3.5	2.5

"T2" TREATMENT DESIGN

• CONFIGURATIONS TE-3 & TE-4

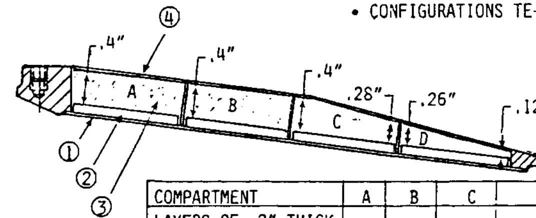

COMPARTMENT	A	B	C	D
LAYERS OF .2" THICK ASTROQUARTZ BLANKET	2	2	1.5	1

EXTENDED LENGTH "L2" EJECTOR TRAY

① PERFORATED SHEET 37% POROSITY, .045"Ø HOLES ON STRAIGHT LINE PATTERN WITH .067" SPACING ON CENTERS, 225 HOLES PER SQUARE INCH, 24 GA.(.025") THICK, INCONEL 625

② .08" THICK RETIMET METAL FOAM GRADE 80NC2, 95% POROUS, TRIMMED TO FIT INDIVIDUAL TRAY CAVITIES

③ ASTROQUARTZ STYLE 550 MAT, PACKED AS SHOWN

④ COVER PLATE, .030" THICK

• CONFIGURATIONS TE-7 & TE-8

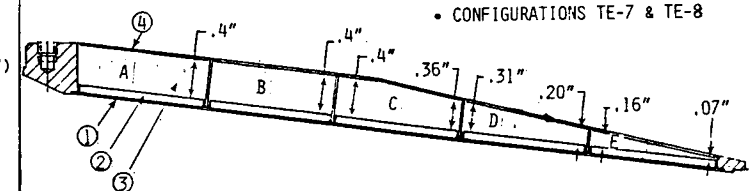

COMPARTMENT	A	B	C	D	E*
LAYERS OF .2" THICK ASTROQUARTZ BLANKET	2	2	2	1.5	1 to.5

* 1 LAYER FWD HALF
.5 LAYER AFT HALF

PLUG TRAY

• CONFIGURATIONS TE-5 & TE-9

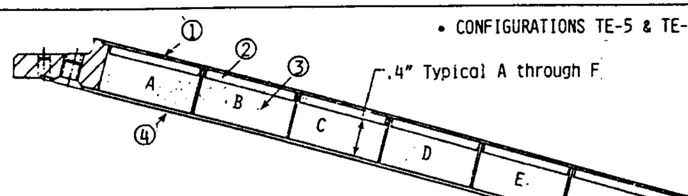

COMPARTMENTS A THROUGH F PACKED WITH 5 LAYERS OF .2" THICK ASTROQUARTZ BLANKET: 2.5#/FT^3 DENS.

• CONFIGURATIONS TE-4, TE-6 & TE-8

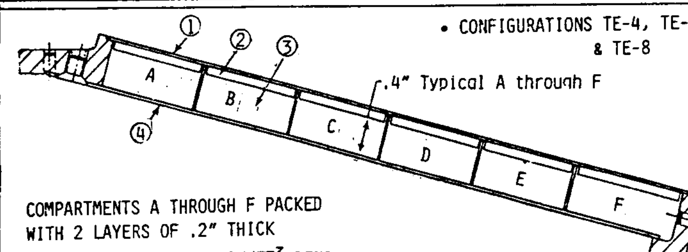

COMPARTMENTS A THROUGH F PACKED WITH 2 LAYERS OF .2" THICK ASTROQUARTZ BLANKET: 1#/FT^3 DENS.

FIGURE 3-32 TREATMENT DESIGN SPECIFICATIONS FOR EJECTOR AND PLUG TRAYS

To convert the ejector internal flow surface to "hardwall", the trays were voided of Astroquartz and Retimet metal foam, fitted with hardwall inserts (see Figures 3-29 and 3-30), then reassembled with metal foam, acoustic treatment and the treatment retainers. The repacking assured compaction and retention of the hardwall inserts against the perforated faceplate. To "hardwall" the plug surface, the treatment trays were directly replaced with a hardwall plug sleeve, per Figure 3-33.

3.2.3 Aerodynamic P_S and T_S Instrumentation

Instrumentation for aerodynamic peformance and thermal environment evaluation was applied to various surfaces of the suppressor-ejector system. Primary purposes of application were:

- o Base pressure measurements for base drag estimation for the 20-Shallow chute suppressor.
- o Skin temperature measurements along the chute forward edge; to verify metal temperatures for mechanical design purposes.
- o Base pressure measurements along the ejector inlet lip and along the length of the ejector inner flowpath, for base drag estimation.
- o Skin temperature measurements along the length of the ejector inner flowpath, to document thermal environment for mechanical design of treatment trays.
- o Static temperature measurements within the packed treatment cavities to aid in treatment performance analysis.

The instrumentation details are described as follows:

On Primary Nozzle System

Figure 3-34 schematically locates a) P_S taps Number 1 through 8 on the 20-chute suppressor in the chute base region, b) T_S Item Numbers 9 and 10 on the chute metal surface, and c) P_S Tap Numbers 11 and 12 on the suppressor nozzle sleeve. Figure 3-35 photo shows instrumentation applied to the base region of the 20-chute suppressor. Figure 3-36 photo shows (2) P_S surface taps applied to the suppressor nozzle sleeve.

On the Ejector Inlet Ring

Figure 3-37 sketch and Figure 3-38 photo show P_S tap Number 13's location on the ejector inlet ring, common to both the nominal and extended length ejector assemblies.

Within the Nominal Length Ejector

Figure 3-39 schematically locates P_S tap Item Numbers 14 through 21 along the ejector inner flowpath, T_S Item Numbers 22 through 27 along the same, and T_S Item Numbers 28 and 29 within the ejector tray Astroquartz material (after tray/shell assembly). The P_S and T_S instrumentation bars for the nominal length ejector are shown unassembled in Figure 3-40 and as applied to the ejector in Figures 3-41 and 3-42 for P_S and T_S, respectively. The two taps within the nominal length ejector shell are shown in Figure 3-43 photo.

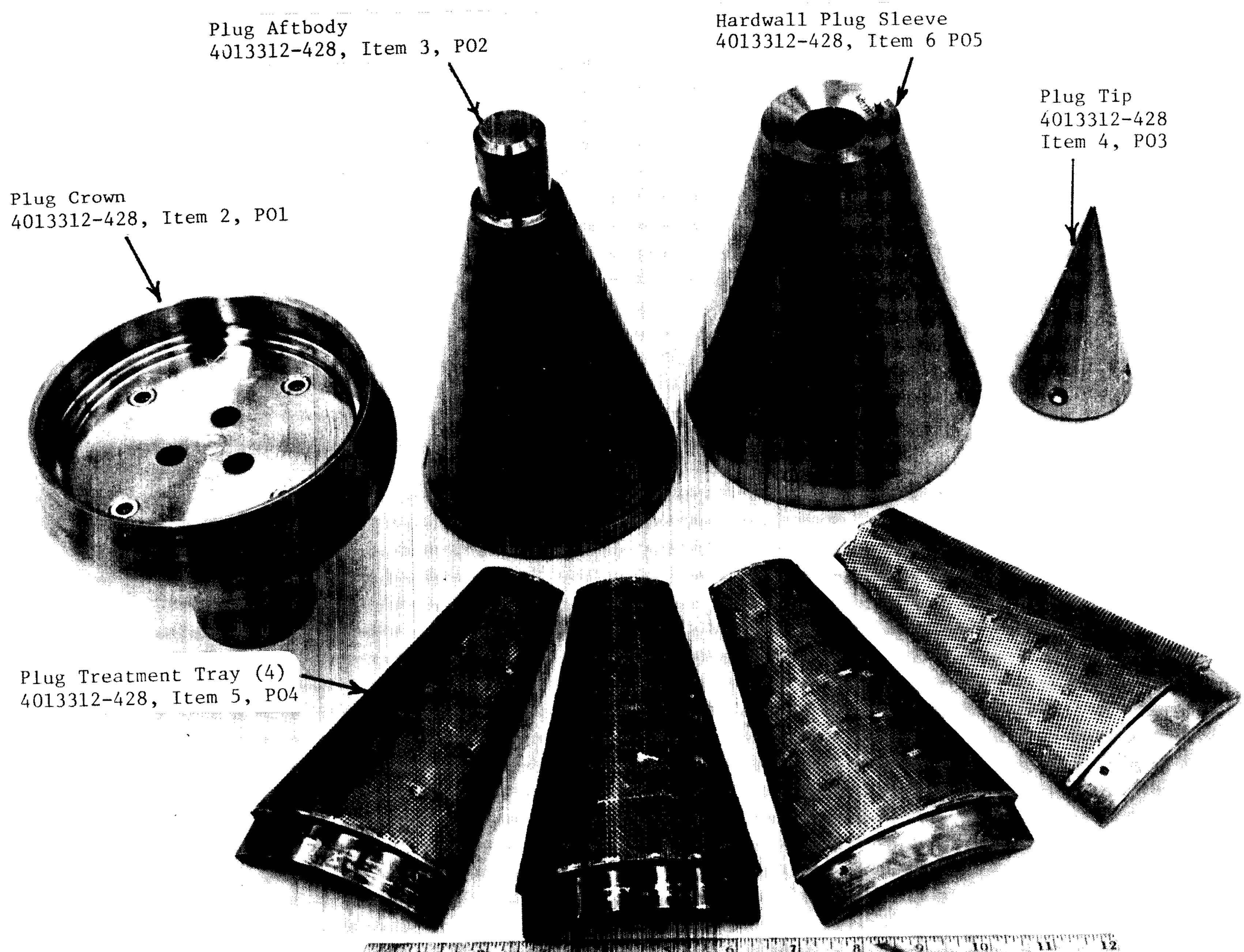

FIGURE 3-33. HARDWARE ITEMS FOR ASSEMBLY OF HARDWALL/TREATED CENTER PLUG

ORIGINAL PAGE IS
OF POOR QUALITY

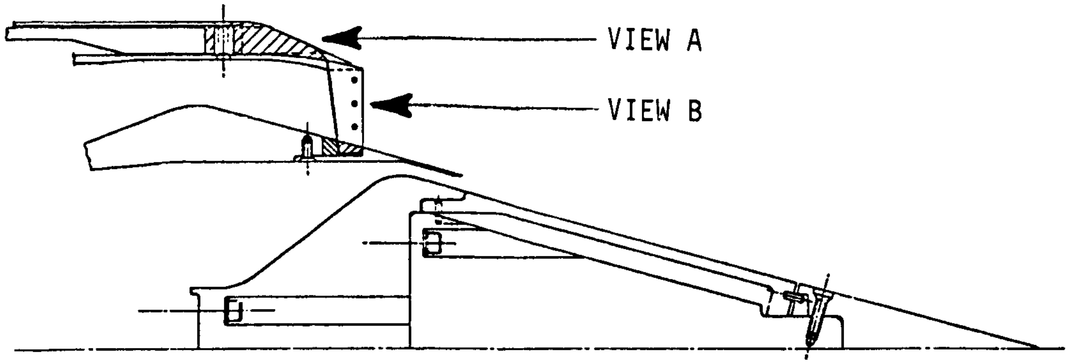

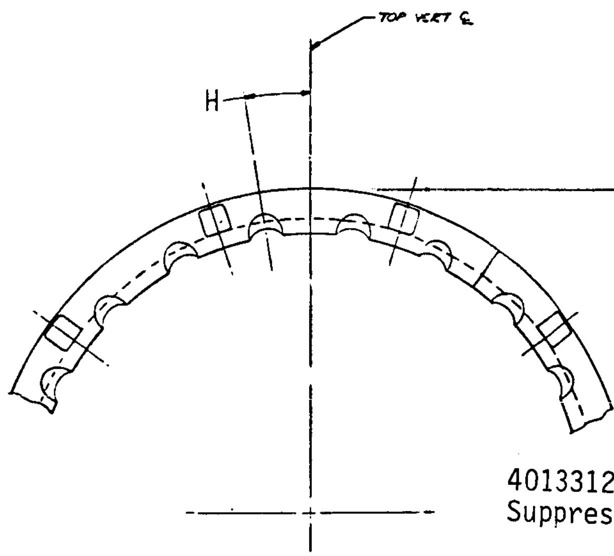

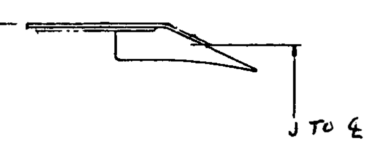

INSTRUMENTATION TABLE			
INSTR ITEM	H	J	ELEMENT TYPE
11	189°	5.403	Ps
12	207°	5.861	Ps

4013312-428 P09
Suppressor Nozzle Sleeve

VIEW A, AFT LOOKING FWD

INSTRUMENTATION TABLE				
INSTR ITEM	CHUTE NO	K	L	ELEMENT TYPE
1	1	9°	3.807	Ps
2	2	27°	4.013	↓
3	3	45°	4.210	↓
4	4	63°	4.398	↓
5	5	81°	4.578	↓
6	6	99°	4.751	↓
7	7	117°	4.918	↓
8	8	135°	5.080	Ps
9	9	153°	4.013	Ts
10	10	171°	4.918	Ts

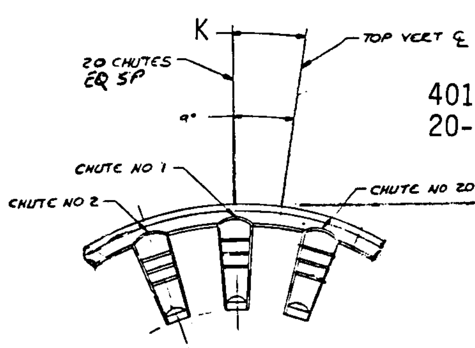

4013312-428 P10
20-Chute Nozzle

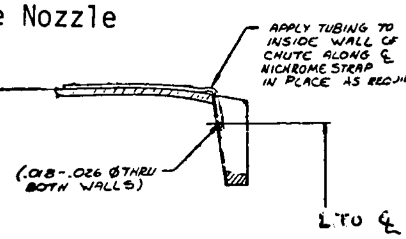

VIEW B, AFT LOOKING FWD

FIGURE 3-34 P_S AND T_S INSTRUMENTATION ON PRIMARY NOZZLE SYSTEM

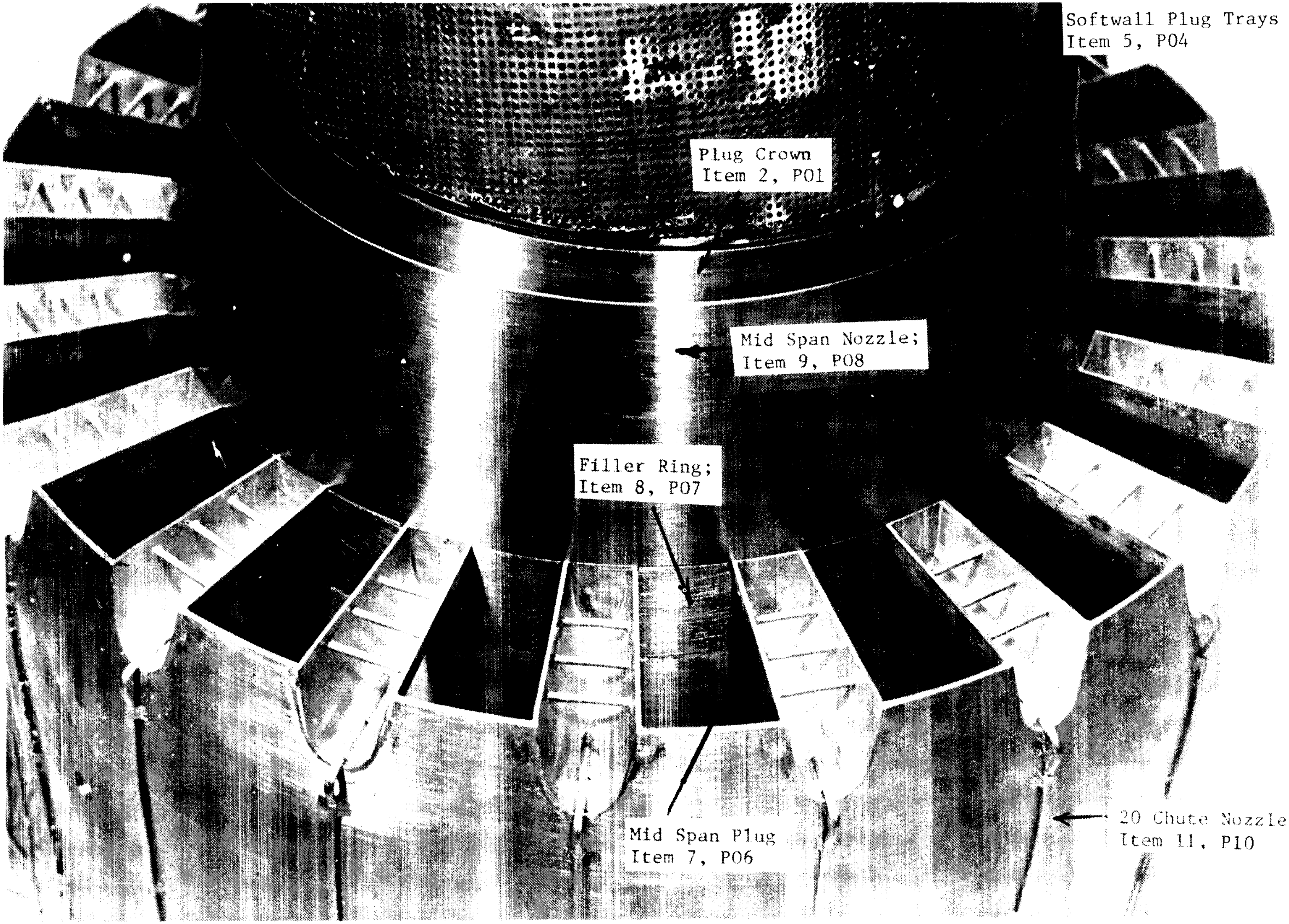

FIGURE 3-35. INSTRUMENTATION APPLICATION TO 20-CHUTE NOZZLE ASSEMBLY

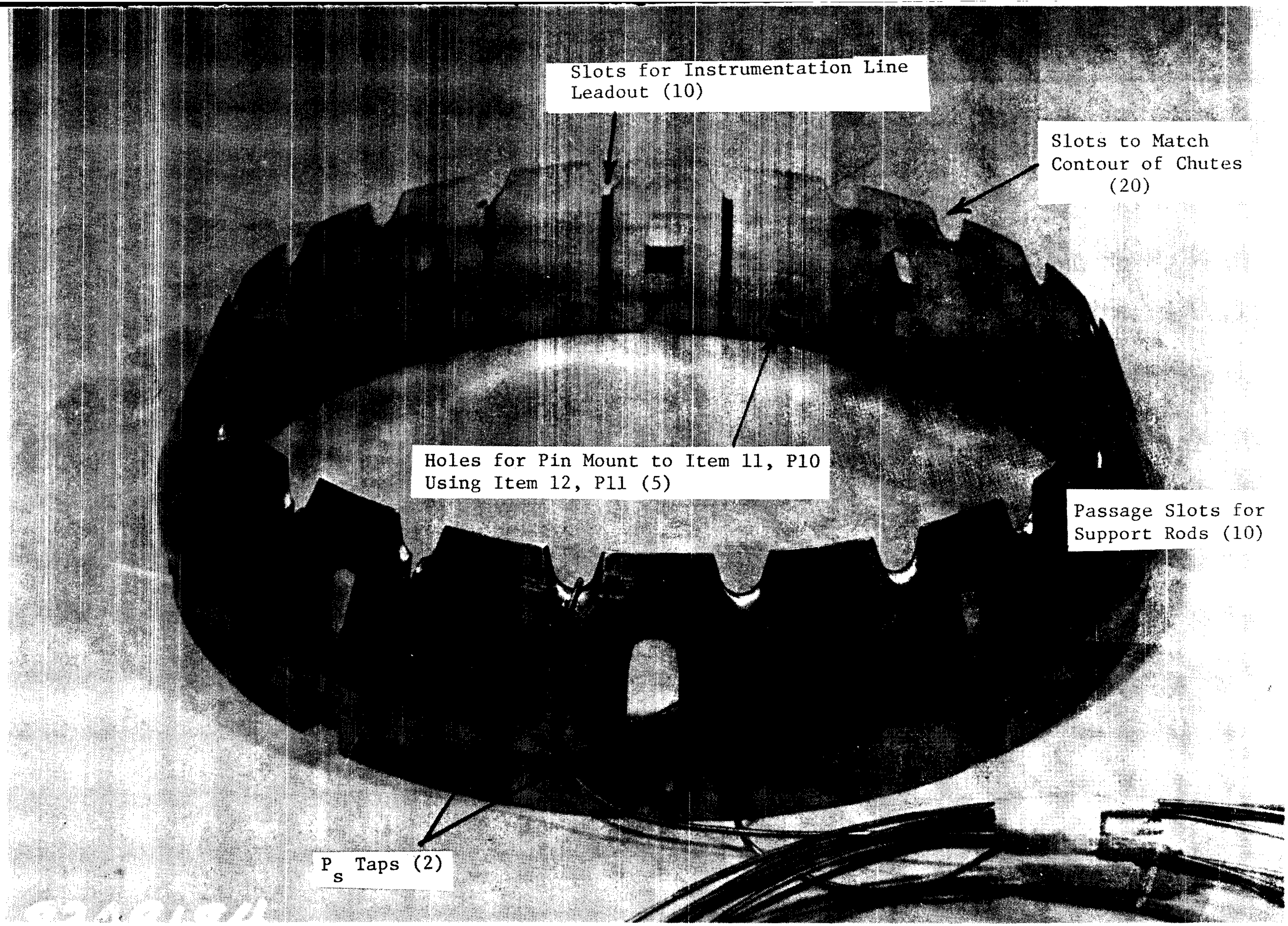

FIGURE 3-36. Ps INSTRUMENTATION APPLICATION TO THE SUPPRESSOR NOZZLE SLEEVE

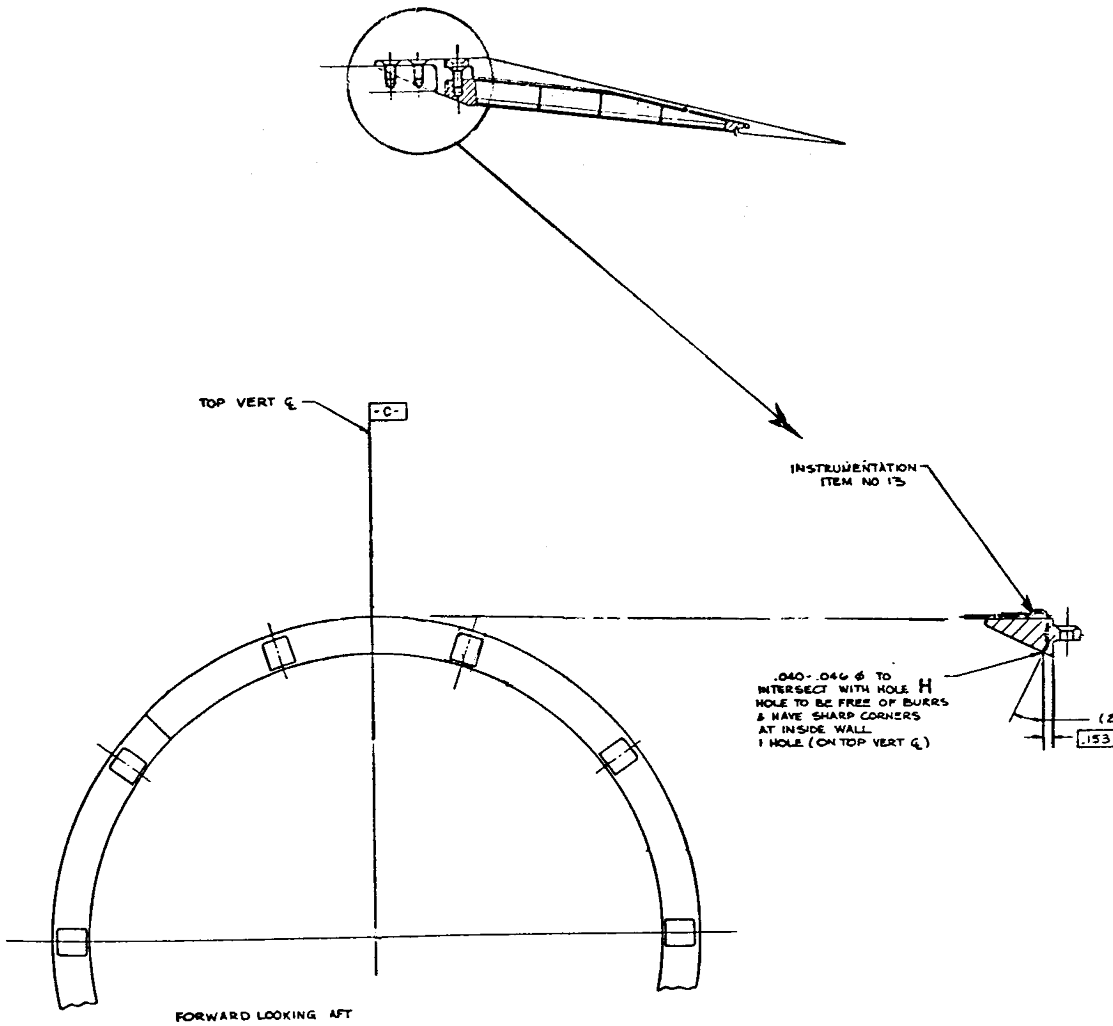

4013312-428 P14 EJECTOR INLET RING

FIGURE 3-37 P_S INSTRUMENTATION ON EJECTOR INLET RING

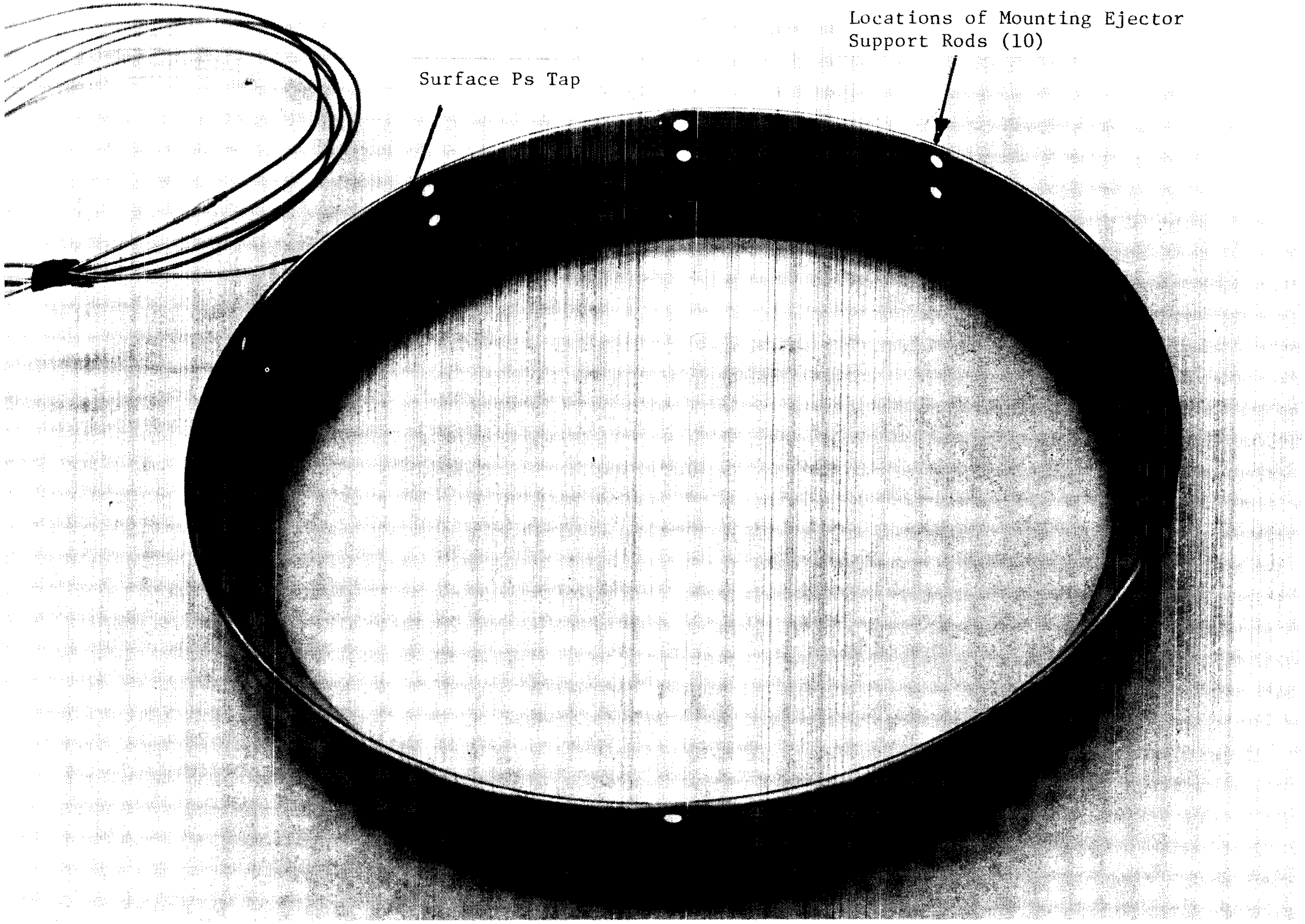

FIGURE 3-38. Ps TAP APPLICATION TO THE EJECTOR INLET RING

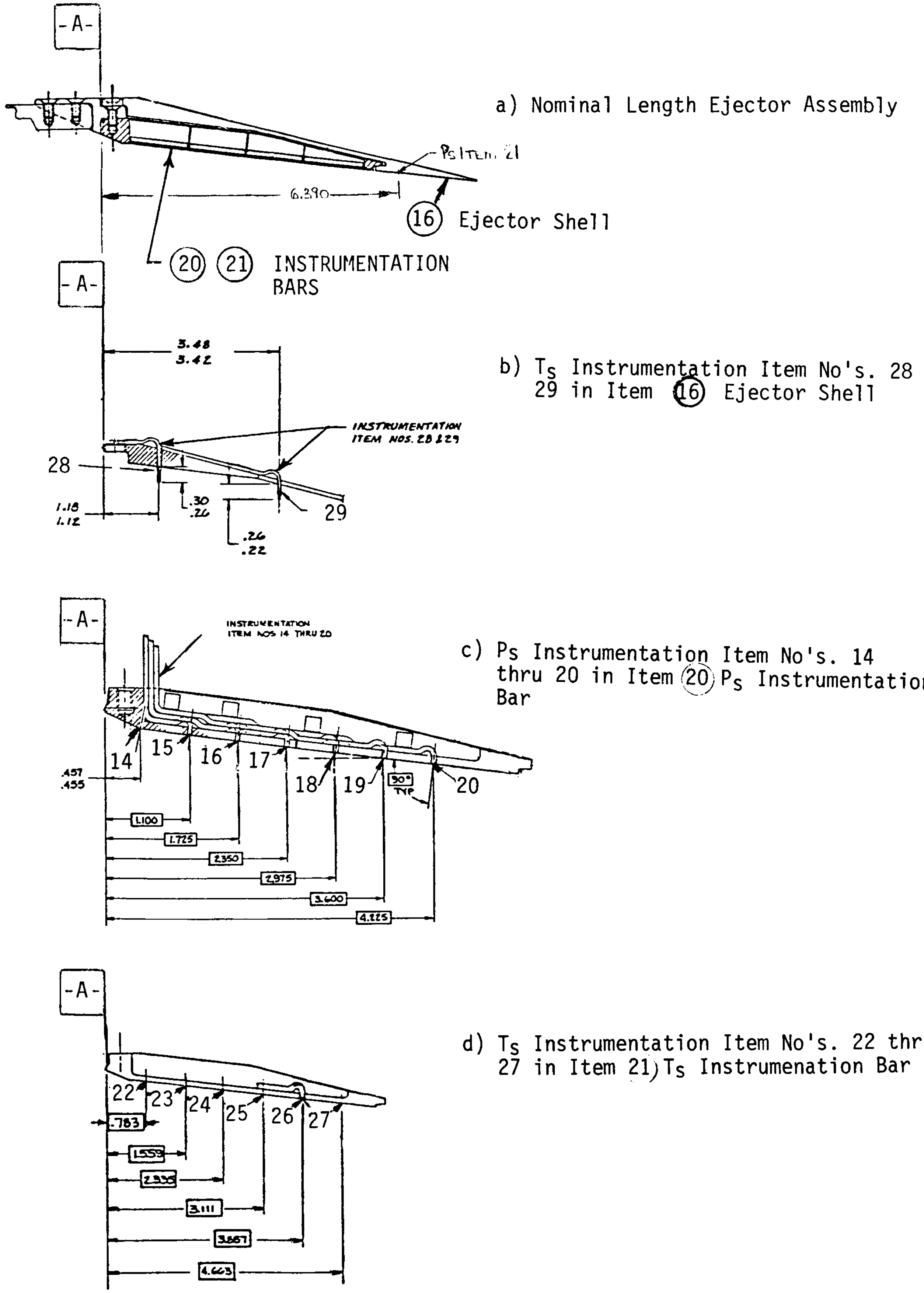

FIGURE 3-39 P_S AND T_S INSTRUMENTATION WITHIN THE NOMINAL LENGTH EJECTOR

ORIGINAL PAGE IS
OF POOR QUALITY

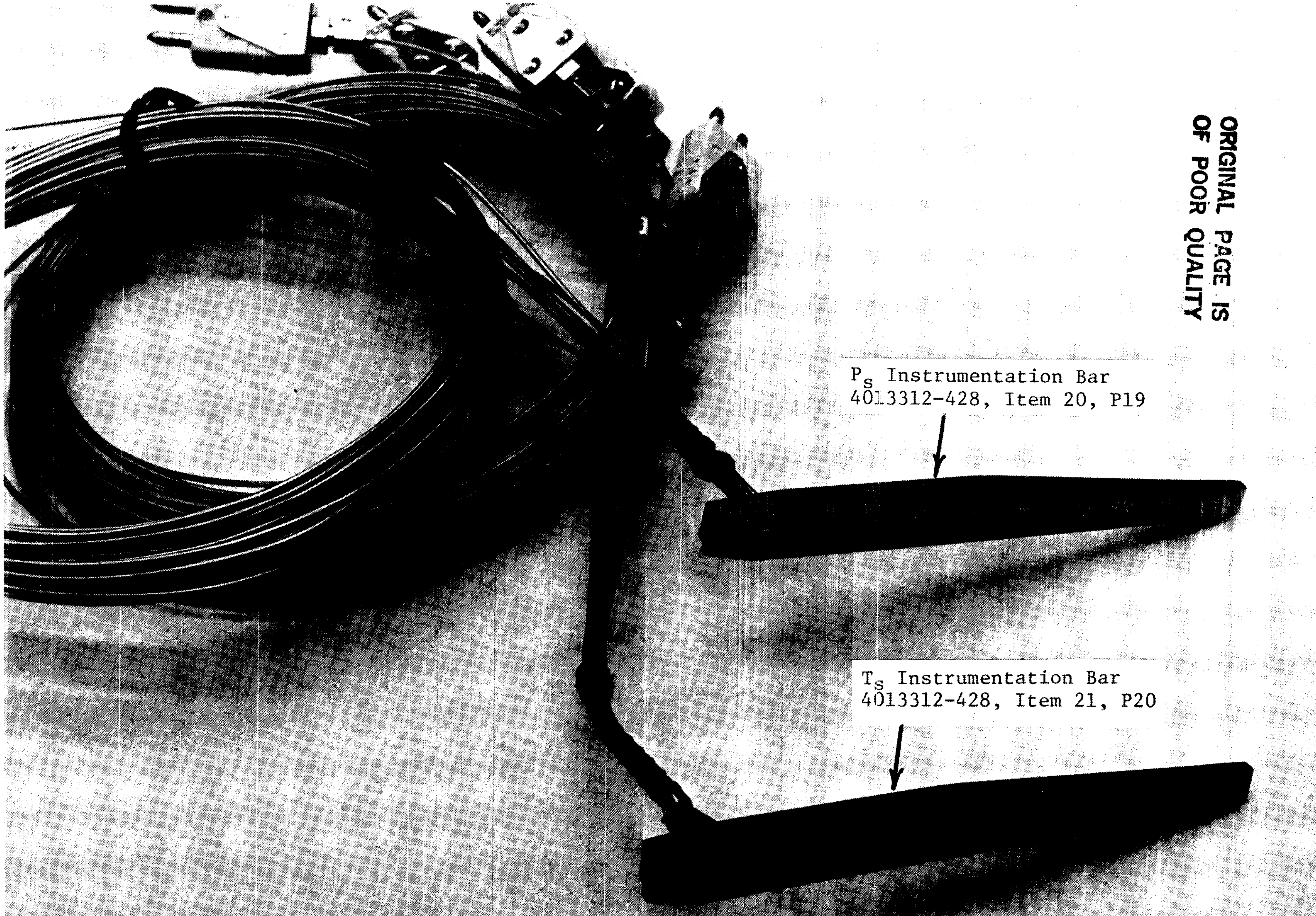

FIGURE 3-40. Ps AND Ts INSTRUMENTATION BARS FOR APPLICATION WITHIN THE NOMINAL LENGTH EJECTOR

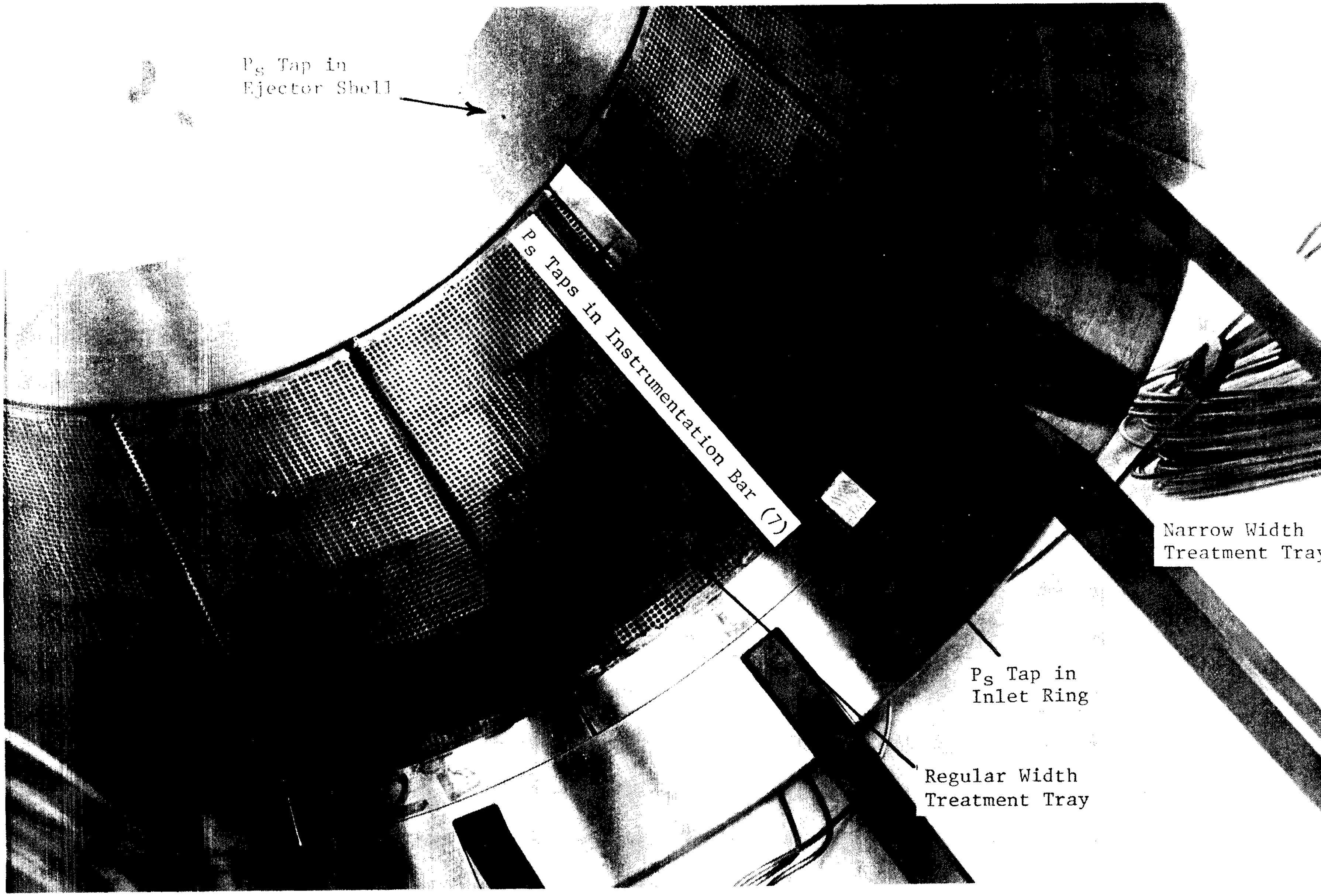

FIGURE 3-41. INSTALLATION OF THE P_S INSTRUMENTAION BAR WITHIN THE NOMINAL LENGTH EJECTOR ASSEMBLY

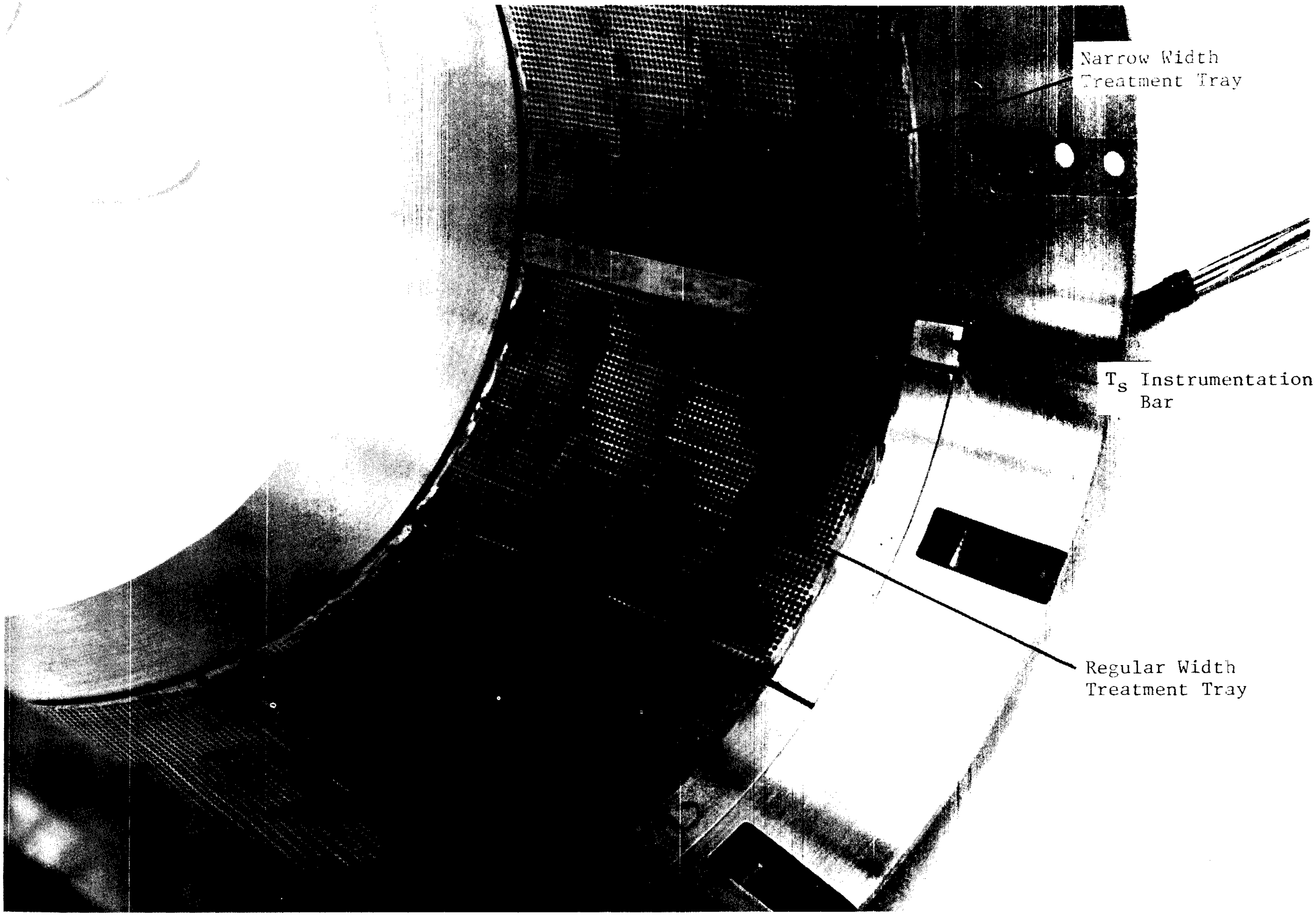

FIGURE 3-42. INSTALLATION OF THE T_S INSTRUMENTATION BAR WITHIN THE NOMINAL LENGTH EJECTOR ASSEMBLY

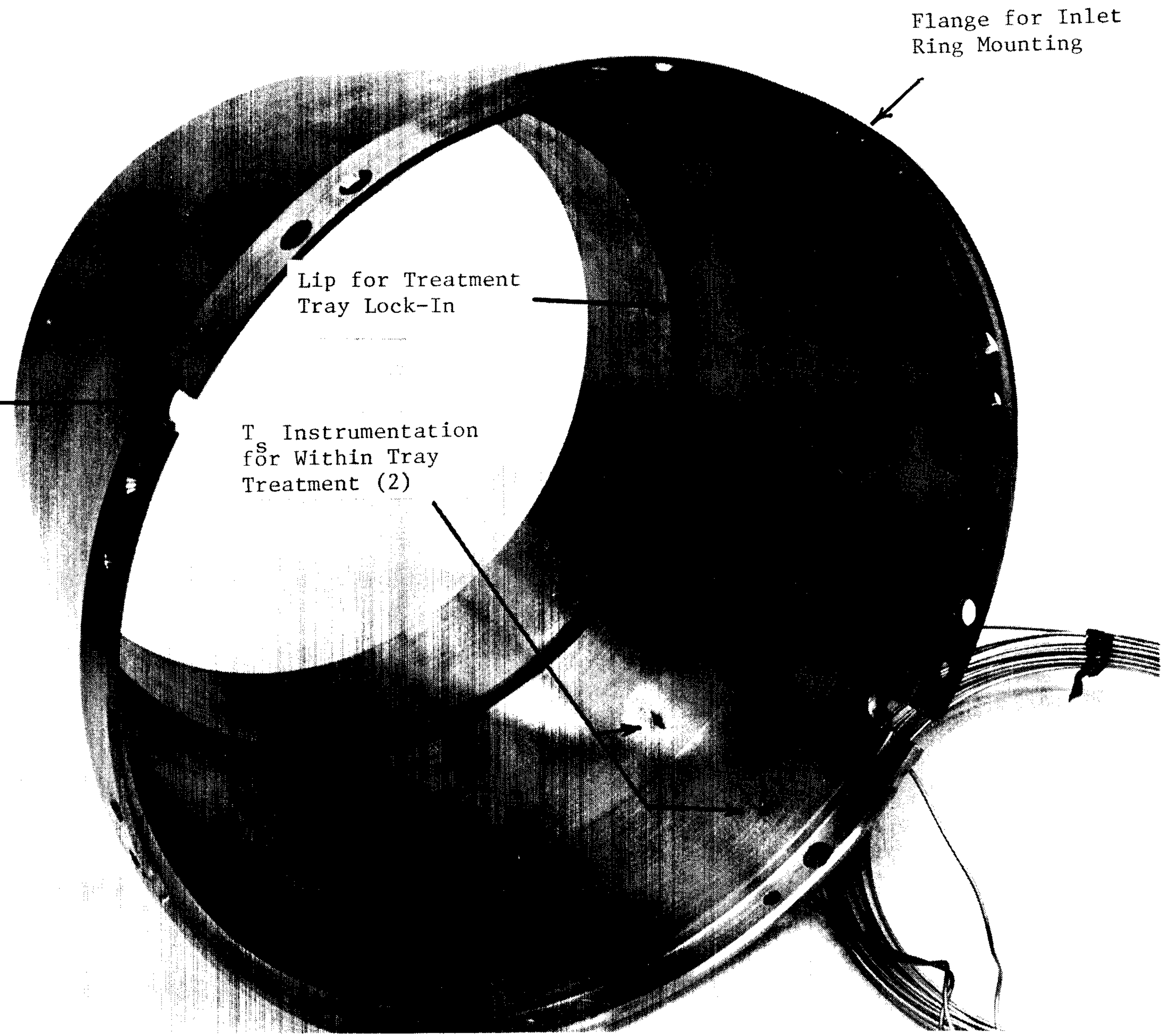

FIGURE 3-43. T_S INSTRUMENTATION APPLICATION TO THE NOMINAL LENGTH EJECTOR SHELL

Within the Extended Length Ejector

Figure 3-44 schematically locates P_S Item Numbers 30 through 37 along the ejector inner flowpath, T_S Item Numbers 38 through 43 along the same, and T_S Item Numbers 44 and 45 within the ejector tray Astroquartz material (after tray/shell assembly). The P_S and T_S instrumentation bars for the extended length ejector are shown unassembled in Figure 3-45 and as applied to the ejector in Figures 3-46 and 3-47 for P_S and T_S, respectively. The two T_S taps within the extended length ejector shell are shown in Figure 3-48 photo.

Measurements obtained during acoustic testing through use of this aerodynamic instrumentation are presented within this report's comprehensive data report, Volume II, Section 6.0, "Aerodynamic Static Pressure and Static Temperature Data Summary".

3.3 ACOUSTIC AND DIAGNOSTIC TEST MATRICES

A summary of the acoustic and diagnostic tests conducted with the ten model configurations is presented in this section. The acoustic test matrices are described in Section 3.3.1, the laser velocimeter tests within Section 3.3.2, the shadowgraph diagnostic tests within Section 3.3.3, and the aerodynamic P_S and T_S tests within Section 3.3.4.

For detailed reduced test data, refer to this contract's comprehensive data report (CDR) as follows:

- o CDR Volume I Section 4.0 Acoustic Test Results
- o CDR Volume II Section 5.0 Laser Velocimeter Tests
- o CDR Volume II Section 6.0 Aerodynamic Static Pressure and Static Temperature Data Summary
- o CDR Volume II Section 7.0 Shadowgraph Tests

3.3.1 Acoustic Test Matrices

The aerodynamic flow conditions corresponding to the acoustic test points taken on each of the test configurations are tabulated in this section. An overview of the test program and details of cycle point selection are included in Section 3.3.1.1. Definition of variables used in data reduction and tabulation is discussed in Section 3.3.1.2. Section 3.3.1.3 presents the aerodynamic test conditions for the 10 individual test configurations, both in International (S.I.) Units and in English Units.

3.3.1.1 Test Matrix Overview

In total, 188 acoustic data points were acquired, distributed over 10 scale model nozzle configurations; 87 points under static and 101 points under simulated flight conditions. These data points are summarized versus nominal cycle conditions and test configurations in Table 3-1. The table is presented in chronological order of test dates (Build Number 1 through 10), rather than in test configuration number numerical order.

As a general guide, typical Advanced Supersonic Technology/Variable Cycle Engine (AST/VCE) cycle conditions for a product GE-21 engine were used in planning the inner and outer stream flow conditions, for a major portion of the test points. The engine operating line was developed utilizing cycle

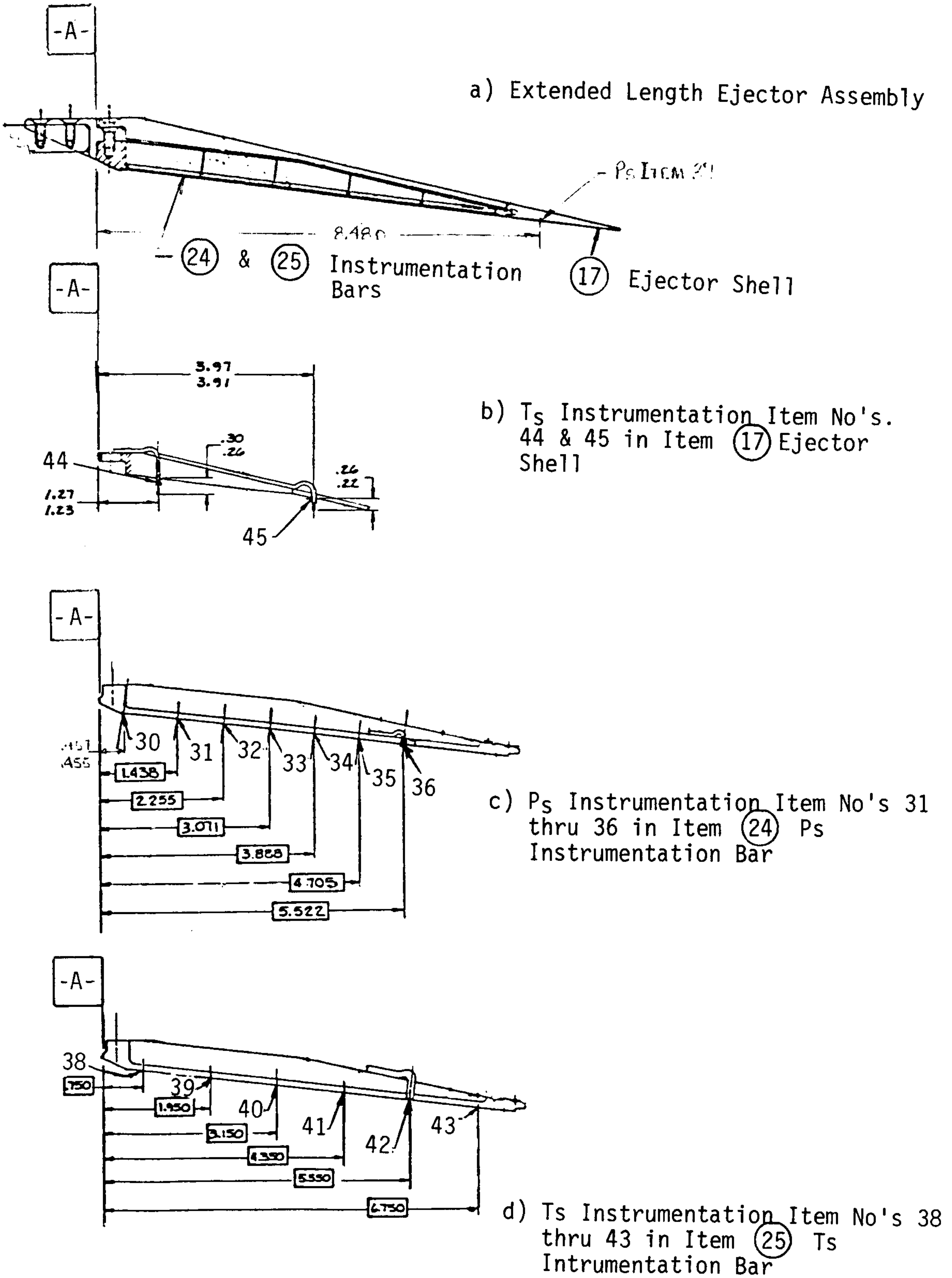

FIGURE 3-44 Ps AND Ts INSTRUMENTATION WITHIN THE EXTENDED LENGTH EJECTOR

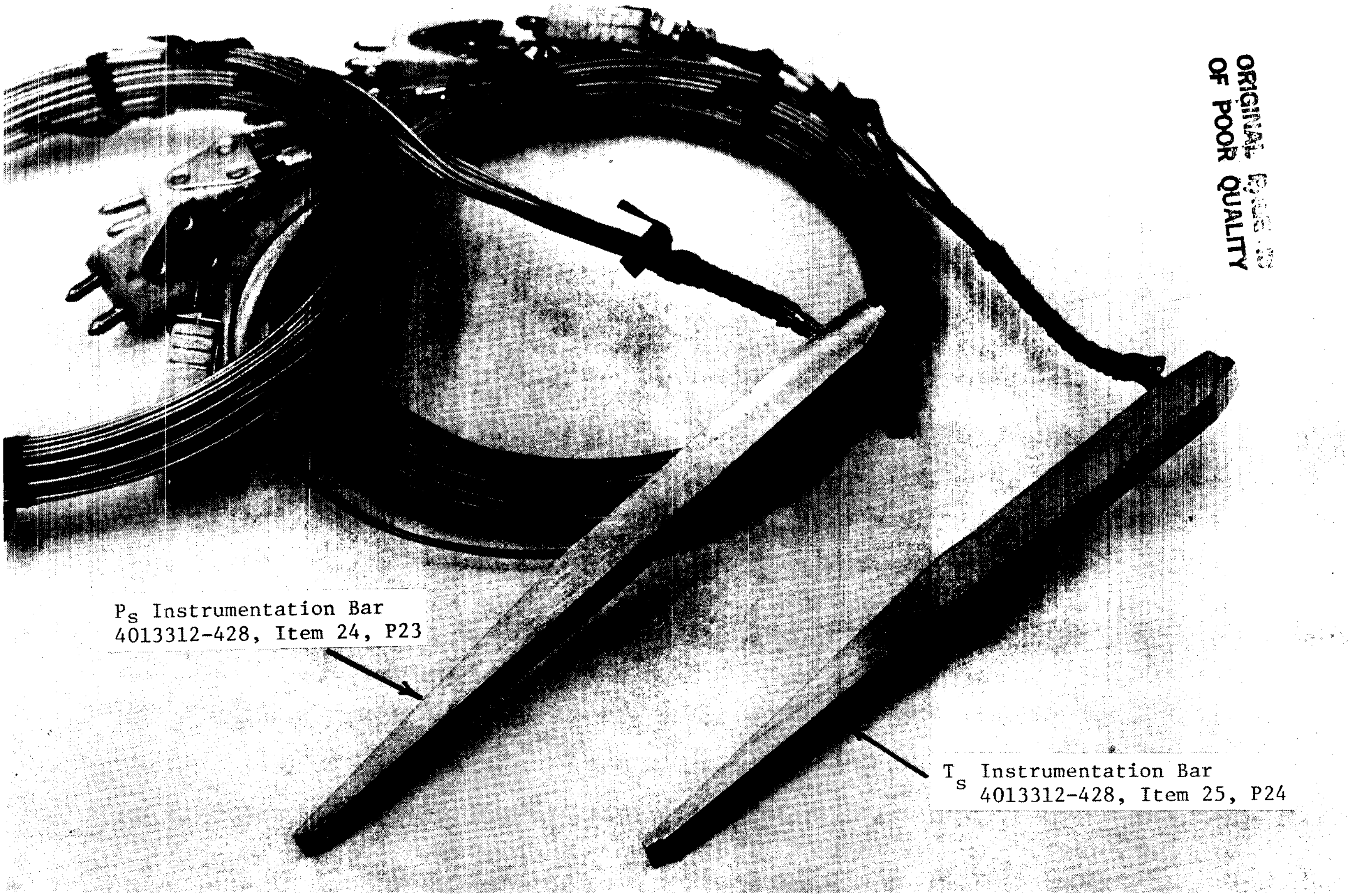

FIGURE 3-45. P_S AND T_S INSTRUMENTATION BARS FOR APPLICATION WITHIN THE EXTENDED LENGTH EJECTOR

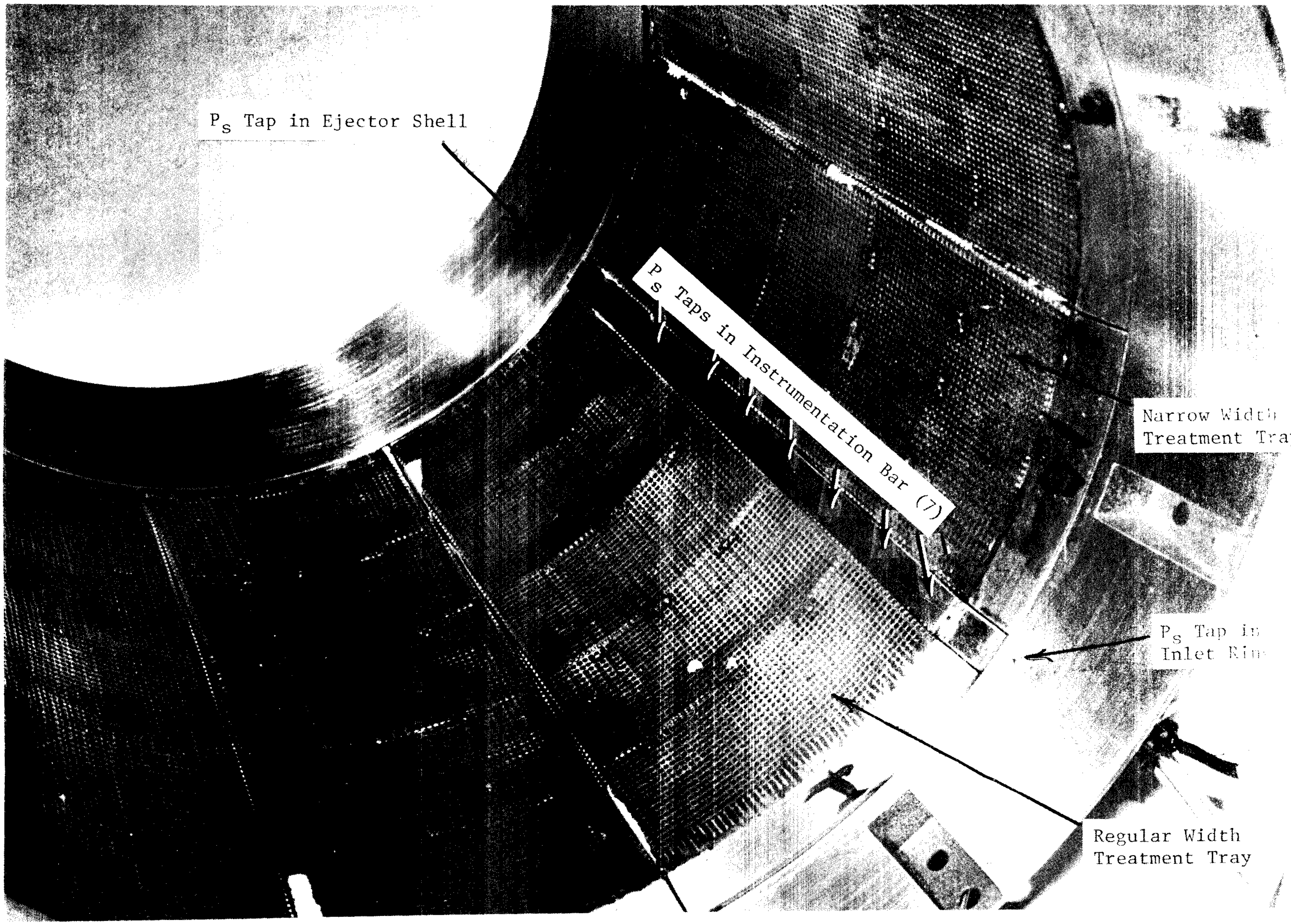

FIGURE 3-46. INSTALLATION OF THE P_S INSTRUMENTATION BAR WITHIN THE EXTENDED LENGTH EJECTOR ASSEMBLY

ORIGINAL PAGE IS OF POOR QUALITY

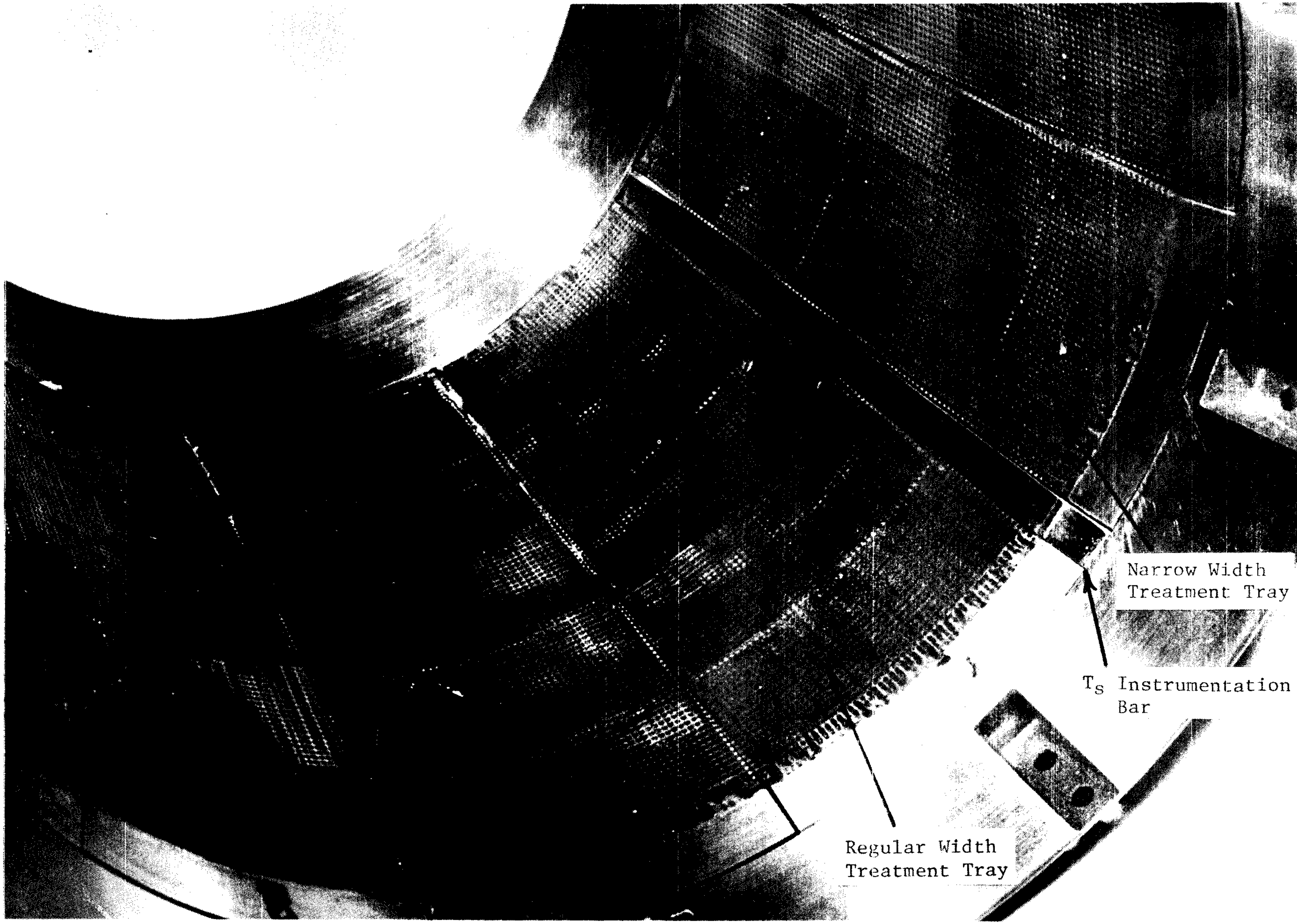

FIGURE 3-47. INSTALLATION OF THE Ts INSTRUMENTATION BAR WITHIN THE EXTENDED LENGTH EJECTOR ASSEMBLY

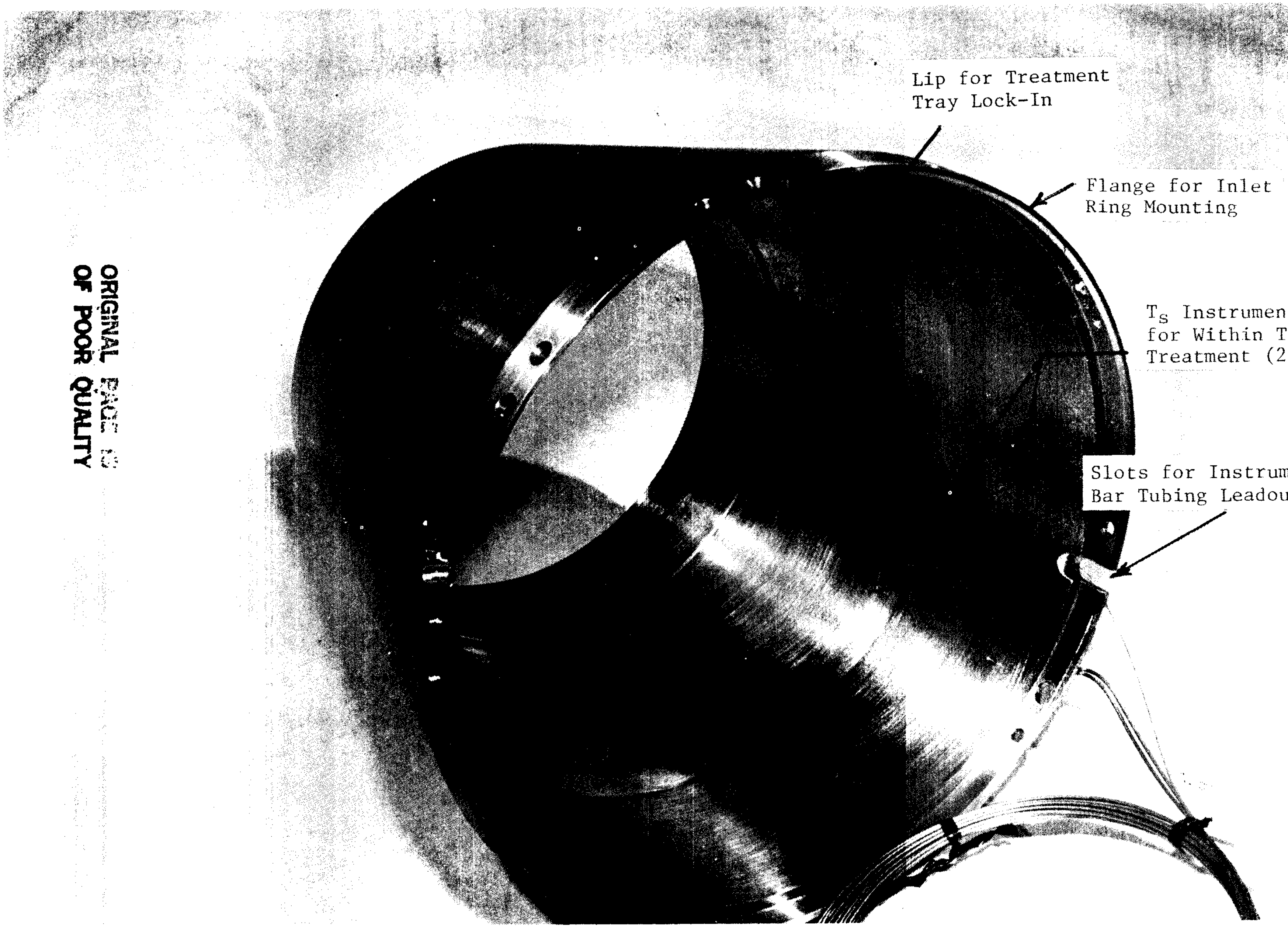

FIGURE 3-48. Ts INSTRUMENTATION APPLICATION TO THE EXTENDED LENGTH EJECTOR SHELL

TABLE 3-1. SUMMARY OF ACQUIRED ACOUSTIC DATA POINTS

- o Numbers in Table Represent Acquired Acoustic Data Points
- o Odd Numbered Test Points Are under Static Conditions.
- o Even Numbered Test Points Are under Simulated Flight Conditions.
- o Second Digit of '2' in Test Point No. Indicates 200'/s Free Jet Vel.
- o Second Digit of '3' in Test Point No. Indicates Repeat Test Point.

TEST POINT NO.		NOMINAL CYCLE CONDITIONS: INNER NOZZLE P_r^i	INNER NOZZLE T_T^i, (°R)	INNER NOZZLE V_j^i, (fps)	OUTER NOZZLE P_r^o	OUTER NOZZLE T_T^o, (°R)	OUTER NOZZLE V_j^o, (fps)	MIXED P_r^m	MIXED T_T^m (°R)	MIXED V_j^m (fps)	BUILD NO. / CONFIG. NO. / TEST DATE / FREE JET VEL. (fps)	1	2	3	4	5	6	7	8	9	10
											CONFIG. NO.	TE-1	TE-5	TE-9	TE-4	TE-3	TE-2	TE-8	TE-7	TE-10	TE-6
											TEST DATE	8/26,27/83	9/1/83	9/6/83	9/8,9,12/83	9/15/83	9/16/83	9/21/83	9/22/83	9/24/83	11/16,18/83
												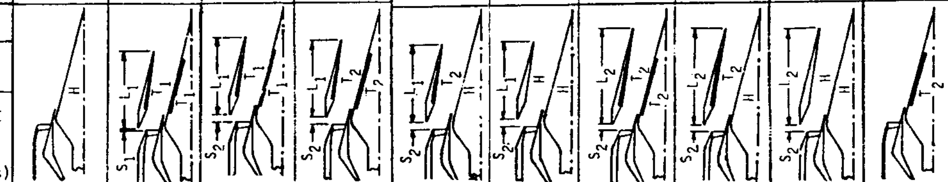									
1	MIXED SUBSONIC	1.85	800	1245	1.90	1420	1695	1.88	1290	1600	0	1001	5001	9001	4001	3001	2001	8001	7001	0001	6001
											400	1002	5002	9002	4002	3002	2002	8002	7002	0002	6002
2	CUTBACK	2.20	800	1390	2.25	1530	1960	2.21	1370	1830	0	1003 1303	5003	9003	4003	3003	2003	8003	7003 7303	0003	6003
											200	1204	5204	9204	4204	-	-	8204	-	-	6204
											400	1004 1304	5004	9004	4004 4304	3004	2004	8004	7004 7304	0004	6004
3	INTERMEDIATE	2.60	810	1525	2.60	1620	2170	2.56	1440	2025	0	1005	5005	9005	4005	3005	2005	8005	7005	0005	6005
											400	1006	5006	9006	4006	3006	2006	8006	7006	0006	6006
4	SIMILAR TO INTER-MEDIATE AT T_T^o=810°R	2.60	810	1525	2.64	810	1550	2.63	810	1545	0	1105	5105	9105	4105	-	-	8105	-	-	6105
											400	1106	5106	9106	4106	-	-	8106	-	-	6106
5	CYCLE LINE POINT	2.90	840	1625	2.90	1730	2350	2.84	1525	2185	0	1007	5007	9007	4007	3007	2007	8007	7007	0007	6007
											400	1008	5008	9008	4008	3008	2008	8008	7008	0008	6008
6	TAKEOFF	3.20	870	1720	3.40	1730	2495	3.29	1540	2320	0	1009	5009	9009	4009 4309	3009	2009	8009	7009 7309	0009	6009
											200	1210	5210	9210	4210	-	-	8210	-	-	6210
											400	1010	5010	9010	4010	3010	2010	8010	7010 7310	0010	6010
7	SIMILAR TO TAKEOFF AT T_T^o = 870°R	3.20	870	1720	3.47	870	1850	3.43	870	1830	0	1109	5109	9109	4109	3109	2109	8109	-	0109	6109
											400	1110	5110	9110	4110	3110	2110	8110	-	0110	6110
8	TAKEOFF OUTER SUBSONIC INNER	1.80	870	1270	3.40	1730	2495	2.97	1555	2245	0	1011	5011	9011	4011	-	-	8011	-	-	6011
											400	1012	5012	9012	4012	-	-	8012	-	-	6012
9	MAX CYCLE	3.40	890	1775	3.70	1730	2565	3.57	1545	2390	0	1013	5013	9013	4013	3013	2013	8013	7013	0013	6013
											400	1014	5014	9014	4014	3014	2014	8014	7014	0014	6014
10	CUTBACK - NO INNER FLOW	-	-	-	2.25	1530	1960	2.25	1530	1960	0	-	-	-	-	-	-	-	-	0403	-
11	TAKEOFF - NO INNER FLOW	-	-	-	3.40	1730	2495	3.40	1730	2495	0	-	-	-	-	-	-	-	-	0409	-
12	FREE JET AMBIENT			≈ 200			≈ 200	—	—	—	200	-	5200	-	-	-	-	8200	-	-	-
				≈ 400			≈ 400	—	—	—	400	-	5400	-	-	-	-	8400	-	-	-

information from preliminary design studies with AST/VCE applications, tempered by facility operating limits. Comparisons of the select test point aerodynamic conditions to those of the GE-21 engine cycle are made in Figures 3-49 and 3-50. Table 3-1's test points 1 through 12 can be categorized as follows:

- Test Point Numbers 1, 2, 3, 5, 6 and 9 - Cycle line points representative of GE-21 operation, tempered at high T_T operation by facility limits; refer to Figures 3-49 and 3-50.

- Test Point Numbers 4 and 7 - Similar to cycle line points 3 and 6 at intermediate and takeoff, respectively, but with $T_T^o = 870^oR$. These points are at outer stream Mach numbers equivalent to the hot flow case, but at low T_T^o to study the effect of shock noise while generating lower jet mixing noise. These low temperature points are also used for shadowgraph plume studies where stream density variations are more readily documented photographically.

- Test Point Number 8 - Outer stream at takeoff cycle, inner stream at subsonic P_r; to study the effect of subsonic inner flow on shock of the supersonic outer stream.

- Test Point Numbers 10 and 11 - Outer stream similar to cycle points 2 and 6 at cutback and takeoff, respectively, however, with inner nozzle flow completely shut off.

- Test Point Number 12 - Free stream at either 200 or 400 ft/sec for measurement of background noise levels of the free-jet facility. Inner and outer nozzles are also set a similar 200 or 400 ft/sec velocity so that no abrupt velocity changes are seen in the vicinity of the nozzle exists.

The majority of the above test conditions were acquired at both static and simulated flight velocity of 400 ft/sec. Cutback and takeoff points were also selectively acquired at 200 ft/sec simulated flight velocity to investigate forward flight effects on noise generation and base drag of the suppressor.

3.3.1.2 Definition of Variables

The presented variables are defined in Table 3-2. Sample sheets specifying the variables listed in the tables that summarize the aerodynamic flow conditions are presented in Tables 3-3 and 3-4. In addition to the inner and outer stream flow parameters, the tabulated data contain the mixed stream conditions that were calculated after assuming that the two streams were mixed perfectly. The mixed stream velocity (V_j^{mix}) and the mixed stream total temperature (T_T^{mix}) were calculated using the following expressions:

$$V_j^{mix} = \frac{V_j^o W^o + V_j^i W^i}{W^o + W^i}$$

and

$$T_T^{mix} = \frac{T_T^o W^o + T_T^i W^i}{W^o + W^i}$$

From the known mixed stream velocity and total temperature, other mixed flow parameters have been calculated by using standard isentropic relations. The ambient pressure and temperature, along with the relative humidity in the GE Anechoic Facility at the time of the test, are presented in these tables.

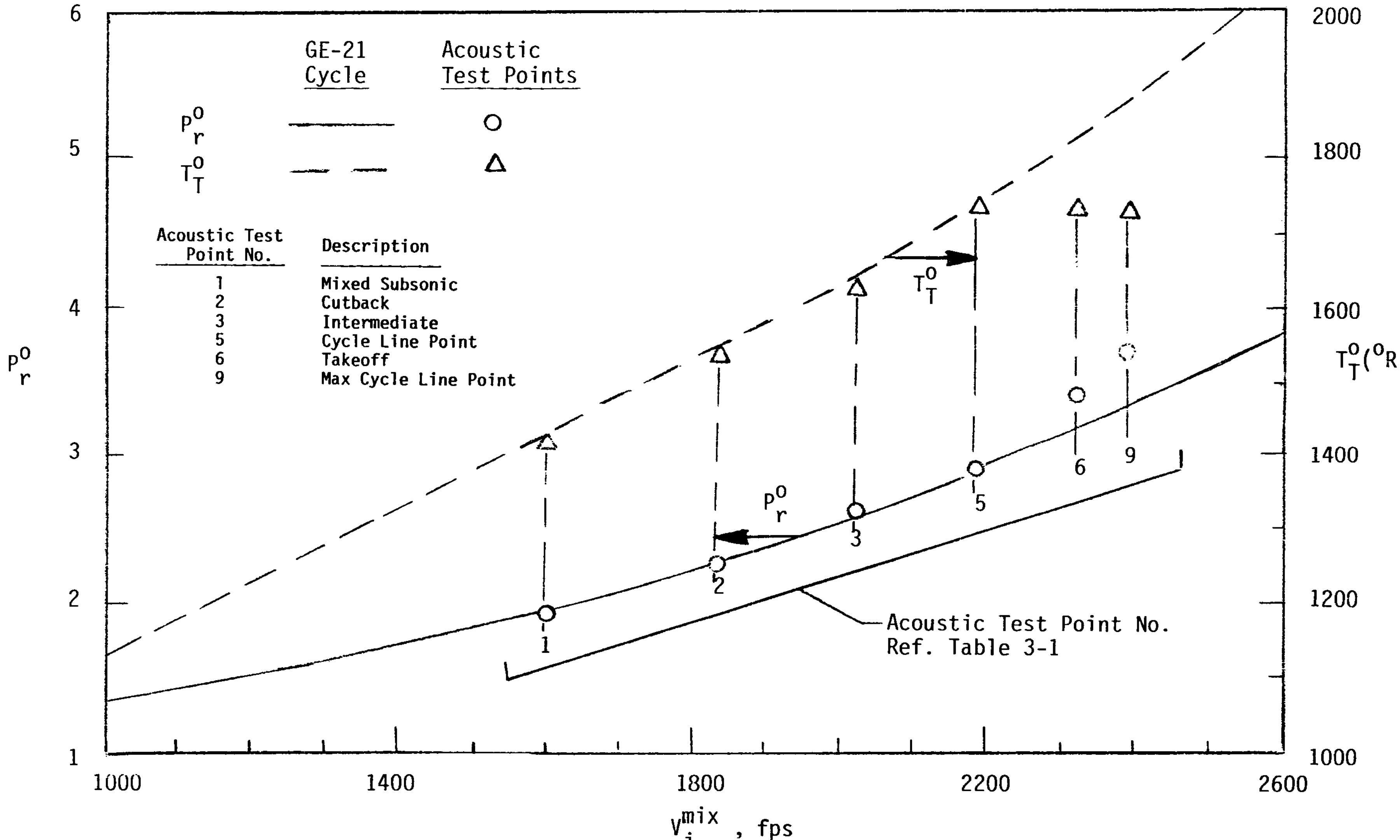

FIGURE 3-49 TYPICAL AST/VCE CYCLE CONDITIONS AND SELECT ACOUSTIC TEST POINTS; VARIATION OF P_r^o AND T_r^o WITH V_j^{mix}

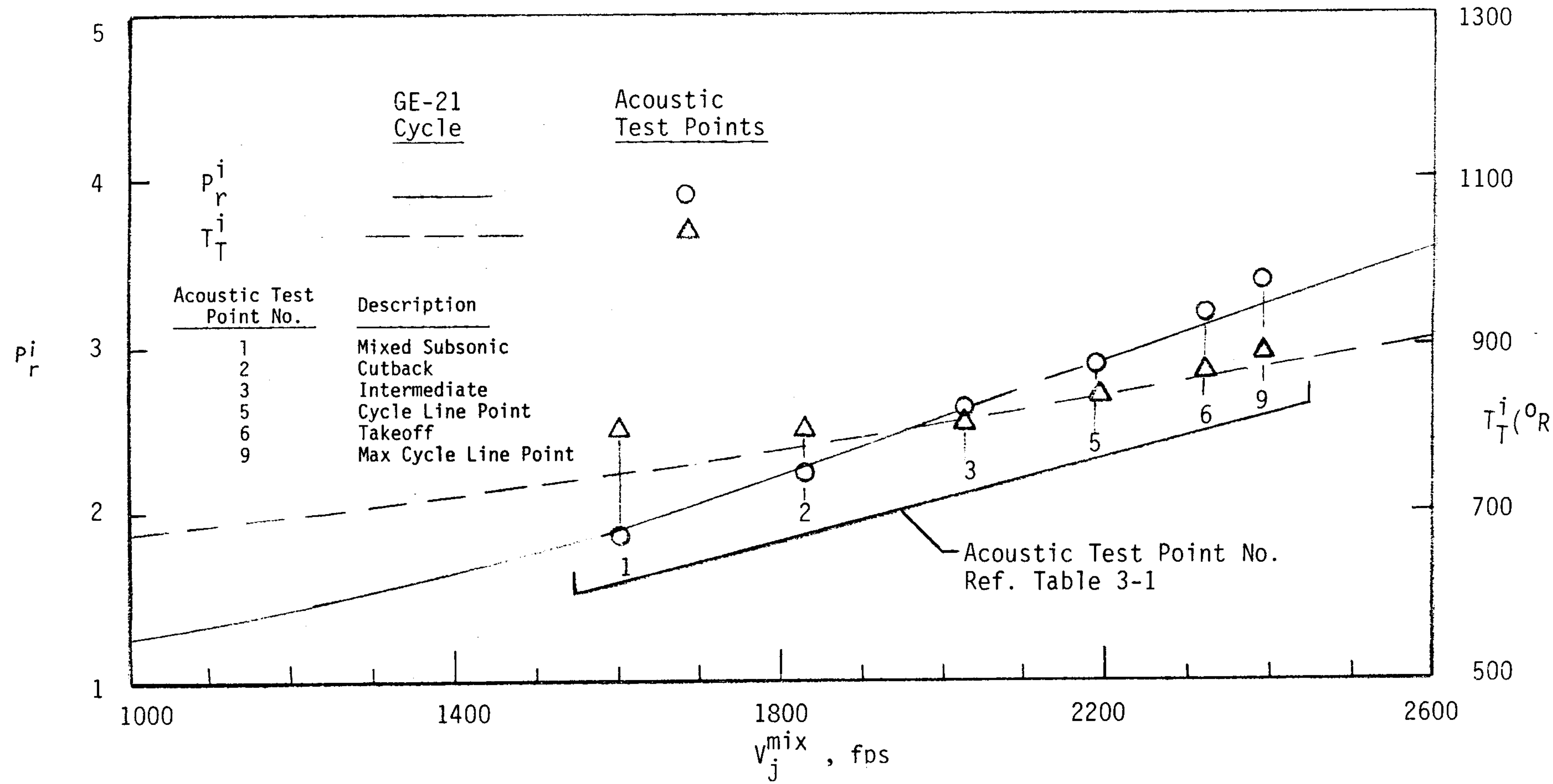

FIGURE 3-50 TYPICAL AST/VCE CONDITIONS AND SELECT ACOUSTIC TEST POINTS; VARIATION OF P_r^i AND T_T^i WITH V_j^{mix}

TABLE 3-2. DEFINITION OF SYMBOLS USED IN AERODYNAMIC DATA TABLES

F	Total thrust; lbs, N
F_{ref}	Reference thrust; 22,820 N (5130 lb)
LVM	Defined as 10 log (V_j^{mix}/a_{amb})
LBM	Defined as 10 log β^{eff},
	where, $\beta^{eff} = \sqrt{(M_j^{eff})^2 - 1}$; $M_j^{eff} = \frac{2}{\gamma-1}\left[(P_r^{eff})^{\frac{\gamma-1}{\gamma}} - 1\right]$; $P_r^{eff} = \frac{P_r^o A^o + P_r^i A^i}{A^o + A^i}$
M	Mach No.
NF	PNL normalization factor; defined as -10 log $\left(\frac{F}{F_{ref}}\right)\left(\frac{\rho}{\rho_{amb}}\right)^{\omega-1}$, dB
OAPWL	Overall Power Level, dB re 10^{-12} watts
P_{amb}	Ambient pressure; Pascal, psia
PNL	Perceived Noise Level, dB
P_r	Nozzle pressure ratio
RH	Relative Humidity, %
T_{amb}	Dry bulb ambient temperature; °K, °R
T_T	Nozzle total temperature; °K, °R
V_{ac}	Free-jet velocity; m/s, ft/sec
V_j	Nozzle exhaust velocity (ideal); m/s, ft/sec
W	Ideal calculated weight flow rate; kg/s, lb/sec
ρ	Density
ω	Density exponent, (Ref. 11, Hoch)

SUPERSCRIPTS

i	Inner Jet (Nozzle) Conditions
mix	Mass Averaged Conditions
o	Outer Jet (Nozzle) Conditions

SUBSCRIPTS

amb	Ambient
j	Jet
r	Ratio
ref	Reference
T	Total (Stagnation)

TABLE 3-3. DESCRIPTION OF AERODYNAMIC DATA SHEET, INTERNATIONAL (S.I.) UNITS

International (S. I.) Units

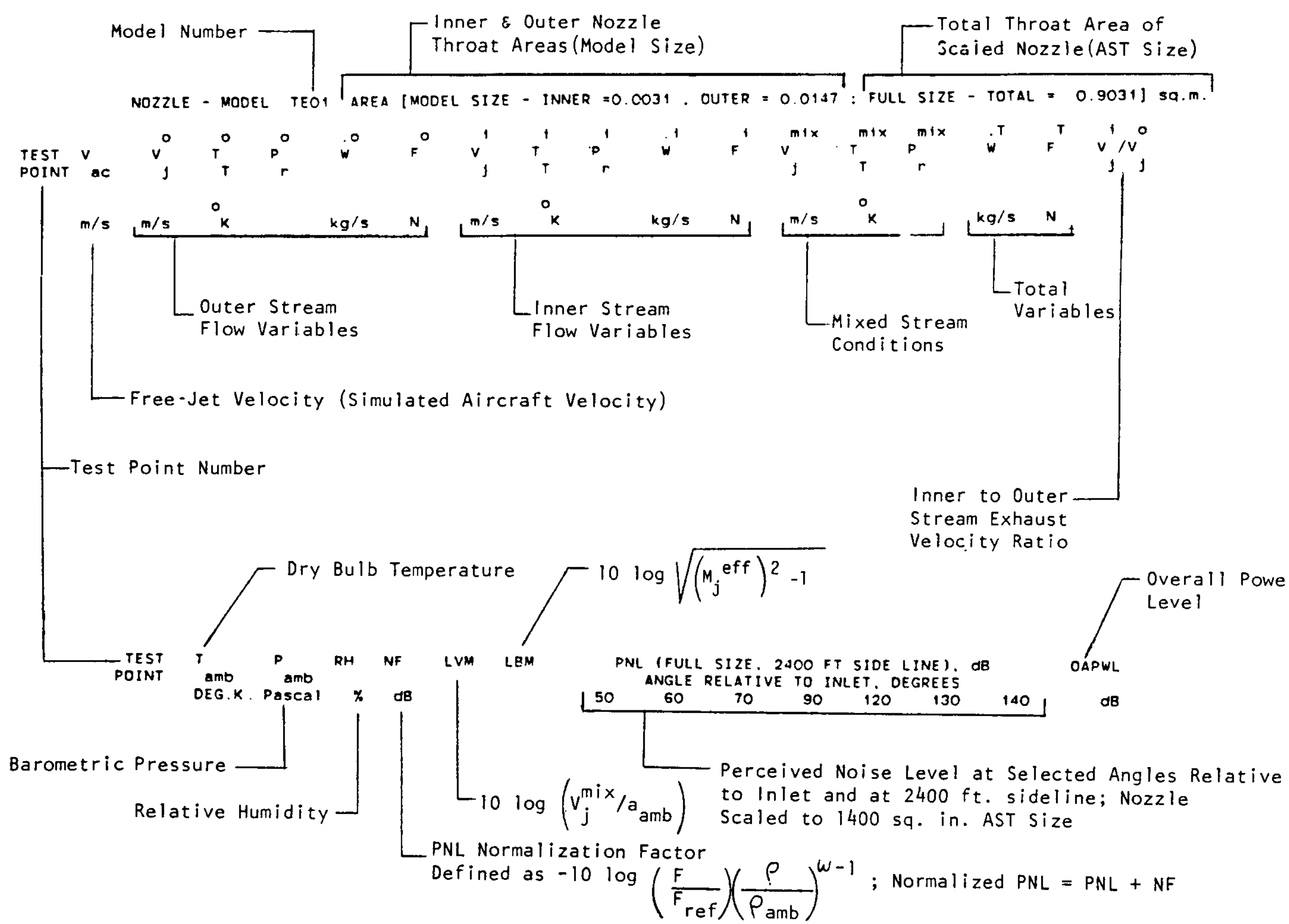

$10 \log \sqrt{\left(M_j^{eff}\right)^2 - 1}$

$10 \log \left(V_j^{mix}/a_{amb}\right)$

PNL Normalization Factor Defined as $-10 \log \left(\frac{F}{F_{ref}}\right)\left(\frac{\rho}{\rho_{amb}}\right)^{\omega - 1}$; Normalized PNL = PNL + NF

TABLE 3-4. DESCRIPTION OF AERODYNAMIC DATA SHEET, ENGLISH UNITS

(English Units)

NOZZLE - MODEL 5 AREA [MODEL SIZE - INNER = 0.00 , OUTER = 20.38 ; FULL SIZE - TOTAL = 1400.00] SQ.IN.

TEST POINT	V_{ac}	P_r^o	T_T^o	V_j^o	W^o	P_r^i	T_T^i	V_j^i	W^i	P_r^{mix}	T_T^{mix}	V_j^{mix}	F	V_j^i/V_j^o
	FT/SEC		DEG R	FT/SEC	LB/SEC		DEG R	FT/SEC	LB/SEC		DEG R	FT/SEC	LB	

- Model Number
- Inner & Outer Nozzle Throat Areas (Model Size)
- Total Throat Area of Scaled Nozzle (AST Size)
- Test Point Number
- Free-Jet Velocity (Simulated Aircraft Velocity)
- Outer Stream Flow Variables
- Inner Stream Flow Variables
- Mixed Stream Conditions
- Total Thrust
- Inner to Outer Stream Exhaust Velocity Ratio

TEST POINT	T_{amb}	P_{amb}	RH	NF	LVM	LBM	PNL (FULL SIZE, 2400 FT SIDE LINE), dB ANGLE RELATIVE TO INLET, DEGREES 50	60	70	90	120	130	140	OAPWL
	DEG R	PSIA	%	dB										dB

- Dry Bulb Temperature
- Barometric Pressure
- Relative Humidity
- PNL Normalization Factor Defined as $-10 \log \left(\frac{F}{F_{ref}}\right)\left(\frac{\rho}{\rho_{amb}}\right)^{\omega-1}$; Normalized PNL = PNL + NF
- LVM: $10 \log\left(V_j^{mix}/a_{amb}\right)$
- LBM: $10 \log \sqrt{\left(M_j^{eff}\right)^2 - 1}$
- Perceived Noise Level at Selected Angles Relative to Inlet and @ 2400 ft. sideline; Nozzle Scaled to 1400 sq. in. AST Size
- Overall Power Level

In addition, the measured far-field PNL data extrapolated to a 731.5-m (2400-ft) sideline and scaled to an AST product size of $0.903m^2$ (1400 $in.^2$) also are presented in the tables. The selected data correspond to microphone locations of θ_i = 50°, 60°, 70°, 90°, 120°, 130° and 140°.

The normalization factor (NF) found in these tables is employed to normalize the measured noise levels to a reference thrust, as an example with PNL, as follows:

$$PNLN = \text{Normalized PNL} = PNL + NF$$

where NF is given by $-10 \log \left(\frac{F}{F_{ref}}\right) \left(\frac{\rho}{\rho_{amb}}\right)^{\omega-1}$

In this case, the normalized data are used to determine the dependence of aft angle jet noise on the acoustic Mach number by plotting PNLN against 10 log (V_j^{mix}/a_{amb}).

The aerodynamic flow conditions and the selected PNL data corresponding to the acoustic test points are presented in the following section.

3.3.1.3 Test Matrices for Scale Model Configurations

The test matrices for the 10 scale model configurations are presented in test configuration number numerical order in Tables 3-5 through 3-24, as follows: the aerodynamic values are presented in both International (SI) units and in English units:

- o Tables 3-5 and 3-6; Test Matrices for TE-1; Baseline Nozzle; Coannular Inverted-Velocity-Profile Plug Nozzle with 20-Shallow Chute Outer Stream Suppressor; Hardwall Plug and no Ejector.
- o Tables 3-7 and 3-8; Test Matrices for TE-2; Baseline Nozzle with Hardwall Plug and with Hardwall Ejector of Nominal Length, L1, at Extended Spacing, S2.
- o Tables 3-9 and 3-10; Test Matrices for TE-3; Baseline Nozzle with Hardwall Plug and with Treated Ejector, T2, of Nominal Length, L1, at Extended Spacing, S2.
- o Tables 3-11 and 3-12; Test Matrices for TE-4; Baseline Nozzle with Treated Plug, T2, and Treated Ejector, T2, of Nominal Length, L1, at Extended Spacing, S2.
- o Tables 3-13 and 3-14; Test Matrices for TE-5; Baseline Nozzle with Treated Plug, T1, and Treated Ejector, T1, of Nominal Length, L1, at Nominal Spacing, S1.
- o Tables 3-15 and 3-16; Test Matrices for TE-6; Baseline Nozzle with Treated Plug, T2; no Ejector.
- o Tables 3-17 and 3-18; Test Matrices for TE-7; Baseline Nozzle with Hardwall Plug and with Treated Ejector, T2, of Extended Length, L2, at Extended Spacing, S2.

TABLES 3-5 TEST MATRICES FOR TE-1; BASELINE NOZZLE; COANNULAR INVERTED-VELOCITY-PROFILE PLUG NOZZLE WITH 20-SHALLOW CHUTE OUTER STREAM SUPPRESSOR; HARDWALL PLUG AND NO EJECTOR. (INTERNATIONAL UNITS)

************** S I.UNITS **************

NOZZLE - MODEL TEO1 AREA [MODEL SIZE - INNER =0.0031 OUTER = 0.0147 ; FULL SIZE - TOTAL = 0.9031] sq.m.

TEST POINT	V_{ac}	V_j^o	T_T^o	P_r^o	$\dot{W}^o$	F^o	V_j^i	T_T^i	P_r^i	$\dot{W}^i$	F^i	V_j^{mix}	T_T^{mix}	P_r^{mix}	$\dot{W}^T$	F^T	V_j^i/V_j^o
	m/s	m/s	°K		kg/s	N	m/s	°K		kg/s	N	m/s	°K		kg/s	N	
1001	0	517	798	1.887	199.0	6442	392	469	1.864	54.1	1325	491	399	1.871	253	7767	0.76
1002	121	526	819	1.899	196.8	6480	380	442	1.861	55.4	1316	494	404	1.875	252	7796	0.72
1003	0	605	878	2.238	224.7	8497	437	470	2.210	64.1	1753	568	432	2.207	288	10250	0.72
1303	0	599	862	2.237	226.2	8472	420	434	2.208	66.5	1746	558	419	2.201	292	10219	0.70
1204	60	597	859	2.230	225.6	8422	429	452	2.207	65.0	1743	559	421	2.199	290	10165	0.72
1004	121	589	833	2.238	230.2	8473	428	450	2.213	65.3	1751	553	410	2.208	295	10225	0.73
1304	121	592	845	2.235	228.1	8454	430	455	2.210	64.9	1747	557	416	2.205	293	10201	0.73
1005	0	662	915	2.564	251.5	10413	468	453	2.620	77.2	2260	616	442	2.527	328	12674	0.71
1006	121	672	938	2.576	248.4	10434	464	447	2.611	77.2	2240	622	450	2.531	325	12675	0.69
1105	0	470	457	2.630	369.9	10887	470	457	2.618	76.8	2256	470	251	2.627	446	13143	1.00
1106	121	468	456	2.612	367.8	10776	465	450	2.608	77.1	2243	468	249	2.611	444	13019	0.99
1007	0	721	981	2.869	271.2	12224	506	484	2.920	83.4	2638	670	474	2.818	354	14863	0.70
1008	121	714	961	2.884	275.0	12285	500	471	2.921	84.2	2631	664	464	2.831	359	14917	0.70
1009	0	760	970	3.363	319.4	15188	530	492	3.227	91.2	3023	709	474	3.269	410	18211	0.70
1210	60	763	976	3.364	317.8	15161	528	489	3.223	91.2	3010	710	475	3.267	409	18172	0.69
1010	121	756	959	3.361	320.8	15164	524	481	3.221	91.9	3013	704	468	3.265	412	18177	0.69
1109	0	537	491	3.365	456.1	15337	527	486	3.225	91.7	3020	536	269	3.341	547	18357	0.98
1110	121	548	504	3.428	458.7	15718	534	500	3.216	90.1	3008	545	276	3.391	548	18727	0.97
1011	0	762	973	3.367	319.3	15221	392	491	1.812	51.3	1257	711	497	3.075	370	16478	0.51
1012	121	755	958	3.356	320.4	15132	389	486	1.808	51.3	1249	705	490	3.066	371	16381	0.52
1013	0	783	974	3.652	346.0	16947	545	500	3.426	96.0	3276	732	478	3.536	442	20223	0.70
1014	121	775	960	3.618	349.6	16950	542	497	3.390	96.5	3270	725	472	3.505	446	20220	0.70

TEST POINT	T_{amb}	P_{amb}	RH	NF	LVM	LBM	PNL (FULL SIZE, 2400 FT SIDE LINE), dB							OAPWL
							ANGLE RELATIVE TO INLET, DEGREES							
	DEG.K	Pascal	%	dB			50	60	70	90	120	130	140	dB
1001	305.1	99738.	63	-5.2	1.47	-10.00	86.1	88.7	91.6	95.3	97.2	94.7	94.2	172.0
1002	302.0	99332.	71	-5.1	1.52	-10.00	91.0	92.0	94.5	95.3	96.7	92.7	89.7	170.6
1003	305.1	99773.	63	-5.4	2.10	-2.69	91.1	93.7	96.4	98.6	100.5	99.2	97.8	176.6
1303	305.1	99535.	63	-5.6	2.03	-2.69	90.3	93.0	95.7	97.9	100.0	98.0	97.3	175.1
1204	303.4	99400.	74	-5.5	2.05	-2.73	92.3	94.6	97.4	98.6	99.0	96.8	94.5	174.3
1004	302.0	99433.	71	-5.7	2.01	-2.68	94.6	95.9	97.5	98.5	99.5	96.8	93.2	174.5
1304	303.4	99433.	74	-5.6	2.03	-2.70	94.8	95.8	97.2	98.1	99.1	96.3	93.1	173.9
1005	305.1	99671.	63	-6.3	2.46	-1.30	95.4	97.6	99.8	101.3	102.5	100.7	100.5	179.6
1006	302.0	99231.	71	-6.2	2.52	-1.27	99.4	100.2	102.7	102.4	103.3	100.5	97.8	179.3
1105	306.5	99603.	74	-9.3	1.28	-1.15	94.6	96.9	99.3	99.7	96.6	94.9	93.7	174.8
1106	306.5	99569.	74	-9.3	1.25	-1.19	98.9	99.7	101.7	100.6	97.9	93.9	89.8	176.9
1007	305.1	99671.	63	-6.9	2.82	-0.59	96.8	99.7	101.9	102.9	104.4	102.4	101.5	181.3
1008	302.0	99366.	71	-6.9	2.80	-0.56	101.5	102.2	104.2	103.9	104.8	102.4	99.6	180.9
1009	305.1	99502.	63	-7.9	3.07	0.12	98.1	100.8	103.7	105.0	105.9	104.7	104.9	183 9
1210	303.4	99265.	74	-7.9	3.09	0.12	99.6	101.8	104.0	105.2	105.3	104.0	101.3	182.3
1010	303.4	99400.	74	-7.9	3.05	0.12	102.4	103.7	105.6	105.0	106.2	103.4	101.7	182.[illegible]
1109	306.5	99502.	74	-10.6	1.84	0.12	97.7	100.1	102.6	103.8	100.7	98.8	98.6	179.0
1110	302.0	99502.	71	-10.5	1.95	0.18	102.9	103.5	104.6	103.9	103.1	100.1	96.7	181.2
1011	305.1	99535.	63	-7.2	3.08	-0.21	97.7	100.6	103.0	104.3	105.5	103.7	102.5	182.5
1012	303.4	99366.	74	-7.2	3.05	-0.23	102.0	103.7	104.9	104.8	105.7	103.6	100.8	181.8
1013	305.1	99467.	63	-8.4	3.20	0.43	98.8	101.2	103.7	105.7	106.7	105.3	106.1	184.3
1014	303.4	100687.	74	-8.5	3.17	0.39	103.1	103.9	105.1	105.6	106.5	104.3	102.0	182.3

TABLES 3-6 TEST MATRICES FOR TE-1; BASELINE NOZZLE; COANNULAR INVERTED-VELOCITY-PROFILE PLUG NOZZLE WITH 20-SHALLOW CHUTE OUTER STREAM SUPPRESSOR; HARDWALL PLUG AND NO EJECTOR. (ENGLISH UNITS)

NOZZLE - MODEL TE01 AREA [MODEL SIZE - INNER = 4.75 , OUTER = 22.75 ; FULL SIZE - TOTAL = 1400.00] SQ.IN.

TEST POINT	V_{ac} FT/SEC	P_r^o	T_T^o DEG R	V_j^o FT/SEC	W^o LB/SEC	P_r^i	T_T^i DEG R	V_j^i FT/SEC	W^i LB/SEC	P_r^{mix}	T_T^{mix} DEG R	V_j^{mix} FT/SEC	F LB	V_j^i/V_j^o
1001	0	1.887	1438	1699	438.8	1.864	845	1286	119.2	1.871	1311	1611	27939	0.76
1002	400	1.899	1475	1729	433.8	1.861	796	1247	122.1	1.875	1325	1622	28043	0.72
1003	0	2.238	1581	1986	495.3	2.210	846	1436	141.3	2.207	1417	1863	36872	0.72
1303	0	2.237	1552	1966	498.7	2.208	782	1379	146.5	2.201	1377	1833	36758	0.70
1204	200	2.230	1547	1960	497.3	2.207	815	1408	143.3	2.199	1383	1836	36564	0.72
1004	400	2.238	1500	1933	507.4	2.213	811	1407	144.0	2.208	1347	1816	36779	0.73
1304	400	2.235	1521	1945	502.9	2.210	820	1413	143.1	2.205	1365	1827	36694	0.73
1005	0	2.564	1648	2173	554.5	2.620	816	1536	170.3	2.527	1452	2023	45590	0.71
1006	400	2.576	1689	2205	547.6	2.611	806	1524	170.1	2.531	1479	2043	45592	0.69
1105	0	2.630	824	1545	815.4	2.618	824	1542	169.3	2.627	823	1544	47278	1.00
1106	400	2.612	821	1538	810.8	2.608	810	1527	170.0	2.611	819	1536	46832	0.99
1007	0	2.869	1767	2366	598.0	2.920	871	1661	183.8	2.818	1556	2200	53463	0.70
1008	400	2.884	1730	2345	606.2	2.921	849	1640	185.7	2.831	1523	2180	53658	0.70
1009	0	3.363	1747	2496	704.1	3.227	885	1739	201.1	3.269	1555	2328	65507	0.70
1210	200	3.364	1757	2504	700.7	3.223	880	1734	201.0	3.267	1561	2332	65365	0.69
1010	400	3.361	1727	2482	707.2	3.221	867	1720	202.7	3.265	1535	2312	65384	0.69
1109	0	3.365	885	1765	1005.6	3.225	875	1729	202.2	3.341	883	1759	66032	0.98
1110	400	3.428	908	1799	1011.3	3.216	901	1752	198.7	3.391	906	1791	67363	0.97
1011	0	3.367	1753	2502	704.0	1.812	884	1288	113.0	3.075	1633	2334	59274	0.51
1012	400	3.356	1725	2479	706.4	1.808	875	1279	113.0	3.066	1608	2313	58923	0.52
1013	0	3.652	1754	2571	762.8	3.426	900	1791	211.7	3.536	1568	2401	72743	0.70
1014	400	3.618	1729	2545	770.8	3.390	895	1779	212.7	3.505	1548	2379	72733	0.70

TEST POINT	T_{amb} DEG R	P_{amb} PSIA	RH %	NF dB	LVM	LBM	PNL (FULL SIZE, 2400 FT SIDE LINE), dB ANGLE RELATIVE TO INLET, DEGREES 50	60	70	90	120	130	140	OAPWL dB
1001	549.2	14.47	63	-5.2	1.47	-10.00	86.1	88.7	91.6	95.3	97.2	94.7	94.2	172.0
1002	543.7	14.41	71	-5.1	1.52	-10.00	91.0	92.0	94.5	95.3	96.7	92.7	89.7	170.6
1003	549.2	14.47	63	-5.4	2.10	-2.69	91.1	93.7	96.4	98.6	100.5	99.2	97.8	176.6
1303	549.2	14.44	63	-5.6	2.03	-2.69	90.3	93.0	95.7	97.9	100.0	98.0	97.3	175.1
1204	546.2	14.42	74	-5.5	2.05	-2.73	92.3	94.6	97.4	98.6	99.0	96.8	94.5	174.3
1004	543.7	14.42	71	-5.7	2.01	-2.68	94.6	95.9	97.5	98.5	99.5	96.8	93.2	174.5
1304	546.2	14.42	74	-5.6	2.03	-2.70	94.8	95.8	97.2	98.1	99.1	96.3	93.1	173.9
1005	549.2	14.46	63	-6.3	2.46	-1.30	95.4	97.6	99.8	101.3	102.5	100.7	100.5	179.6
1006	543.7	14.39	71	-6.2	2.52	-1.27	99.4	100.2	102.7	102.4	103.3	100.5	97.8	179.3
1105	551.7	14.45	74	-9.3	1.28	-1.15	94.6	96.9	99.3	99.7	96.6	94.9	93.7	174.8
1106	551.7	14.44	74	-9.3	1.25	-1.19	98.9	99.7	101.7	100.6	97.9	93.9	89.8	176.9
1007	549.2	14.46	63	-6.9	2.82	-0.59	96.8	99.7	101.9	102.9	104.4	102.4	101.5	181.3
1008	543.7	14.41	71	-6.9	2.80	-0.56	101.5	102.2	104.2	103.9	104.8	102.4	99.6	180.9
1009	549.2	14.43	63	-7.9	3.07	0.12	98.1	100.8	103.7	105.0	105.9	104.7	104.9	183.9
1210	546.2	14.40	74	-7.9	3.09	0.12	99.6	101.8	104.0	105.2	105.3	104.0	101.3	182.9
1010	546.2	14.42	74	-7.9	3.05	0.12	102.4	103.7	105.6	105.0	106.2	103.4	101.7	182.1
1109	551.7	14.43	74	-10.6	1.84	0.12	97.7	100.1	102.6	103.8	100.7	98.8	98.6	179.0
1110	543.7	14.43	71	-10.5	1.95	0.18	102.9	103.5	104.6	103.9	103.1	100.1	96.7	181.2
1011	549.2	14.44	63	-7.2	3.08	-0.21	97.7	100.6	103.0	104.3	105.5	103.7	102.5	182.5
1012	546.2	14.41	74	-7.2	3.05	-0.23	102.0	103.7	104.9	104.8	105.7	103.6	100.8	181.8
1013	549.2	14.43	63	-8.4	3.20	0.43	98.8	101.2	103.7	105.7	106.7	105.3	106.1	184.3
1014	546.2	14.60	74	-8.5	3.17	0.39	103.1	103.9	105.1	105.6	106.5	104.3	102.0	182.3

TABLES 3-7 TEST MATRICES FOR TE-2; BASELINE NOZZLE WITH HARDWALL PLUG AND WITH HARDWALL EJECTOR OF NOMI LENGTH, L1, AT EXTENDED SPACING, S2. (INTERNATIONAL UNITS)

************** S.I.UNITS ***************

NOZZLE - MODEL AX. AREA [MODEL SIZE - INNER =0.0031 , OUTER = 0.0147 ; FULL SIZE - TOTAL = 0.9031] sq.m.

TEST POINT	V_{ac}	V_j^o	T_T^o	P_r^o	$\dot{W}^o$	F^o	V_j^i	T_T^i	P_r^i	$\dot{W}^i$	F^i	V_j^{mix}	T_T^{mix}	P_r^{mix}	$\dot{W}^T$	F^T	V_j^i/V_j^o
	m/s	m/s	°K		kg/s	N	m/s	°K		kg/s	N	m/s	°K		kg/s	N	
2001	0	517	801	1.882	197.6	6393	377	442	1.843	54.9	1295	487	396	1.860	252	7688	0.73
2002	121	521	808	1.888	197.6	6436	387	462	1.850	54.0	1306	492	402	1.868	251	7742	0.74
2003	0	594	852	2.223	226.0	8390	420	438	2.190	65.6	1723	554	416	2.188	291	10113	0.71
2004	121	598	863	2.224	224.9	8406	427	454	2.184	64.3	1718	560	424	2.190	289	10125	0.71
2005	0	657	902	2.558	252.5	10368	464	451	2.588	76.5	2218	612	437	2.519	328	12587	0.71
2006	121	661	915	2.553	250.2	10341	467	456	2.588	76.0	2219	615	443	2.515	326	12560	0.71
2007	0	712	966	2.841	270.5	12045	495	468	2.886	83.6	2591	661	465	2.788	354	14637	0.70
2008	121	713	966	2.850	271.4	12098	499	475	2.887	83.1	2593	663	466	2.798	354	14692	0.70
2009	0	753	959	3.329	318.5	15008	521	480	3.188	91.3	2978	702	467	3.234	409	17986	0.69
2010	121	757	966	3.336	317.8	15040	523	484	3.189	91.0	2978	705	471	3.239	408	18018	0.69
2109	0	560	528	3.411	446.0	15622	526	488	3.194	90.6	2982	554	286	3.373	536	18604	0.94
2110	121	557	523	3.402	447.2	15581	526	489	3.192	90.6	2982	552	284	3.366	537	18564	0.95
2013	0	779	967	3.627	345.4	16815	541	495	3.389	95.6	3233	727	474	3.510	440	20048	0.69
2014	121	777	965	3.616	344.9	16762	540	495	3.387	95.6	3232	726	473	3.501	440	19995	0.70

TEST POINT	T_{amb}	P_{amb}	RH	NF	LVM	LBM	PNL (FULL SIZE, 2400 FT SIDE LINE), dB ANGLE RELATIVE TO INLET, DEGREES							OAPWL
	DEG.K	Pascal	%	dB			50	60	70	90	120	130	140	dB
2001	299.3	99517.	85	-5.1	1.47	-10.00	81.3	83.8	86.3	91.3	91.7	87.2	83.8	165.8
2002	298.2	99586.	87	-5.0	1.53	-10.00	86.0	87.7	89.0	91.4	91.7	85.5	81.0	165.6
2003	299.3	99495.	85	-5.5	2.04	-2.78	84.3	87.5	89.9	95.1	94.9	92.7	89.5	170.4
2004	298.2	99662.	87	-5.4	2.09	-2.79	89.9	92.3	93.2	95.5	95.1	89.6	85.9	170.1
2005	299.3	99550.	85	-6.3	2.47	-1.33	87.8	91.2	93.4	98.0	98.1	96.8	95.4	174.6
2006	299.3	99581.	85	-6.2	2.50	-1.34	92.9	94.7	95.9	98.1	97.3	93.7	90.4	173.4
2007	299.3	99520.	85	-6.8	2.80	-0.64	90.5	94.3	96.2	100.0	100.8	100.0	99.0	177.7
2008	299.3	99513.	85	-6.8	2.82	-0.63	93.9	96.5	97.5	99.8	99.5	96.3	93.7	175.1
2009	299.3	99653.	85	-7.8	3.06	0.08	96.2	98.7	100.1	102.9	104.8	104.7	105.2	181.7
2010	299.3	99595.	85	-7.8	3.08	0.08	99.7	101.2	101.8	102.8	103.4	101.3	98.5	179.5
2109	298.2	99544.	87	-10.3	2.05	0.16	96.2	98.5	99.8	101.3	100.3	99.1	98.5	178.1
2110	298.2	99621.	87	-10.3	2.03	0.15	100.7	102.1	102.2	102.3	98.5	95.2	91.5	178.4
2013	299.3	99591.	85	-8.3	3.22	0.40	96.6	99.1	100.6	103.1	105.7	106.2	107.6	183.5
2014	299.3	99650.	85	-8.3	3.21	0.39	101.0	102.5	102.9	103.8	104.3	102.2	100.9	180.5

TABLES 3-8 TEST MATRICES FOR TE-2; BASELINE NOZZLE WITH HARDWALL PLUG AND WITH HARDWALL EJECTOR OF NOMINAL LENGTH, L1, AT EXTENDED SPACING, S2. (ENGLISH UNITS)

NOZZLE - MODEL AX. AREA [MODEL SIZE - INNER = 4.75 , OUTER = 22.75 ; FULL SIZE - TOTAL = 1400.00] SQ.IN.

TEST POINT	V_{ac} FT/SEC	P^o_r	T^o_T DEG R	V^o_j FT/SEC	W^o LB/SEC	P^i_r	T^i_T DEG R	V^i_j FT/SEC	W^i LB/SEC	P^{mix}_r	T^{mix}_T DEG R	V^{mix}_j FT/SEC	F LB	V^i_j/V^o_j
2001	0	1.882	1443	1698	435.7	1.843	796	1238	121.1	1.860	1302	1598	27655	0.73
2002	400	1.888	1455	1710	435.6	1.850	832	1270	119.0	1.868	1321	1615	27849	0.74
2003	0	2.223	1535	1949	498.3	2.190	788	1378	144.6	2.188	1367	1820	36377	0.71
2004	400	2.224	1555	1962	495.8	2.184	818	1402	141.8	2.190	1391	1837	36420	0.71
2005	0	2.558	1625	2156	556.7	2.588	811	1523	168.6	2.519	1436	2008	45276	0.71
2006	400	2.553	1648	2169	551.7	2.588	821	1532	167.6	2.515	1455	2020	45181	0.71
2007	0	2.841	1740	2338	596.3	2.886	842	1626	184.4	2.788	1528	2169	52650	0.70
2008	400	2.850	1739	2340	598.4	2.887	855	1638	183.1	2.798	1532	2175	52847	0.70
2009	0	3.329	1727	2473	702.2	3.188	865	1712	201.3	3.234	1535	2303	64698	0.69
2010	400	3.336	1740	2484	700.7	3.189	871	1718	200.6	3.239	1546	2313	64812	0.69
2109	0	3.411	952	1839	983.2	3.194	879	1727	199.8	3.373	939	1820	66921	0.94
2110	400	3.402	943	1829	985.8	3.192	881	1728	199.7	3.366	933	1812	66775	0.95
2013	0	3.627	1741	2556	761.4	3.389	891	1775	210.7	3.510	1557	2386	72114	0.69
2014	400	3.616	1738	2551	760.4	3.387	891	1774	210.8	3.501	1554	2382	71921	0.70

TEST POINT	T_{amb} DEG R	P_{amb} PSIA	RH %	NF dB	LVM	LBM	PNL (FULL SIZE, 2400 FT SIDE LINE), dB ANGLE RELATIVE TO INLET, DEGREES 50	60	70	90	120	130	140	OAPWL dB
2001	538.7	14.43	85	-5.1	1.47	-10.00	81.3	83.8	86.3	91.3	91.7	87.2	83.8	165.8
2002	536.7	14.44	87	-5.0	1.53	-10.00	86.0	87.7	89.0	91.4	91.7	85.5	81.0	165.6
2003	538.7	14.43	85	-5.5	2.04	-2.78	84.3	87.5	89.9	95.1	94.9	92.7	89.5	170.4
2004	536.7	14.45	87	-5.4	2.09	-2.79	89.9	92.3	93.2	95.5	95.1	89.6	85.9	170.1
2005	538.7	14.44	85	-6.3	2.47	-1.33	87.8	91.2	93.4	98.0	98.1	96.8	95.4	174.6
2006	538.7	14.44	85	-6.2	2.50	-1.34	92.9	94.7	95.9	98.1	97.3	93.7	90.4	173.4
2007	538.7	14.43	85	-6.8	2.80	-0.64	90.5	94.3	96.2	100.0	100.8	100.0	99.0	177.7
2008	538.7	14.43	85	-6.8	2.82	-0.63	93.9	96.5	97.5	99.8	99.5	96.3	93.7	175.1
2009	538.7	14.45	85	-7.8	3.06	0.08	96.2	98.7	100.1	102.9	104.8	104.7	105.2	181.7
2010	538.7	14.45	85	-7.8	3.08	0.08	99.7	101.2	101.8	102.8	103.4	101.3	98.5	179.5
2109	536.7	14.44	87	-10.3	2.05	0.16	96.2	98.5	99.8	101.3	100.3	99.1	98.5	178.1
2110	536.7	14.45	87	-10.3	2.03	0.15	100.7	102.1	102.2	102.3	98.5	95.2	91.5	178.4
2013	538.7	14.44	85	-8.3	3.22	0.40	96.6	99.1	100.6	103.1	105.7	106.2	107.6	183.5
2014	538.7	14.45	85	-8.3	3.21	0.39	101.0	102.5	102.9	103.8	104.3	102.2	100.9	180.5

TABLES 3-9 TEST MATRICES FOR TE-3; BASELINE NOZZLE WITH HARDWALL PLUG AND WITH TREATED EJECTOR, T2, OF NOMINAL LENGTH, L1, AT EXTENDED SPACING, S2. (INTERNATIONAL UNITS)

************** S.I.UNITS **************

NOZZLE - MODEL TEO3 AREA [MODEL SIZE - INNER =0.0031 , OUTER = 0.0147 ; FULL SIZE - TOTAL = 0.9031] sq.m.

TEST POINT	V_{ac}	V^o_j	T^o_T	P^o_r	$\dot{W}^o$	F^o	V^i_j	T^i_T	P^i_r	$\dot{W}^i$	F^i	V^{mix}_j	T^{mix}_T	P^{mix}_r	$\dot{W}^T$	F^T	V^i_j/V^o_j
	m/s	m/s	°K		kg/s	N	m/s	°K		kg/s	N	m/s	°K		kg/s	N	
3001	0	519	803	1.889	198.8	6455	374	430	1.854	56.2	1313	487	395	1.866	255	7769	0.72
3002	121	521	808	1.890	197.8	6446	381	449	1.845	54.6	1299	491	400	1.867	252	7745	0.73
3003	0	598	863	2.230	225.7	8443	415	425	2.202	67.1	1742	556	418	2.192	292	10185	0.69
3004	121	594	848	2.233	227.7	8455	424	446	2.195	65.2	1731	556	416	2.199	292	10187	0.72
3005	0	660	907	2.574	253.8	10478	459	440	2.603	78.0	2242	613	437	2.530	331	12721	0.70
3006	121	664	918	2.571	252.0	10458	469	459	2.593	76.0	2229	618	445	2.530	327	12688	0.71
3007	0	714	962	2.874	274.2	12242	488	451	2.909	85.8	2621	660	461	2.813	360	14863	0.68
3008	121	717	971	2.869	272.4	12211	495	465	2.902	84.4	2611	664	467	2.811	356	14823	0.69
3009	0	757	963	3.358	320.3	15170	525	484	3.215	91.6	3010	706	470	3.262	411	18181	0.69
3010	121	755	960	3.354	320.6	15147	526	486	3.209	91.3	3002	705	469	3.260	411	18150	0.70
3109	0	567	538	3.439	446.7	15834	517	469	3.218	93.4	3022	558	288	3.398	540	18856	0.91
3110	121	566	538	3.417	442.3	15644	527	488	3.206	90.9	2996	559	290	3.379	533	18641	0.93
3013	0	777	960	3.654	349.1	16967	534	480	3.418	97.8	3267	724	469	3.531	446	20235	0.69
3014	121	779	961	3.674	351.1	17107	535	482	3.411	97.5	3262	726	470	3.547	448	20370	0.69

TEST POINT	T_{amb}	P_{amb}	RH	NF	LVM	LBM	PNL (FULL SIZE, 2400 FT SIDE LINE), dB — ANGLE RELATIVE TO INLET, DEGREES							OAPWL
	DEG.K	Pascal	%	dB			50	60	70	90	120	130	140	dB
3001	295.9	99836.	72	-5.1	1.50	-10.00	81.4	83.3	86.5	89.9	90.8	86.8	83.9	166.2
3002	296.8	99586.	68	-5.0	1.53	-10.00	86.0	87.2	89.7	90.6	90.2	84.6	80.4	165.7
3003	295.9	99684.	72	-5.4	2.08	-2.74	83.9	86.6	90.2	94.0	94.4	92.3	90.9	171.2
3004	296.8	99618.	68	-5.5	2.07	-2.73	88.5	89.8	92.8	93.9	93.8	89.1	85.5	170.5
3005	295.9	99745.	72	-6.3	2.50	-1.28	87.1	90.2	94.1	97.4	97.8	96.8	95.3	175.1
3006	296.8	99726.	68	-6.2	2.53	-1.29	91.3	93.0	95.3	97.7	97.1	92.8	90.9	175.4
3007	295.9	99524.	72	-6.8	2.82	-0.58	90.0	93.2	97.2	99.5	100.6	99.7	99.3	177.7
3008	296.8	99517.	68	-6.8	2.84	-0.59	94.4	96.0	98.4	99.8	99.8	96.3	94.7	177.7
3009	295.9	99577.	72	-7.8	3.11	0.11	95.1	97.5	100.5	102.2	104.4	103.8	104.8	181.8
3010	296.8	99559.	68	-7.8	3.10	0.11	98.9	100.8	102.7	102.7	103.4	100.7	99.3	181.2
3109	295.9	99838.	72	-10.3	2.09	0.19	96.4	98.4	100.9	101.3	100.0	99.1	99.3	179.2
3110	296.8	99517.	68	-10.2	2.09	0.17	100.9	101.6	103.5	102.3	98.7	95.0	92.5	179.9
3013	295.9	99508.	72	-8.4	3.22	0.43	96.6	98.9	102.1	103.1	105.7	105.8	110.2	184.5
3014	296.8	99595.	68	-8.4	3.23	0.44	100.4	101.9	104.1	104.0	104.5	102.6	101.5	181.7

TABLES 3-10 TEST MATRICES FOR TE-3; BASELINE NOZZLE WITH HARDWALL PLUG AND WITH TREATED EJECTOR, T2, OF NOMINAL LENGTH, L1, AT EXTENDED SPACING, S2.(ENGLISH UNITS)

NOZZLE - MODEL TEO3 AREA [MODEL SIZE - INNER = 4.75 , OUTER = 22.75 ; FULL SIZE - TOTAL = 1400.00] SQ.IN.

TEST POINT	V_{ac} FT/SEC	P^o_r	T^o_T DEG R	V^o_j FT/SEC	W^o LB/SEC	P^i_r	T^i_T DEG R	V^i_j FT/SEC	W^i LB/SEC	P^{mix}_r	T^{mix}_T DEG R	V^{mix}_j FT/SEC	F LB	V^i_j/V^o_j
3001	0	1.889	1446	1705	438.3	1.854	775	1227	123.9	1.866	1298	1599	27945	0.72
3002	400	1.890	1455	1711	436.0	1.845	809	1250	120.3	1.867	1315	1611	27861	0.73
3003	0	2.230	1554	1964	497.5	2.202	765	1362	147.9	2.192	1373	1826	36638	0.69
3004	400	2.233	1528	1949	502.1	2.195	803	1394	143.8	2.199	1367	1825	36644	0.72
3005	0	2.574	1634	2167	559.5	2.603	792	1508	172.0	2.530	1435	2012	45757	0.70
3006	400	2.571	1653	2179	555.5	2.593	827	1539	167.6	2.530	1461	2030	45639	0.71
3007	0	2.874	1732	2343	604.6	2.909	813	1603	189.2	2.813	1513	2166	53463	0.68
3008	400	2.869	1749	2353	600.6	2.902	837	1625	186.0	2.811	1533	2180	53319	0.69
3009	0	3.358	1735	2486	706.1	3.215	872	1724	202.0	3.262	1543	2316	65397	0.69
3010	400	3.354	1728	2480	706.8	3.209	876	1727	201.2	3.260	1538	2313	65285	0.70
3109	0	3.439	969	1861	984.8	3.218	845	1697	206.0	3.398	947	1832	67824	0.91
3110	400	3.417	970	1857	975.0	3.206	880	1730	200.5	3.379	954	1835	67051	0.93
3013	0	3.654	1728	2552	769.6	3.418	864	1753	215.6	3.531	1538	2377	72785	0.69
3014	400	3.674	1730	2558	774.0	3.411	868	1756	215.0	3.547	1542	2383	73270	0.69

TEST POINT	T_{amb} DEG R	P_{amb} PSIA	RH %	NF dB	LVM	LBM	PNL (FULL SIZE, 2400 FT SIDE LINE), dB ANGLE RELATIVE TO INLET, DEGREES 50	60	70	90	120	130	140	OAPWL dB
3001	532.7	14.48	72	-5.1	1.50	-10.00	81.4	83.3	86.5	89.9	90.8	86.8	83.9	166.2
3002	534.2	14.44	68	-5.0	1.53	-10.00	86.0	87.2	89.7	90.6	90.2	84.6	80.4	165.7
3003	532.7	14.46	72	-5.4	2.08	-2.74	83.9	86.6	90.2	94.0	94.4	92.3	90.9	171.2
3004	534.2	14.45	68	-5.5	2.07	-2.73	88.5	89.8	92.8	93.9	93.8	89.1	85.5	170.5
3005	532.7	14.47	72	-6.3	2.50	-1.28	87.1	90.2	94.1	97.4	97.8	96.8	95.3	175.1
3006	534.2	14.46	68	-6.2	2.53	-1.29	91.3	93.0	95.3	97.7	97.1	92.8	90.9	175.4
3007	532.7	14.43	72	-6.8	2.82	-0.58	90.0	93.2	97.2	99.5	100.6	99.7	99.3	177.7
3008	534.2	14.43	68	-6.8	2.84	-0.59	94.4	96.0	98.4	99.8	99.8	96.3	94.7	177.7
3009	532.7	14.44	72	-7.8	3.11	0.11	95.1	97.5	100.5	102.2	104.4	103.8	104.8	181.8
3010	534.2	14.44	68	-7.8	3.10	0.11	98.9	100.8	102.7	102.7	103.4	100.7	99.3	181.2
3109	532.7	14.48	72	-10.3	2.09	0.19	96.4	98.4	100.9	101.3	100.0	99.1	99.3	179.2
3110	534.2	14.43	68	-10.2	2.09	0.17	100.9	101.6	103.5	102.3	98.7	95.0	92.5	179.9
3013	532.7	14.43	72	-8.4	3.22	0.43	96.6	98.9	102.1	103.1	105.7	105.8	110.2	184.5
3014	534.2	14.45	68	-8.4	3.23	0.44	100.4	101.9	104.1	104.0	104.5	102.6	101.5	181.7

TABLES 3-11 TEST MATRICES FOR TE-4; BASELINE NOZZLE WITH TREATED PLUG, T2, AND TREATED EJECTOR, T2, OF NOMINAL LENGTH, L1, AT EXTENDED SPACING, S2. (INTERNATIONAL UNITS)

************** S.I.UNITS ***************

NOZZLE - MODEL AX. AREA [MODEL SIZE - INNER =0.0031 , OUTER = 0.0147 ; FULL SIZE - TOTAL = 0.9031] sq.m.

TEST POINT	V_{ac}	V_j^o	T_T^o	P_r^o	$\dot{W}^o$	F^o	V_j^i	T_T^i	P_r^i	$\dot{W}^i$	F^i	V_j^{mix}	T_T^{mix}	P_r^{mix}	$\dot{W}^T$	F^T	V_j^i/V_j^o
	m/s	m/s	°K		kg/s	N	m/s	°K		kg/s	N	m/s	°K		kg/s	N	
4001	0	521	806	1.894	198.9	6486	376	436	1.855	55.9	1315	489	398	1.870	254	7802	0.72
4002	121	511	782	1.881	200.7	6411	380	449	1.845	54.7	1302	483	390	1.861	255	7714	0.75
4003	0	598	865	2.227	225.4	8438	423	441	2.207	66.1	1750	559	422	2.193	291	10188	0.71
4204	60	606	882	2.236	224.1	8494	433	464	2.199	64.2	1742	568	433	2.202	288	10236	0.72
4004	121	597	860	2.231	226.5	8461	419	433	2.203	66.6	1745	557	418	2.195	293	10207	0.70
4304	121	599	866	2.229	223.3	8369	425	446	2.202	64.9	1727	560	423	2.195	288	10096	0.71
4005	0	663	913	2.576	253.5	10508	459	438	2.612	78.5	2256	615	439	2.532	332	12764	0.69
4006	121	662	913	2.574	251.2	10406	464	448	2.607	76.8	2231	616	441	2.532	328	12637	0.70
4105	0	477	473	2.614	362.3	10820	459	438	2.612	78.5	2255	474	256	2.613	440	13075	0.96
4106	121	480	480	2.605	355.4	10672	461	442	2.606	77.3	2228	477	259	2.604	432	12901	0.96
4007	0	714	965	2.869	274.0	12241	490	455	2.913	85.9	2633	661	462	2.810	359	14874	0.69
4008	121	719	977	2.868	271.9	12221	495	462	2.919	85.3	2638	665	468	2.810	357	14860	0.69
4009	0	758	965	3.360	320.9	15211	519	472	3.222	93.2	3024	704	468	3.259	414	18235	0.68
4309	0	760	971	3.351	318.7	15142	519	474	3.212	92.6	3010	706	471	3.250	411	18153	0.68
4210	60	762	975	3.360	316.7	15094	524	482	3.209	91.1	2984	709	474	3.259	407	18079	0.69
4010	121	758	967	3.345	319.2	15132	520	476	3.201	92.2	3000	705	470	3.245	411	18132	0.69
4109	0	560	526	3.423	450.1	15756	519	473	3.215	93.0	3021	553	284	3.386	543	18777	0.93
4110	121	549	505	3.443	457.7	15729	517	469	3.215	92.6	2992	544	274	3.403	550	18721	0.94
4011	0	755	961	3.344	320.2	15121	389	489	1.801	51.1	1246	705	491	3.055	371	16368	0.52
4012	121	758	965	3.352	320.3	15175	387	484	1.797	51.3	1241	706	493	3.060	371	16416	0.51
4013	0	778	962	3.644	348.5	16953	535	483	3.410	97.5	3266	725	470	3.522	446	20219	0.69
4014	121	784	974	3.660	347.7	17041	535	482	3.415	97.7	3270	729	475	3.533	445	20311	0.68

TEST POINT	T_{amb}	P_{amb}	RH	NF	LVM	LBM	PNL (FULL SIZE, 2400 FT SIDE LINE), dB ANGLE RELATIVE TO INLET, DEGREES							OAPWL
	DEG.K	Pascal	%	dB			50	60	70	90	120	130	140	dB
4001	301.5	99886.	32	-5.2	1.48	-10.00	81.8	83.5	85.4	89.6	90.3	87.0	84.5	164.3
4002	295.4	99816.	57	-5.2	1.47	-10.00	85.7	85.6	86.5	88.8	88.9	83.3	79.0	162.7
4003	301.5	99842.	32	-5.5	2.06	-2.75	83.8	85.7	88.6	93.5	94.5	92.4	90.6	169.2
4204	295.4	99916.	57	-5.2	2.17	-2.71	85.3	87.5	89.9	93.8	93.8	89.1	85.7	167.0
4004	295.4	99845.	57	-5.4	2.09	-2.73	88.2	89.3	90.6	93.5	93.4	88.3	84.9	167.1
4304	297.6	98886.	87	-5.4	2.10	-2.74	88.2	90.3	91.6	94.3	95.1	89.4	86.7	168.2
4005	301.5	99884.	32	-6.4	2.47	-1.27	86.8	89.2	92.4	97.1	98.1	97.1	95.4	173.2
4006	297.6	99029.	87	-6.2	2.51	-1.28	92.0	93.8	95.1	98.2	98.0	94.0	91.1	172.0
4105	301.5	99848.	32	-9.2	1.35	-1.19	89.1	91.5	94.5	97.0	94.0	91.0	89.5	172.0
4106	297.6	99000.	87	-9.0	1.40	-1.21	92.1	95.2	96.2	98.0	94.9	88.3	84.8	173.0
4007	301.5	99786.	32	-6.9	2.79	-0.59	89.7	92.3	95.8	99.3	100.5	100.0	98.5	176.1
4008	295.4	99688.	57	-6.8	2.86	-0.59	94.0	95.0	96.8	99.4	99.9	97.1	93.5	173.9
4009	301.5	99755.	32	-7.9	3.06	0.12	93.1	95.9	98.9	101.7	103.9	104.0	103.7	180.2
4309	295.4	99680.	57	-7.8	3.12	0.10	94.2	96.9	99.6	102.6	105.0	104.4	104.1	180.7
4210	297.6	98980.	87	-7.8	3.12	0.11	97.1	100.7	102.6	104.4	104.6	102.7	100.7	180.6
4010	295.4	99833.	57	-7.8	3.11	0.10	97.7	99.5	101.4	102.8	103.5	100.9	98.0	177.7
4109	301.5	99910.	32	-10.4	2.01	0.18	96.0	97.9	100.2	101.9	99.8	98.8	98.0	178.0
4110	297.6	98972.	87	-10.5	1.97	0.20	100.7	102.7	103.7	104.5	100.0	94.9	91.6	179.5
4011	295.4	99810.	57	-7.1	3.11	-0.24	93.1	96.1	99.2	102.5	104.6	104.0	103.5	179.4
4012	295.4	99815.	57	-7.1	3.12	-0.23	96.8	98.0	99.8	102.1	102.7	100.3	97.4	176.7
4013	295.4	99779.	57	-8.4	3.23	0.42	98.0	99.9	102.2	104.4	106.9	106.6	107.4	183.3
4014	295.4	99713.	57	-8.3	3.26	0.43	100.7	102.8	103.6	104.6	105.6	103.1	101.3	180.1

TABLES 3-12 TEST MATRICES FOR TE-4; BASELINE NOZZLE WITH TREATED PLUG, T2, AND TREATED EJECTOR, T2, OF NOMINAL LENGTH, L1, AT EXTENDED SPACING, S2. (ENGLISH UNITS)

NOZZLE - MODEL AX. AREA [MODEL SIZE - INNER = 4.75 , OUTER = 22.75 ; FULL SIZE - TOTAL = 1400.00] SQ.IN.

TEST POINT	V_{ac} FT/SEC	P_r^o	T_T^o DEG R	V_j^o FT/SEC	W^o LB/SEC	P_r^i	T_T^i DEG R	V_j^i FT/SEC	W^i LB/SEC	P_r^{mix}	T_T^{mix} DEG R	V_j^{mix} FT/SEC	F LB	V_j^i/V_j^o
4001	0	1.894	1452	1712	438.6	1.855	786	1236	123.2	1.870	1306	1607	28066	0.72
4002	400	1.881	1408	1677	442.5	1.845	809	1249	120.6	1.861	1279	1585	27747	0.75
4003	0	2.227	1558	1965	496.9	2.207	794	1390	145.7	2.193	1384	1834	36648	0.71
4204	200	2.236	1589	1990	494.1	2.199	836	1423	141.6	2.202	1421	1863	36820	0.72
4004	400	2.231	1549	1961	499.3	2.203	780	1376	146.8	2.195	1374	1828	36716	0.70
4304	400	2.229	1560	1968	492.2	2.202	803	1396	143.1	2.195	1389	1839	36316	0.71
4005	0	2.576	1645	2176	558.9	2.612	789	1508	173.1	2.532	1442	2018	45913	0.69
4006	400	2.574	1644	2174	553.9	2.607	807	1524	169.4	2.532	1447	2022	45455	0.70
4105	0	2.614	852	1568	798.7	2.612	788	1507	173.1	2.613	841	1557	47033	0.96
4106	400	2.605	864	1576	783.6	2.606	796	1513	170.4	2.604	852	1565	46405	0.96
4007	0	2.869	1737	2345	604.1	2.913	819	1610	189.3	2.810	1518	2169	53503	0.69
4008	400	2.868	1759	2360	599.4	2.919	832	1624	188.0	2.810	1537	2184	53452	0.69
4009	0	3.360	1737	2488	707.5	3.222	850	1704	205.4	3.259	1537	2311	65593	0.68
4309	0	3.351	1748	2494	702.6	3.212	854	1705	204.2	3.250	1546	2316	65296	0.68
4210	200	3.360	1756	2502	698.1	3.209	868	1719	200.9	3.259	1557	2327	65030	0.69
4010	400	3.345	1742	2488	703.8	3.201	858	1707	203.3	3.245	1543	2313	65223	0.69
4109	0	3.423	948	1838	992.3	3.215	852	1704	205.1	3.386	931	1814	67541	0.93
4110	400	3.443	910	1804	1009.0	3.215	845	1697	204.1	3.403	899	1786	67341	0.94
4011	0	3.344	1730	2479	705.9	1.801	880	1279	112.7	3.055	1613	2313	58875	0.52
4012	400	3.352	1738	2487	706.1	1.797	871	1270	113.0	3.060	1618	2319	59051	0.51
4013	0	3.644	1733	2554	768.3	3.410	870	1758	215.0	3.522	1544	2379	72728	0.69
4014	400	3.660	1754	2573	766.5	3.415	868	1756	215.4	3.533	1559	2393	73060	0.68

TEST POINT	T_{amb} DEG R	P_{amb} PSIA	RH %	NF dB	LVM	LBM	PNL (FULL SIZE, 2400 FT SIDE LINE), dB ANGLE RELATIVE TO INLET, DEGREES 50	60	70	90	120	130	140	OAPWL dB
4001	542.7	14.49	32	-5.2	1.48	-10.00	81.8	83.5	85.4	89.6	90.3	87.0	84.5	164.3
4002	531.7	14.48	57	-5.2	1.47	-10.00	85.7	85.6	86.5	88.8	88.9	83.3	79.0	162.7
4003	542.7	14.48	32	-5.5	2.06	-2.75	83.8	85.7	88.6	93.5	94.5	92.4	90.6	169.2
4204	531.7	14.49	57	-5.2	2.17	-2.71	85.3	87.5	89.9	93.8	93.8	89.1	85.7	167.0
4004	531.7	14.48	57	-5.4	2.09	-2.73	88.2	89.3	90.6	93.5	93.4	88.3	84.9	167.1
4304	535.7	14.34	87	-5.4	2.10	-2.74	88.2	90.3	91.6	94.3	95.1	89.4	86.7	168.2
4005	542.7	14.49	32	-6.4	2.47	-1.27	86.8	89.2	92.4	97.1	98.1	97.1	95.4	173.2
4006	535.7	14.36	87	-6.2	2.51	-1.28	92.0	93.8	95.1	98.2	98.0	94.0	91.1	172.0
4105	542.7	14.48	32	-9.2	1.35	-1.19	89.1	91.5	94.5	97.0	94.0	91.0	89.5	172.0
4106	535.7	14.36	87	-9.0	1.40	-1.21	92.1	95.2	96.2	98.0	94.9	88.3	84.8	173.0
4007	542.7	14.47	32	-6.9	2.79	-0.59	89.7	92.3	95.8	99.3	100.5	100.0	98.5	176.1
4008	531.7	14.46	57	-6.8	2.86	-0.59	94.0	95.0	96.8	99.4	99.9	97.1	93.5	173.9
4009	542.7	14.47	32	-7.9	3.06	0.12	93.1	95.9	98.9	101.7	103.9	104.0	103.7	180.2
4309	531.7	14.46	57	-7.8	3.12	0.10	94.2	96.9	99.6	102.6	105.0	104.4	104.1	180.7
4210	535.7	14.36	87	-7.8	3.12	0.11	97.1	100.7	102.6	104.4	104.6	102.7	100.7	180.6
4010	531.7	14.48	57	-7.8	3.11	0.10	97.7	99.5	101.4	102.8	103.5	100.9	98.0	177.7
4109	542.7	14.49	32	-10.4	2.01	0.18	96.0	97.9	100.2	101.9	99.8	98.8	98.0	178.0
4110	535.7	14.35	87	-10.5	1.97	0.20	100.7	102.7	103.7	104.5	100.0	94.9	91.6	179.5
4011	531.7	14.48	57	-7.1	3.11	-0.24	93.1	96.1	99.2	102.5	104.6	104.0	103.5	179.4
4012	531.7	14.48	57	-7.1	3.12	-0.23	96.8	98.0	99.8	102.1	102.7	100.3	97.4	176.7
4013	531.7	14.47	57	-8.4	3.23	0.42	98.0	99.9	102.2	104.4	106.9	106.6	107.4	183.3
4014	531.7	14.46	57	-8.3	3.26	0.43	100.7	102.8	103.6	104.6	105.6	103.1	101.3	180.1

TABLES 3-13 TEST MATRICES FOR TE-5; BASELINE NOZZLE WITH TREATED PLUG, T1, AND TREATED EJECTOR, T1, OF NOMIN. LENGTH, L1, AT NOMINAL SPACING, S1. (INTERNATIONAL UNITS)

ORIGINAL PAGE IS OF POOR QUALITY

************** S.I.UNITS **************

NOZZLE - MODEL TEO5 AREA [MODEL SIZE - INNER =0.0031 , OUTER = 0.0147 ; FULL SIZE - TOTAL = 0.9031] sq.m.

TEST POINT	V_{ac}	V_j^o	T_T^o	P_r^o	$\dot{W}^o$	F^o	V_j^i	T_T^i	P_r^i	$\dot{W}^i$	F^i	V_j^{mix}	T_T^{mix}	P_r^{mix}	$\dot{W}^T$	F^T	V_j^i/V_j^o
	m/s	m/s	°K		kg/s	N	m/s	°K		kg/s	N	m/s	°K		kg/s	N	
5001	0	519	804	1.888	197.5	6417	374	436	1.843	55.2	1293	488	397	1.864	252	7710	0.72
5002	121	520	800	1.898	199.1	6473	380	444	1.856	55.1	1308	489	396	1.875	254	7782	0.73
5003	0	597	860	2.231	225.6	8429	419	435	2.201	66.1	1735	557	419	2.195	291	10165	0.70
5204	60	597	858	2.234	226.1	8441	423	441	2.200	65.5	1733	558	419	2.198	291	10174	0.71
5004	121	597	855	2.240	226.7	8464	424	443	2.207	65.5	1739	558	418	2.205	292	10203	0.71
5005	0	659	903	2.574	253.1	10428	456	432	2.605	78.3	2232	611	434	2.529	331	12661	0.69
5006	121	661	906	2.584	253.7	10489	464	447	2.610	77.2	2238	615	438	2.542	330	12728	0.70
5105	0	472	462	2.608	363.5	10725	464	448	2.607	77.0	2236	470	252	2.608	440	12962	0.98
5106	121	482	481	2.615	357.5	10774	463	446	2.615	77.5	2247	478	260	2.615	435	13022	0.96
5007	0	715	966	2.871	272.9	12200	493	461	2.911	84.9	2617	662	464	2.814	357	14817	0.69
5008	121	714	963	2.872	273.2	12198	495	464	2.910	84.5	2615	662	464	2.816	357	14814	0.69
5009	0	750	944	3.359	322.8	15130	515	466	3.222	93.3	3008	697	459	3.260	416	18139	0.69
5210	60	758	966	3.356	319.2	15142	520	476	3.210	92.2	3000	705	470	3.255	411	18142	0.69
5010	121	754	956	3.361	321.1	15148	521	476	3.214	92.1	3000	702	465	3.262	413	18149	0.69
5109	0	575	579	3.222	401.2	14419	526	502	3.083	86.2	2839	566	310	3.195	487	17258	0.92
5110	121	573	579	3.193	397.0	14227	536	521	3.082	84.5	2836	566	312	3.172	481	17063	0.94
5011	0	754	957	3.355	320.2	15105	385	475	1.806	51.8	1245	703	488	3.062	371	16351	0.51
5012	121	754	955	3.361	321.1	15143	387	479	1.809	51.6	1249	703	487	3.069	372	16393	0.51
5013	0	778	960	3.655	348.4	16943	533	479	3.412	97.5	3253	724	469	3.530	445	20196	0.69
5014	121	779	963	3.652	347.8	16938	536	484	3.418	97.3	3263	726	471	3.531	445	20202	0.69

TEST POINT	T_{amb}	P_{amb}	RH	NF	LVM	LBM	PNL (FULL SIZE, 2400 FT SIDE LINE), dB ANGLE RELATIVE TO INLET, DEGREES							OAPWL
	DEG.K	Pascal	%	dB			50	60	70	90	120	130	140	dB
5001	299.0	99325.	70	-5.1	1.49	-10.00	79.4	81.6	84.4	90.3	91.4	88.1	85.8	164.8
5002	301.5	99289.	53	-5.2	1.48	-10.00	84.5	85.1	86.1	90.1	89.9	84.9	81.3	163.7
5003	299.0	99428.	70	-5.5	2.06	-2.73	83.0	85.9	88.7	94.0	95.1	93.4	90.9	169.3
5204	301.5	99393.	53	-5.5	2.05	-2.72	84.9	87.8	90.2	94.4	93.5	90.9	87.8	168.8
5004	301.5	99225.	53	-5.6	2.06	-2.68	87.8	89.6	90.8	94.0	94.4	90.7	87.1	168.6
5005	299.0	99212.	70	-6.3	2.46	-1.28	89.1	92.2	95.4	99.0	98.5	97.6	95.0	174.3
5006	301.2	99235.	78	-6.4	2.48	-1.25	91.4	93.7	94.3	97.2	97.0	94.1	91.0	171.6
5105	299.0	99287.	70	-9.2	1.33	-1.20	91.9	94.3	96.3	98.9	96.6	92.8	90.7	174.6
5106	301.5	99349.	53	-9.1	1.39	-1.18	95.5	97.5	99.0	100.0	95.7	90.3	86.1	175.8
5007	299.0	99320.	70	-6.8	2.81	-0.59	94.0	96.2	98.2	101.7	102.6	102.0	100.2	178.0
5008	301.2	99268.	78	-6.9	2.80	-0.59	97.7	98.9	99.8	101.9	101.2	98.0	95.6	176.2
5009	299.0	99253.	70	-7.9	3.04	0.11	96.5	98.5	100.7	103.8	105.7	105.5	106.2	182.1
5210	301.5	99455.	53	-7.9	3.07	0.11	98.0	100.3	102.2	104.6	105.2	103.6	103.4	181.4
5010	301.2	99298.	78	-7.9	3.05	0.11	99.5	100.7	101.6	103.6	104.2	101.6	99.4	178.7
5109	299.0	99480.	70	-9.5	2.13	-0.07	96.1	98.5	100.8	102.6	101.3	100.7	99.6	178.5
5110	301.5	99376.	53	-9.5	2.12	-0.10	98.2	99.4	100.9	102.8	98.8	95.2	92.0	177.8
5011	299.0	99251.	70	-7.1	3.07	-0.23	94.1	96.5	98.8	102.1	104.7	104.9	104.7	180.4
5012	301.2	99253.	78	-7.2	3.06	-0.22	98.1	99.0	100.4	102.4	102.2	100.7	98.2	177.3
5013	299.0	99324.	70	-8.4	3.20	0.43	96.7	98.9	101.1	104.0	106.9	107.7	109.5	184.2
5014	299.0	99386.	70	-8.4	3.21	0.43	100.4	101.8	102.3	104.5	105.6	104.0	102.9	180.4

TABLES 3-14 TEST MATRICES FOR TE-5; BASELINE NOZZLE WITH TREATED PLUG, T1, AND TREATED EJECTOR, T1, OF NOMINAL LENGTH, L1, AT NOMINAL SPACING, S1. (ENGLISH UNITS)

NOZZLE - MODEL TEO5 AREA [MODEL SIZE - INNER = 4.75 , OUTER = 22.75 ; FULL SIZE - TOTAL = 1400.00] SQ.IN.

TEST POINT	V_{ac} FT/SEC	P_r^o	T_T^o DEG R	V_j^o FT/SEC	W^o LB/SEC	P_r^i	T_T^i DEG R	V_j^i FT/SEC	W^i LB/SEC	P_r^{mix}	T_T^{mix} DEG R	V_j^{mix} FT/SEC	F LB	V_j^i/V_j^o
5001	0	1.888	1448	1705	435.5	1.843	785	1229	121.7	1.864	1303	1601	27735	0.72
5002	400	1.898	1440	1707	438.9	1.856	800	1248	121.4	1.875	1301	1607	27992	0.73
5003	0	2.231	1549	1961	497.4	2.201	783	1377	145.7	2.195	1375	1829	36563	0.70
5204	200	2.234	1545	1960	498.4	2.200	795	1388	144.5	2.198	1376	1831	36598	0.71
5004	400	2.240	1540	1960	499.7	2.207	799	1394	144.4	2.205	1373	1833	36703	0.71
5005	0	2.574	1626	2163	558.0	2.605	779	1496	172.6	2.529	1426	2005	45541	0.69
5006	400	2.584	1632	2170	559.3	2.610	805	1523	170.1	2.542	1439	2019	45782	0.70
5105	0	2.608	833	1549	801.4	2.607	808	1524	169.7	2.608	829	1544	46624	0.98
5106	400	2.615	867	1582	788.2	2.615	803	1522	170.9	2.615	855	1571	46840	0.96
5007	0	2.871	1739	2347	601.6	2.911	830	1619	187.1	2.814	1523	2174	53299	0.69
5008	400	2.872	1735	2344	602.2	2.910	836	1626	186.2	2.816	1522	2174	53286	0.69
5009	0	3.359	1700	2461	711.6	3.222	839	1692	205.7	3.260	1507	2288	65247	0.69
5210	200	3.356	1740	2490	703.8	3.210	857	1708	203.3	3.255	1542	2314	65259	0.69
5010	400	3.361	1721	2477	707.8	3.214	858	1710	203.0	3.262	1528	2305	65281	0.69
5109	0	3.222	1043	1887	884.5	3.083	903	1728	190.1	3.195	1018	1858	62079	0.92
5110	400	3.193	1043	1881	875.3	3.082	938	1761	186.4	3.172	1025	1859	61375	0.94
5011	0	3.355	1723	2476	705.9	1.806	855	1263	114.1	3.062	1602	2307	58816	0.51
5012	400	3.361	1719	2475	708.0	1.809	862	1270	113.8	3.069	1600	2308	58965	0.51
5013	0	3.655	1729	2553	768.1	3.412	863	1751	215.0	3.530	1539	2377	72647	0.69
5014	400	3.652	1735	2557	766.7	3.418	872	1761	214.4	3.531	1546	2383	72667	0.69

TEST POINT	T_{amb} DEG R	P_{amb} PSIA	RH %	NF dB	LVM	LBM	PNL (FULL SIZE, 2400 FT SIDE LINE), dB ANGLE RELATIVE TO INLET, DEGREES 50	60	70	90	120	130	140	OAPWL dB
5001	538.2	14.41	70	-5.1	1.49	-10.00	79.4	81.6	84.4	90.3	91.4	88.1	85.8	164.8
5002	542.7	14.40	53	-5.2	1.48	-10.00	84.5	85.1	86.1	90.1	89.9	84.9	81.3	163.7
5003	538.2	14.42	70	-5.5	2.06	-2.73	83.0	85.9	88.7	94.0	95.1	93.4	90.9	169.3
5204	542.7	14.42	53	-5.5	2.05	-2.72	84.9	87.8	90.2	94.4	93.5	90.9	87.8	168.8
5004	542.7	14.39	53	-5.6	2.06	-2.68	87.8	89.6	90.8	94.0	94.4	90.7	87.1	168.6
5005	538.2	14.39	70	-6.3	2.46	-1.28	89.1	92.2	95.4	99.0	98.5	97.6	95.0	174.3
5006	542.2	14.39	78	-6.4	2.48	-1.25	91.4	93.7	94.3	97.2	97.0	94.1	91.0	171.6
5105	538.2	14.40	70	-9.2	1.33	-1.20	91.9	94.3	96.3	98.9	96.6	92.8	90.7	174.6
5106	542.7	14.41	53	-9.1	1.39	-1.18	95.5	97.5	99.0	100.0	95.7	90.3	86.1	175.8
5007	538.2	14.41	70	-6.8	2.81	-0.59	94.0	96.2	98.2	101.7	102.6	102.0	100.2	178.0
5008	542.2	14.40	78	-6.9	2.80	-0.59	97.7	98.9	99.8	101.9	101.2	98.0	95.6	176.2
5009	538.2	14.40	70	-7.9	3.04	0.11	96.5	98.5	100.7	103.8	105.7	105.5	106.2	182.1
5210	542.7	14.42	53	-7.9	3.07	0.11	98.0	100.3	102.2	104.6	105.2	103.6	103.4	181.4
5010	542.2	14.40	78	-7.9	3.05	0.11	99.5	100.7	101.6	103.6	104.2	101.6	99.4	178.7
5109	538.2	14.43	70	-9.5	2.13	-0.07	96.1	98.5	100.8	102.6	101.3	100.7	99.6	178.5
5110	542.7	14.41	53	-9.5	2.12	-0.10	98.2	99.4	100.9	102.8	98.8	95.2	92.0	177.8
5011	538.2	14.40	70	-7.1	3.07	-0.23	94.1	96.5	98.8	102.1	104.7	104.9	104.7	180.4
5012	542.2	14.40	78	-7.2	3.06	-0.22	98.1	99.0	100.4	102.4	102.2	100.7	98.2	177.3
5013	538.2	14.41	70	-8.4	3.20	0.43	96.7	98.9	101.1	104.0	106.9	107.7	109.5	184.2
5014	538.2	14.41	70	-8.4	3.21	0.43	100.4	101.8	102.3	104.5	105.6	104.0	102.9	180.4

TABLES 3-15 TEST MATRICES FOR TE-6; BASELINE NOZZLE WITH TREATED PLUG, T2; NO EJECTOR. (INTERNATIONAL UNITS)

************** S.I.UNITS ***************

NOZZLE - MODEL AX. AREA [MODEL SIZE - INNER =0.0031 , OUTER = 0.0147 ; FULL SIZE - TOTAL = 0.9031] sq.m.

TEST POINT	V_{ac}	V_j^o	T_T^o	P_r^o	$\dot{W}^o$	F^o	V_j^i	T_T^i	P_r^i	$\dot{W}^i$	F^i	V_j^{mix}	T_T^{mix}	P_r^{mix}	$\dot{W}^T$	F^T	V_j^i/V_j^o
	m/s	m/s	°K		kg/s	N	m/s	°K		kg/s	N	m/s	°K		kg/s	N	
6001	0	509	778	1.882	198.8	6334	375	436	1.845	54.8	1285	480	386	1.861	253	7620	0.74
6002	121	520	800	1.899	198.4	6457	380	446	1.852	54.6	1298	490	397	1.876	253	7755	0.73
6003	0	591	841	2.234	226.4	8370	422	439	2.201	65.1	1719	553	412	2.200	291	10089	0.71
6204	60	606	877	2.251	224.4	8513	433	459	2.214	64.5	1745	568	430	2.216	288	10258	0.71
6004	121	598	851	2.259	228.6	8553	425	446	2.203	65.0	1729	560	417	2.222	293	10282	0.71
6005	0	658	903	2.573	251.3	10351	465	451	2.599	76.0	2209	613	438	2.533	327	12560	0.71
6006	121	661	902	2.598	255.1	10547	467	453	2.606	76.3	2229	616	438	2.555	331	12776	0.71
6105	0	476	469	2.625	360.6	10746	467	452	2.614	76.3	2228	475	256	2.623	436	12974	0.98
6106	121	478	467	2.664	367.9	11011	464	448	2.610	76.8	2231	476	254	2.654	444	13242	0.97
6007	0	708	949	2.870	273.3	12107	496	467	2.900	83.3	2585	659	459	2.817	356	14693	0.70
6008	121	718	962	2.920	276.7	12429	498	469	2.909	83.6	2602	667	465	2.856	360	15032	0.69
6009	0	757	954	3.398	322.3	15247	525	484	3.210	90.5	2971	706	466	3.296	412	18219	0.69
6210	60	756	957	3.371	320.6	15157	524	483	3.217	91.3	2992	705	467	3.274	411	18149	0.69
6010	121	754	952	3.373	321.7	15168	526	486	3.213	90.9	2989	704	466	3.277	412	18158	0.70
6109	0	549	506	3.430	453.3	15571	523	480	3.207	90.8	2967	545	275	3.391	544	18538	0.95
6110	121	563	524	3.505	457.4	16100	523	480	3.218	91.5	2995	556	283	3.455	548	19096	0.93
6011	0	754	950	3.392	322.2	15204	386	483	1.793	50.5	1218	704	486	3.095	372	16423	0.51
6012	121	760	961	3.403	323.0	15346	387	480	1.809	51.4	1246	709	491	3.104	374	16592	0.51
6013	0	775	951	3.667	348.5	16882	548	506	3.409	94.0	3224	726	470	3.555	442	20107	0.71
6014	121	780	958	3.700	352.3	17180	539	488	3.419	96.6	3255	728	470	3.573	448	20435	0.69

TEST POINT	T_{amb}	P_{amb}	RH	NF	LVM	LBM	PNL (FULL SIZE, 2400 FT SIDE LINE), dB ANGLE RELATIVE TO INLET, DEGREES							OAPWL
	DEG.K	Pascal	%	dB			50	60	70	90	120	130	140	dB
6001	279.3	98552.	89	-4.8	1.57	-10.00	86.3	89.8	91.5	95.1	99.8	97.2	94.8	171.9
6002	285.1	98878.	62	-4.8	1.61	-10.00	90.4	93.0	92.9	94.5	97.3	92.0	87.7	170.3
6003	279.3	98521.	89	-5.1	2.18	-2.72	91.2	94.4	95.4	98.6	102.8	100.8	98.7	175.6
6204	284.8	99074.	76	-5.1	2.25	-2.62	92.0	95.8	96.8	99.0	102.8	98.6	95.7	176.7
6004	285.1	98918.	62	-5.3	2.19	-2.59	94.0	96.9	96.7	98.5	101.1	97.3	93.6	174.8
6005	279.3	98547.	89	-6.0	2.63	-1.29	95.2	98.4	99.2	101.1	104.7	103.2	101.1	178.2
6006	284.8	99000.	76	-6.1	2.61	-1.22	97.9	100.5	100.6	101.9	104.0	100.5	97.1	178.6
6105	279.3	98554.	89	-8.8	1.52	-1.16	94.5	93.6	98.7	100.1	100.6	98.6	96.5	175.6
6106	285.1	98876.	62	-9.0	1.48	-1.08	98.2	100.1	100.2	100.7	100.5	95.6	91.2	177.1
6007	279.3	98592.	89	-6.6	2.94	-0.59	97.2	100.6	101.3	103.1	106.5	105.0	103.0	180.0
6008	284.8	98827.	76	-6.7	2.95	-0.51	100.2	103.3	103.2	103.7	106.5	102.8	99.9	180.9
6009	279.3	98483.	89	-7.6	3.24	0.15	98.9	102.0	103.2	105.2	107.9	106.6	105.8	182.1
6210	284.8	98928.	76	-7.7	3.19	0.13	99.7	103.0	103.9	105.2	107.5	105.6	103.1	182.7
6010	284.8	98955.	76	-7.7	3.18	0.13	101.3	104.0	104.7	105.1	107.6	104.7	101.2	182.1
6109	279.3	98493.	89	-10.1	2.12	0.18	98.7	101.7	102.3	104.2	104.4	102.7	100.7	179.6
6110	285.1	98937.	62	-10.2	2.16	0.26	101.7	103.5	103.1	103.6	104.6	100.5	96.8	180.6
6011	279.3	98411.	89	-6.9	3.23	-0.18	98.5	101.9	103.2	105.1	107.6	106.2	104.7	181.4
6012	284.8	98936.	76	-7.0	3.21	-0.17	101.9	104.3	104.2	105.0	108.0	104.4	101.2	182.2
6013	279.3	98513.	89	-8.1	3.37	0.44	99.7	102.7	103.7	105.8	108.7	107.8	108.1	183.3
6014	284.8	99095..	76	-8.3	3.33	0.47	102.3	104.4	104.6	105.7	108.6	105.3	102.5	182.7

TABLES 3-16 TEST MATRICES FOR TE-6; BASELINE NOZZLE WITH TREATED PLUG, T2; NO EJECTOR. (ENGLISH UNITS)

NOZZLE - MODEL AX. AREA [MODEL SIZE - INNER = 4.75 , OUTER = 22.75 ; FULL SIZE - TOTAL = 1400.00] SQ.IN.

TEST POINT	V_{ac} FT/SEC	P_r^o	T_T^o DEG R	V_j^o FT/SEC	W^o LB/SEC	P_r^i	T_T^i DEG R	V_j^i FT/SEC	W^i LB/SEC	P_r^{mix}	T_T^{mix} DEG R	V_j^{mix} FT/SEC	F LB	V_j^i/V_j^o
6001	0	1.882	1401	1673	438.2	1.845	785	1230	120.9	1.861	1268	1577	27410	0.74
6002	400	1.899	1440	1708	437.5	1.852	803	1248	120.4	1.876	1302	1608	27896	0.73
6003	0	2.234	1514	1940	499.2	2.201	791	1385	143.6	2.200	1352	1816	36291	0.71
6204	200	2.251	1580	1991	494.8	2.214	827	1421	142.2	2.216	1411	1864	36901	0.71
6004	400	2.259	1532	1964	504.0	2.203	804	1397	143.2	2.222	1370	1838	36987	0.71
6005	0	2.573	1626	2162	554.1	2.599	812	1526	167.5	2.533	1437	2014	45181	0.71
6006	400	2.598	1624	2170	562.4	2.606	816	1532	168.3	2.555	1438	2023	45956	0.71
6105	0	2.625	845	1564	795.0	2.614	814	1532	168.3	2.623	839	1558	46668	0.98
6106	400	2.664	842	1571	811.1	2.610	807	1525	169.3	2.654	835	1563	47633	0.97
6007	0	2.870	1709	2326	602.5	2.900	841	1628	183.7	2.817	1506	2162	52850	0.70
6008	400	2.920	1732	2358	610.0	2.909	845	1634	184.3	2.856	1526	2190	54071	0.69
6009	0	3.398	1718	2484	710.5	3.210	871	1722	199.6	3.296	1532	2316	65534	0.69
6210	200	3.371	1723	2481	706.9	3.217	869	1721	201.2	3.274	1534	2313	65284	0.69
6010	400	3.373	1714	2475	709.3	3.213	875	1727	200.3	3.277	1529	2310	65315	0.70
6109	0	3.430	912	1803	999.3	3.207	865	1715	200.1	3.391	904	1788	66682	0.95
6110	400	3.505	944	1848	1008.4	3.218	865	1718	201.7	3.455	930	1826	68688	0.93
6011	0	3.392	1710	2477	710.4	1.793	869	1267	111.3	3.095	1596	2312	59073	0.51
6012	400	3.403	1730	2494	712.0	1.809	865	1272	113.3	3.104	1611	2326	59682	0.51
6013	0	3.667	1712	2543	768.3	3.409	912	1799	207.3	3.555	1542	2385	72324	0.71
6014	400	3.700	1726	2560	776.6	3.419	879	1769	212.9	3.573	1543	2390	73507	0.69

TEST POINT	T_{amb} DEG R	P_{amb} PSIA	RH %	NF dB	LVM	LBM	PNL (FULL SIZE, 2400 FT SIDE LINE), dB ANGLE RELATIVE TO INLET, DEGREES 50	60	70	90	120	130	140	OAPWL dB
6001	502.7	14.29	89	-4.8	1.57	-10.00	86.3	89.8	91.5	95.1	99.8	97.2	94.8	171.9
6002	513.2	14.34	62	-4.8	1.61	-10.00	90.4	93.0	92.9	94.5	97.3	92.0	87.7	170.3
6003	502.7	14.29	89	-5.1	2.18	-2.72	91.2	94.4	95.4	98.6	102.8	100.8	98.7	175.6
6204	512.7	14.37	76	-5.1	2.25	-2.62	92.0	95.8	96.8	99.0	102.8	98.6	95.7	176.7
6004	513.2	14.35	62	-5.3	2.19	-2.59	94.0	96.9	96.7	98.5	101.1	97.3	93.6	174.8
6005	502.7	14.29	89	-6.0	2.63	-1.29	95.2	98.4	99.2	101.1	104.7	103.2	101.1	178.2
6006	512.7	14.36	76	-6.1	2.61	-1.22	97.9	100.5	100.6	101.9	104.0	100.5	97.1	178.6
6105	502.7	14.29	89	-8.8	1.52	-1.16	94.5	93.6	98.7	100.1	100.6	98.6	96.5	175.6
6106	513.2	14.34	62	-9.0	1.48	-1.08	98.2	100.1	100.2	100.7	100.5	95.6	91.2	177.1
6007	502.7	14.30	89	-6.6	2.94	-0.59	97.2	100.6	101.3	103.1	106.5	105.0	103.0	180.0
6008	512.7	14.33	76	-6.7	2.95	-0.51	100.2	103.3	103.2	103.7	106.5	102.8	99.9	180.9
6009	502.7	14.28	89	-7.6	3.24	0.15	98.9	102.0	103.2	105.2	107.9	106.6	105.8	182.1
6210	512.7	14.35	76	-7.7	3.19	0.13	99.7	103.0	103.9	105.2	107.5	105.6	103.1	182.7
6010	512.7	14.35	76	-7.7	3.18	0.13	101.3	104.0	104.7	105.1	107.6	104.7	101.2	182.1
6109	502.7	14.29	89	-10.1	2.12	0.18	98.7	101.7	102.3	104.2	104.4	102.7	100.7	179.6
6110	513.2	14.35	62	-10.2	2.16	0.26	101.7	103.5	103.1	103.6	104.6	100.5	96.8	180.6
6011	502.7	14.27	89	-6.9	3.23	-0.18	98.5	101.9	103.2	105.1	107.6	106.2	104.7	181.4
6012	512.7	14.35	76	-7.0	3.21	-0.17	101.9	104.3	104.2	105.0	108.0	104.4	101.2	182.2
6013	502.7	14.29	89	-8.1	3.37	0.44	99.7	102.7	103.7	105.8	108.7	107.8	108.1	183.3
6014	512.7	14.37	76	-8.3	3.33	0.47	102.3	104.4	104.6	105.7	108.6	105.3	102.5	182.7

TABLES 3-17 TEST MATRICES FOR TE-7; BASELINE NOZZLE WITH HARDWALL PLUG AND WITH TREATED EJECTOR, T2, OF EXTENDED LENGTH, L2, AT EXTENDED SPACING, S2. (INTERNATIONAL UNITS)

************** S.I.UNITS ***************

NOZZLE - MODEL TE07 AREA [MODEL SIZE - INNER =0.0031 , OUTER = 0.0147 ; FULL SIZE - TOTAL = 0.9031] sq.m.

TEST POINT	V_{ac}	V^o_j	T^o_T	P^o_r	$\dot{W}^o$	F^o	V^i_j	T^i_T	P^i_r	$\dot{W}^i$	F^i	V^{mix}_j	T^{mix}_T	P^{mix}_r	$\dot{W}^T$	F^T	V^i_j/V^o_j
	m/s	m/s	°K		kg/s	N	m/s	°K		kg/s	N	m/s	°K		kg/s	N	
7001	0	515	795	1.882	199.7	6433	378	440	1.853	55.7	1315	485	393	1.861	255	7749	0.73
7002	121	518	802	1.885	198.8	6441	376	440	1.844	55.3	1302	487	396	1.862	254	7743	0.73
7003	0	594	855	2.220	226.3	8410	419	434	2.196	66.4	1739	554	417	2.186	292	10150	0.71
7303	0	594	854	2.222	226.7	8421	420	437	2.189	65.9	1730	555	417	2.187	292	10151	0.71
7004	121	597	862	2.224	225.7	8431	418	434	2.191	66.3	1732	556	419	2.187	291	10163	0.70
7304	121	598	864	2.225	225.2	8421	420	439	2.188	65.6	1726	558	421	2.188	290	10147	0.70
7005	0	657	901	2.563	254.5	10451	461	443	2.601	77.9	2246	611	435	2.523	332	12697	0.70
7006	121	660	907	2.570	253.8	10473	463	448	2.596	77.2	2235	614	439	2.529	330	12709	0.70
7007	0	713	963	2.862	274.1	12219	493	461	2.904	85.2	2625	661	463	2.805	359	14845	0.69
7008	121	713	963	2.863	273.9	12217	495	466	2.897	84.4	2615	662	464	2.807	358	14832	0.69
7009	0	758	967	3.349	320.6	15195	521	478	3.202	92.4	3009	705	470	3.249	412	18205	0.69
7309	0	756	965	3.338	319.3	15105	523	483	3.201	91.7	3003	704	470	3.243	411	18109	0.69
7010	121	755	959	3.347	321.3	15163	520	476	3.201	92.3	3003	702	467	3.249	413	18166	0.69
7310	121	756	964	3.342	320.2	15150	524	483	3.204	91.9	3012	705	470	3.246	412	18162	0.69
7013	0	778	962	3.643	348.6	16959	536	485	3.407	97.3	3264	725	471	3.523	445	20223	0.69
7014	121	779	964	3.647	348.7	16983	537	487	3.403	97.0	3259	726	472	3.525	445	20243	0.69

TEST POINT	T_{amb} DEG.K	P_{amb} Pascal	RH %	NF dB	LVM	LBM	PNL (FULL SIZE, 2400 FT SIDE LINE), dB ANGLE RELATIVE TO INLET, DEGREES 50	60	70	90	120	130	140	OAPWL dB
7001	288.7	100128.	84	-5.0	1.54	-10.00	82.5	79.8	85.2	89.7	90.7	88.0	85.3	166.6
7002	286.8	99916.	66	-4.9	1.57	-10.00	86.5	86.7	86.6	89.9	91.1	85.6	81.4	165.1
7003	288.7	99984.	84	-5.3	2.12	-2.79	84.4	83.3	88.2	94.0	94.6	93.4	91.5	171.3
7303	286.8	99962.	66	-5.3	2.14	-2.79	84.9	86.7	88.4	94.0	95.2	94.0	91.6	169.9
7004	286.8	99950.	66	-5.2	2.15	-2.78	89.3	90.0	90.4	94.3	95.0	90.4	86.3	169.5
7304	286.8	99776.	66	-5.2	2.16	-2.78	89.7	90.1	90.5	94.3	95.1	90.4	86.4	169.4
7005	288.7	100075.	84	-6.2	2.54	-1.31	86.7	85.3	91.0	97.0	98.5	98.2	96.2	175.1
7006	287.6	99870.	67	-6.1	2.57	-1.29	91.8	92.4	93.1	97.8	98.4	94.2	90.8	173.5
7007	288.7	99945.	84	-6.7	2.88	-0.60	89.2	91.3	93.6	99.4	101.3	101.1	100.3	178.3
7008	287.6	99882.	67	-6.7	2.90	-0.61	93.2	94.2	95.0	99.6	100.6	97.3	94.3	175.3
7009	288.7	100095.	84	-7.7	3.16	0.10	92.5	94.2	96.0	101.4	104.6	104.7	106.2	181.8
7309	286.8	99922.	66	-7.6	3.17	0.09	92.8	94.4	96.1	101.5	105.0	105.2	105.8	181.2
7010	288.7	99946.	84	-7.7	3.15	0.10	95.2	96.7	97.4	101.6	103.0	100.6	98.2	178.9
7310	286.8	100073.	66	-7.7	3.17	0.09	95.9	96.9	97.9	101.5	102.7	101.1	98.6	177.5
7013	288.7	99838.	84	-8.3	3.28	0.42	94.5	96.2	97.5	102.1	105.5	106.0	108.2	183.2
7014	287.6	99851.	67	-8.2	3.30	0.42	96.5	97.9	98.5	102.3	104.5	102.6	101.1	179.4

TABLES 3-18 TEST MATRICES FOR TE-7; BASELINE NOZZLE WITH HARDWALL PLUG AND WITH TREATED EJECTOR, T2, OF EXTENDED LENGTH, L2, AT EXTENDED SPACING, S2. (ENGLISH UNITS)

NOZZLE - MODEL TE07 AREA [MODEL SIZE - INNER = 4.75 , OUTER = 22.75 ; FULL SIZE - TOTAL = 1400.00] SQ.IN.

TEST POINT	V_{ac} FT/SEC	P^o_r	T^o_T DEG R	V^o_j FT/SEC	W^o LB/SEC	P^i_r	T^i_T DEG R	V^i_j FT/SEC	W^i LB/SEC	P^{mix}_r	T^{mix}_T DEG R	V^{mix}_j FT/SEC	F LB	V^i_j/V^o_j
7001	0	1.882	1432	1691	440.2	1.853	792	1240	122.8	1.861	1292	1593	27874	0.73
7002	400	1.885	1444	1701	438.2	1.844	792	1235	122.0	1.862	1301	1599	27853	0.73
7003	0	2.220	1540	1951	499.0	2.196	782	1375	146.4	2.186	1368	1820	36510	0.71
7303	0	2.222	1538	1950	499.8	2.189	788	1378	145.3	2.187	1369	1821	36515	0.71
7004	400	2.224	1553	1961	497.6	2.191	781	1372	146.1	2.187	1377	1827	36559	0.70
7304	400	2.225	1556	1963	496.4	2.188	791	1380	144.7	2.188	1383	1831	36501	0.70
7005	0	2.563	1623	2156	561.0	2.601	798	1514	171.7	2.523	1430	2005	45673	0.70
7006	400	2.570	1634	2166	559.5	2.596	807	1521	170.1	2.529	1441	2016	45716	0.70
7007	0	2.862	1734	2340	604.2	2.904	830	1618	187.8	2.805	1519	2169	53397	0.69
7008	400	2.863	1735	2342	603.8	2.897	840	1626	186.1	2.807	1524	2173	53353	0.69
7009	0	3.349	1741	2488	706.7	3.202	861	1711	203.6	3.249	1544	2314	65483	0.69
7309	0	3.338	1738	2483	703.9	3.201	869	1718	202.2	3.243	1543	2312	65138	0.69
7010	400	3.347	1727	2478	708.3	3.201	858	1707	203.5	3.249	1533	2305	65345	0.69
7310	400	3.342	1736	2483	706.0	3.204	869	1719	202.7	3.246	1543	2313	65328	0.69
7013	0	3.643	1733	2554	768.6	3.407	874	1761	214.5	3.523	1545	2380	72744	0.69
7014	400	3.647	1736	2557	768.8	3.403	877	1764	213.8	3.525	1549	2384	72816	0.69

TEST POINT	T_{amb} DEG R	P_{amb} PSIA	RH %	NF dB	LVM	LBM	PNL (FULL SIZE, 2400 FT SIDE LINE), dB ANGLE RELATIVE TO INLET, DEGREES 50	60	70	90	120	130	140	OAPWL dB
7001	519.7	14.52	84	-5.0	1.54	-10.00	82.5	79.8	85.2	89.7	90.7	88.0	85.3	166.6
7002	516.2	14.49	66	-4.9	1.57	-10.00	86.5	86.7	86.6	89.9	91.1	85.6	81.4	165.1
7003	519.7	14.50	84	-5.3	2.12	-2.79	84.4	83.3	88.2	94.0	94.6	93.4	91.5	171.3
7303	516.2	14.50	66	-5.3	2.14	-2.79	84.9	86.7	88.4	94.0	95.2	94.0	91.6	169.9
7004	516.2	14.50	66	-5.2	2.15	-2.78	89.3	90.0	90.4	94.3	95.0	90.4	86.3	169.5
7304	516.2	14.47	66	-5.2	2.16	-2.78	89.7	90.1	90.5	94.3	95.1	90.4	86.4	169.4
7005	519.7	14.51	84	-6.2	2.54	-1.31	86.7	85.3	91.0	97.0	98.5	98.2	96.2	175.1
7006	517.7	14.48	67	-6.1	2.57	-1.29	91.8	92.4	93.1	97.8	98.4	94.2	90.8	173.5
7007	519.7	14.50	84	-6.7	2.88	-0.60	89.2	91.3	93.6	99.4	101.3	101.1	100.3	178.3
7008	517.7	14.49	67	-6.7	2.90	-0.61	93.2	94.2	95.0	99.6	100.6	97.3	94.3	175.3
7009	519.7	14.52	84	-7.7	3.16	0.10	92.5	94.2	96.0	101.4	104.6	104.7	106.2	181.8
7309	516.2	14.49	66	-7.6	3.17	0.09	92.8	94.4	96.1	101.5	105.0	105.2	105.8	181.2
7010	519.7	14.50	84	-7.7	3.15	0.10	95.2	96.7	97.4	101.6	103.0	100.6	98.2	178.9
7310	516.2	14.51	66	-7.7	3.17	0.09	95.9	96.9	97.9	101.5	102.7	101.1	98.6	177.5
7013	519.7	14.48	84	-8.3	3.28	0.42	94.5	96.2	97.5	102.1	105.5	106.0	108.2	183.2
7014	517.7	14.48	67	-8.2	3.30	0.42	96.5	97.9	98.5	102.3	104.5	102.6	101.1	179.4

OF EXTENDED LENGTH, L2, AT EXTENDED SPACING, S2. (INTERNATIONAL UNITS)

************** S.I.UNITS ***************

NOZZLE - MODEL TE08 AREA [MODEL SIZE - INNER =0.0031 , OUTER = 0.0147 ; FULL SIZE - TOTAL = 0.9031] sq.m.

TEST POINT	V_{ac}	V_j^o	T_T^o	P_r^o	$\dot{W}^o$	F^o	V_j^i	T_T^i	P_r^i	W^i	F^i	V_j^{mix}	T_T^{mix}	P_r^{mix}	W^T	F^T	V_j^i/V_j^o
	m/s	m/s	°K		kg/s	N	m/s	°K		kg/s	N	m/s	°K		kg/s	N	
8001	0	521	808	1.890	197.4	6435	383	455	1.847	54.2	1299	491	401	1.868	251	7735	0.74
8002	121	517	797	1.888	198.7	6430	383	452	1.852	54.6	1306	488	396	1.868	253	7736	0.74
8003	0	599	865	2.229	224.8	8419	430	456	2.206	64.8	1742	561	424	2.198	289	10162	0.72
8204	60	596	860	2.222	225.0	8390	431	460	2.197	64.3	1733	560	423	2.192	289	10124	0.72
8004	121	598	864	2.225	224.6	8399	431	459	2.202	64.4	1737	561	424	2.195	288	10136	0.72
8005	0	659	907	2.564	252.3	10398	469	459	2.604	76.2	2237	615	440	2.528	328	12636	0.71
8006	121	661	909	2.572	252.6	10436	471	463	2.601	75.7	2232	617	442	2.534	328	12669	0.71
8105	0	472	463	2.608	364.0	10745	468	454	2.611	76.7	2245	471	253	2.609	440	12991	0.99
8106	121	474	466	2.612	362.8	10753	469	459	2.600	76.0	2228	473	255	2.610	438	12982	0.99
8007	0	712	962	2.859	272.8	12152	501	476	2.904	83.5	2614	663	465	2.809	356	14766	0.70
8008	121	714	966	2.864	272.2	12159	498	470	2.904	83.8	2610	663	466	2.810	356	14770	0.70
8009	0	758	965	3.352	319.0	15113	530	494	3.213	90.5	3003	707	472	3.260	409	18116	0.70
8210	60	759	968	3.353	318.8	15133	528	491	3.211	90.9	3003	708	473	3.258	409	18137	0.70
8010	121	758	967	3.352	318.3	15097	528	490	3.205	90.6	2990	707	472	3.257	408	18088	0.70
8109	0	543	497	3.417	460.4	15649	527	487	3.222	91.5	3015	541	271	3.384	551	18665	0.97
8110	121	544	498	3.424	460.4	15683	529	492	3.212	90.7	3001	542	273	3.387	551	18685	0.97
8011	0	755	959	3.351	319.8	15102	391	494	1.800	50.6	1239	705	491	3.062	370	16342	0.52
8012	121	759	967	3.360	319.3	15154	391	494	1.797	50.5	1236	709	495	3.069	369	16390	0.52
8013	0	779	965	3.640	346.8	16885	547	504	3.412	95.3	3261	729	475	3.528	442	20146	0.70
8014	121	778	962	3.649	347.7	16917	541	493	3.412	96.2	3254	727	472	3.532	443	20172	0.70

TEST POINT	T_{amb}	P_{amb}	RH	NF	LVM	LBM	PNL (FULL SIZE, 2400 FT SIDE LINE), dB ANGLE RELATIVE TO INLET, DEGREES							OAPWL
	DEG.K	Pascal	%	dB			50	60	70	90	120	130	140	dB
8001	287.6	99414.	89	-4.8	1.60	-10.00	82.8	83.2	84.6	88.8	90.1	88.5	85.8	164.7
8002	288.2	99478.	89	-4.9	1.57	-10.00	85.5	84.2	85.7	88.3	88.2	84.1	79.8	164.3
8003	287.6	99467.	89	-5.2	2.18	-2.74	84.6	83.4	87.9	92.5	94.5	93.9	91.3	169.3
8204	287.6	99573.	72	-5.2	2.17	-2.78	87.1	87.7	88.9	93.1	91.6	89.8	87.0	168.4
8004	287.6	99478.	72	-5.2	2.18	-2.76	88.9	88.4	89.3	92.4	93.6	89.6	86.0	168.6
8005	287.6	99518.	89	-6.1	2.58	-1.30	86.9	87.0	90.5	96.2	98.0	98.3	96.1	173.7
8006	288.2	99442.	89	-6.1	2.59	-1.29	90.8	89.8	91.5	95.4	96.0	93.8	90.2	172.0
8105	287.6	99463.	89	-9.0	1.42	-1.20	83.5	84.3	87.3	92.1	93.7	91.8	89.7	169.4
8106	287.6	99348.	72	-9.0	1.44	-1.20	87.2	86.5	88.5	92.4	94.0	88.9	83.8	170.7
8007	287.6	99504.	89	-6.6	2.90	-0.61	89.6	89.3	92.8	98.2	101.0	101.6	100.7	177.3
8008	288.2	99336.	89	-6.6	2.90	-0.60	93.1	92.3	94.6	97.8	98.9	97.2	94.0	174.5
8009	287.6	99441.	89	-7.6	3.19	0.10	92.8	92.9	95.5	100.5	104.3	105.2	105.3	181.0
8210	287.6	99538.	72	-7.6	3.19	0.11	92.8	94.5	96.8	101.0	103.1	102.7	101.8	179.1
8010	288.2	99344.	89	-7.6	3.18	0.10	95.9	95.2	97.8	100.4	101.7	100.8	98.6	177.9
8109	287.6	99457.	89	-10.4	2.02	0.17	90.3	91.3	93.7	98.0	98.2	98.3	97.0	175.6
8110	288.2	99435.	89	-10.4	2.03	0.18	92.6	92.8	94.1	97.9	98.3	94.4	90.7	176.0
8011	287.6	99390.	89	-6.9	3.17	-0.24	92.1	92.4	94.9	100.0	103.7	104.5	104.8	180.3
8012	287.6	99372.	89	-6.9	3.19	-0.22	95.2	94.6	97.2	99.7	101.6	100.3	97.7	176.5
8013	287.6	99533.	89	-8.2	3.31	0.41	94.4	94.8	97.1	101.5	105.5	106.8	108.2	182.7
8014	287.6	99376.	89	-8.2	3.30	0.42	96.4	96.2	98.2	100.8	103.3	102.9	100.9	179.2

TABLES 3-20 TEST MATRICES FOR TE-8; BASELINE NOZZLE WITH TREATED PLUG, T2, AND WITH TREATED EJECTOR, T2, OF EXTENDED LENGTH, L2, AT EXTENDED SPACING, S2. (ENGLISH UNITS)

NOZZLE - MODEL TEO8 AREA [MODEL SIZE - INNER = 4.75 , OUTER = 22.75 ; FULL SIZE - TOTAL = 1400.00] SQ.IN.

TEST POINT	V_{ac} FT/SEC	P_r^o	T_T^o DEG R	V_j^o FT/SEC	W^o LB/SEC	P_r^i	T_T^i DEG R	V_j^i FT/SEC	W^i LB/SEC	P_r^{mix}	T_T^{mix} DEG R	V_j^{mix} FT/SEC	F LB	V_j^i/V_j^o
8001	0	1.890	1455	1711	435.3	1.847	820	1258	119.5	1.868	1318	1613	27823	0.74
8002	400	1.888	1436	1699	438.1	1.852	815	1257	120.3	1.868	1302	1603	27829	0.74
8003	0	2.229	1557	1966	495.6	2.206	820	1412	142.8	2.198	1392	1842	36555	0.72
8204	200	2.222	1549	1958	496.0	2.197	828	1415	141.7	2.192	1389	1837	36416	0.72
8004	400	2.225	1556	1963	495.1	2.202	827	1416	141.9	2.195	1393	1841	36462	0.72
8005	0	2.564	1633	2163	556.3	2.604	826	1541	168.0	2.528	1446	2018	45451	0.71
8006	400	2.572	1637	2169	556.9	2.601	834	1547	166.9	2.534	1452	2025	45572	0.71
8105	0	2.608	835	1550	802.4	2.611	818	1535	169.2	2.609	831	1547	46728	0.99
8106	400	2.612	840	1556	799.8	2.600	826	1540	167.5	2.610	837	1553	46698	0.99
8007	0	2.859	1733	2339	601.4	2.904	856	1644	184.1	2.809	1527	2175	53116	0.70
8008	400	2.864	1739	2345	600.1	2.904	846	1634	184.8	2.810	1529	2177	53127	0.70
8009	0	3.352	1738	2487	703.2	3.213	890	1741	199.6	3.260	1550	2322	65165	0.70
8210	200	3.353	1744	2492	702.8	3.211	884	1735	200.3	3.258	1553	2324	65240	0.70
8010	400	3.352	1742	2490	701.8	3.205	883	1733	199.7	3.257	1551	2322	65063	0.70
8109	0	3.417	895	1784	1015.0	3.222	876	1729	201.7	3.384	892	1775	67137	0.97
8110	400	3.424	898	1788	1015.0	3.212	886	1737	200.0	3.387	895	1779	67211	0.97
8011	0	3.351	1727	2479	705.1	1.800	889	1285	111.6	3.062	1612	2315	58782	0.52
8012	400	3.360	1741	2491	704.0	1.797	890	1284	111.4	3.069	1624	2326	58957	0.52
8013	0	3.640	1738	2556	764.5	3.412	908	1796	210.1	3.528	1558	2392	72466	0.70
8014	400	3.649	1732	2554	766.5	3.412	888	1776	212.0	3.532	1549	2385	72561	0.70

TEST POINT	T_{amb} DEG R	P_{amb} PSIA	RH %	NF dB	LVM	LBM	PNL (FULL SIZE, 2400 FT SIDE LINE), dB ANGLE RELATIVE TO INLET, DEGREES 50	60	70	90	120	130	140	OAPWL dB
8001	517.7	14.42	89	-4.8	1.60	-10.00	82.8	83.2	84.6	88.8	90.1	88.5	85.8	164.7
8002	518.7	14.43	89	-4.9	1.57	-10.00	85.5	84.2	85.7	88.3	88.2	84.1	79.8	164.3
8003	517.7	14.43	89	-5.2	2.18	-2.74	84.6	83.4	87.9	92.5	94.5	93.9	91.3	169.3
8204	517.7	14.44	72	-5.2	2.17	-2.78	87.1	87.7	88.9	93.1	91.6	89.8	87.0	168.4
8004	517.7	14.43	72	-5.2	2.18	-2.76	88.9	88.4	89.3	92.4	93.6	89.6	86.0	168.6
8005	517.7	14.43	89	-6.1	2.58	-1.30	86.9	87.0	90.5	96.2	98.0	98.3	96.1	173.7
8006	518.7	14.42	89	-6.1	2.59	-1.29	90.8	89.8	91.5	95.4	96.0	93.8	90.2	172.0
8105	517.7	14.43	89	-9.0	1.42	-1.20	83.5	84.3	87.3	92.1	93.7	91.8	89.7	169.4
8106	517.7	14.41	72	-9.0	1.44	-1.20	87.2	86.5	88.5	92.4	94.0	88.9	83.8	170.7
8007	517.7	14.43	89	-6.6	2.90	-0.61	89.6	89.3	92.8	98.2	101.0	101.6	100.7	177.3
8008	518.7	14.41	89	-6.6	2.90	-0.60	93.1	92.3	94.6	97.8	98.9	97.2	94.0	174.5
8009	517.7	14.42	89	-7.6	3.19	0.10	92.8	92.9	95.5	100.5	104.3	105.2	105.3	181.0
8210	517.7	14.44	72	-7.6	3.19	0.11	92.8	94.5	96.8	101.0	103.1	102.7	101.8	179.1
8010	518.7	14.41	89	-7.6	3.18	0.10	95.9	95.2	97.8	100.4	101.7	100.8	98.6	177.9
8109	517.7	14.42	89	-10.4	2.02	0.17	90.3	91.3	93.7	98.0	98.2	98.3	97.0	175.6
8110	518.7	14.42	89	-10.4	2.03	0.18	92.6	92.8	94.1	97.9	98.3	94.4	90.7	176.0
8011	517.7	14.42	89	-6.9	3.17	-0.24	92.1	92.4	94.9	100.0	103.7	104.5	104.8	180.3
8012	517.7	14.41	89	-6.9	3.19	-0.22	95.2	94.6	97.2	99.7	101.6	100.3	97.7	176.5
8013	517.7	14.44	89	-8.2	3.31	0.41	94.4	94.8	97.1	101.5	105.5	106.8	108.2	182.7
8014	517.7	14.41	89	-8.2	3.30	0.42	96.4	96.2	98.2	100.8	103.3	102.9	100.9	179.2

TABLES 3-21 TEST MATRICES FOR TE-9; BASELINE NOZZLE WITH TREATED PLUG, T1, AND WITH TREATED EJECTOR, T1, OF NOMINAL LENGTH, L1, AT EXTENDED SPACING, S2. (INTERNATIONAL UNITS)

************** S.I.UNITS ***************

NOZZLE - MODEL AX. AREA [MODEL SIZE - INNER =0.0031 , OUTER = 0.0147 ; FULL SIZE - TOTAL = 0.9031] sq.m.

TEST POINT	V_{ac}	V^o_j	T^o_T	P^o_r	$\dot{W}^o$	F^o	V^i_j	T^i_T	P^i_r	$\dot{W}^i$	F^i	V^{mix}_j	T^{mix}_T	P^{mix}_r	$\dot{W}^T$	F^T	V^i_j/V^o_j
	m/s	m/s	°K		kg/s	N	m/s	°K		kg/s	N	m/s	°K		kg/s	N	
9001	0	509	773	1.888	200.7	6388	383	452	1.853	54.2	1299	482	386	1.869	254	7687	0.75
9002	121	523	812	1.891	196.0	6406	380	449	1.846	54.2	1291	492	402	1.868	250	7697	0.73
9003	0	597	859	2.231	224.5	8384	420	436	2.203	65.7	1727	557	418	2.196	290	10111	0.70
9204	60	602	872	2.237	223.5	8420	425	447	2.197	64.8	1722	562	426	2.201	288	10142	0.71
9004	121	595	852	2.232	225.5	8389	423	443	2.197	65.0	1721	556	417	2.198	290	10111	0.71
9005	0	660	907	2.570	251.4	10374	463	445	2.605	76.9	2226	614	438	2.529	328	12600	0.70
9006	121	661	910	2.570	250.6	10356	468	456	2.597	75.6	2212	616	441	2.530	326	12568	0.71
9105	0	478	476	2.609	357.1	10687	455	432	2.600	77.9	2217	474	256	2.607	434	12905	0.95
9106	121	485	489	2.610	352.5	10695	465	451	2.607	76.5	2228	481	264	2.609	429	12923	0.96
9007	0	713	961	2.870	272.1	12130	493	461	2.905	84.2	2597	661	462	2.813	356	14727	0.69
9009	0	761	973	3.355	315.9	15033	519	475	3.208	91.6	2977	707	472	3.253	407	18010	0.68
9210	60	762	975	3.355	315.9	15053	524	483	3.198	90.7	2969	709	475	3.254	406	18023	0.69
9010	121	758	965	3.358	317.8	15066	516	470	3.200	91.9	2970	704	468	3.254	409	18036	0.68
9109	0	559	525	3.437	447.6	15665	530	494	3.209	89.9	2980	555	285	3.398	537	18645	0.95
9110	121	557	522	3.415	446.7	15552	525	484	3.207	90.8	2980	551	282	3.379	537	18533	0.94
9011	0	759	968	3.353	316.8	15030	383	473	1.802	51.5	1235	706	493	3.058	368	16266	0.51
9012	121	758	967	3.351	316.8	15025	381	469	1.797	51.6	1229	705	492	3.055	368	16255	0.50
9013	0	778	962	3.650	345.9	16834	534	481	3.400	96.5	3224	725	470	3.525	442	20058	0.69
9014	121	778	961	3.649	345.7	16815	532	477	3.405	97.0	3226	724	469	3.523	442	20042	0.68

TEST POINT	T_{amb} DEG.K	P_{amb} Pascal	RH %	NF dB	LVM	LBM	PNL (FULL SIZE, 2400 FT SIDE LINE), dB ANGLE RELATIVE TO INLET, DEGREES 50	60	70	90	120	130	140	OAPWL dB
9001	302.6	98840.	84	-5.3	1.41	-10.00	81.2	82.7	84.7	89.0	90.2	86.7	84.3	163.2
9002	303.7	98885.	67	-5.1	1.49	-10.00	85.5	85.9	86.7	89.1	89.1	81.7	79.7	162.8
9003	302.6	98865.	84	-5.5	2.04	-2.73	84.0	85.8	88.3	93.3	94.5	92.8	90.4	168.2
9204	303.4	98927.	79	-5.5	2.07	-2.70	85.5	87.4	89.5	93.7	93.7	87.4	86.7	167.0
9004	303.7	98852.	67	-5.6	2.03	-2.73	87.8	88.7	90.1	93.0	93.3	87.7	85.3	166.8
9005	302.6	98927.	84	-6.3	2.46	-1.29	87.0	89.3	92.2	96.8	98.0	97.0	95.1	172.5
9006	303.7	98772.	67	-6.3	2.47	-1.29	91.8	92.7	94.1	97.2	97.1	92.0	90.2	171.2
9105	302.6	98876.	84	-9.1	1.34	-1.20	89.6	91.7	94.4	96.6	94.0	91.2	89.6	170.7
9106	303.4	98903.	79	-9.0	1.40	-1.20	91.9	93.7	94.9	96.7	93.7	87.0	84.1	170.9
9007	302.6	98821.	84	-6.9	2.78	-0.59	90.1	92.7	95.8	99.0	100.9	100.1	98.7	176.0
9009	302.6	98774.	84	-7.8	3.07	0.11	95.0	97.9	100.2	102.6	104.4	104.4	103.7	180.7
9210	303.4	98929.	79	-7.8	3.08	0.10	97.5	100.1	101.9	103.5	104.0	102.6	100.4	179.9
9010	303.7	98864.	67	-7.9	3.04	0.11	96.6	99.1	100.4	102.2	103.3	100.1	97.6	177.5
9109	302.6	98803.	84	-10.4	2.02	0.19	96.1	98.2	100.6	101.8	100.0	98.6	97.7	177.4
9110	303.4	98920.	79	-10.4	1.99	0.17	100.5	101.3	102.2	103.3	98.6	93.2	90.7	177.5
9011	302.6	98844.	84	-7.1	3.07	-0.23	92.6	95.0	98.2	101.5	103.8	103.5	103.1	179.1
9012	303.7	98878.	67	-7.1	3.06	-0.24	96.7	98.0	99.4	101.7	103.1	100.1	97.3	176.5
9013	302.6	98854.	84	-8.4	3.18	0.42	96.6	99.5	101.2	103.1	105.0	106.0	104.5	181.8
9014	303.7	98780.	67	-8.5	3.17	0.42	92.4	105.1	104.8	104.6	105.4	103.3	101.4	180.6

TABLE 3-22 TEST MATRICES FOR TE-9; BASELINE NOZZLE WITH TREATED PLUG, T1, AND WITH TREATED EJECTOR, T1, OF NOMINAL LENGTH, L1, AT EXTENDED SPACING, S2. (ENGLISH UNITS)

NOZZLE - MODEL AX. AREA [MODEL SIZE - INNER = 4.75 , OUTER = 22.75 ; FULL SIZE - TOTAL = 1400.00] SQ.IN.

TEST POINT	V_{ac} FT/SEC	P_r^o	T_T^o DEG R	V_j^o FT/SEC	W^o LB/SEC	P_r^i	T_T^i DEG R	V_j^i FT/SEC	W^i LB/SEC	P_r^{mix}	T_T^{mix} DEG R	V_j^{mix} FT/SEC	F LB	V_j^i/V_j^o
9001	0	1.888	1392	1671	442.4	1.853	815	1257	119.5	1.869	1269	1583	27652	0.75
9002	400	1.891	1462	1716	432.1	1.846	809	1249	119.6	1.868	1320	1614	27687	0.73
9003	0	2.231	1547	1960	495.0	2.203	785	1380	144.8	2.196	1374	1829	36372	0.70
9204	200	2.237	1570	1978	492.7	2.197	804	1395	142.8	2.201	1397	1847	36483	0.71
9004	400	2.232	1535	1953	497.2	2.197	799	1390	143.2	2.198	1370	1827	36369	0.71
9005	0	2.570	1634	2166	554.2	2.605	802	1519	169.6	2.529	1439	2014	45323	0.70
9006	400	2.570	1639	2170	552.4	2.597	822	1535	166.7	2.530	1449	2022	45208	0.71
9105	0	2.609	857	1571	787.3	2.600	778	1494	171.7	2.607	843	1557	46421	0.95
9106	400	2.610	881	1593	777.2	2.607	812	1528	168.7	2.609	868	1581	46486	0.96
9007	0	2.870	1730	2340	599.9	2.905	831	1619	185.6	2.813	1517	2169	52973	0.69
9009	0	3.355	1752	2498	696.5	3.208	855	1706	202.0	3.253	1550	2320	64783	0.68
9210	200	3.355	1756	2501	696.5	3.198	870	1719	199.9	3.254	1558	2326	64828	0.69
9010	400	3.358	1737	2488	700.7	3.200	846	1695	202.7	3.254	1537	2310	64878	0.68
9109	0	3.437	945	1837	986.7	3.209	889	1740	198.2	3.398	936	1821	67068	0.95
9110	400	3.415	940	1828	984.7	3.207	872	1723	200.2	3.379	928	1810	66663	0.94
9011	0	3.353	1743	2491	698.4	1.802	852	1259	113.6	3.058	1618	2318	58510	0.51
9012	400	3.351	1741	2489	698.5	1.797	844	1250	113.8	3.055	1615	2315	58470	0.50
9013	0	3.650	1733	2555	762.6	3.400	867	1753	212.8	3.525	1543	2380	72149	0.69
9014	400	3.649	1731	2553	762.1	3.405	859	1746	213.8	3.523	1540	2376	72092	0.68

TEST POINT	T_{amb} DEG R	P_{amb} PSIA	RH %	NF dB	LVM	LBM	PNL (FULL SIZE, 2400 FT SIDE LINE), dB ANGLE RELATIVE TO INLET, DEGREES 50	60	70	90	120	130	140	OAPWL dB
9001	544.7	14.34	84	-5.3	1.41	-10.00	81.2	82.7	84.7	89.0	90.2	86.7	84.3	163.2
9002	546.7	14.34	67	-5.1	1.49	-10.00	85.5	85.9	86.7	89.1	89.1	81.7	79.7	162.8
9003	544.7	14.34	84	-5.5	2.04	-2.73	84.0	85.8	88.3	93.3	94.5	92.8	90.4	168.2
9204	546.2	14.35	79	-5.5	2.07	-2.70	85.5	87.4	89.5	93.7	93.7	87.4	86.7	167.0
9004	546.7	14.34	67	-5.6	2.03	-2.73	87.8	88.7	90.1	93.0	93.3	87.7	85.3	166.8
9005	544.7	14.35	84	-6.3	2.46	-1.29	87.0	89.3	92.2	96.8	98.0	97.0	95.1	172.5
9006	546.7	14.33	67	-6.3	2.47	-1.29	91.8	92.7	94.1	97.2	97.1	92.0	90.2	171.2
9105	544.7	14.34	84	-9.1	1.34	-1.20	89.6	91.7	94.4	96.6	94.0	91.2	89.6	170.7
9106	546.2	14.34	79	-9.0	1.40	-1.20	91.9	93.7	94.9	96.7	93.7	87.0	84.1	170.9
9007	544.7	14.33	84	-6.9	2.78	-0.59	90.1	92.7	95.8	99.0	100.9	100.1	98.7	176.0
9009	544.7	14.33	84	-7.8	3.07	0.11	95.0	97.9	100.2	102.6	104.4	104.4	103.7	180.7
9210	546.2	14.35	79	-7.8	3.08	0.10	97.5	100.1	101.9	103.5	104.0	102.6	100.4	179.9
9010	546.7	14.34	67	-7.9	3.04	0.11	96.6	99.1	100.4	102.2	103.3	100.1	97.6	177.5
9109	544.7	14.33	84	-10.4	2.02	0.19	96.1	98.2	100.6	101.8	100.0	98.6	97.7	177.4
9110	546.2	14.35	79	-10.4	1.99	0.17	100.5	101.3	102.2	103.3	98.6	93.2	90.7	177.5
9011	544.7	14.34	84	-7.1	3.07	-0.23	92.6	95.0	98.2	101.5	103.8	103.5	103.1	179.1
9012	546.7	14.34	67	-7.1	3.06	-0.24	96.7	98.0	99.4	101.7	103.1	100.1	97.3	176.5
9013	544.7	14.34	84	-8.4	3.18	0.42	96.6	99.5	101.2	103.1	105.0	106.0	104.5	181.8
9014	546.7	14.33	67	-8.5	3.17	0.42	92.4	105.1	104.8	104.6	105.4	103.3	101.4	180.6

TABLES 3-23 TEST MATRICES FOR TE-10; BASELINE NOZZLE WITH HARDWALL PLUG AND WITH HARDWALL EJECTOR OF EXTENDED LENGTH, L2, AT EXTENDED SPACING, S2. (INTERNATIONAL UNITS)

************** S.I.UNITS ***************

NOZZLE - MODEL TE10 AREA [MODEL SIZE - INNER =0. OUTER = 0.0147 ; FULL SIZE - TOTAL = 0.9031] sq.m.

TEST POINT	V_{ac}	V^o_j	T^o_T	P^o_r	$\dot{W}^o$	F^o	V^i_j	T^i_T	P^i_r	$\dot{W}^i$	F^i	V^{mix}_j	T^{mix}_T	P^{mix}_r	$\dot{W}^T$	F^T	V^i_j/V^o_j
	m/s	m/s	°K		kg/s	N	m/s	°K		kg/s	N	m/s	°K		kg/s	N	
1	0	516	802	1.872	200.2	6457	373	431	1.852	57.0	1332	484	395	1.852	257	7790	0.72
2	121	518	806	1.877	199.3	6453	382	451	1.848	55.2	1319	488	400	1.858	254	7772	0.74
3	0	594	852	2.224	223.4	8483	422	440	2.200	66.4	1753	555	417	2.191	294	10236	0.71
4	121	594	854	2.224	229.5	8529	423	445	2.186	66.0	1745	556	418	2.190	295	10275	0.71
5	0	656	906	2.542	256.2	10508	457	439	2.577	78.9	2255	609	436	2.501	335	12763	0.70
6	121	657	905	2.556	255.8	10515	463	448	2.591	77.9	2255	612	438	2.517	333	12770	0.70
7	0	715	968	2.867	275.1	12309	495	464	2.907	85.3	2642	663	466	2.810	360	14951	0.69
8	121	716	969	2.867	276.6	12381	494	465	2.894	85.4	2641	664	466	2.809	361	15022	0.69
9	0	757	963	3.357	322.5	15276	521	477	3.215	93.0	3033	705	469	3.258	415	18309	0.69
10	121	755	960	3.346	324.1	15301	521	479	3.195	92.8	3023	703	467	3.248	416	18325	0.69
109	0	561	528	3.421	452.3	15862	528	491	3.202	91.7	3028	555	286	3.383	544	18890	0.94
110	121	555	517	3.423	458.8	15920	528	490	3.201	91.9	3034	550	281	3.384	550	18955	0.95
13	0	775	953	3.650	352.4	17071	541	493	3.416	97.2	3290	724	468	3.535	449	20362	0.70
14	121	774	953	3.651	352.7	17080	543	497	3.416	96.8	3290	725	469	3.537	449	20370	0.70
403	0	598	866	2.225	274.6	10277	0	255	1.000	0.0	0	598	475	2.225	274	10277	0.00
409	0	760	972	3.354	389.5	18522	0	255	1.000	0.0	0	760	533	3.354	389	18522	0.00

TEST POINT	T_{amb}	P_{amb}	RH	NF	LVM	LBM	PNL (FULL SIZE, 2400 FT SIDE LINE), dB ANGLE RELATIVE TO INLET, DEGREES							OAPWL
	DEG.K	Pascal	%	dB			50	60	70	90	120	130	140	dB
1	277.6	101388.	92	-4.7	1.62	-10.00	84.0	85.0	86.9	93.3	92.6	89.1	86.0	166.6
2	288.7	100857.	78	-4.9	1.57	-10.00	87.8	87.3	88.2	92.6	91.5	85.9	81.8	167.5
3	277.6	100526.	92	-5.1	2.21	-2.77	86.0	87.7	90.4	96.8	96.1	94.1	91.6	170.7
4	277.6	101104.	92	-5.1	2.22	-2.78	91.3	91.6	93.0	96.4	95.3	90.6	86.5	169.9
5	277.6	101824.	92	-6.0	2.61	-1.37	88.4	90.4	93.0	99.8	99.6	99.0	97.2	174.6
6	277.6	101070.	92	-6.0	2.63	-1.33	93.0	93.7	94.7	99.7	98.3	94.8	91.2	173.0
7	277.6	100421.	92	-6.5	2.98	-0.60	90.7	92.5	95.1	101.3	102.5	101.9	100.6	177.7
8	277.6	101006.	92	-6.6	2.98	-0.60	94.5	95.4	96.6	101.0	100.6	97.8	94.7	174.9
9	277.6	100301.	92	-7.6	3.25	0.11	93.5	94.9	97.1	102.9	105.0	105.1	106.3	181.2
10	277.6	100887.	92	-7.6	3.23	0.10	96.6	97.7	99.0	102.7	103.2	101.3	98.7	177.3
109	288.7	100691.	78	-10.2	2.13	0.17	91.2	92.9	95.4	100.6	99.2	98.5	97.8	177.9
110	288.7	100979.	78	-10.3	2.09	0.17	95.1	96.0	97.5	101.5	100.4	96.2	92.5	178.7
13	277.6	100264.	92	-8.1	3.36	0.42	95.4	96.6	98.4	103.7	106.3	106.7	108.3	182.8
14	277.6	100273.	92	-8.1	3.37	0.42	98.3	98.8	100.1	103.7	104.7	102.7	100.9	178.7
403	288.7	100768.	78	-4.7	2.45	-2.74	85.3	86.9	89.2	96.3	95.8	93.6	91.7	172.2
409	288.7	100756.	78	-7.2	3.49	0.14	92.7	94.7	97.3	102.9	104.7	104.7	104.9	181.9

C-2

TABLES 3-24 TEST MATRICES FOR TE-10; BASELINE NOZZLE WITH HARDWALL PLUG AND WITH HARDWALL EJECTOR OF EXTENDED LENGTH, L2, AT EXTENDED SPACING, S2. (ENGLISH UNITS)

NOZZLE - MODEL TE10 AREA [MODEL SIZE - INNER = 0. , OUTER = 22.75 ; FULL SIZE - TOTAL = 1400.00] SQ.IN.

TEST POINT	V_{ac} FT/SEC	P_r^o	T_T^o DEG R	V_j^o FT/SEC	W^o LB/SEC	P_r^i	T_T^i DEG R	V_j^i FT/SEC	W^i LB/SEC	P_r^{mix}	T_T^{mix} DEG R	V_j^{mix} FT/SEC	F LB	V_j^i/V_j^o
1	0	1.872	1445	1693	441.4	1.852	775	1226	125.7	1.852	1296	1589	28021	0.72
2	400	1.877	1451	1700	439.3	1.848	813	1254	121.8	1.858	1312	1603	27958	0.74
3	0	2.224	1535	1949	503.6	2.200	793	1386	146.4	2.191	1368	1822	36821	0.71
4	400	2.224	1538	1951	505.9	2.186	802	1389	145.4	2.190	1373	1825	36960	0.71
5	0	2.542	1631	2153	564.8	2.577	790	1500	174.0	2.501	1433	1999	45910	0.70
6	400	2.556	1630	2158	563.9	2.591	807	1519	171.8	2.517	1437	2009	45936	0.70
7	0	2.867	1744	2349	606.4	2.907	836	1625	188.1	2.810	1529	2177	53780	0.69
8	400	2.867	1745	2350	609.7	2.894	837	1623	188.3	2.809	1531	2178	54035	0.69
9	0	3.357	1735	2486	711.0	3.215	860	1712	205.0	3.258	1539	2313	65859	0.69
10	400	3.346	1728	2478	714.5	3.195	862	1710	204.6	3.248	1535	2307	65916	0.69
109	0	3.421	952	1841	997.2	3.202	884	1733	202.2	3.383	940	1822	67947	0.94
110	400	3.423	932	1822	1011.5	3.201	883	1732	202.7	3.384	923	1806	68182	0.95
13	0	3.650	1717	2543	777.0	3.416	888	1777	214.3	3.535	1538	2377	73241	0.70
14	400	3.651	1716	2542	777.6	3.416	894	1783	213.5	3.537	1539	2378	73273	0.70
403	0	2.225	1559	1965	605.3	1.000	460	0	0.0	2.225	1558	1964	36967	0.00
409	0	3.354	1750	2496	858.8	1.000	460	0	0.0	3.354	1749	2496	66626	0.00

TEST POINT	T_{amb} DEG R	P_{amb} PSIA	RH %	NF dB	LVM	LBM	PNL (FULL SIZE, 2400 FT SIDE LINE), dB ANGLE RELATIVE TO INLET, DEGREES 50	60	70	90	120	130	140	OAPWL dB
1	499.7	14.71	92	-4.7	1.62	-10.00	84.0	85.0	86.9	93.3	92.6	89.1	86.0	166.6
2	519.7	14.63	78	-4.9	1.57	-10.00	87.8	87.3	88.2	92.6	91.5	85.9	81.8	167.5
3	499.7	14.58	92	-5.1	2.21	-2.77	86.0	87.7	90.4	96.8	96.1	94.1	91.6	170.7
4	499.7	14.66	92	-5.1	2.22	-2.78	91.3	91.6	93.0	96.4	95.3	90.6	86.5	169.9
5	499.7	14.77	92	-6.0	2.61	-1.37	88.4	90.4	93.0	99.8	99.6	99.0	97.2	174.6
6	499.7	14.66	92	-6.0	2.63	-1.33	93.0	93.7	94.7	99.7	98.3	94.8	91.2	173.0
7	499.7	14.56	92	-6.5	2.98	-0.60	90.7	92.5	95.1	101.3	102.5	101.9	100.6	177.7
8	499.7	14.65	92	-6.6	2.98	-0.60	94.5	95.4	96.6	101.0	100.6	97.8	94.7	174.9
9	499.7	14.55	92	-7.6	3.25	0.11	93.5	94.9	97.1	102.9	105.0	105.1	106.3	181.2
10	499.7	14.63	92	-7.6	3.23	0.10	96.6	97.7	99.0	102.7	103.2	101.3	98.7	177.3
109	519.7	14.60	78	-10.2	2.13	0.17	91.2	92.9	95.4	100.6	99.2	98.5	97.8	177.9
110	519.7	14.65	78	-10.3	2.09	0.17	95.1	96.0	97.5	101.5	100.4	96.2	92.5	178.7
13	499.7	14.54	92	-8.1	3.36	0.42	95.4	96.6	98.4	103.7	106.3	106.7	108.3	182.8
14	499.7	14.54	92	-8.1	3.37	0.42	98.3	98.8	100.1	103.7	104.7	102.7	100.9	178.7
403	519.7	14.62	78	-4.7	2.45	-2.74	85.3	86.9	89.2	96.3	95.8	93.6	91.7	172.2
409	519.7	14.61	78	-7.2	3.49	0.14	92.7	94.7	97.3	102.9	104.7	104.7	104.9	181.9

- o Tables 3-19 and 3-20, Test Matrices for TE-8; Baseline Nozzle with Treated Plug, T2, and with Treated Ejector, T2, of Extended Length, L2, at Extended Spacing, S2.
- o Tables 3-21 and 3-22, Test Matrices for TE-9; Baseline Nozzle with Treated Plug, T1, and with Treated Ejector, T1, of Nominal Length, L1, at Extended Spacing, S2.
- o Tables 3-23 and 3-24, Test Matrices for TE-10; Baseline Nozzle with Hardwall Plug and with Hardwall Ejector of Extended Length, L2, at Extended Spacing, S2.

3.3.2 Laser Velocimeter Test Summary

Mean velocity (axial component) and turbulent velocity (axial component) measurements of twenty-one (21) selected flow conditions with five (5) test configurations were performed employing the laser velocimeter (LV). Measurements were acquired on Configurations TE-1, TE-4, TE-5, TE-6 and TE-8. The nominal aerodynamic flow conditions of the LV test points are summarized in Table 3-25. Twenty-one (21) aero plumes were LV studied in varying degrees of detail; these 21 configuration/plume combinations being identified by "LV Test Point No." for ease of reference in the Table 3-25 summary. "Match Acoustic Test Point Number", also in the table, is a cross reference to the same acoustic test point number of Section 3.3.1's Table 3-1 ; the same nominal aerodynamic flow conditions being maintained. As noted from the table, 7 plumes were documented on Configuration TE-1, 4 on TE-6, 6 on TE-4, and 2 each on TE-8 and TE-5. A brief description of the test point is also included.

The detailed LV measurements are included in this contract's comprehensive data report. Select data are included within the reports Section 4.0, "Acoustic and Diagnostic Test Results".

3.3.3 Shadowgraph-Photograph Test Summary

In addition to the acoustic, LV and aerodynamic instrumentation performance tests, diagnostic shadowgraph-photography testing was conducted on Configurations TE-1, TE-4 and TE-6. Table 3-26 summarizes the shadowgraph test matrix, covering (6) similar plume/aero cycle conditions on each of the (3) test configurations. The nominal aerodynamic flow conditions are summarized in this table. Test point numbers again match the acoustic test points of Section 3.3.1's Table 3-1 ; the same aerodynamic flow conditions being maintained. The detailed shadowgraph-photographs are included in this contracts comprehensive data report. Results of these data are referenced within Section 4.0, "Acoustic and Diagnostic Test Results".

3.3.4 Aerodynamic Ps and Ts Test Summary

Instrumentation for aerodynamic performance and thermal environment evaluation were applied to various surfaces of the suppressor/ejector systems in order to a) estimate chute base drag, b) measure chute metal temperature and skin temperature along the ejector inner flowpath plus cavity temperature within the packed treatment trays, and c) measure static pressure along the ejector inner flowpath. To acquire said measurements, this instrumentation was utilized, whenever possible, during the prime acoustic test matrices as

TABLE 3-25. LASER VELOCIMETER TEST MATRIX

	TEST POINT DESCRIPTION	LV TEST POINT NO.	MATCH ACOUSTIC TEST POINT NO.	NOMINAL AERODYNAMIC CYCLE: INNER P/R	INNER T_T, °R	INNER V_j, fps	INNER W, pps	OUTER P/R	OUTER T_T, °R	OUTER V_j, fps	OUTER W, pps	V_{fs}, fps
CONFIG. TE-1	T/O, HOT, STATIC	1	1009	3.20	870	1720	4.0	3.40	1730	2495	13.9	0
	T/O, HOT, FLIGHT	2	1010	3.20	870	1720	4.0	3.40	1730	2495	13.9	400
	T/O, $T_T^i=T_T^o=$ 870°R, STATIC	3	1109	3.20	870	1720	4.0	3.47	870	1850	19.5	0
	T/O, $T_T^i=T_T^o=$ 870°R, FLIGHT	4	1110	3.20	870	1720	4.0	3.47	870	1850	19.5	400
	T/O, SUBSONIC INNER, STATIC	5	1011	1.80	870	1270	2.3	3.40	1730	2495	13.9	0
	T/O OUTER, NO INNER, STATIC	6	1409	-	-	-	0	3.40	1730	2495	13.9	0
	C/B, FLIGHT	7	1004	2.20	800	1390	2.9	2.25	1530	1960	9.8	400
CONFIG. TE-6	T/O, HOT, STATIC	8	6009	3.20	870	1720	4.0	3.40	1730	2495	13.9	0
	T/O, HOT, FLIGHT	9	6010	3.20	870	1720	4.0	3.40	1730	2495	13.9	400
	T/O, SUBSONIC INNER, STATIC	10	6011	1.80	870	1270	2.3	3.40	1730	2495	13.9	0
	T/O, OUTER, NO INNER, STATIC	11	6409	-	-	-	0	3.40	1730	2495	13.9	0
CONFIG. TE-4	T/O, HOT, STATIC	12	4009	3.20	870	1720	4.0	3.40	1730	2495	13.9	0
	T/O, HOT, FLIGHT	13	4010	3.20	870	1720	4.0	3.40	1730	2495	13.9	400
	T/O, $T_T^i=T_T^o=$ 870°R, STATIC	14	4109	3.20	870	1720	4.0	3.47	870	1850	19.5	0
	T/O, $T_T^i=T_T^o=$ 870°R, FLIGHT	15	4110	3.20	870	1720	4.0	3.47	870	1850	19.5	400
	T/O OUTER, NO INNER, STATIC	16	4409	-	-	-	0	3.40	1730	2495	13.9	0
	C/B, FLIGHT	17	4004	2.20	800	1390	2.9	2.25	1530	1960	9.8	400
CONFIG. TE-8	T/O, HOT, STATIC	18	8009	3.20	870	1720	4.0	3.40	1730	2495	13.9	0
	T/O, HOT, FLIGHT	19	8010	3.20	870	1720	4.0	3.40	1730	2495	13.9	400
CONFIG. TE-5	T/O, HOT, STATIC	20	5009	3.20	870	1720	4.0	3.40	1730	2495	13.9	0
	T/O, HOT, FLIGHT	21	5010	3.20	870	1720	4.0	3.40	1730	2495	13.9	400

TABLE 3-26. SHADOWGRAPH-PHOTOGRAPH TEST SEQUENCE AND DATA SUMMARY

	SHADOWGRAPH AERO DATA			INNER			OUTER			
	DMS NO.	POINT NO.	$V_{a/c}$	V^i_j	T^i_T	P^i_r	V^o_j	T^o_T	P^o_r	V^{mix}_j
CONFIGURATION			Ft/Sec	Ft/Sec	Deg.R		Ft/Sec	Deg.R		Ft/Sec
TE-1	223	1409	0	0.0	1183	1.000	2469.0	1705	3.375	2469.0
	224	1409	0	0.0	1366	1.000	2501.5	1742	3.395	2501.5
	225	1011	0	1261.9	859	1.798	2500.1	1745	3.381	2328.3
	226	1009	0	1720.9	870	3.210	2496.8	1740	3.384	2325.5
	227	1109	0	1725.5	875	3.208	1782.7	882	3.480	1773.4
	228	1110	400	1728.8	876	3.217	1804.8	906	3.471	1792.3
	229	1010	400	1736.4	886	3.209	2506.1	1740	3.419	2338.8
TE-6	230	6010	400	1738.2	892	3.189	2487.8	1727	3.386	2325.4
	231	6110	400	1740.5	894	3.189	1779.7	881	3.470	1773.4
	232	6109	0	1736.5	891	3.185	1802.9	903	3.478	1792.2
	233	6009	0	1752.6	905	3.195	2504.8	1743	3.405	2342.6
	234	6011	0	1286.4	894	1.796	2494.1	1733	3.392	2330.0
	235	6409	0	0.0	766	1.000	2493.4	1734	3.387	2493.4
TE-4	236	4009	0	1727.8	880	3.194	2485.3	1726	3.377	2319.8
	237	4109	0	1713.9	867	3.186	1794.5	899	3.454	1781.3
	238	4110	400	1712.8	866	3.189	1789.5	895	3.447	1776.9
	239	4010	400	1725.5	878	3.190	2505.4	1750	3.389	2334.6
	240	4011	0	1285.1	887	1.803	2495.5	1737	3.386	2328.9
	241	4409	0	7161.8	789	0.994	2500.4	1743	3.389	2500.4

described in Section 3.3.1 Table 3-1. Aerodynamic data were acquired and reduced to engineering units, along with the standard aerodynamic flow monitoring instrumentation for both flow streams, on the Data Management (DMS) System. Detailed Ps and Ts measurements are tabularized in this contract's comprehensive data report, Section 4.7, "Aerodynamic Static Pressure and Static Temperature Data Summary". Select results of these measurements are within this report's Section 5.8, "Aerodynamic Performance Evaluation from Chute Base Pressure Measurements" for chute base drag impact on nozzle thrust coefficient and within Section 4.0, "Acoustic and Diagnostic Test Results".

4.0 ACOUSTIC AND DIAGNOSTIC TEST RESULTS

Within this section, the acquired acoustic and diagnostic data are analyzed and results reported. As discussed in Section 3.1, "Scale Model Test Hardware", a chronology of test configurations was developed to systematically evaluate parameters which were judged influential to suppressor/ejector acoustic performance. This chronology, diagrammed in Figure 4-1, was also followed in identifying the methodology of comparisons for analysis and presentation of results. The following report subsections present results of various study areas, as follows:

Section 4.1: Establish performance of the baseline TE-1 unejected nozzle in relation to a previous similarly designed 20-chute coannular nozzle of NASA-GE Contract NAS3-21608. Additionally, as no conic nozzle data were acquired within the current program, establish conical nozzle acoustic performance curves for reference in evaluating suppressor/ejector effectiveness.

Section 4.2: Provide an overview of effectiveness of parameters influencing suppressor/ejector acoustic performance and summarize the impact of geometric/aerodynamic variables.

Section 4.3: Verify the on-test selections of optimum peformance of ejector axial position S2 (TE-9) over S1 (TE-5) and treatment application T2 (TE-4) over T1 (TE-9).

Section 4.4: Rank and quantatively evaluate the individual sources of ejector effectiveness, i.e., a) application of hardwall ejector, b) application of acoustic treatment to ejector flow surface, and c) application of acoustic treatment to plug surface. These are reviewed within the nominal length ejector set; TE-4, TE-3 and TE-2, and within the extended length ejector set; TE-8, TE-7 and TE-10.

Section 4.5: Evaluation of effectiveness of ejector length variation within the comparisons of a) hardwall ejector TE-2 and TE-10, b) treated ejector flowsurfaces, TE-3 and TE-7, and c) fully treated ejector/plug, TE-4 and TE-8.

Section 4.6: Review effectiveness of softwall plug surface for potential of diminishing shock-cell strength and subsequently alleviating shock-cell related noise.

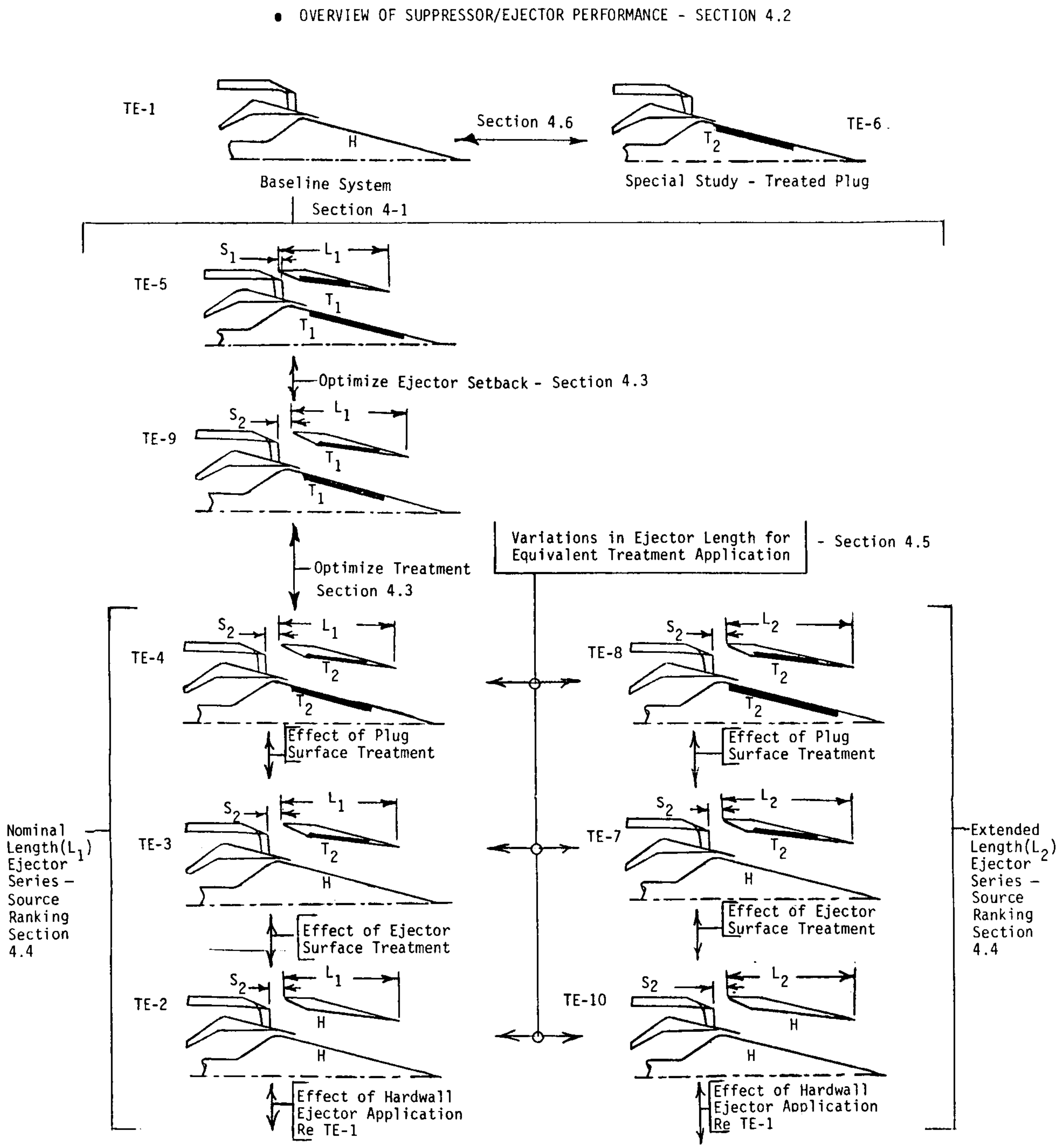

FIGURE 4-1 FLOW SCHEMATIC OF TEST CONFIGURATIONS RELATIVE TO EVALUATION OF ACOUSTIC PERFORMANCE

As acoustic performance can be gauged through comparison of a variety of standard noise parameters, i.e., PWL, PNL, OASPL, EPNL, and basic spectra, it is of interest to present representative samples of these types of data sets for overall trend evaluation. Many of the physical changes incorporated in ejector model variations produced minor changes in acoustic levels and in many cases the changes are not methodically consistent. For example, as primary nozzle thermodynamic cycle is changed or as simulated flight is introduced, mechanisms of noise generation and subsequent ejector suppression are altered. Therefore, to gauge effectiveness of a physical change in ejector design, i.e., length increase, ejector axial location, hardwall, ejector flowpath treatment, or plug surface treatment, review of a representative sample of comparisons is generally warranted to discern general trends of effectiveness. More specifically, if a select cycle condition and acoustic parameter is of interest, exact comparisons at those conditions are most helpful. Therefore, for evaluation of acoustic peformance of the baseline and treated ejector variations, this section will present an array of detailed data comparisons, primarily to augment observation of trends, but also to benefit the readers future use. General peformance trends elicited from the comparisons are then summarized.

4.1 EFFECTIVENESS OF BASELINE CONFIGURATION TE-1 RELATIVE TO CONICAL NOZZLE AND TO PREVIOUS MULTI-CHUTE INVERTED-VELOCITY-PROFILE SUPPRESSOR SYSTEM

Within this section, the baseline TE-1 unejected 20-chute suppressor nozzle is compared to a reference conical nozzle for establishing its level of suppression. It is also compared to a previously tested, similarly designed 20-chute outer annular suppressor to validate consistency of jet noise suppression level attained, plus, to evaluate whether additional forward quadrant shock noise suppression was achieved. Prior to this presentation, however, conical nozzle data from previous NASA-Lewis sponsored contracts are summarized in order to document reference nozzle performance curves for use throughout the report.

4.1.1 Conical Nozzle Baseline Substantiation

This program's test effort did not include testing of a reference conical nozzle. As acoustic performance of jet noise suppressors is always referenced to a baseline conical nozzle, previous NASA sponsored test efforts on conic nozzles within the General Electric Anechoic Free-Jet Facility and a full scale conic nozzle engine test are summarized within this report section to provide said baseline. Data from References 5 and 12 through 14 have been reviewed and used to establish nominal performance curves, the nominal curves then used as reference to which suppressor/ejector systems' suppression is quoted in various report sections. Except for the Reference 14 YJ101 engine test static data, the conic nozzle data have been acquired and reduced in the same manner described in Section 3.1 of this report. The YJ101 data have acquired, reduced and scaled in similar manner and represent compatible conic nozzle data for a full scale engine sized to the AST/VCE study system. Unless otherwise stated, presented data are for a full scale 1400 in^2 exhaust nozzle total area, corrected to a 59^{o}F 70% relative humidity standard day and presented on a 2400' sideline.

The conic nozzle performance summaries, where applicable, are presented as direct comparisons of static and simulated flight. The simulated flight range being 370 to 400 ft/sec, representative of takeoff flight speed for an AST/VCE system. Compared as such, influence of flight can readily be seen on all presented parameters, i.e., spectra, OASPL, PNL and PWL. These results will be later referenced in relation to flight influence on the suppressor/ejector acoustic performance.

A quick review of flight effects on jet noise may be in order for the sake of qualitatively understanding the major changes seen in static-to-flight data comparisons. Flight effects can be examined by reviewing the methodology in which the General Electric M*G*B prediction model, Reference 15, handles said effects on the basic noise generation/emission mechanisms of a) basic turbulent mixing, b) convective amplification of the turbulent eddy sources, c) fluid shielding and refraction of mixing noise, and d) shock cell associated noise.

First, the basic turbulent mixing noise generation is altered in several ways. The forward flight is seen in a nozzle-fixed reference frame as a co-flowing medium; hence the shear between the jet flow and the ambient medium is reduced. Simultaneously, the mixing rate coefficients are reduced which tends to elongate or stretch out the jet. The result of these competing effects is a reduction in the basic turbulent mixing noise level (typified by the $\theta_I = 90^o$ spectrum), but more reduction occurs at high frequencies than at low frequencies. In addition, the "source" frequencies, which are determined by intensities and length scales of the generated jet shear layer turbulence, become smaller so the resultant spectrum shifts to lower frequencies. This is illustrated qualitatively in Figure 4-2a.

The second mechanism which is altered by forward flight is the convective amplification of the turbulent eddy sources due to motion relative to the observer. Typical convective amplification trends on OASPL are shown in Figure 4-2b. The effect of forward flight is to change the convection speed of the eddies relative to the observer from M_c (relative to the nozzle) to M_c-M_o. Thus, the "observed" convection speed $M_{co} = M_c-M_o$ is reduced, and the directivity pattern due to convection becomes less steep. This results in an increase in the forward-arc level relative to the 90^o level, and a corresponding decrease in the aft-arc level relative to the 90^o level, as compared to the static levels.

The third mechanism which is altered by forward flight is the fluid shielding and refraction of the mixing noise as it propagates through the jet flow itself to the ambient field. This mechanism only plays an important role in the aft quadrant, above $\theta_I = 120^o$ to 130^o, depending on the jet velocity. Since the amount of shielding or attenuation provided by the jet flow itself increases with increasing jet velocity, the effect of forward flight is to reduce the flow shielding, since the jet flow velocity level relative to the ambient medium is reduced. This results in an increase in noise in the aft arc, above the critical angle or "zone of silence" where shielding occurs, $\theta_I = 120^o$ to 130^o. This effect is illustrated qualitatively in Figure 4-2c. The shielding effect diminishes at low frequencies, having negligible impact below about 1/2 the peak noise frequency at 90^o.

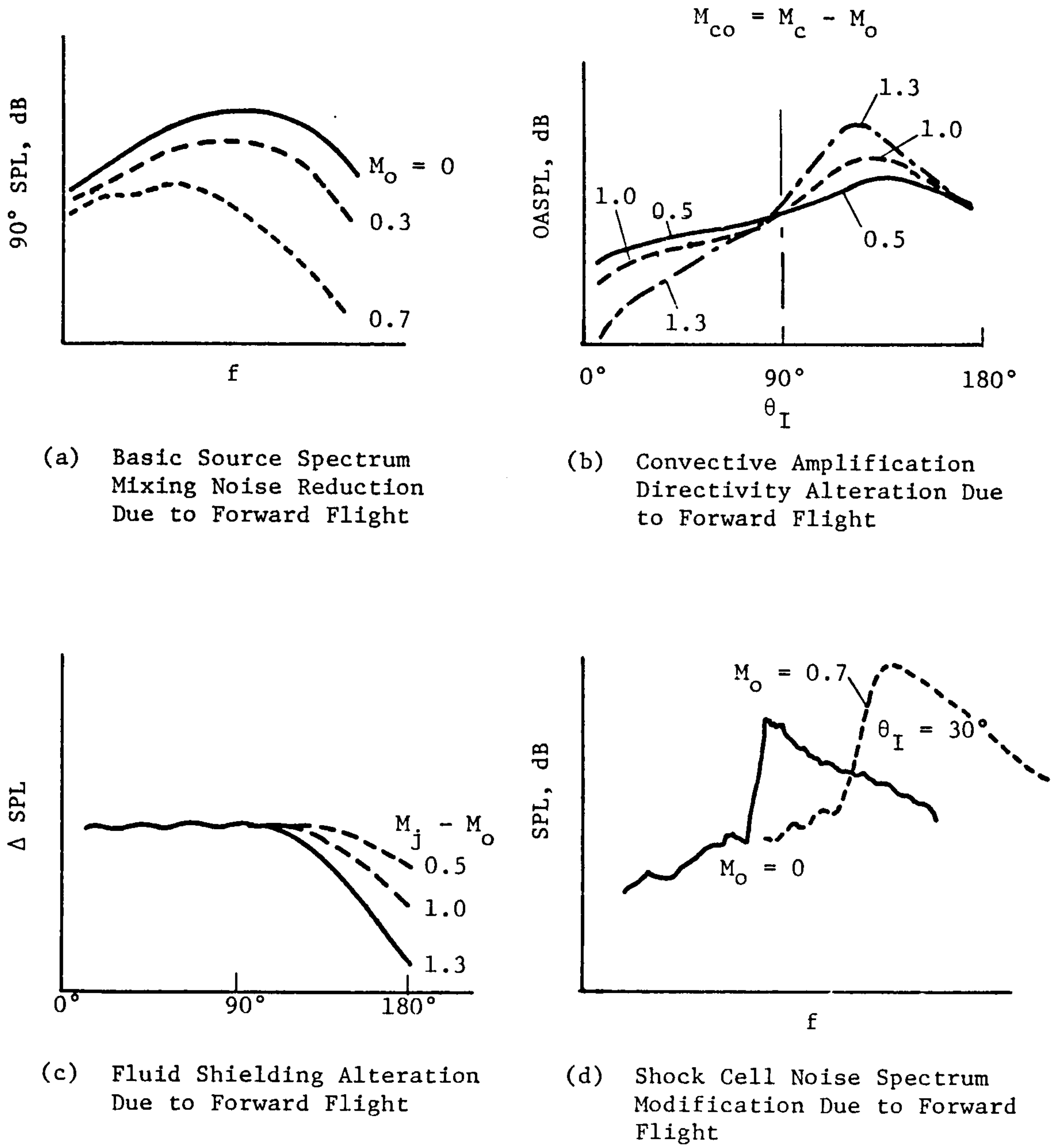

FIGURE 4-2 QUALITATIVE EFFECTS OF FORWARD FLIGHT ON VARIOUS JET NOISE EMISSION/GENERATION MECHANISMS.

Finally, the fourth mechanism of jet noise generation which is altered by forward flight is shock cell noise generation. The shock cell noise generation "sources" are fixed (on a time-averaged basis) to the nozzle reference frame, i.e., they are not convected sources. This is because the nozzle plume shock fronts formed in the jet flow at supersonic pressure ratios are the noise radiators, producing acoustic emission as a result of jet flow turbulence convecting through and over the shock cell fronts. The noise "source" locations, i.e., the shock fronts, are fixed relative to the nozzle, but the emission spectrum shape depends upon the turbulence characteristics (intensity, length scale and convection speed). To the extent that forward motion modifies these turbulence characteristics, the shock cell noise emission spectrum will also be altered. For low flight speeds ($M_0 < 0.3$), this effect will be small, since we are concerned with changes close to the jet exit plane where flow velocities are high. For high flight speeds ($M_0 > 0.5$), this effect could be substantial.

In addition to the above effects (modification of shock-cell noise source spectrum due to changes in turbulence characteristics), the shock-cell noise spectrum suffers a dynamic and doppler effect due to source motion similar to that of a moving point source, of the form

$$SPL_{static} - SPL_{flight} = 40 \log_{10} (1-M_0 \cos \theta_I)$$

$$f_{flight} = f_{static}/(1-M_0 \cos \theta_I)$$

Again, for large M_0, these level and frequency corrections can be quite substantial. This effect is illustrated qualitatively in Figure 4-2d.

For presentation of the summarized conic nozzle data, standard methods for correlating jet mixing noise are followed and resultant curves presented in the following:

- o Figure 4-3: Normalized OAPWL versus normalized jet velocity for static and simulated-flight.

- o Figure 4-4 and 4-5: Normalized OASPL and PNL, respectively, versus normalized jet velocity parameter, static and flight, for $\theta_I = 60^o$, 90^o, 130^o and peak value.

Noteworthy in reviewing these figures are the following:

- o Substantial reduction of flight OAPWL for all but the highest velocity test points. At the high velocity points, forward quadrant shock noise amplification overrides influence of aft quadrant jet noise reduction.

- o For OASPL and PNL, a) the significant aft quadrant ($\theta_I = 130^o$ and peak value) reduction of jet mixing noise over the entire jet velocity range of operation, and b) the flight amplification of forward quadrant, $\theta_I = 60^o$, and broadside, $\theta_I = 90^o$, noise levels at cycle conditions above critical nozzle pressure ratio ($10_{log}(V_j/A_o) \geq 3.0$), due to influence of shock noise.

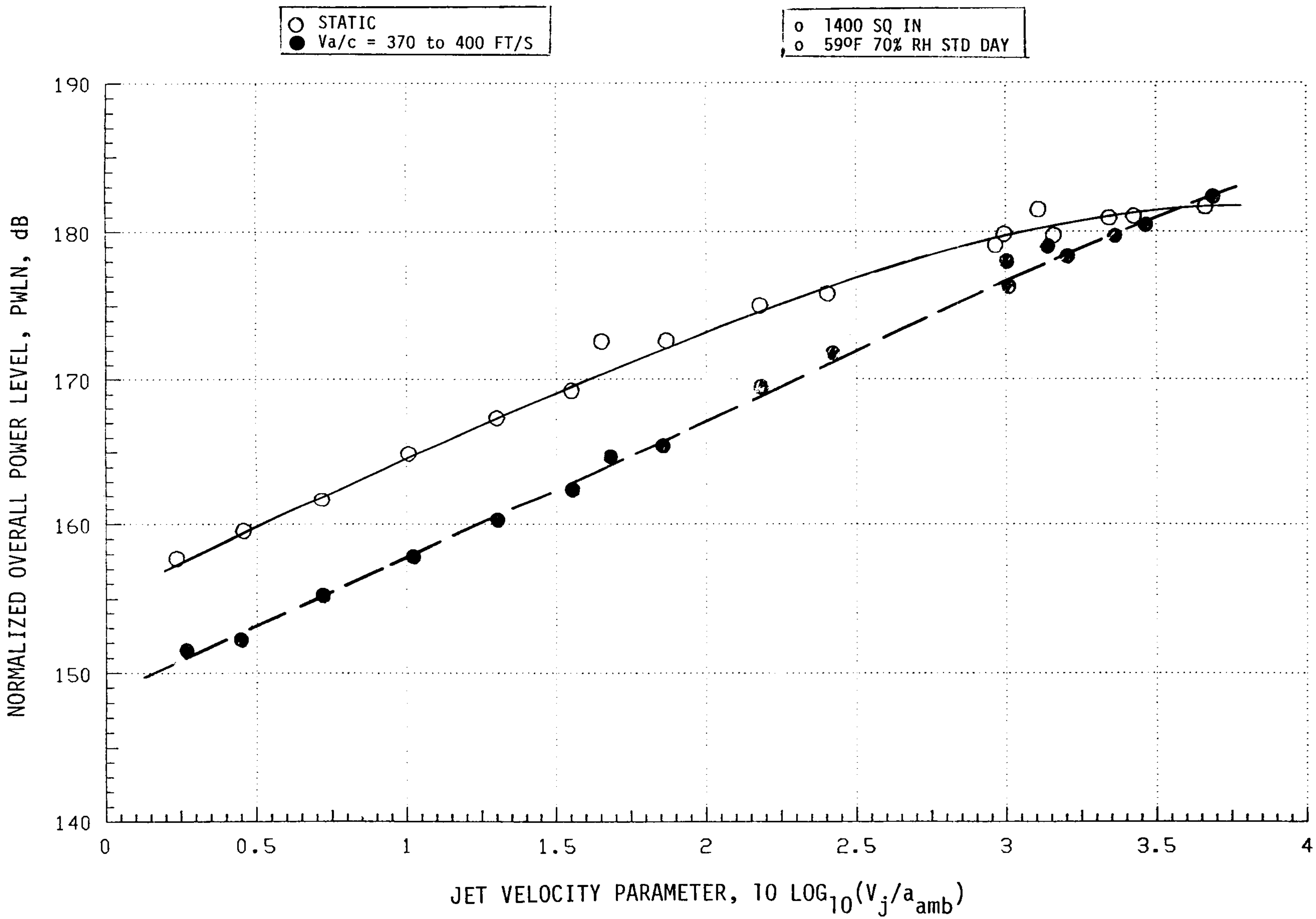

FIGURE 4-3 CONICAL NOZZLE NORMALIZED OAPWL AS A FUNCTION OF JET VELOCITY PARAMETER, STATIC AND SIMULATED-FLIGHT.

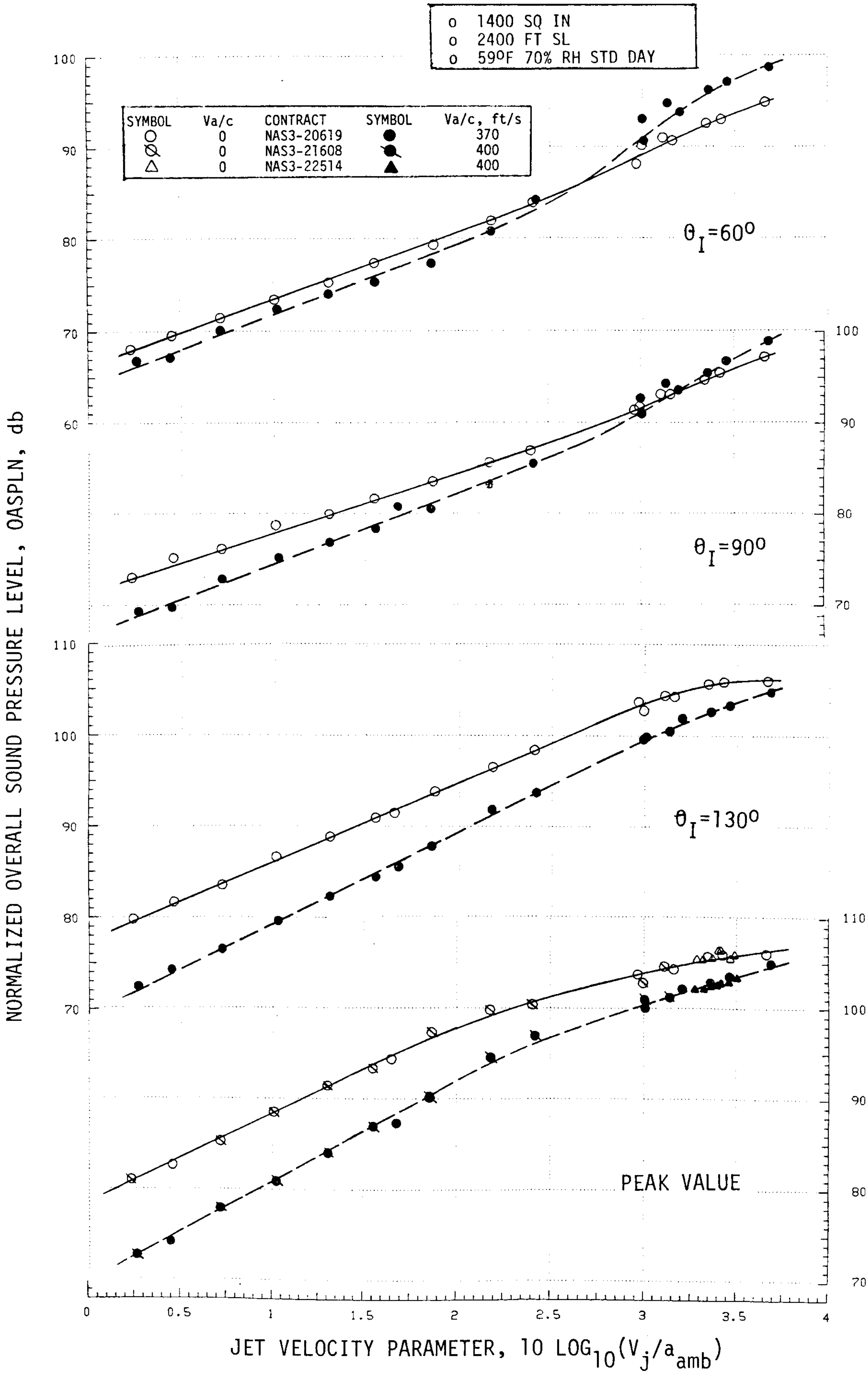

FIGURE 4-4 CONICAL NOZZLE NORMALIZED OASPL AS A FUNCTION OF JET VELOCITY PARAMETER, STATIC AND SIMULATED-FLIGHT AT $\theta_I = 60^o$, 90^o, 130^o AND PEAK VALUE.

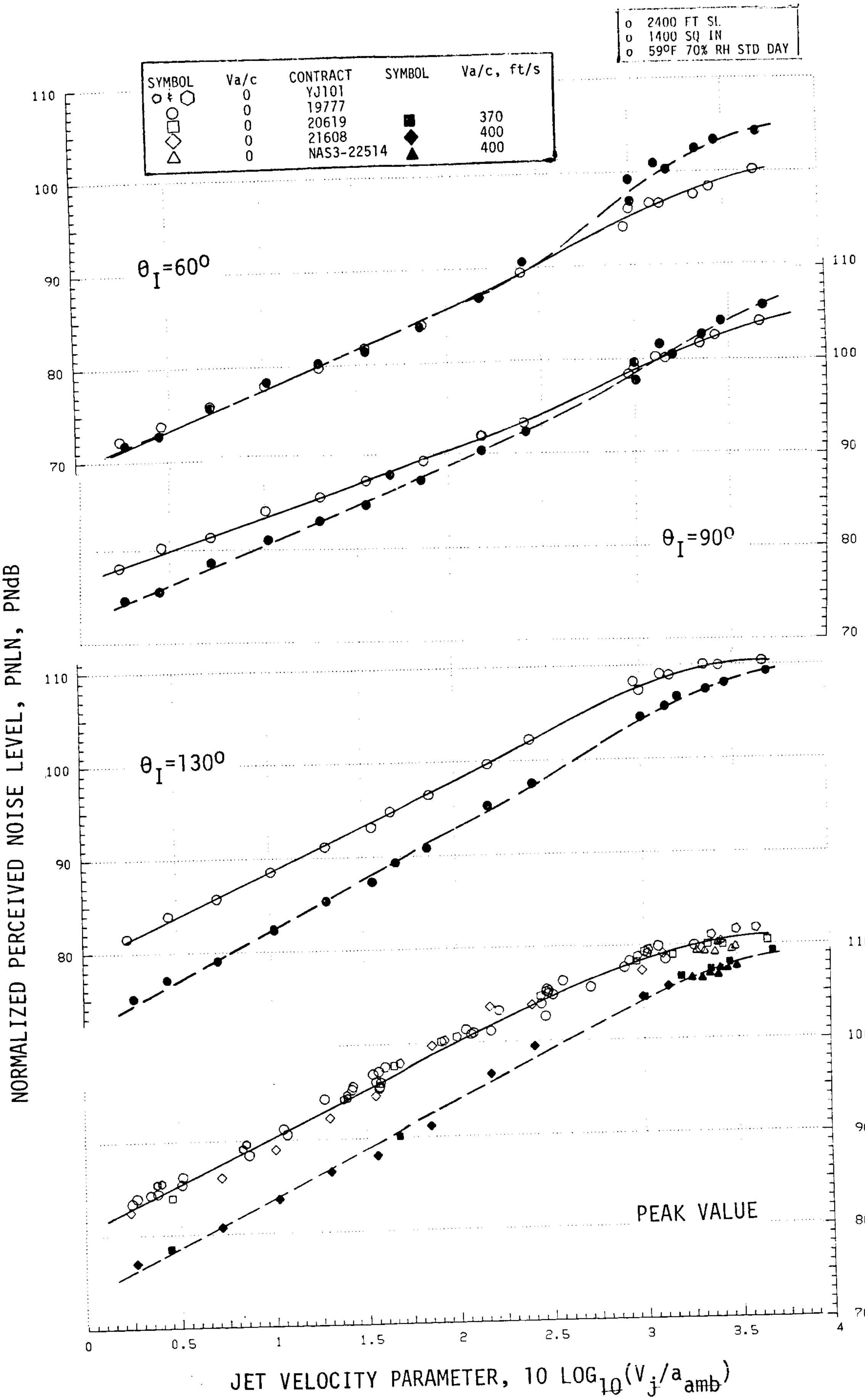

FIGURE 4-5 CONICAL NOZZLE NORMALIZED PNL AS A FUNCTION OF JET VELOCITY PARAMETER, STATIC AND SIMULATED-FLIGHT AT θ_I=60°, 90°, 130° AND PEAK VALUE.

To exemplify flight noise influence on conical nozzle spectral content, Figures 4-6, 4-7 and 4-8 present static to flight comparisons at $\theta_I = 60^o$, 90^o and 130^o for three cycle points. The points have been selected as nearest match to the suppressor/ejector coannular nozzle's mixed jet aerodynamic cycle at "cutback", "intermediate" and "takeoff" power settings for the study AST/VCE system (see Section 3.3.1 for test point definition). Conic nozzle cycle parameters are noted on the figure and have pressure ratio ranging from 2.16 at cutback to 2.92 for takeoff; from slightly supersonic where shock noise is non-influential to highly super-critical where shock noise is quite dominant. Review of these figures elicits the following influences of flight on conic nozzle noise:

- o Aft quadrant jet-mixing-noise-dominated spectra are significantly reduced for all frequencies at all three cycle points.
- o 90^o spectra show slight reduction for all frequency bands for cutback and intermediate cycle, but amplification of the peak shock broadband frequencies and above for the takeoff cycle point.
- o Forward quadrant mid-to-high frequency noise is amplified for all three cases; for the intermediate and takeoff cases where shock peaks are seen in the static spectrum, flight amplifies the level and shifts these peaks to higher frequencies, as would be expected from the dynamic and doppler effects discussed earlier.

A further comparison of general data trends and influence of flight can be seen in Figure 4-9, presenting directivity patterns of OASPL and PNL at the representative cycle points of cutback, intermediate and takeoff for both static and flight. Trends in this data follow those previously observed, i.e.:

- o Aft angles controlled by jet mixing noise (for all three cycle points) are substantially reduced by flight effects.
- o Forward quadrant OASPL and PNL for cutback and intermediate are of similar level due to the offsetting balance of slight low-frequency reduction and slight high-frequency amplification, PNL being amplified slightly more than OASPL due to its mid-to-high frequency weighting.
- o For takeoff, the forward quadrant PNL and OASPL are substantially amplified, primarily due to the strong influence of shock cell noise amplification, even though very low frequency jet mixing noise is still slightly reduced.

A further correlation of conical nozzle shock noise influence can be seen in Figures 4-10 and 4-11 where forward quadrant measured OASPL and PNL are presented as a function of the shock strength parameter, β. Harper-Bourne and Fisher, Reference 16, have developed theoretical and experimental guidelines for estimating the characteristics of broadband shock noise for jets operating above critical pressure ratio. They suggest that shock noise can be correlated on the basis of the shock strength parameter, β, defined as $\sqrt{M_j^2 - 1}$, and used in plotting as $10\text{Log}_{10}\beta$. The graphs presented correlate data at angles of θ_I = 50, 60, 80, 90 and 100^o and directly compare static to flight data. Previous correlations have shown static data to have a β dependency of near 4.0. Figures 4-9 and 4-10 data show:

SYMBOL	TEST POINT	PR	T_T, °R	V_j, ft/s	NF	Va/c, ft/s
○	561	2.16	1472	1876	-4.9	0
●	562	2.16	1464	1871	-4.9	400

o 1400 SQ IN
o 2400 FT SL
o 59°F 70% RH STD DAY

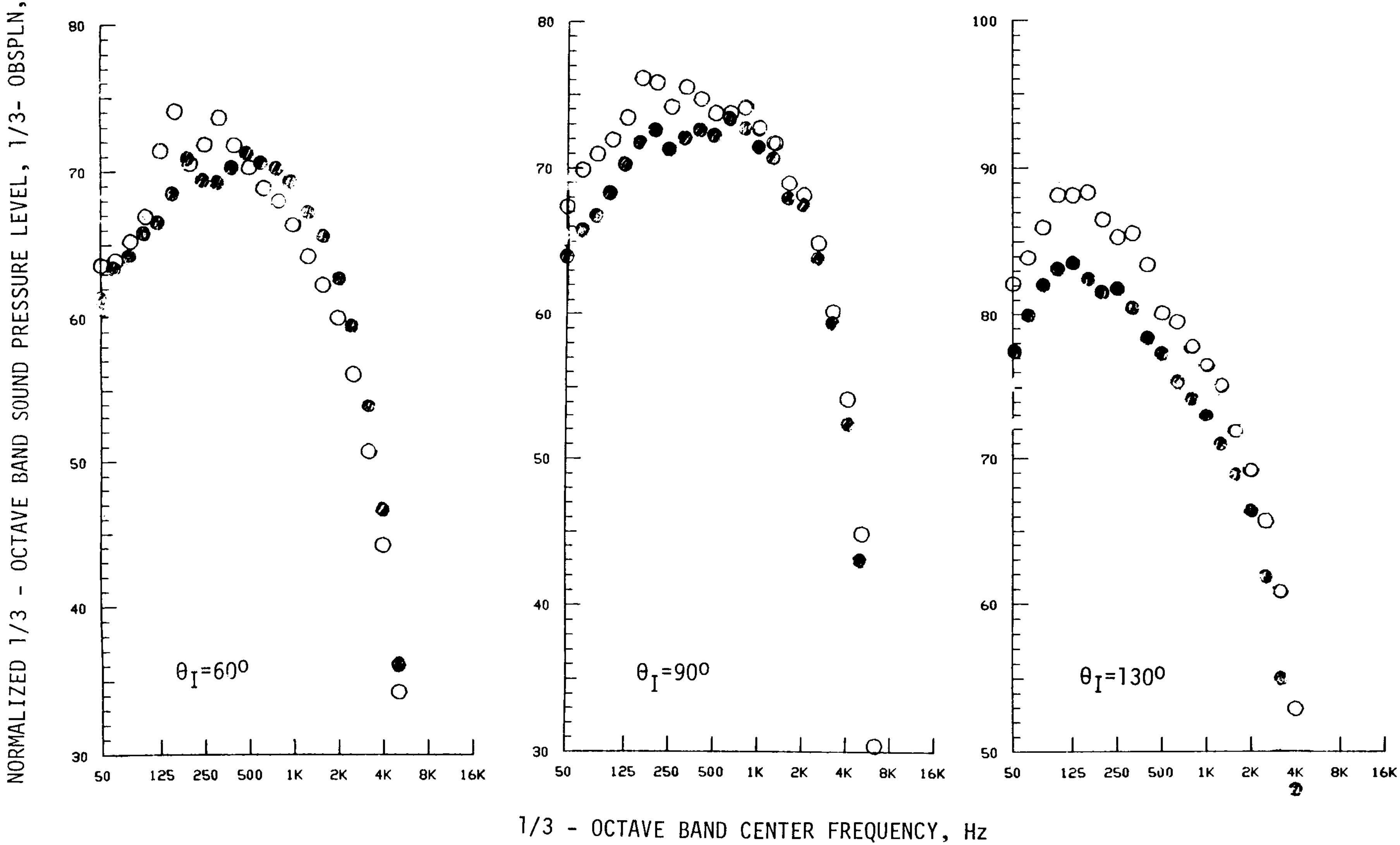

FIGURE 4-6 CONIC NOZZLE STATIC-TO-FLIGHT SPECTRA COMPARISONS AT REPRESENTATIVE CUTBACK CYCLE

SYMBOL	TEST POINT	PR	T_T, °R	V_j, ft/s	NF	Va/c, ft/s
○	563	2.32	1508	1976	-5.3	0
●	564	2.32	1507	1977	-5.3	0

o 2400 FT SL
o 1400 SQ IN
o 59°F 70% RH STD DAY

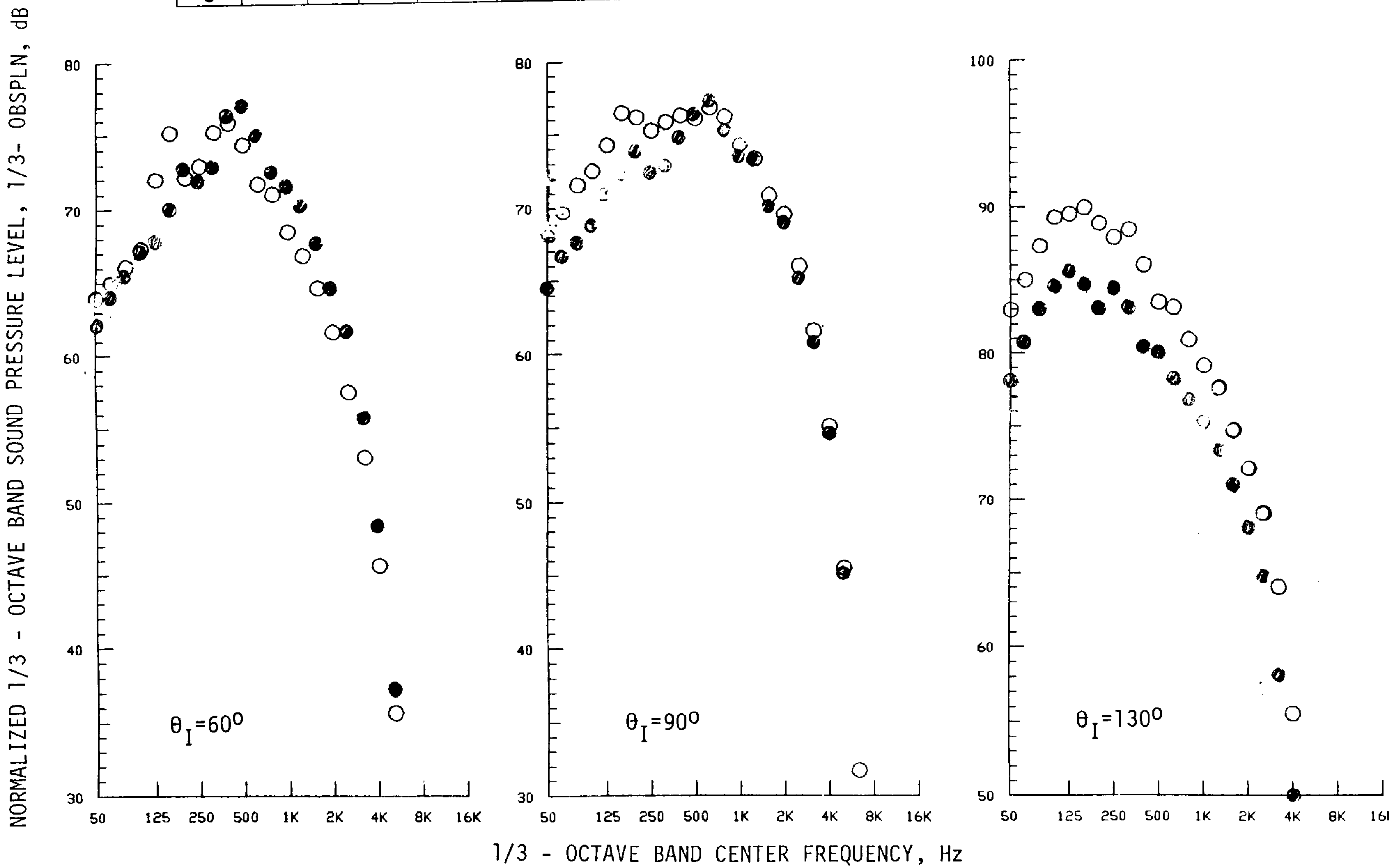

FIGURE 4-7 CONIC NOZZLE STATIC-TO-FLIGHT SPECTRA COMPARISONS AT REPRESENTATIVE INTERMEDIATE CYCLE

SYMBOL	TEST POINT	PR	T_T, °R	V_j, ft/s	NF	Va/c, ft/s
○	567	2.91	1685	2324	-6.5	0
●	568	2.92	1689	2327	-6.5	400

o 1400 SQ IN
o 2400 FT SL
o 59°F 70% RH STD DAY

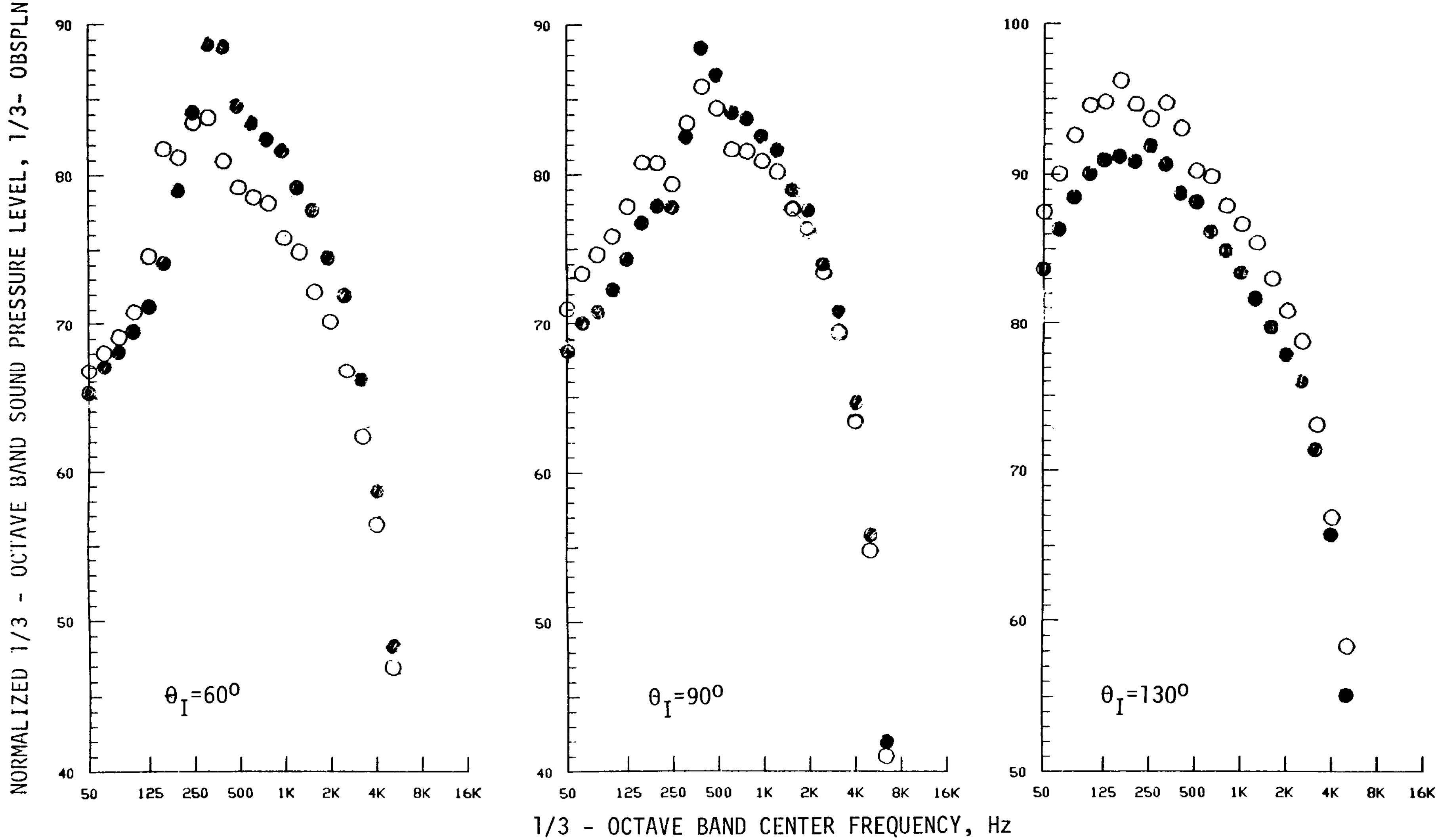

FIGURE 4-8 CONIC NOZZLE STATIC-TO-FLIGHT SPECTRA COMPARISON AT REPRESENTATIVE TAKEOFF CYCLE

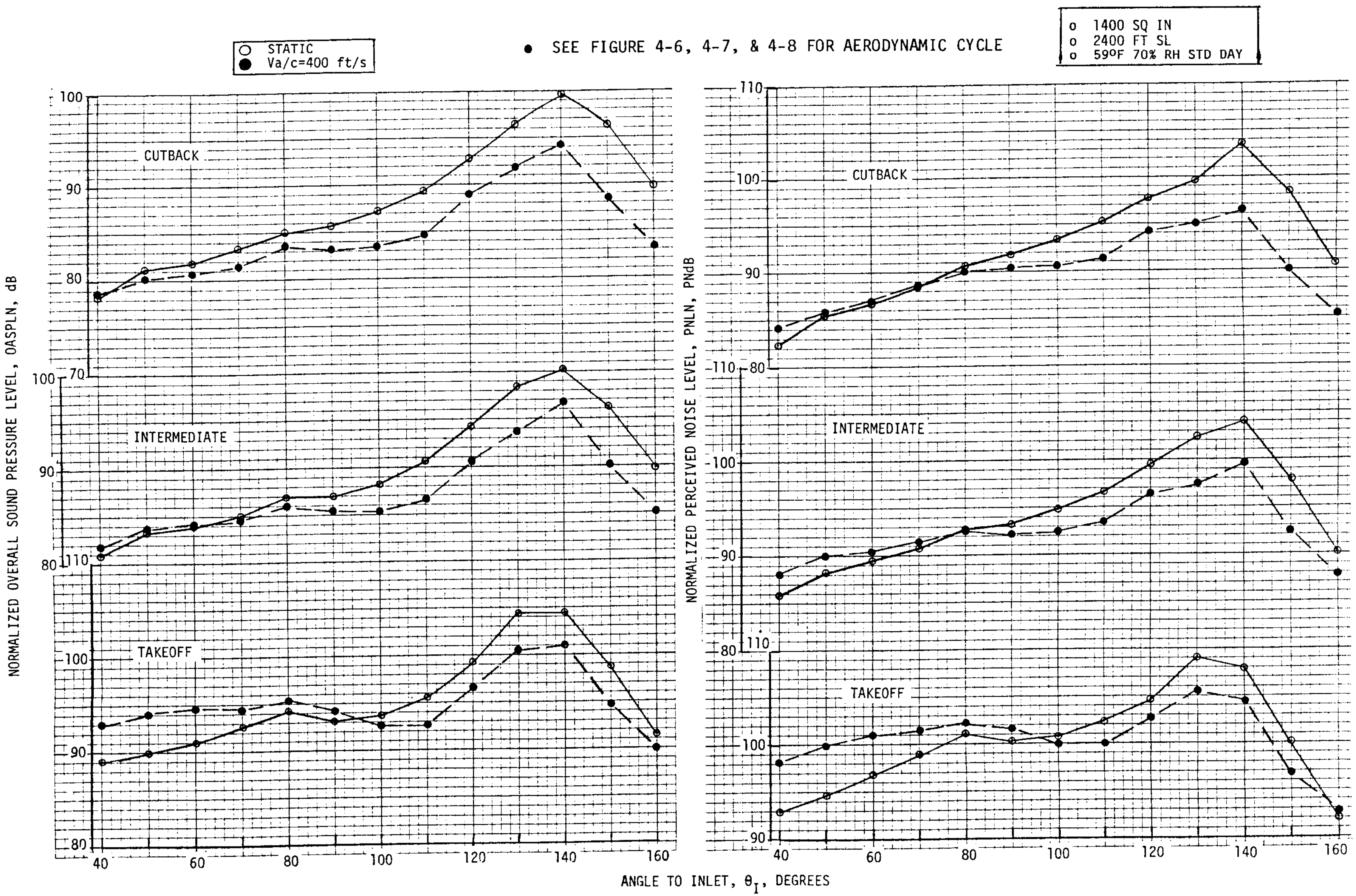

FIGURE 4-9 CONIC NOZZLE STATIC-TO-FLIGHT DIRECTIVITY COMPARISONS OF OASPL AND PNL AT

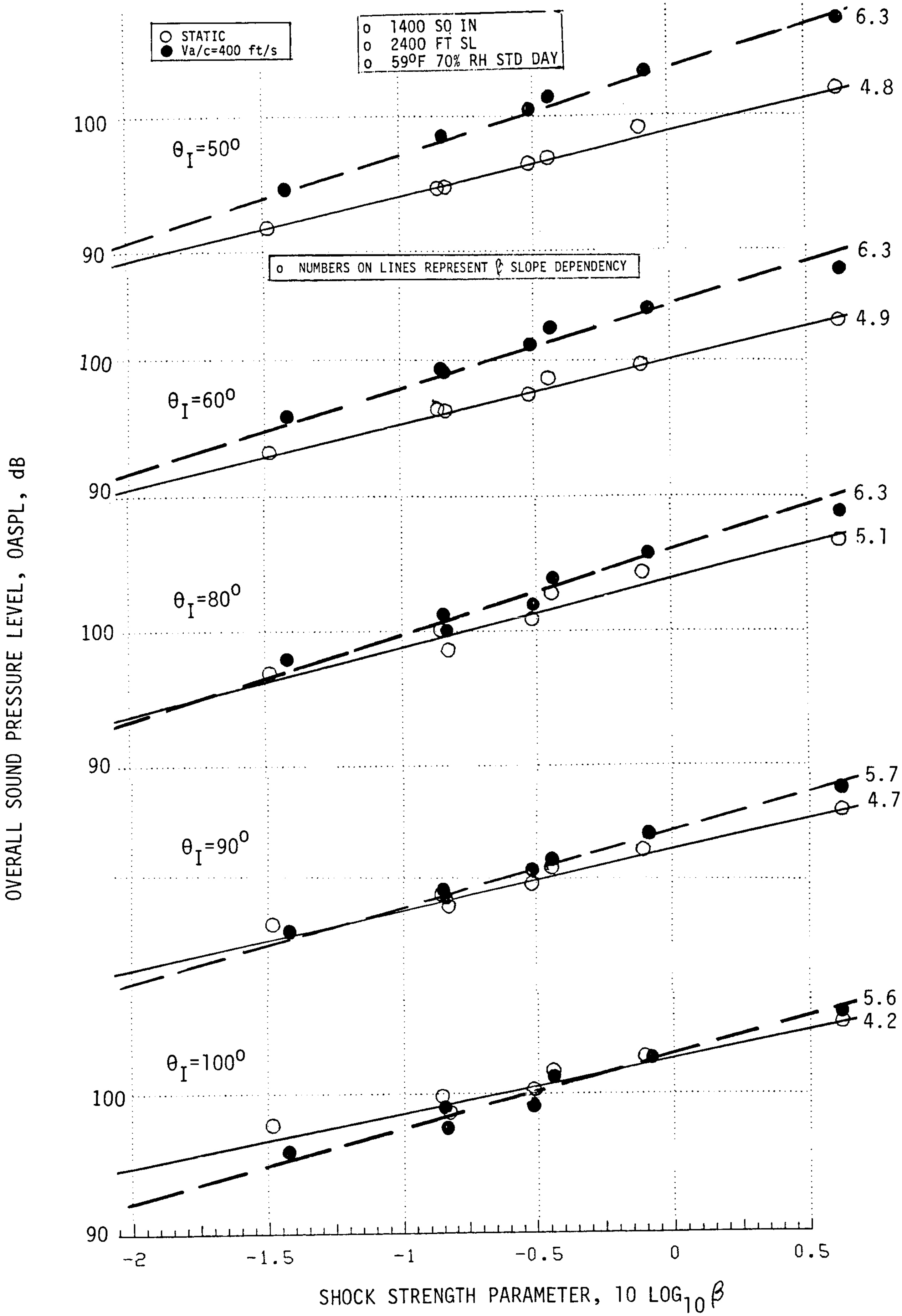

FIGURE 4-10 CONIC NOZZLE STATIC AND FLIGHT CORRELATION OF FORWARD QUADRANT PNL DEPENDENCY ON SHOCK STRENGTH PARAMETER

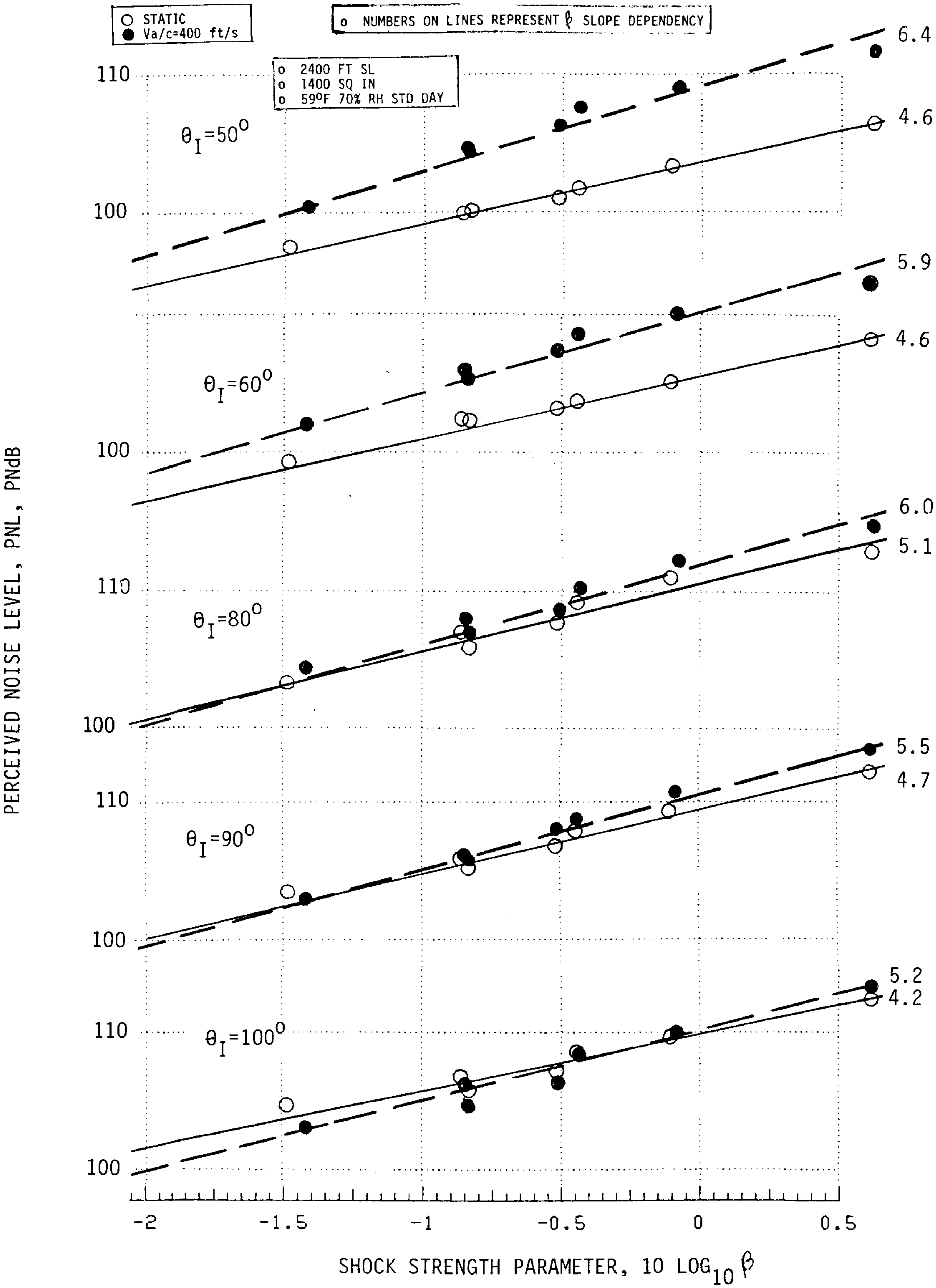

FIGURE 4-11 CONIC NOZZLE STATIC AND FLIGHT CORRELATION OF FORWARD QUADRANT OASPL DEPENDENCY ON SHOCK STRENGTH PARAMETER.

- o Static OASPL and PNL correlate in the range of $\beta^{4.2}$ to $\beta^{5.1}$ for the shown angles in which shock noise is present.
- o Flight OASPL and PNL correlate on slightly higher slopes, from $\beta^{5.2}$ to $\beta^{6.4}$, due to a) the basic forward quadrant amplification of shock by flight, and b) the stronger intensity of shock influence at higher β (pressure ratio) values relative to the diminished shock at low β values.
- o As shock cell-noise spectrum suffers a dynamic effect of $-10\text{Log}_{10}(1 - M_0 \cos \theta_I)$ due to flight; more forward quadrant levels are more severely amplified by flight, therefore, the flight noise lines should progressively increase above the static lines as viewed from $\theta_I = 90^o$ to 50^o; which they do by observation.

Note that these correlations and trends will be compared to the suppressor/ejector data in later text.

A final conical nozzle acoustic performance correlation is presented in Figure 4-12 as normalized EPNL as a function of normalized jet velocity. The calculated EPNL are based on simulated-flight measured data projected to a 2400' sideline and are for two nominal flight speeds, i.e., a) 370 to 400 ft/sec, and b) 280 ft/sec. Presented on this basis the EPNL correlate as a straight line dependency on velocity to an approximate V^{10} slope.

4.1.2 Effectiveness of Baseline Configuration TE-1

4.1.2.1 Comparison of NAS3-23275 Configuration TE-1 to NAS3-21608 Model 10.1

The TE-1 baseline suppressor design is detail-defined in Section 3.2.1, sketch and photo being repeated herein as Figure 4-13, for easy reference. The nozzle essentially duplicates the full scale study nozzle of Contract NAS3-23038 (Reference 1 and Figure 2-1). The details of the full scale nozzle, as far as parameters judged to influence potential for jet noise suppression, were heavily influenced by results of previous test programs, primarily Contract NAS3-20582, Reference 17, "Core Driven YJ101 AST/VCE Coannular Plug Nozzle Investigation" and its scale model counterpart, Contract NAS3-21608, Reference 8, "Free-Jet Investigation of Mechanically Suppressed High-Radius Ratio Coannular Plug Model Nozzles". The coannular nozzle developed under these two contract efforts was a pseudo-optimum jet noise suppressor, implemented in an inverted-velocity-profile exhaust nozzle of the AST/VCE concept. Its model test results, per Reference 8, showed strong peak jet noise suppression, but retention of some forward quadrant shock-cell noise, though substantially reduced below the level of a reference conical nozzle. The NAS3-23038 full scale study nozzle, and therefore the TE-1 baseline nozzle for the treated ejector study, maintained the physical parameters of the pseudo-optimum suppressor that were most influential in jet mixing noise suppression, i.e.:

- 20-shallow chutes
- Suppressor area ratio near 1.75
- Suppressor radius ratio = .72
- Inner-to-outer nozzle area ratio ≈ 0.2

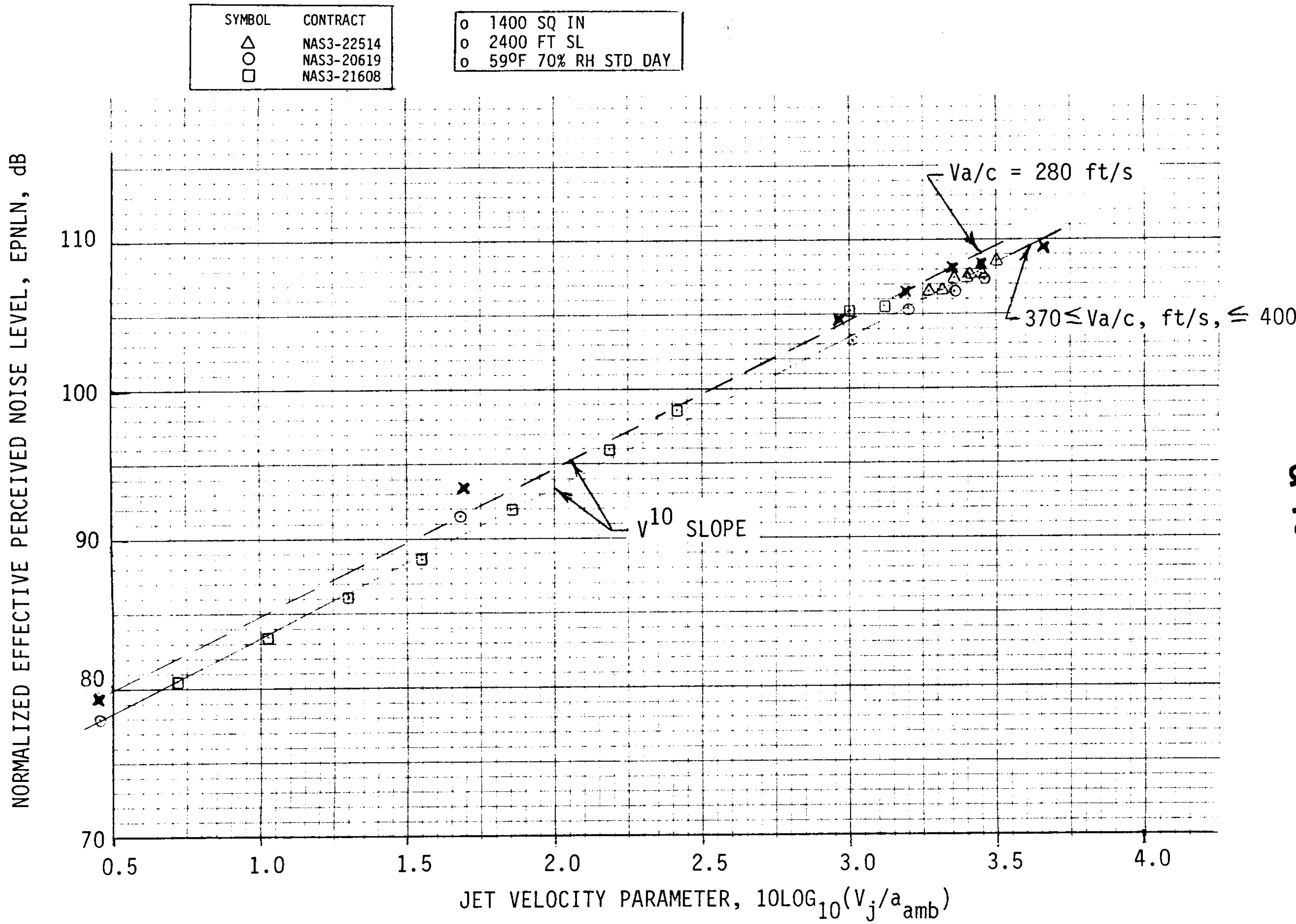

FIGURE 4-12 CONIC NOZZLE EPNL CORRELATION WITH JET VELOCITY PARAMETER.

"AS BUILT" PARAMETERS

Parameter	Outer Nozzle	Inner Nozzle
Type	20-Chute	Annular
A_{flow}, in.^{2}	22.75	4.747
$D_{flow,eq}$, in.	5.382	2.458
$A_{blocked}$, in.^{2}	17.634	-
Area Ratio	1.775	-
Throat Plane Angle Re Vert., Degrees	0	15
R_{tip}, in.	5.162	3.190
R_{hub}, in.	3.713	2.952
Radius Ratio	.719	.926
A_{inner}/A_{outer}	.21	

• All Items Dwg No. 4013312-428

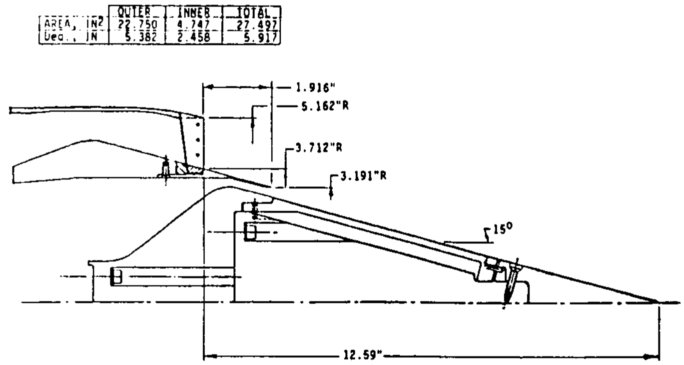

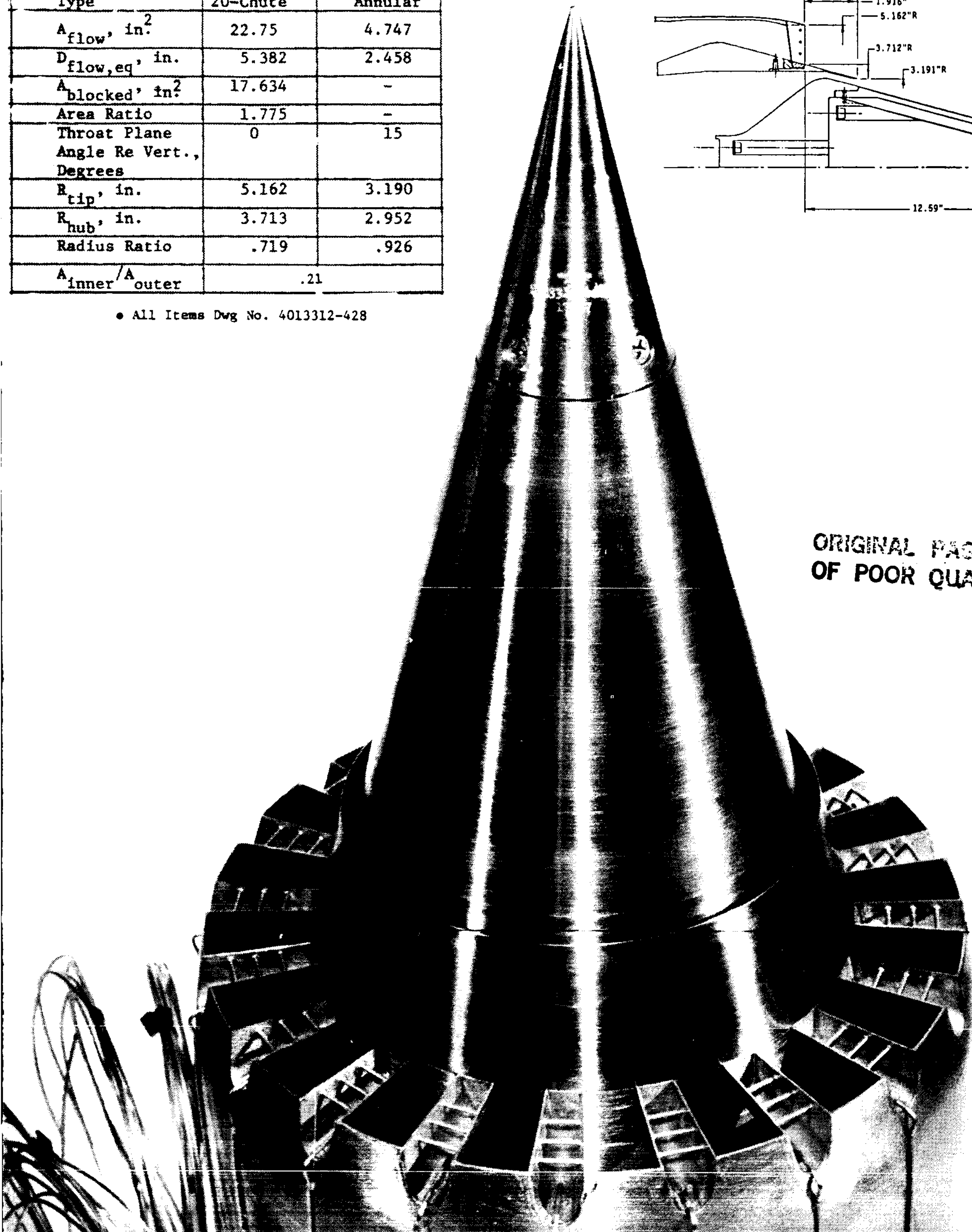

FIGURE 4-13. CONFIGURATION TE-1; BASELINE COANNULAR INVERTED-VELOCITY-PROFILE PLUG NOZZLE WITH 20-SHALLOW CHUTE OUTER STREAM SUPPRESSOR, HARDWALL PLUG AND NO EJECTOR

However, the chute cross sections and the plug closure were altered to attempt to further weaken shock structure and associated shock-cell noise. This report section, therefore, has a twofold purpose, i.e., a) to document the suppression levels and noise characteristics of the baseline TE-1 configuration, and b) to compare its acoustic/aerodynamic performance levels to that of its similarly designed predecessor, Model 10.1 of Contract NAS3-21608.

A schematic and photograph of the Model 10.1 are per Figure 4-14. The following is a comparison of pertinent geometric parameters:

PARAMETER	NAS3-23275 CONFIG. TE-1		NAS3-21608 MODEL 10.1	
	OUTER NOZZLE	INNER NOZZLE	OUTER NOZZLE	INNER NOZZLE
Type	20-Chute	Annular	20-Chute	Annular
A_{flow}, in.^{2}	22.75	4.747	19.88	4.00
$D_{flow, eq.}$, in.	5.382	2.458	5.03	2.25
Area Ratio-Suppressor	1.775	-	1.75	-
Radius Ratio	.719	.926	.718	.941
Throat Plane ∡ Re Vert., Degrees	0	15	0	15
Plug Truncation	-	Sharp Tip	-	Truncated
A_{TOTAL}, in.^{2}	27.497		23.88	
D_{TOTAL}, eq., in.	5.917		5.514	
A_{inner}/A_{outer}	.21		.20	

The primary differences between the two nozzles are a) chute cross section contours, b) contour-truncated plug termination versus sharp-tipped truncation, and c) flow areas. The difference in flow areas is compensated for within the method of scaling to a full size engine; described in Section 3.1.

4.1.2.2 Acoustic Comparison of Configuration TE-1 to Model 10.1 and to Conic

On the basis of normalized power level, per Figure 4-15, the new TE-1 configuration is seen to be approximately 1 dB noisier than the previous Model 10.1 at static. In flight, it has slightly higher total acoustic energy at low and intermediate velocities, is similar at takeoff, and just slightly lower at max cycle.

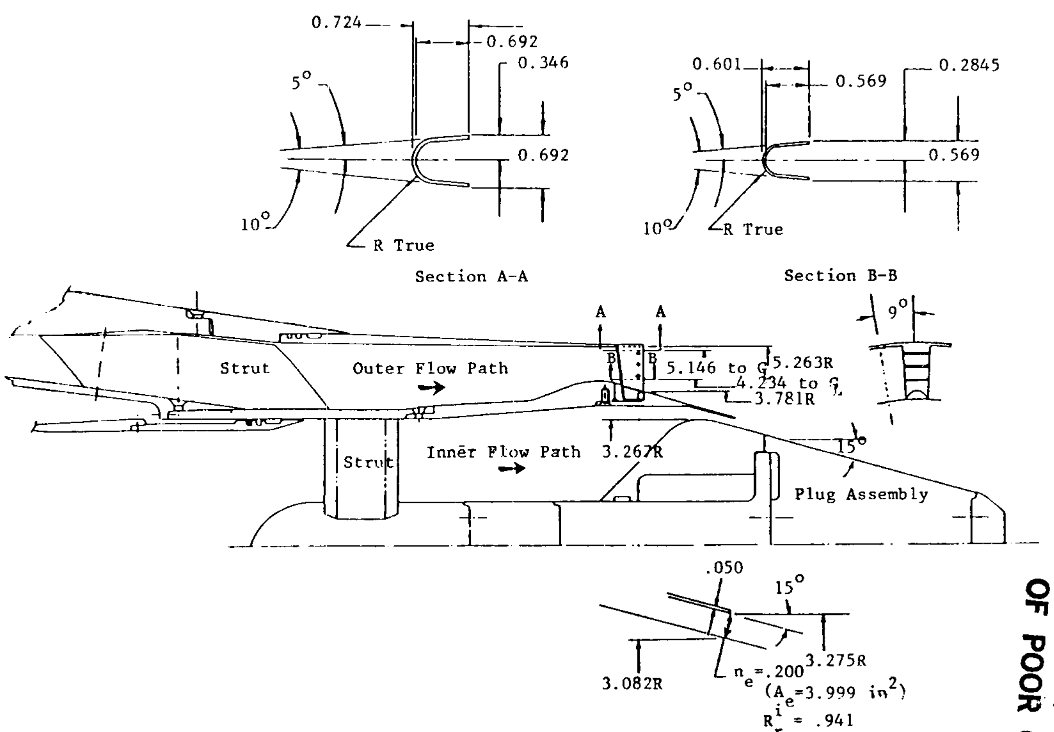

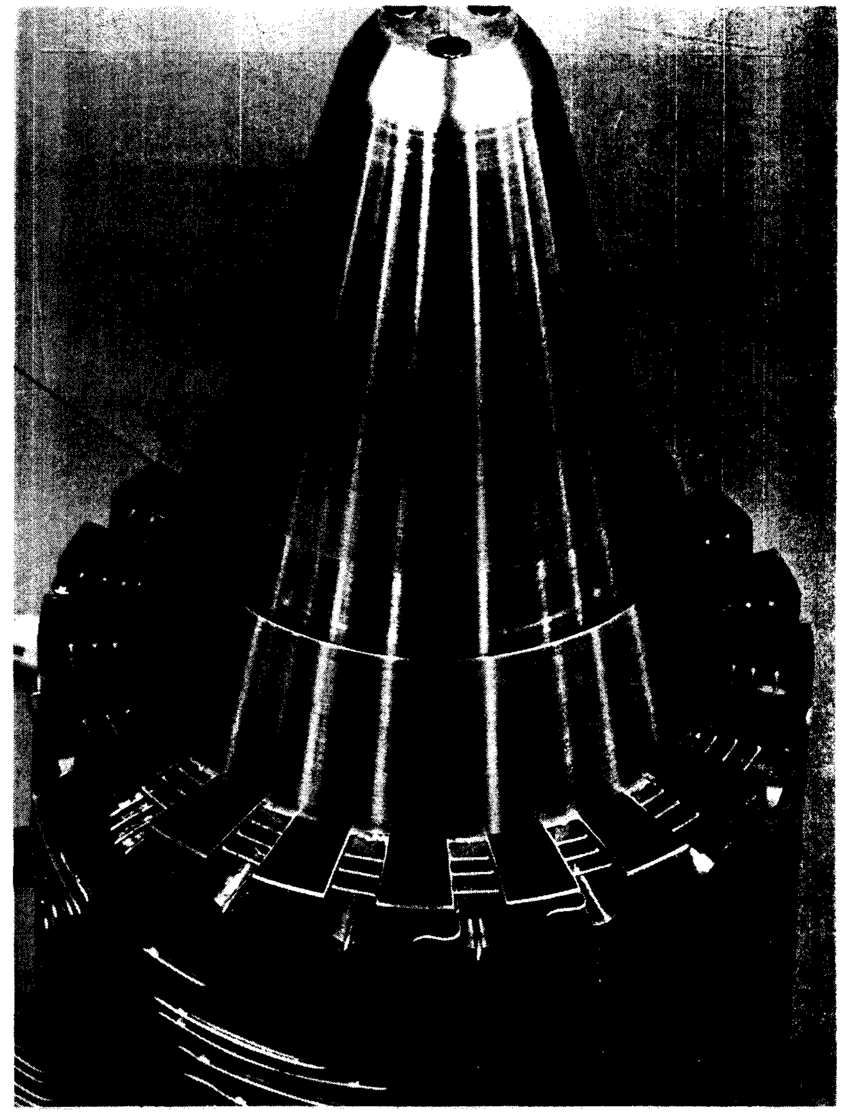

FIGURE 4-14. CONTRACT NAS3-21608 MODEL 10.1 COANNULAR INVERTED-VELOCITY-PROFILE NOZZLE WITH 20-CHUTE OUTER STREAM SUPPRESSOR

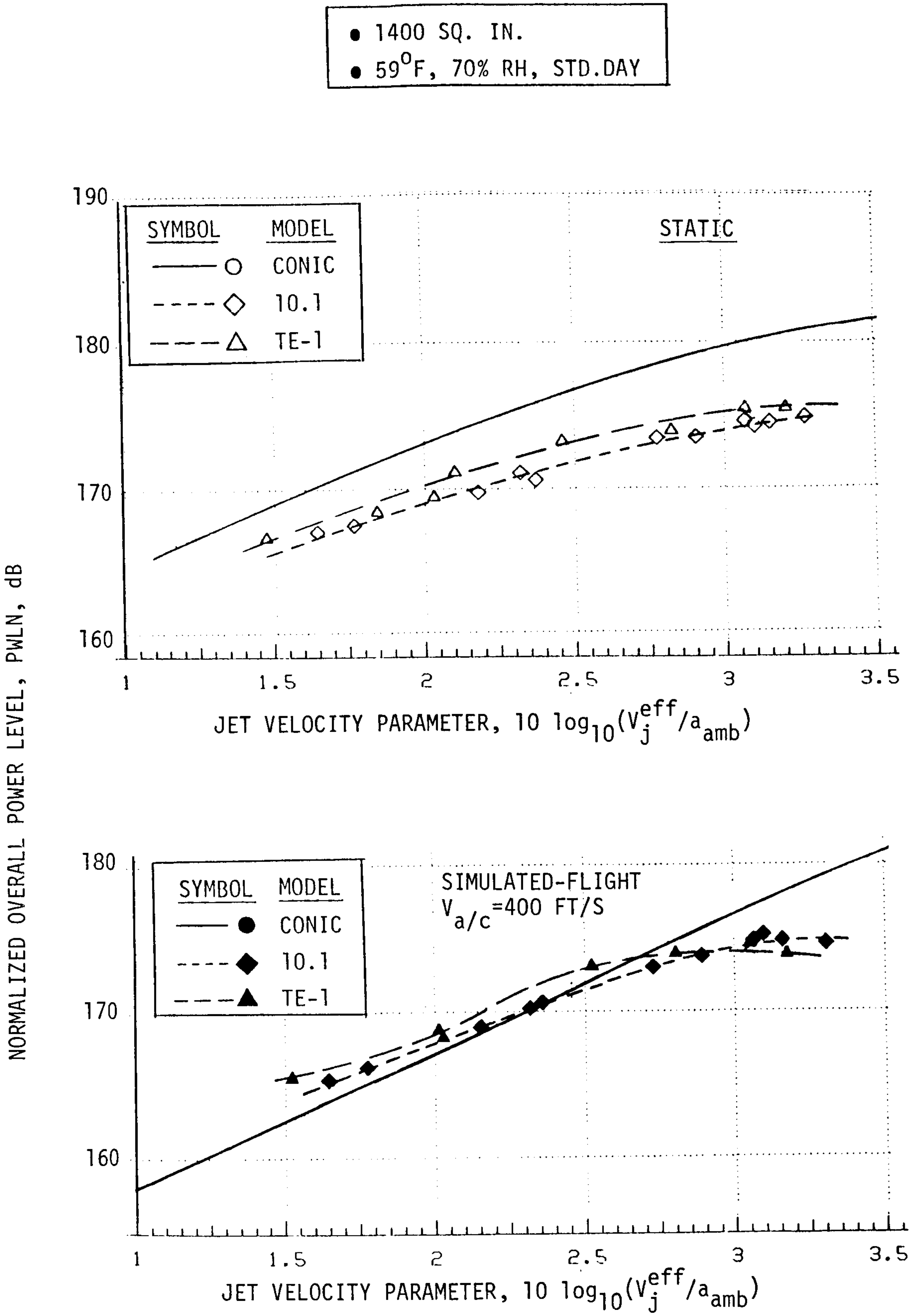

FIGURE 4-15 NORMALIZED PWL AS A FUNCTION OF JET VELOCITY PARAMETER FOR COMPARISON OF CONFIGURATION TE-1 TO MODEL 10.1, STATIC AND SIMULATED-FLIGHT

A second basis of comparison is presented in Figures 4-16 through 4-19; normalized OASPL and PNL versus jet velocity parameter for static and flight at θ_I = 60°, 90°, 130° and peak value. On a peak noise level basis, the two configurations are very repetitive in suppression level, the nominal suppression levels relative to a conic nozzle summarized at the takeoff and cutback cycles as follows:

	$(10\log_{10}(V_j^{mix}/a_{amb}))$	ΔPOASPL		ΔPPNL	
		Static	Flight	Static	Flight
Takeoff	≈ 3.0	11.2	10.7	10.5	5.8
Cutback	≈ 2.1	11.3	7.5	6.2	0.5

At broadside, θ_I = 90°, and forward quadrant, θ_I = 60°, the TE-1 OASPL and PNL levels are normally slightly above those of Model 10.1

More thorough noise level comparisons at cutback, intermediate and takeoff are afforded in the following graphs:

- o Figures 4-20, 4-23 and 4-26: Directivity patterns of OASPL and PNL at cutback, intermediate, and takeoff cycles, respectively, for both static and flight.

- o Figures 4-21/-22, 4-24/-25 and 4-27/-28: Sets of spectra at θ_I = 60°, 90° and 130° for cutback, intermediate and takeoff, respectively, for both static and flight.

The data comparisons indicate, in general:

- o Peak noise levels are very similar for TE-1 and 10.1 for all comparisons.

- o Forward quadrant noise levels are normally slightly higher for TE-1 and aft quadrant levels are normally slightly lower.

- o Spectra comparisons generally indicate very similar frequency distribution of noise levels with no major shape differences. Minor differences between TE-1 and 10.1 are seen for all static and flight comparisons and all cycle points, but no consistent pattern is obvious. The most consistent data repetition is at the highest takeoff cycle comparison.

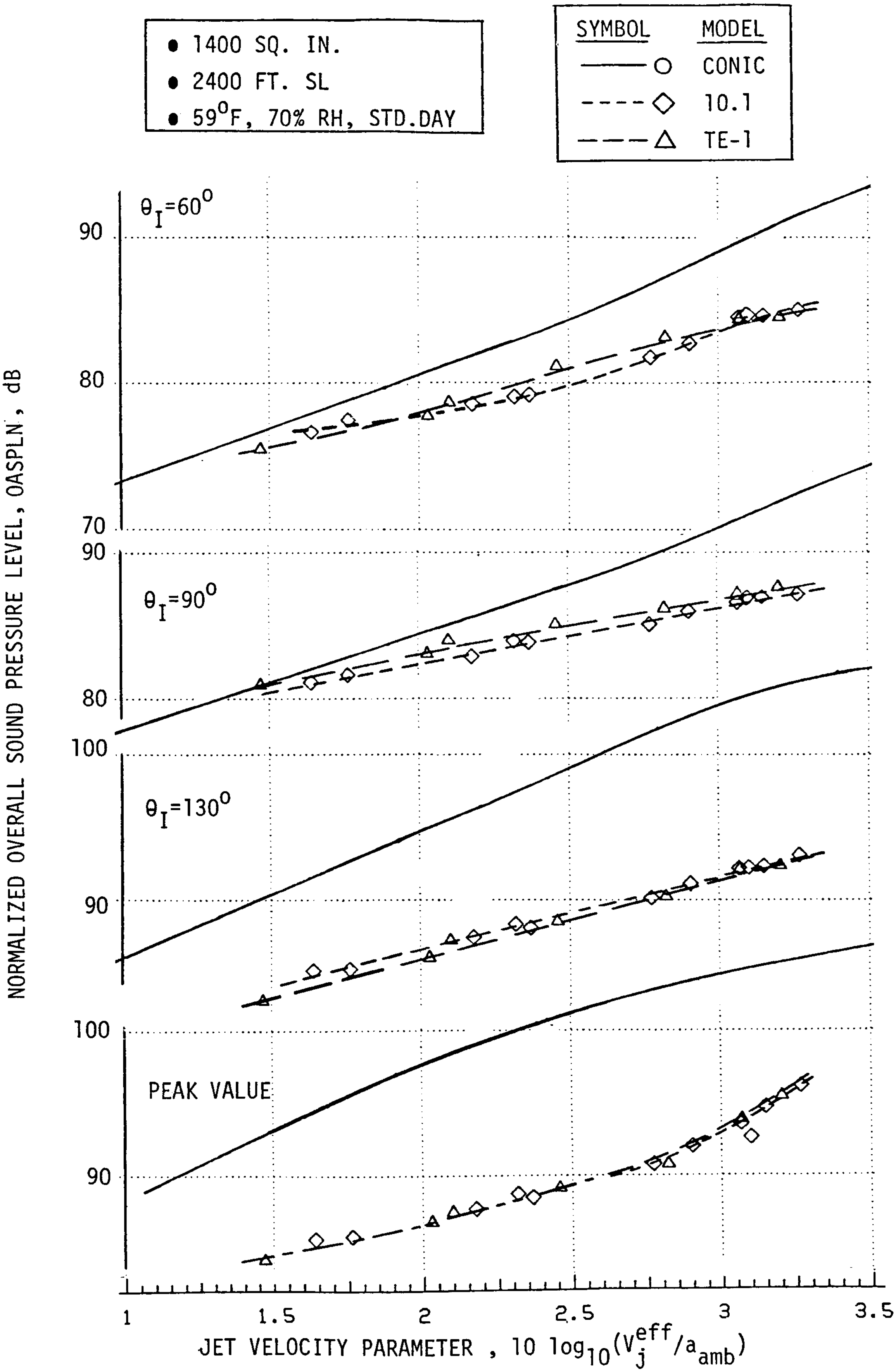

FIGURE 4-16 NORMALIZED OASPL AS A FUNCTION OF JET VELOCITY PARAMETER FOR COMPARISON OF CONFIGURATION TE-1 TO MODEL 10.1, STATIC, AT $\theta_I = 60^0$, 90^0, 130^0, and PEAK VALUE

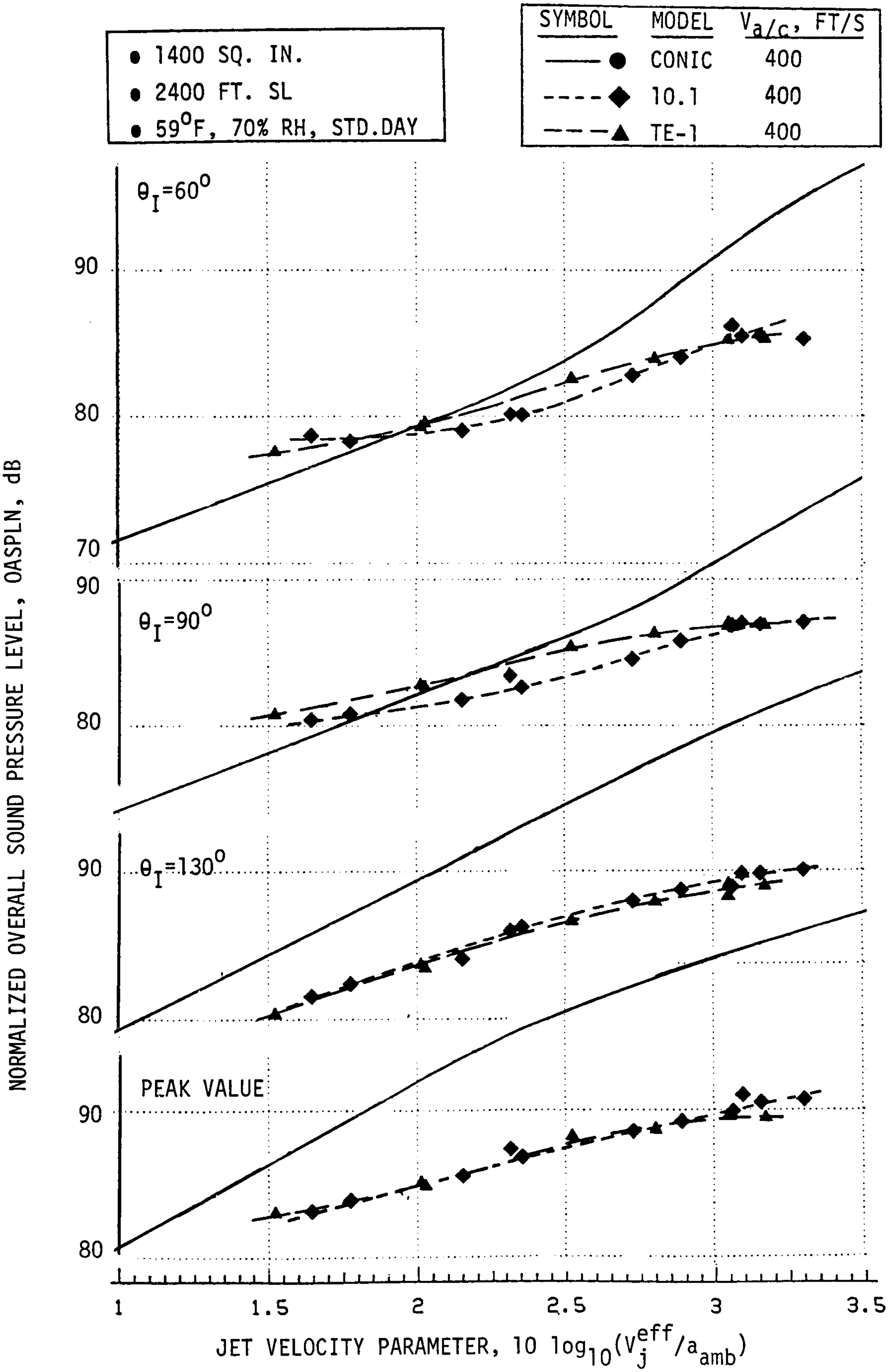

FIGURE 4-17 NORMALIZED OASPL AS A FUNCTION OF JET VELOCITY PARAMETER FOR COMPARISON OF CONFIGURATION TE-1 TO MODEL 10.1, SIMULATED-FLIGHT, AT θ_I=60°, 90°, 130° AND PEAK VALUE

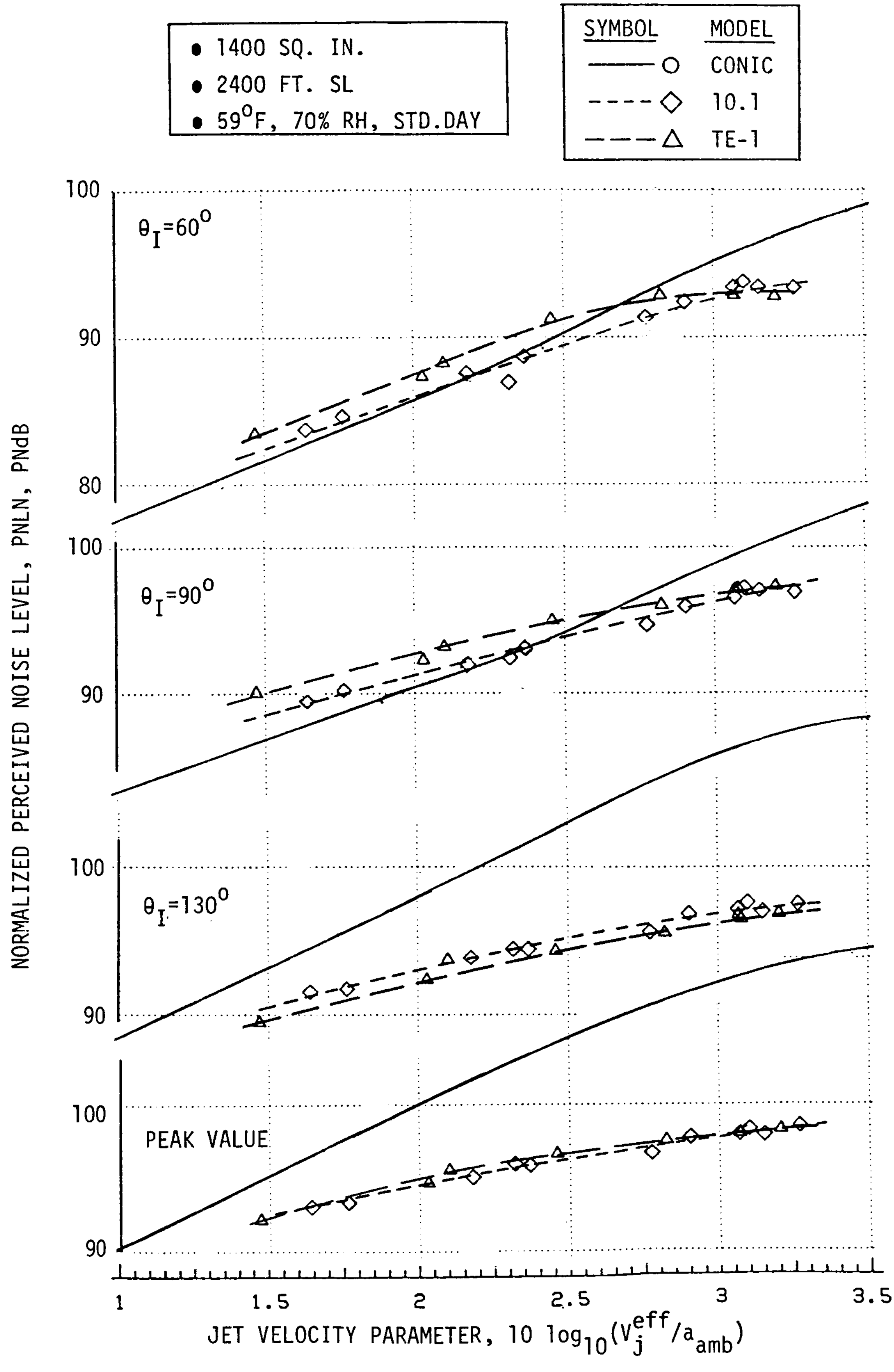

FIGURE 4-18 NORMALIZED PNL AS A FUNCTION OF JET VELOCITY PARAMETER FOR COMPARISON OF CONFIGURATION TE-1 TO MODEL 10.1, STATIC, AT θ_I =60°, 90°, 130° AND PEAK VALUE

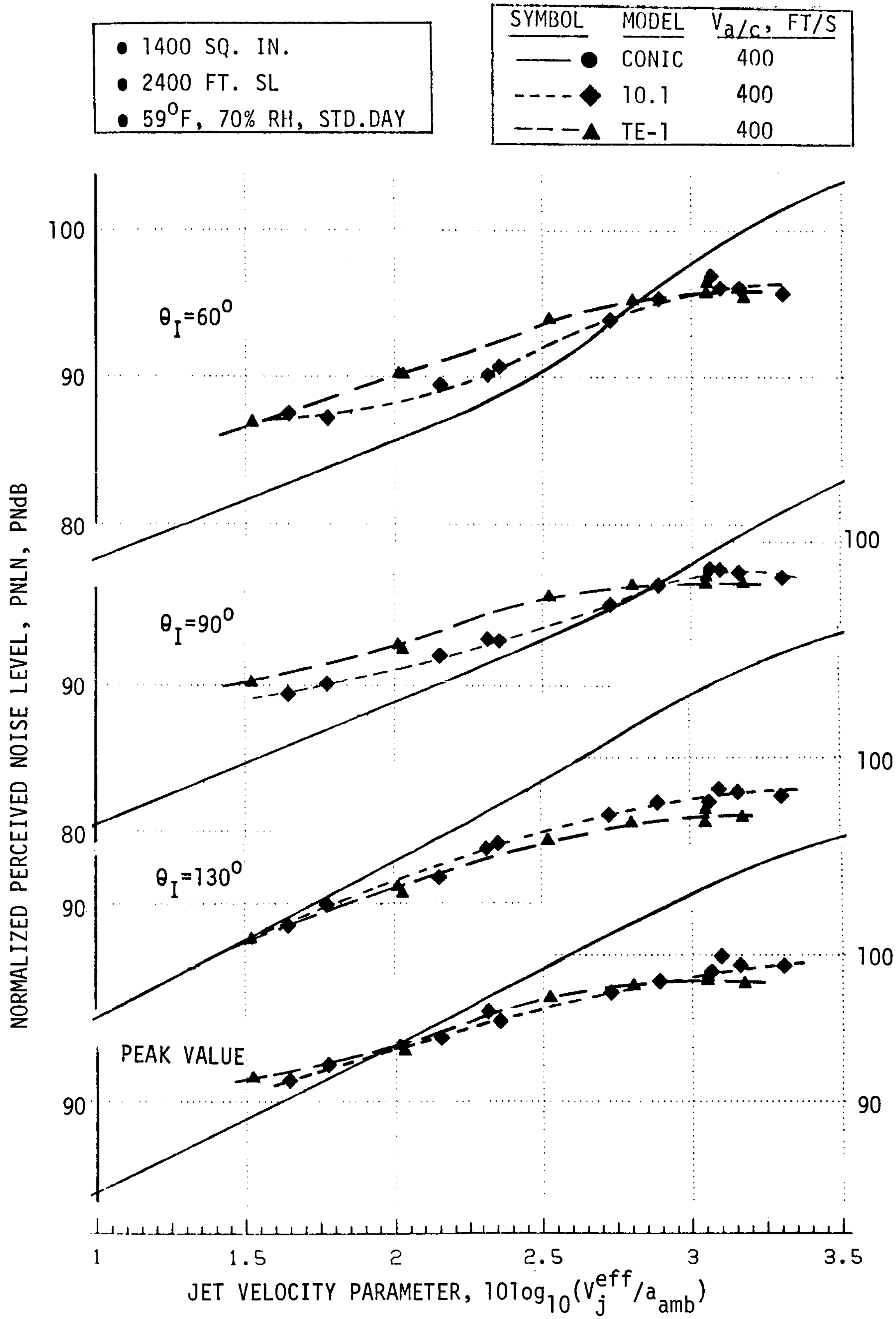

FIGURE 4-19 NORMALIZED PNL AS A FUNCTION OF JET VELOCITY PARAMETER FOR COMPARISON OF CONFIGURATION TE-1 TO MODEL 10.1, SIMULATED-FLIGHT, AT θ_I=60°, 90°, 130° AND PEAK VALUE

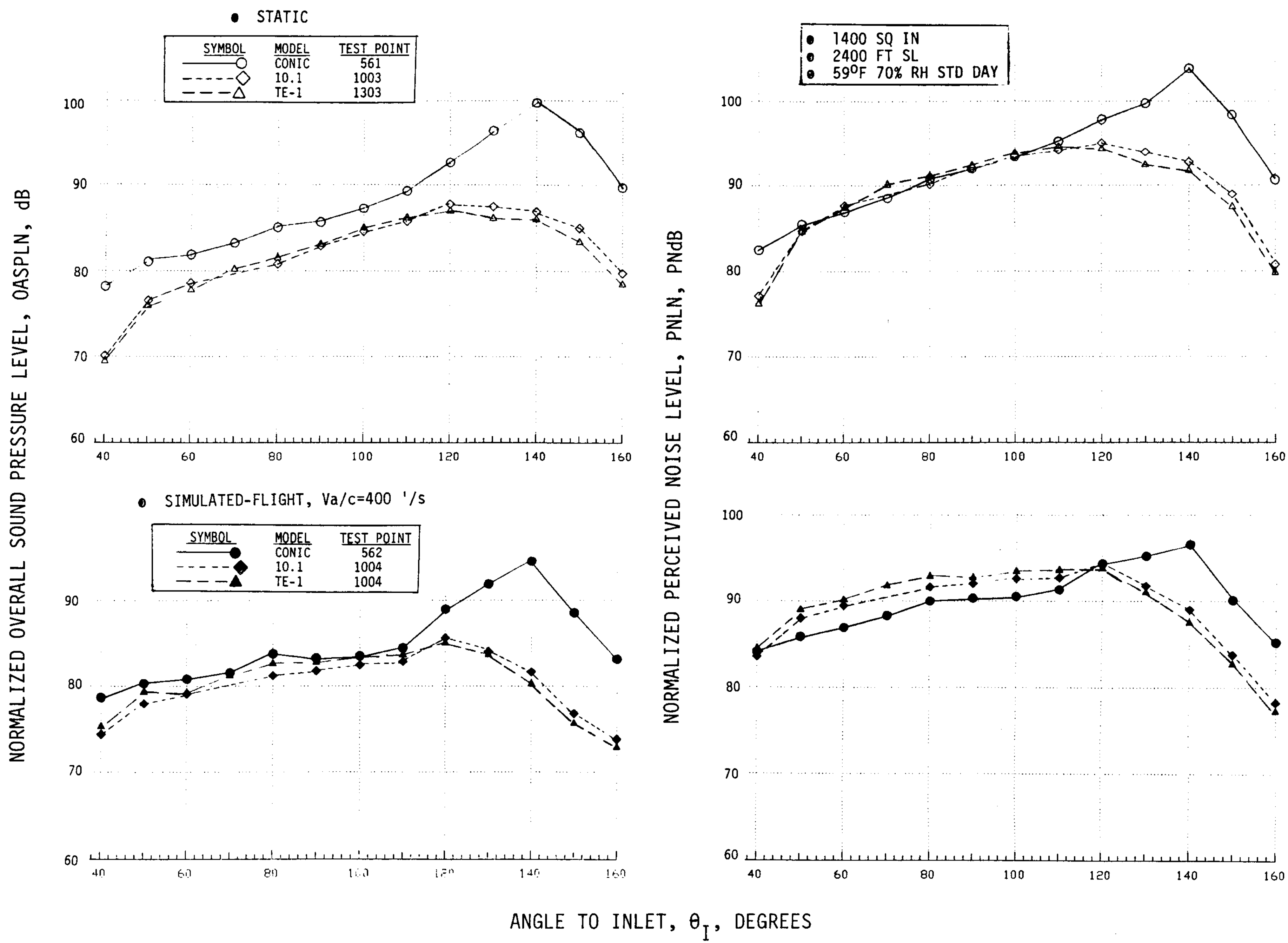

• STATIC
SYMBOL MODEL TEST POINT
CONIC 561
10.1 1003
TE-1 1303
• SIMULATED-FLIGHT, Va/c=400 '/s
SYMBOL MODEL TEST POINT
CONIC 562
10.1 1004
TE-1 1004
• 1400 SQ IN
• 2400 FT SL
• 59°F 70% RH STD DAY
NORMALIZED OVERALL SOUND PRESSURE LEVEL, OASPLN, dB
NORMALIZED PERCEIVED NOISE LEVEL, PNLN, PNdB
ANGLE TO INLET, θI, DEGREES

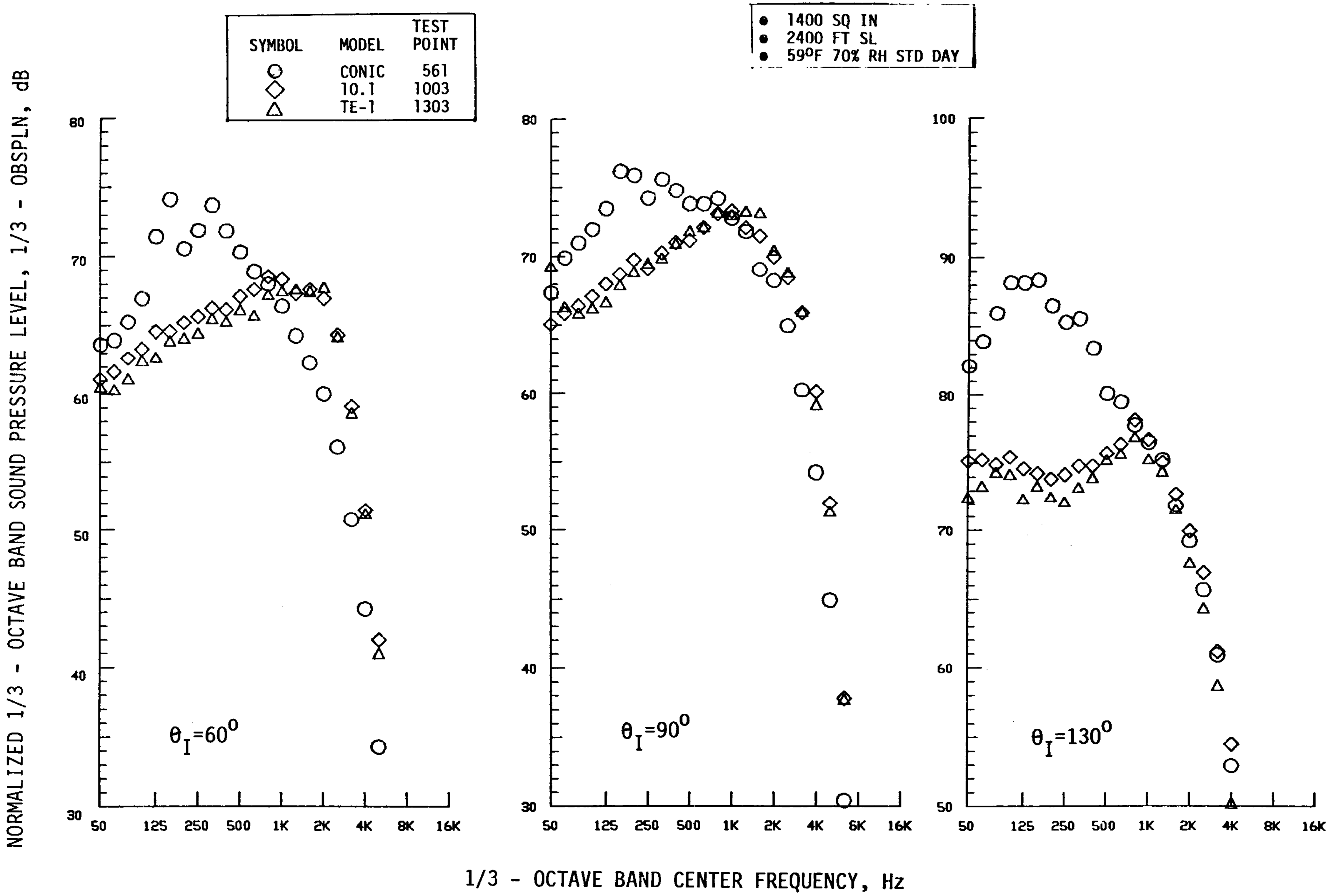

FIGURE 4-21. NORMALIZED SPECTRA AT $\theta_I=60^0$, 90^0 & 130^0 FOR COMPARISON OF CONFIGURATION TE-1 TO MODEL 10.1 AT CUTBACK, STATIC

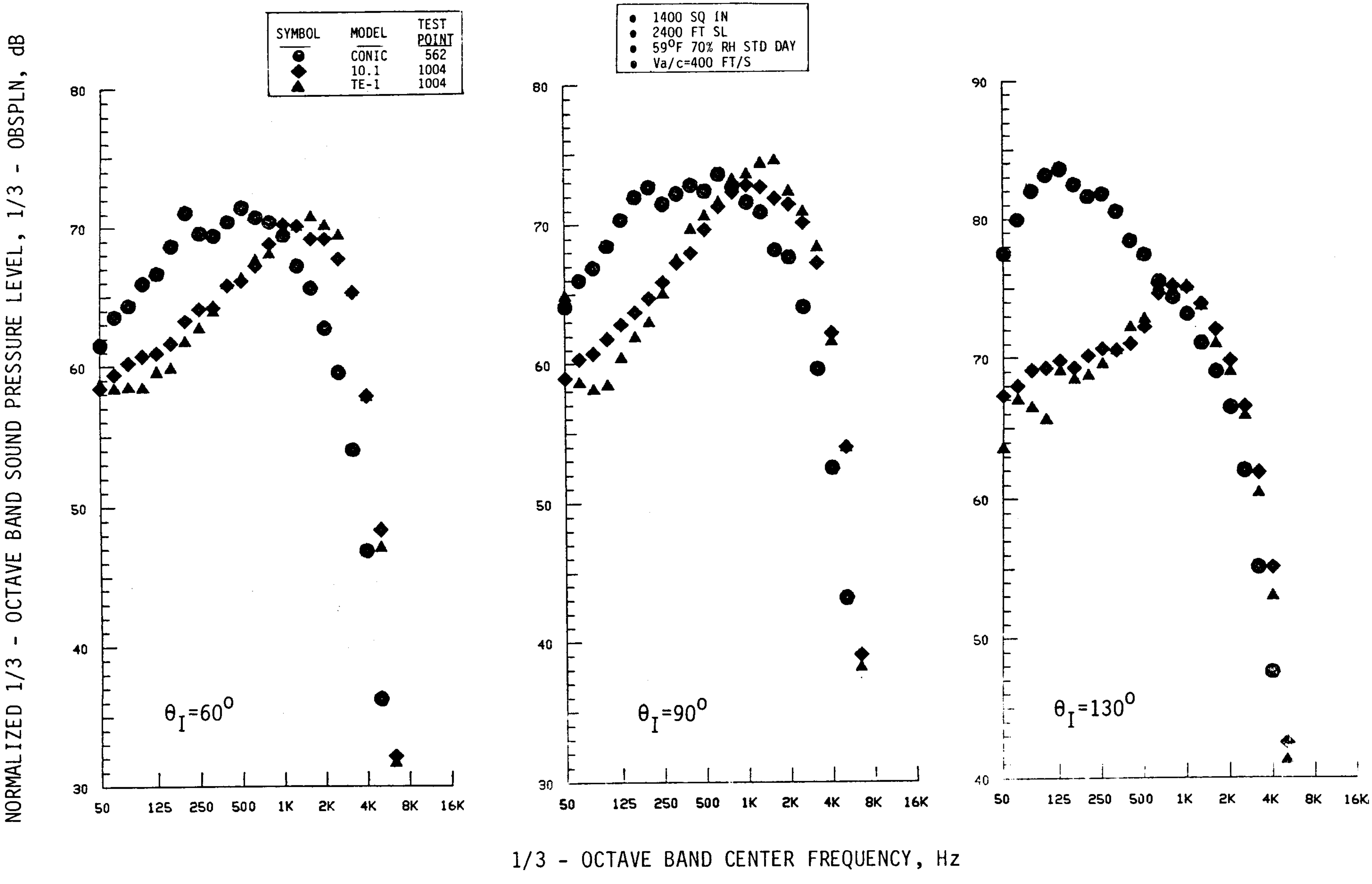

FIGURE 4-22. NORMALIZED SPECTRA AT $\theta_I=60^0$, 90^0 & 130^0 FOR COMPARISON OF CONFIGURATION TE-1

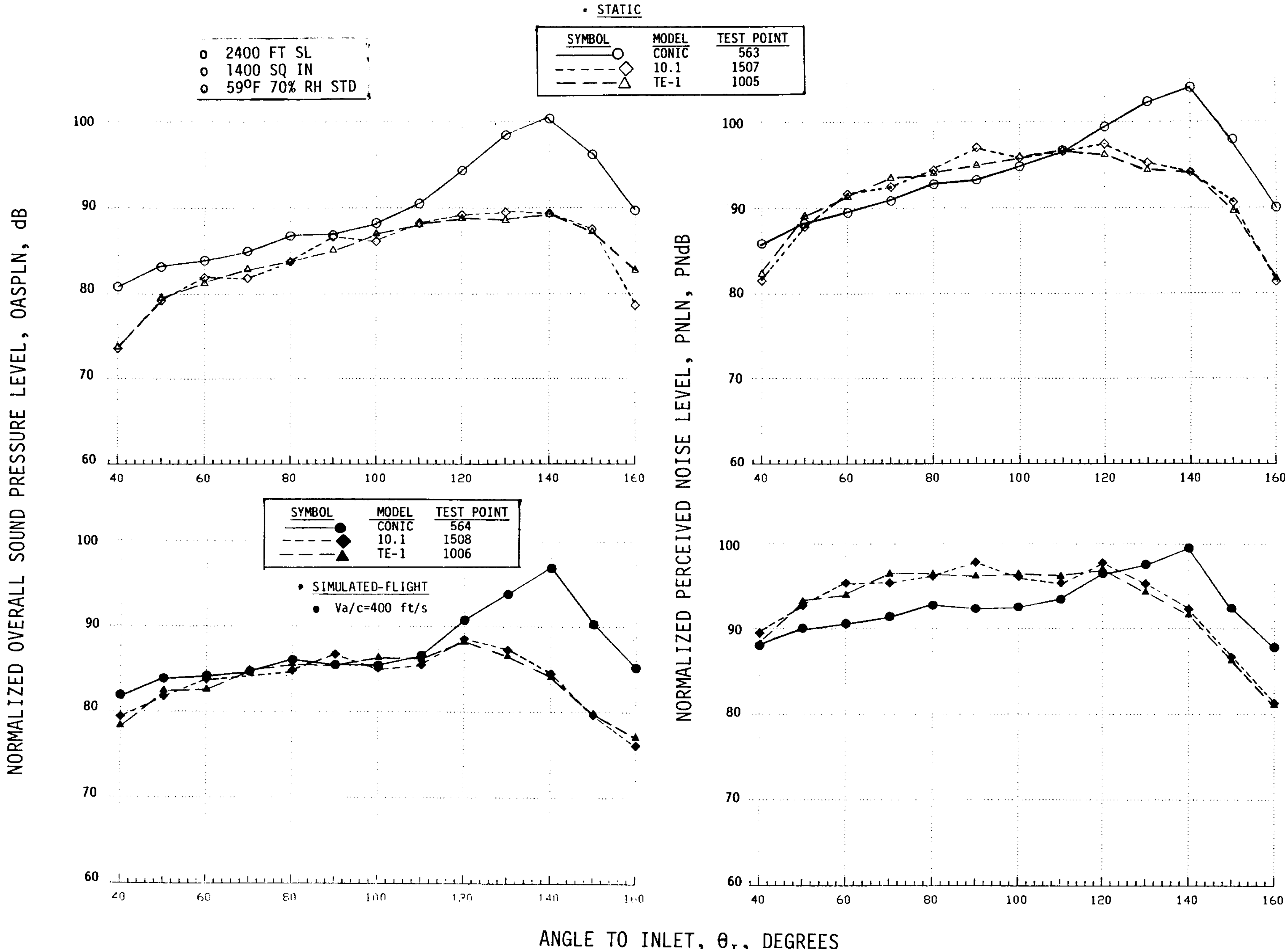

FIGURE 4-23. STATIC AND SIMULATED FLIGHT DIRECTIVITY COMPARISONS OF OASPL AND PNL AT INTERMEDIATE FOR COMPARISION OF CONFIGURATION TE-1 TO MODEL 10.1.

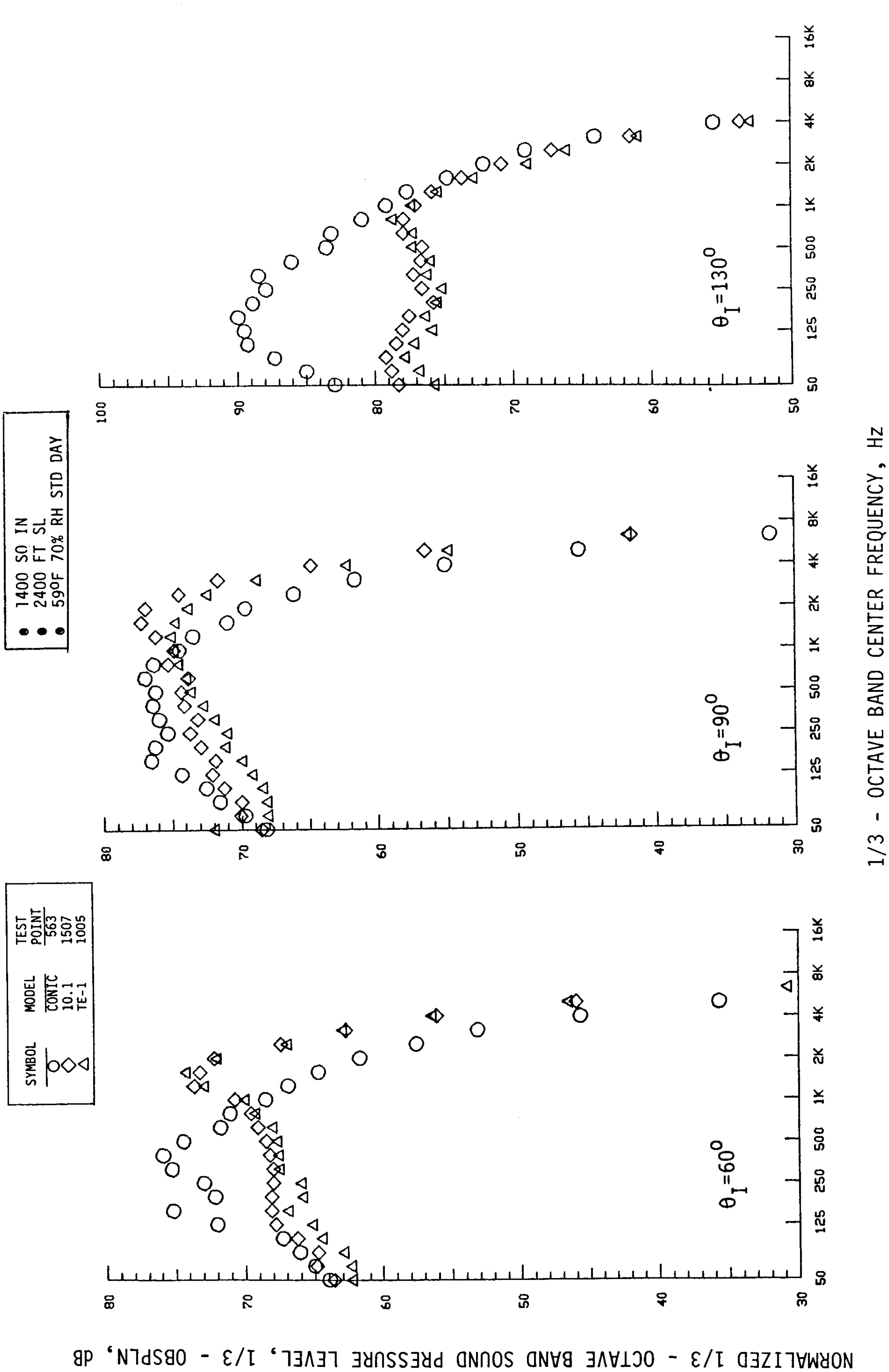

SYMBOL MODEL TEST POINT
○ CONIC 563
◇ 10.1 1507
△ TE-1 1005
1400 SQ IN
2400 FT SL
59°F 70% RH STD DAY
θI=60°
θI=90°
θI=130°
1/3 - OCTAVE BAND CENTER FREQUENCY, Hz
NORMALIZED 1/3 - OCTAVE BAND SOUND PRESSURE LEVEL, 1/3 - OBSPLN, dB

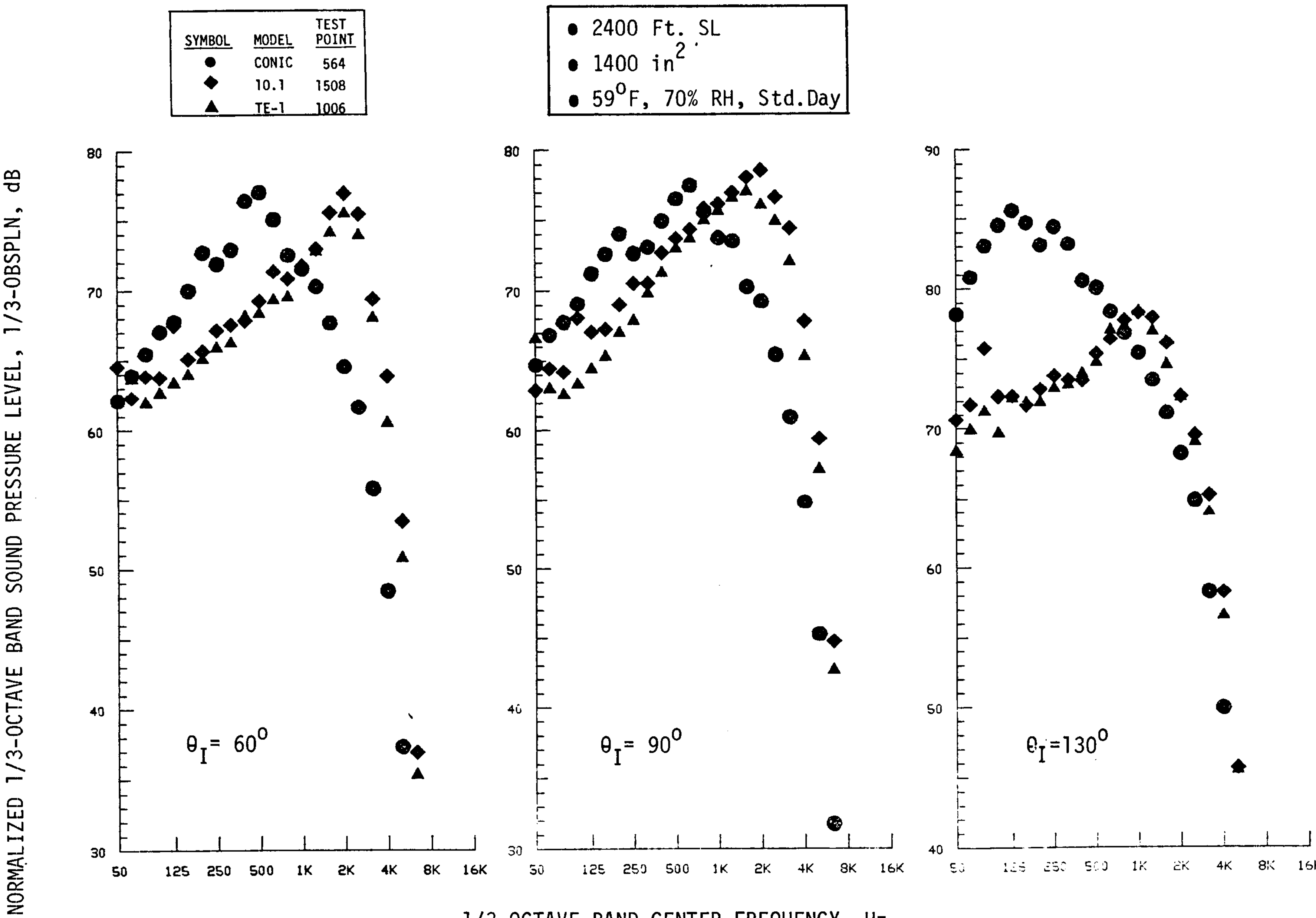

FIGURE 4-25 NORMALIZED SPECTRA AT θ_I=60°, 90°, AND 130° FOR COMPARISON OF CONFIGURATION TE-1 TO MODEL 10.1 AT INTERMEDIATE, SIMULATED-FLIGHT

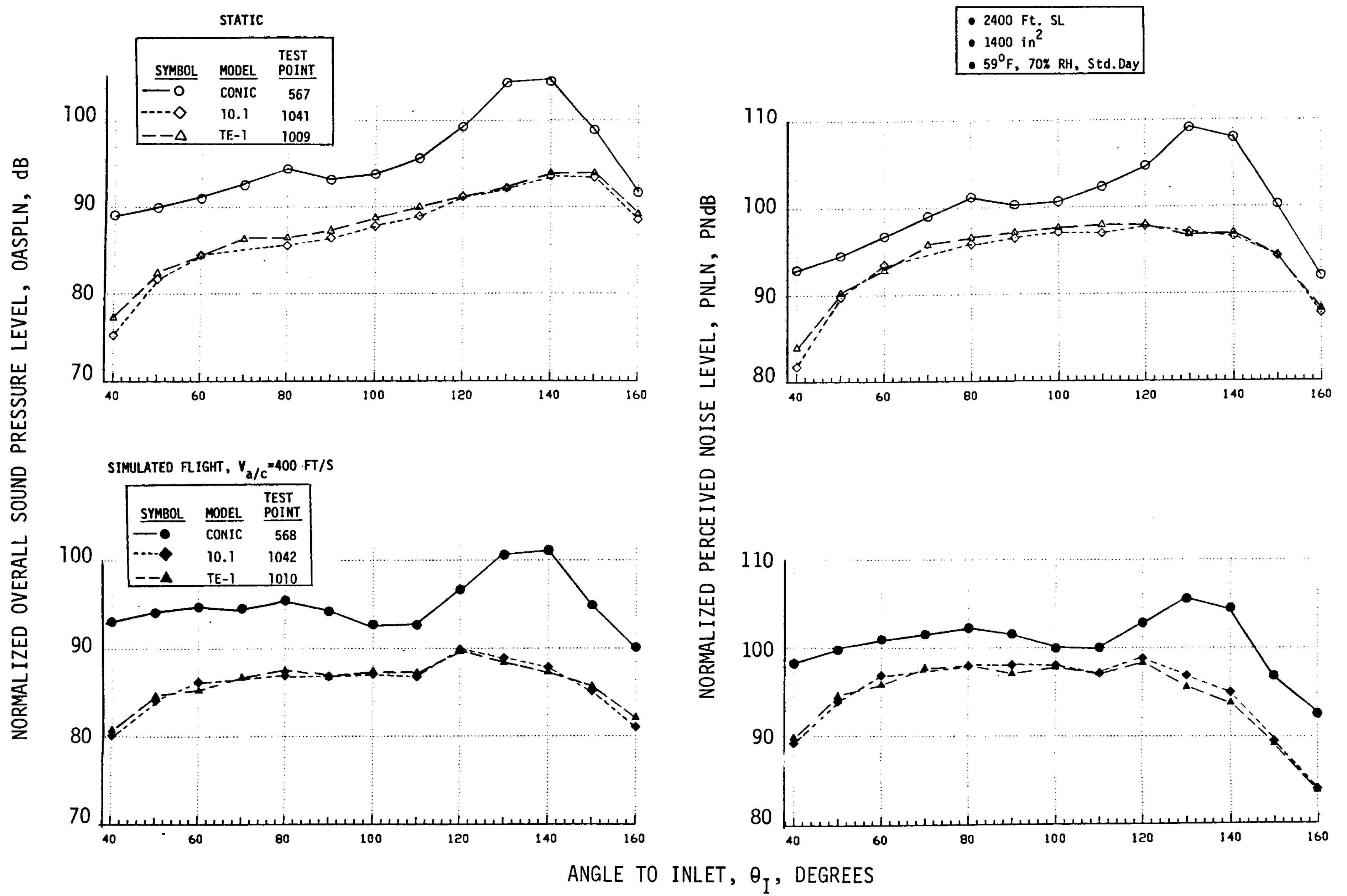

FIGURE 4-26 STATIC AND SIMULATED-FLIGHT DIRECTIVITY COMPARISONS OF OASPL AND PNL AT TAKEOFF FOR COMPARISON OF CONFIGURATION TE-1 TO MODEL 10.1

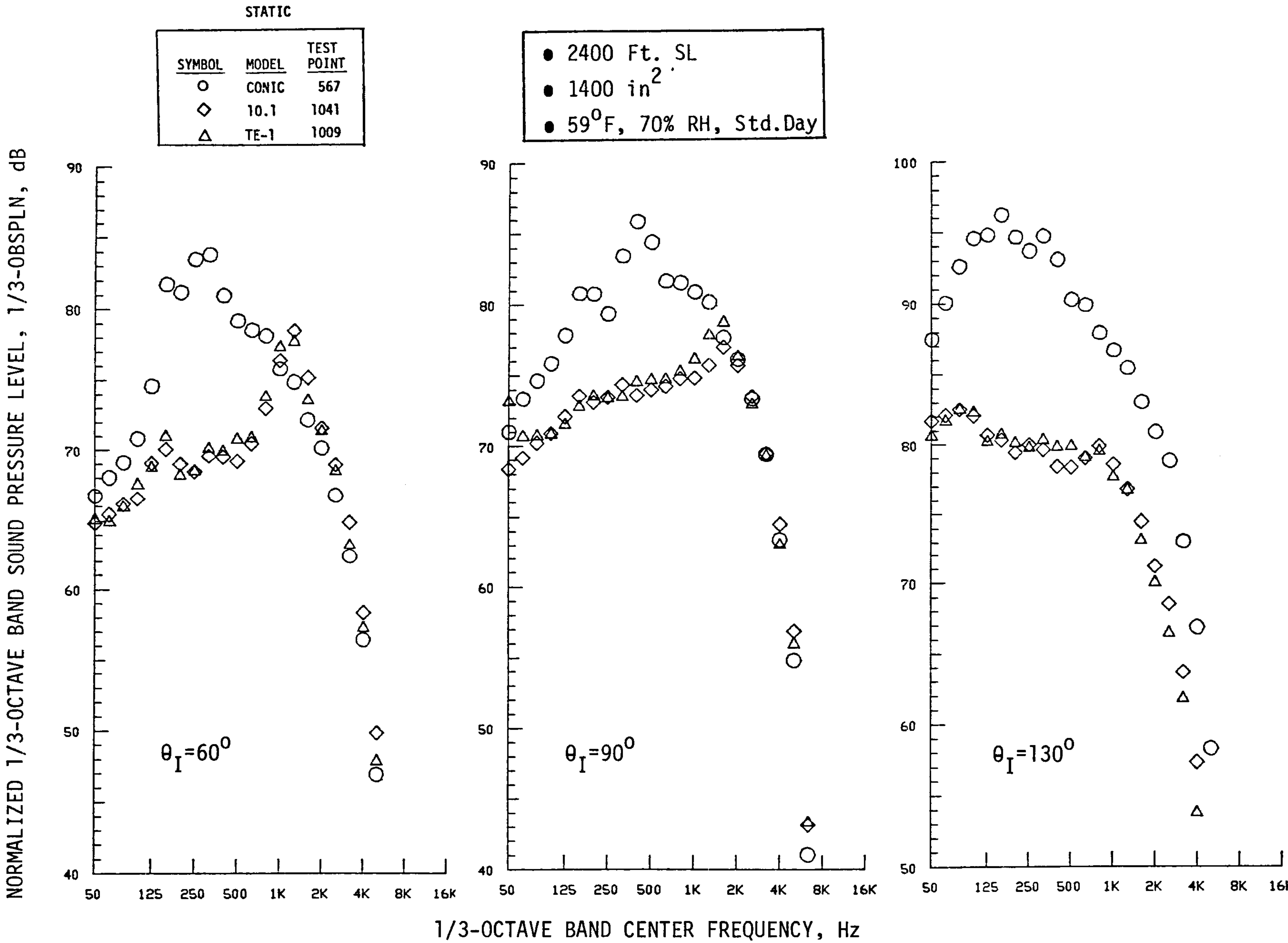

FIGURE 4-27 NORMALIZED SPECTRA AT θ_I=60^0, 90^0, AND 130^0 FOR COMPARISON OF CONFIGURATION TE-1 TO MODEL 10.1 AT TAKEOFF, STATIC

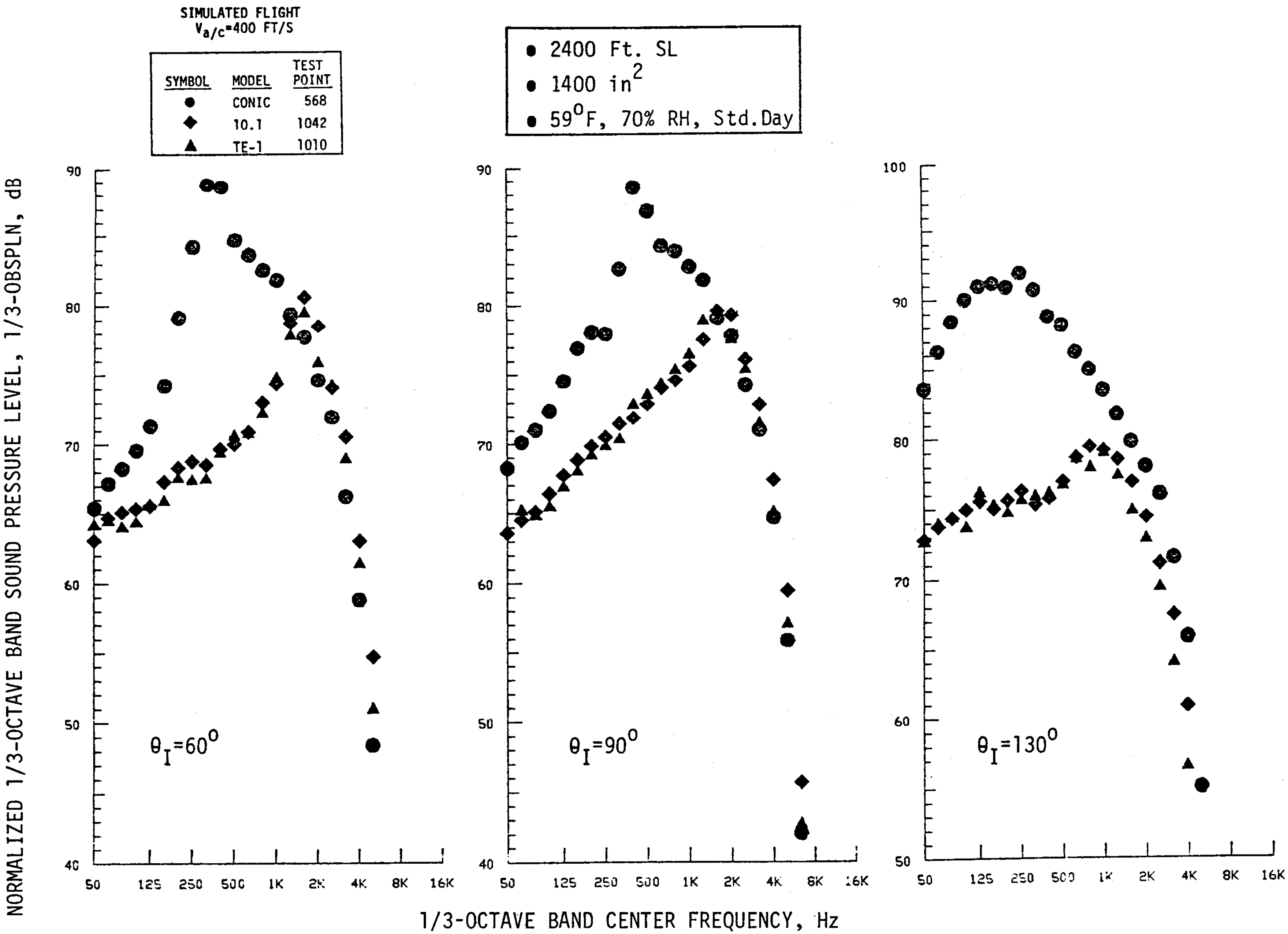

FIGURE 4-28 NORMALIZED SPECTRA AT $\theta_I=60^0$, 90^0, and 130^0 FOR COMPARISON OF CONFIGURATION TE-1 TO MODEL 10.1 AT TAKEOFF, SIMULATED-FLIGHT

- The suppressor nozzle spectra, particularly at takeoff, show less of a peakness than the conic nozzle. The conic nozzle spectra are very peaked at 400 to 500 Hz from broadband shock noise. The suppressor spectra do show a slight peak at 1250 to 1600 Hz, possibly from the shadowgraph-observed less intense shock structure.

As a gauge of shock noise control effectiveness, Figures 4-29 and 4-30 present measured OASPL and PNL as a function of shock strength parameter, β . To directly gauge changes relative to a reference nozzle, conic nozzle correlations of Section 4.1.1's Figures 4-10 and 4-11 are included. Also, to directly evaluate impact of simulated-flight, data are correlated for both static and flight for conic, TE-1 and 10.1. Reviewing the two figures, the following are noteworthy:

- Forward quadrant noise levels, particularly at higher values of β (higher nozzle pressure ratio) are very substantially reduced by the multi-element suppressor nozzle systems. As an example, at $\theta_I = 60^o$ for takeoff cycle ($10 \log_{10} \beta = 0.1$), OASPL is reduced by 7 dB static and 12 dB flight whereas PNL are reduced by 5 dB static and 7 dB flight. Suppression levels relative to conic are less at lower β values as shock noise is less dominant at lower pressure ratio.

- Suppressor nozzles' forward quadrant data correlate at a much lower slope, i.e., β dependency, than do conic measurements, again indicative of the sharp reduction in shock noise content. Conic nozzle data correlated with β within a range of a 4.2 to 5.1 power for static and 5.2 to 6.4 for flight. TE-1 and 10.1 data correlate with β to the 2.0 to 3.0 power for OASPL and PNL, static and flight.

- For both OASPL and PNL, static and flight, TE-1 forward quadrant levels are seen to be equivalent to slightly higher than those of 10.1, indicative of no further reduction of shock cell noise, as originally hoped for during design.

  A review of the comprehensive data report's (Reference 3) shadowgraph documentation for TE-1 test points 1009 and 1010 shows fairly strong shock structure just aft of the suppressor nozzle exit plane, for the extent of the plug structure, but no shock structure aft of the plug tip. The shock structure is not as intense as conic nozzle shock at similar jet Mach No.

- As noted previously, shock cell noise spectrum suffers a dynamic effect of $-10 \text{Log}_{10} (1 - M_o \cos \theta_I)$ due to flight; far forward quadrant levels are more highly amplified by flight. Therefore, the flight noise correlated data lines should progressively increase in level above the static lines as viewed from θ_I of 90^o toward 50^o; presuming shock noise is present. This progression is very dramatically seen for the conic nozzle, for OASPL and PNL; flight data lines being near similar to static at $\theta_I = 90^o$ and progressing to well above static at 50^o. The slopes of the flight data lines also increase due to the higher shock noise content at high β (pressure ratio) values. For the suppressor data, however, the progressively larger separation between flight and static data is not as readily observed nor is a noticable change in slope. This is attributed to the lower shock noise content. For OASPL, the static and flight levels are very similar from 90^o through 60^o and show slight increase at 50^o. For PNL the increase is more noticable for 80^o to 50^o as suppressor spectra are high frequency dominated and the slight amplification due to flight is more readily seen in the PNL weighting.

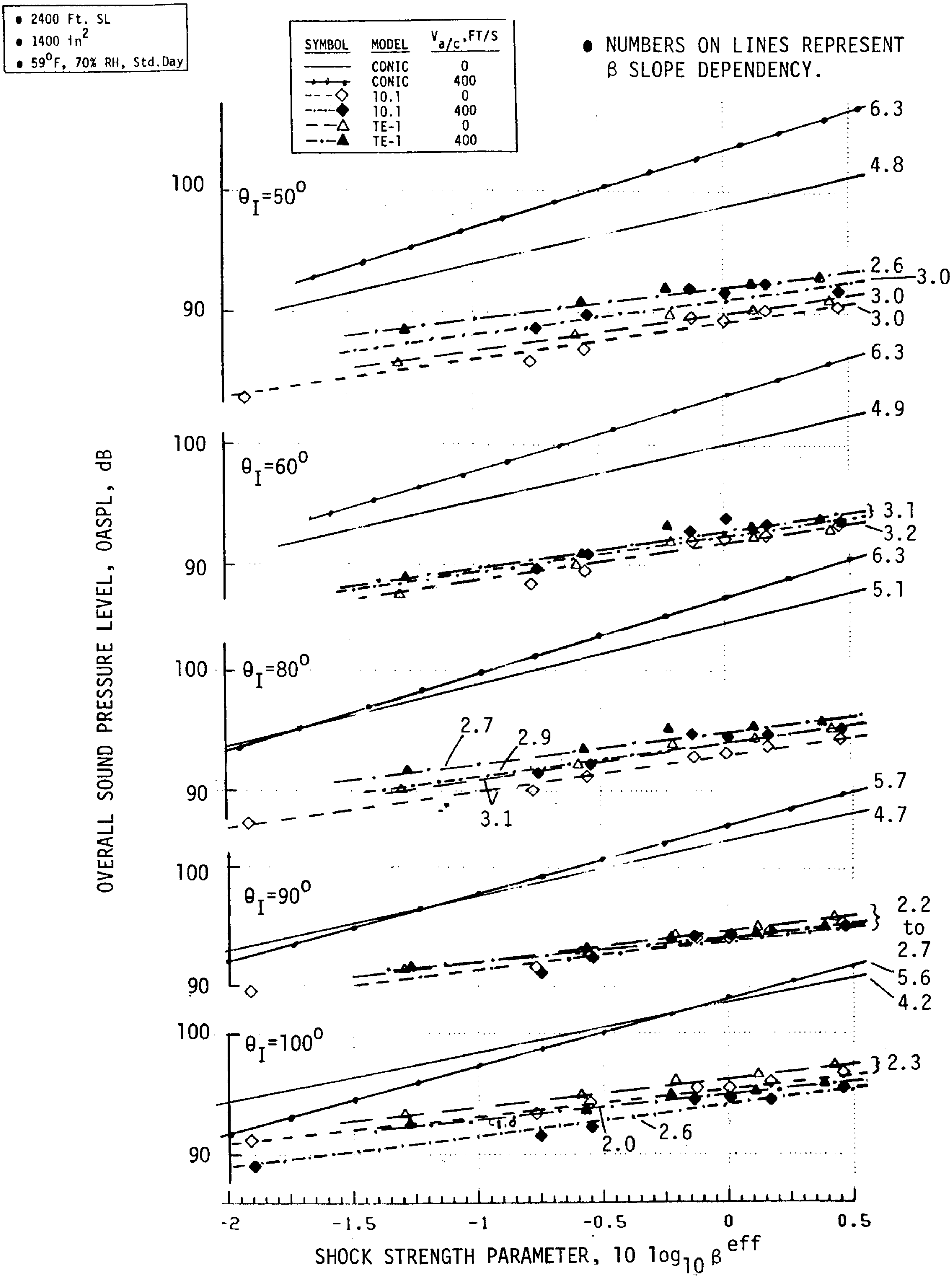

FIGURE 4-29 STATIC AND SIMULATED-FLIGHT CORRELATION OF FORWARD QUADRANT OASPL DEPENDENCY ON SHOCK STRENGTH PARAMETER FOR COMPARISON OF CONFIGURATION TE-1 TO MODEL 10.1

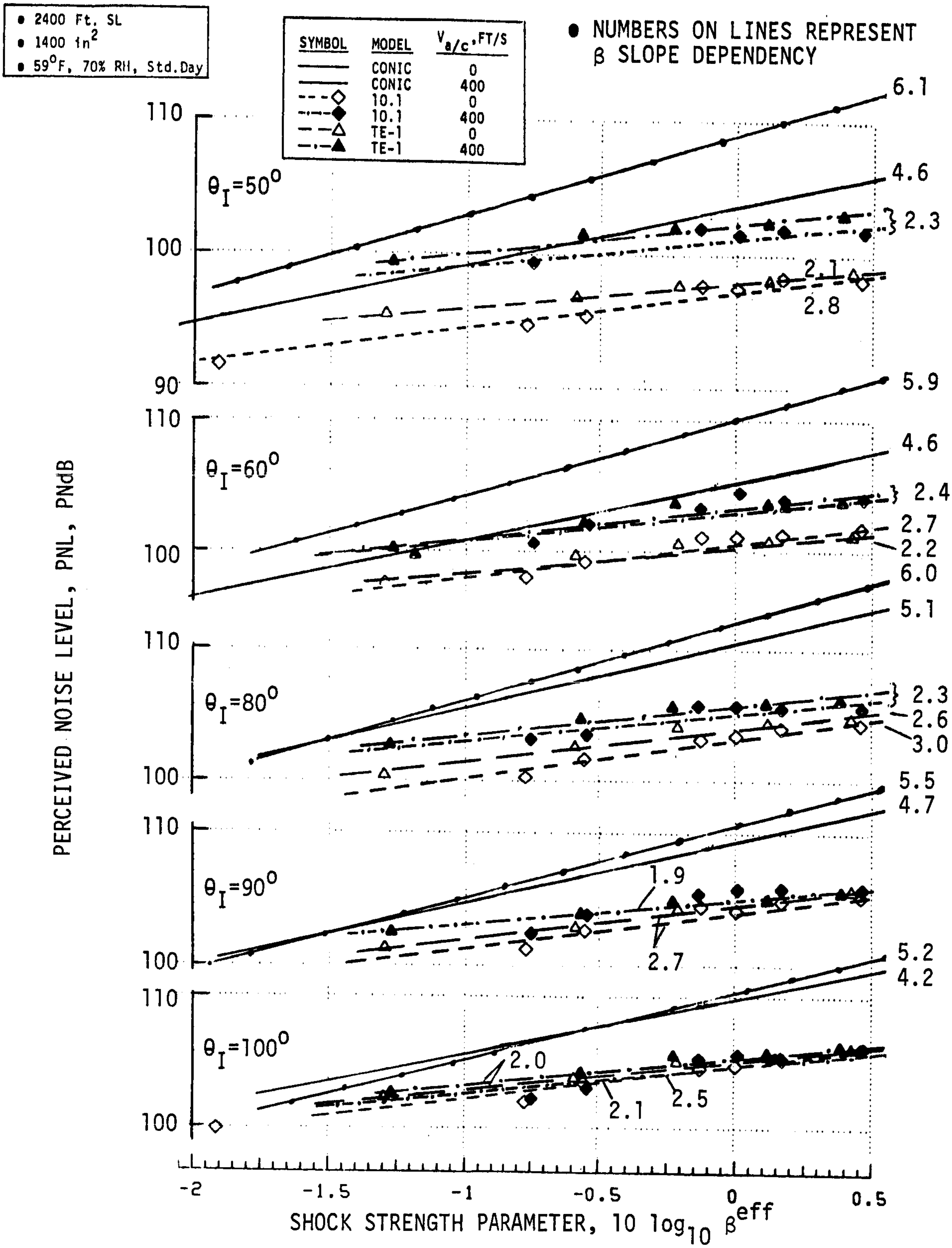

FIGURE 4-30 STATIC AND SIMULATED-FLIGHT CORRELATION OF FORWARD QUADRANT PNL DEPENDENCY ON SHOCK STRENGTH PARAMETER FOR COMPARISON OF CONFIGURATION TE-1 TO MODEL 10.1

Further comparisons for flight effect trends on the TE-1 suppressor are shown in Figures 4-31 through 4-34. Figure 4-31 presents directivity patterns of static and flight OASPL and PNL at cutback, intermediate and takeoff. Figures 4-32, -33 and -34 similarly present θ_I = 60°, 90° and 130° spectra. Flight influences observed are:

- o Aft angle OASPL and PNL, controlled by jet mixing noise, are all reduced by flight effects. Aft angle low-frequency spectra are very significantly reduced and high-frequency levels remain similar to slightly amplified.

- o Forward quadrant OASPL and PNL levels are all amplified by flight, by fairly similar levels for each cycle point. Conic nozzle trends of Figure 4-9 showed this forward quadrant magnitude of amplification to be cycle/pressure ratio/shock noise dependent. Forward quadrant high frequency spectra are all flight amplified and low frequency are lowered.

4.1.2.3 Diagnostic Data Presentation

As an indication of simulated-flight effects on jet plume characteristics, Figures 4-35 and 4-36 compare select laser velocimeter mean velocity traces for static and flight operation of Configuration TE-1 at takeoff. The axial traces of Figure 4-35, along and parallel to the nozzle centerline at three radial locations, in general show a stretching of the jet. This is due to reduced shear between the jet flow and the ambient medium. The mixing rates are lowered by flight motion and this tends to elongate or stretch-out the jet. Jet exit close proximity velocity levels are relatively unaffected, whereas higher velocity levels are maintained quite further aft. Figure 4-36, showing radial variations of mean velocity at select axial locations, mimics the trends of the axial traverse data, showing flight plume-velocity-levels to be near similar to static near the jet exhaust (with some slight peak variance possibly due to exact measurement location within the shock structure) and higher in level at all further aft locations.

4.1.2.4 Aerodynamic Base Pressure/Chute Drag Comparisons; TE-1 to 10-1

Figure 4-37 presents the Configuration TE-1 calculated thrust loss coefficient variance with outer stream pressure ratio (Refer to Section 4.7 for detailed method of calculation). Additionally, it compares Model 10.1 static data from Reference 8. The comparison indicates that the two model designs are essentially compatible in ability to ventilate the chute base region and, therefore, have near similar levels of thrust loss due to chute base drag.

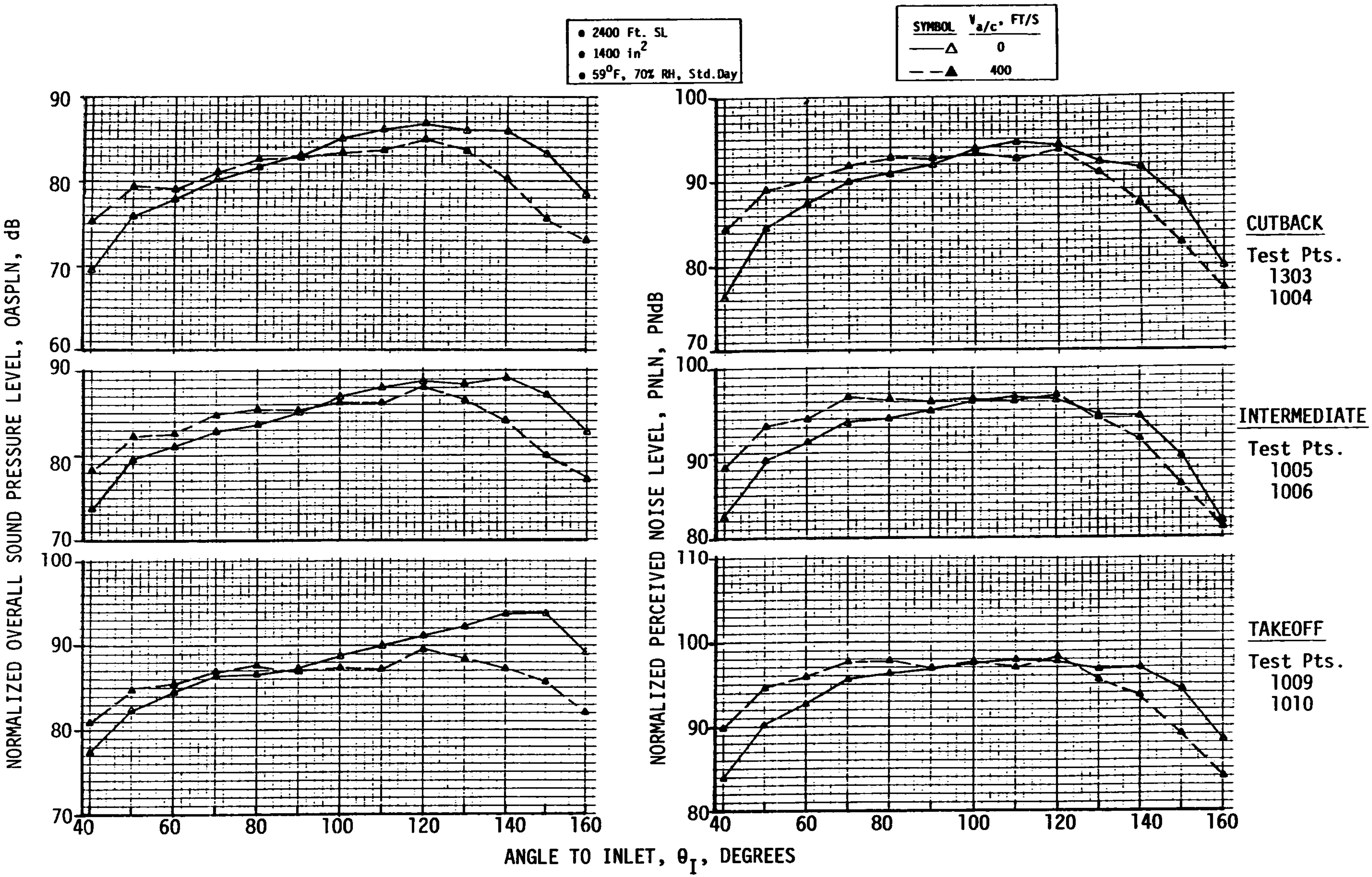

FIGURE 4-31 CONFIGURATION TE-1 STATIC-TO-FLIGHT DIRECTIVITY COMPARISON OF NORMALIZED OASPL AND PNL AT CUTBACK, INTERMEDIATE, AND TAKEOFF CYCLE

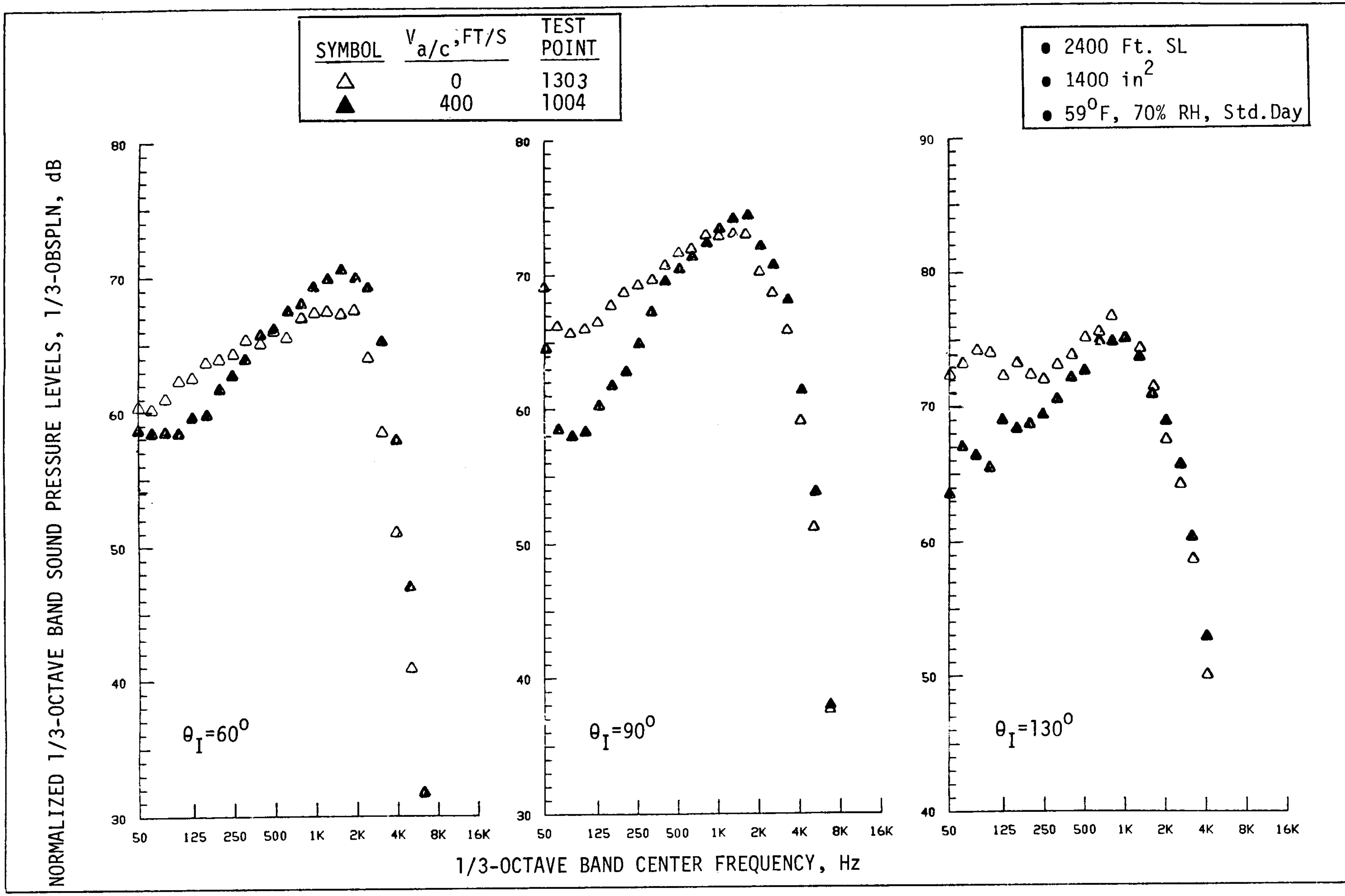

FIGURE 4-32 CONFIGURATION TE-1 STATIC-TO-FLIGHT NORMALIZED SPECTRA COMPARISONS AT CUTBACK, $\theta_I=60^0$, 90^0, 130^0

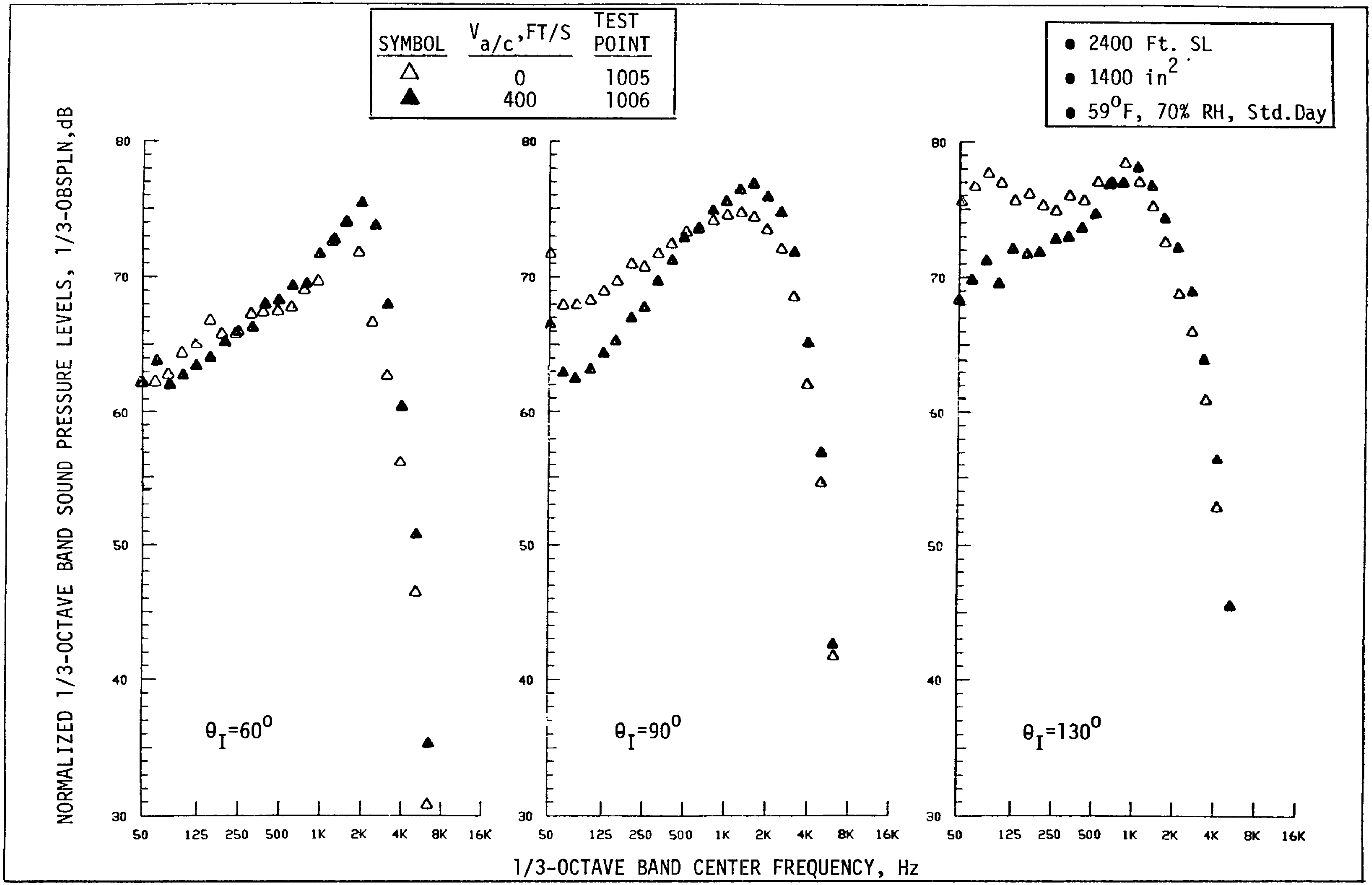

FIGURE 4-33 CONFIGURATION TE-1 STATIC-TO-FLIGHT NORMALIZED SPECTRA COMPARISONS AT INTERMEDIATE, $\theta_I=60^0$, 90^0, AND 130^0

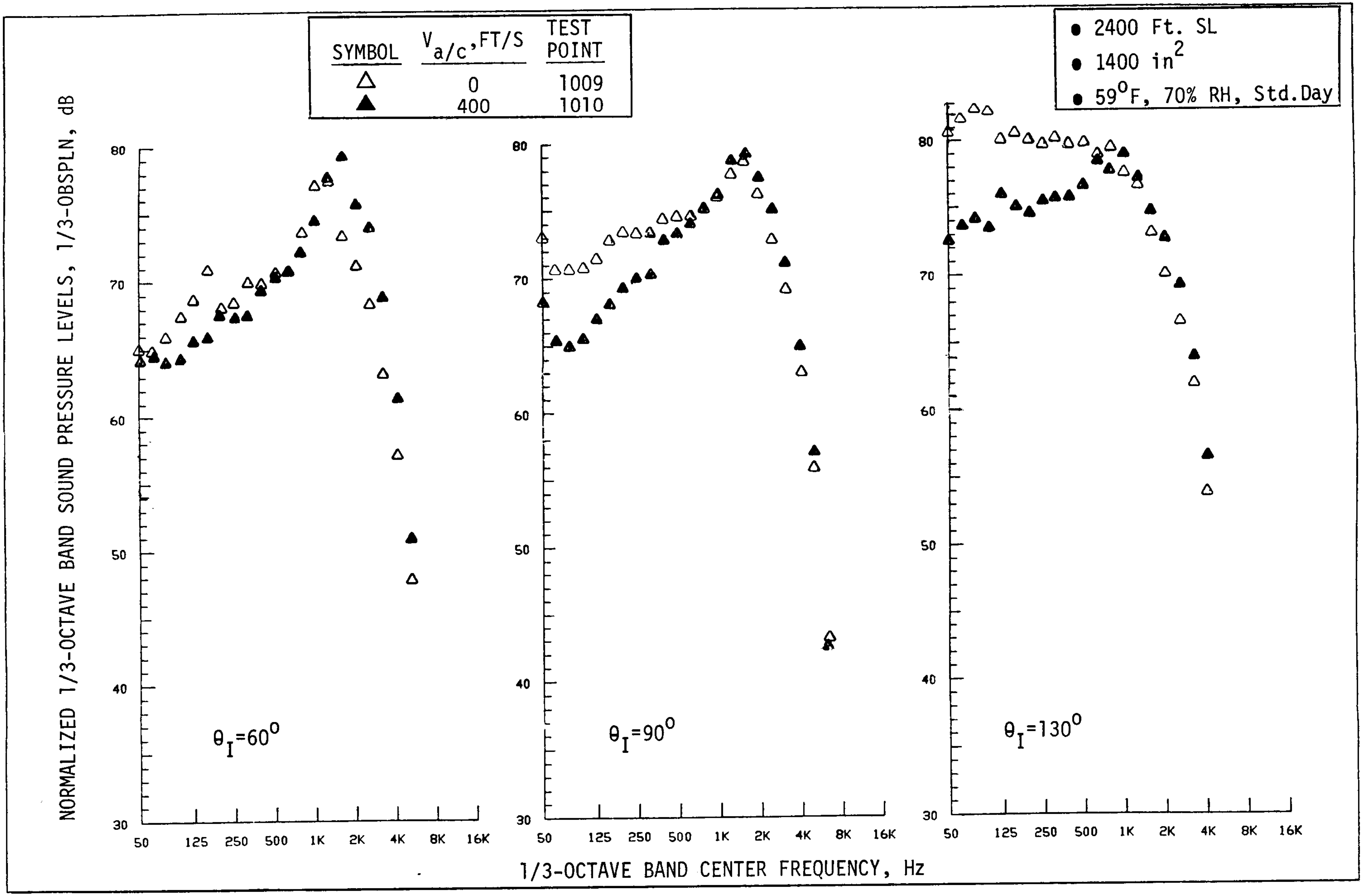

FIGURE 4-34 CONFIGURATION TE-1 STATIC-TO-FLIGHT NORMALIZED SPECTRA COMPARISONS AT TAKEOFF, θ_I=60°, 90°, AND 130°

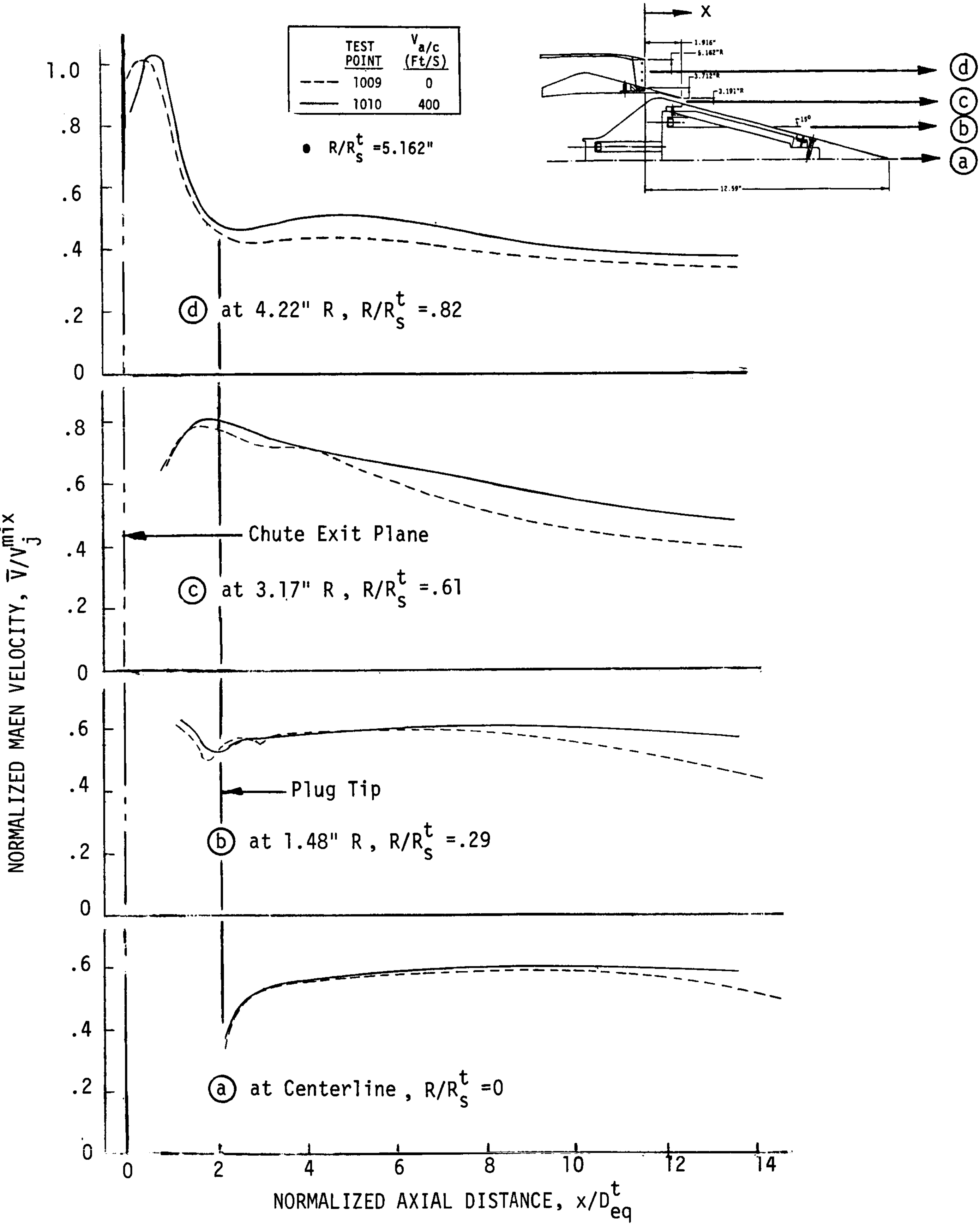

FIGURE 4-35 AXIAL VARIATION OF THE MEAN VELICITY (AXIAL COMPONENT) IN THE PLUME OF CONFIGURATION TE-1 AT TAKEOFF CONDITION, STATIC VS. FLIGHT, TEST POINTS 1009 AND 1010

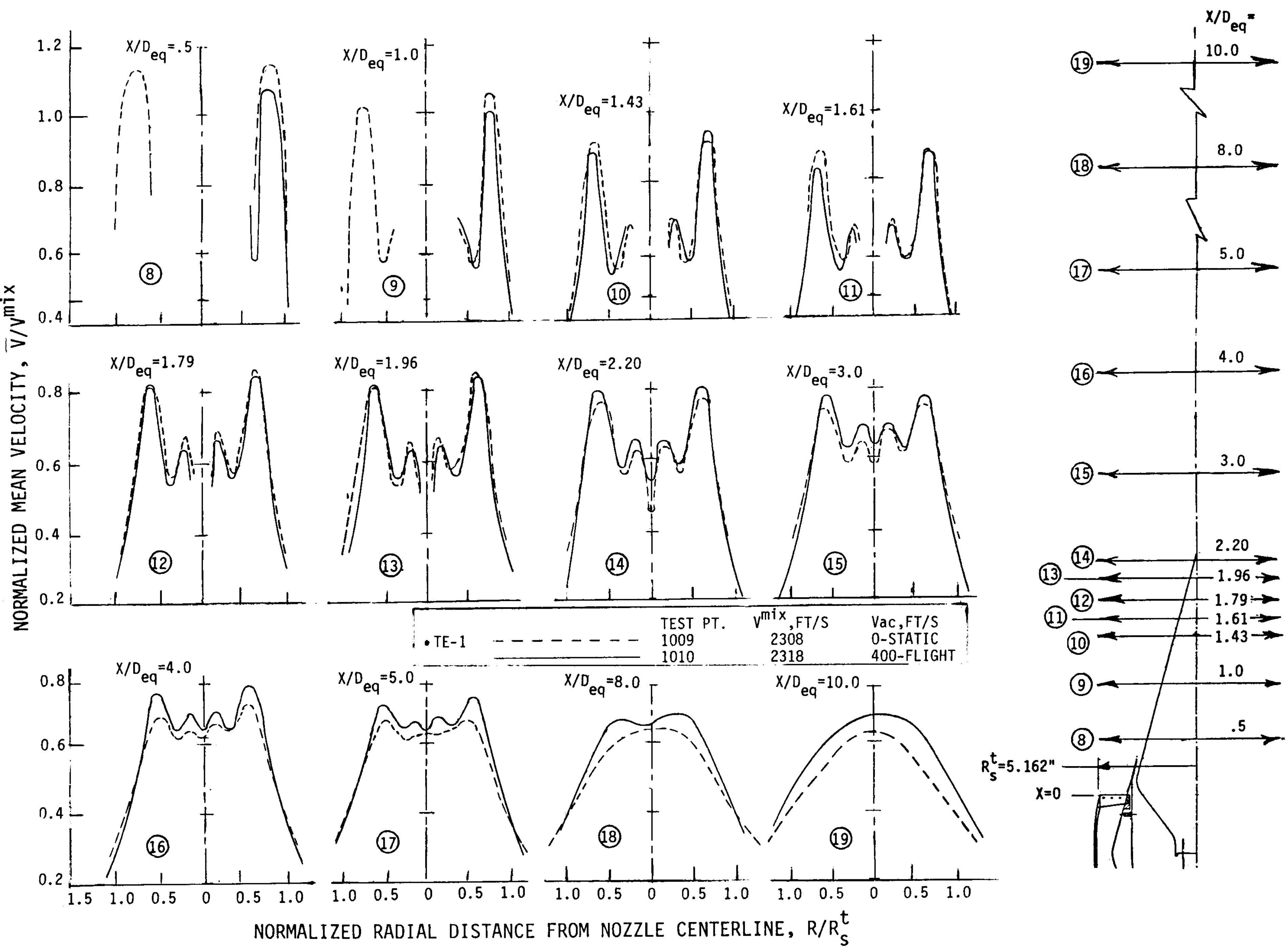

FIGURE 4.26 RADIAL VARIATION OF THE MEAN VELOCITY (AXIAL COMPONENT) IN THE PLUME OF CONFIGURATION TE-1

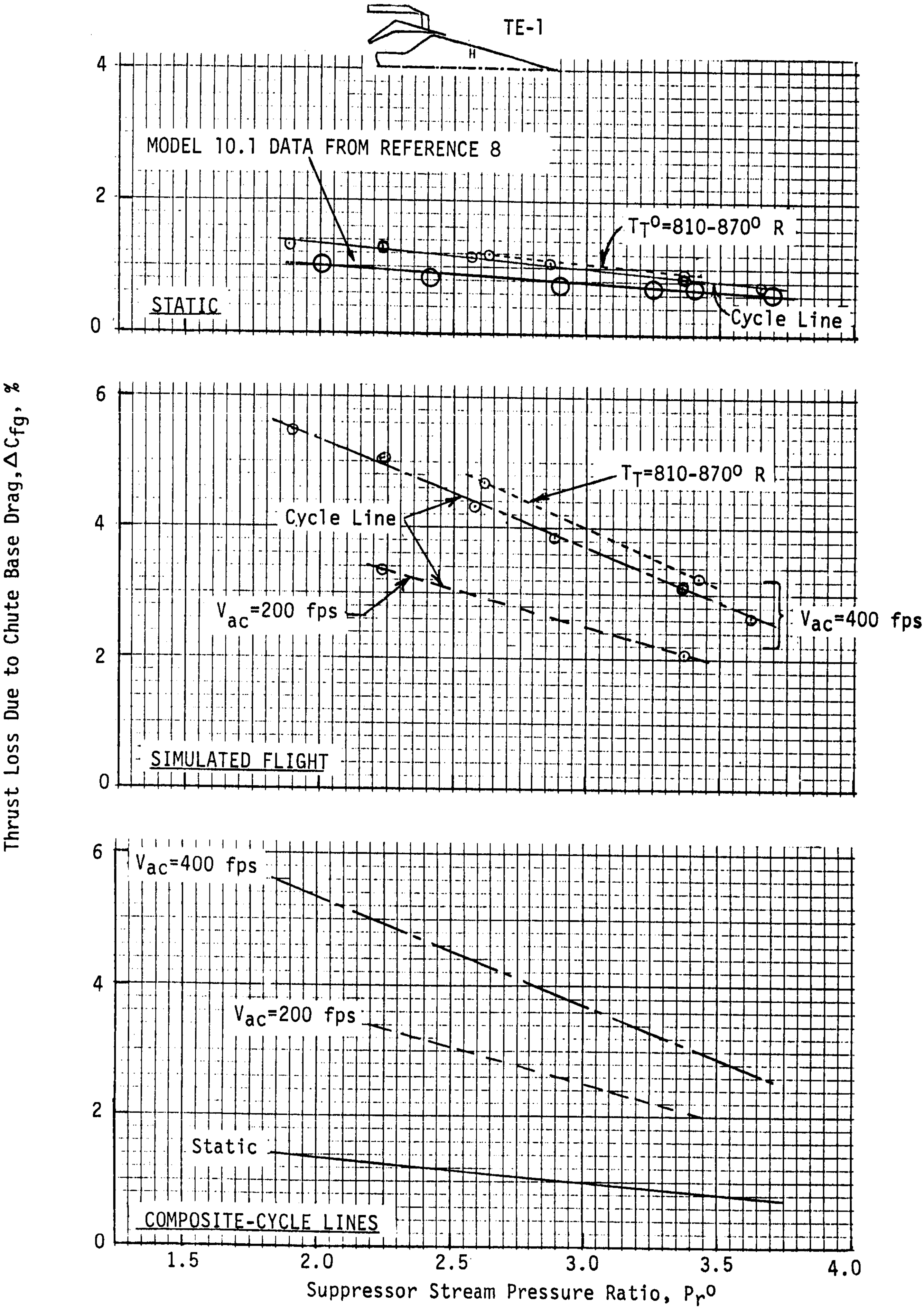

FIGURE 4-37 THRUST LOSS COEFFICIENT DUE TO CHUTE BASE DRAG OF CONFIGURATION TE-1 & MODEL 10.1

4.2 OVERVIEW OF TREATED EJECTOR APPLICATIONS EFFECTIVENESS

The previous section summarized acoustic performance of the baseline 20-chute coannular nozzle and reviewed previously accumulated reference conical nozzle data; both for the purpose of establishing baselines to which ejector and special study acoustic measurements could be referenced. Later report sections discuss detailed analyses of various acquired data bases to establish the impact of ejector geometric variations on performance. This section, however, is intended as an overview, i.e., a brief summary establishing ejector maximum effectiveness and presenting trends of performance for ejector system design variables. The design variables overviewed will include ejector axial location, treatment design, ejector length, and extent of treatment application within the ejector/plug flowpaths.

4.2.1 Ejector System Maximum Effectiveness

Ejector geometry and treatment design variations were limited to the extent accomplishable within eight model test configurations. Variables investigated were, therefore, "optimized" only within the limited range of geometry and design tested. Two axial locations, S1 and S2, and two treatment designs, T1 and T2, were tested. Extended axial location, S2, and less dense treatment, T2, were judged optimum and maintained for all further test configurations. Verification of these selections will be accomplished by data presentations in later report sections. The later test configurations varied ejector length, L1-nominal and L2-extended, and region of treatment application, i.e., a) hardwall-no treatment applied, b) treated ejector flowsurface only, and c) treated ejector and plug flowsurfaces; these variations intended to isolate the individual sources of ejector acoustic effectiveness.

The L1 ejector length duplicated the full scale study nozzle design length, Reference Figure 2-1 of Section 2.1, however, in model size the treatment application was not feasible along its entire length, as the full scale study nozzle called for, due to thin-walled closure. A longer ejector, L2, was therefore tested to extend length beyond that allowed in the full scale nozzle. It was anticipated that additional length would allow greater suppression due to more extensive physical shielding and greater area of treatment application. If so, a practical design may precipitate from further noise/weight/performance trade studies. The L2 ejector applied treatment to a length equivalent to the entire ejector length of the L1 model. Untreated closure length of the ejector was similar to that of the shorter system, therefore, total length increased 24%.

In final analysis, the L2 ejector system in the TE-8 configuration with S2 ejector-axial positioning and with T2 treatment applied to ejector and plug flowsurfaces, was most effective in suppression. Its characteristics are summarized in terms of normalized peak OASPL and PNL plus EPNL in Figure 4-38, 4-39 and 4-40, respectively. If reviewed at nominal takeoff and cutback cycles, i.e., at jet velocity parameter of approximately 3.1 and 2.15, suppression performance relative to the reference conical nozzle can be summarized as follows; suppression levels for the baseline unejected TE-1 configuration are also included:

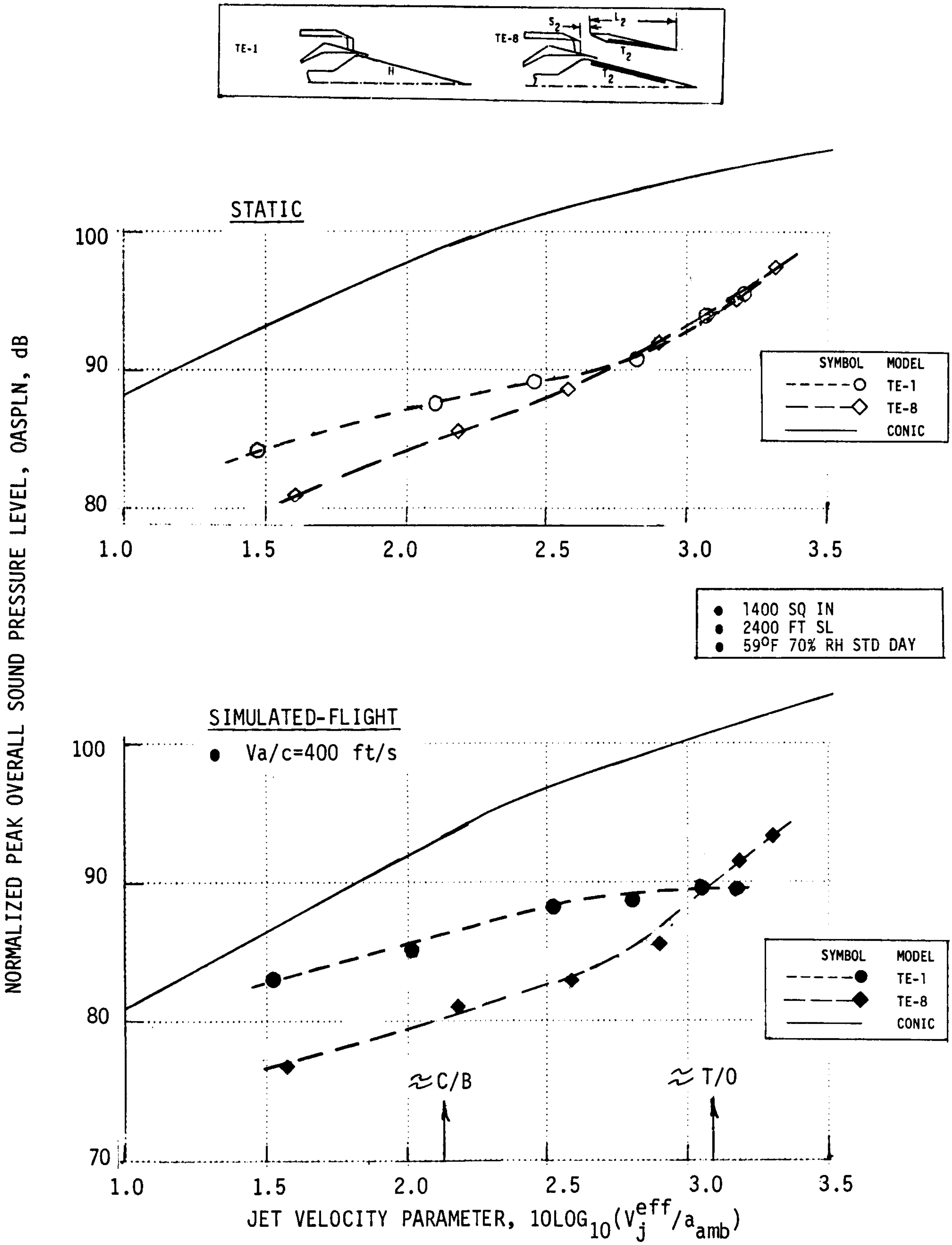

FIGURE 4-38. NORMALIZED PEAK OASPL AS A FUNCTION OF JET VELOCITY PARAMETER FOR COMPARISON OF CONFIGURATION TE-1 AND TE-8 TO SHOW EJECTOR MAXIMUM EFFECTIVENESS, STATIC AND SIMULATED-FLIGHT.

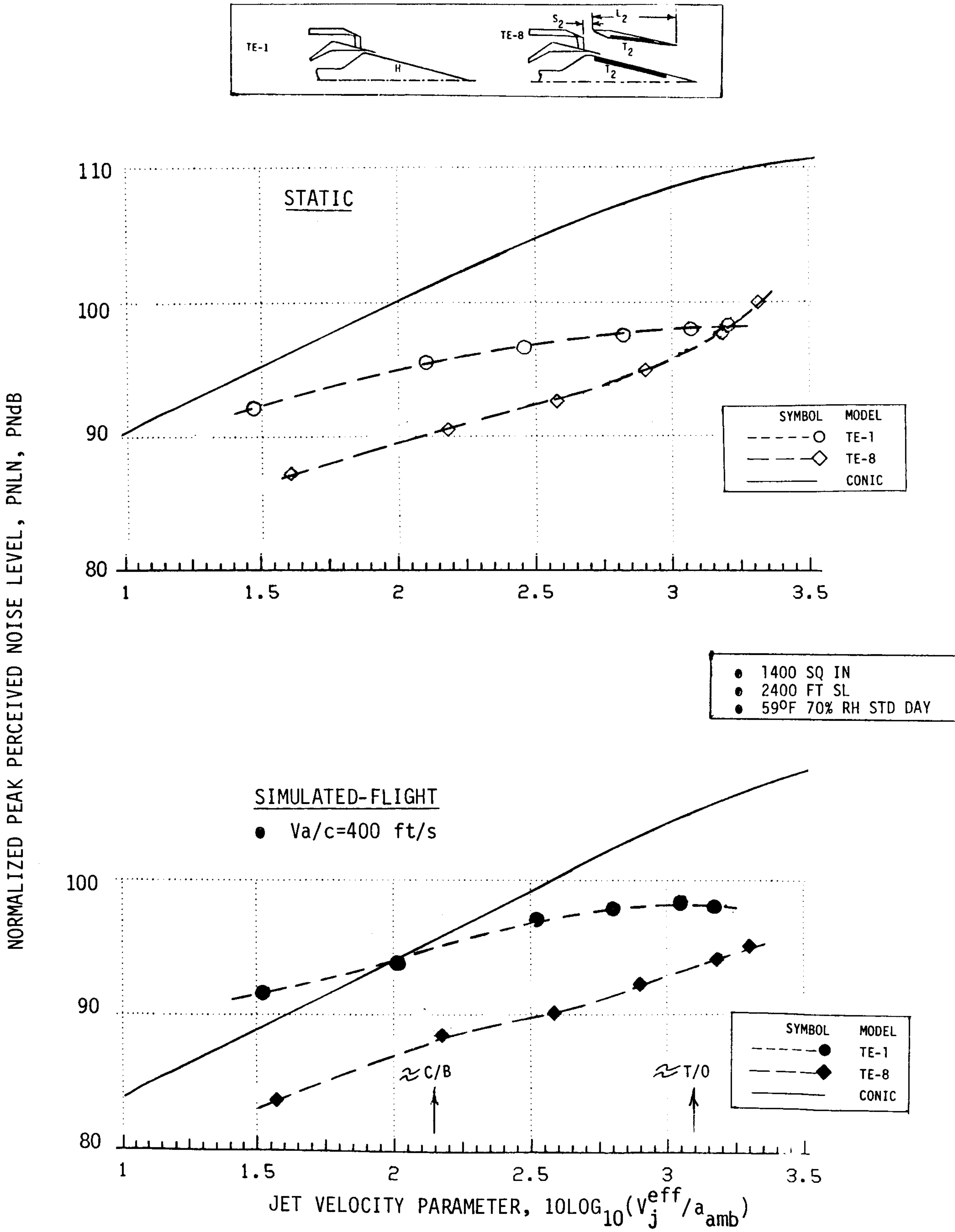

FIGURE 4-39. NORMALIZED PEAK PNL AS A FUNCTION OF JET VELOCITY PARAMETER FOR COMPARISON OF CONFIGURATION TE-1 AND TE-8 TO SHOW EJECTOR MAXIMUM EFFECTIVENESS, STATIC AND SIMULATED-FLIGHT

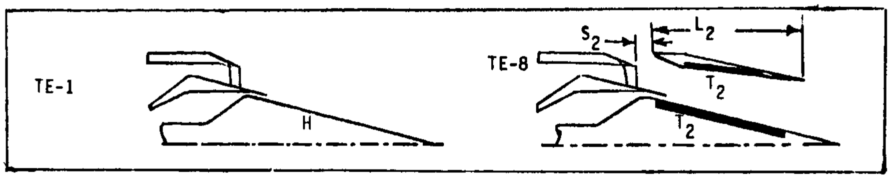

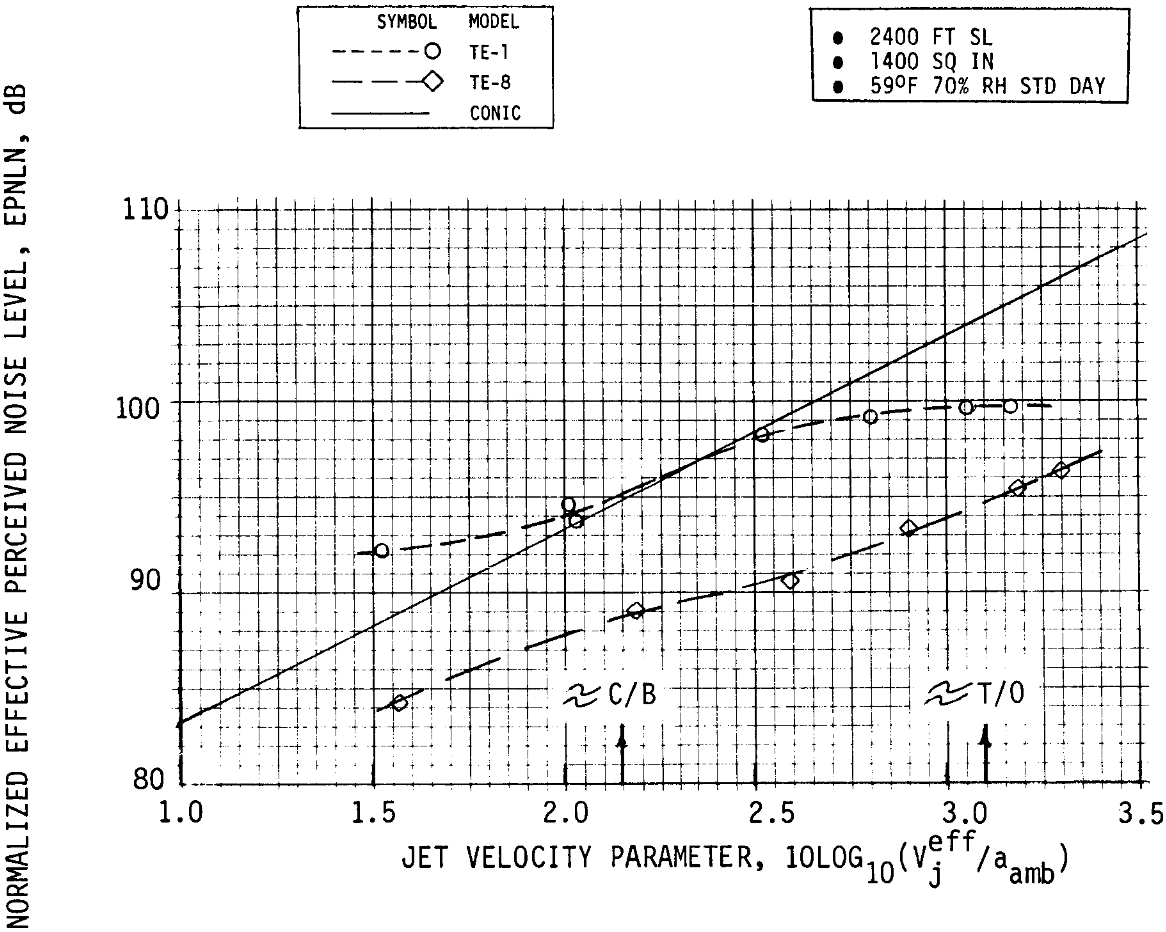

FIGURE 4-40. EPNL CORRELATION WITH JET VELOCITY PARAMETER FOR COMPARISON OF CONFIGURATION TE-1 AND TE-8 TO SHOW EJECTOR MAXIMUM EFFECTIVENESS

	NOMINAL CYCLE	$10 Log_{10}$ (V_{jeff}/a_{amb})	△ PEAK OASPL		△ PEAK PNL		△ EPNL
			STATIC	FLIGHT	STATIC	FLIGHT	FLIGHT
TE-1	Cutback	2.15	11.0	7.0	5.7	0.5	- 0.3
	Takeoff	3.1	10.4	11.2	10.6	6.6	4.6
TE-8	Cutback	2.15	13.5	13.0	10.8	7.3	6.0
	Takeoff	3.1	10.2	10.7	12.0	11.4	9.8

Review of the above figures and table yields the following interesting observations:

- At takeoff cycle, peak PNL suppression referenced to the conic nozzle is 11.4 △PNdB, a very significant 4.8 △ PNL greater than the baseline 20-chute suppressor.

- At the 400 ft/sec simulated-flight speed and 2400 ft. sideline distance, the △ PNL values translate into 4.6 △ EPNL for the TE-1 baseline and 9.8 △EPNL for the suppressor/ejector system, an addition of 5.2 △ EPNL attributable to the treated ejector/treated plug system.

- Ejector performance at lower velocity, i.e., cutback cycle, is even more significant, 6.8 △ peak PNL and 6.3 △ EPNL relative to the TE-1 performance. The retention of acoustic suppression effectiveness to very low operating cycles is uncharacteristic of most mechanical jet noise suppressor (unejected) systems previously investigated. Most have followed the pattern exhibited by the TE-1 nozzle, where suppressor absolute noise levels approach those of the reference conic nozzle at low jet velocity. Retention of suppression at low cycles offers a significant advantage for quiet part power, e.g., cutback, operation.

- Comparing static to flight performance on a peak PNL basis, Figure 4-39, the TE-8 ejector system does not lose suppression nearly as rapidly as the TE-1 baseline nozzle. For example, at takeoff, the TE-1 suffers 4.0 △ PNL static-to-flight loss and the TE-8 loses only 0.6 △ PNL. At cutback, similar comparisons show 5.2 and 3.5 △ PNL losses for TE-1 and TE-8, respectively.

Inspection of PNL directivity patterns and spectral content aid in understanding ejector peformance characteristics. Figures 4-41 through 4-44 present static and simulated-flight normalized PNL and normalized spectra at takeoff and cutback cycles. Review indicates:

- At takeoff, per Figure 4-41, peak static PNL levels are near similar, however, the ejector alters the directivity pattern significantly, moving the peak from near 100° for the unejected to 130°/140° for the long ejector. Simulated-flight, Figure 4-42, lowers ejector noise levels substantially further than the TE-1 nozzle, allowing significant peak noise reduction of approximately 4.8 △ PNL due to ejector application. Of primary significance is the high level of forward quadrant suppression afforded by the ejector, both static and flight,

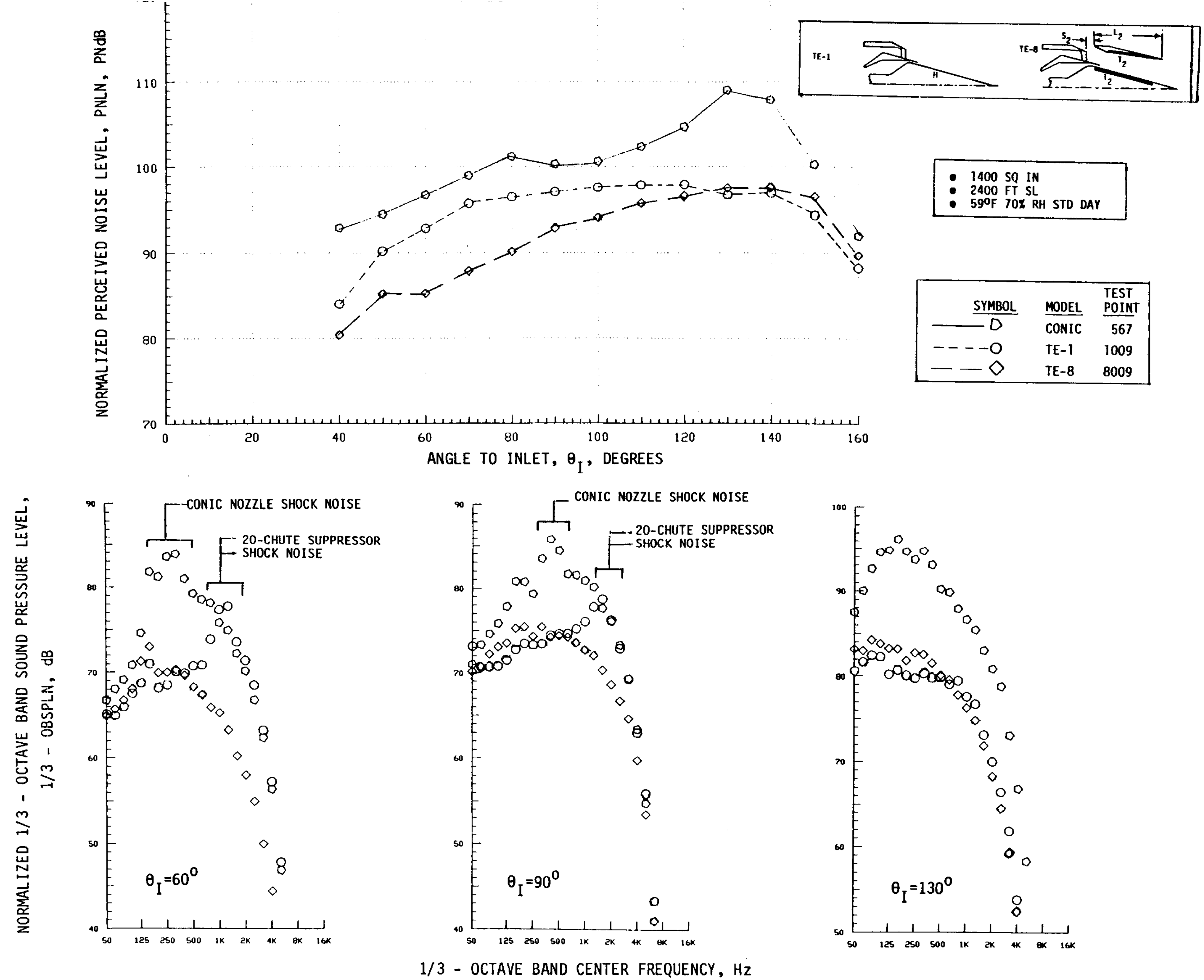

FIGURE 4-41. PNL DIRECTIVITY AND SPECTRA COMPARISON AT θ_I =60°, 90° AND 130°, TAKEOFF, STATIC, FOR COMPARISON OF CONFIGURATION TE-1 AND TE-8

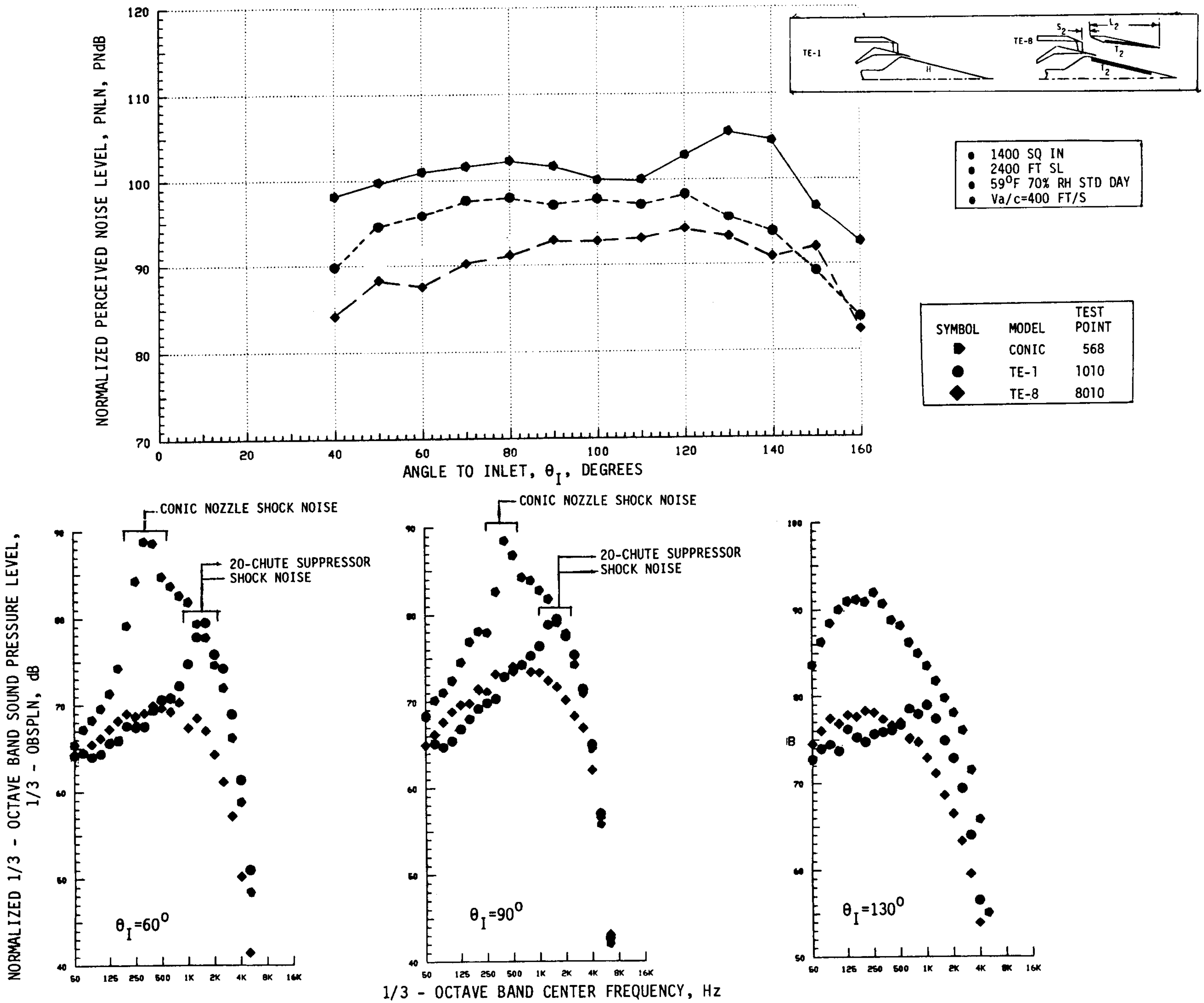

FIGURE 4-42. PNL DIRECTIVITY AND SPECTRA COMPARISON AT $\Theta_I = 60^0$, 90^0, AND 130^0, TAKEOFF.

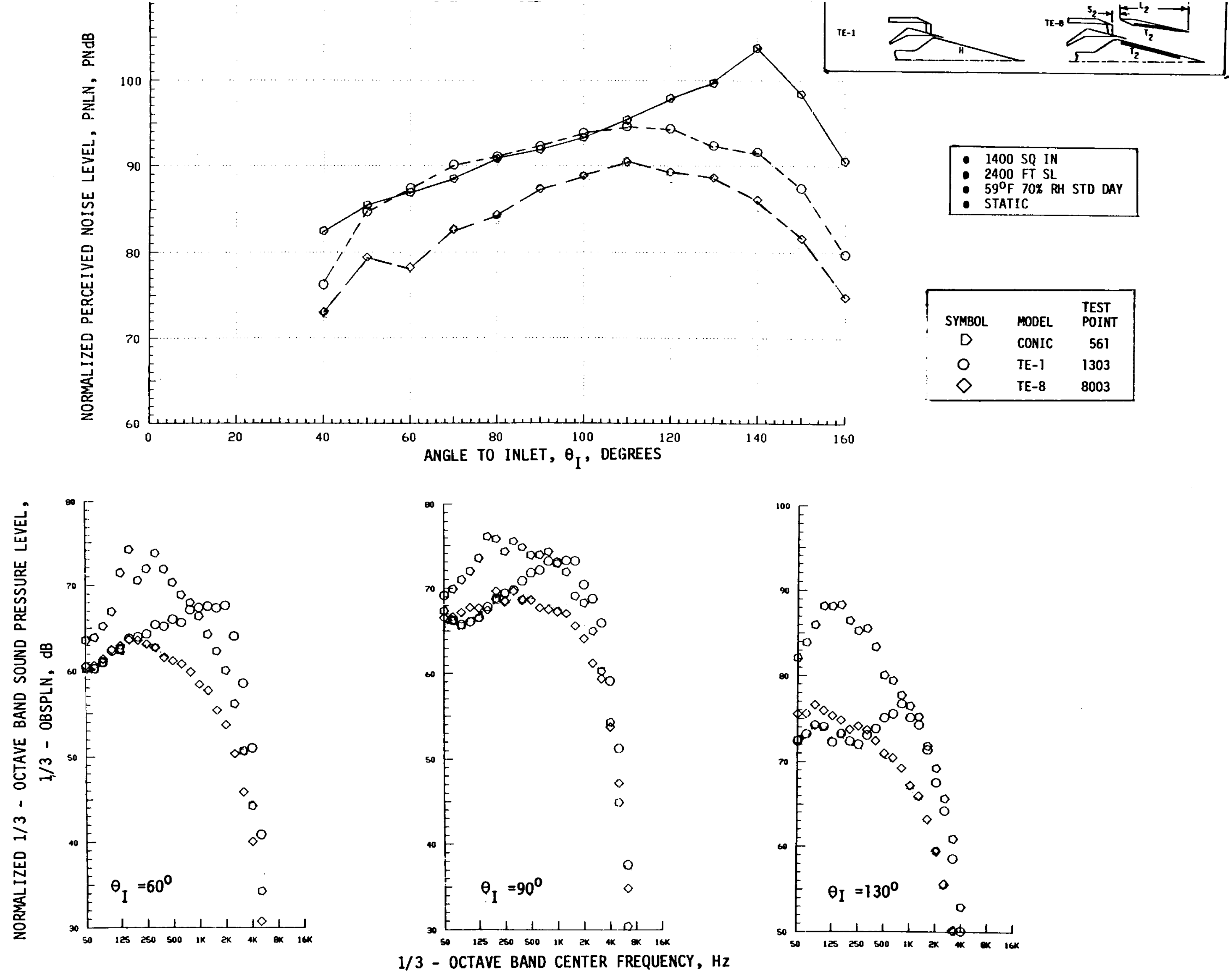

FIGURE 4-43. PNL DIRECTIVITY AND SPECTRA COMPARISON AT θ_I =60°, 90°, AND 130°, CUTBACK, STATIC, FOR COMPARISON OF CONFIGURATION TE-1 AND TE-8

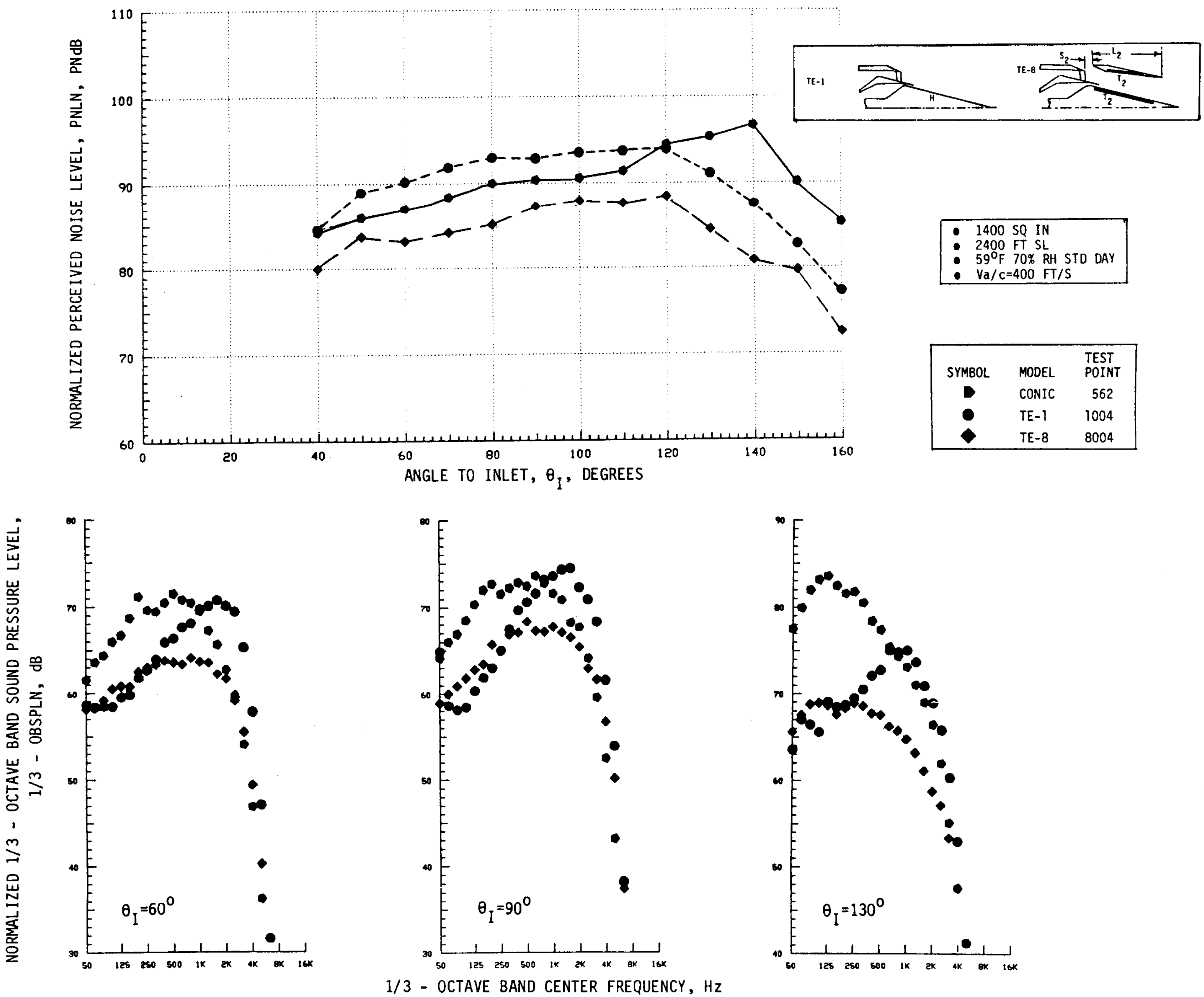
NORMALIZED PERCEIVED NOISE LEVEL, PNLN, PNdB
ANGLE TO INLET, θ_I, DEGREES
TE-1
TE-8
S_2
L_2
T_2
H
1400 SQ IN
2400 FT SL
59°F 70% RH STD DAY
Va/c=400 FT/S
SYMBOL
MODEL
TEST POINT
CONIC
562
TE-1
1004
TE-8
8004
NORMALIZED 1/3 - OCTAVE BAND SOUND PRESSURE LEVEL, 1/3 - OBSPLN, dB
θ_I=60°
θ_I=90°
θ_I=130°
1/3 - OCTAVE BAND CENTER FREQUENCY, Hz

per Figures 4-41 and 4-42. The basic unejected suppressor significantly lowers the forward quadrant shock noise content relative to the conical nozzle, approximately 3 dB at $\theta_I = 60^o$. The ejector, however, further reduces shock and jet mixing noise by a substantial 5 to 7 Δ PNL.

- o At cutback cycle, Figures 4-43 and 4-44, the ejector allows an additional 4.0 peak PNL suppression statically and approximately 6.0 in flight, again beyond that exhibited by the 20-chute suppressor. Forward quadrant suppression is again significant and of magnitude similar to the takeoff cycle. The flight TE-8 noise levels are reduced below that of the conic whereas the unejected TE-1 model was noisier than the conic baseline.

- o Review of spectral content shows that the 20-chute TE-1 suppressor substantially reduces the low and mid-range frequency levels relative to the conic nozzle. It, however, has little effect on the high frequency energy as the multi-jet segmentation transfers energy to the high frequency range, characteristic to the dimensions of the smaller segmented jets.

On occasion, such as cutback cycle of Figure 4-43, high frequency energy levels exceed that of the conical nozzle. The 20-chute suppressor is very effective in reducing the takeoff cycle conic nozzle shock noise as seen in Figure 4-41. In itself, it still exhibits slight shock noise, but in a much higher frequency range, more characteristic of the smaller dimensions of the segmented jet. No low frequency shock noise is seen in the TE-1 spectra as no post-merged stream shock structure is present in the jet plume past the nozzle's plug tip region, verified by shadowgraph photographs within CDR Volume II.

Application of the TE-8 ejector, reference to all spectra plots of Figures 4-41 through 4-44, is seen very effective in reducing the high frequency content of the 20-chute suppressor nozzle. The high frequency noise sources, due to jet segmentation, are sufficiently contained within the ejector to allow treatment effectiveness. In itself, however, a hardwall ejector, due to physical shielding and noise redirection, lends to a major portion of the ejector's effectiveness, as will be seen later.

Of further aid in understanding ejector application effectiveness are the laser velocimeter plume surveys of Figures 4-45 and 4-46. Figure 4-45 displays normalized mean velocity data acquired during axial traverses within the plume of Configurations TE-1 and TE-8 at takeoff cycle. Traces are at radial locations of a) centerline, b) 1.54", c) 3.07" and d) 4.09/4.22" for $R/R_S^{\mathfrak{t}}$ values of 0, .3, .6 and .79/.82, respectively. Figure 4-46 presents normalized mean velocity data acquired during radial traverses at various axial locations, as noted on the figure. From the axial traverses at $R/R_S^{\mathfrak{t}}$ = .79/.82, it it seen that the unejected plume decays quite rapidly by nature of free-mixing with ambient air. The ejected plume also decays quite rapidly within the length of the ejector, but not to the level of the free mixer. The higher velocity of the ejector plume persists for quite some distance before decaying to similar levels at far aft distances. These results indicate that forced mixing of ejected ambient air does not readily occur within the ejector and does not allow substantially reduced mean velocity at the ejector exit.

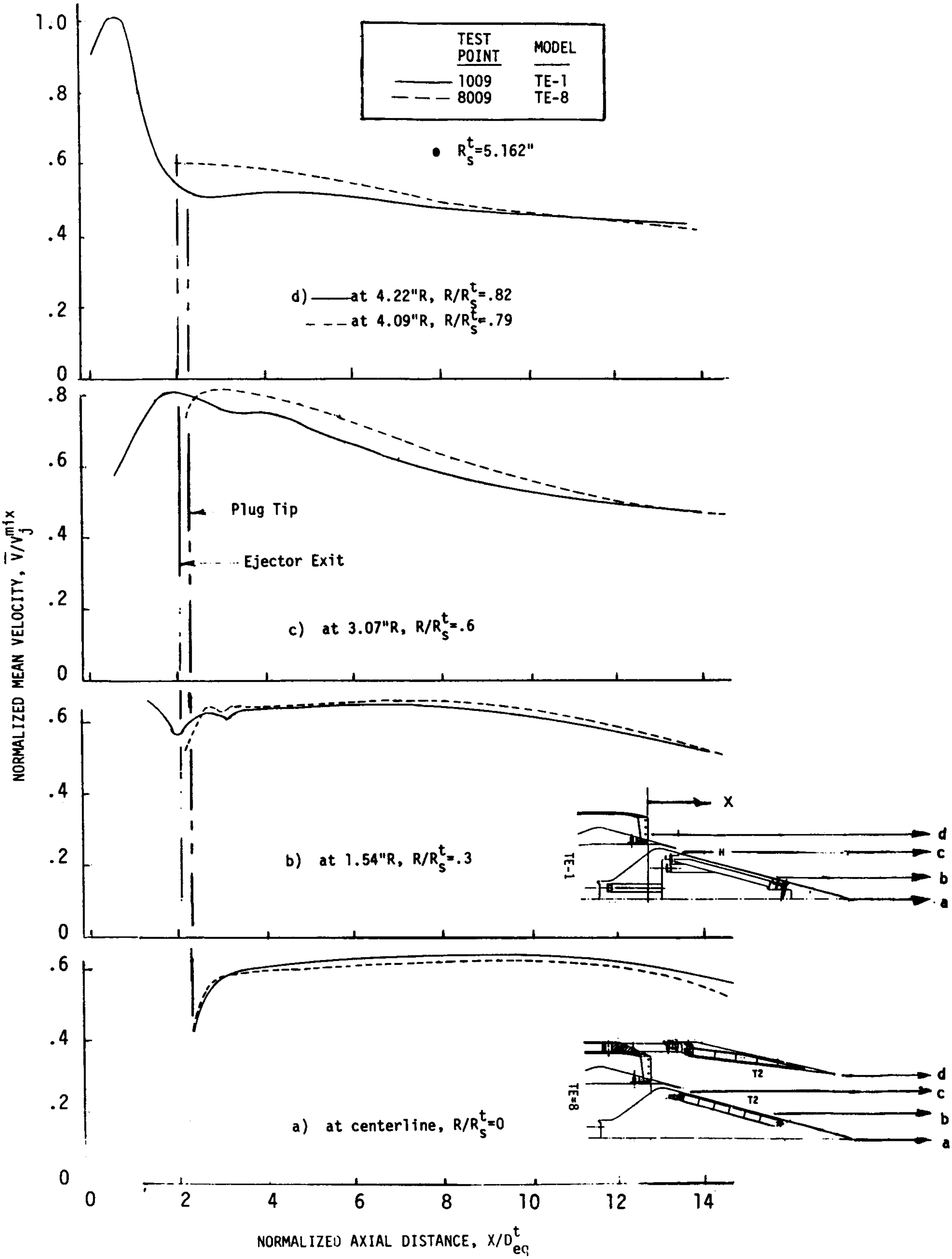

FIGURE 4-45. AXIAL VARIATION OF THE MEAN VELOCITY (AXIAL COMPONENT) IN THE PLUME OF CONFIGURATIONS TE-1 AND TE-8 AT TAKEOFF, STATIC, TEST POINTS 1009 AND 8009, FOR COMPARISON OF EJECTOR APPLICATION TO 20-CHUTE NOZZLE

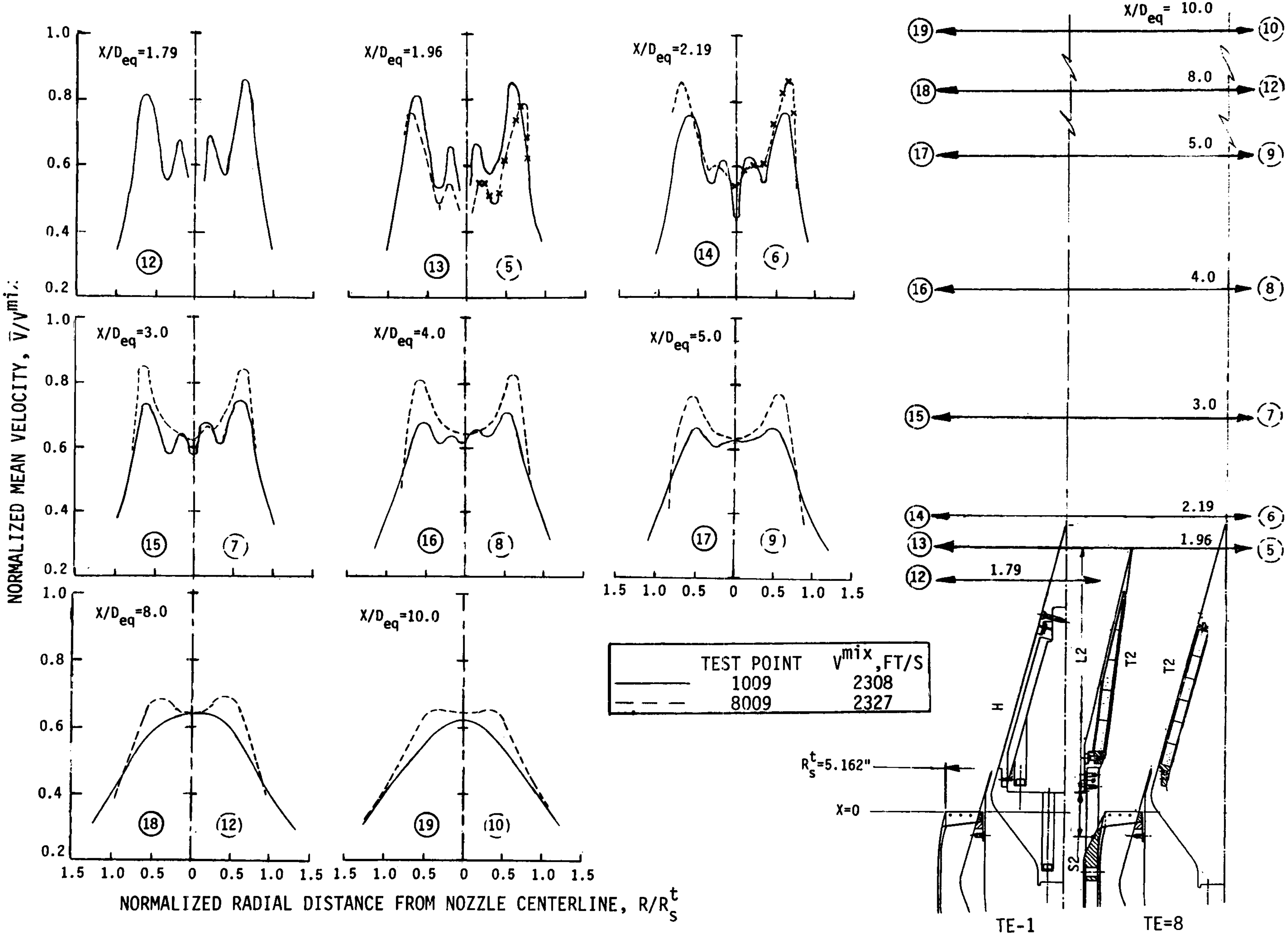

FIGURE 4-46. RADIAL VARIATION OF THE MEAN VELOCITY (AXIAL COMPONENT) IN THE PLUME OF CONFIGURATIONS TE-1 AND TE-8 AT TAKEOFF, STATIC, TEST POINTS 1009 AND 8009, FOR COMPARISON OF EJECTOR APPLICATION TO 20-CHUTE NOZZLE

Enhanced mixing was initially anticipated to occur and would be accompanied by lower levels of jet mixing noise. The somewhat higher velocity levels are felt to account for the aft quadrant (Figure 4-41, $\theta_I = 130^o$) noise increase in low-to-mid frequency range.

Axial traces at $R/R_s^{\mathfrak{t}} = .3$ and at centerline show unejected and ejected plumes to be of identical velocity levels, again indicating no forced mixing of ambient air to the center of the jet.

Review of the Figure 4-45 radial traverses fairly well substantiates the axial traverse data. At the first comparison location, approximately 1/8" aft of the ejector exit, the TE-8 velocity levels are somewhat below those of TE-1. At further aft locations, all peak velocity levels are above those of the TE-1 and near-centerline levels are fairly similar. The lower initial levels of TE-8 may be measurements within an area of shock structure at the ejector exit. Review of shadowgraph photographs within CDR Volume II shows presence of shock at the ejector exit for the takeoff cycle operation.

4.2.2 Ejector Axial Spacing Variation

Configurations TE-5 and TE-9 varied ejector axial spacing, within a nominal length, L1, ejector system using T1 treatment design applied to ejector and plug flowsurfaces. The S1 ejector setback distance (1.484" model scale/11.0" full scale) was compatible with the original full scale design of Figure 2-1, Section 2.1. The S2 position (2.496" model scale/18.5" full scale) was that found optimum among the locations tested for aerodynamic performance at takeoff cycle pressure ratio during conduct of the NAS3-23038 wind tunnel test effort (Reference 1). Details of the many acoustic data comparisons are found in Section 4.3.

Acoustic performance comparisons on the basis of peak normalized OASPL and PNL, static and simulated-flight, are presented in Figure 4-47 and 4-48; accompanied by the TE-1 and reference conic nozzle baseline data. S1 setback, Configuration TE-5, is normally slightly less efficient in suppression for lower velocity conditions and is particularly poorer at higher cycle conditions when evaluated on a PNL basis. At takeoff cycle, nearly 2 dB increased suppression is noted for static and 1 dB for flight PNL by using the S2/TE-9 ejector position.

Laser velocimeter plume measurement comparisons for the two ejector locations are shown for the static takeoff cycle in Figure 4-49 and 4-50 and for the simulated flight takeoff cycle in Figures 4-51 and 4-52. Note that these comparisons are for Configurations TE-5 (S1) and TE-4 (S2), not for TE-9; however, the only variances between TE-9 and TE-4 is treatment design, not anticipated to influence plume mixing and decay characteristics.

The axial traverses, Figures 4-49 and 4-51, particularly at $R/R_s^{\mathfrak{t}} = .3$ and .6 locations, indicate that a) the initial velocity at the ejector exit for the S1 spacing is somewhat higher than for the further aft S2 position, and the higher velocity levels continue for a substantial distance downstream, b) mild shock structure is present in the plume aft of the ejector exit for the tigher-spaced ejector. This is as observed in shadowgraph photographs included in CDR Volume II. The centerline-plume decay rates are similar for both ejector locations.

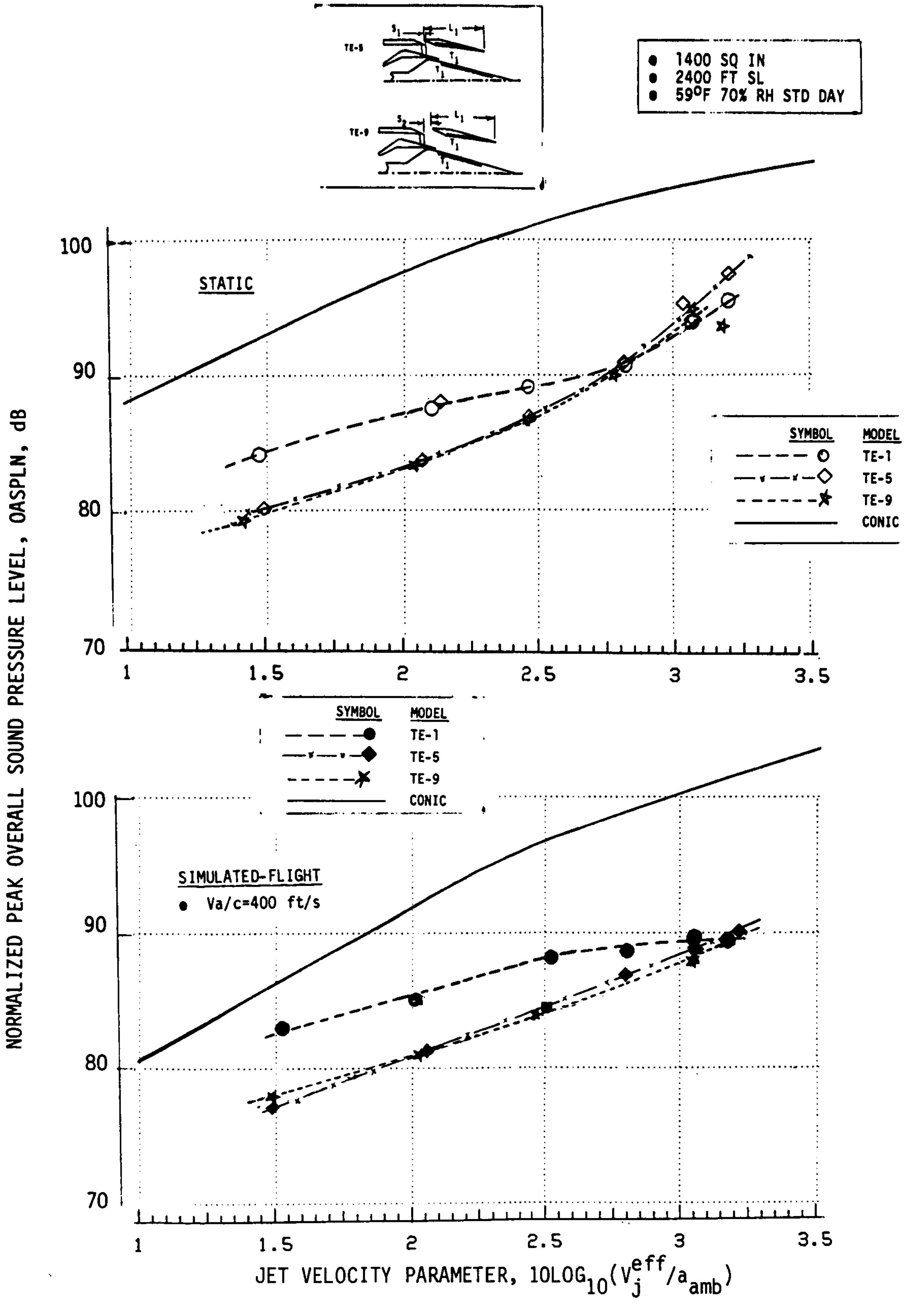

FIGURE 4-47. NORMALIZED PEAK OASPL AS A FUNCTION OF JET VELOCITY PARAMETER, STATIC AND SIMULATED-FLIGHT, FOR COMPARISON OF EJECTOR SETBACK, S1-CONFIGURATION TE-5 VERSUS S2-CONFIGURATION TE-9

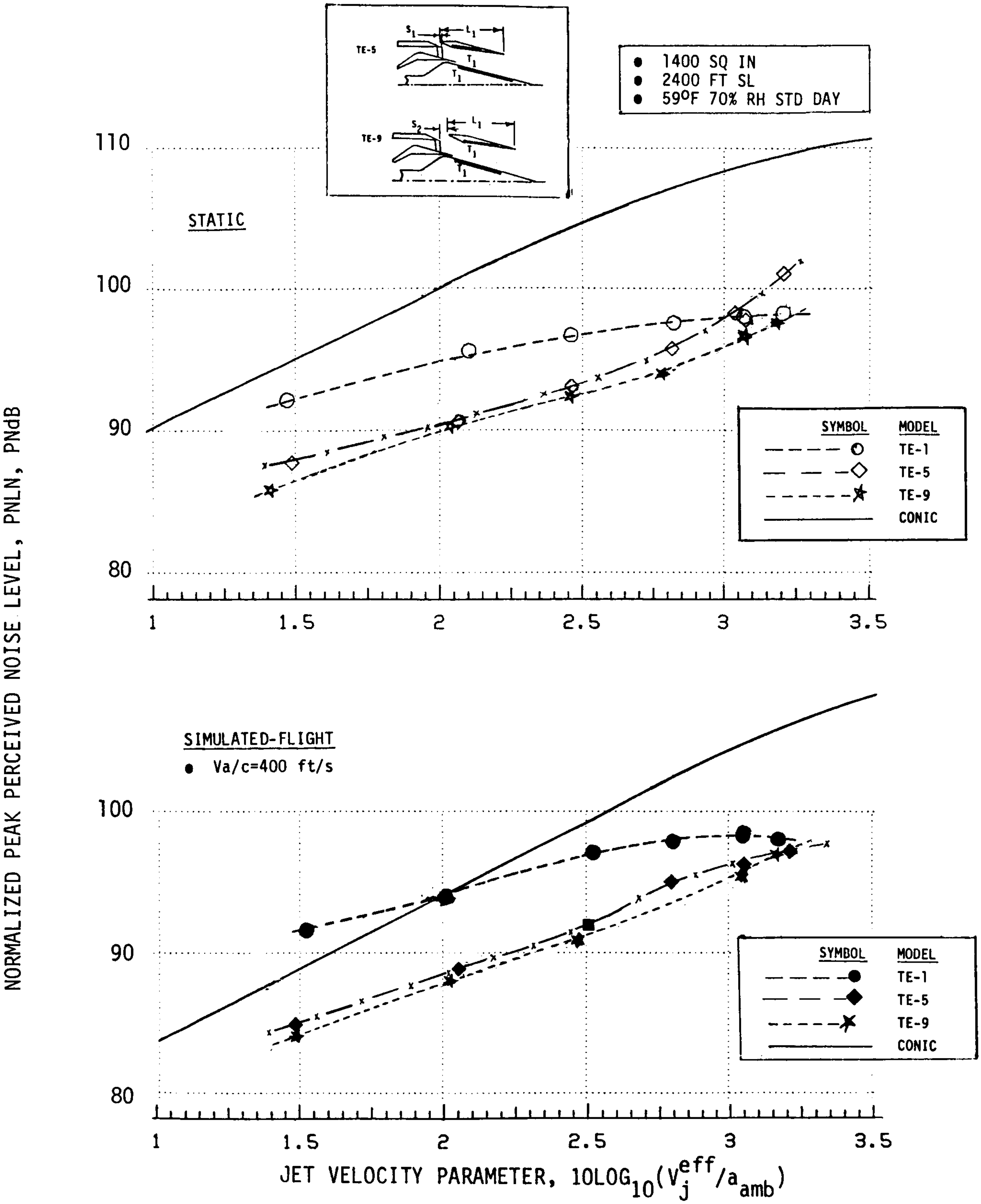

FIGURE 4-48 NORMALIZED PEAK PNL AS A FUNCTION OF JET VELOCITY PARAMETER, STATIC AND SIMULATED-FLIGHT, FOR COMPARISON OF EJECTOR SETBACK, S1-CONFIGURATION TE-5 VERSUS S2-CONFIGURATION TE-9

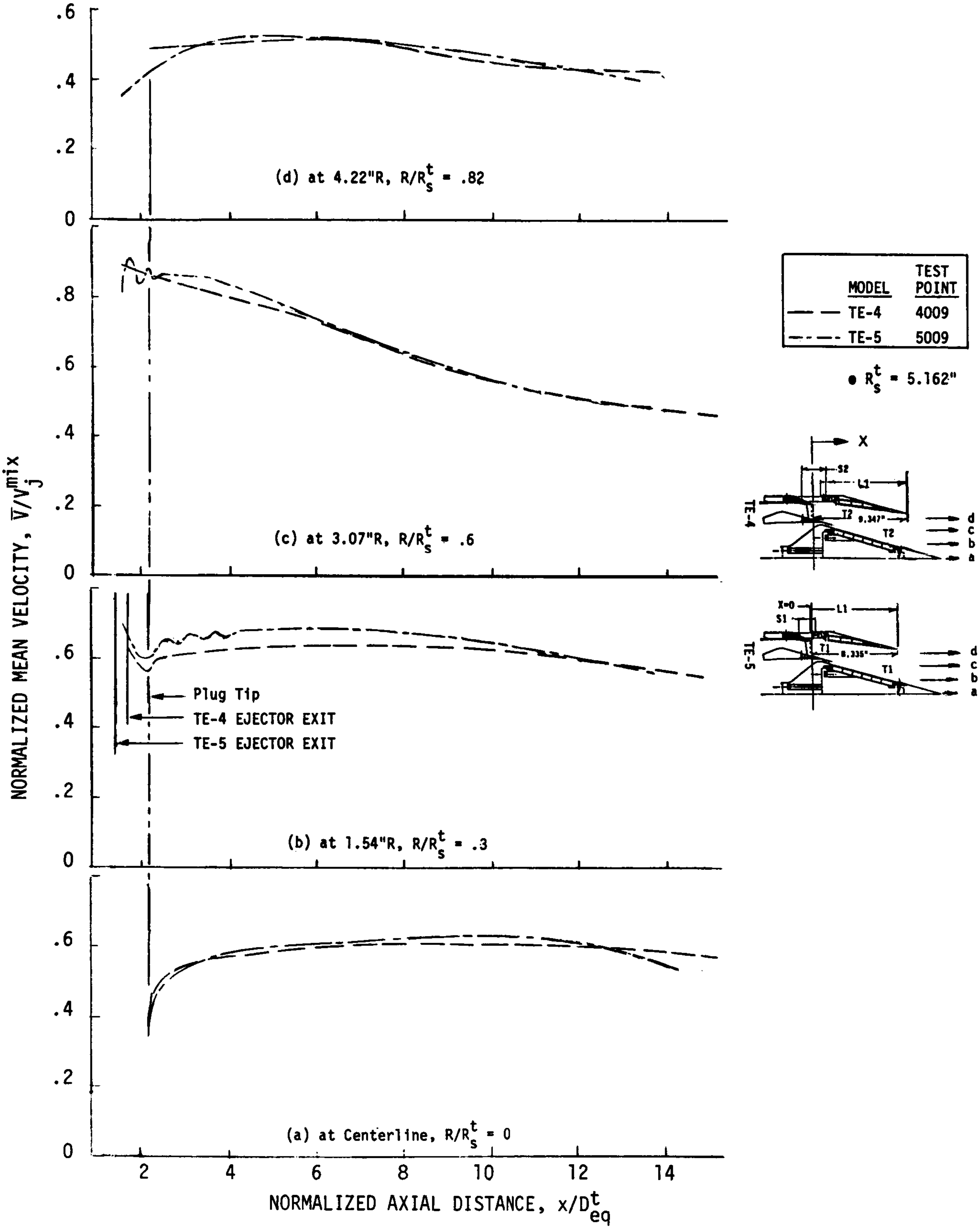

FIGURE 4-49 AXIAL VARIATION OF THE MEAN VELICITY (AXIAL COMPONENT) IN THE PLUME OF CONFIGURATIONS TE-4 & TE-5 AT TAKEOFF, STATIC, TEST POINTS 4009 & 5009, FOR COMPARISON OF EJECTOR SETBACK S1 & S2

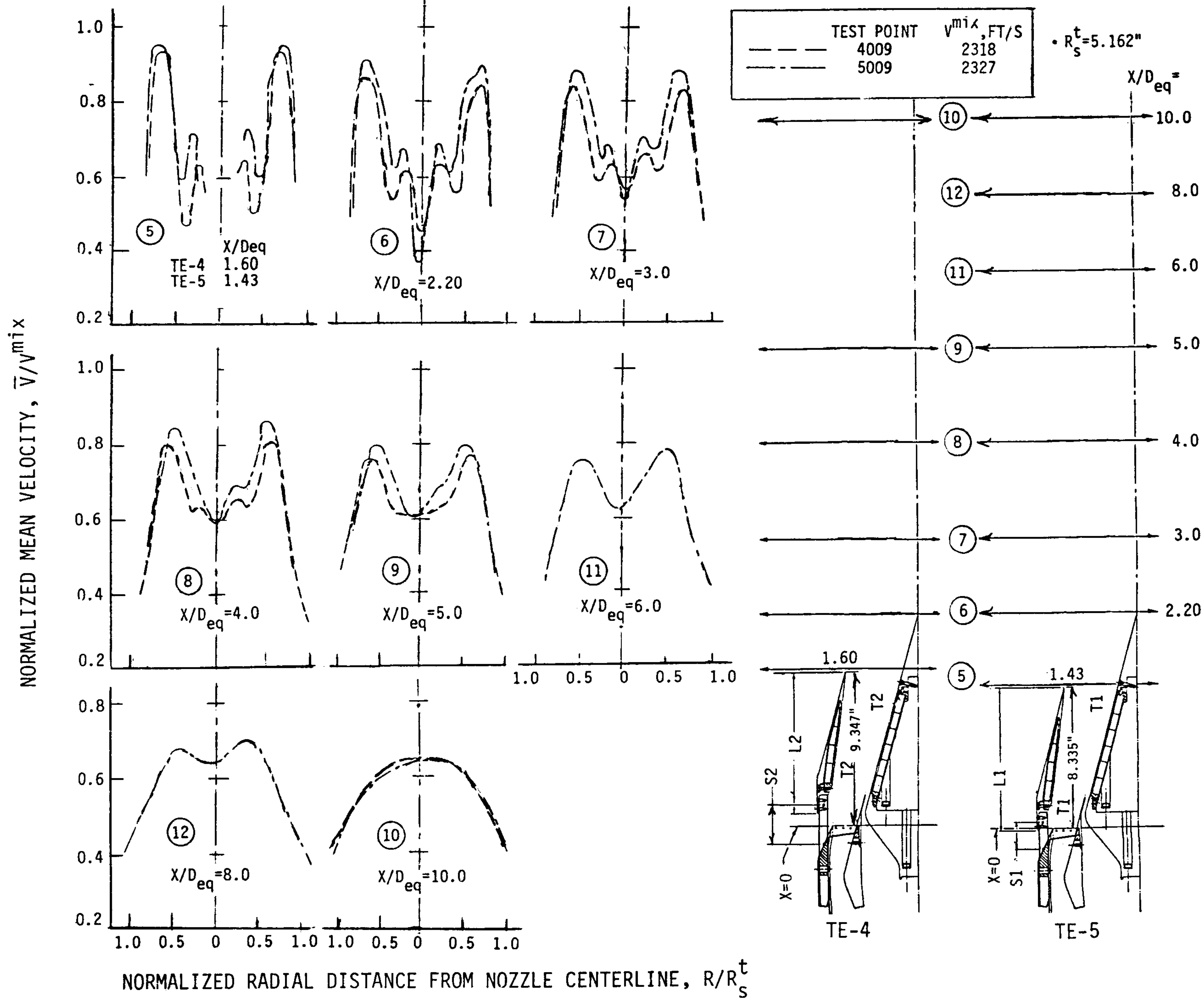

FIGURE 4-50 RADIAL VARIATION OF THE MEAN VELOCITY (AXIAL COMPONENT) IN THE PLUME OF CONFIGURATIONS TE-4 & TE-5 AT TAKEOFF CONDITION, STATIC. TEST POINTS

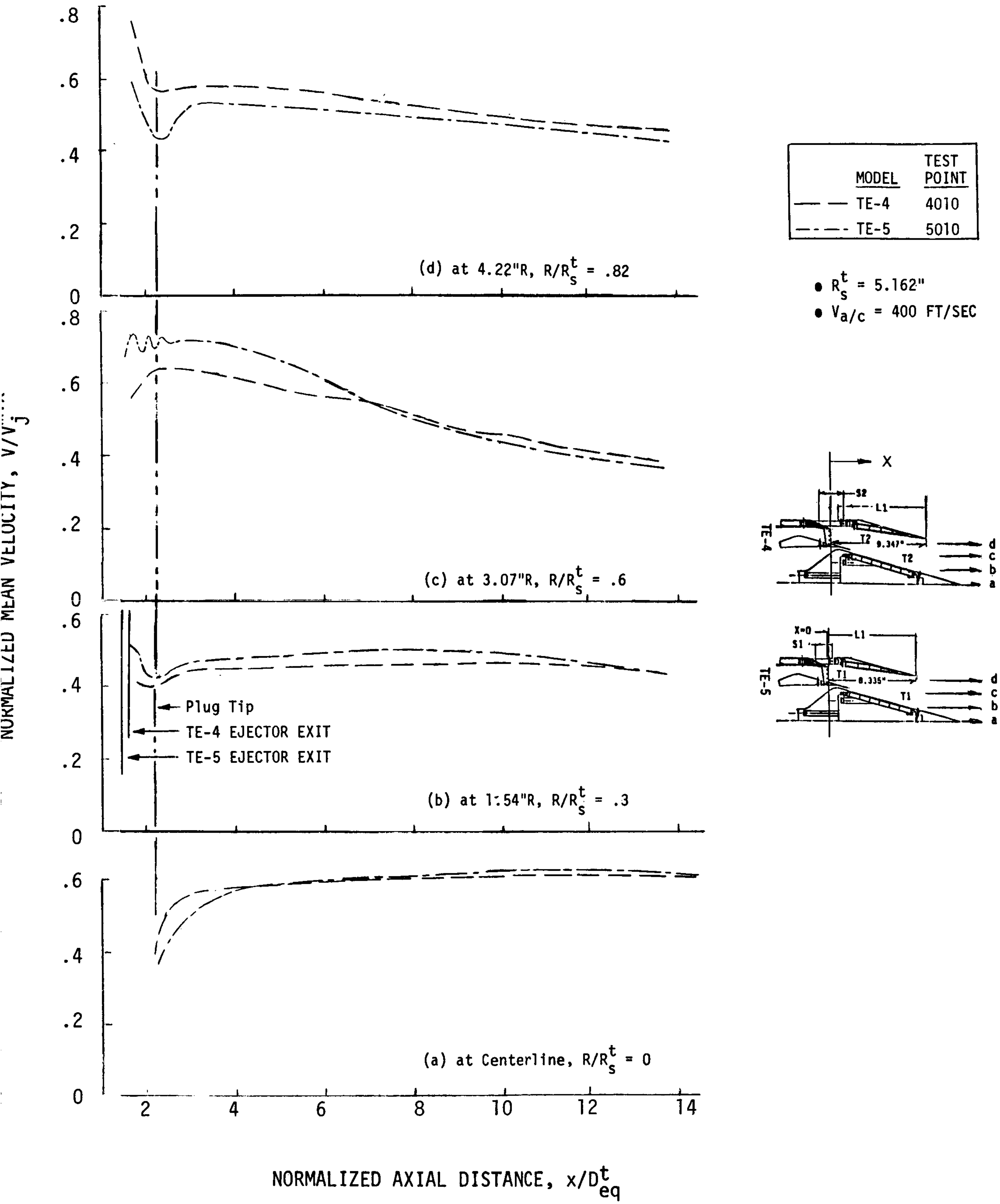

FIGURE 4-51 AXIAL VARIATION OF THE MEAN VELOCITY (AXIAL COMPONENT) IN THE PLUME OF CONFIGURATIONS TE-4 & TE-5 AT TAKEOFF, SIMULATED-FLIGHT, TEST POINTS 4010 & 5010, FOR COMPARISON OF EJECTOR SETBACK S1 & S2

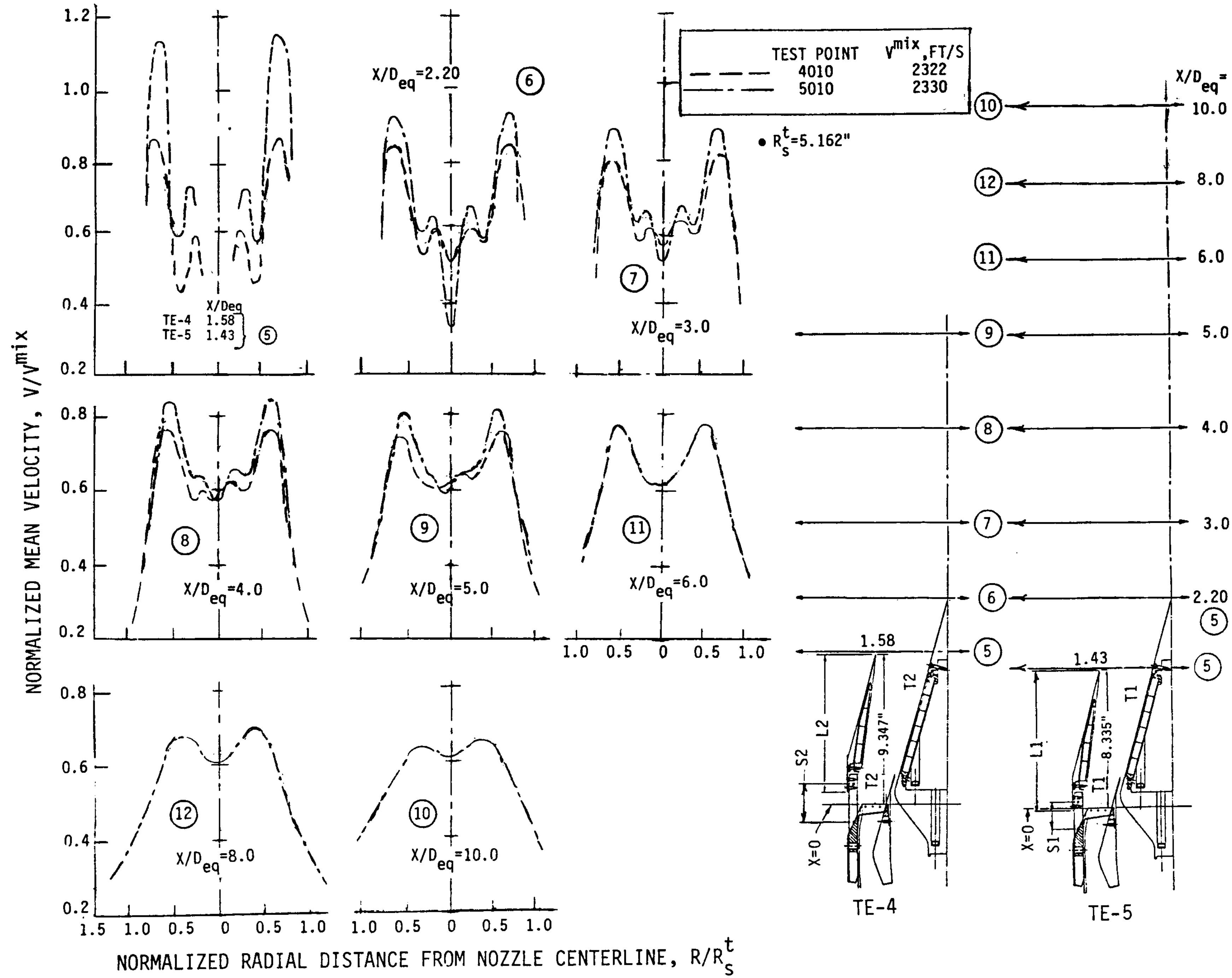

FIGURE 4-52 RADIAL VARIATION OF THE MEAN VELOCITY (AXIAL COMPONENT) IN THE PLUME OF CONFIGURATIONS TE-4 & TE-5 AT TAKEOFF, SIMULATED-FLIGHT, TEST POINTS 4010 & 5010, FOR COMPARISON OF EJECTOR SETBACK S1 & S2

The radial cross section mean velocity traverses substantiate the axial traverses; i.e., peak velocity levels are normally considerably higher for the TE-5 configuration and near-centerline levels are similar for both configurations.

As seen in later Section 4.3 Figure 4-75, aerodynamic performance in the form of ΔC_{fg} attributable to chute base drag is dramatically improved for the S2 ejector location. The aft ejector location allows for improved chute ventilation, decreased base drag and, therefore, less C_{fg} degradation.

In summary, the aft ejector S2 location is both aerodynamically and acoustically superior to the closer S1 spacing.

4.2.3 Treatment Design Variation

Within the fully treated ejector/plug system of L1 ejector length, two variations of treatment design were investigated. The selections were made with the intent of achieving acoustic resistance of approximately 1 ρc and reactance as close to zero as possible in the frequency range of interest for the temperature and pressure of the test conditions. Because the test conditions within the ejector depended upon the simulated engine power setting, two treatment designs were selected to achieve or bracket the intended values of acoustic impedance. In both cases, the nominal thickness of the model treatment in the full-depth regions was 1.016 cm (0.4 inch). The first design, treatment T1, used an Astroquartz density of 0.0401 gm/cc (2.50 lb/cu. ft.) and the second, treatment T2, used 0.0160 gm/cc (1.00 lb/cu. ft.). The laboratory values of D.C. flow resistance for these two designs were 41.0 and 12.5 Rayls (cgs), respectively. Details of ejector and plug surface "tray packing" to achieve T1 and T2 treatment designs are described in Section 3.2.2 and in particular in Figure 3-32.

For direct comparison of treatment effectiveness, Configurations TE-9 and TE-4 were evaluated, each using the L1 ejector system at S2 ejector spacing. Treatments T1 and T2 were alternately applied to effect Configurations TE-9 and TE-4, respectively. Application was to the full ejector flowsurface as well as to the plug. Details of various data comparisons are found in Section 4.3.

Overview data comparisons in terms of peak OASPL and PNL, static and flight, are presented in Figures 4-53 and 4-54. On an OASPL basis, static and flight, T2 performs very similar to T1, showing only very slight improvement at the higher velocity region. On a PNL basis, statically T1 and T2 perform nominally similar for all cycle conditions. In simulated-flight, T2 is seen more effective by approximately 1 ΔPNL near the takeoff cycle point.

More detailed comparisons within Section 4.3 will view impact of treatment design on spectral suppression, directivity alterations, and changes in effectiveness of flight relative to static. An example of treatment effectiveness on spectral suppression is shown in Figure 4-55 for the takeoff cycle during static and simulated-flight operation. The graph exhibits the effect of treatment only, comparing TE-9 and TE-4 spectra directly to those of TE-2, the hardwall plug/hardwall ejector system. Treatment effectiveness is seen primarily in the 500 to 8 KHz frequency range with shapes of effectiveness patterns being fairly similar for both treatments. In this takeoff case, the T2 treatment shows slightly greater suppression for static, whereas, in flight, the T1 treatment is slightly more effective.

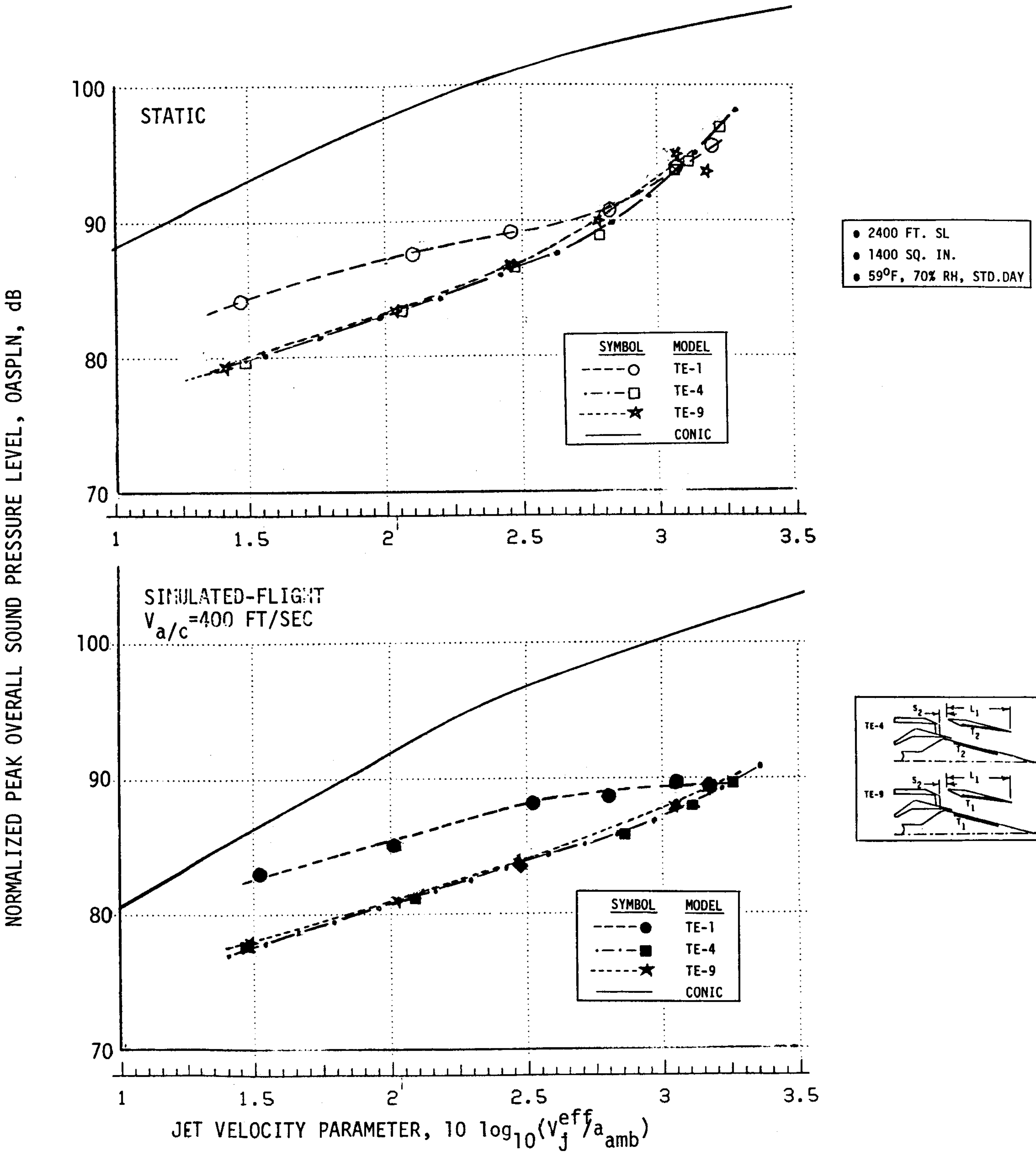

FIGURE 4-53 NORMALIZED PEAK OASPL AS A FUNCTION OF JET VELOCITY PARAMETER, STATIC AND SIMULATED-FLIGHT, FOR COMPARISON OF TREATMENT T1-CONFIGURATION TE-9 TO TREATMENT T2-CONFIGURATION TE-4

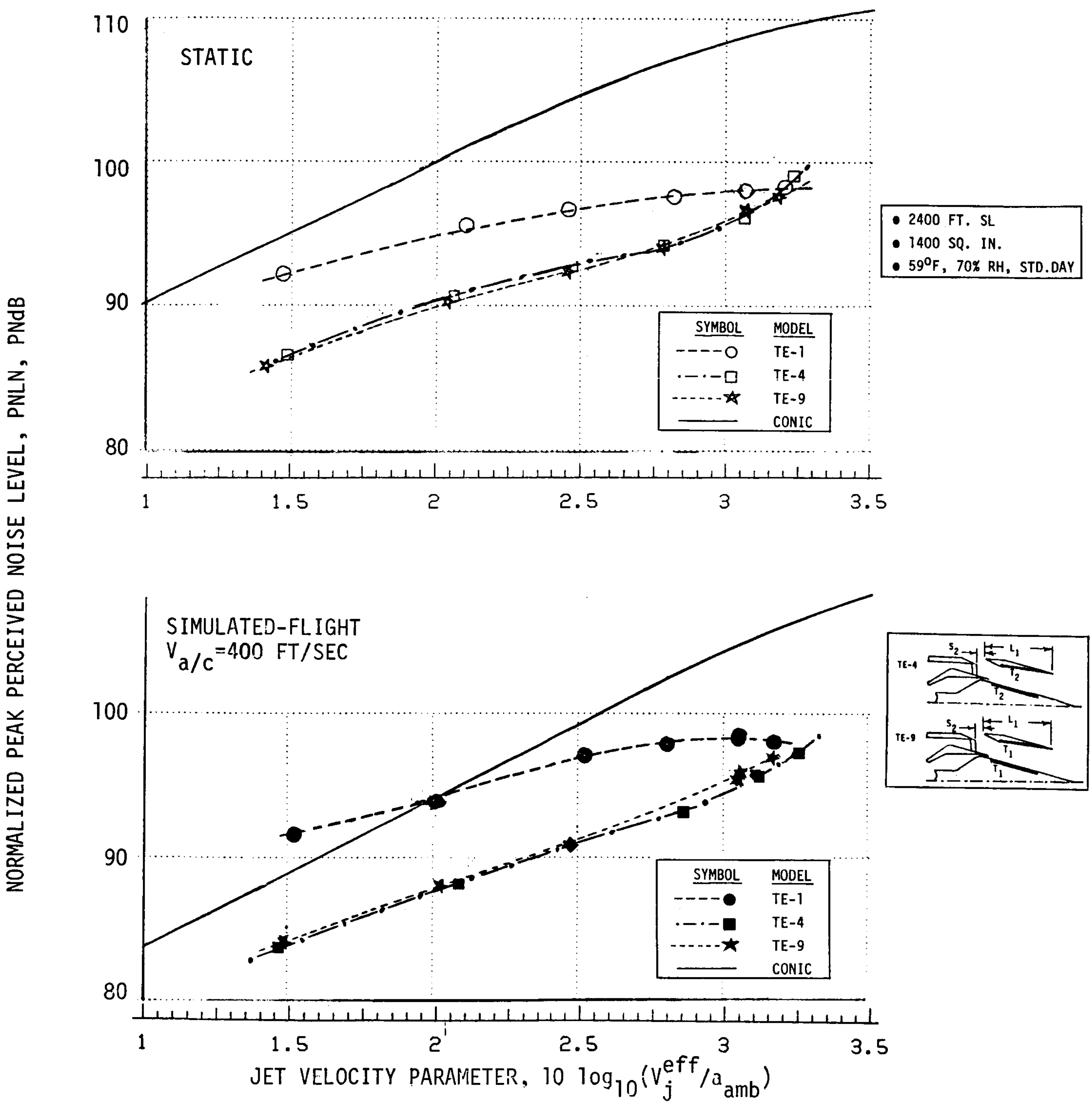

FIGURE 4-54 NORMALIZED PEAK PNL AS A FUNCTION OF JET VELOCITY PARAMETER STATIC AND SIMULATED-FLIGHT, FOR COMPARISON OF TREATMENT T1-CONFIGURATION TE-9 TO TREATMENT T2-CONFIGURATION TE-4

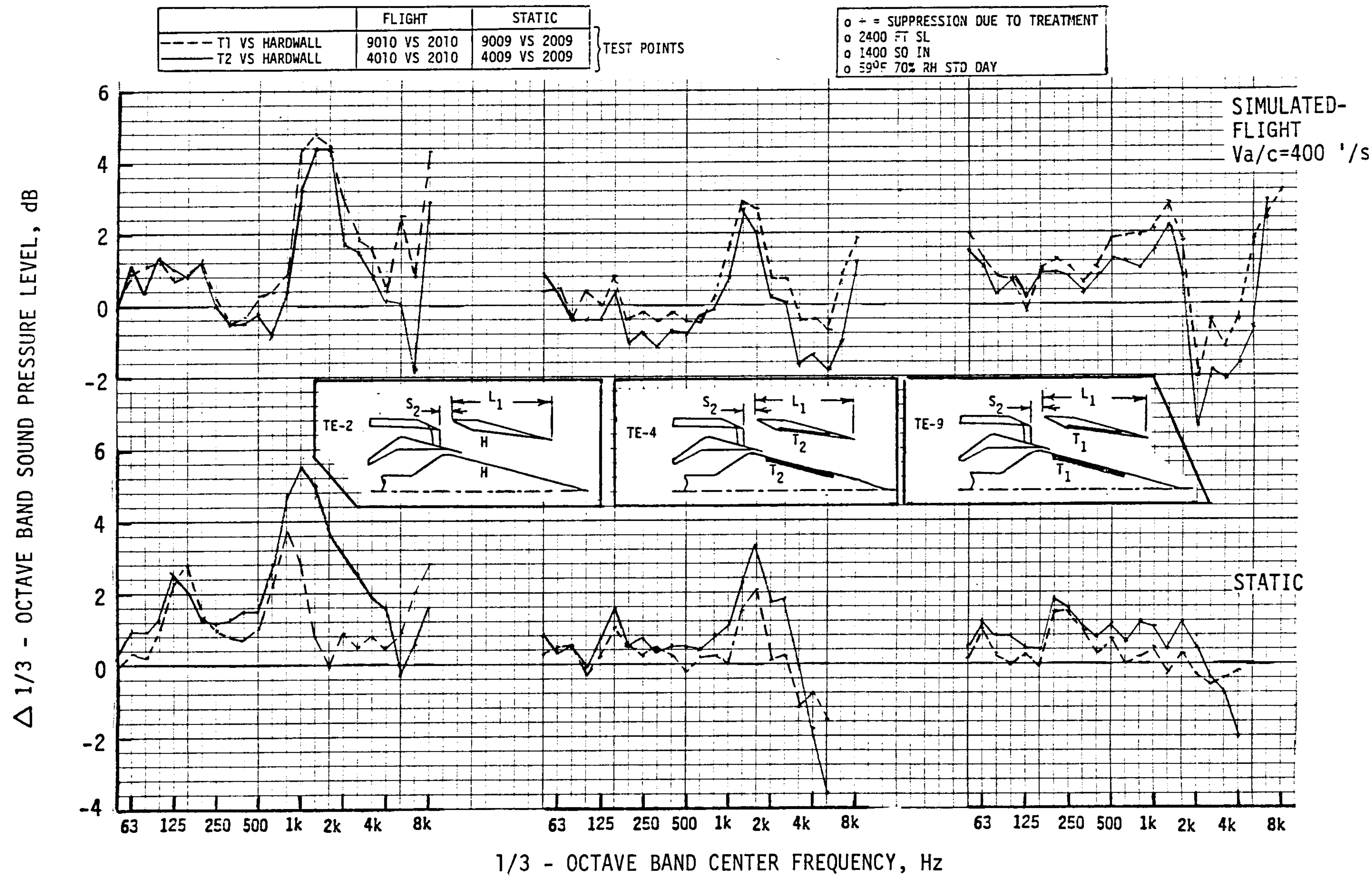

FIGURE 4-55. TREATMENT EFFECTIVENESS, T1 & T2 VS HARDWALL, AS A FUNCTION OF 1/3-OCTAVE BAND FREQ. AT TAKEOFF, STATIC AND SIMULATED-FLIGHT, θ_I = 60°, 90°, and 130°

Later results will also show the T1 and T2 treatments equally effective on an EPNL basis. In summary, T1 versus T2 treatment selection was not a critical parameter in providing total ejector system acoustic effectiveness.

4.2.4 Ejector Length Variation

Ejector length was varied within three comparative model sets, i.e., a) hardwall ejector and plug systems using TE-2 and TE-10, b) treated-ejector-surface systems using TE-3 and TE-7, and c) fully treated ejector/plug systems using TE-4 and TE-8. All ejector axial locations for these models were set at the S2 extended position. The L1-nominal length ejector was 8.68" long model-scale and was scaled from the full scale nozzle design of Reference 1 shown in Figure 2-1. It had acoustic treatment application over approximately 70% of its flap length. The L2-extended length ejector was 10.8" long model-scale and had treatment applied to a length equivalent to the full flap length of the L1 ejector system, for an increase in treated surface area of approximately 35%.

As discussed in detail within Section 4.5, primary effectiveness of the extended length system was seen in the forward quadrant with up to 3 ΔPNL additional suppression gained for the takeoff case at $\theta_I = 60^o$ due to ejector length increase, for both static and flight. In most cases, added length was most beneficial in the fully treated plug/ejector system. At broadside, e.g., $\theta_I = 90^o$, the longer ejector showed only slight improvement and only for the fully treated system. At the $\theta_I = 130^o$ aft quadrant location, all three long ejector systems created noise levels in excess of the shorter ejectors, by up to 1 to 1.5 ΔPNL.

Peak noise level comparisons are shown in Figure 4-56 and 4-57 for normalized OASPL and normalized PNL, static and flight, for the TE-4 and TE-8 model set. The comparisons show mostly mixed results relative to length effectiveness for the aft quadrant peak noise levels. Peak PNL is, however, reduced by approximately 1.5 ΔPNL near takeoff cycle.

On a spectral suppression basis, the longer ejector normally increases low frequency noise levels by 1 to 2 dB for 50 to 500 Hz. This can be correlated to LV plume decay data which show mean velocity to decay less rapidly for long ejectors than for short ejectors, thereby allowing longer zones of turbulent mixing noise generation of low frequency. Maximum spectral suppression due to ejector length is in the forward quadrant for the frequency range of 800 to 8 KHz, reaching suppression of 6 to 8 ΔdB near 2 KHz.

On the basis of aerodynamic performance, the extended length ejector system's thrust loss attributable to chute base drag is significantly below that of the nominal length ejector, indicating that it has better pumping/ventilating characteristics which raise chute base pressure and lower base drag.

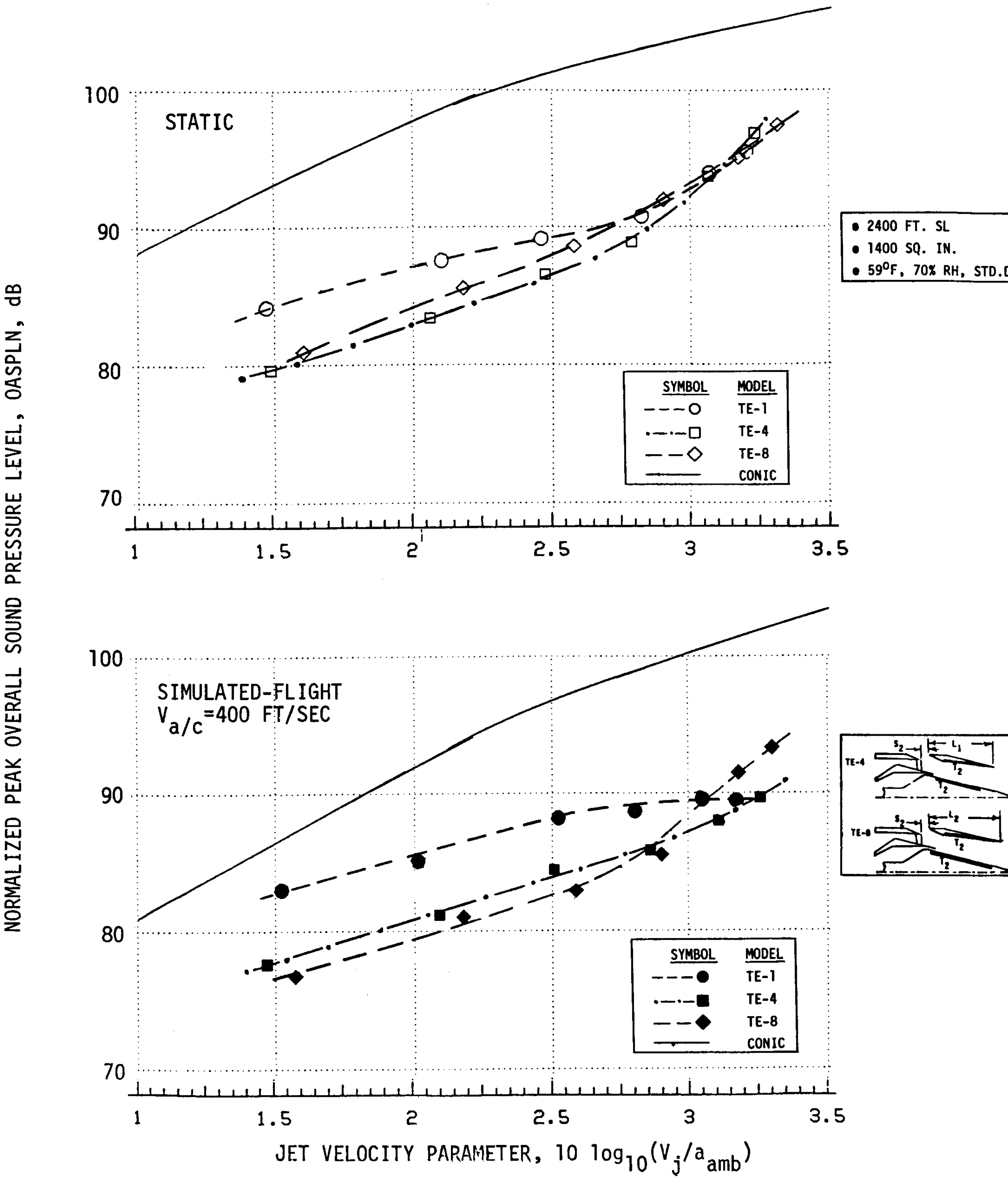

FIGURE 4-56 NORMALIZED PEAK OASPL AS A FUNCTION OF JET VELOCITY PARAMETER, STATIC AND SIMULATED-FLIGHT, FOR COMPARISON OF EJECTOR LENGTH, L1-CONFIGURATION TE-4 VERSUS L2-CONFIGURATION TE-8

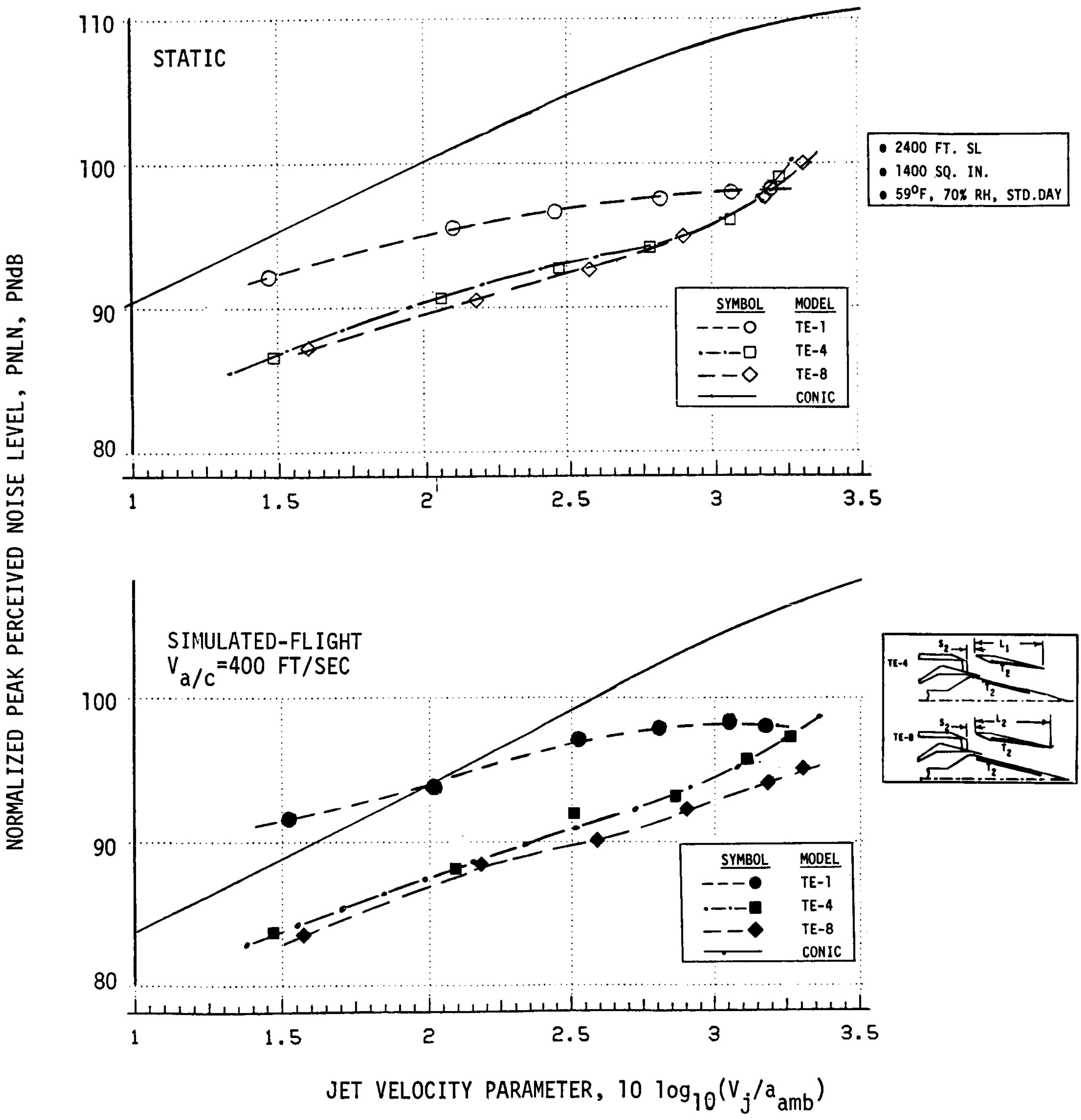

FIGURE 4-57 NORMALIZED PEAK PNL AS A FUNCTION OF JET VELOCITY PARAMETER, STATIC AND SIMULATED-FLIGHT, FOR COMPARISON OF EJECTOR LENGTH, L1-CONFIGURATION TE-4 VERSUS L2-CONFIGURATION TE-8

4.2.5 Extent of Treatment Application Within the Plug/Ejector System

The ejector system's acoustic effectiveness can be attributed to three individual sources, i.e.:

a. application of hardwall ejector

b. application of treatment to the ejector inner flowsurface, and

c. application of treatment to the plug surface, in conjunction with the ejector treatment.

The extended length, L2, and nominal length, L1, ejector sets, comprised of Configurations TE-7, TE-8, TE-10 and TE-2, TE-3, TE-4, respectively, allowed for evaluation of these individual suppression sources within two ejector length systems. Detailed data are presented and discussed in Section 4.4.

Static and flight peak PNL comparisons for the extended length ejector in Figure 4-58 are good examples of trends exhibited by more detailed data comparisons. They indicate that a) hardwall and treatment applications are more effective for flight PNL and in the low-to-moderately high velocity range, b) the hardwall ejector application, TE-10, provides a significant portion of the ejector system's aft quadrant PNL suppression effectiveness in flight and a small portion statically, c) application of treatment to the ejector inner flowsurface, TE-7, very effectively further reduces PNL levels except at high cycle conditions, and d) further treatment application to the plug surface, TE-8, allows still further static and primarily flight PNL reduction.

A broader view of individual source effectiveness is seen in Figure 4-59's ΔPNL suppression plot. This figure compares the extended and nominal length ejector configurations directly to the baseline TE-1 configuration, showing PNL suppression as a function of θ_I for three cycle conditions of cutback, intermediate and takeoff at simulated-flight. The Δ's represent incremental changes in suppression due to a) hardwall ejector applications, b) treated ejector applications, and c) treated ejector/treated plug applications. When comparing effectiveness between individual lines on the graph, incremental changes can be seen for a) treatment application to ejector surface relative to hardwall, and b) treatment application to the plug surface relative to treated ejector flowsurfaces only. The graphs reveal:

- The hardwall ejector, due to its physical shielding, provides the major portion of the ejector system's suppression effectiveness. In itself, it contributes substantially in both forward and aft quadrant suppression. Loss of effectiveness, particularly in the aft peak noise quadrant, is at the higher jet velocity takeoff cycle. Absolute levels of inlet quadrant suppression are normally somewhat greater than broadside and aft quadrant, particularly as the cycle is increased from cutback to takeoff. Of major significance is that the forward radiated jet noise is still reduced substantially at all cycle conditions, even though aft quadrant suppression levels diminish.

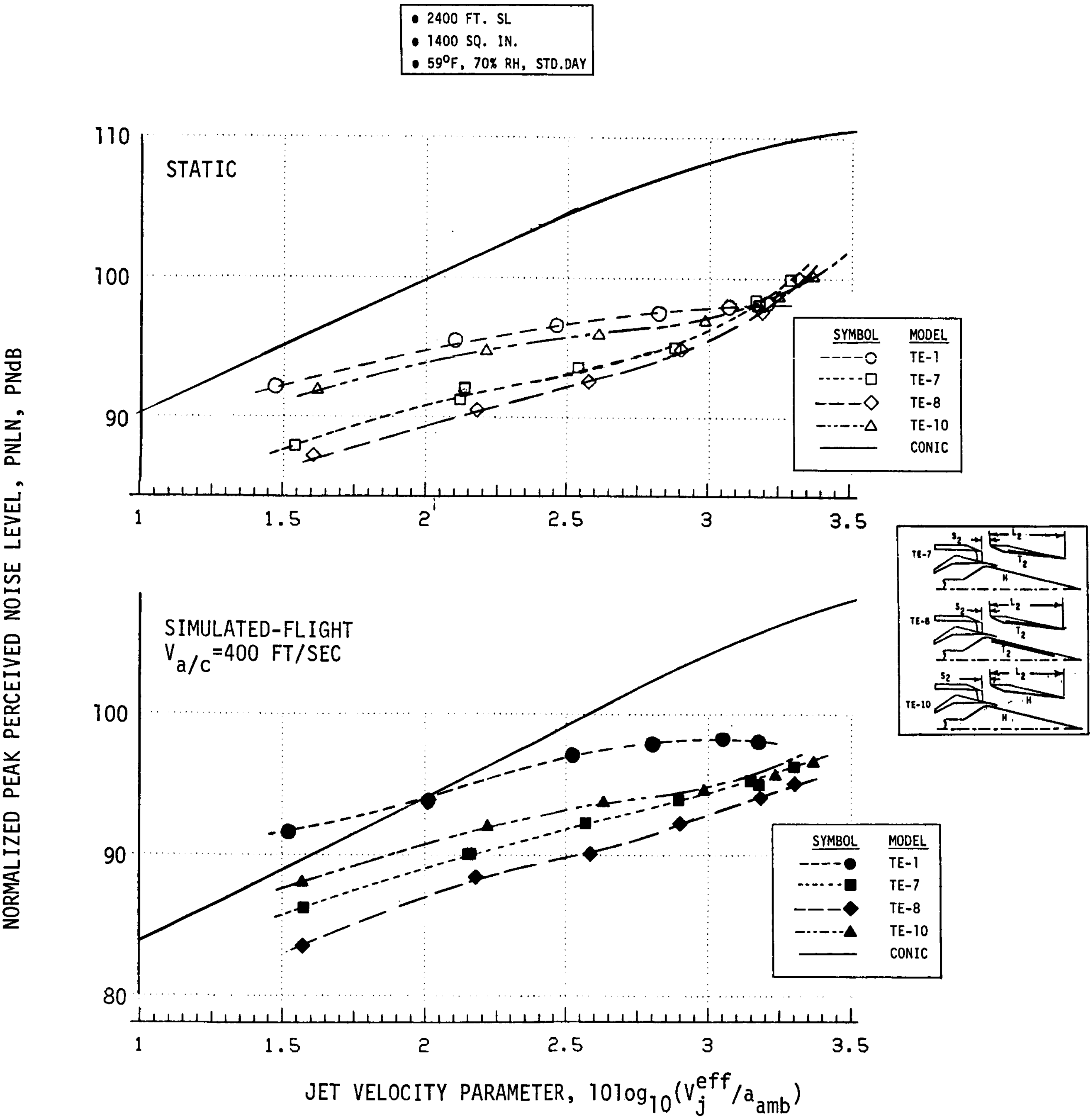

FIGURE 4-58 NORMALIZED PEAK PNL AS A FUNCTION OF JET VELOCITY PARAMETER, STATIC AND SIMULATED-FLIGHT, FOR IDENTIFICATION OF INDIVIDUAL SUPPRESSION SOURCE EFFECTIVENESS, CONFIGURATIONS TE-7, TE-8, AND TE-10.

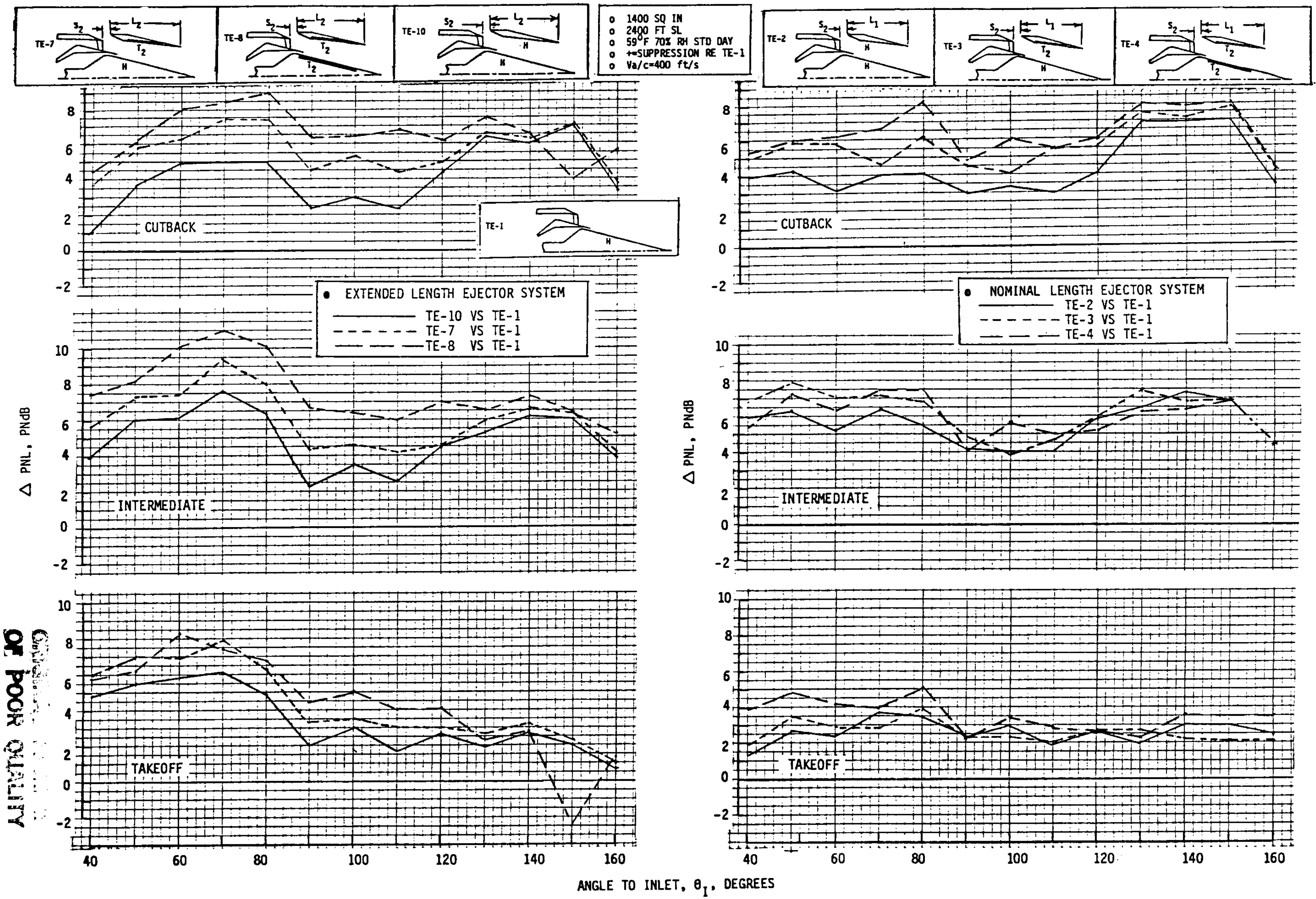

FIGURE 4-59. INDIVIDUAL SUPPRESSION SOURCE EFFECTIVENESS ON PNL SUPPRESSION, SIMULATED-FLIGHT, AT CUTBACK, INTERMEDIATE AND TAKEOFF.

ORIGINAL PAGE IS OF POOR QUALITY

- o Application of treatment to the ejector inner flowsurface is primarily effective within the extended length ejector, effectiveness being marginal within the nominal length ejector as many of these data comparisons show minimal to no increase in Δ PNL when the single surface treatment is added. For the extended length ejector system, the single surface treatment, however, is seen primarily effective on forward angle radiated noise suppression, peak noise angles being minimally effected.

- o Addition of further treatment to the plug surface significantly improves suppression of both L1 and L2 systems, the magnitude of improvement varying with cycle as internal flow conditions change, but showing no trend to implicate either ejector length or cycle as a dependent variable regulating improvement. The plug surface treatment again is more beneficial to forward quadrant suppression, aft quadrant peak noise being reduced just slightly further. In general, the conclusion can be drawn that plug surface treatment improves acoustic performance by a noteworthy amount, however, levels and trends are not easily predictable from the data comparisons.

4.3 VARIATIONS OF EJECTOR AXIAL SPACING AND TREATMENT DESIGN

Reference to Section 4.0 and Figure 4-1 indicates that chronology of tests was developed in order to reflect optimum ejector setback and treatment design during conduct of the test series. Optimum in these analyses are interpreted as "best between set comparions", S1 to S2 and T1 to T2, not absolute optimum available. The selections of optimum were to be made based on evaluation of on-line model size OASPL and spectra, the final full scale spectra and PNL values not being available in real-time. The test chronology and selections of optimum proceeded as follows:

- o TE-5, Ejector L1 of treatment T1 at axial spacing S1

- o TE-9, Ejector L1 of treatment T1 at axial spacing S2

- o TE-4, Ejector L1 of treatment T2 at axial spacing S2

From Configurations TE-5 and TE-9, varying ejector axial spacing, the on-line acoustic data indicated slightly better suppression performance for the S2 ejector positioning, thus it was retained for all further testing. From Configuration TE-9 and TE-4, varying ejector treatment design, the on-line acoustic data indicated slightly better performance for T2 treatment, thus this design was retained for all further testing. This report section presents final scaled, flight transformed (where applicable), extrapolated data comparisons for these three configurations to substantiate whether initial selections of S2 and T2 were accurate. In retrospect, the final processed data bear out the on-line selections and verify that a) S2 ejector setback is superior in both acoustic suppression and aerodynamic performance above the S1 location, and, b) T1 versus T2 treatment designs present mixed results, in some areas the T1 showing slightly increased suppression and in other areas T2 being slightly superior.

4.3.1 Acoustic Data Presentation and Evaluation

Examination of acoustic data is introduced with comparisons of normalized PWL for static and flight in Figure 4-60. Using this overview parameter, the conclusions are:

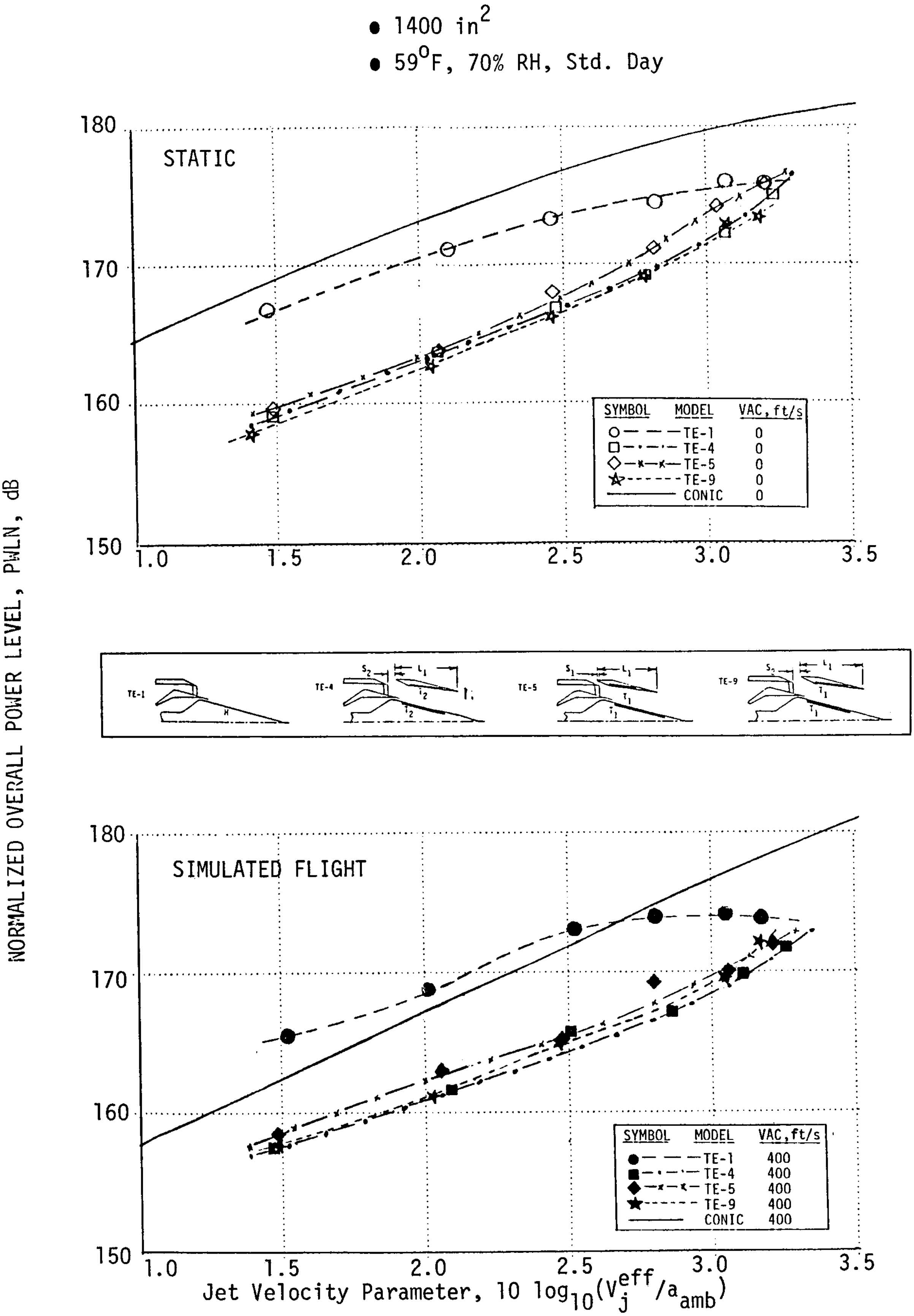

FIGURE 4-60. NORMALIZED PWL AS A FUNCTION OF JET VELOCITY PARAMETER FOR COMPARISON OF EJECTOR SETBACK, S1 VS. S2, AND EJECTOR/PLUG TREATMENT, T1 vs. T2; STATIC & SIMULATED FLIGHT

- o Ejector setback S2 allows more efficient suppression over S1, the trend maintained for all cycle conditions and for both static and flight.

- o Ejector treatments T1 and T2 are marginally similar for static, the T1 showing less than .5 dB greater suppression, however, in flight PWL suppression is more efficient using T2 design, particularly at high V_j values with approximately .7 dB Δ at takeoff.

Further acoustic performance comparisons are presented for OASPL and PNL, static and flight, in Figures 4-61 through 4-64. Each of these graphs presents θ_I = 60°, 90°, 130° and peak values for TE-5, TE-9 and TE-4. Additionally, each contains conic nozzle and TE-1 baseline data. Scanning the graphs for comparisons of TE-9 versus TE-5 indicates:

- o S1 setback, TE-5, is normally slightly less efficient at low jet velocity settings for all parameter comparisons and is particularly poorer at higher cycle settings when evaluated on PNL basis. At takeoff cycle, nearly 2 dB increased suppression is noted for static and 1 dB for flight PNL using the S2/TE-9 ejector position.

Examining the same graphs for comparisons of TE-4 to TE-9 concludes:

- o On an OASPL basis, static and flight, T2 performs very similar to T1, showing only very slight improvement for most angles in the higher velocity region. This would be expected as the treatment is designed primarily for high frequency suppression, normally beyond peak frequency of jet-controlled spectra where little impact on OASPL is expected.

- o On a PNL basis, statically T1 and T2 perform nominally similar for all angles at all cycle conditions. In flight, T2 is seen more effective only at forward quadrant and peak values and then by 1 or less ΔPNL.

More detailed comparisons of data on a directivity basis are shown in Fiures 4-65, 4-66 and 4-67 for three cycle points of cutback, intermediate and takeoff, respectively. Each graph presents both normalized OASPL and PNL versus angle relative to inlet, θ_I, and for both static and flight. TE-1 and conic nozzle baselines at similar cycle conditions are also included. Detailed review of ejector setback comparisons of TE-9 versus TE-5 indicate:

- o For all comparisons, the S2 setback's suppression exceeds that of S1, particularly so for the high jet velocity takeoff cycle. At takeoff, the S2 improvement is exemplified by a Δ plot in Figure 4-68. The figure shows improved PNL and OASPL suppression as a function of θ_I for S2 spacing for both static and flight.

Examining the same Figure 4-65 through 4-67 graphs for comparison of TE-4 to TE-9 for treatment effectiveness indicates:

- o Mixed regions of effectiveness for optimizing T1 versus T2.

- o At cutback and intermediate, statically T1 and T2 perform similarly; in-flight, T1 is slightly more efficient for OASPL and PNL.

- o At takeoff, T2 is slightly more efficient statically and T1 is slightly superior in flight; each on both PNL and OASPL.

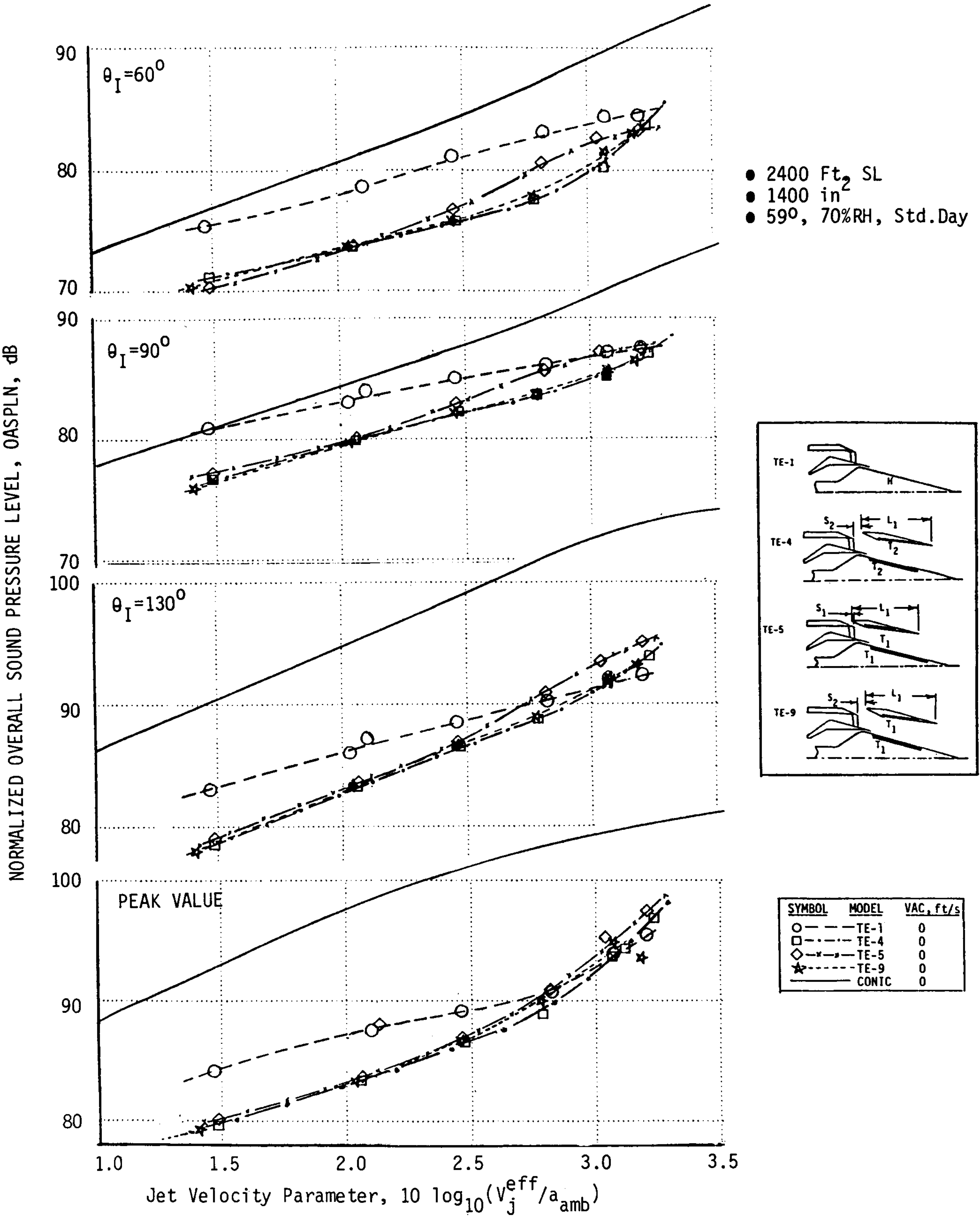

FIGURE 4-61. NORMALIZED OASPL AS A FUNCTION OF JET VELOCITY PARAMETER FOR COMPARISON OF EJECTOR SETBACK, S1 VS. S2, AND EJECTOR/PLUG TREATMENT, T1 VS. T2; STATIC, AT θ_I=60°, 90°, 130° & PEAK VALUE

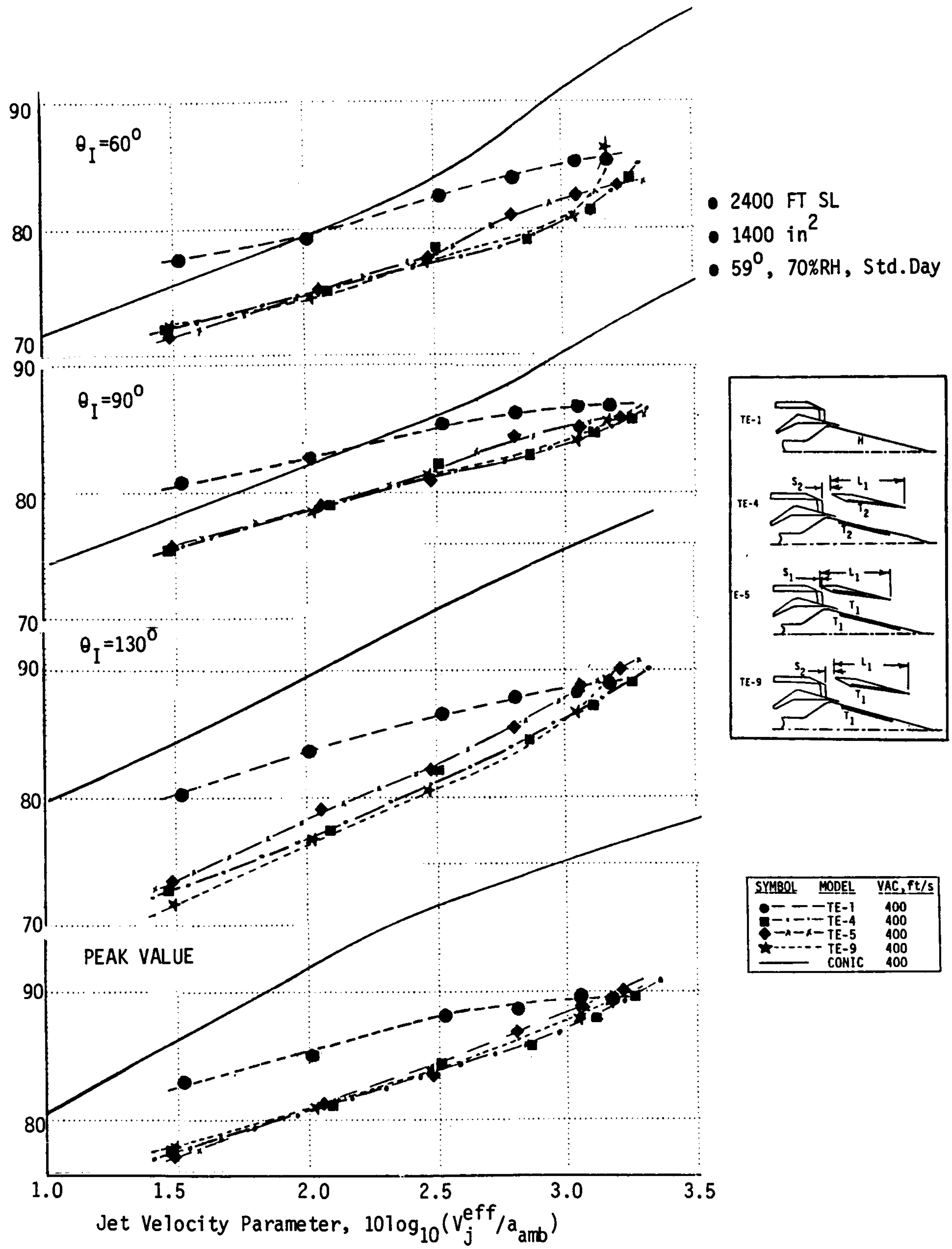

FIGURE 4-62. NORMALIZED OASPL AS A FUNCTION OF JET VELOCITY PARAMETER FOR COMPARISON OF EJECTOR SETBACK, S1 vs S2, AND EJECTOR/PLUG TREATMENT, T1 vs T2; SIMULATED FLIGHT, AT $\theta_I = 60^o$, 90^o, 130^o & PEAK VALUE

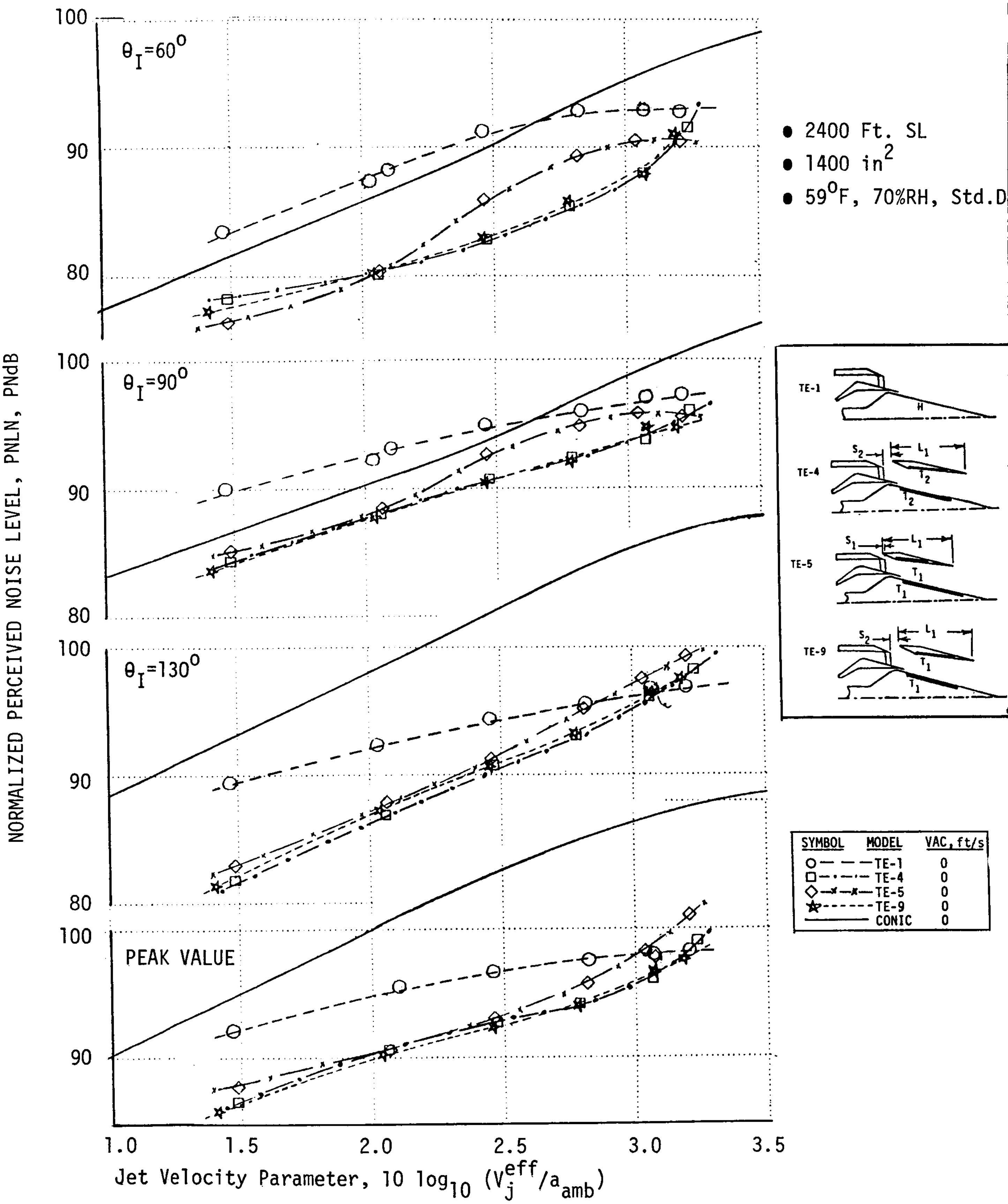

FIGURE 4-63. NORMALIZED PNL AS A FUNCTION OF JET VELOCITY PARAMETER FOR COMPARISON OF EJECTOR SETBACK, S1 vs S2, AND EJECTOR/PLUG TREATMENT, T1 vs T2; STATIC, AT θ_I=60°, 90°, 130°, AND PEAK VALUE

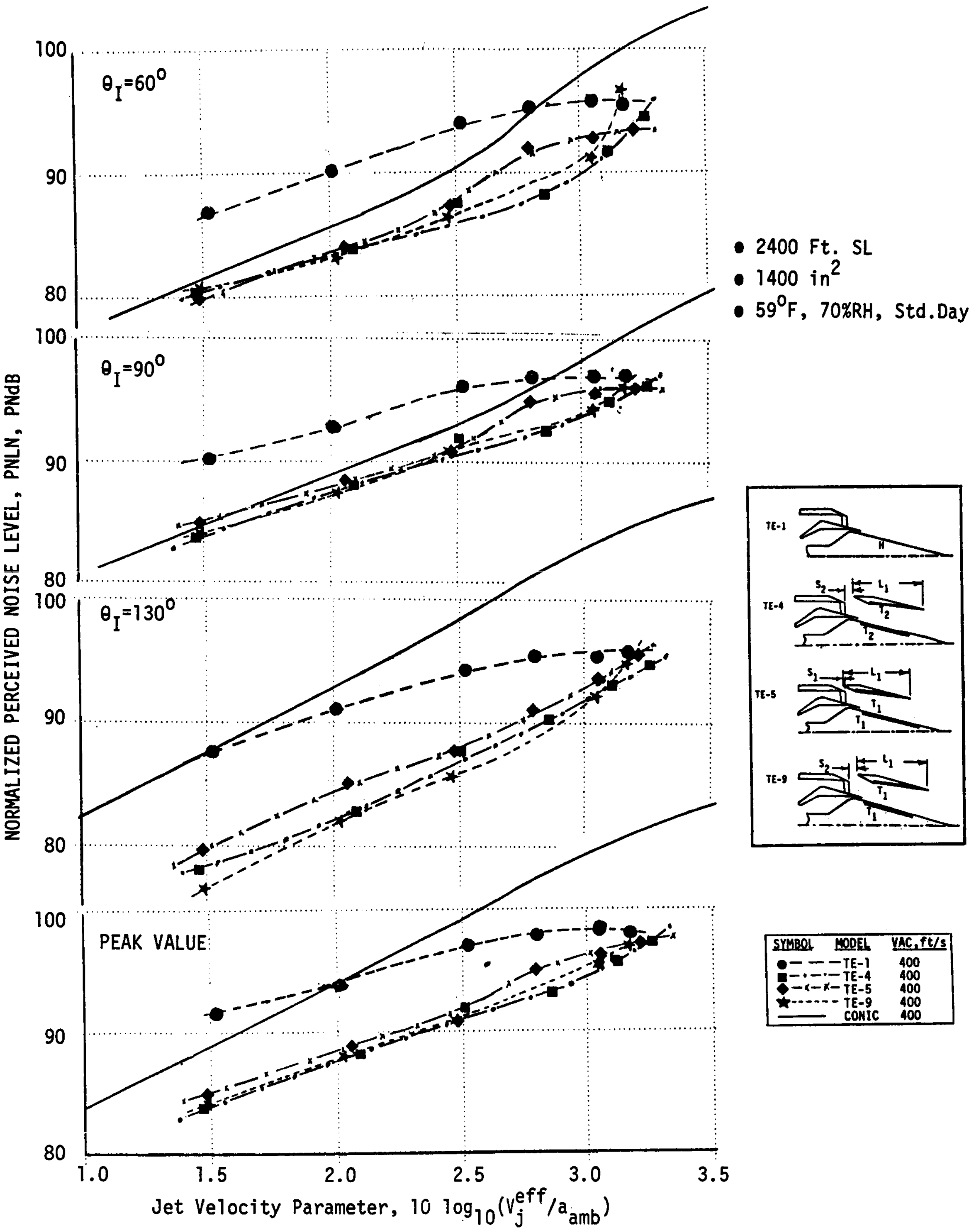

FIGURE 4-64. NORMALIZED PNL AS A FUNCTION OF JET VELOCITY PARAMETER FOR COMPARISON OF EJECTOR SETBACK, S1 vs S2, AND EJECTOR/PLUG TREATMENT, T1 vs T2; SIMULATED FLIGHT, AT $\theta_I = 60^0$, 90^0, 130^0 AND PEAK VALUE

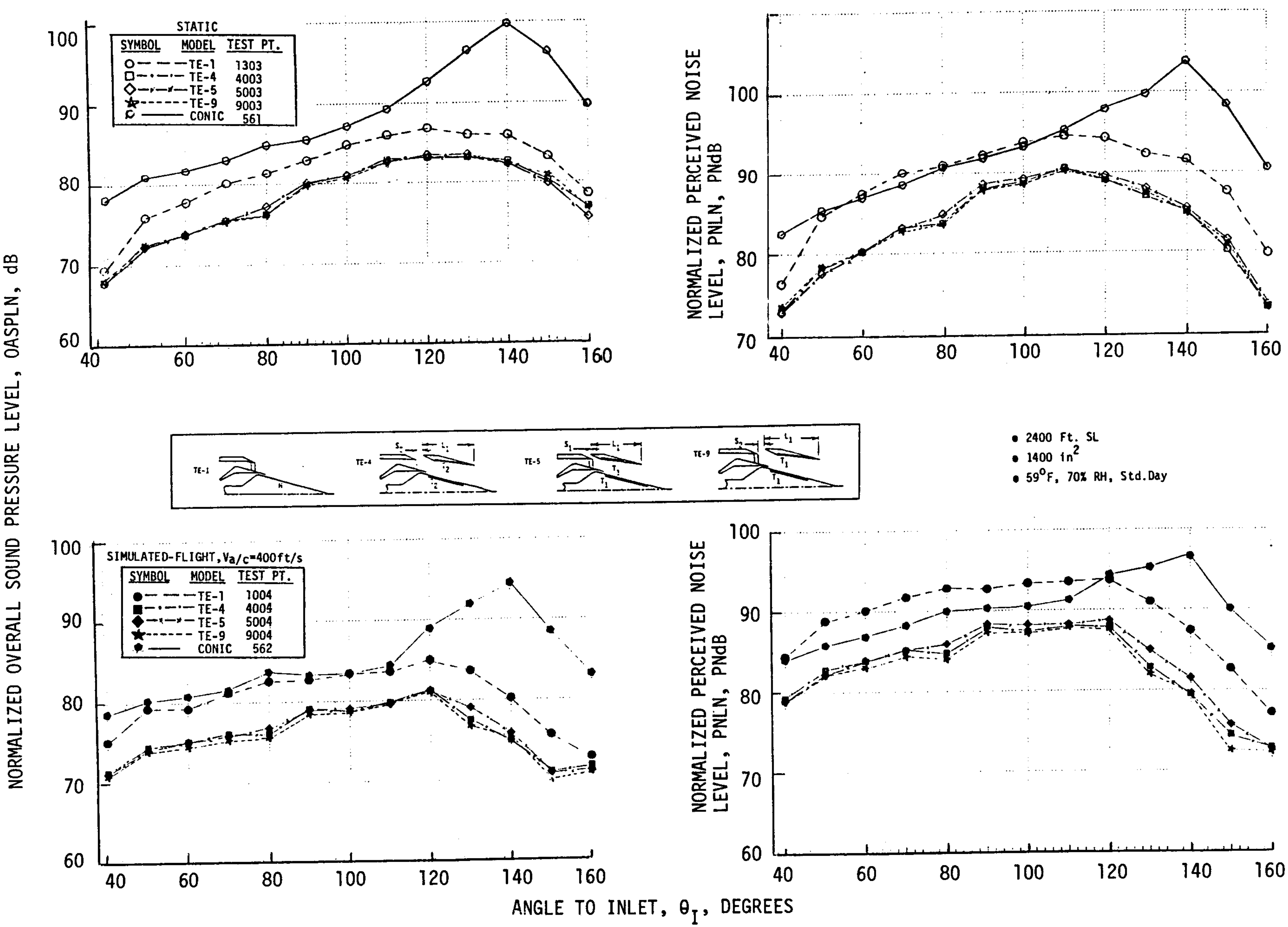

FIGURE 4-65. STATIC AND SIMULATED-FLIGHT DIRECTIVITY COMPARISONS OF OASPL AND PNL AT CUTBACK FOR COMPARISON OF EJECTOR SETBACK, S1 vs S2, AND EJECTOR/PLUG TREATMENT, T1 vs T2

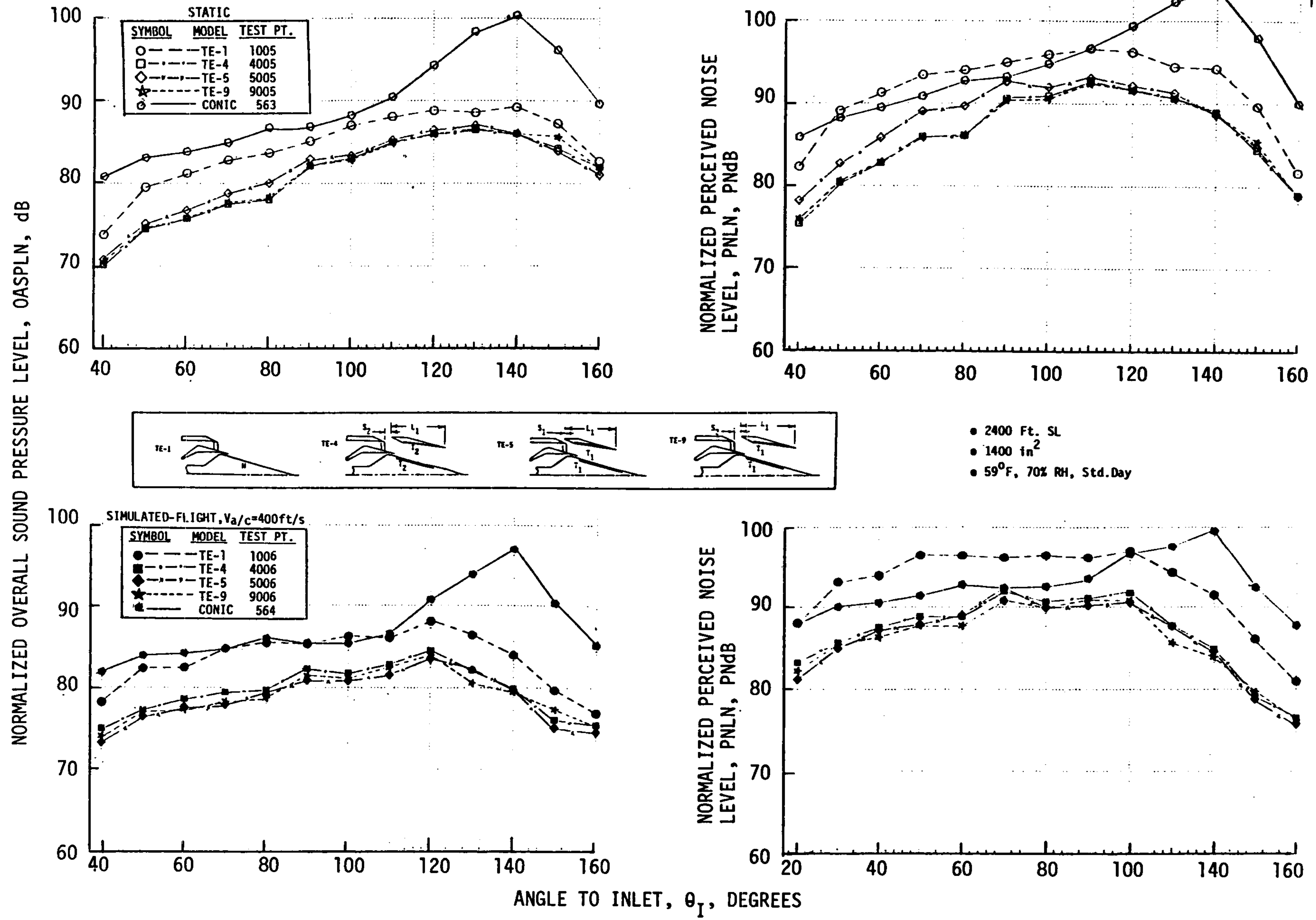

FIGURE 4-66. STATIC AND SIMULATED-FLIGHT DIRECTIVITY COMPARISONS OF OASPL AND PNL AT INTERMEDIATE FOR EJECTOR SETBACK, S1 vs S2, AND EJECTOR/PLUG TREATMENT, T1 vs T2

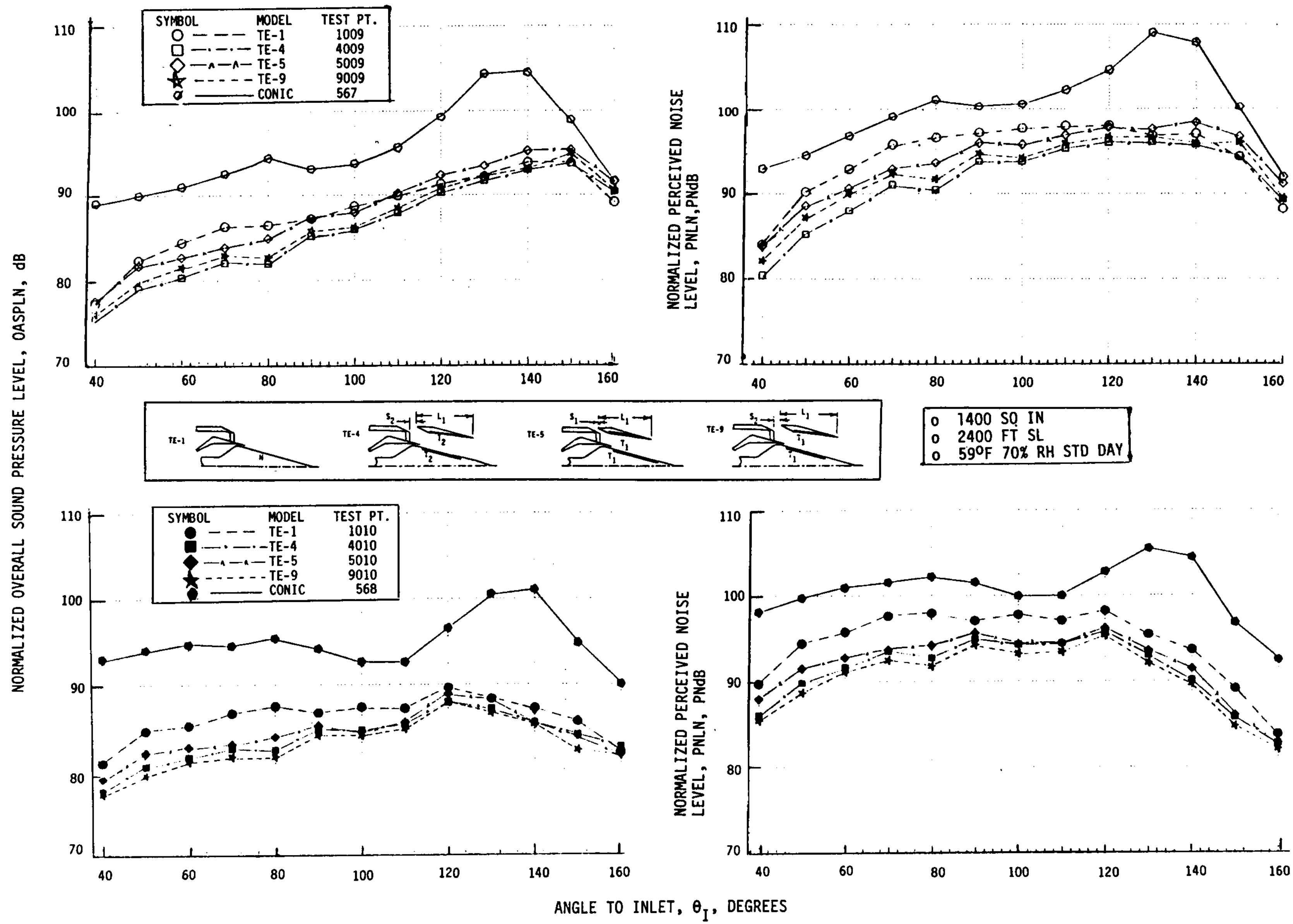

FIGURE 4-67. STATIC AND SIMULATED-FLIGHT DIRECTIVITY COMPARISONS OF OASPL AND PNL AT TAKEOFF FOR COMPARISON OF EJECTOR SETBACK, S1 VS S2, AND EJECTOR/PLUG TREATMENT, T1 VS T2.

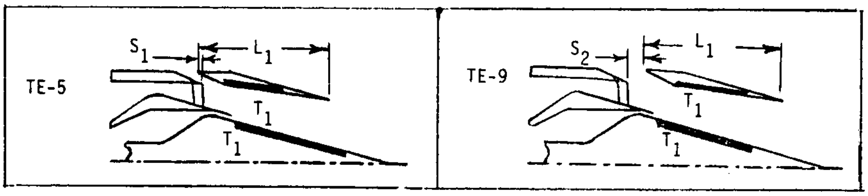

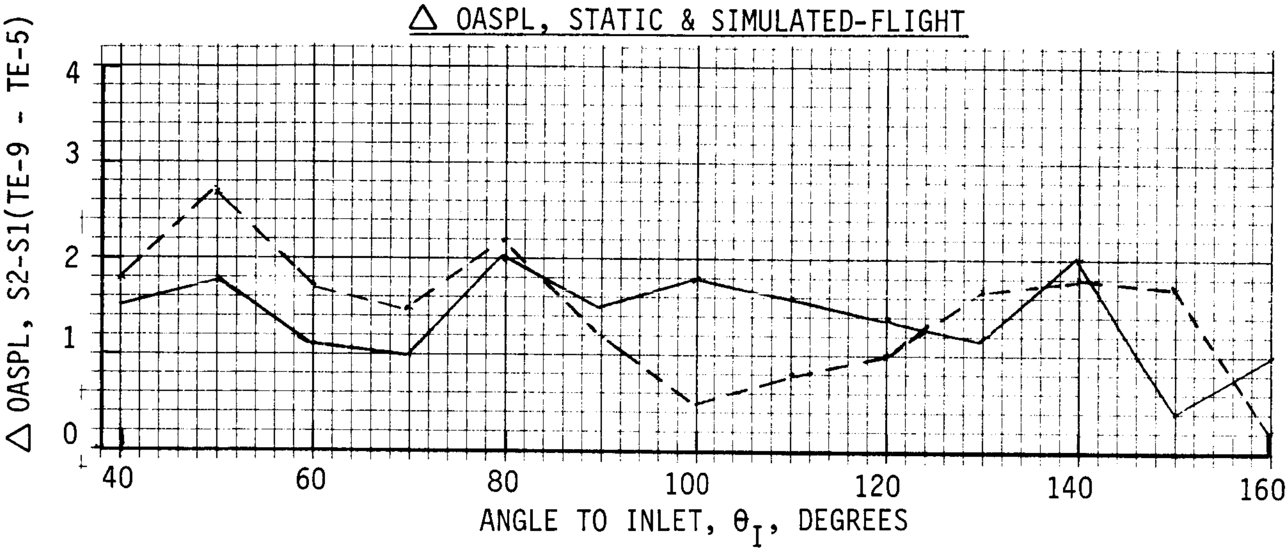

	TE-9	TE-5	
——— STATIC	9009	5009	TEST POINTS
– – – SIMULATED-FLIGHT	9010	5010	

- o 1400 SQ IN
- o 2400 FT SL
- o 59°F 70% RH STD DAY

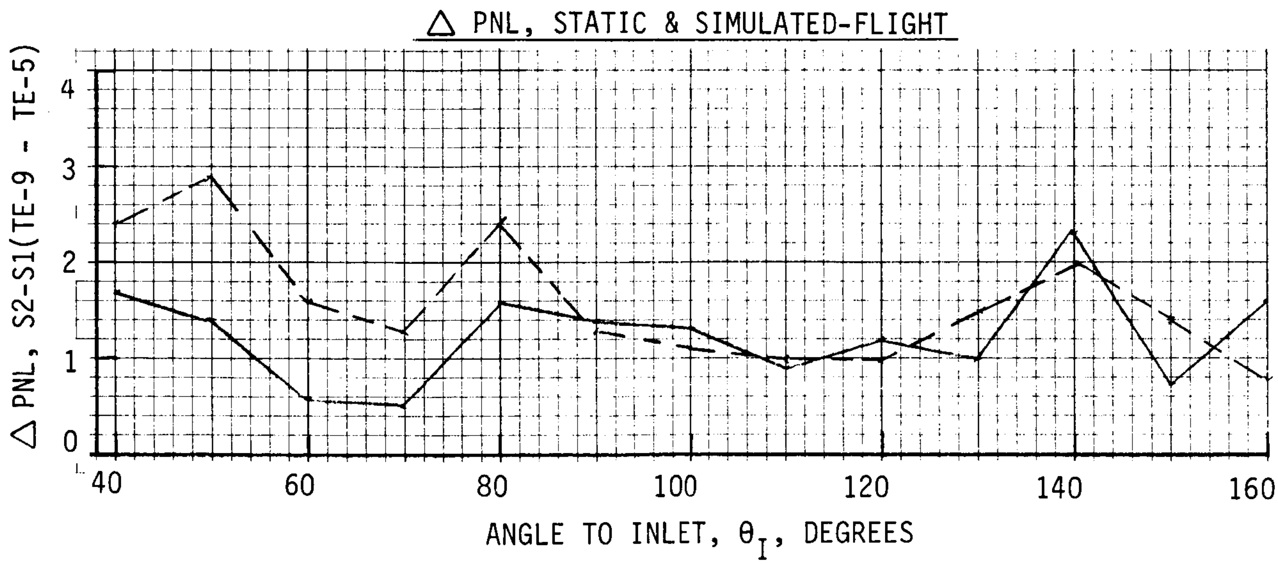

FIGURE 4-68. PNL AND OASPL SUPPRESSION BENEFIT OF EJECTOR SETBACK, S2 VS S1, AT TAKEOFF, STATIC & SIMULATED-FLIGHT

In the previous comparisons of OASPL and PNL directivities for S1 versus S2 and T1 versus T2, the largest variations for the three cycle conditions were seen at takeoff. Figures 4-69 and 4-70 present spectra comparisons at that condition, for static and flight, respectively. The figures exemplify select angles of θ_I = 60°, 90° and 130°. Observations from these data are:

- TE-5 spectra for S1 spacing are significantly above the levels of TE-9 with S2 spacing, for all three angles, static and flight; therefore, again indicating S2 as more effective.

- Low frequency humps occur for TE-5, levels being substantially above those of the TE-1 baseline unejected model, indicative of potential induced shock noise. The peaks, particularly in the forward quadrant, are well above those of TE-9, although still slightly present in TE-9 spectra.

- In comparing TE-4/T2 treatment versus TE-9/T1 treatment, the results bear out the observations made from the PNL and OASPL directivity graphs, i.e., statically the T2 treatment is more effective, particularly in mid-to-high-frequency and at sideline to inlet angles. In-flight, the T1 treatment is slightly more effective in the mid-to-high-frequency spectra.

To further exemplify the effect of treatment design, Figures 4-71, 4-72 and 4-73 show treatment effectiveness as a function of 1/3-octave band frequency at cutback, intermediate and takeoff cycle cases, respectively. The graphs were developed to show the effect of treatment only, therefore, TE-9 and TE-4 spectra were compared directly to those of TE-2, the hardwall plug/hardwall ejector system. Each model was, therefore, of L1 ejector length and S2 spacing; the only variation being application of either T1 or T2 treatment versus hardwall.

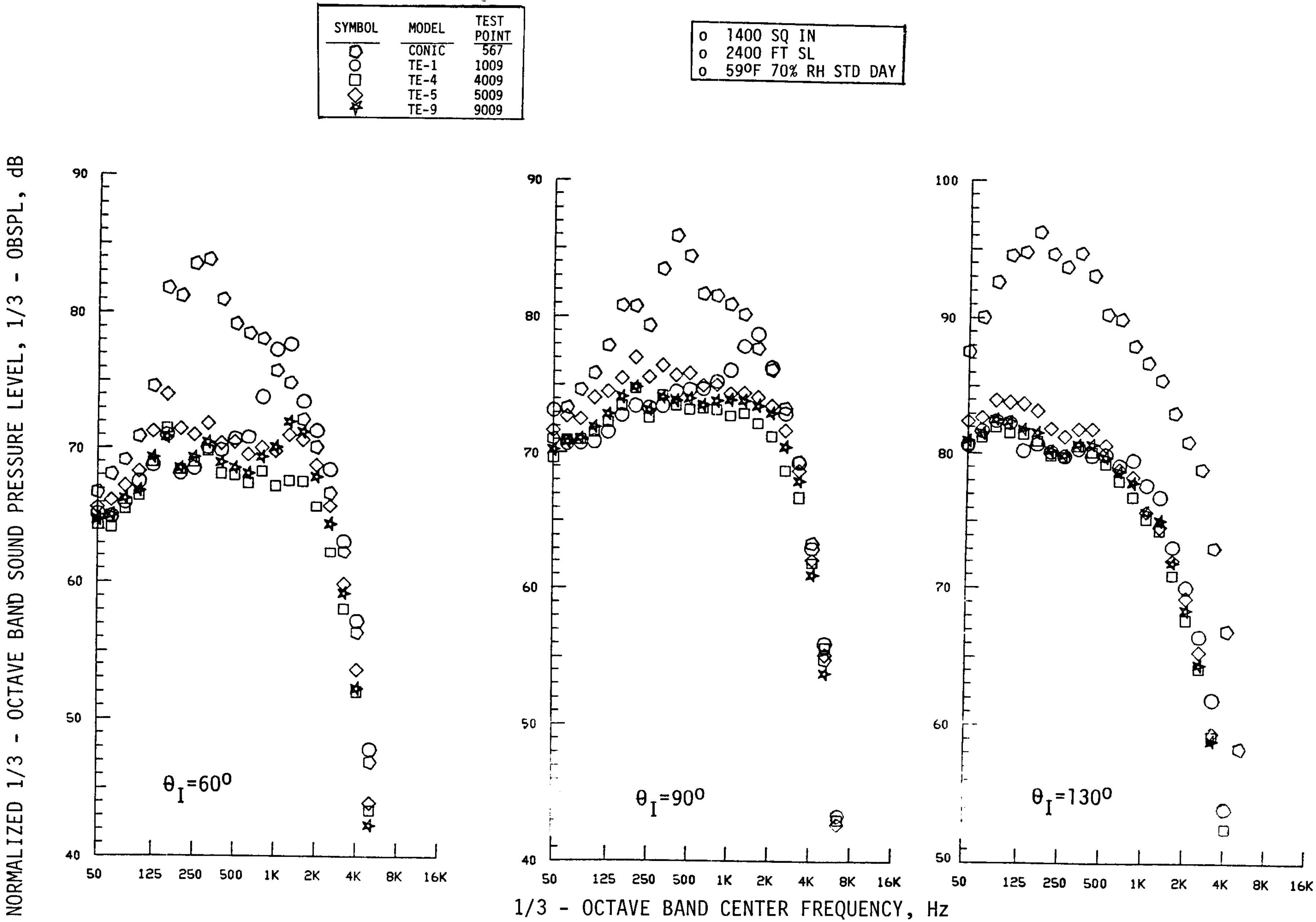

FIGURE 4-69. NORMALIZED SPECTRA AT θ_I=60°, 90° & 130° FOR COMPARISON OF EJECTOR SETBACK, S1 VS S2 AND EJECTOR/PLUG TREATMENT, T1 VS T2, STATIC, AT TAKEOFF

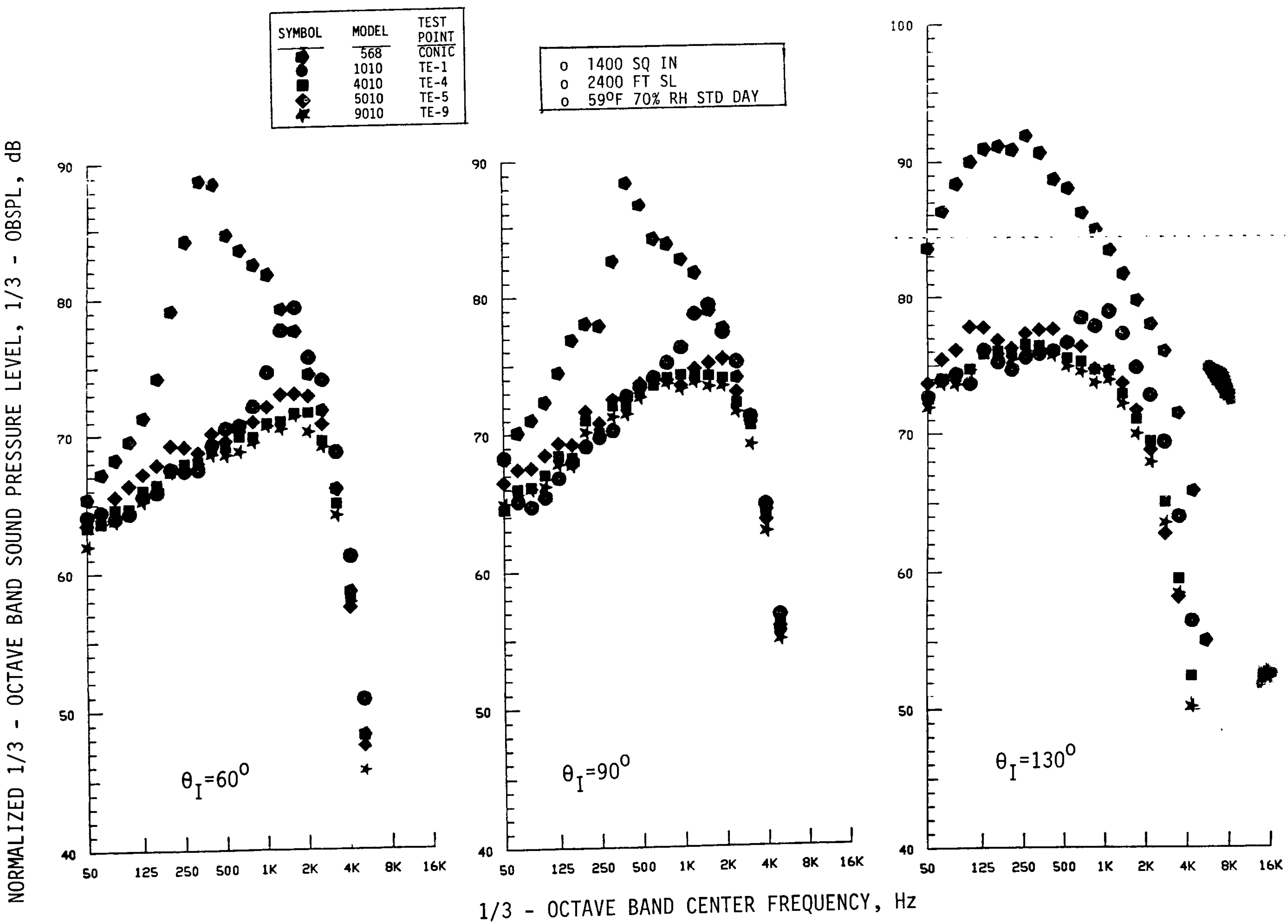

FIGURE 4-70 NORMALIZED SPECTRA AT $\theta_I=60^0$, 90^0 & 130^0 FOR COMPARISON OF EJECTOR SETBACK, S1 VS S2, AND EJECTOR/PLUG TREATMENT, T1 VS T2. SIMULATED-FLIGHT, AT TAKEOFF.

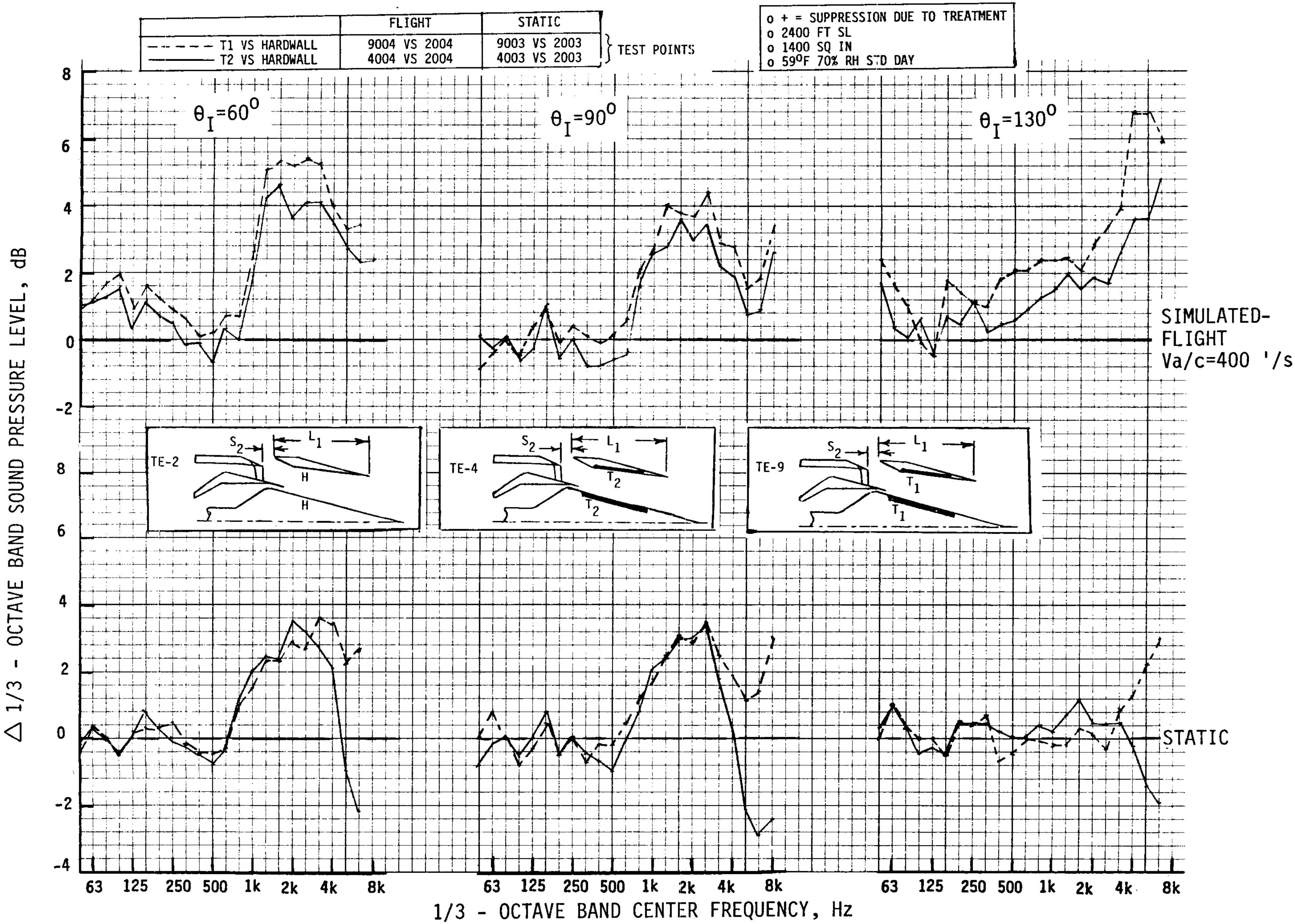

FIGURE 4-71. TREATMENT EFFECTIVENESS, T1 AND T2 VS HARDWALL, AS A FUNCTION OF 1/3 - OCTAVE BAND FREQUENCY AT CUTBACK, STATIC AND SIMULATED-FLIGHT, $\theta_I=60^o$, 90^o & 130^o.

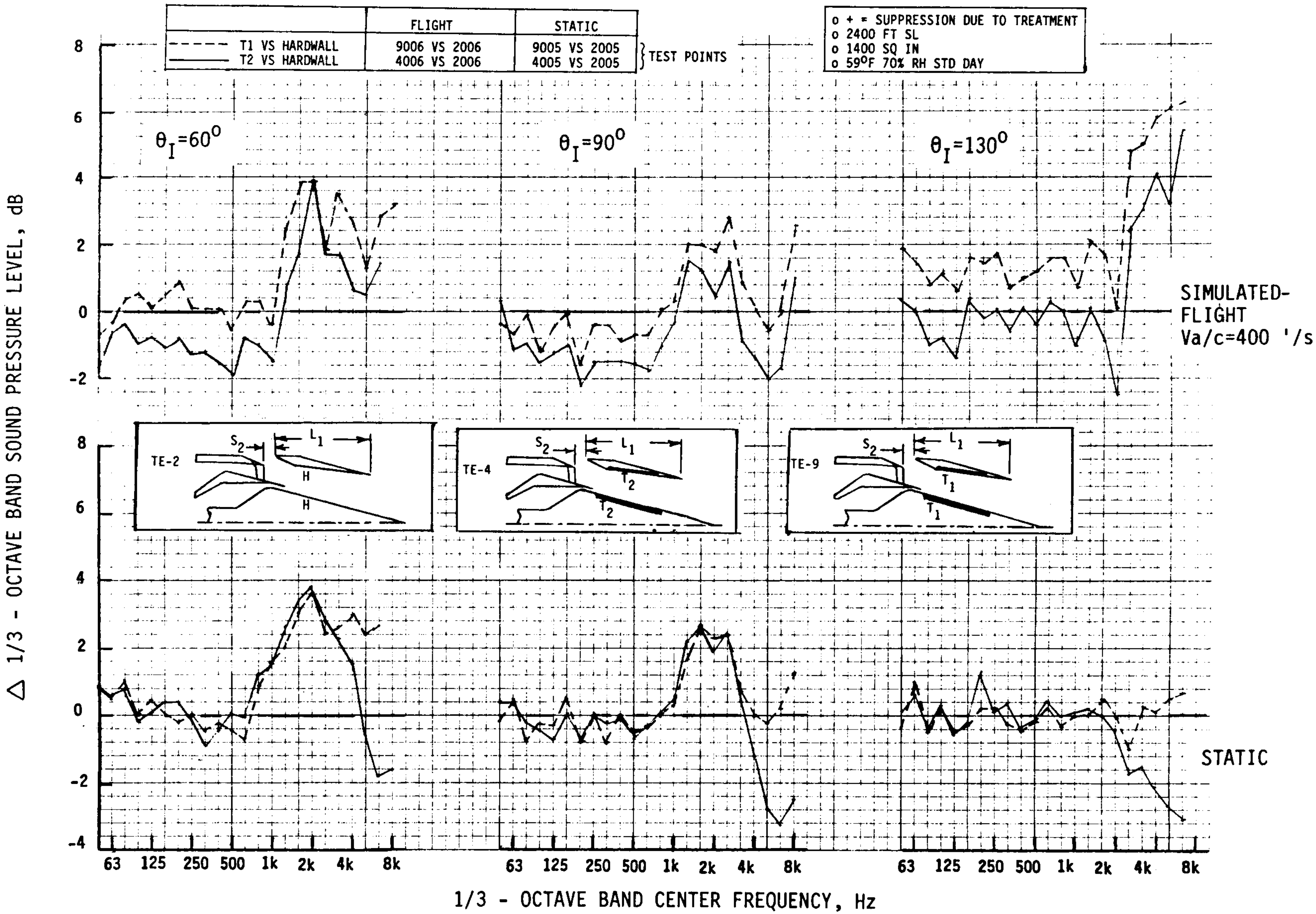

FIGURE 4-72. TREATMENT EFFECTIVENESS, T1 AND T2 VS HARDWALL, AS A FUNCTION OF 1/3 - OCTAVE BAND FREQUENCY AT INTERMEDIATE, STATIC AND SIMULATED-FLIGHT, θ_I=60°, 90°, & 130°.

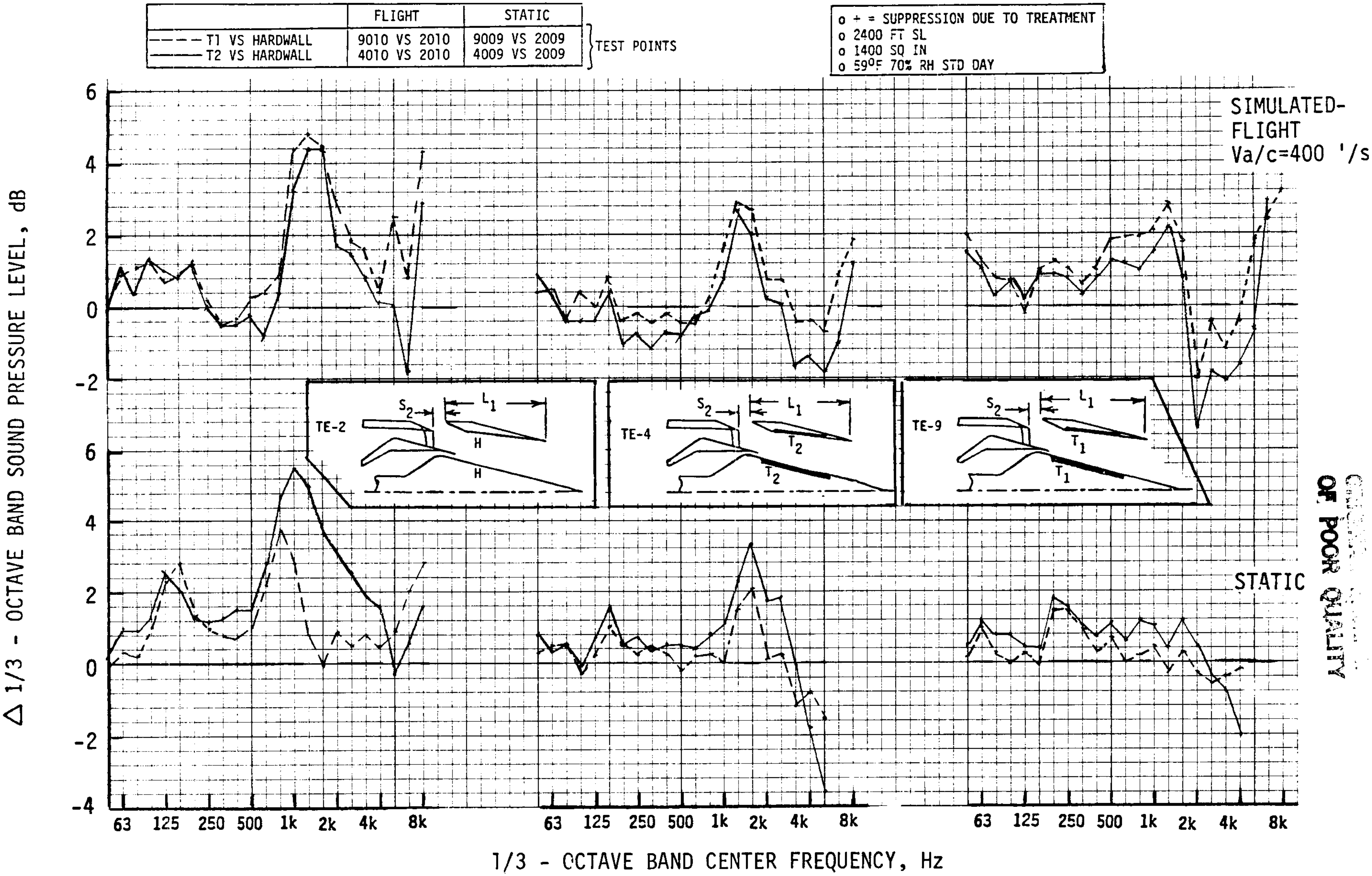

FIGURE 4-73. TREATMENT EFFECTIVENESS, T1 & T2 VS HARDWALL, AS A FUNCTION OF 1/3-OCTAVE BAND FREQ. AT TAKEOFF, STATIC AND SIMULATED-FLIGHT, θ_I = 60°, 90°, and 130°

Data are presented at θ_I = 60°, 90° and 130° and for static and flight; observations indicate:

- o In all cases, suppression of either T1 or T2 occurs primarily in the 500 to 8 KHz frequency range; shapes of effectiveness patterns are generally the same for both.
- o Static results for all three conditions are generally a mixed choice of optimal effectiveness, both designs performing near similarly with the exception of slightly improved suppression for T2 at takeoff.
- o In-flight results for all three cycle points and at all three presented angles, however, show slightly increased effectiveness of the T1 treatment.

A final acoustic comparison of the three models is presented in Figure 4-74 as normalized EPNL variation against the jet velocity parameter. The EPNL calculations are based on the 2400 ft sideline PNL directivity patterns and are for a nominal aircraft (simulated-flight) speed of 400 ft/sec. Conical nozzle and baseline TE-1 data are included for reference. Observations elicit:

- o Comparison of S2/TE-9 versus S1/TE-5 show the S2 setback superior to S1, by approximately 1 ΔEPNL at cutback and takeoff.
- o T1 and T2 treatments perform equally on the basis of EPNL.

Laser velocimeter plume measurements for comparison of the two ejector axial locations were previously presented in Section 4.2's Figures 4-49 through 4-52. The data indicated that a) the initial velocity levels at the ejector exit for S1 spacing are somewhat higher than for the S2 position and the higher velocity levels persist for a substantial distance aft of the exit, and b) mild shock structure is present in the plume just aft of the S1-located ejector, however, none is seen in the S2-located ejector plume. These observations aid in understanding the source of higher noise levels for the S1 positioned ejector model.

4.3.2 Aerodynamic Performance Data

As an indication of relative aerodynamic performance, Figure 4-75 compares thrust loss due to base drag for the TE-4, TE-5 and TE-9 configurations. Section 4.8, "Aerodynamic Performance Evaluation" describes how chute base pressure instrumentation is used to calculate base drag. This is subsequently used as an indication of thrust coefficient degredation, expressed as a percentage of outer stream (suppressor) ideal thrust.

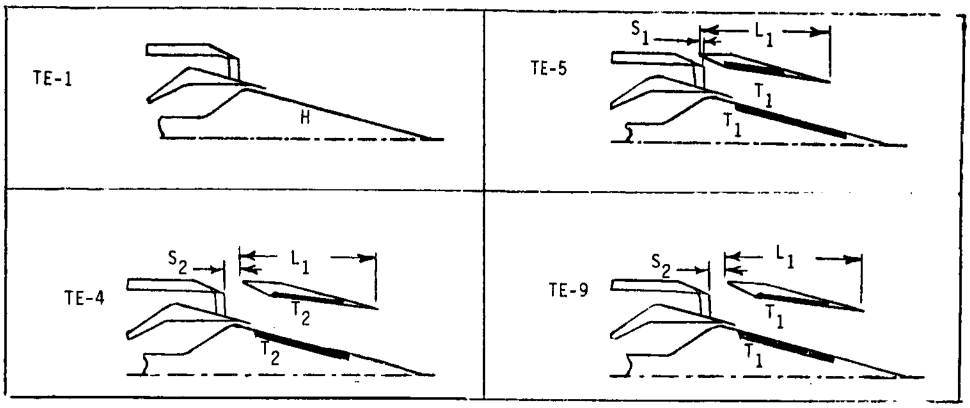

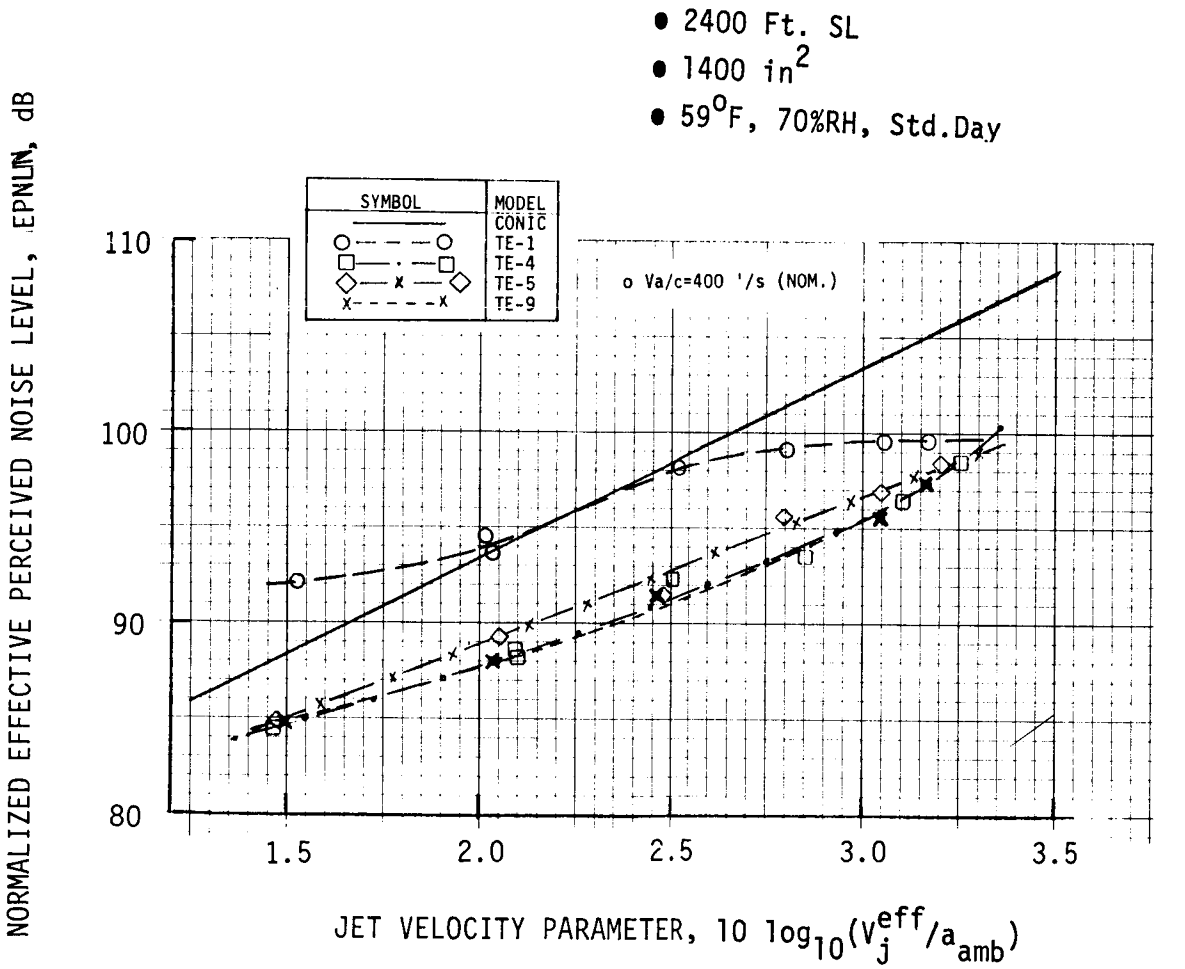

FIGURE 4-74. EPNL CORRELATION WITH JET VELOCITY PARAMETER FOR COMPARISON OF EJECTOR SETBACK, S1 VS S2, AND EJECTOR/PLUG TREATMENT, T1 VS T2.

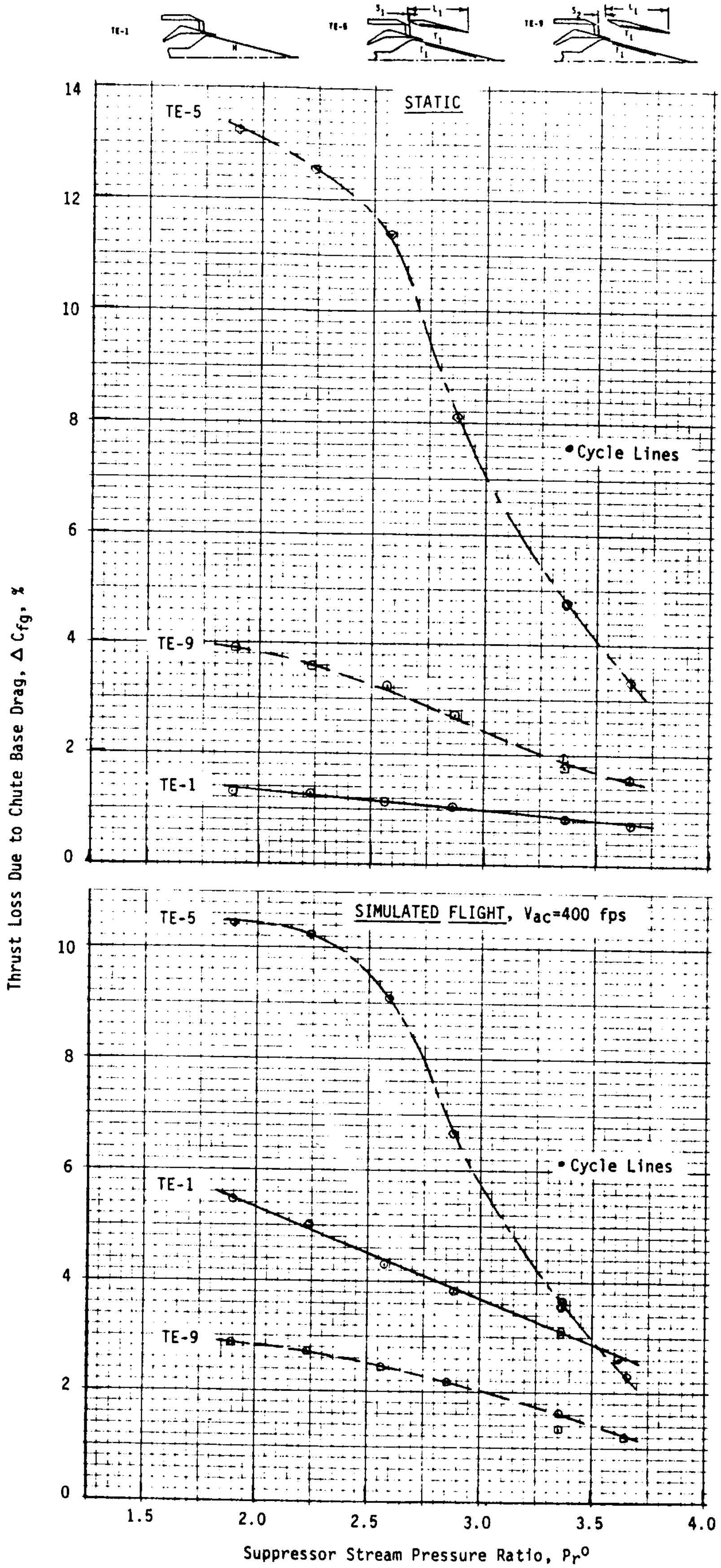

FIGURE 4-75. VARIATION IN THRUST LOSS COEFFICIENT DUE TO CHUTE BASE DRAG AS A FUNCTION OF a) ADDITION OF EJECTOR TO BASELINE, AND b) EJECTOR AXIAL LOCATION; TE-1, TE-5 AND TE-9

Chute base drag is a major portion of the total thrust loss of mechanical chute suppressors. The base drag results from low static pressure on the chute surface, low pressure indicative of inability to well-ventilate the chute. The Figure 4-75 comparison can be summarized as follows:

- o The unejected TE-1 configuration, trendwise, performs similarly to previous chute models by exhibiting substantially greater thrust loss in flight than statically. This results from the forward velocity over the chute tips not readily allowing flow to turn and ventilate the chute base area; thus causing lower base pressure and increased drag.

- o Application of TE-5 ejector with close, S1, spacing dramatically increases base drag, both static and in flight, resulting from poorer chute ventilation. Levels as high as 12.5% ΔC_{fg} static at cutback and 4.6% at takeoff are seen.

- o Axially relocating the ejector to S2 location (18.5" full scale; 2.496" model scale) from the S1 location (11" full scale; 1.484" model scale) allowed for substantial improvement in chute ventilation capability and decreased base drag to even below that of Configuration TE-1 in simulated-flight. A summarization at cutback and takeoff shows:

	ΔC_{fg}			
	C/B, PR $\approx$ 2.25		T/O, PR $\approx$ 3.4	
	STATIC	FLIGHT	STATIC	FLIGHT
TE-1	1.2	3.9	0.8	3.0
TE-5 (S1)	12.5	10.2	4.6	3.4
TE-9 (S2)	3.6	2.7	1.8	1.5

The ejector application, properly spaced, thus enhances flight aerodynamic performance in this $V_{a/c} \approx 400$ ft/sec operational range.

4.4 RANKING OF INDIVIDUAL SUPPRESSION SOURCES OF EJECTOR APPLICATION

This report section isolates the effectiveness of individual aspects of ejector/treatment application to the primary 20-chute suppressor nozzle. Reference to Section 4.0 and in particular to Figure 4-1 indicates from the test chronology that two model sets were tested to isolate suppression sources, i.e.:

- o Extended length ejector set: TE-7, TE-8 and TE-10.

- o Nominal length ejector set: TE-2, TE-3 and TE-4.

Within the comparisons for each test set was envisioned the capability of isolating effects of:

- o Application of hardwall ejector to primary nozzle system

- o Application of treatment to ejector inner flowsurface

- o Application of treatment to both the ejector and plug flowsurfaces

By comparison of test data among the three models of each set and then back to the reference TE-1 model, magnitudes of suppression attributable to each source were evactuated; results are discussed in this section.

4.4.1 Overview of Individual Suppression Source Effectiveness

As the primary gauge of acoustic effectiveness is PNL suppression, an overview of individual suppression source effectiveness can be gleaned by review of ΔPNL comparisons in Figures 4-76 and 4-77. The two figures each compare the extended and nominal length ejector sets directly to baseline Model TE-1 on the basis of 2400' sideline PNL suppression as a function of angle to inlet, θ_I. The first figure is a static data comparison and the second is for simulated-flight. Each figure presents data for the three cycle conditions of cutback, intermediate and takeoff. As the presented ΔPNL's are directly in comparison to the TE-1 noise levels, they represent incremental suppression changes due to:

a) Application of extended and nominal length hardwall ejectors

b) Application of extended and nominal length treated ejectors while maintaining a hardwall plug surface.

c) Application of extended and nominal length treated ejectors plus treatment to the plug surface.

Comparison of Δ's between the individual lines on the graphs then represents the incremental changes in noise levels due to:

a) Treatment application to the ejector surface relative to hardwall

b) Treatment application to the plug surface relative to treated ejector flowsurface only.

Review of the graphs reveals the following interesting results:

o The hardwall ejector, due to its physical shielding, provides the major portion of the ejector system's suppression effectiveness. In itself, it contributes substantially in both forward and aft quadrant suppression, levels being fairly consistent from static to flight and with loss of effectiveness, particularly in the aft peak noise quadrant, at the higher jet velocity takeoff cycle. Absolute levels of inlet quadrant suppression are normally somewhat greater than broadside and aft quadrant, particularly as the cycle is increased from cutback to takeoff. Of major significance is that the forward radiated jet noise is still reduced substantially at all cycle conditions, even though aft quadrant suppression levels diminish.

o Application of treatment to the ejector inner flowsurface is primarily effective within the extended length ejector, effectiveness being marginal within the nominal length ejector as many of these data comparisons show minimal to no increase in ΔPNL when the single surface treatment is added. For the extended length ejector system, the single surface treatment, however, is seen primarily effective on forward angle radiated noise suppression, peak noise angles being minimally effected.

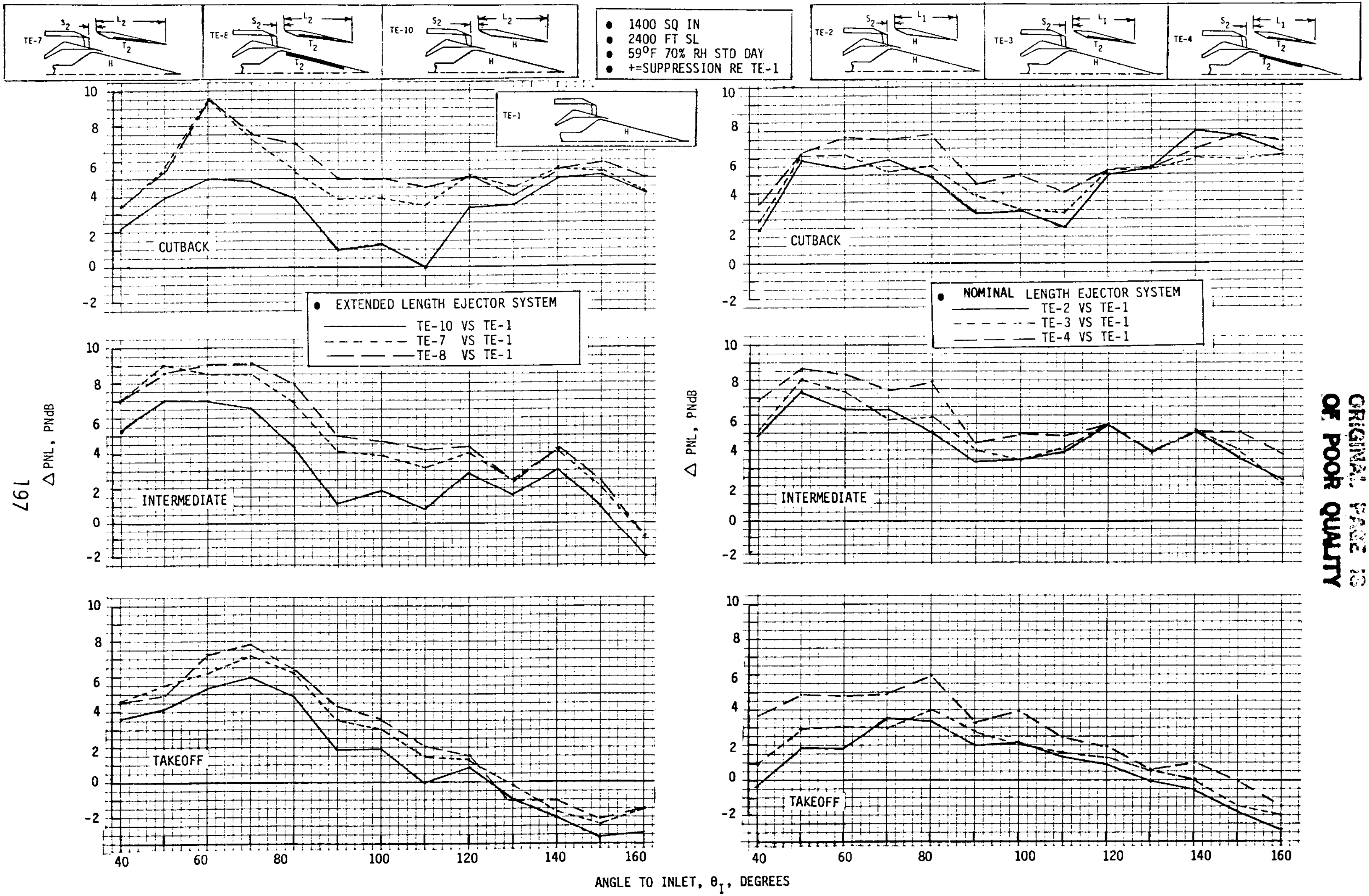

FIGURE 4-76. INDIVIDUAL SUPPRESSION SOURCE EFFECTIVENESS ON PNL SUPPRESSION, STATIC, AT CUTBACK, INTERMEDIATE AND TAKEOFF.

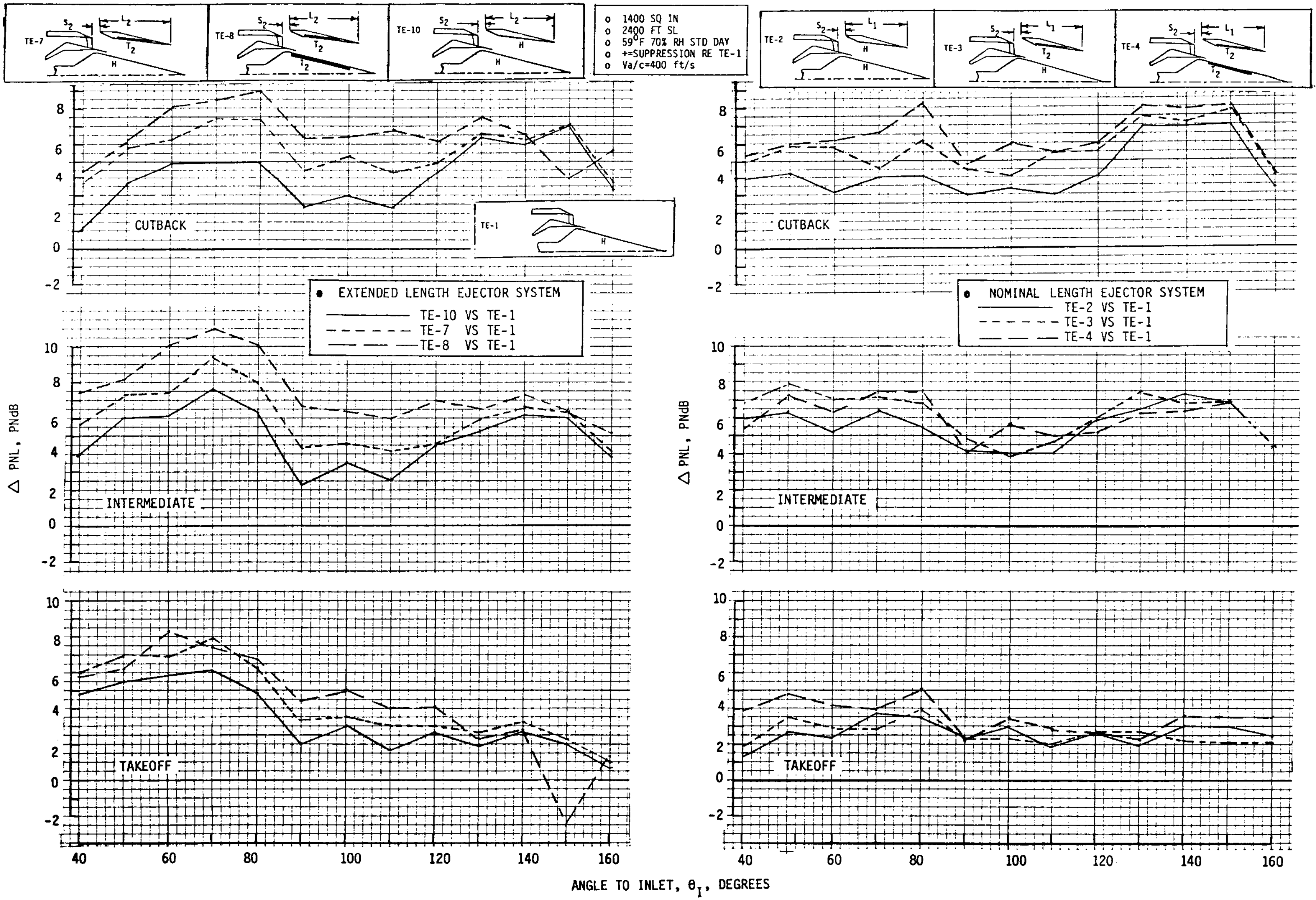

FIGURE 4-77. INDIVIDUAL SUPPRESSION SOURCE EFFECTIVENESS ON PNL SUPPRESSION, SIMULATED-FLIGHT, AT CUTBACK, INTERMEDIATE AND TAKEOFF.

- Addition of further treatment to the plug surface significantly improves suppression of both L1 and L2 systems, the magnitude of improvement varying with cycle as internal flow conditions change, but showing no trend to implicate either ejector length or cycle as a dependent variable regulating improvement. The plug surface treatment again is more beneficial to forward quadrant suppression, aft quadrant peak noise being reduced just slightly further. In general, the conclusion can be drawn that plug surface treatment improves acoustic peformance by a noteworthy amount, however, levels and trends are not readily predictable from the data comparisons.

A further overview parameter to gauge suppression source effectiveness is presented in Figure 4-78, i.e., normalized EPNL as a function of cycle operation. The EPNL values are based on 2400' sideline data with nominal 400 ft/sec simulated flight speed. The top of the graph presents the extended length ejector set; TE-10, TE-7 and TE-8. The lower half presents the nominal length ejector set, TE-2, TE-3 and TE-4. Conic nozzle and baseline TE-1 data are included. Relative to reviewing for ejector source effectiveness, these EPNL comparisons indicate:

- For the extended length ejector, approximately 4.2 ΔEPNL is gained relative to the baseline suppressor at takeoff by application of the hardwall ejector. An additional 1.3 ΔEPNL suppression is gained by treating the ejector flowsurface, for an ejector/treatment system effectiveness of 5.5 ΔEPNL. Plug treatment is of no further benefit. Total suppression relative to the conical nozzle is 9.3 ΔEPNL.

- The nominal length hardwall ejector at the same takeoff cycle afforded 3.5 ΔEPNL suppression relative to the baseline suppressor. Addition of ejector flowsurface treatment further improved suppression by 0.5Δ EPNL, yielding a total of 4.0 ΔEPNL for the ejector/treatment package. Plug treatment application is again of no further benefit. Total suppression relative to the conical nozzle is 7.8 ΔEPNL.

- At cutback cycle, gain similar to takeoff is afforded by the hardwall ejector application, i.e., 4 ΔEPNL for both extended and nominal length systems. Ejector shell treatment improves the long ejector by about 2 ΔEPNL and the short ejector by about 1.5 ΔEPNL. Plug surface treatment is, however, effective at this cycle setting by 2Δ EPNL for the long ejector and 0.5 ΔEPNL for the short ejector. Total suppression relative to the conic nozzle is 6.5 ΔEPNL for both systems.

4.4.2 Detailed Data Comparisons Relative to Individual Suppression Source Effectiveness

As mentioned previously, acoustic peformance can be gauged through comparison of a variety of noise parameters. Additionally, physical changes incorporated in ejector model variations often produce minor variations in acoustic levels and in many cases the changes are not methodically consistent. This is the case for analysis of individual suppression source effectiveness in this section. Therefore, the following text presents an array of detailed data comparisons, general review of the data then necessary to discern trends of effectiveness. The general trends are summarized after the data presentation.

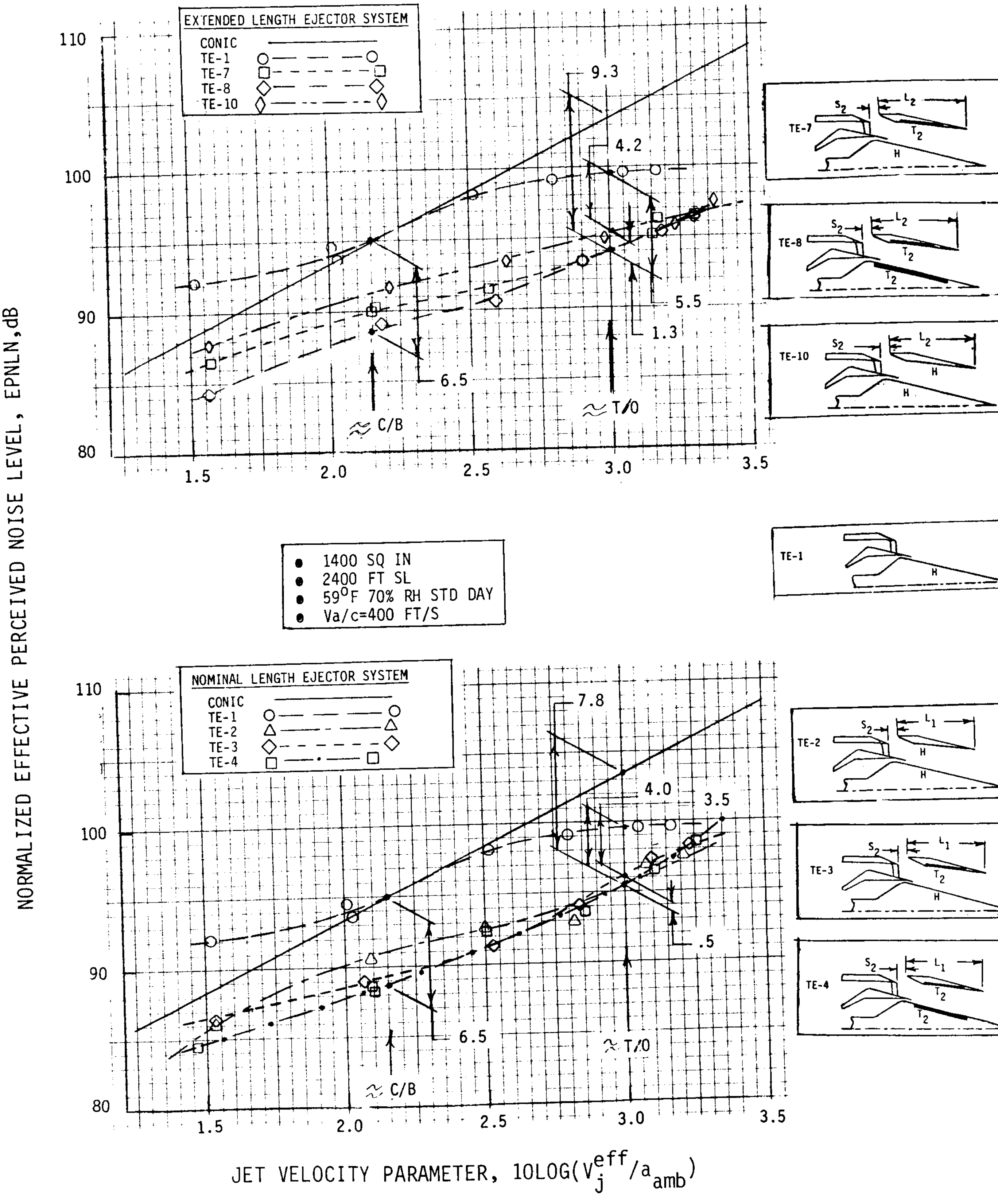

FIGURE 4-78. EPNL CORRELATION WITH JET VELOCITY PARAMETER FOR INDIVIDUAL SUPPRESSION SOURCE EFFECTIVENESS, NOMINAL AND EXTENDED LENGTH EJECTOR SYSTEMS.

4.4.2.1 Data Comparisons for the Extended Length Ejector System: TE-7, TE-8 and TE-10

The following data comparisons are included for the extended length, L2, ejector systems, comparing Configurations TE-10, hardwall, TE-7, treated ejector flowsurface, and TE-8, treated ejector and plug. The data graphs additionally include Configuration TE-1 baseline unejected suppressor and the reference conical nozzle.

- o Figure 4-79; Normalized PWL for static and flight as a function of cycle line of operation.
- o Figures 4-80 and 4-81; Normalized OASPL for static and flight, respectively, at $\theta_I = 60^o, 90^o, 130^o$ and peak value, as a function of cycle line of operation.
- o Figures 4-82 and 4-83; Normalized PNL for static and flight, respectively, at $\theta_I = 60^o, 90^o, 130^o$ and peak value, as a function of cycle line of operation.
- o Figures 4-84, 4-85 and 4-86; OASPL and PNL directivity for static and flight, for select cycle points of cutback, intermediate and takeoff.
- o Figures 4-87 through 4-92; 1/3-OBSPL spectra for static and flight, for select angles of $\theta_I = 60^o, 90^o$ and 130^o, for cutback, intermediate and takeoff cycle points.

4.4.2.2 Data Comparisons for the Nominal Length Ejector System: TE-2, TE-3 and TE-4

Similar to those for the extended length ejector system, the following data comparisons are included for the nominal length, L1, ejector system, comparing Configurations TE-2, hardwall, TE-3, treated ejector flowsurface, and TE-4, treated ejector and plug. As previously, the graphs include baseline unejected suppressor TE-1 and the reference conical nozzle.

- o Figure 4-93; Normalized PWL for static and flight as a function of cycle line of operation.
- o Figures 4-94 and 4-95; Normalized OASPL for static and flight, respectively, at $\theta_I = 60^o, 90^o, 130^o$ and peak value, as a function of cycle line of operation.
- o Figures 4-96 and 4-97; Normalized PNL for static and flight, respectively, at $\theta_I = 60^o, 90^o, 130^o$ and peak value, as a function of cycle line of operation.
- o Figures 4-98, 4-99 and 4-100; OASPL and PNL directivity for static and flight, for select cycle points of cutback, intermediate and takeoff.
- o Figures 4-101 through 4-106; 1/3-OBSPL spectra for static and flight, for select angles of $\theta_I = 60^o, 90^o$ and 130^o, for cutback, intermediate and takeoff cycle points.

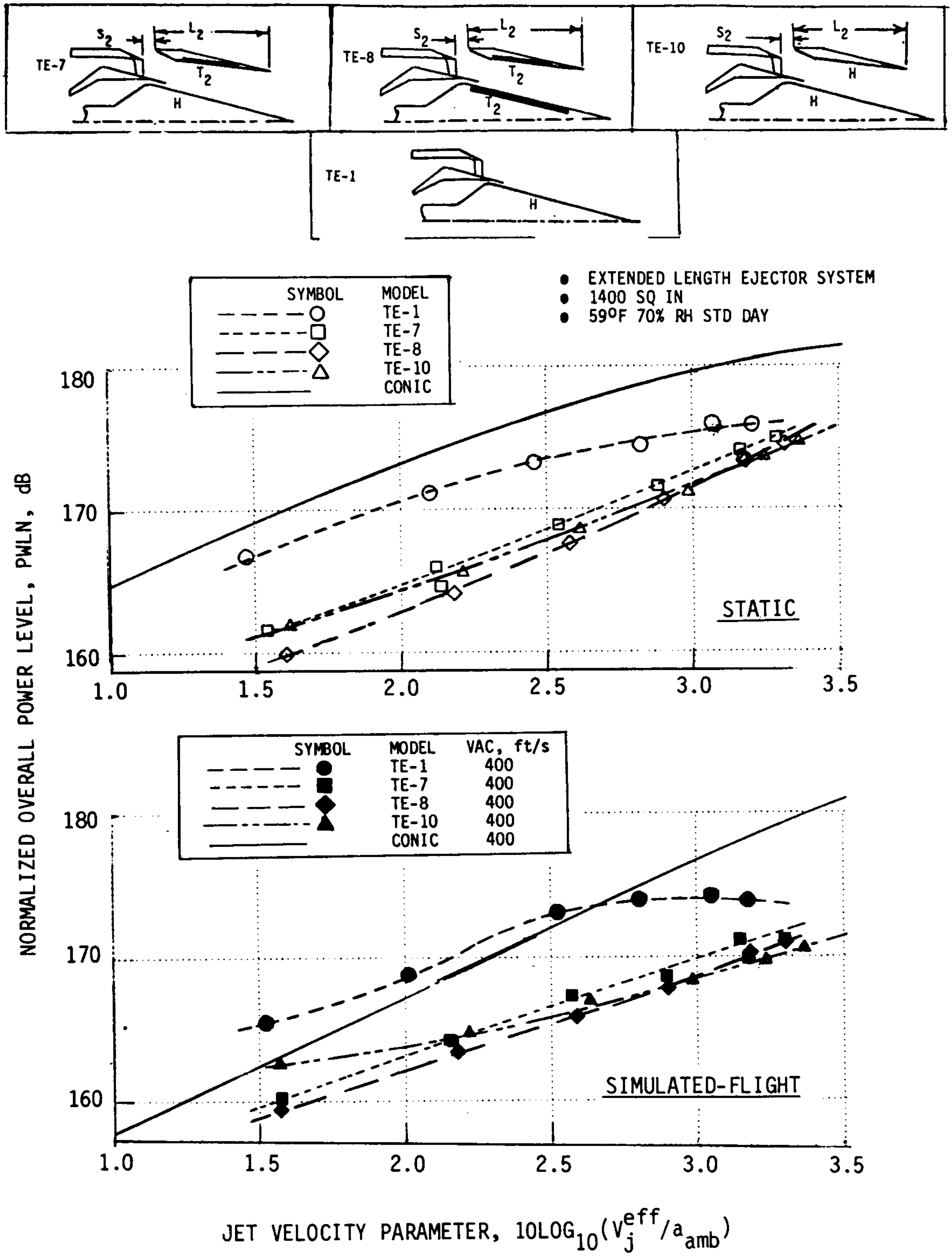

FIGURE 4-79. NORMALIZED PWL AS A FUNCTION OF JET VELOCITY PARAMETER FOR IDENTIFICATION OF INDIVIDUAL SUPPRESSION SOURCE EFFECTIVENESS WITHIN THE EXTENDED LENGTH EJECTOR SYSTEM.

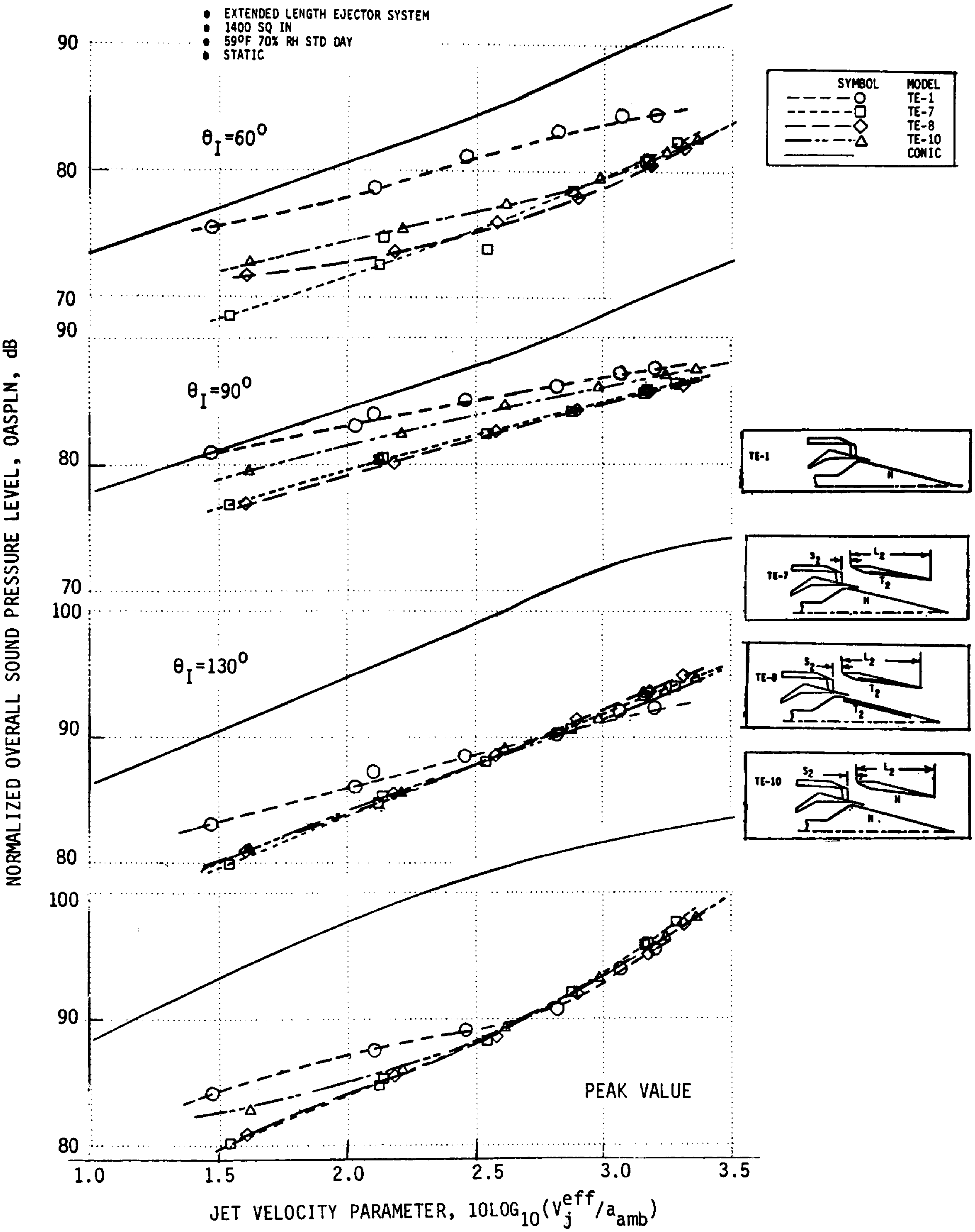

FIGURE 4-80. NORMALIZED OASPL AS A FUNCTION OF JET VELOCITY PARAMETER FOR IDENTIFICATION OF INDIVIDUAL SUPPRESSION SOURCE EFFECTIVENESS WITHIN THE EXTENDED LENGTH EJECTOR SYSTEM, STATIC, AT θ_I=60°, 90°, 130° AND PEAK VALUE

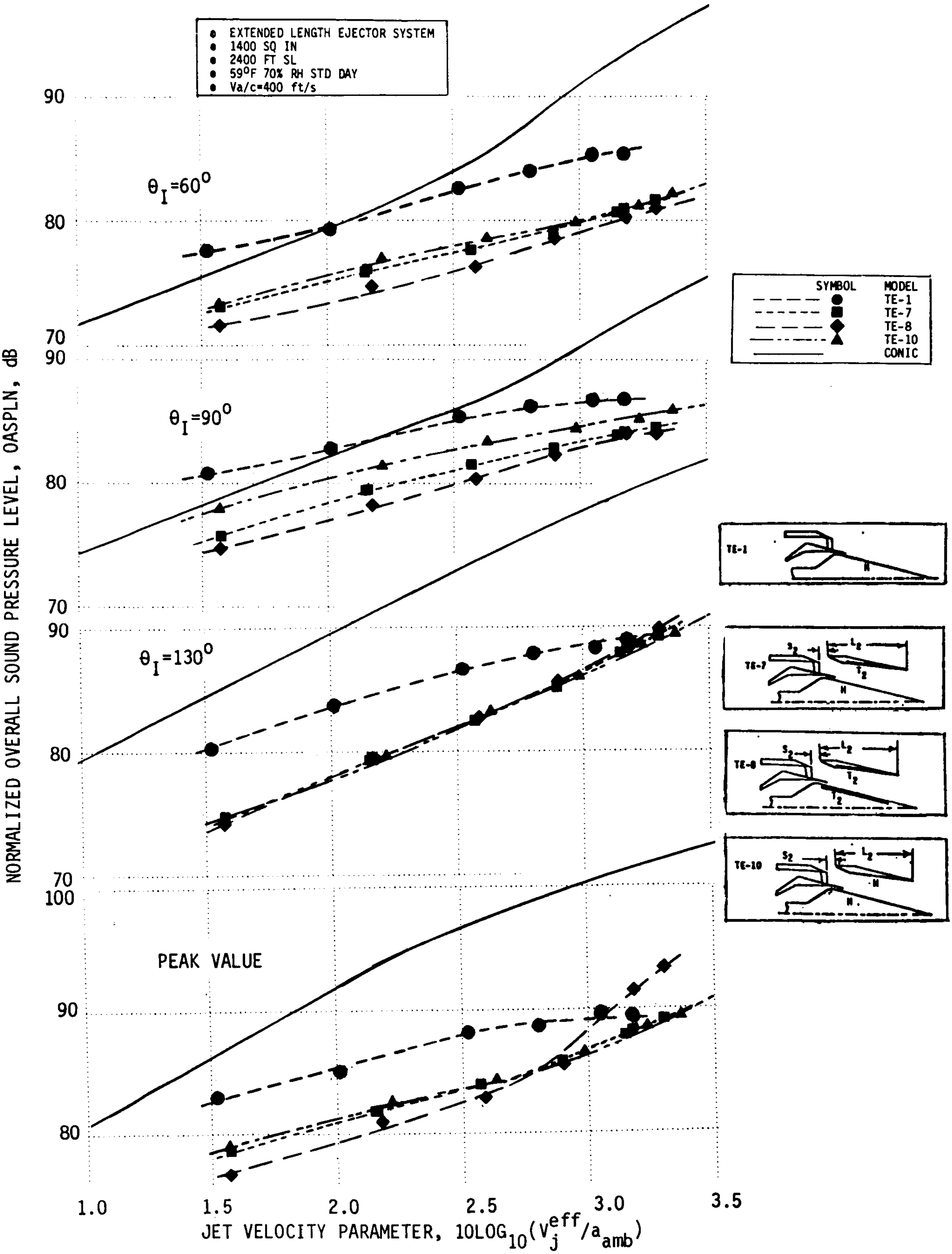

FIGURE 4-81. NORMALIZED OASPL AS A FUNCTION OF JET VELOCITY PARAMETER FOR IDENTIFICATION OF INDIVIDUAL SUPPRESSION SOURCE EFFECTIVENESS WITHIN THE EXTENDED LENGTH EJECTOR SYSTEM, SIMULATED-FLIGHT, AT θ_I=60°, 90°, 130° AND PEAK VALUE.

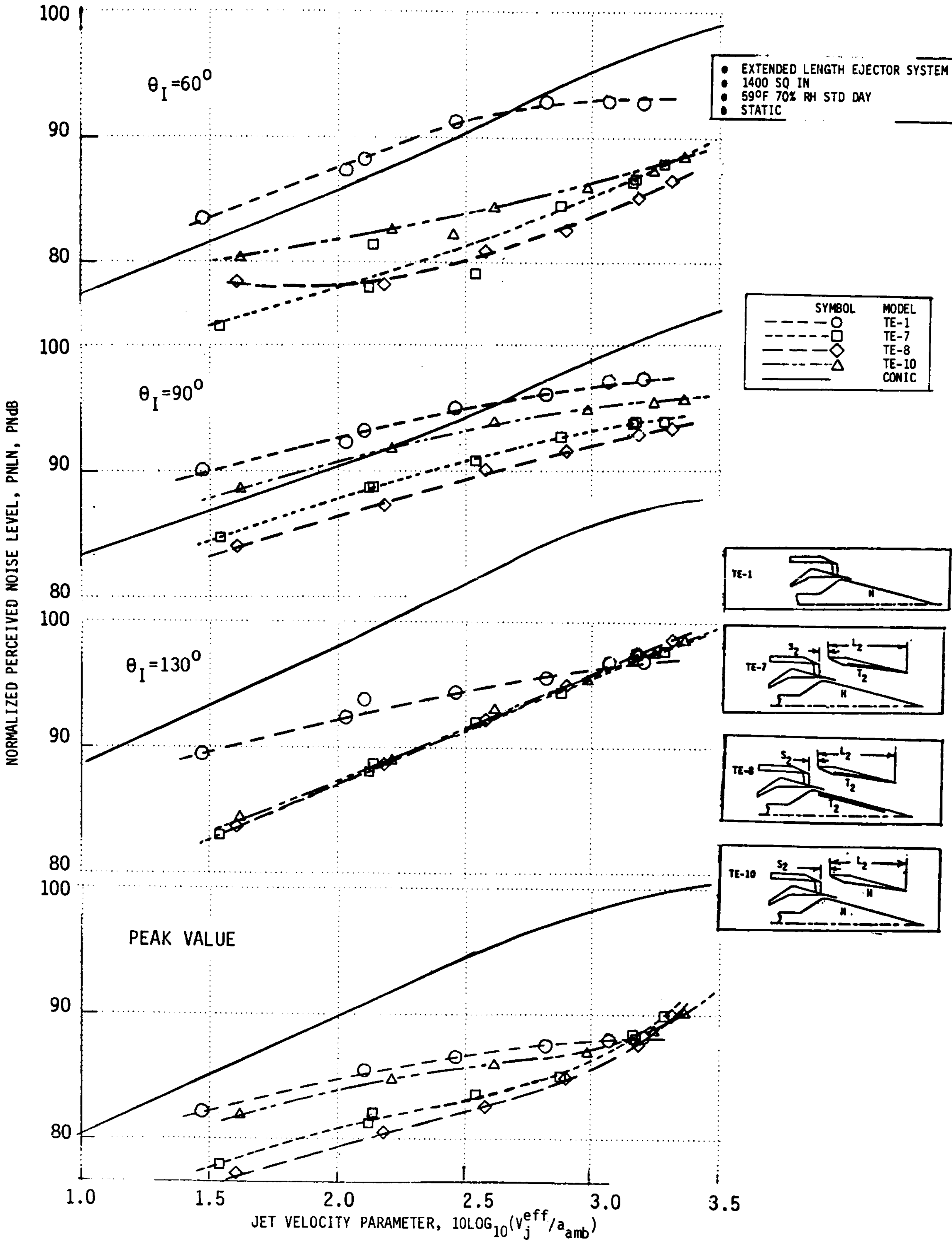

FIGURE 4-82. NORMALIZED PNL AS A FUNCTION OF JET VELOCITY PARAMETER FOR IDENTIFICATION OF INDIVIDUAL SUPPRESSION SOURCE EFFECTIVENESS WITHIN THE EXTENDED LENGTH EJECTOR SYSTEM, STATIC, AT $\theta_I=60^0$, 90^0, 130^0 AND PEAK VALUE.

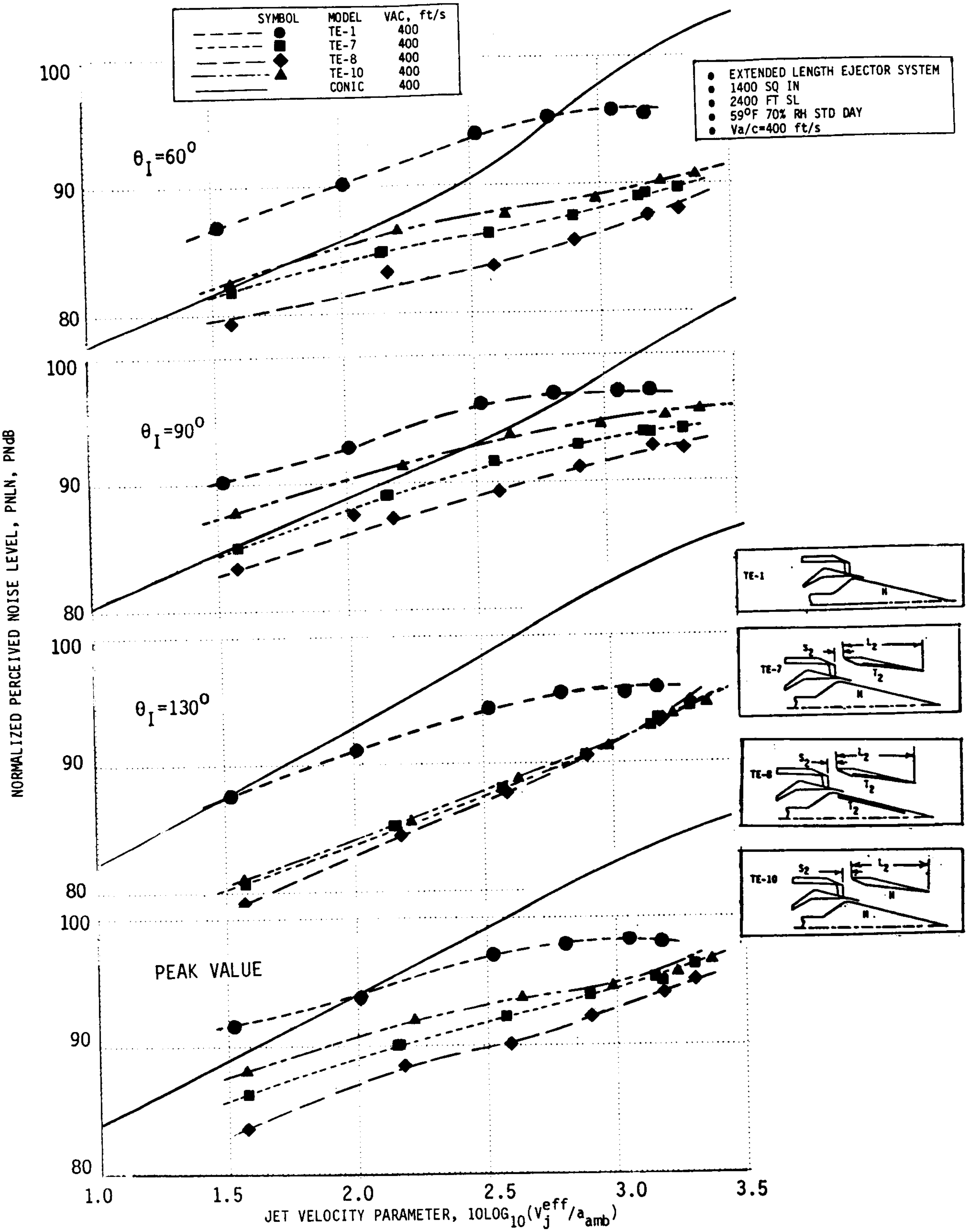

FIGURE 4-83. NORMALIZED PNL AS A FUNCTION OF JET VELOCITY PARAMETER FOR INDENTIFICATION OF INDIVIDUAL SUPPRESSION SOURCE EFFECTIVENESS WITHIN THE EXTENDED LENGTH EJECTOR SYSTEM, SIMULATED-FLIGHT, AT θ_I=60°, 90°, 130° AND PEAK VALUE.

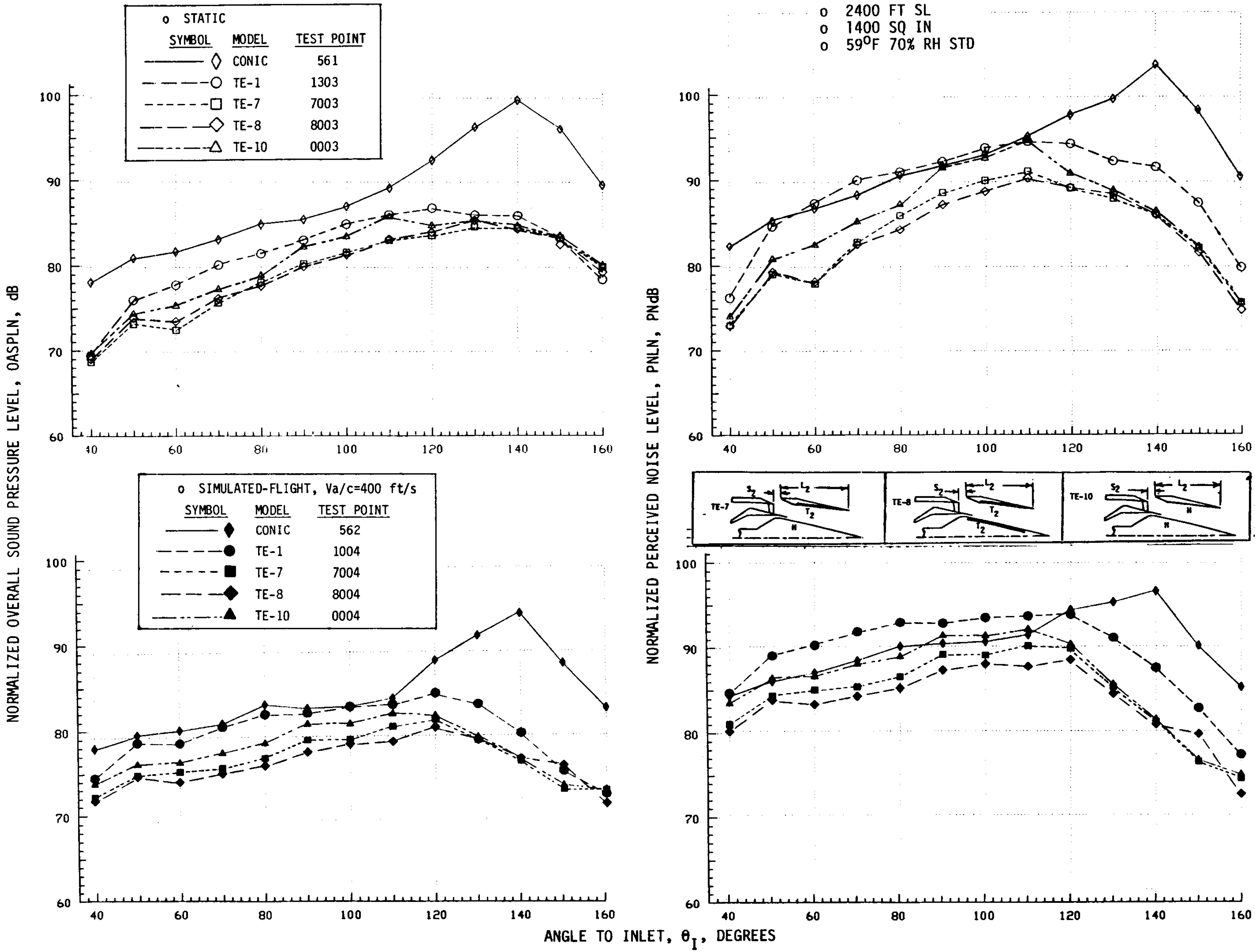

FIGURE 4-84. STATIC AND SIMUALTED-FLIGHT DIRECTIVITY COMPARISONS OF OASPL AND PNL AT CUTBACK FOR IDENTIFICATION OF INDIVIDUAL SUPPRESSION SOURCE EFFECTIVENESS WITHIN THE EXTENDED LENGTH EJECTOR SYSTEM.

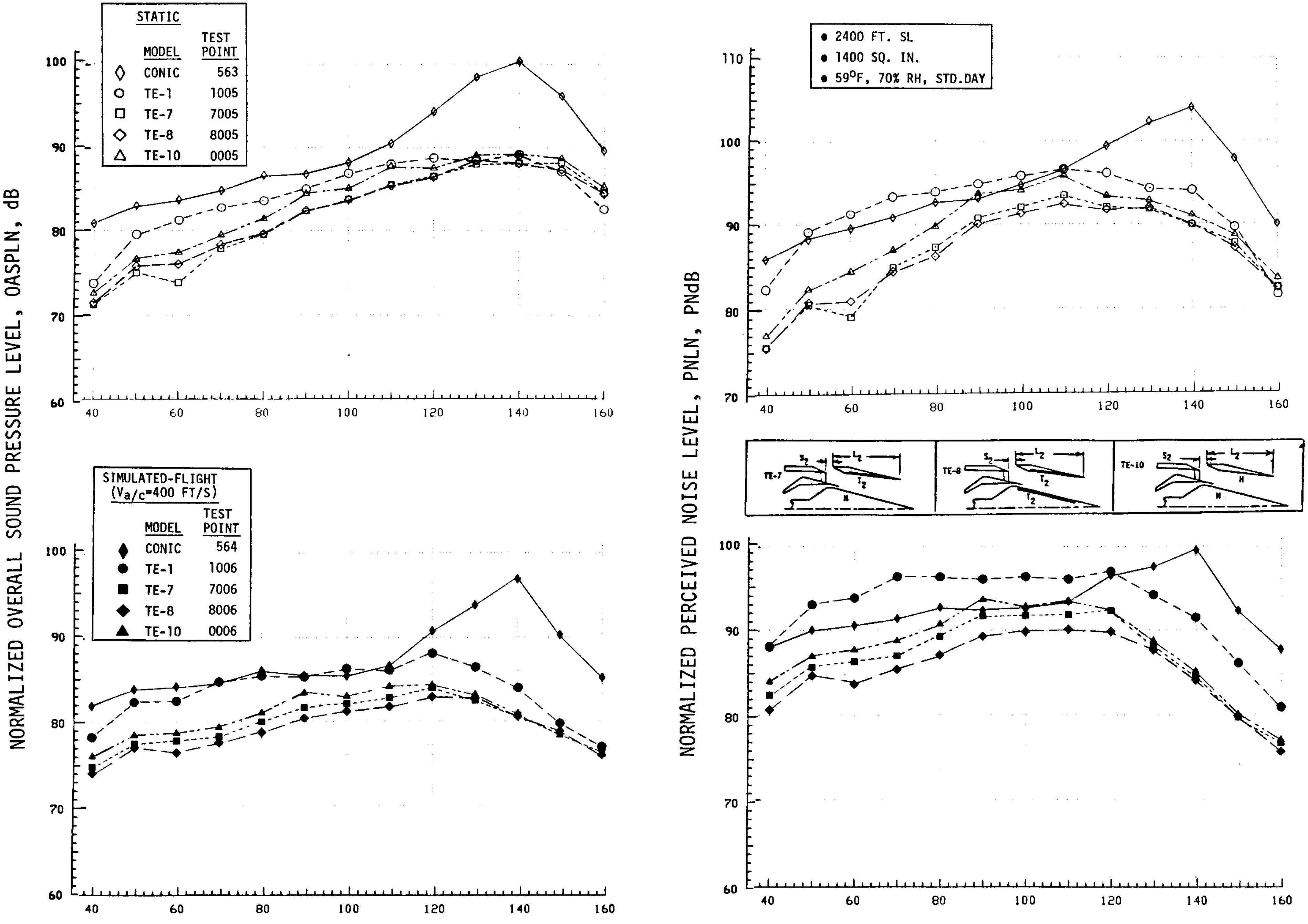

FIGURE 4-85. STATIC AND SIMULATED-FLIGHT DIRECTIVITY COMPARISONS OF OASPL AND PNL AT INTERMEDIATE FOR IDENTIFICATION OF INDIVIDUAL SUPPRESSION SOURCE EFFECTIVENESS WITHIN THE EXTENDED LENGTH EJECTOR SYSTEM

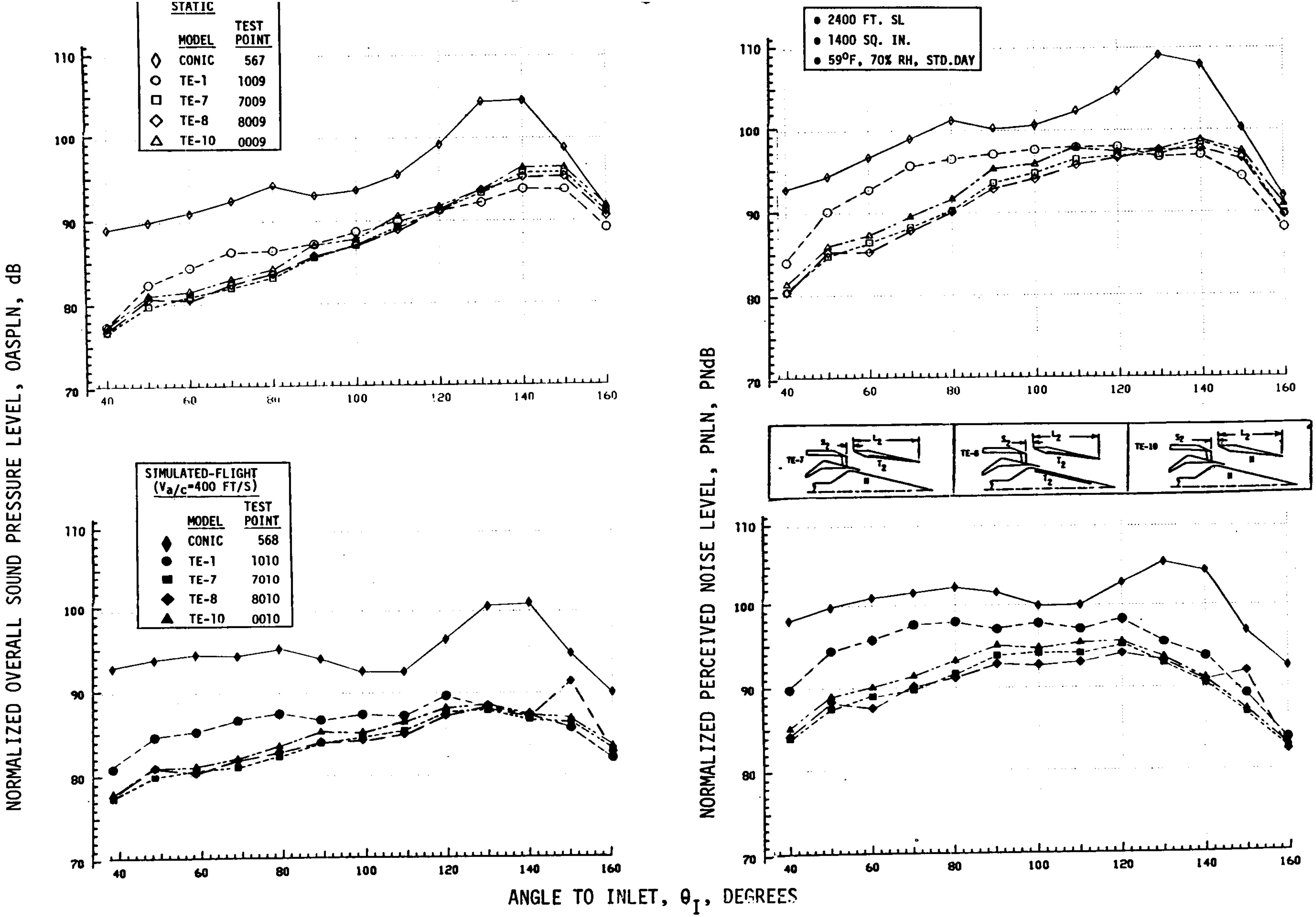

FIGURE 4-86. STATIC AND SIMULATED-FLIGHT DIRECTIVITY COMPARISONS OF OASPL AND PNL AT TAKEOFF FOR IDENTIFICATION OF INDIVIDUAL SUPPRESSION SOURCE EFFECTIVENESS WITHIN THE EXTENDED LENGTH EJECTOR SYSTEM

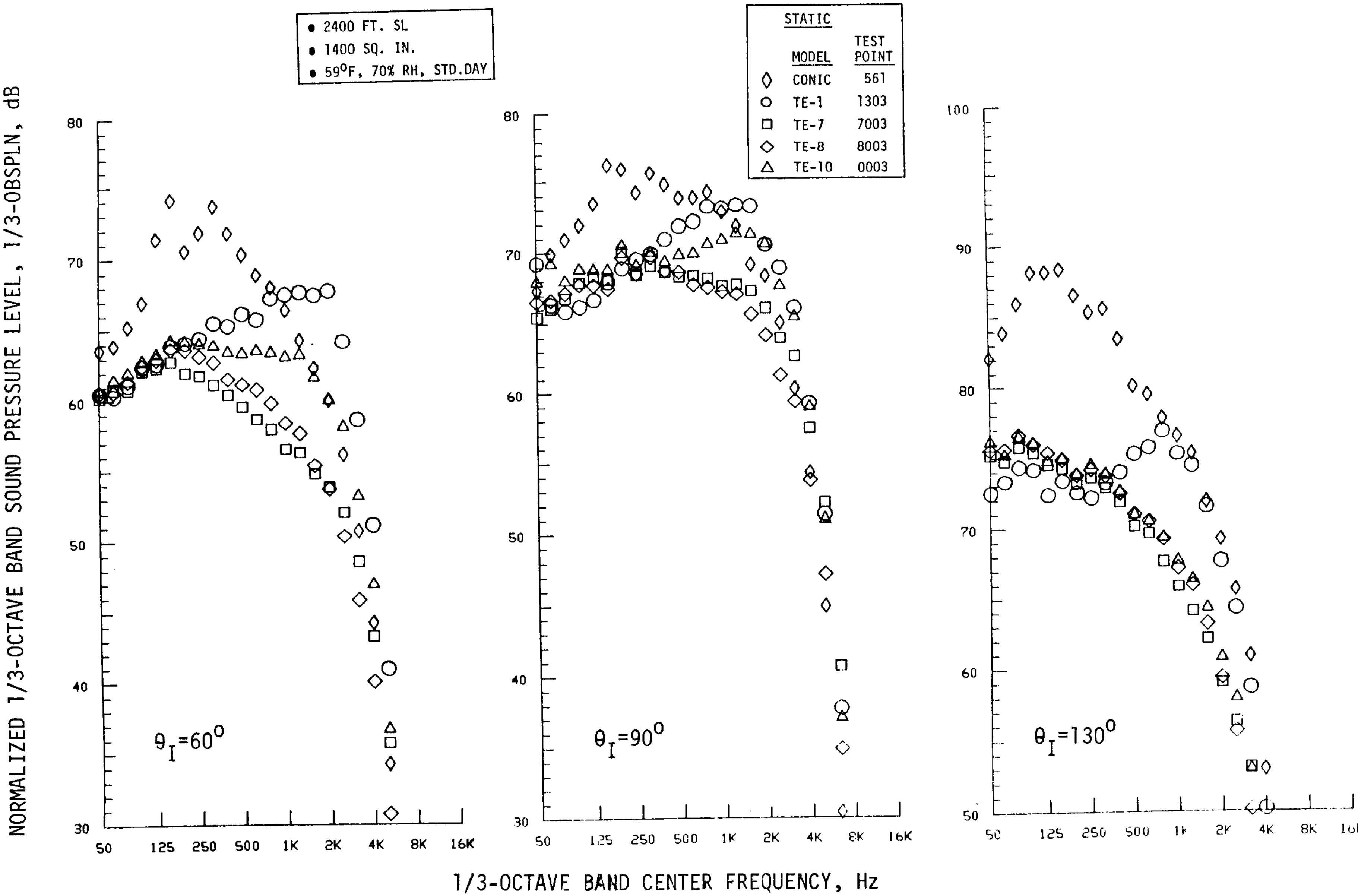

FIGURE 4-87. NORMALIZED SPECTRA AT θ_I=60°, 90°, AND 130° FOR IDENTIFICATION OF INDIVIDUAL SUPPRESSION SOURCE EFFECTIVENESS WITHIN THE EXTENDED LENGTH EJECTOR SYSTEM, STATIC, AT CUTBACK

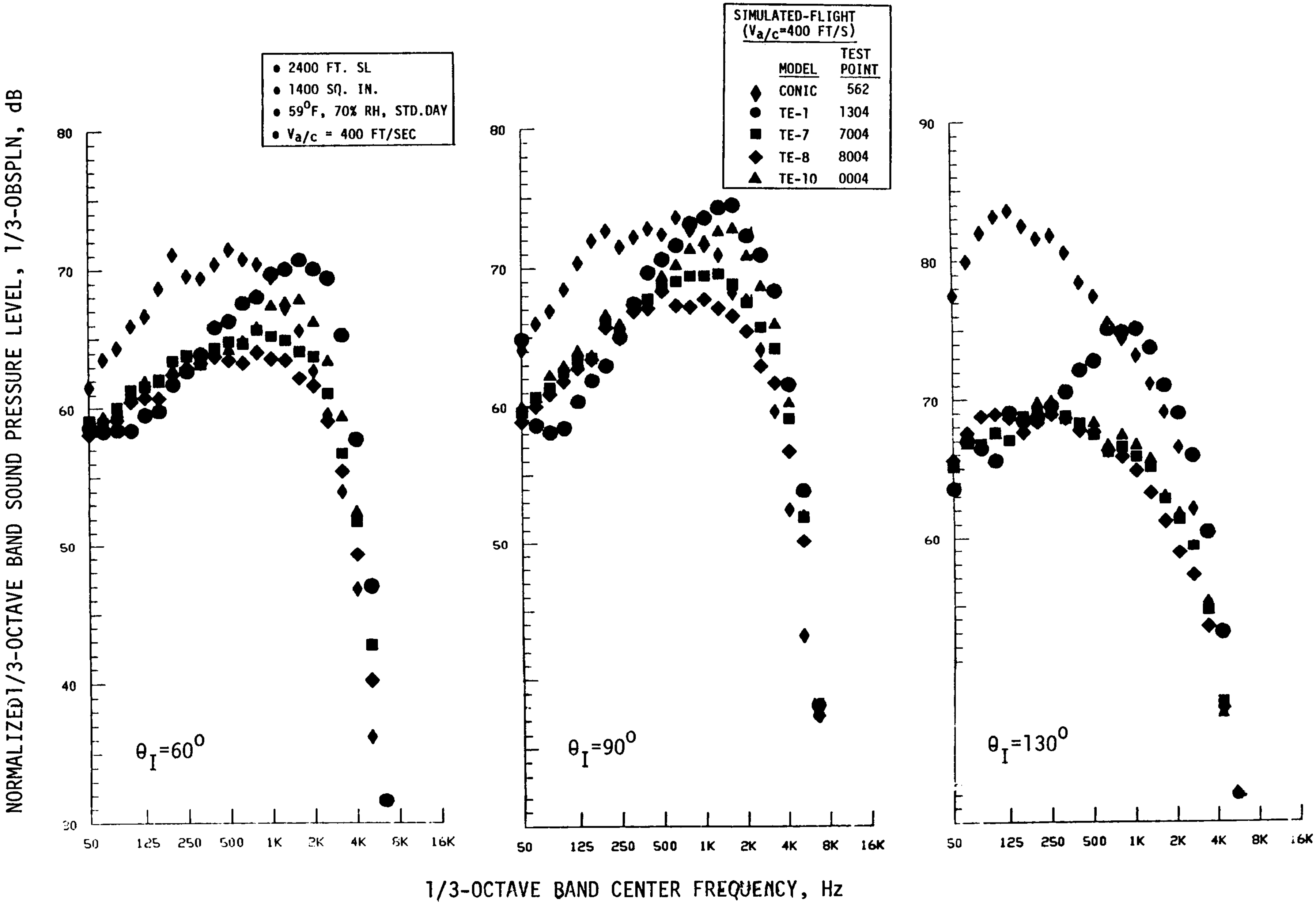

FIGURE 4-88. NORMALIZED SPECTRA AT θ_I=60°, 90°, AND 130° FOR IDENTIFICATION OF INDIVIDUAL SUPPRESSION SOURCE EFFECTIVENESS WITHIN THE EXTENDED LENGTH EJECTOR SYSTEM, SIMULATED-FLIGHT, AT CUTBACK

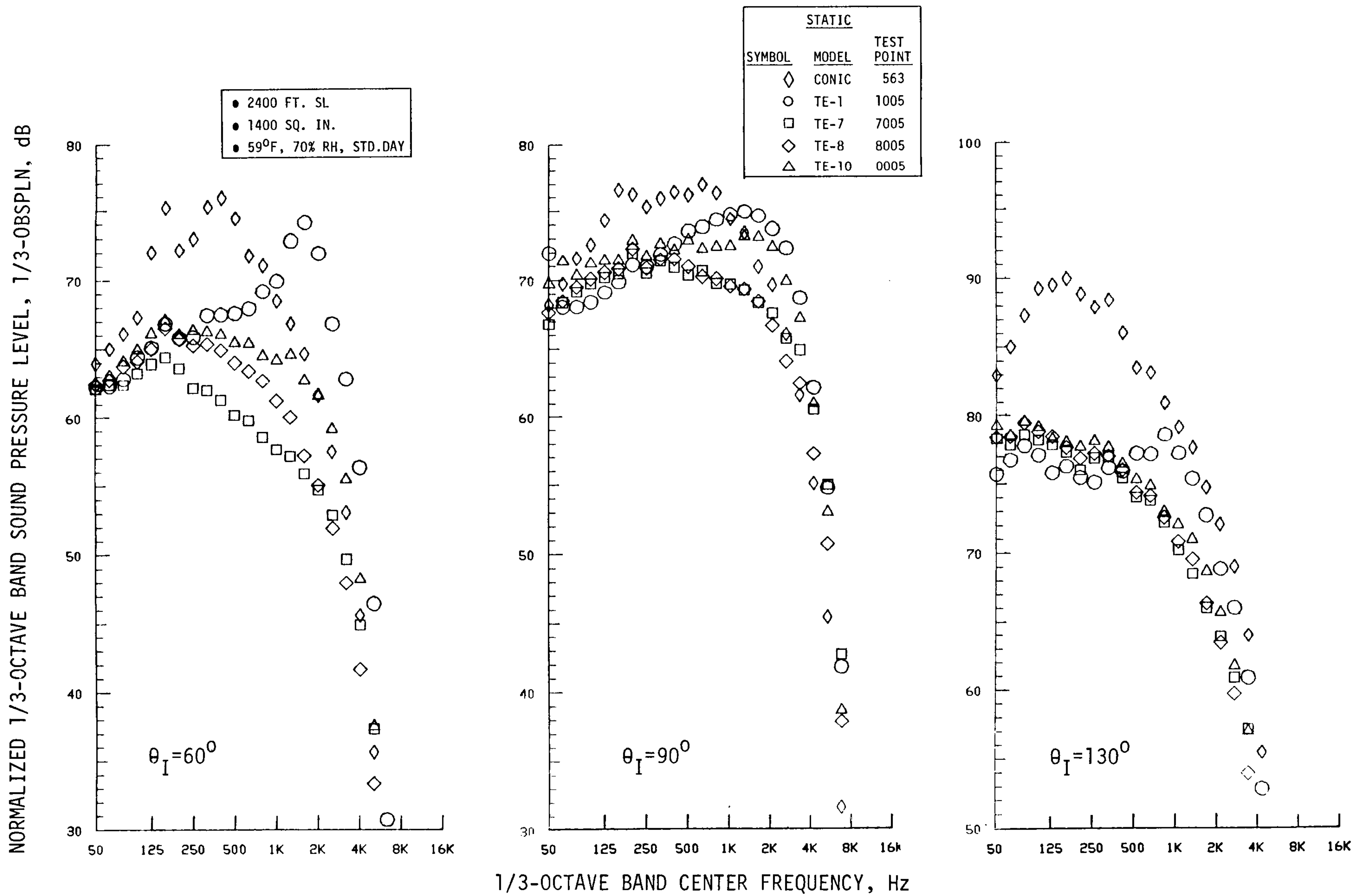

FIGURE 4-89. NORMALIZED SPECTRA AT θ_I=60°, 90°, AND 130° FOR IDENTIFICATION OF INDIVIDUAL SUPPRESSION SOURCE EFFECTIVENESS WITHIN THE EXTENDED LENGTH EJECTOR SYSTEM, STATIC, AT INTERMEDIATE

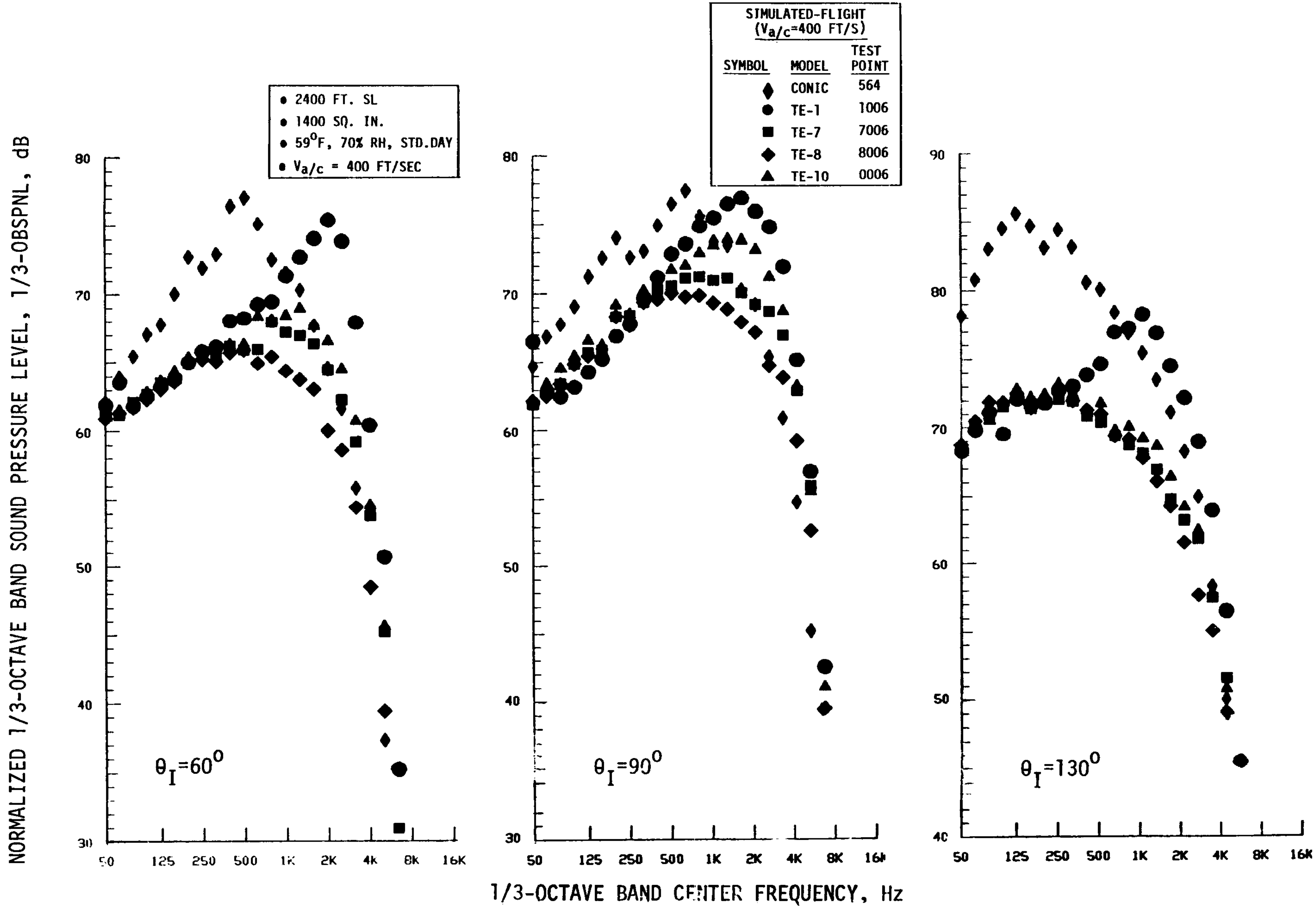

FIGURE 4-90. NORMALIZED SPECTRA AT θ_I=60°, 90°, AND 130° FOR IDENTIFICATION OF INDIVIDUAL SUPPRESSION SOURCE EFFECTIVENESS WITHIN THE EXTENDED LENGTH EJECTOR SYSTEM, SIMULATED-FLIGHT, AT INTERMEDIATE

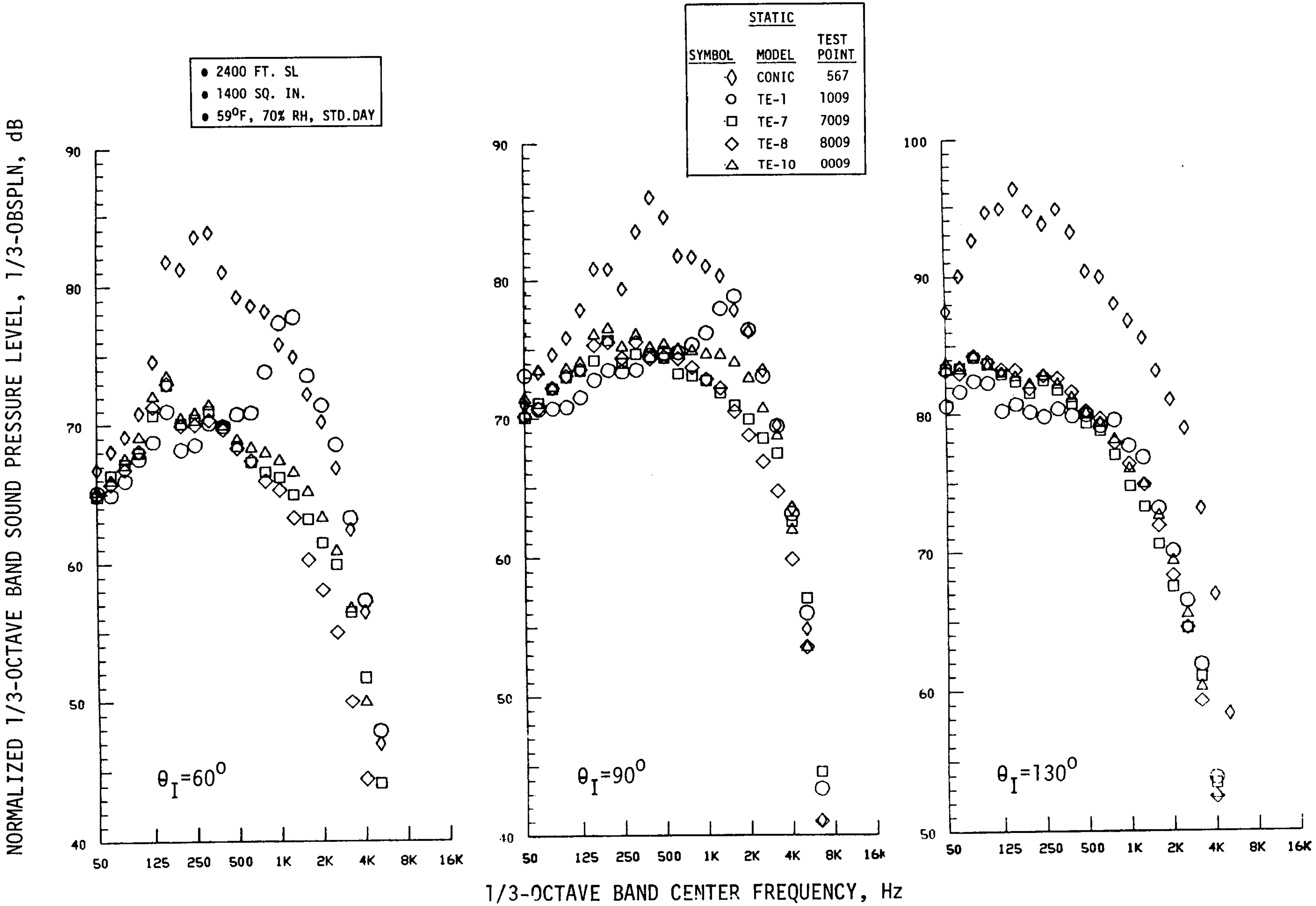

FIGURE 4-91. NORMALIZED SPECTRA AT $\theta_I=60^0$, 90^0, AND 130^0 FOR IDENTIFICATION OF INDIVIDUAL SUPPRESSION SOURCE EFFECTIVENESS WITHIN THE EXTENDED LENGTH EJECTOR SYSTEM, STATIC, AT TAKEOFF

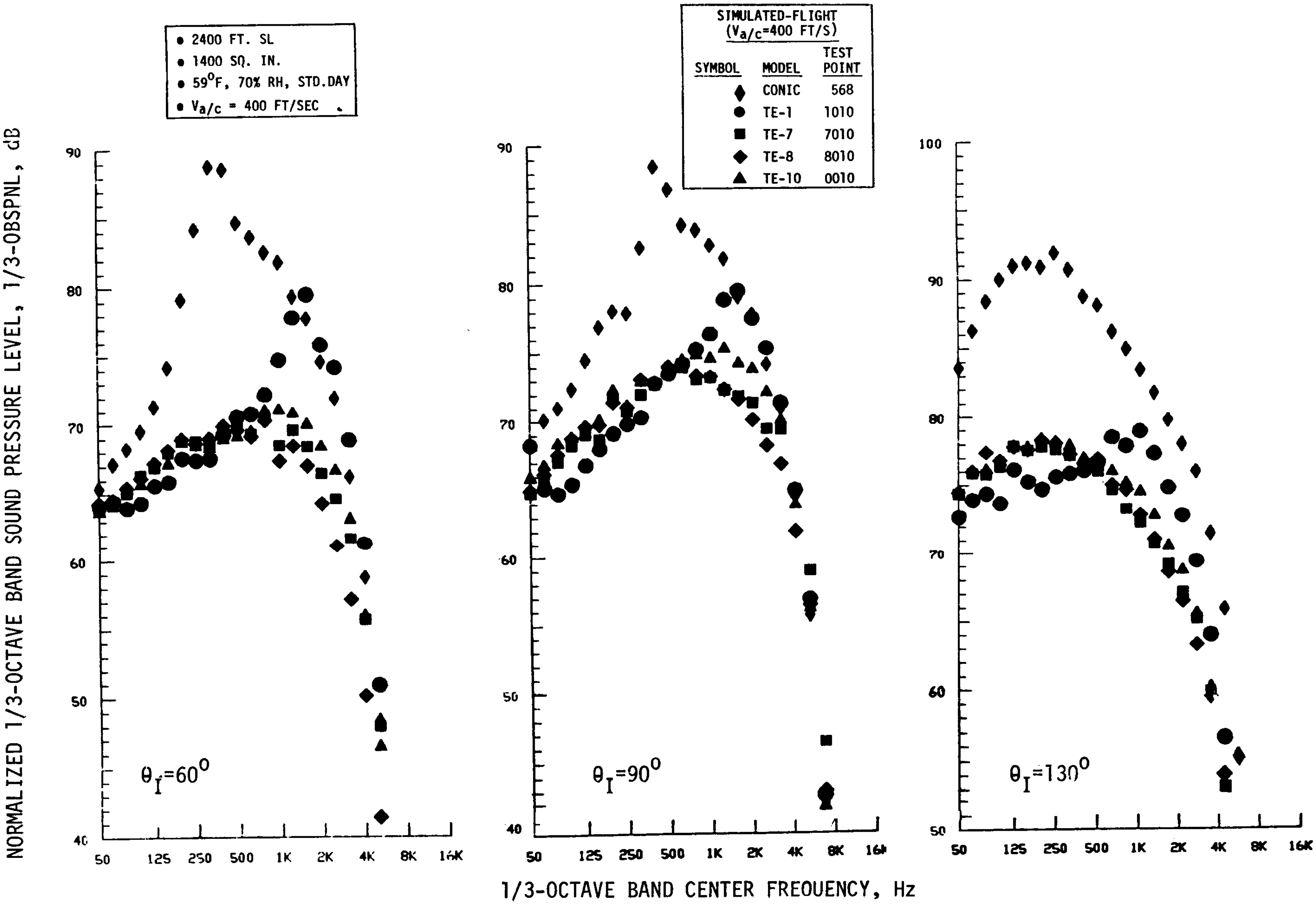

FIGURE 4-92. NORMALIZED SPECTRA AT θ_I=60°, 90°, AND 130° FOR IDENTIFICATION OF INDIVIDUAL SUPPRESSION SOURCE EFFECTIVENESS WITHIN THE EXTENDED LENGTH EJECTOR SYSTEM, SIMULATED-FLIGHT, AT TAKEOFF

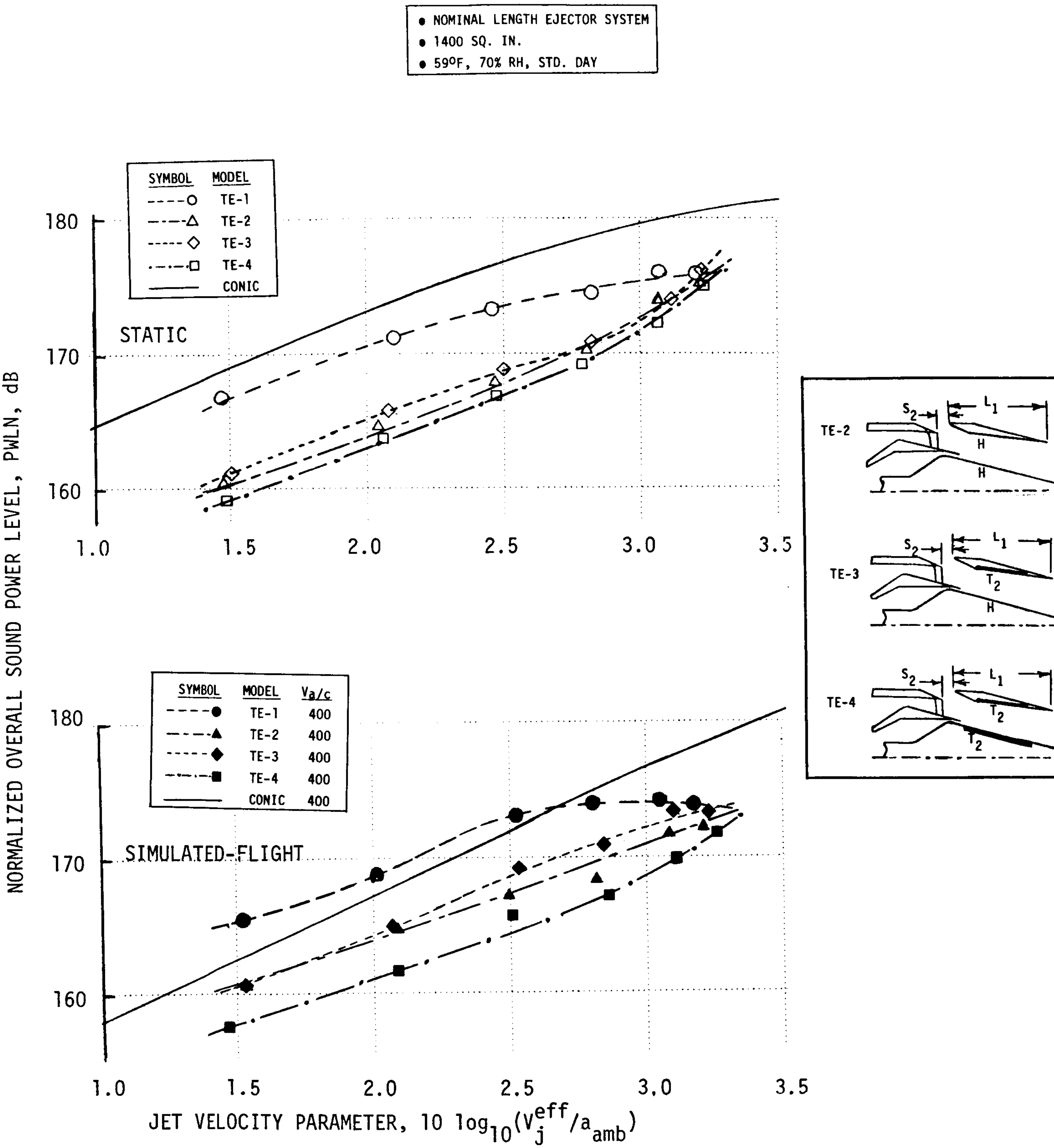

FIGURE 4-93. NORMALIZED PWL AS A FUNCTION OF JET VELOCITY PARAMETER FOR IDENTIFICATION OF INDIVIDUAL SUPPRESSION SOURCE EFFECTIVENESS WITHIN THE NOMINAL LENGTH EJECTOR SYSTEM

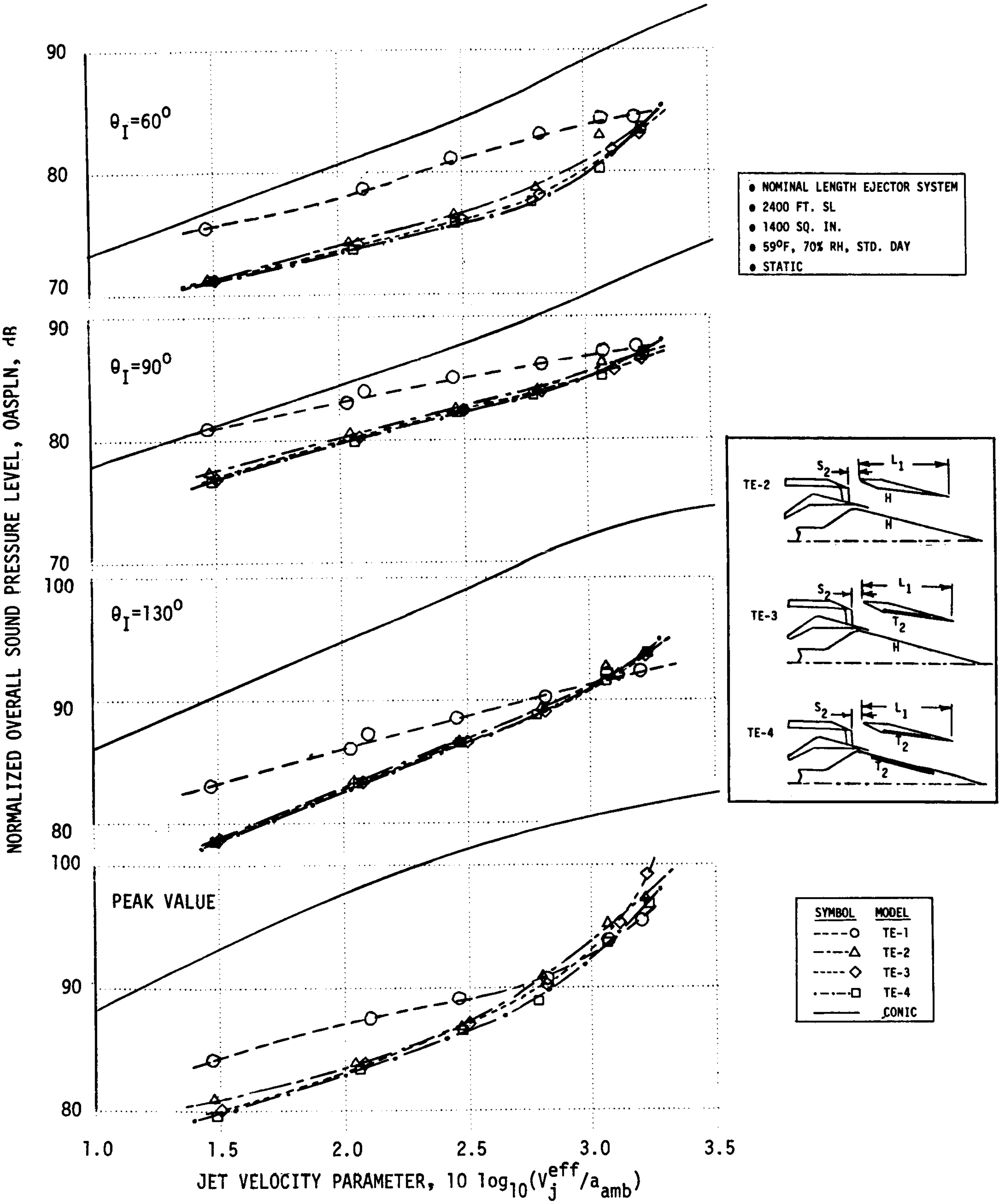

FIGURE 4-94. NORMALIZED OASPL AS A FUNCTION OF JET VELOCITY PARAMETER FOR IDENTIFICATION OF INDIVIDUAL SUPPRESSION SOURCE EFFECTIVENESS WITHIN THE NOMINAL LENGTH EJECTOR SYSTEM, STATIC, AT θ_I=60°, 90°, 130° AND PEAK VALUE

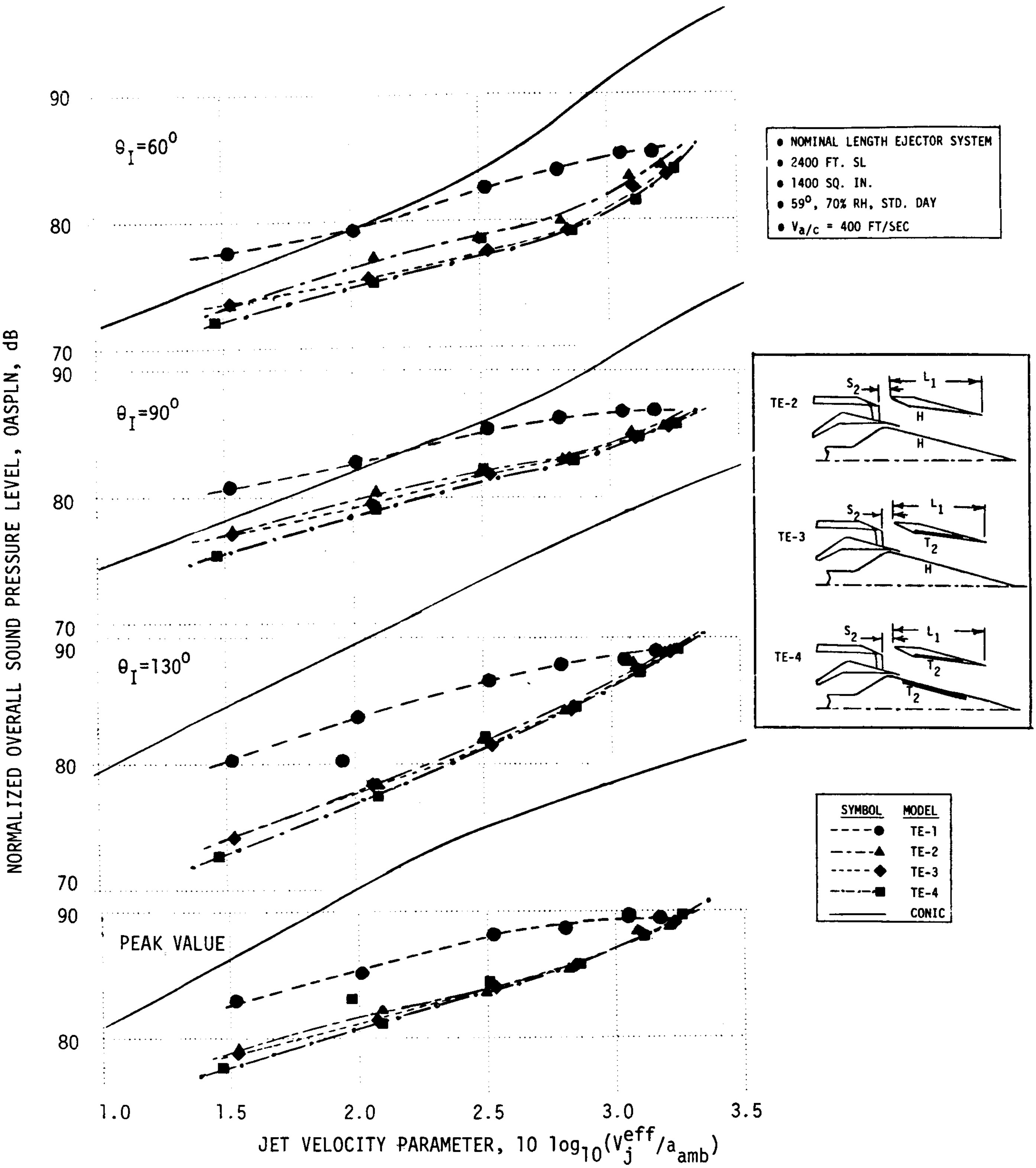

FIGURE 4-95. NORMALIZED OASPL AS A FUNCTION OF JET VELOCITY PARAMETER FOR IDENTIFICATION OF INDIVIDUAL SUPPRESSION SOURCE EFFECTIVENESS WITHIN THE NOMINAL LENGTH EJECTOR SYSTEM, SIMULATED FLIGHT, AT θ_I=60°, 90°, 130°, AND PEAK VALUE

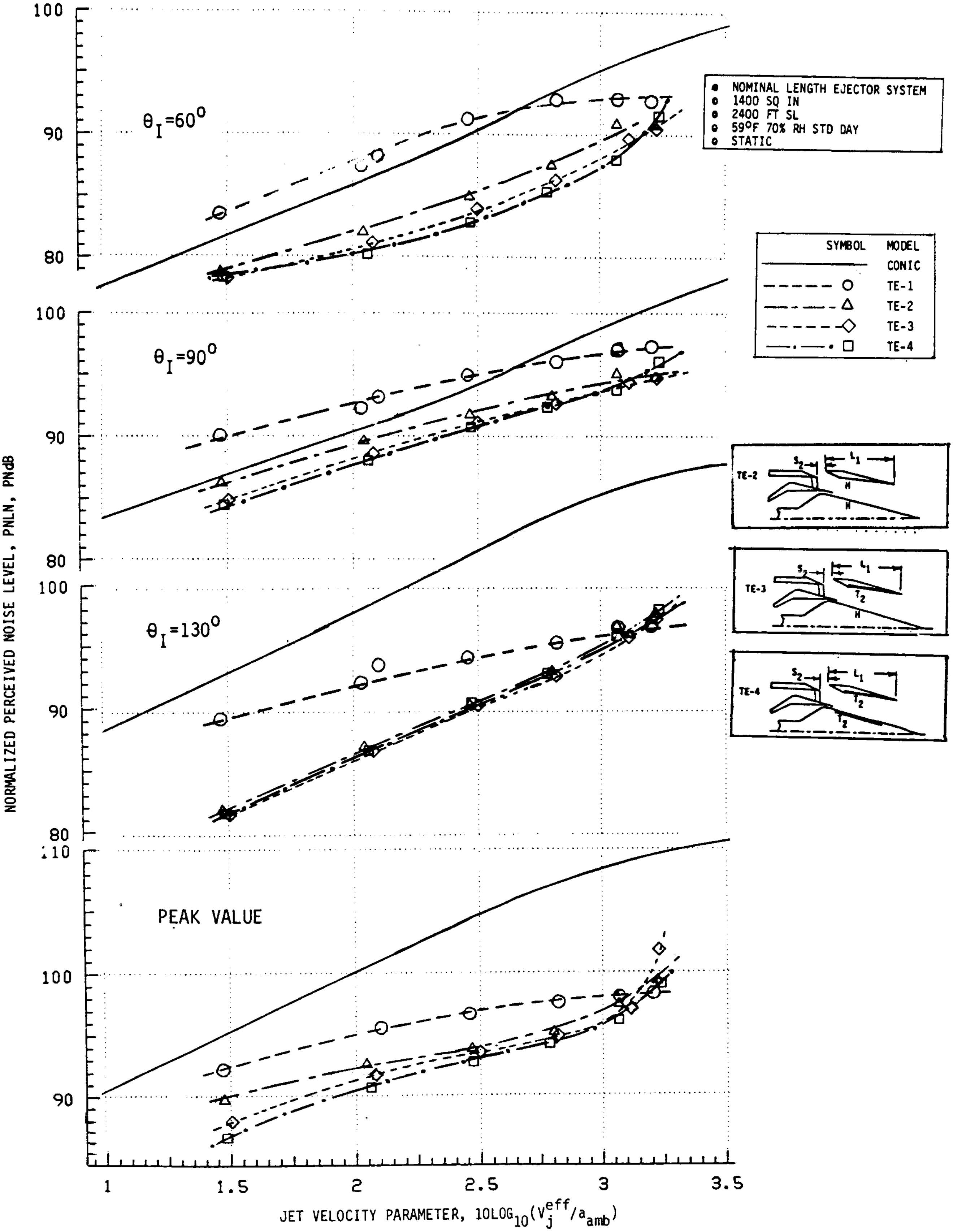

FIGURE 4-96. NORMALIZED PNL AS A FUNCTION OF JET VELOCITY PARAMETER FOR IDENTIFICATION OF INDIVIDUAL SUPPRESSION SOURCE EFFECTIVENESS WITHIN THE NOMINAL LENGTH EJECTOR SYSTEM, STATIC, AT θ_I=60°, 90°, 130° AND PEAK VALUE.

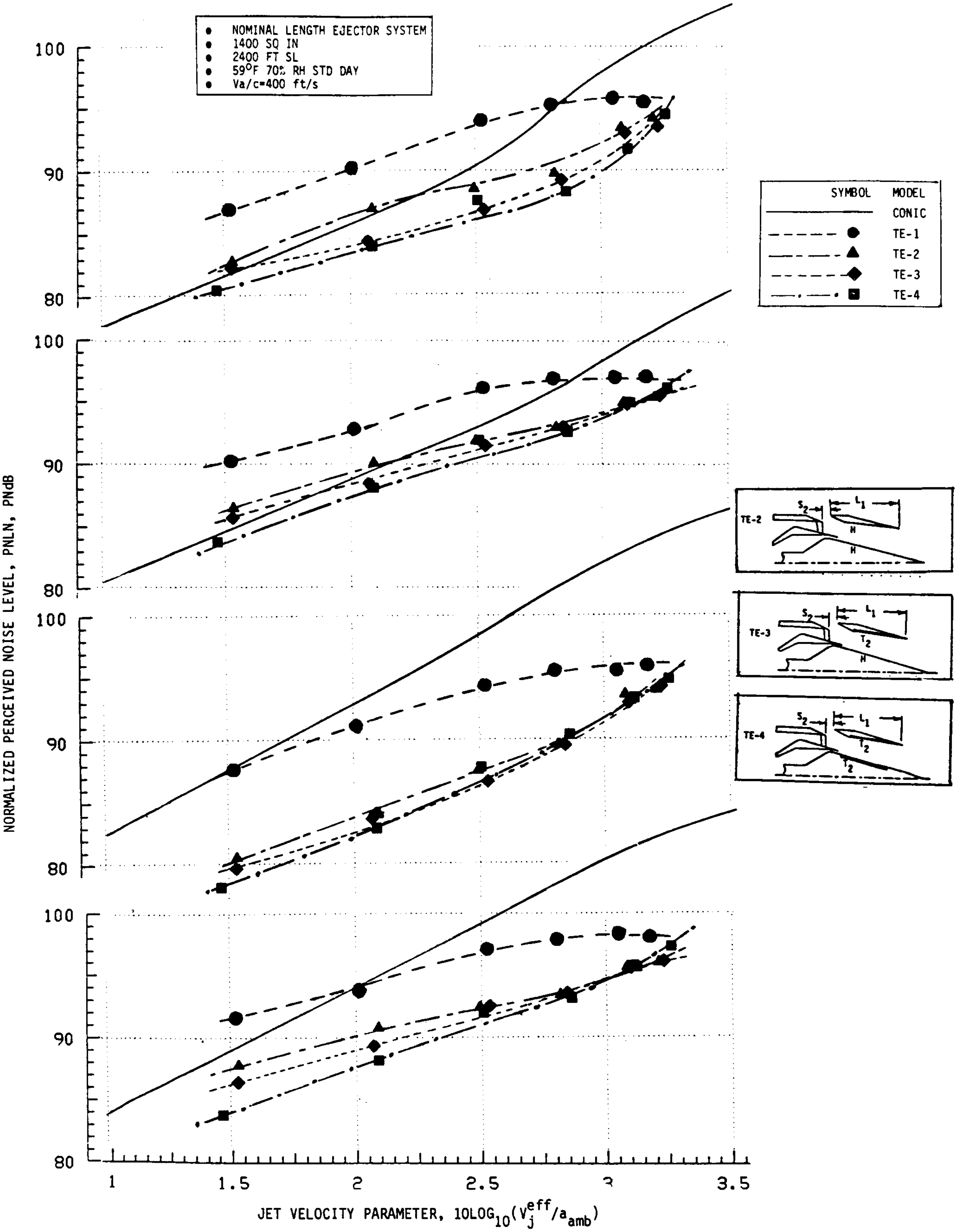

FIGURE 4-97. NORMALIZED PNL AS A FUNCTION OF JET VELOCITY PARAMETER FOR IDENTIFICATION OF INDIVIDUAL SUPPRESSION SOURCE EFFECTIVENESS WITHIN THE NOMINAL LENGTH EJECTOR SYSTEM, SIMULATED-FLIGHT, AT θ_I=60°, 90°, 130° AND PEAK VALUE.

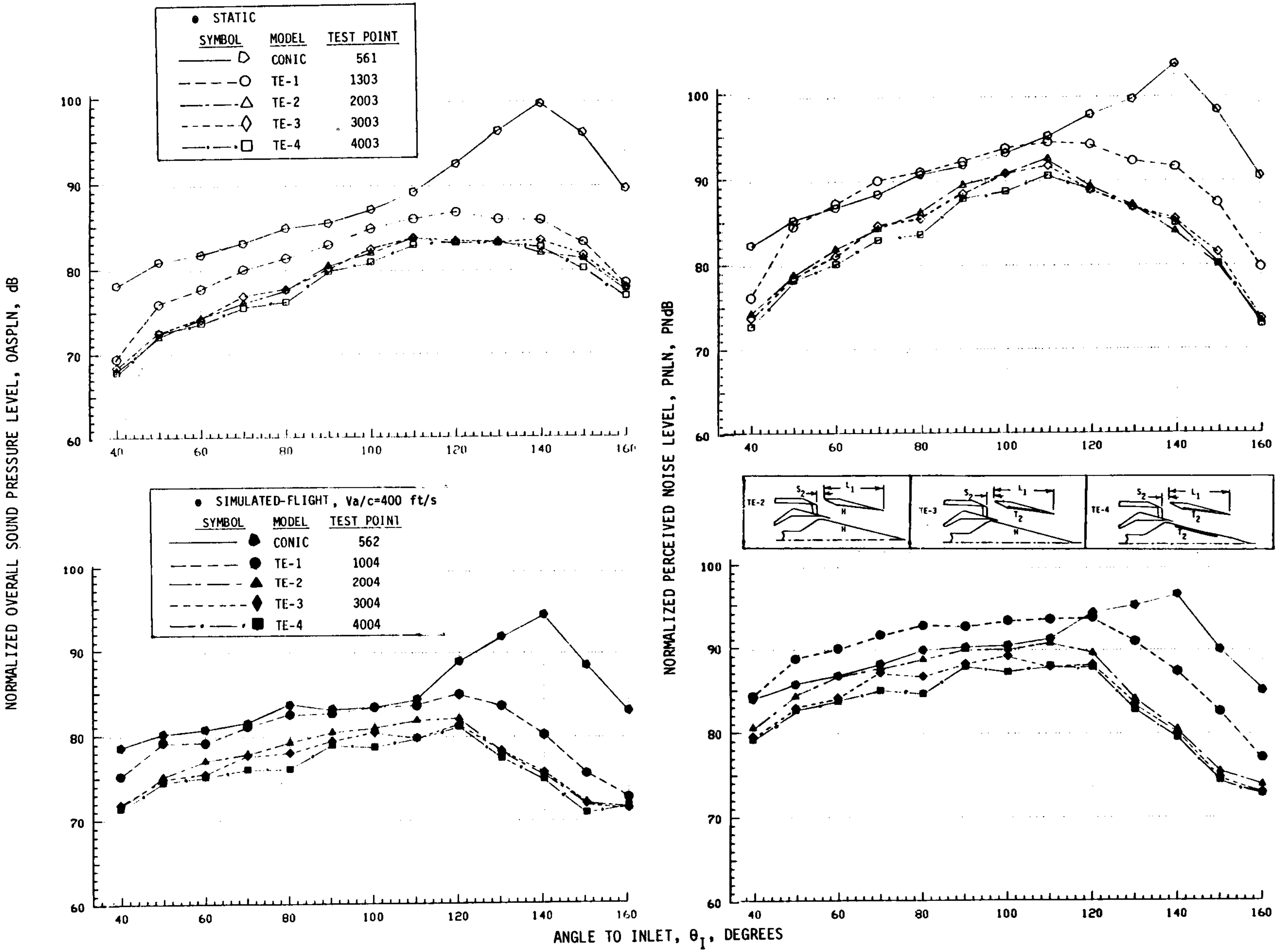

FIGURE 4-98. STATIC AND SIMULATED-FLIGHT DIRECTIVITY COMPARISONS OF OASPL AND PNL AT CUTBACK FOR IDENTIFICATION OF INDIVIDUAL SUPPRESSION SOURCE EFFECTIVENESS WITHIN THE NOMINAL LENGTH EJECTOR SYSTEM.

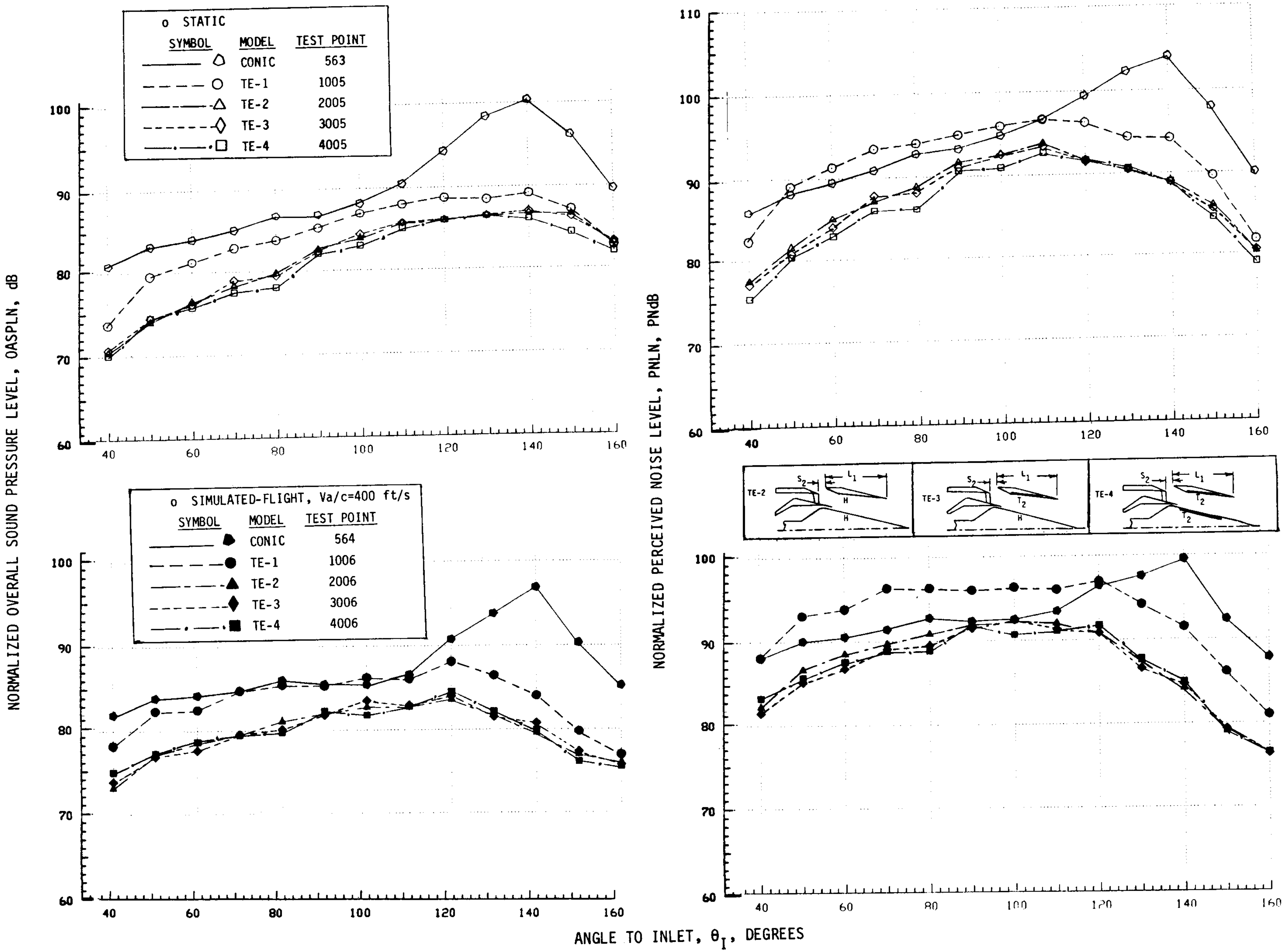

FIGURE 4-99. STATIC AND SIMULATED-FLIGHT DIRECTIVITY COMPARISONS OF OASPL AND PNL AT INTERMEDIATE FOR IDENTIFICATION OF INDIVIDUAL SUPPRESSION SOURCE EFFECTIVENESS WITHIN THE NOMINAL LENGTH EJECTOR SYSTEM

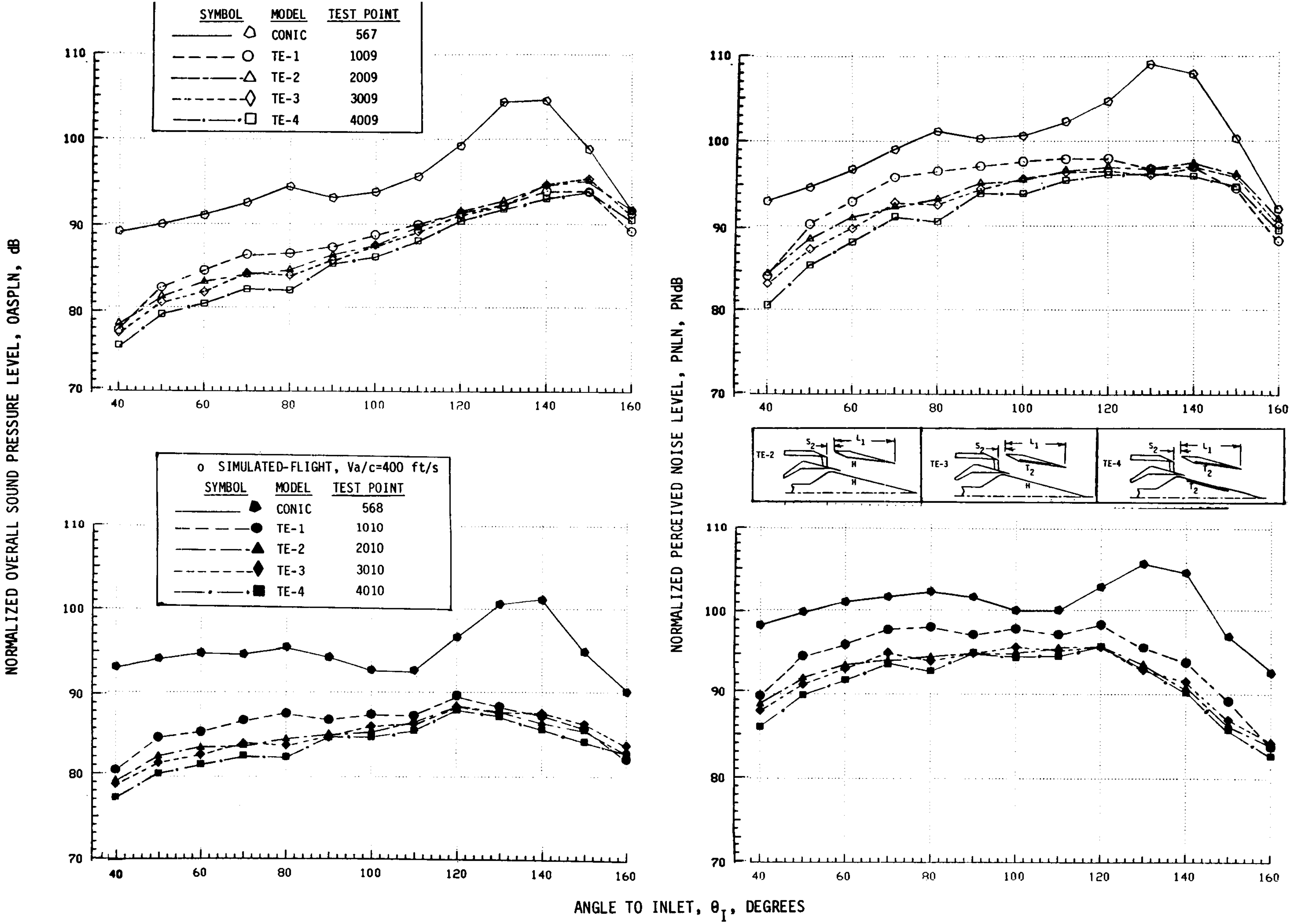

FIGURE 4-100. STATIC AND SIMULATED-FLIGHT DIRECTIVITY COMPARISONS OF OASPL AND PNL AT TAKEOFF FOR IDENTIFICATION OF INDIVIDUAL SUPPRESSION SOURCE EFFECTIVENESS WITHIN THE NOMINAL LENGTH EJECTOR SYSTEM.

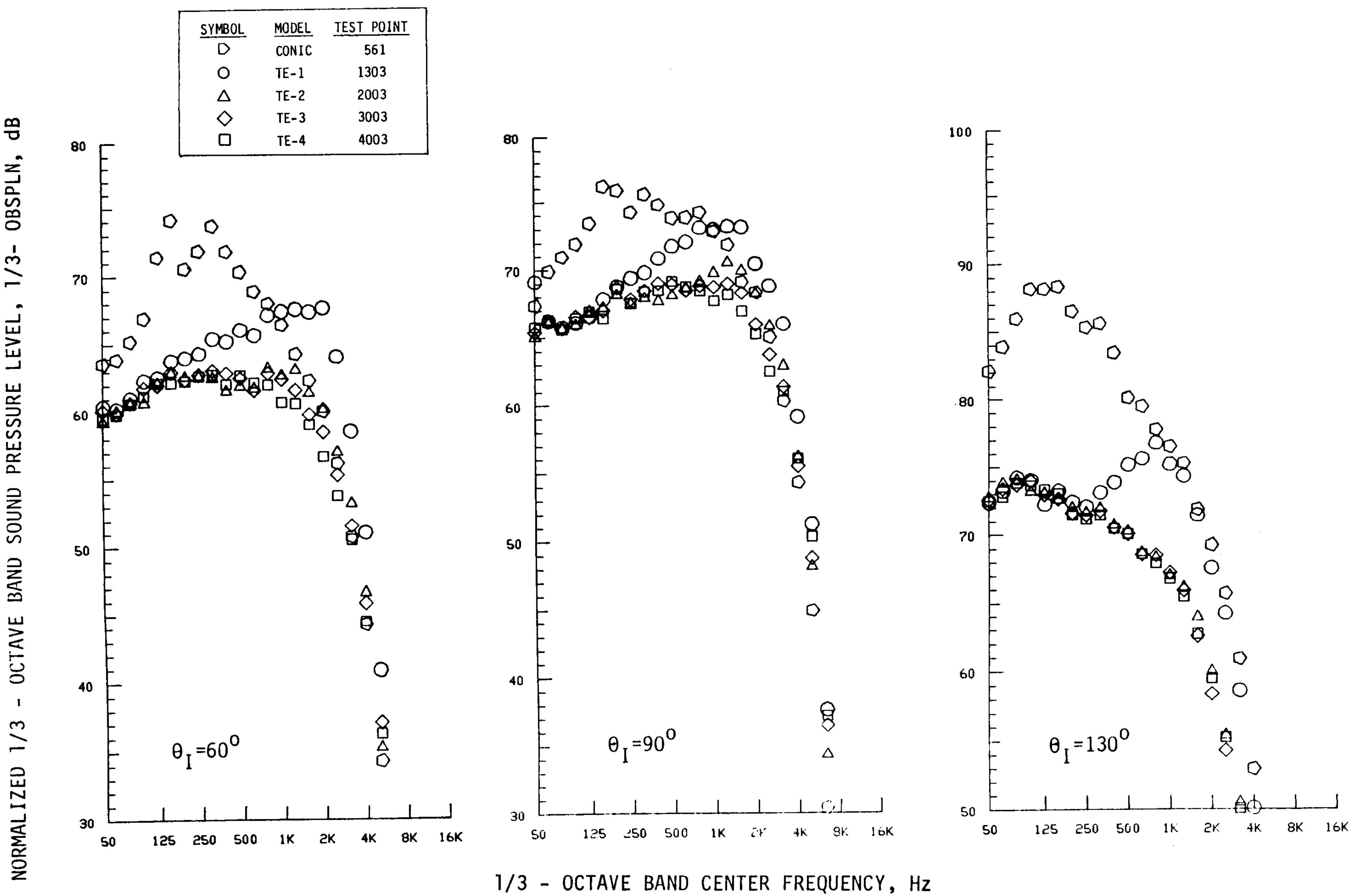

FIGURE 4-101. NORMALIZED SPECTRA @ θ_I=60°, 90° AND 130° FOR IDENTIFICATION OF INDIVIDUAL SUPPRESSION SOURCE EFFECTIVENESS WITHIN THE NOMINAL LENGTH EJECTOR SYSTEM, STATIC, AT CUTBACK.

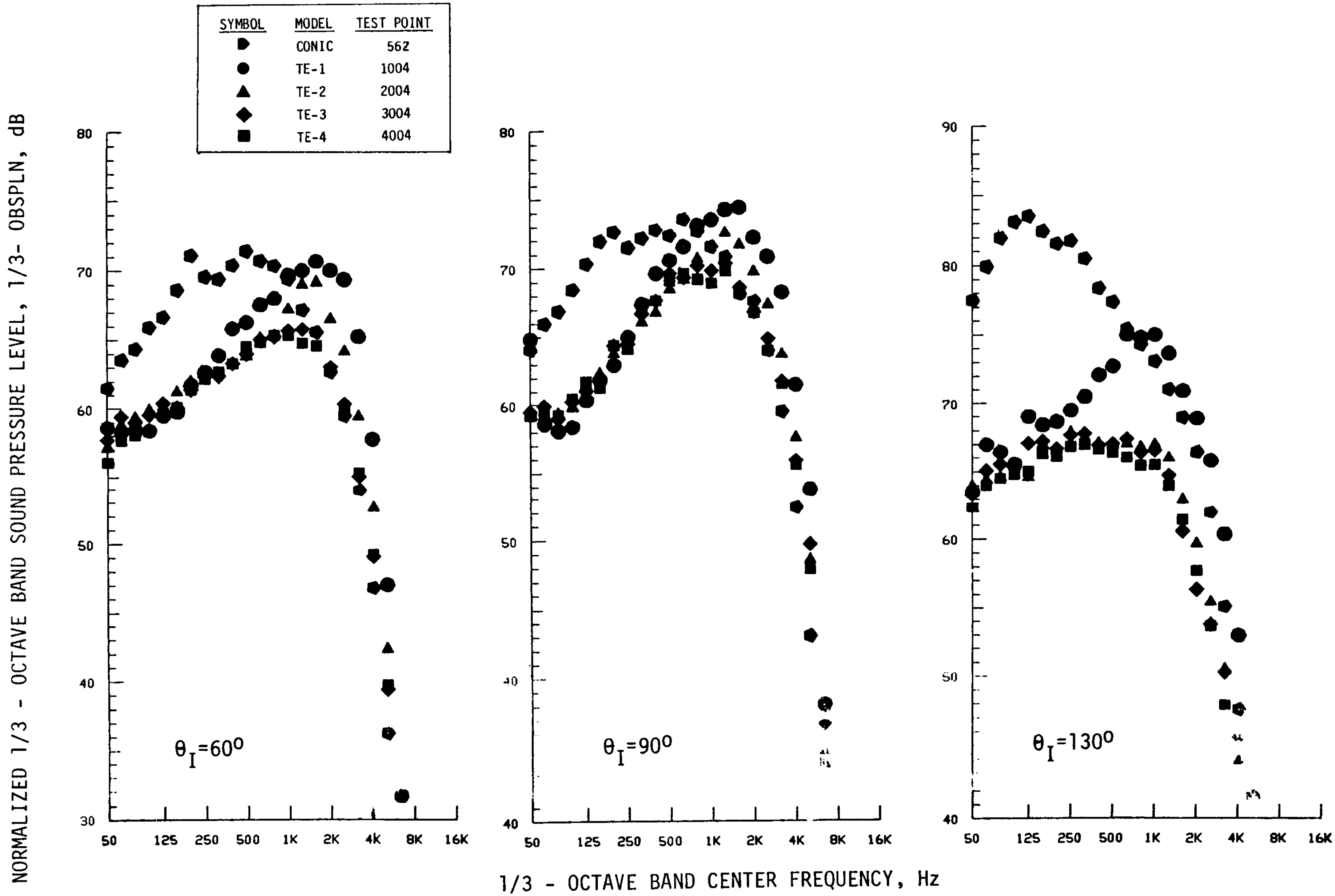

FIGURE 4-102. NORMALIZED SPECTRA @ $\theta_I=60^o$, 90^o AND 130^o FOR IDENTIFICATION OF INDIVIDUAL SUPPRESSION SOURCE EFFECTIVENESS WITHIN THE NOMINAL LENGTH EJECTOR SYSTEM, SIMULATED-FLIGHT, AT CUTBACK.

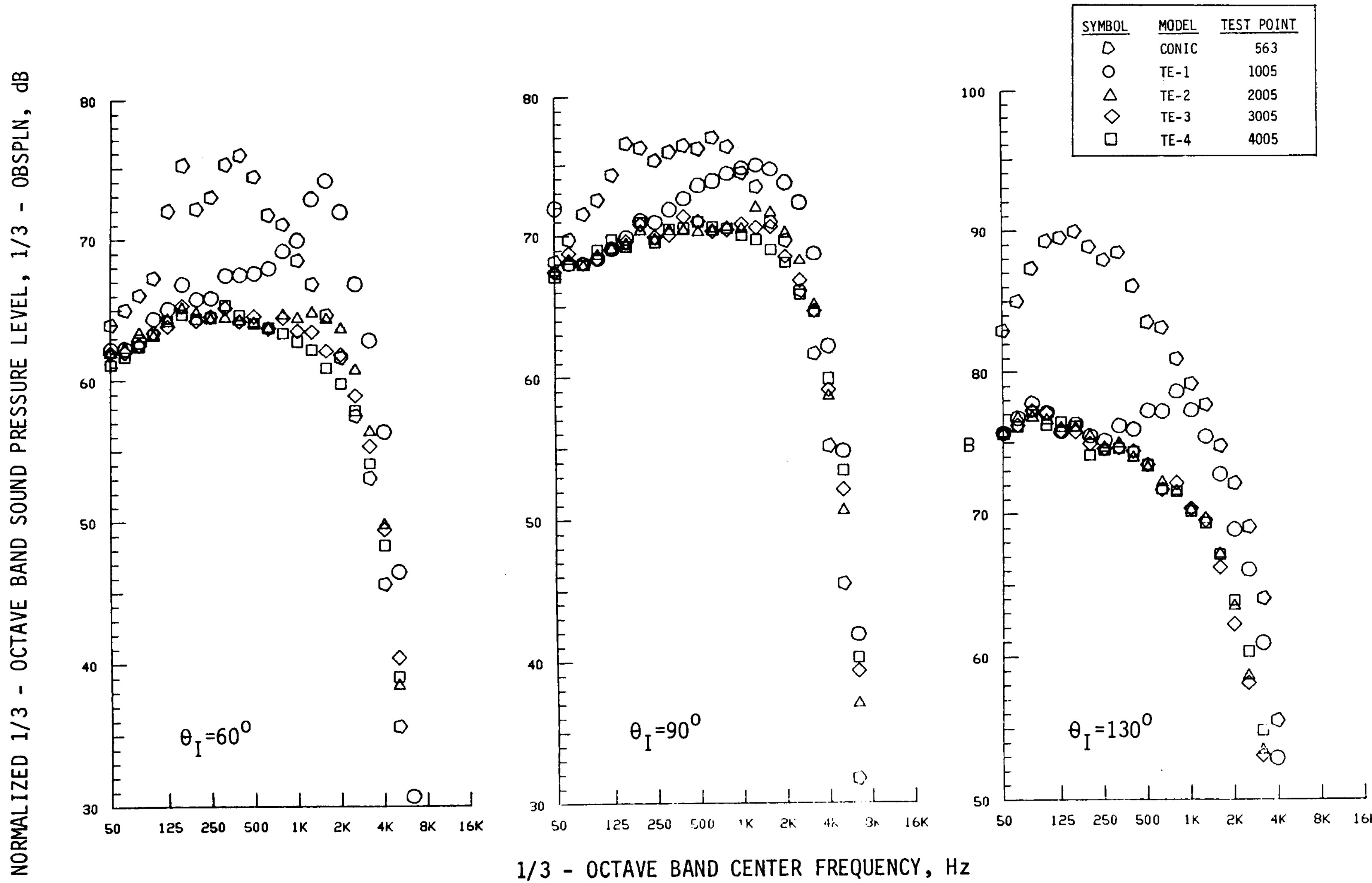

FIGURE 4-103. NORMALIZED SPECTRA @ $\theta_I=60^0$, 90^0 AND 130^0 FOR IDENTIFICATION OF INDIVIDUAL SUPPRESSION SOURCE EFFECTIVENESS WITHIN THE NOMINAL LENGTH EJECTOR SYSTEM, STATIC, AT INTERMEDIATE.

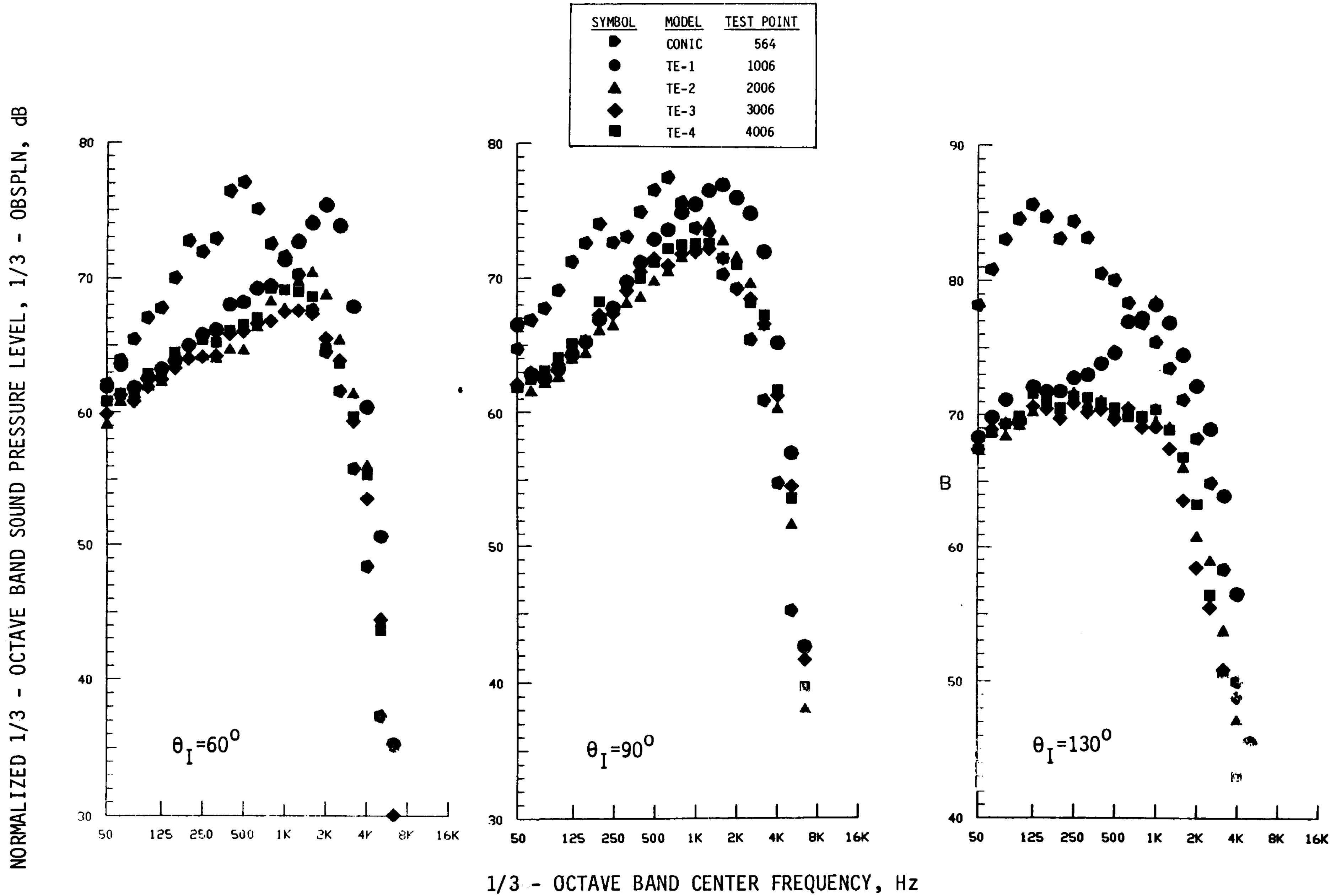

FIGURE 4-104. NORMALIZED SPECTRA @ $\theta_I=60^o$, 90^o AND 130^o FOR IDENTIFICATION OF INDIVIDUAL SUPPRESSION SOURCE EFFECTIVENESS WITHIN THE NOMINAL LENGTH EJECTOR SYSTEM, SIMULATED-FLIGHT, AT INTERMEDIATE.

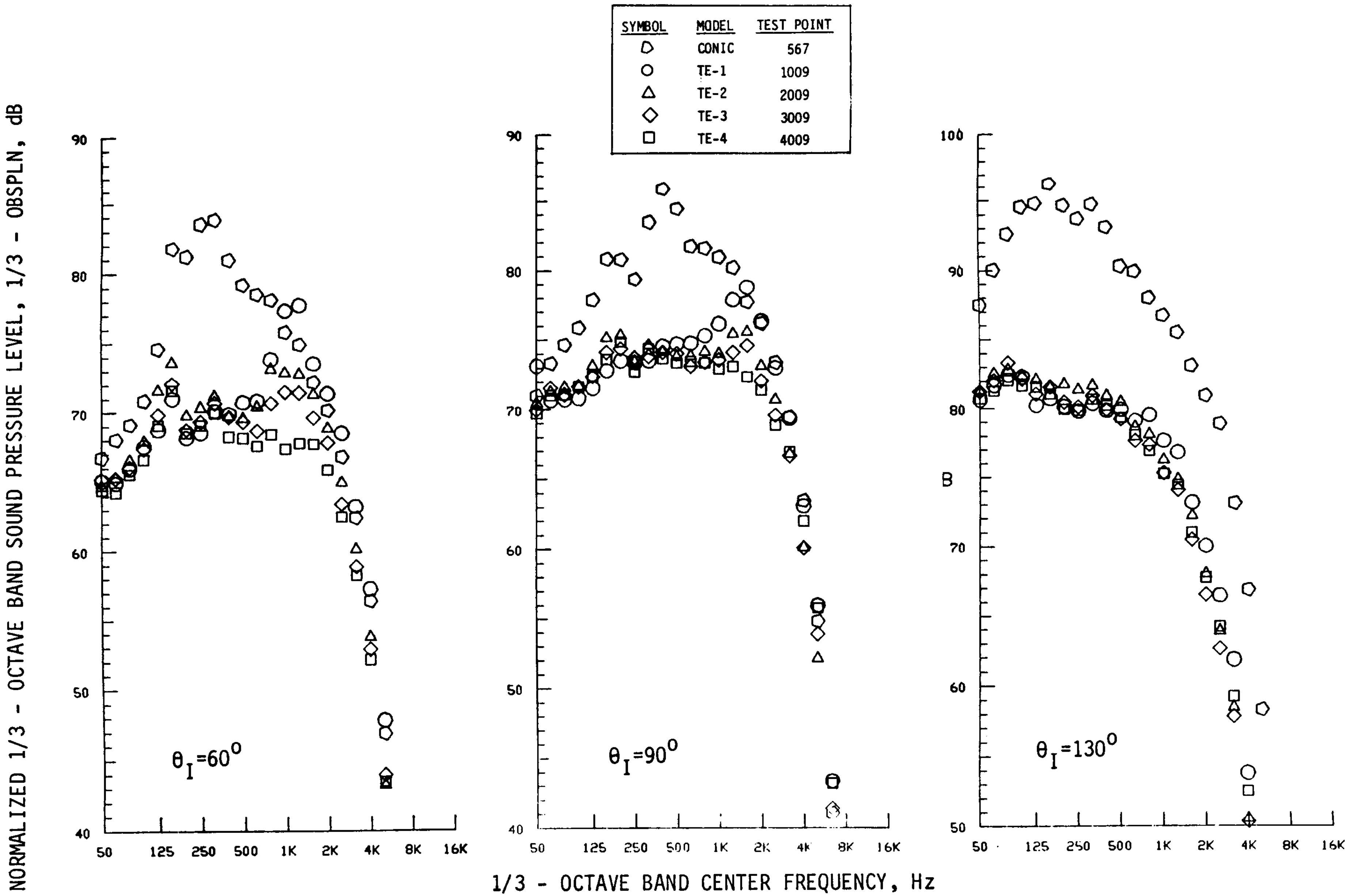

FIGURE 4-105. NORMALIZED SPECTRA @ $\theta_I=60^o$, 90^o AND 130^o FOR IDENTIFICATION OF INDIVIDUAL SUPPRESSION SOURCE EFFECTIVENESS WITHIN THE NOMINAL LENGTH EJECTOR SYSTEM, STATIC, AT TAKEOFF.

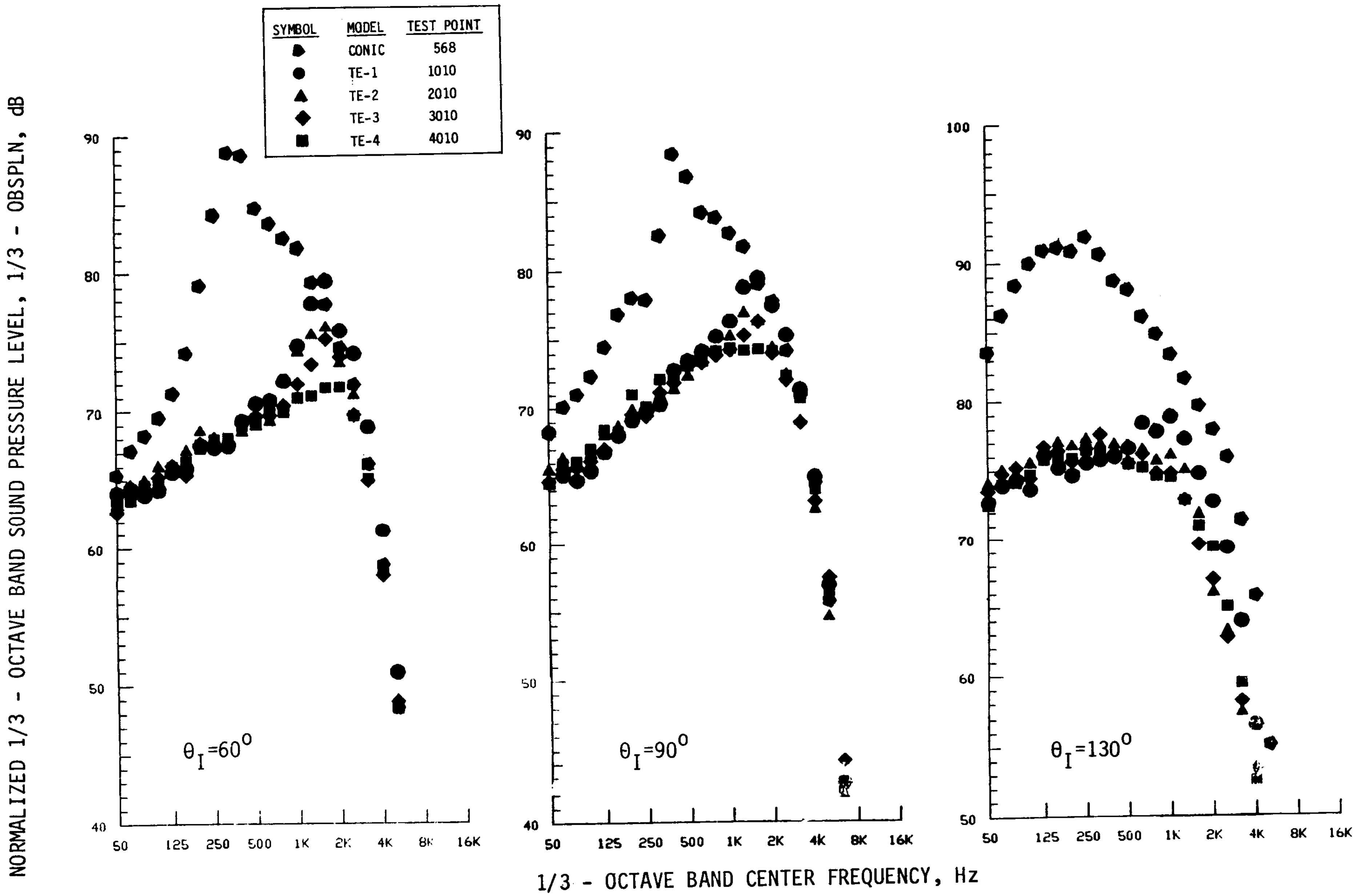

FIGURE 4-106. NORMALIZED SPECTRA @ θ_I=60°, 90° AND 130° FOR IDENTIFICATION OF INDIVIDUAL SUPPRESSION SOURCE EFFECTIVENESS WITHIN THE NOMINAL LENGTH EJECTOR SYSTEM, SIMULATED-FLIGHT, AT TAKEOFF.

4.4.2.3 Review of Detailed Data Comparisons for Nominal and Extended Length Ejector Systems

The power level graphs of Figures 4-79 and 4-93 show that total acoustic energy is reduced quite substantially by the hardwall ejector applications, i.e., TE-10 and TE-2. In each comparison, however, the ejector treatment application, TE-7 and TE-3, decreased the level of PWL reduction to below that of the hardwall. Treatment on both surfaces, TE-8 and TE-4, further reduced the total acoustic energy to below that of the hardwall system. Changes of PWL are most dramatic at low to intermediate cycle points, compared to TE-1 unejected system, and diminish to minimal at highest cycle points.

As the greatest benefit of ejector and treatment application is in the mid-to-high frequency regions of the spectra for most all presented comparisons, Figures 4-87 through 4-92 and 4-101 through 4-106, impact on PNL suppression is normally greater than on OASPL. However, as seen from many of the spectra plots, the effectiveness is sufficiently broad to extend to low frequency peaks which control OASPL, therefore, OASPL reduction is also significant.

The most significant review of individual suppression source effectiveness is afforded by scanning the PNL and OASPL directivity plots for static and flight; Figures 4-84, -85 and -86 at cutback, intermediate and takeoff for the long ejector models and Figures 4-98, -99 and -100, similarly, for the shorter ejector models. In most all comparisons, the pattern of trends is consistent, i.e.:

- Application of the hardwall ejectors substantially reduce both OASPL and PNL, both static and flight. Levels of reduction are most significant in the forward quadrant and broadside angles.

- Applications of ejector and then plug treatments allow incremental steps of additional OASPL and PNL suppression, primarily in the forward and broadside angles for the long ejectors; aft angle levels being altered little. Levels at angles of peak noise, however, are still reduced by the treatment. For the shorter ejectors, these incremental steps of ΔOASPL and ΔPNL are much less than those of the extended length system and are not as systematically identifiable.

- In most all comparisons, however, the fully treated ejector system is judged most effective on both OASPL and PNL bases.

4.5 EJECTOR LENGTH VARIATION

This report section isolates the impact of ejector length variation. Reference to Section 4.0, and in particular Figure 4-1's test chronology, indicates that three model sets were tested within which ejector length variation may be influential. These were:

- o Hardwall ejector/plug systems: TE-2 of L1 and TE-10 of L2 (Reference Figures 3-10 and 3-18).
- o Treated ejector flow surface systems: TE-3 of L1 and TE-7 of L2 (Reference Figures 3-11 and 3-15)
- o Fully treated ejector/plug systems: TE-4 of L1 and TE-8 of L2 (Reference Figures 3-12 and 3-16)

Within the comparisons for each test set, the impact which ejector length variation has on acoustic and aerodynamic (base pressure) performance can be evaluated. All ejector axial locations were maintained at the S2 (extended) position, the optimum of the two locations evaluated; see Section 4.3 "Variations of Ejector Axial Spacing and Treatment Design" for details. In review, the L1-nominal length ejector was 8.68" long model-scale and was scaled from the full scale nozzle design of Reference 1, shown in Figure 2-1. It had acoustic treatment applied over approximately 70% of its flap length. The L2-extended length ejector was 10.8" long model-scale and treatment was applied to a length equivalent to that of the full flap length of the nominal length ejector system. The additional untreated closure length is similar to that of the nominal length ejector.

4.5.1 Overview of Ejector Length Variation Acoustic Impact

To gauge ejector length impact on an overview acoustic parameter, EPNL is presented as a function of the jet velocity parameter in Figure 4-107. The EPNL values are based on 2400' sideline data with nominal 400 ft/sec simulated-flight speed. The figure compares a) TE-2 to TE-10, bottom, b) TE-3 to TE-7, center, and c) TE-4 to TE-8, top, and includes nominal lines for conic and TE-1 reference nozzles. Reviewing the curves for ejector length impact reveals:

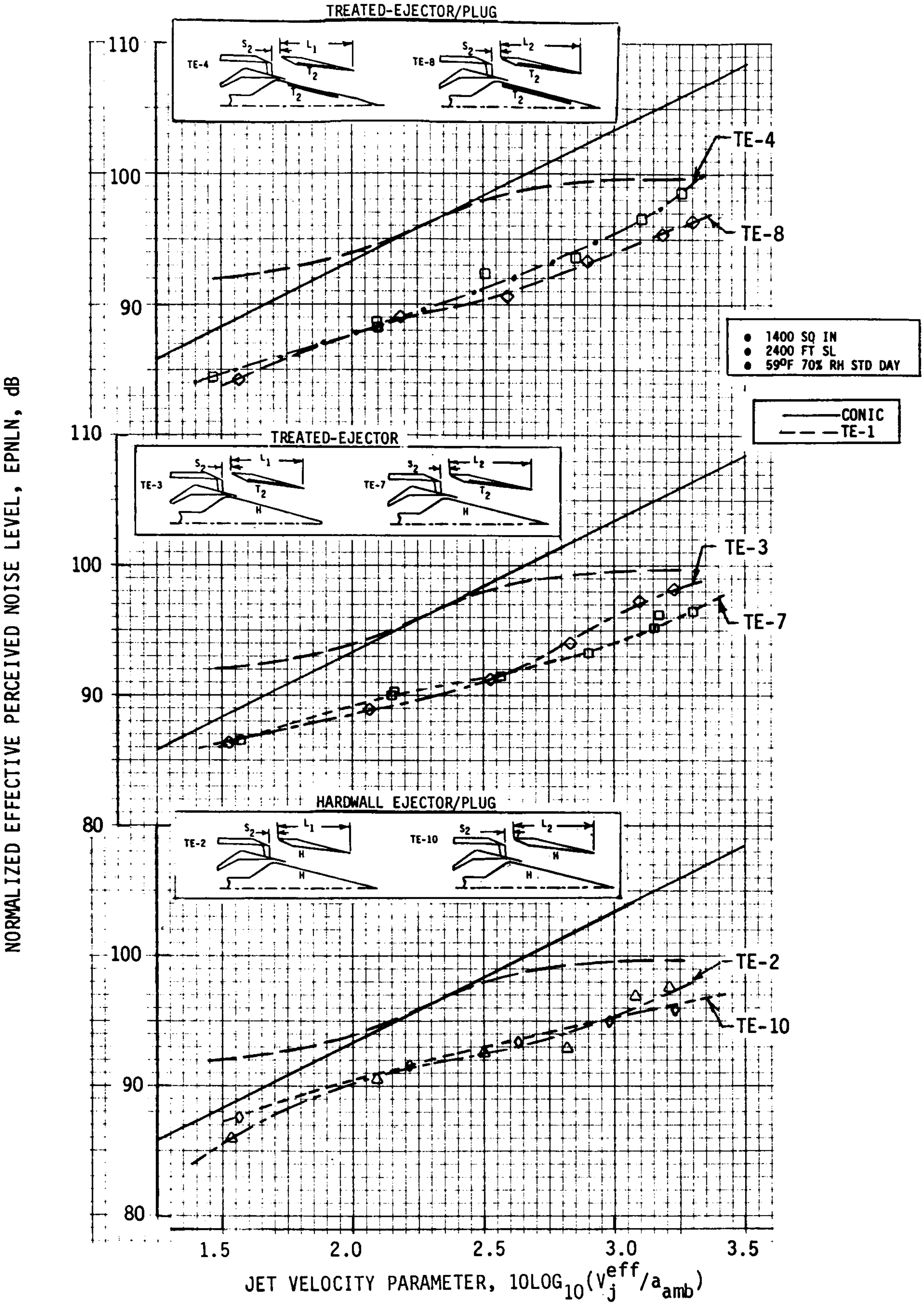

FIGURE 4-107. EPNL CORRELATION WITH JET VELOCITY PARAMETER FOR COMPARISONS OF EJECTOR LENGTH VARIATION.

- o Ejector length variation, from L1 to L2, has insignificant impact for mixed subsonic to intermediate cycle operation, $1.5 \leq 10\log_{10} (V_j^{eff}/a_{amb}) \leq 2.6$, but definitely shows bias toward longer ejector length to improve suppression at takeoff through maximum-cycle operation.

- o At takeoff cycle and above (mixed velocity parameter $\cong$3.0) the longer ejector gains a) up to 1 ΔEPNL in a hardwall version, b) approximately 2 ΔEPNL for the treated ejector system, and c) from 1.5 to 3.0 ΔEPNL for the treated ejector/treated plug system.

A primary gauge of acoustic effectiveness is PNL suppression. An additional overview of ejector length impact can be gleaned from ΔPNL comparisons within Figures 4-108 and 4-109, for static and simulated-flight, for θ_I = 60°, 90°, 130° and peak value. Further similar comparisons on a OASPL basis are in Figures 4-110 and 4-111. Each graph shows the change in PNL/OASPL as effected by ejector length change alone, i.e., by comparing TE-2 to TE-10, TE-3 to TE-7 and TE-4 to TE-8. Positive values indicate suppression increase due to length increase, negative values indicate greater noise levels with the longer ejector. In review:

- o Forward quadrant, θ_I = 60°, suppression is increased quite substantially with ejector length increase; near takeoff, up to 3 dB additional ΔPNL is gained for static and flight. Progression of increased effectiveness, from hardwall to treated ejector to treated plug and ejector is fairly systematic; in most comparisons the fully treated system is most beneficial.

- o Broadside, at θ_I = 90°, length increase impact is very consistent though not as beneficial. The fully treated ejector/plug shows slight improvement with extended length; approximately 2.0 PNL near takeoff cycle for static and flight. The treated ejector/hardwall plug shows similar results with both ejectors and the hardwall long ejector increases PNL/OASPL levels by 0.5 to 1.0 dB for most cycle points.

- o Aft quadrant, θ_I = 130°, comparisons show all long ejectors to degrade acoustic performance, each being 1.0 to 1.5 ΔPNL/ ΔOASPL noisier than short ejectors.

- o Peak value comparisons are similar to θ_I = 130° data. On the ΔPNL basis the fully treated system shows slightly greater suppression for the long ejector. The partially treated and hardwall systems are equivalent and noisier, respectively, for length increase.

ORIGINAL PAGE IS OF POOR QUALITY

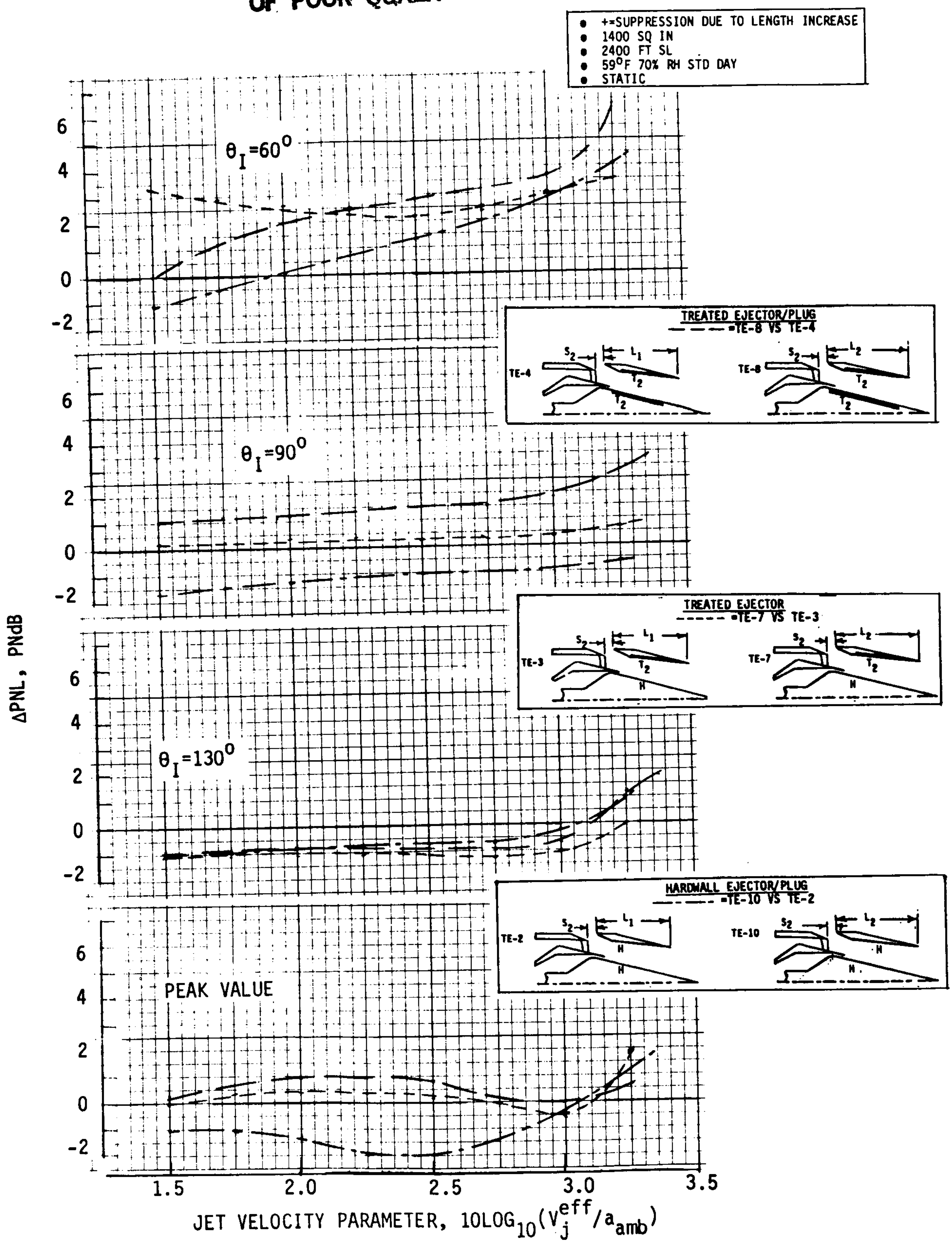

FIGURE 4-108. PNL SUPPRESSION CHANGE DUE TO EJECTOR LENGTH INCREASE; TE-8 VERSUS TE-4, TE-7 VERSUS TE-3, AND TE-10 VERSUS TE-2, STATIC, AT θ_I = 60°, 90°, 130° AND PEAK VALUE

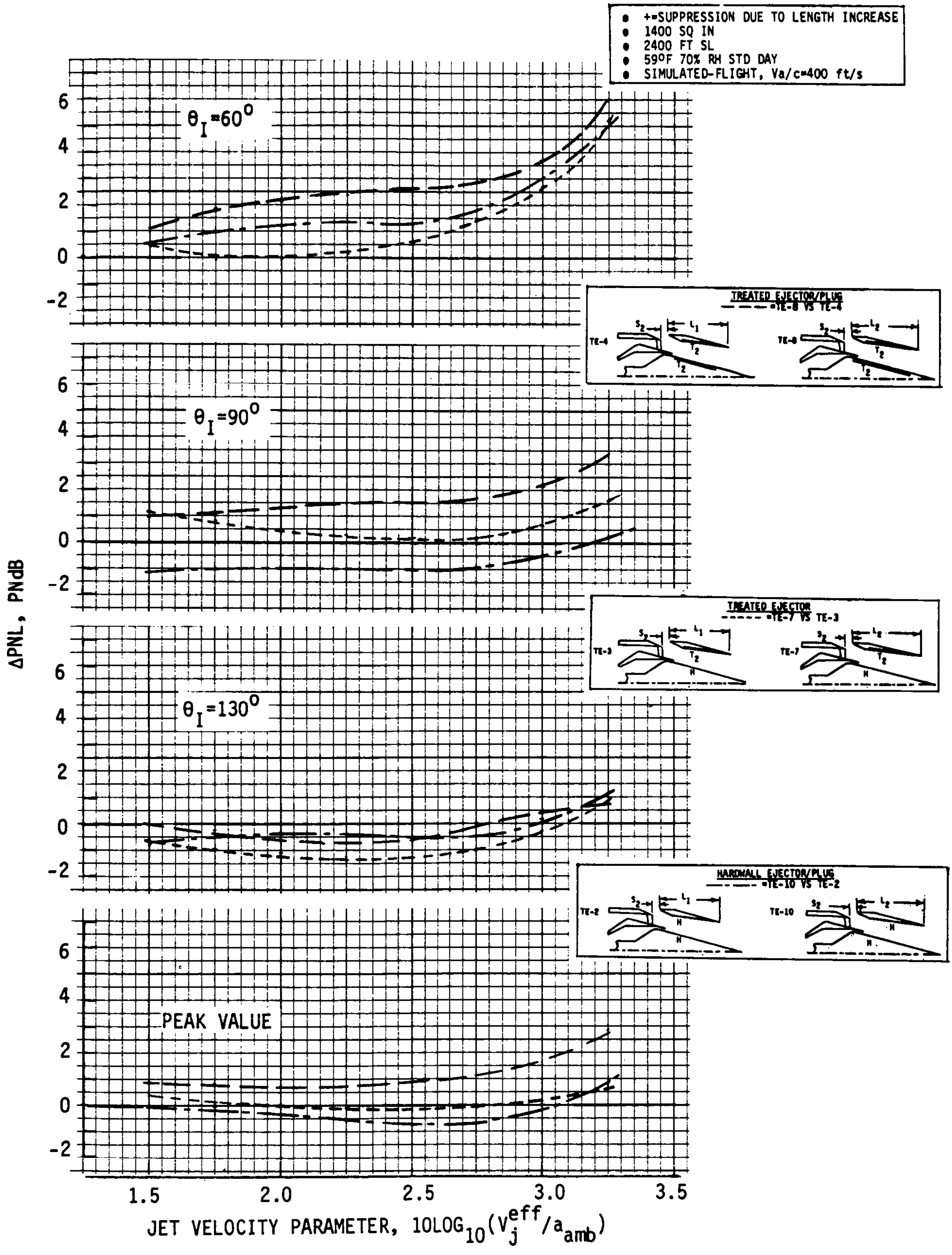

FIGURE 4-109. PNL SUPPRESSION CHANGE DUE TO EJECTOR LENGTH INCREASE; TE-8 VERSUS TE-4, TE-7 VERSUS TE-3, AND TE-10 VERSUS TE-2, SIMULATED-FLIGHT, AT Θ_I= 60°, 90°, 130° AND PEAK VALUE

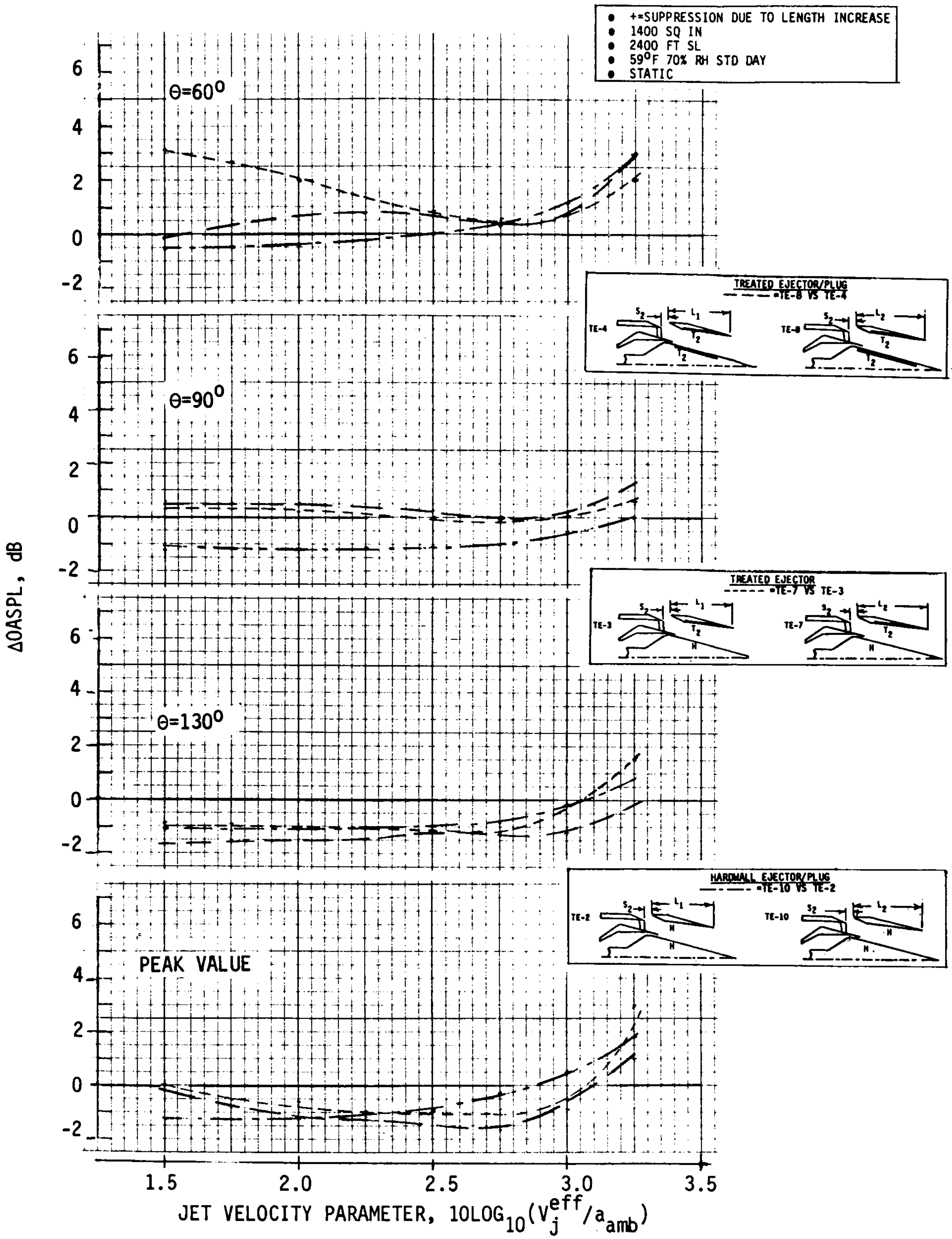

FIGURE 4-110. OASPL SUPPRESSION CHANGE DUE TO EJECTOR LENGTH INCREASE; TE-8 VERSUS TE-4, TE-7 VERSUS TE-3, AND TE-10 VERSUS TE-2, STATIC, AT θ_I = 60°, 90°, 130° AND PEAK VALUE

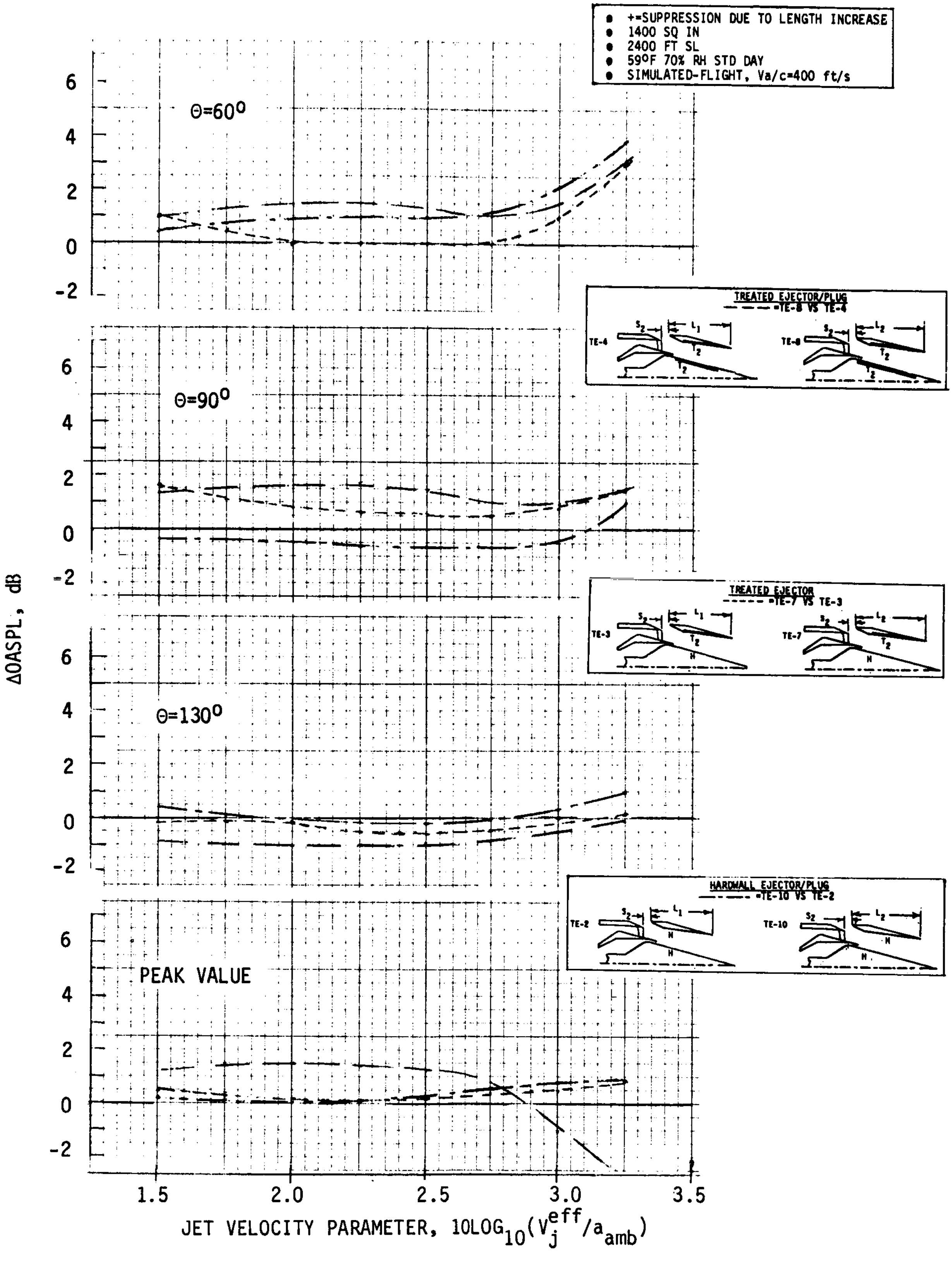

FIGURE 4-111. PNL SUPPRESSION CHANGE DUE TO EJECTOR LENGTH INCREASE; TE-8 VERSUS TE-4, TE-7 VERSUS TE-3, AND TE-10 VERSUS TE-2, SIMULATED-FLIGHT, AT Θ_I = 60°, 90°, 130° AND PEAK VALUE

A final overview evaluation of ejector length is seen per Figures 4-112 through 4-114's spectral suppression comparisons. The graphs show Δ1/3-OBSPL versus frequency at θ_I = 60°, 90° and 130°, for static and flight, at cutback, intermediate and takeoff. Again, the Δ's are from direct comparisons of TE-2 to TE-10, TE-3 to TE-7 and TE-4 to TE-8; positive values indicating increased suppression from length increase and negative values indicating higher noise levels with longer ejectors. Trends are similar to those of the ΔPNL/ ΔOASPL comparisons but on a spectral basis now indicate:

- o For most all comparisons the longer ejector increases low frequency noise levels by 1 to 2 dB for 50 to 500 Hz. (This can be correlated with later presented LV plume decay plots which show the plumes for a long ejector to decay less rapidly than for the short ejector, thus, allowing longer zones of turbulent mixing noise generation of low frequency.)

- o Maximum increase in spectral suppression due to ejector length is seen in the forward quadrant and for the frequency range of approximately 800 to 8 KHz, reaching suppression of 6 to 8 ΔdB near 2 KHz.

- o Moving broadside, 90°, and toward the aft quadrant, 130°, most of the high frequency suppression due to ejector length increase diminishes. Statically, all long ejector systems generate higher aft quadrant noise levels for all frequencies at all three cycle points; simulated-flight shows only light mid-frequency suppression for the higher cycle condition and greater noise for all others.

- o Where increased ejector length does increase spectral suppression, the fully treated plug/ejector system is normally most beneficial.

4.5.2 Detailed Data Comparisons for Ejector Length Variations

In order to view ejector length acoustic impact within a more detailed data base, the following data sets are presented for review:

- o For comparison of TE-2 to TE-10, for length variation within the hardwall ejector/plug geometry, Figures 4-115 through 4-119 present normalized PWL, OASPL and PNL correlated with the jet velocity parameter, for static and simulated-flight. The OASPL and PNL are presented at θ_I = 60°, 90°, 130° and peak value.

- o For comparison of TE-3 to TE-7, for length variation within a treated ejector/hardwall plug system, Figures 4-120 through 4-124 present data similar to that above for TE-2/TE-10.

- o For comparison of TE-4 to TE-8, for length variation within a fully treated ejector/plug geometry, Figures 4-125 through 4-129 do likewise to those above.

These data sets are included primarily for the readers extended use as a detailed data base. Trends from the PNL and OASPL data, in regards to ejector length impact, were summarized and reviewed in the previous ΔPNL/ ΔOASPL graphs of Figures 4-108 through 4-111.

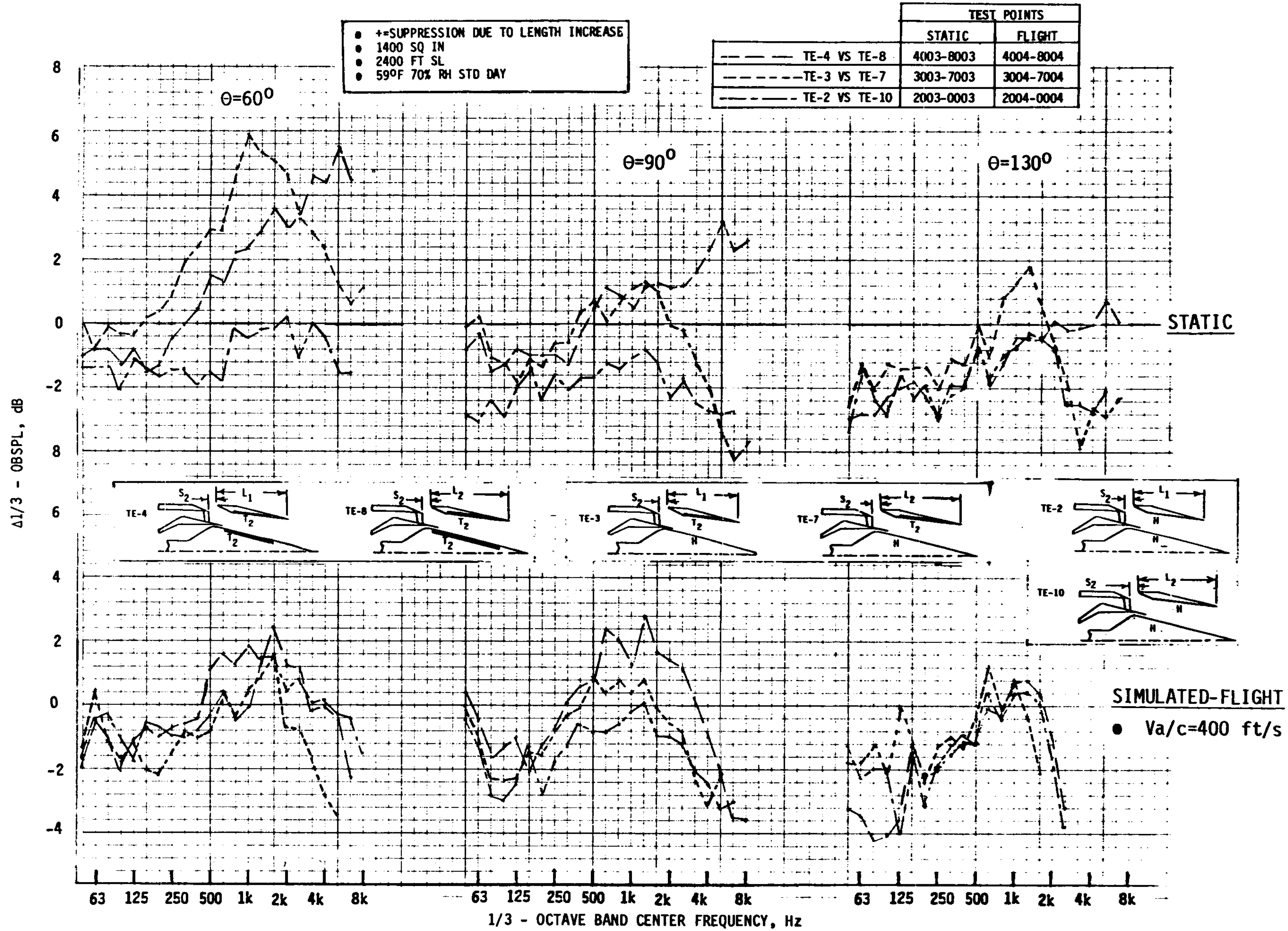

FIGURE 4-112. EJECTOR LENGTH INCREASE EFFECTIVENESS AS A FUNCTION OF 1/3-OCTAVE BAND FREQUENCY AT CUTBACK, STATIC AND SIMULATED-FLIGHT, θ_I =60°, 90° AND 130°

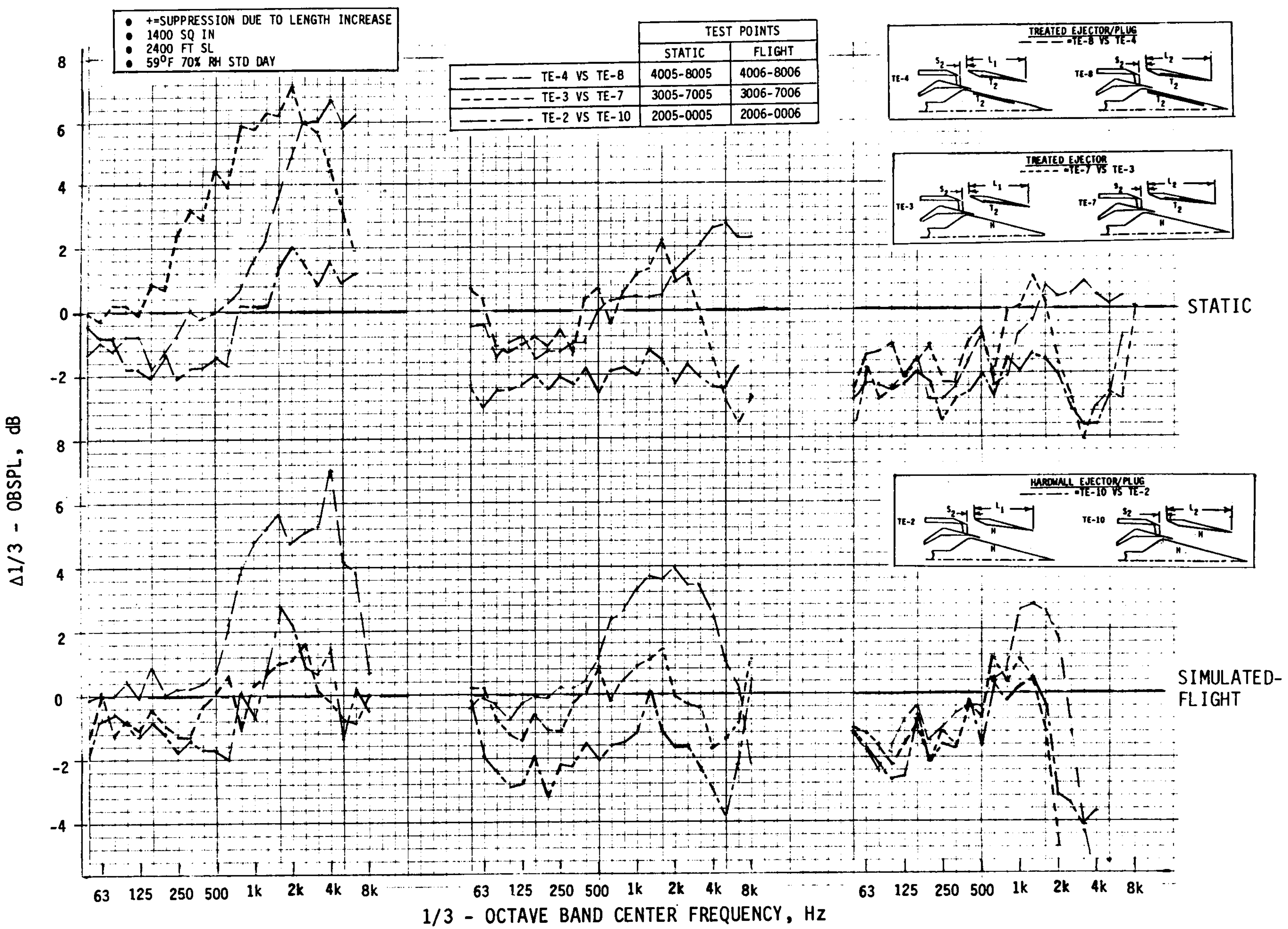

FIGURE 4-113. EJECTOR LENGTH INCREASE EFFECTIVENESS AS A FUNCTION OF 1/3-OCTAVE BAND FREQUENCY AT INTERMEDIATE, STATIC AND SIMULATED-FLIGHT, Θ_I = 60°, 90° AND 130°

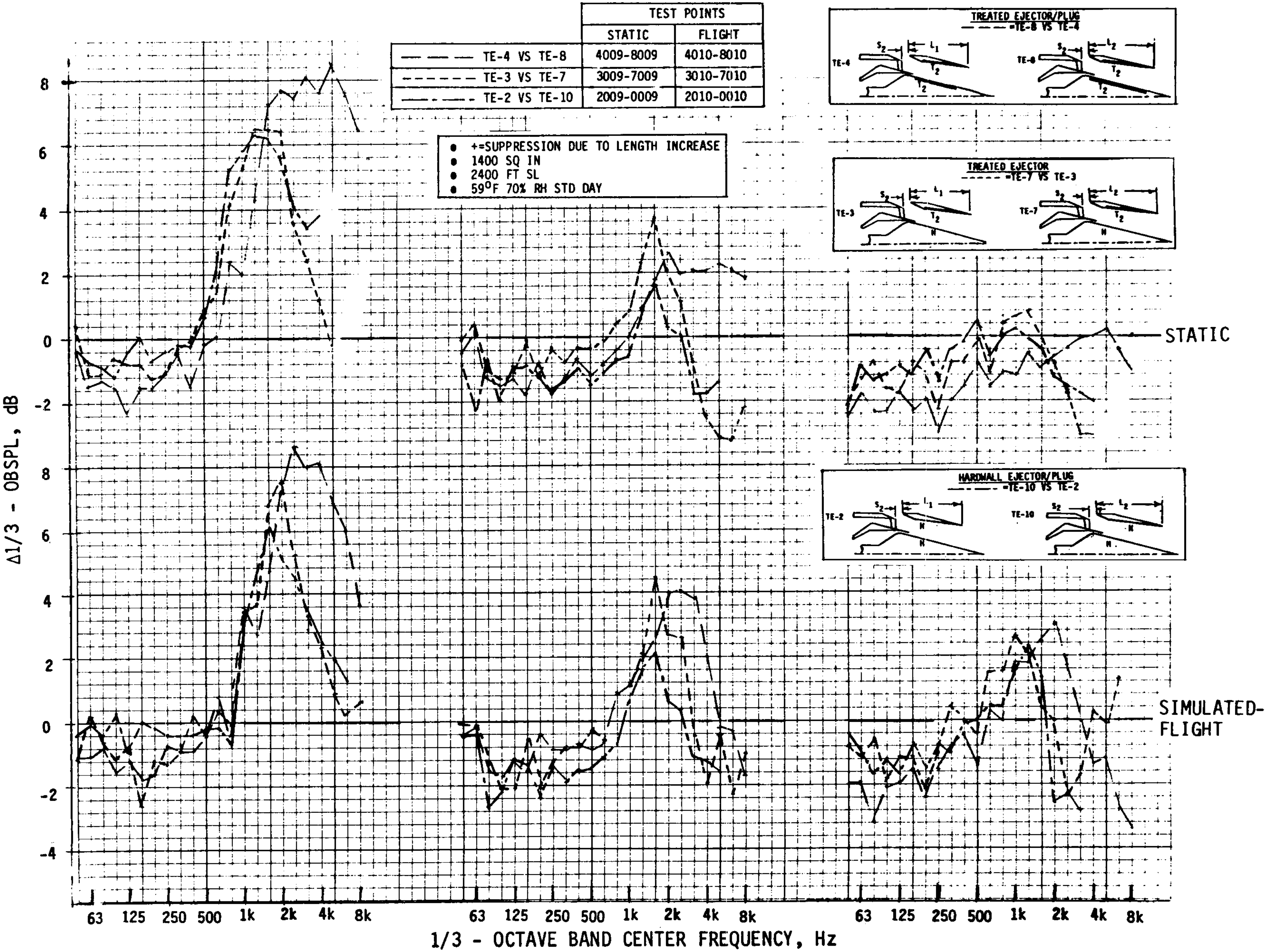

FIGURE 4-114. EJECTOR LENGTH INCREASE EFFECTIVENESS AS A FUNCTION OF 1/3-OCTAVE BAND FREQUENCY AT TAKEOFF, STATIC AND SIMULATED-FLIGHT, θ_I = 60°, 90° AND 130°

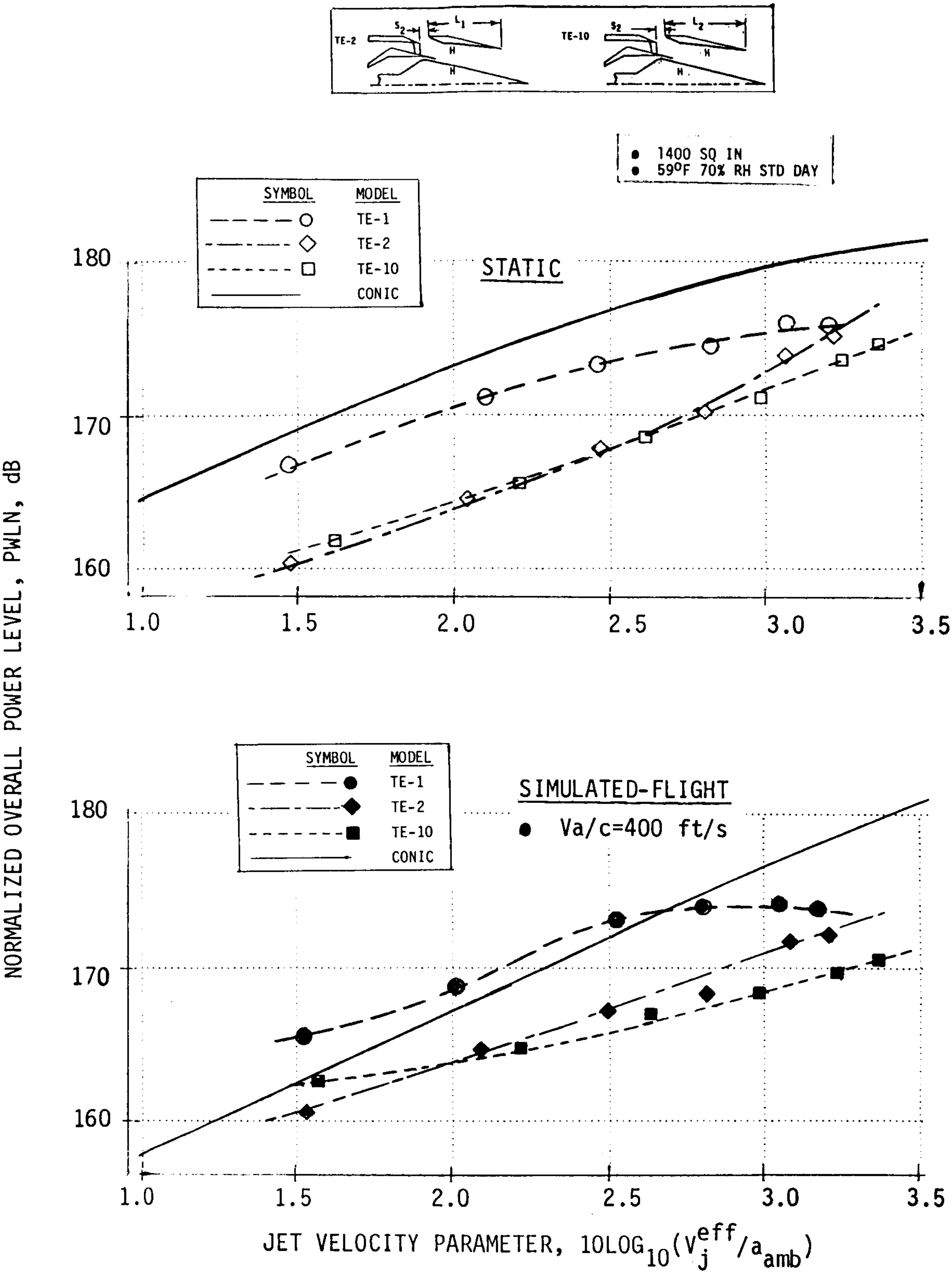

FIGURE 4-115. NORMALIZED PWL AS A FUNCTION OF JET VELOCITY PARAMETER FOR COMPARISON OF EJECTOR LENGTH VARIATION, HARDWALL EJECTOR/PLUG, TE-2 VERSUS TE-10, STATIC AND SIMULATED-FLIGHT

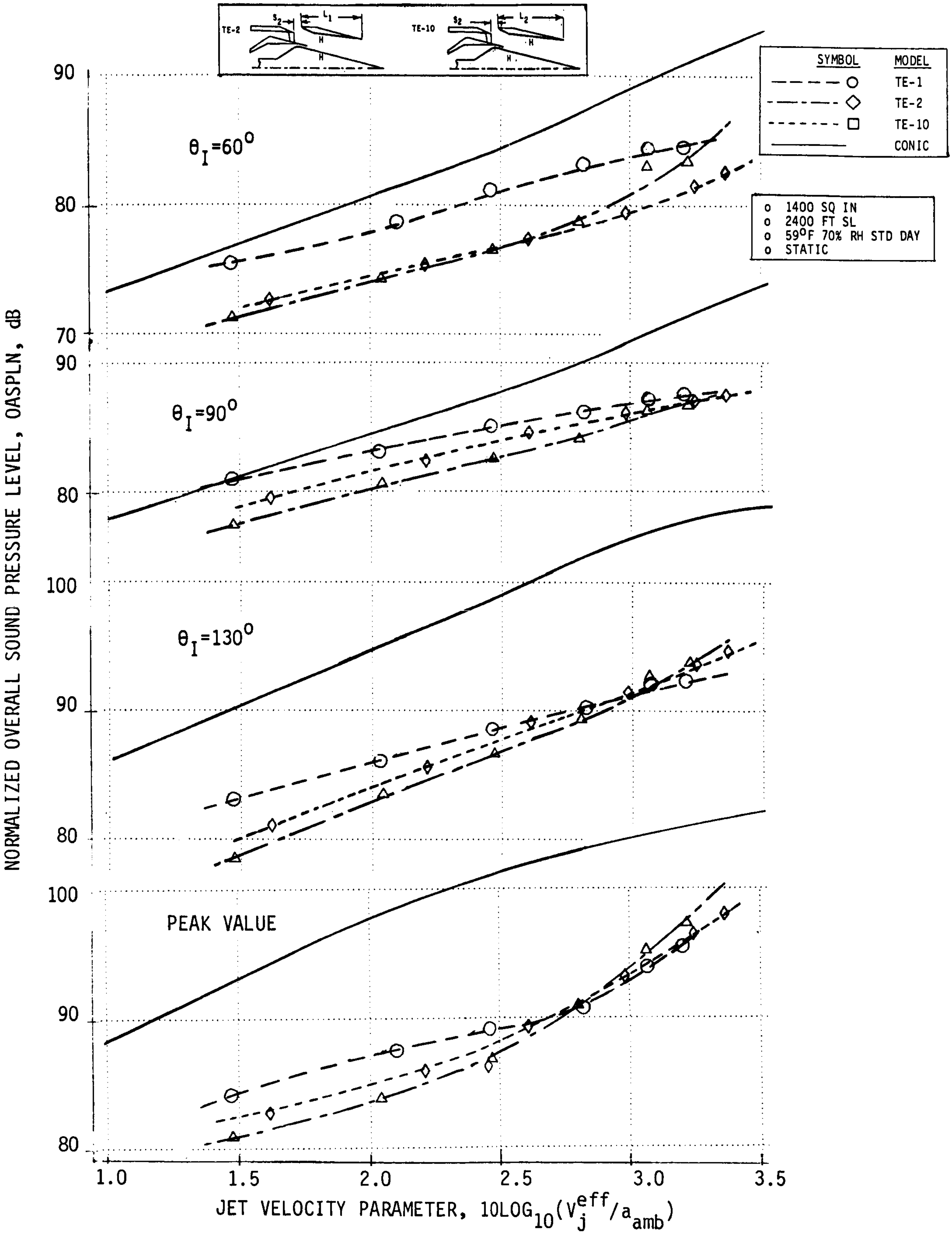

FIGURE 4-116. NORMALIZED OASPL AS A FUNCTION OF JET VELOCITY PARAMETER FOR COMPARISON OF EJECTOR LENGTH VARIATION, HARDWALL EJECTOR/PLUG, TE-2 VERSUS TE-10, STATIC, AT θ_I = 60°, 90°, 130° AND PEAK VALUE

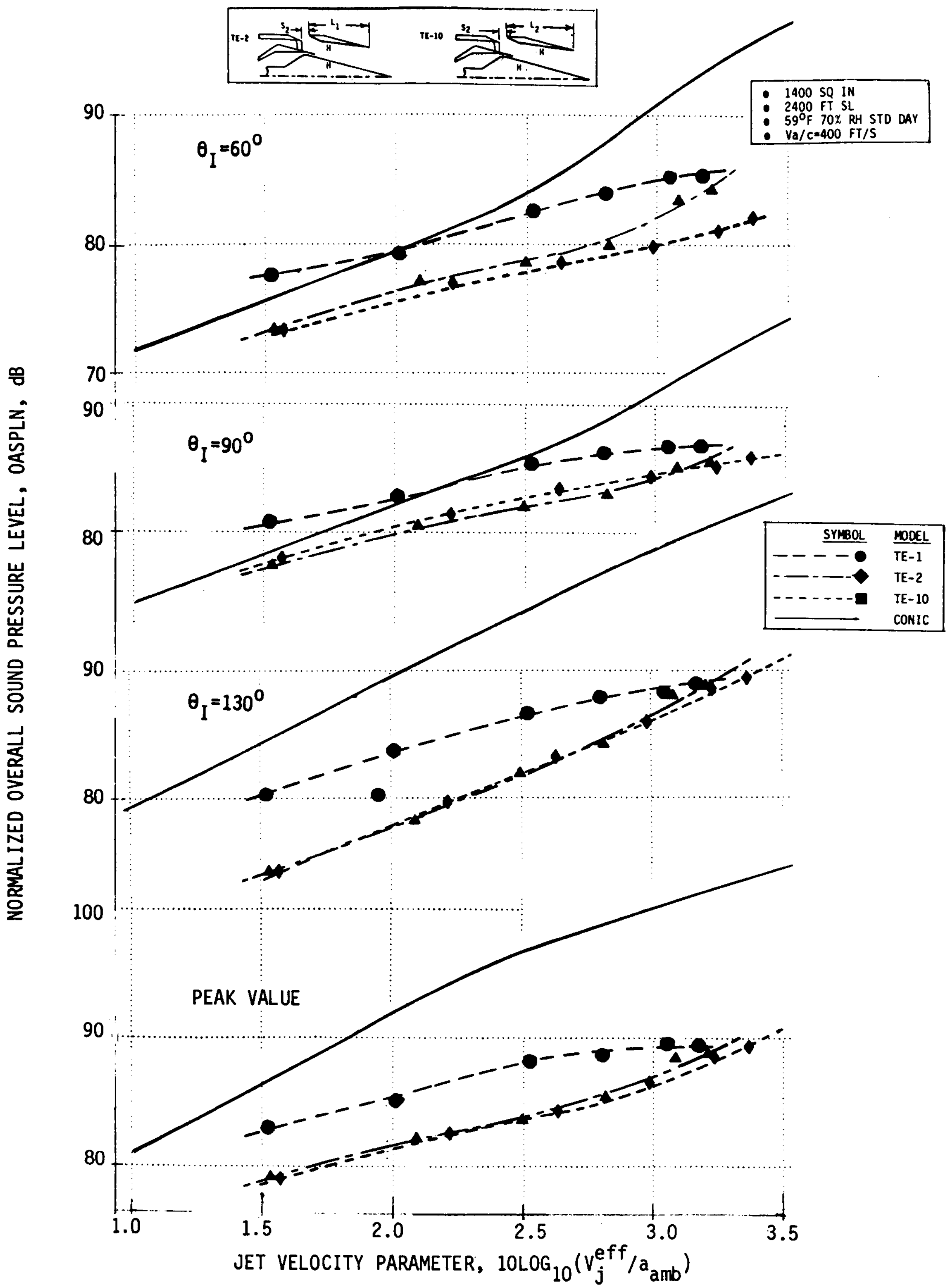

FIGURE 4-117. NORMALIZED OASPL AS A FUNCTION OF JET VELOCITY PARAMETER FOR COMPARISON OF EJECTOR LENGTH VARIATION, HARDWALL EJECTOR/PLUG, TE-2 VERSUS TE-10, SIMULATED-FLIGHT, AT θ_I = 60°, 90°, 130° AND PEAK VALUE

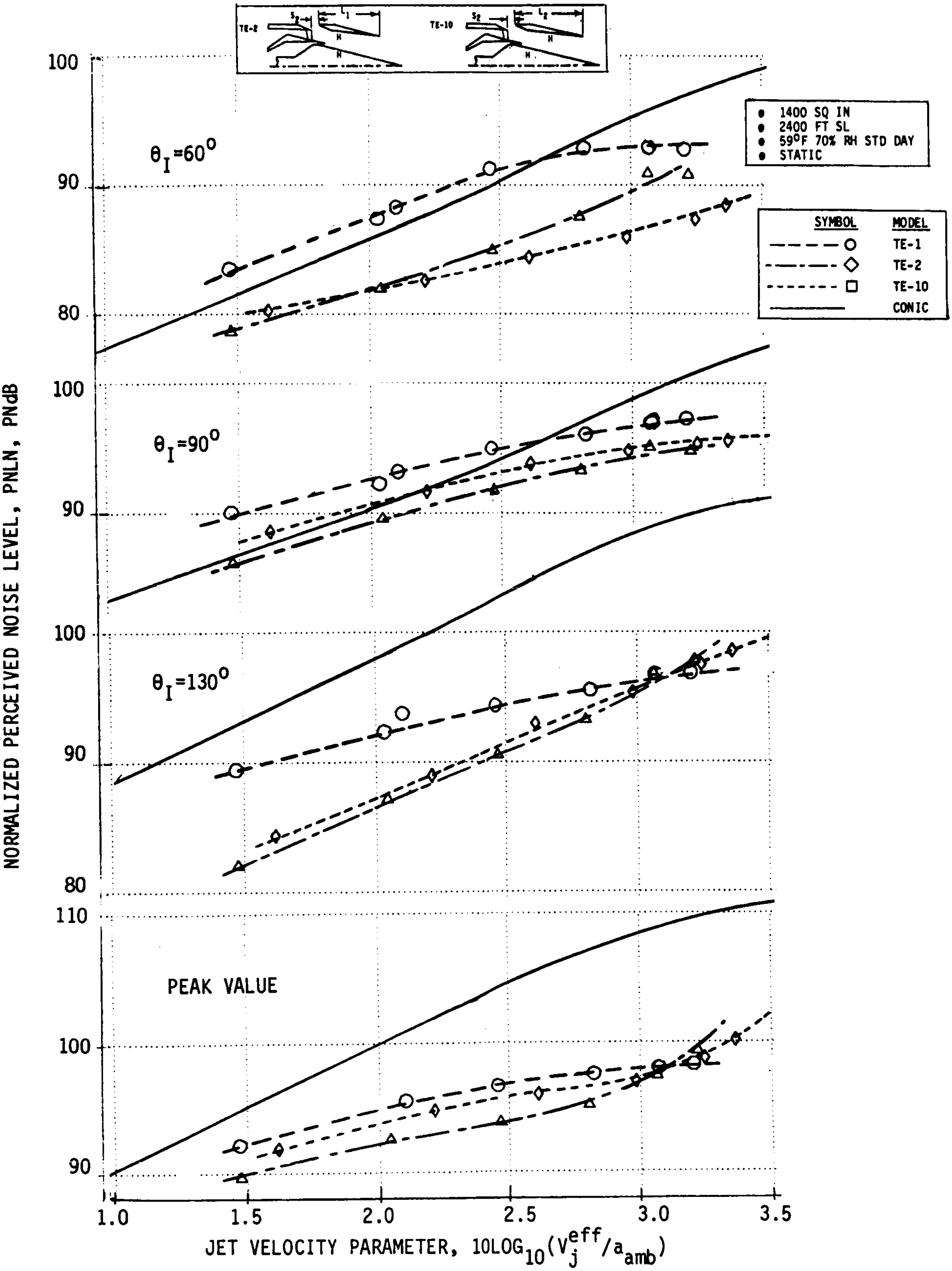

FIGURE 4-118. NORMALIZED PNL AS A FUNCTION OF JET VELOCITY PARAMETER FOR COMPARISON OF EJECTOR LENGTH VARIATION, HARDWALL EJECTOR/PLUG, TE-2 VERSUS TE-10, STATIC, AT θ_I = 60°, 90°, 130° AND PEAK VALUE

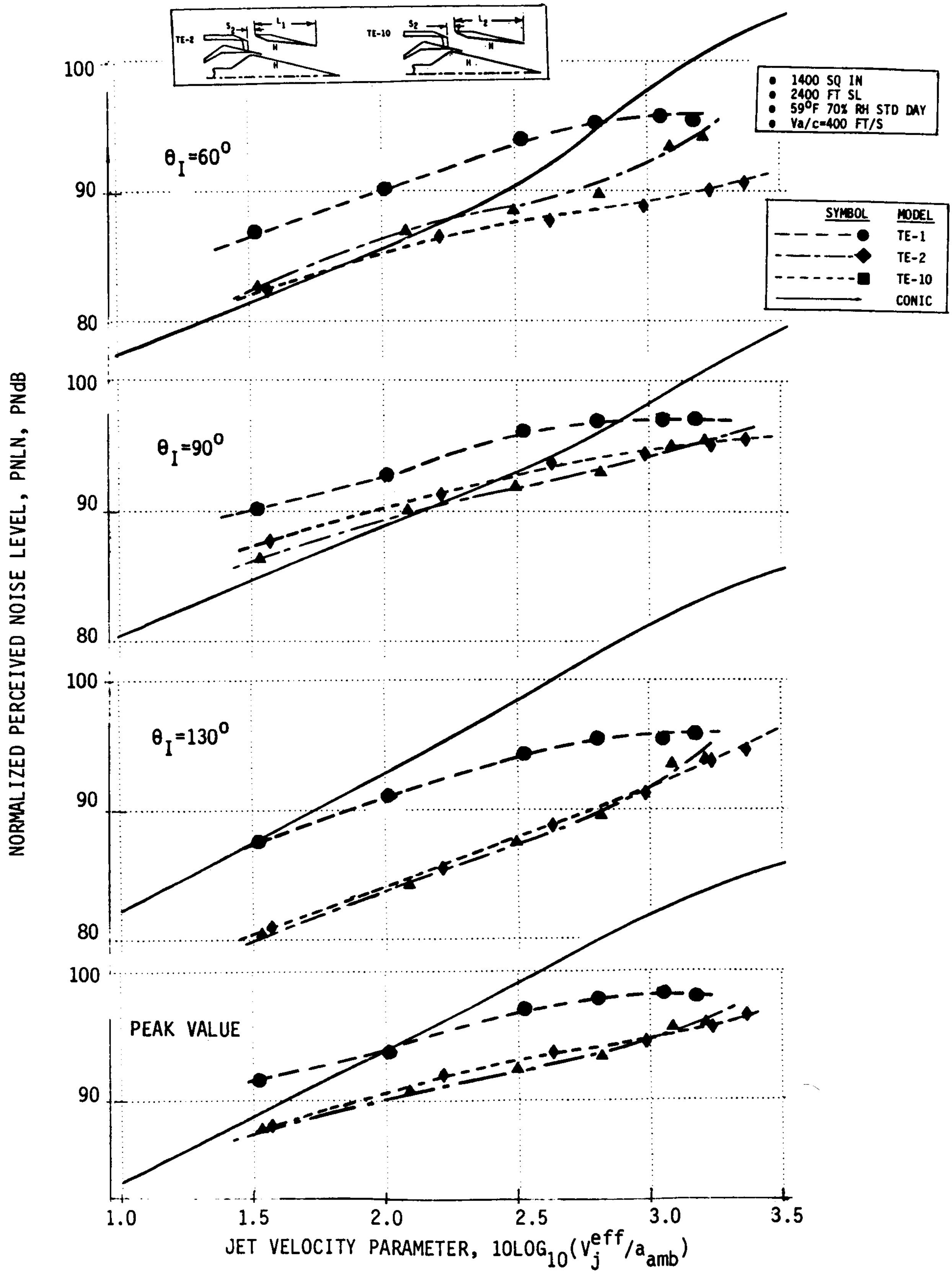

FIGURE 4-119. NORMALIZED PNL AS A FUNCTION OF JET VELOCITY PARAMETER FOR COMPARISON OF EJECTOR LENGTH VARIATION, HARDWALL EJECTOR/PLUG, TE-2 VERSUS TE-10, SIMULATED-FLIGHT, AT Θ_I = 60°, 90°, 130° AND PEAK VALUE

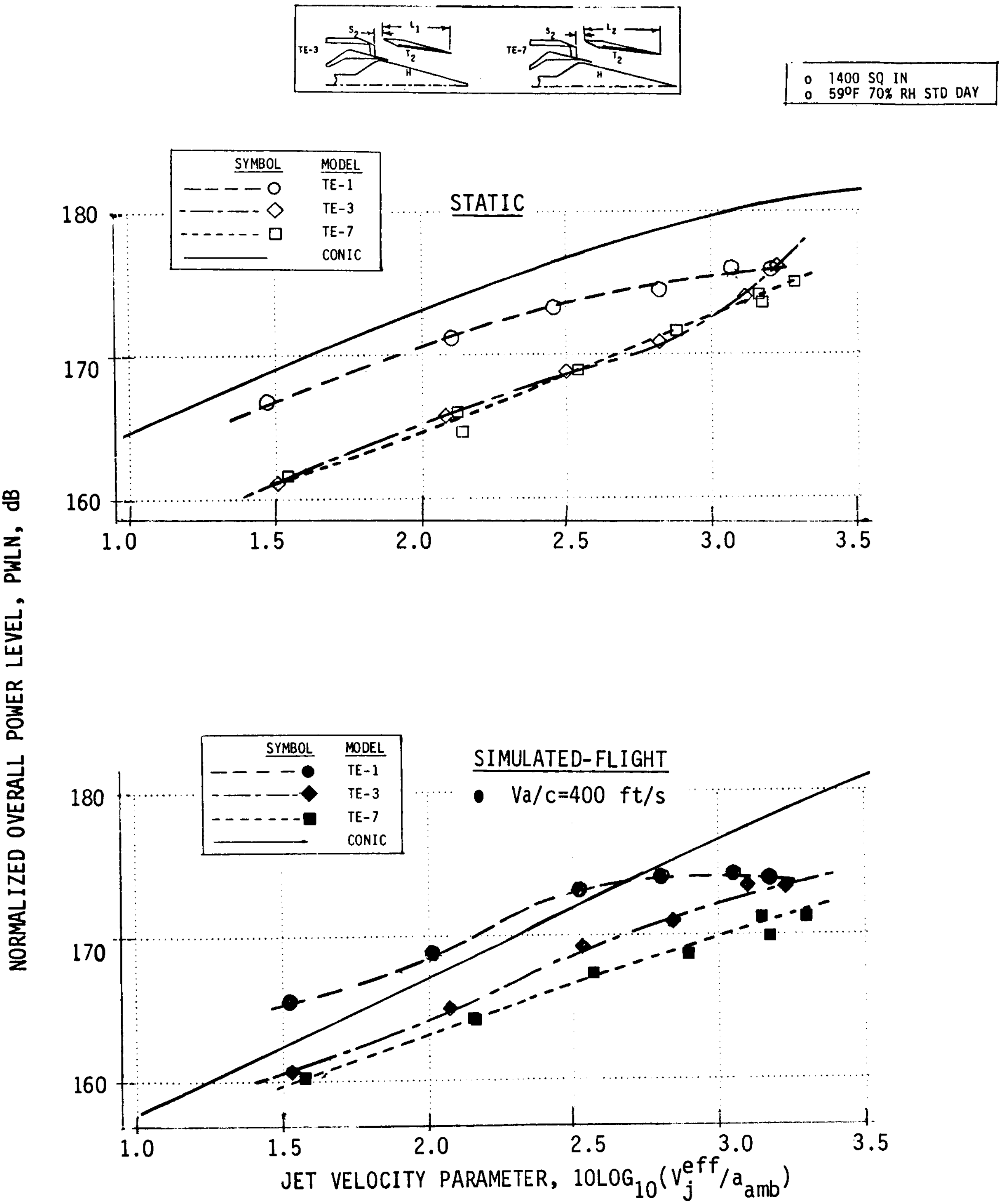

FIGURE 4-120. NORMALIZED PWL AS A FUNCTION OF JET VELOCITY PARAMETER FOR COMPARISON OF EJECTOR LENGTH VARIATION, TREATED EJECTOR, TE-3 VERSUS TE-7, STATIC AND SIMULATED-FLIGHT

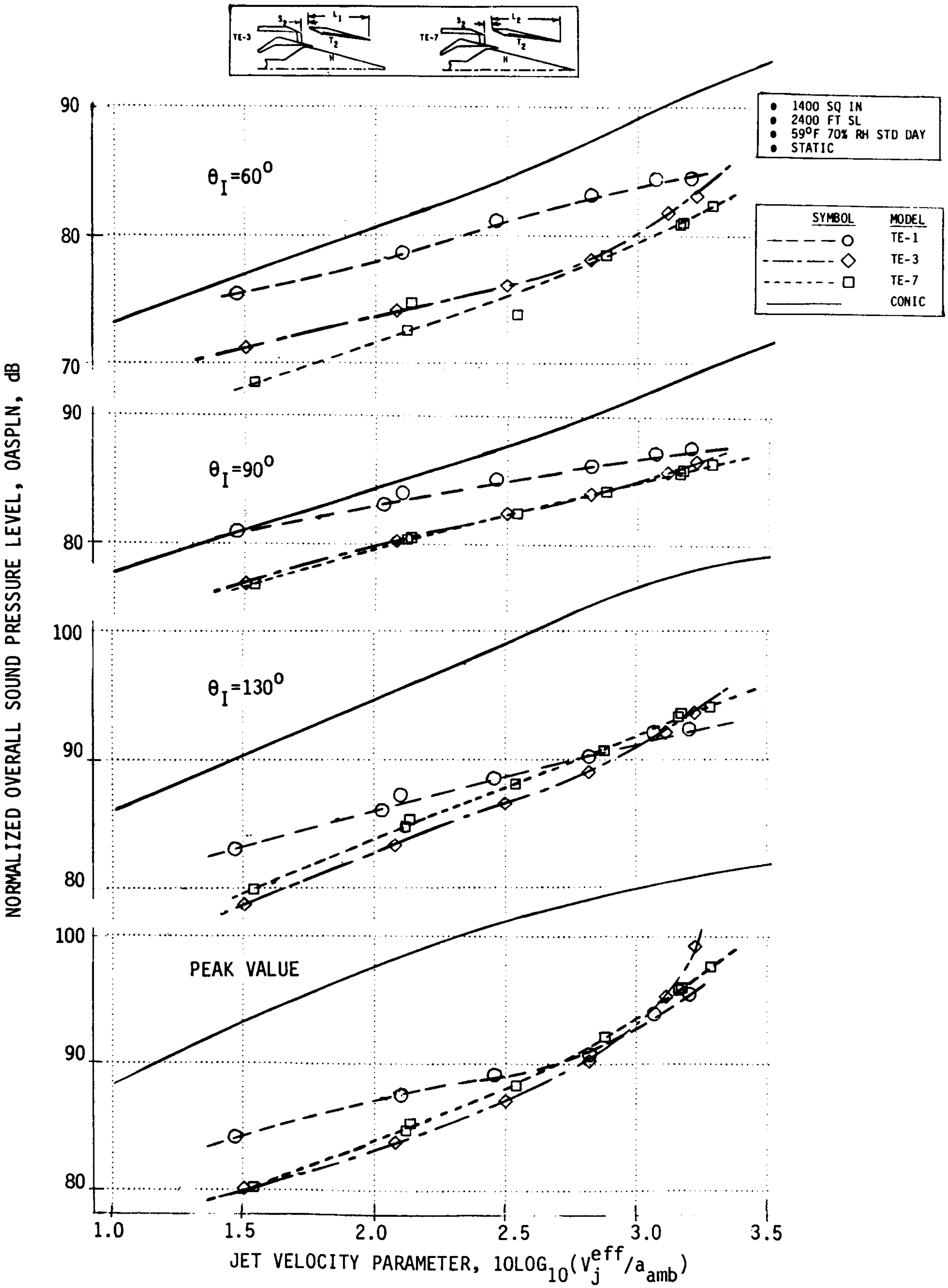

FIGURE 4-121. NORMALIZED OASPL AS A FUNCTION OF JET VELOCITY PARAMETER FOR COMPARISON OF EJECTOR LENGTH VARIATION, TREATED EJECTOR, TE-3 VERSUS TE-7, STATIC, AT Θ_I = 60°, 90°, 130° AND PEAK VALUE

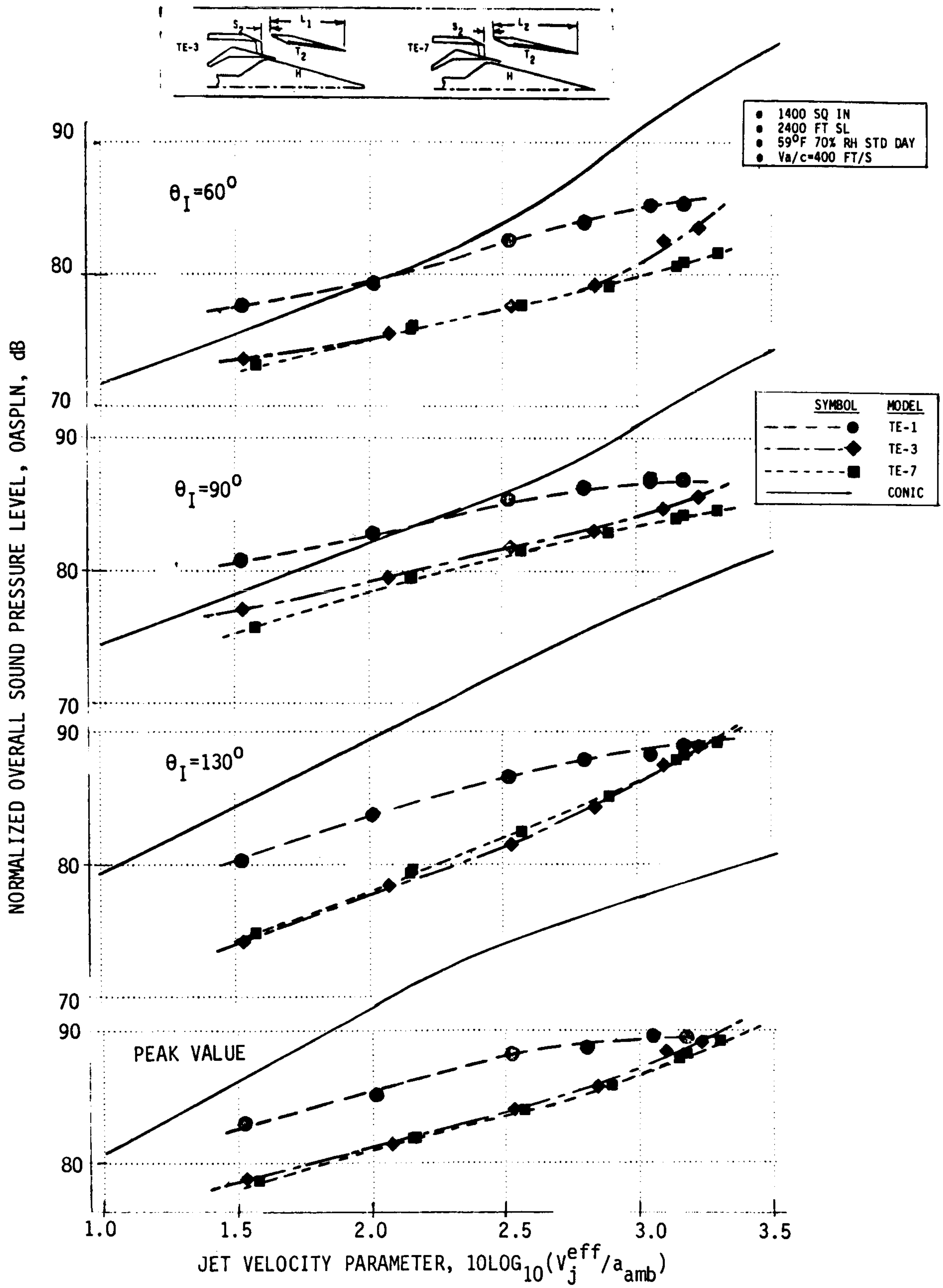

FIGURE 4-122. NORMALIZED OASPL AS A FUNCTION OF JET VELOCITY PARAMETER FOR COMPARISON OF EJECTOR LENGTH VARIATION, TREATED EJECTOR, TE-3 VERSUS TE-7, SIMULATED-FLIGHT, AT Θ_I = 60o, 90o, 130o AND PEAK VALUE

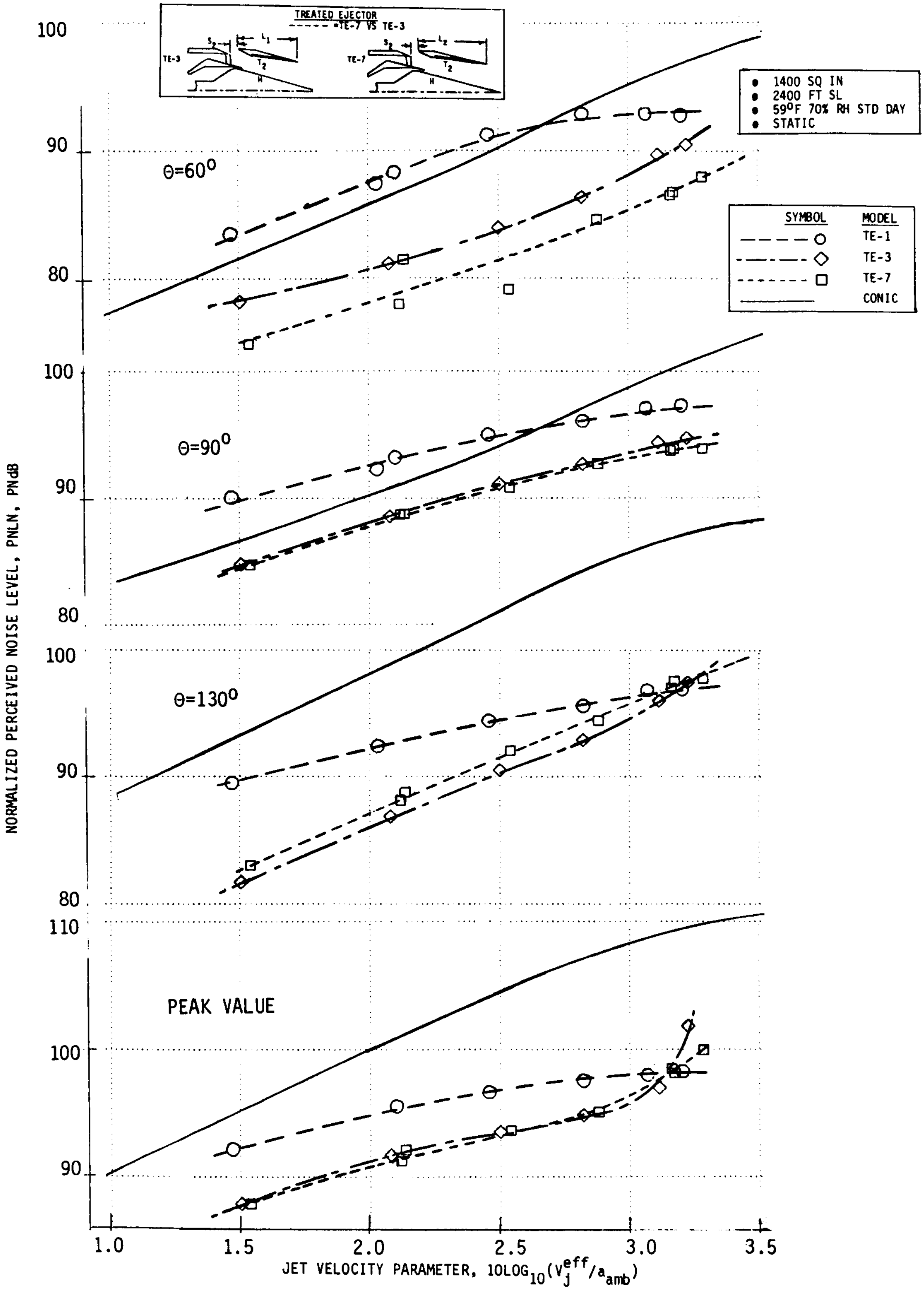

FIGURE 4-123. NORMALIZED PNL AS A FUNCTION OF JET VELOCITY PARAMETER FOR COMPARISON OF EJECTOR LENGTH VARIATION, TREATED EJECTOR, TE-3 VERSUS TE-7, STATIC, AT Θ_I = 60°, 90°, 130° AND PEAK VALUE

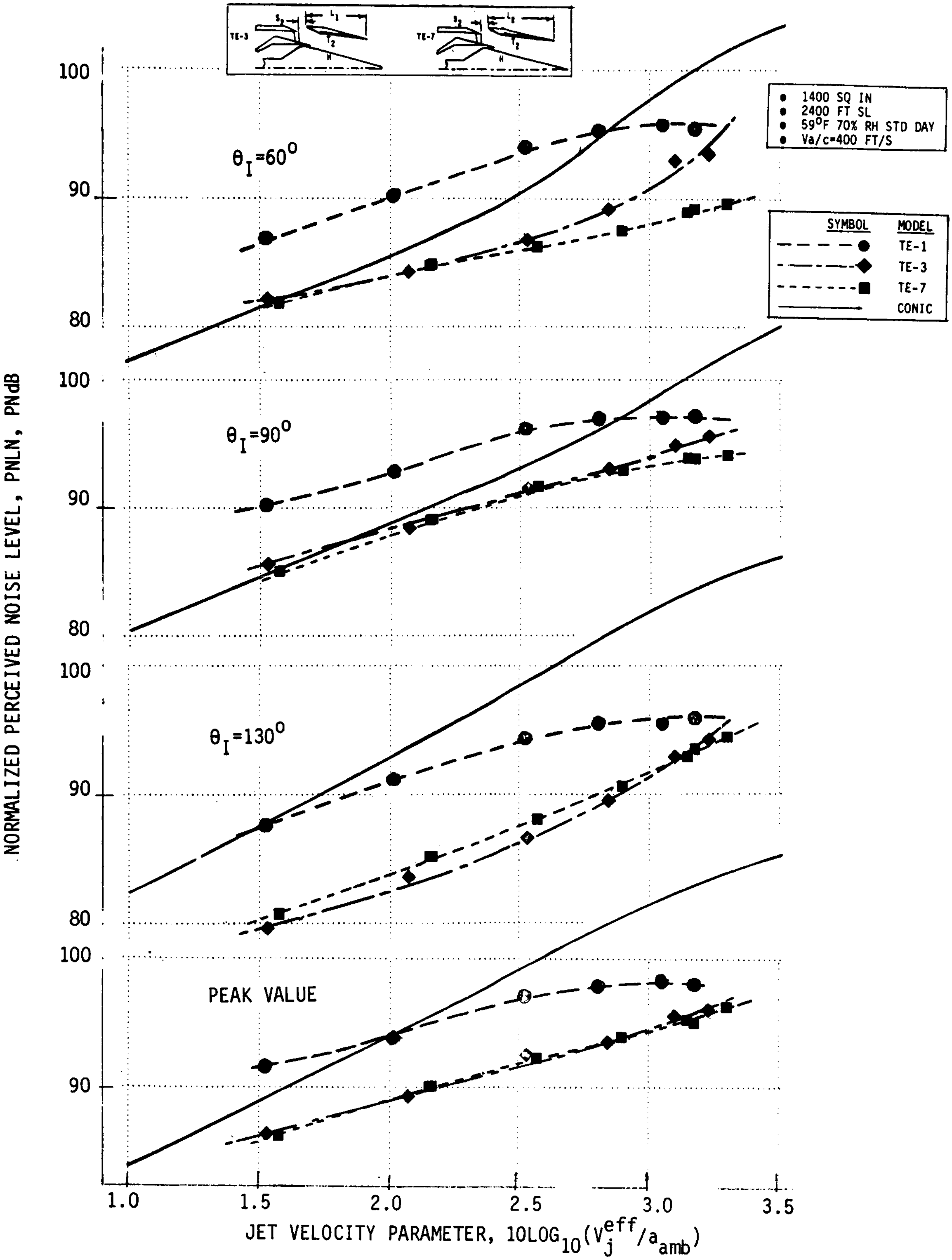

FIGURE 4-124. NORMALIZED PNL AS A FUNCTION OF JET VELOCITY PARAMETER FOR COMPARISON OF EJECTOR LENGTH VARIATION, TREATED EJECTOR, TE-3 VERSUS TE-7, SIMULATED-FLIGHT, AT Θ_I = 60°, 90°, 130° AND PEAK VALUE

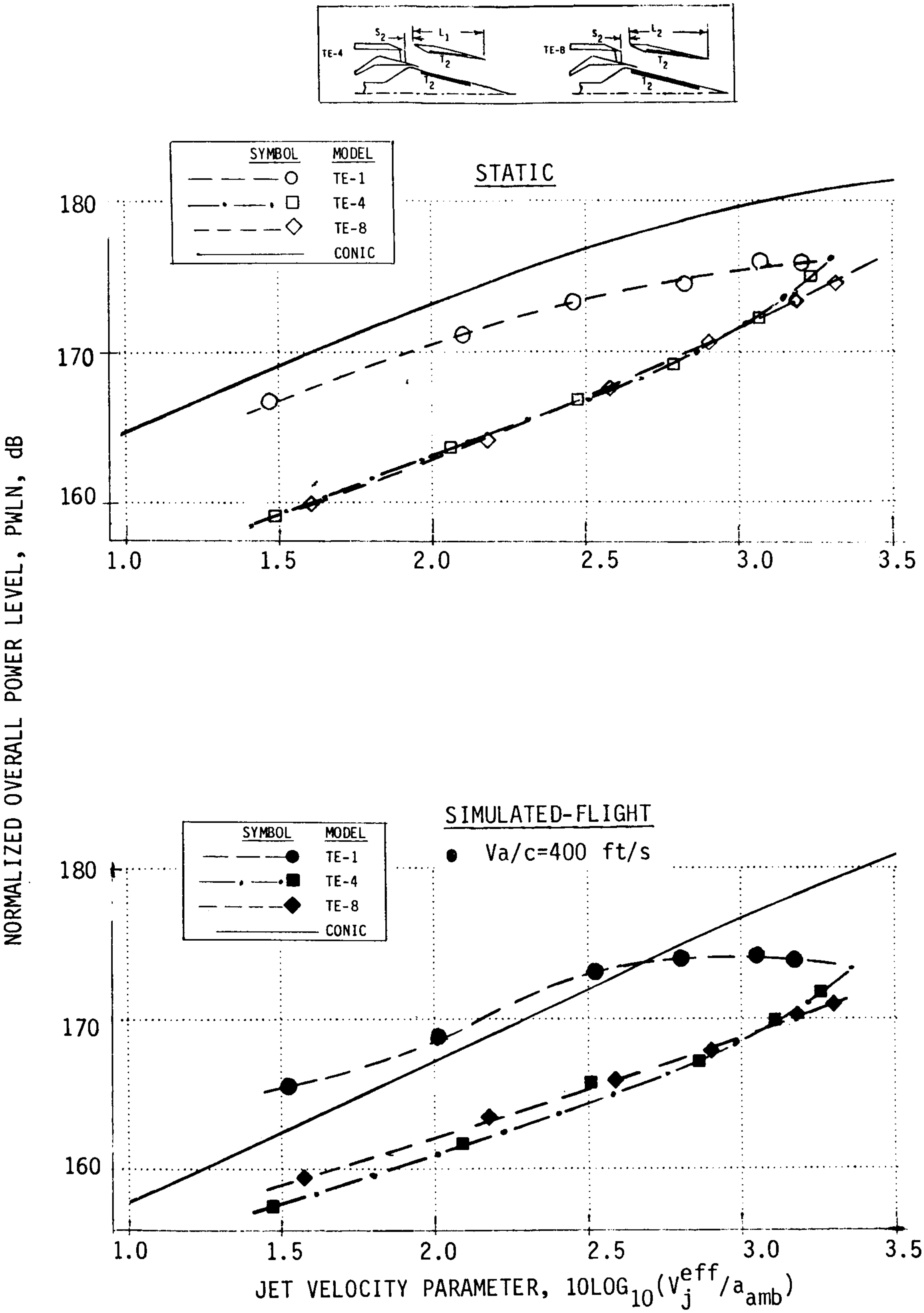

FIGURE 4-125. NORMALIZED PWL AS A FUNCTION OF JET VELOCITY PARAMETER FOR COMPARISON OF EJECTOR LENGTH VARIATION, TREATED EJECTOR/PLUG, TE-4 VERSUS TE-8, STATIC AND SIMULATED-FLIGHT

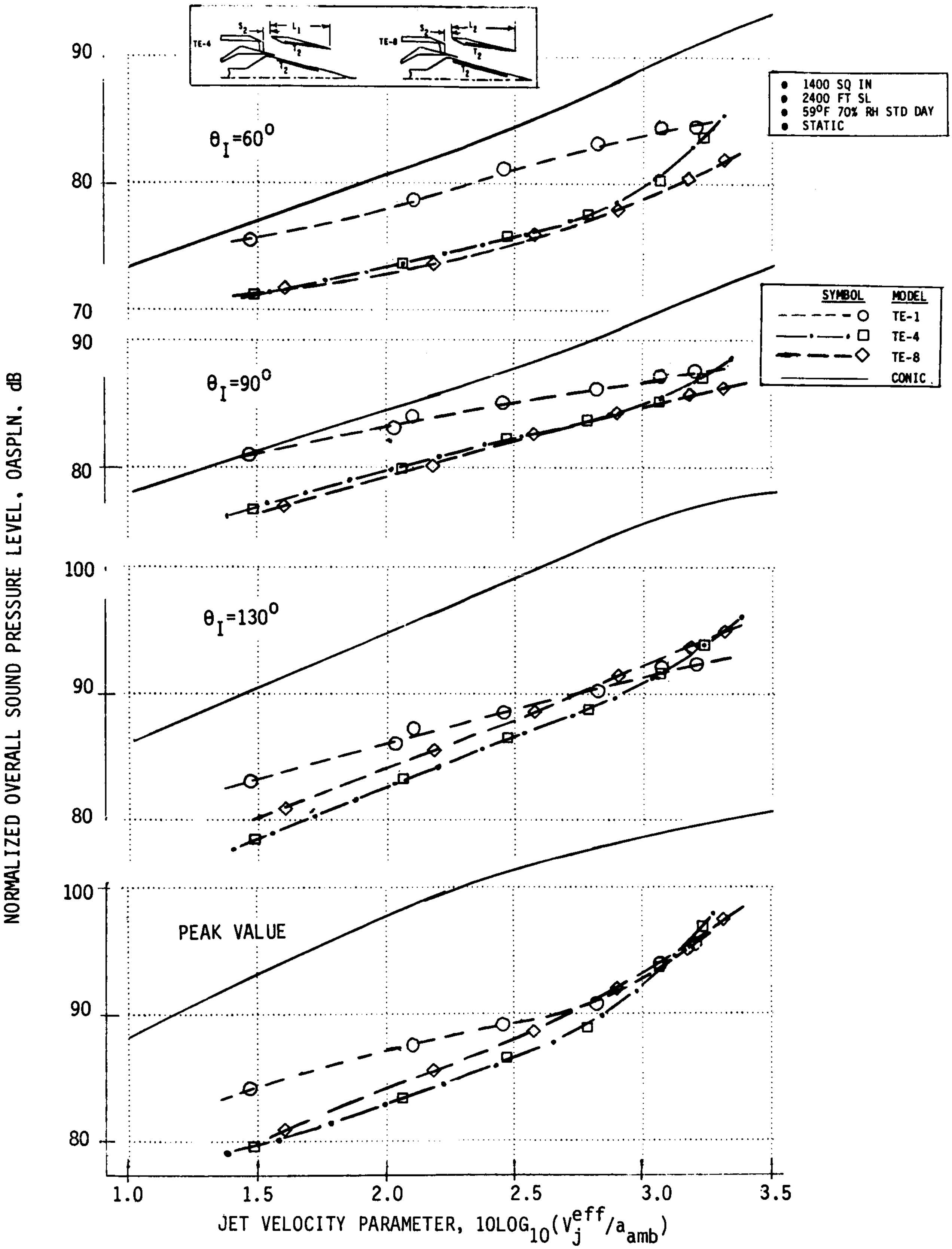

FIGURE 4-126. NORMALIZED OASPL AS A FUNCTION OF JET VELOCITY PARAMETER FOR COMPARISON OF EJECTOR LENGTH VARIATION, TREATED EJECTOR/PLUG, TE-4 VERSUS TE-8, STATIC, AT θ_I = 60°, 90°, 130° AND PEAK VALUE

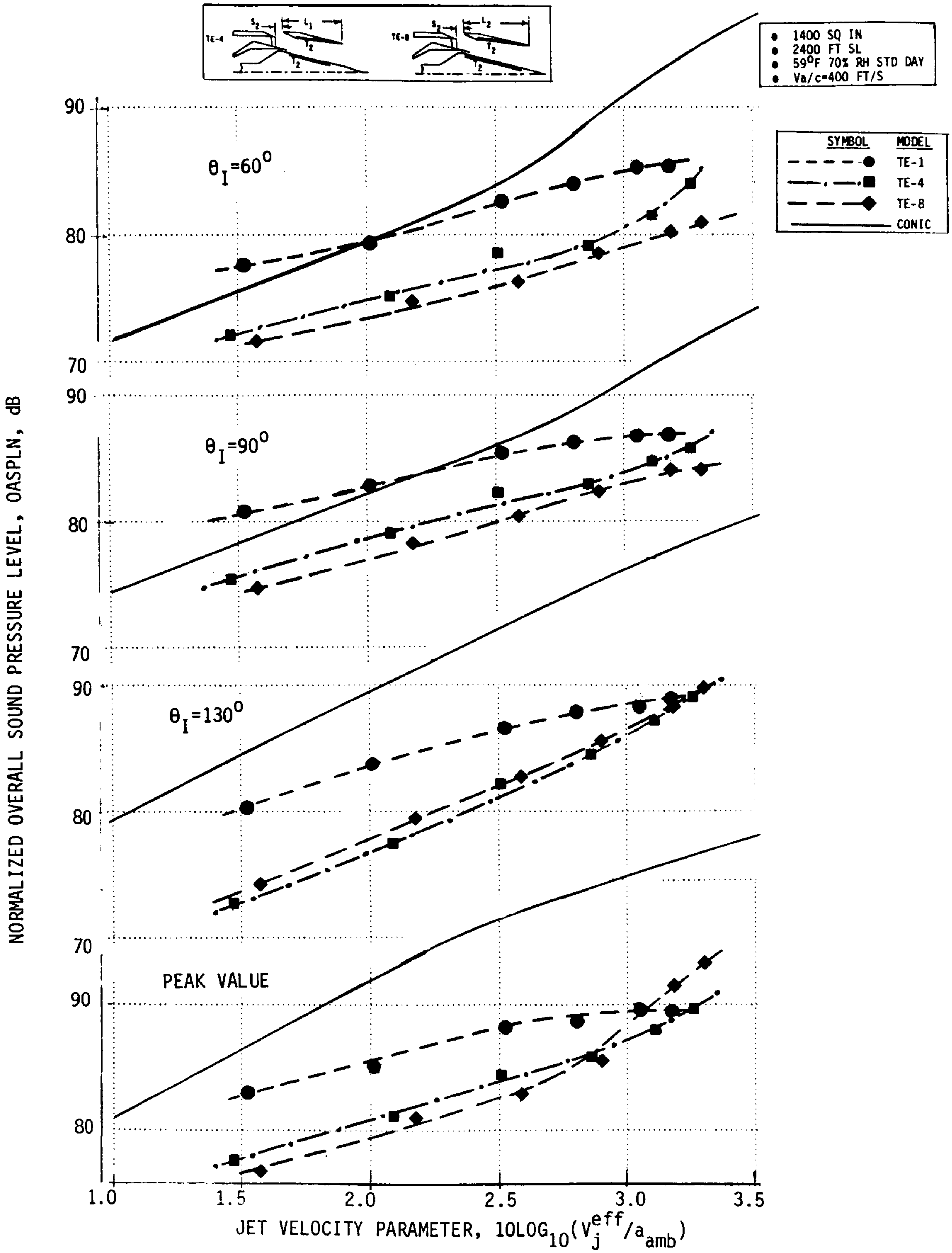

FIGURE 4-127 NORMALIZED OASPL AS A FUNCTION OF JET VELOCITY PARAMETER FOR COMPARISON OF EJECTOR LENGTH VARIATION, TREATED EJECTOR/PLUG, TE-4 VERSUS TE-8, SIMULATED-FLIGHT, AT Θ_I = 60°, 90°, 130° AND PEAK VALUE

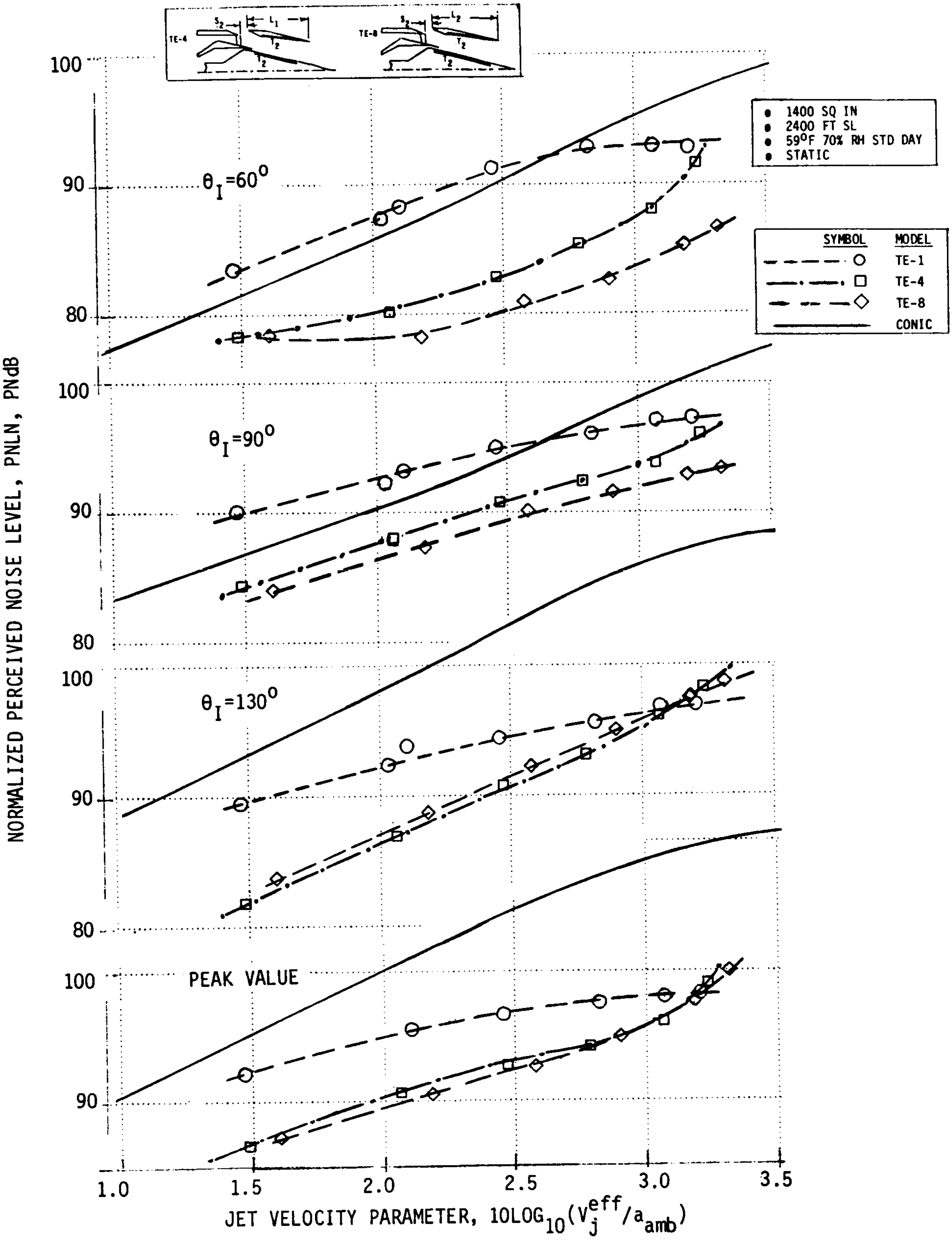

FIGURE 4-128. NORMALIZED PNL AS A FUNCTION OF JET VELOCITY PARAMETER FOR COMPARISON OF EJECTOR LENGTH VARIATION, TREATED EJECTOR/PLUG, TE-4 VERSUS TE-8, STATIC, AT Θ_I = 60°, 90°, 130° AND PEAK VALUE

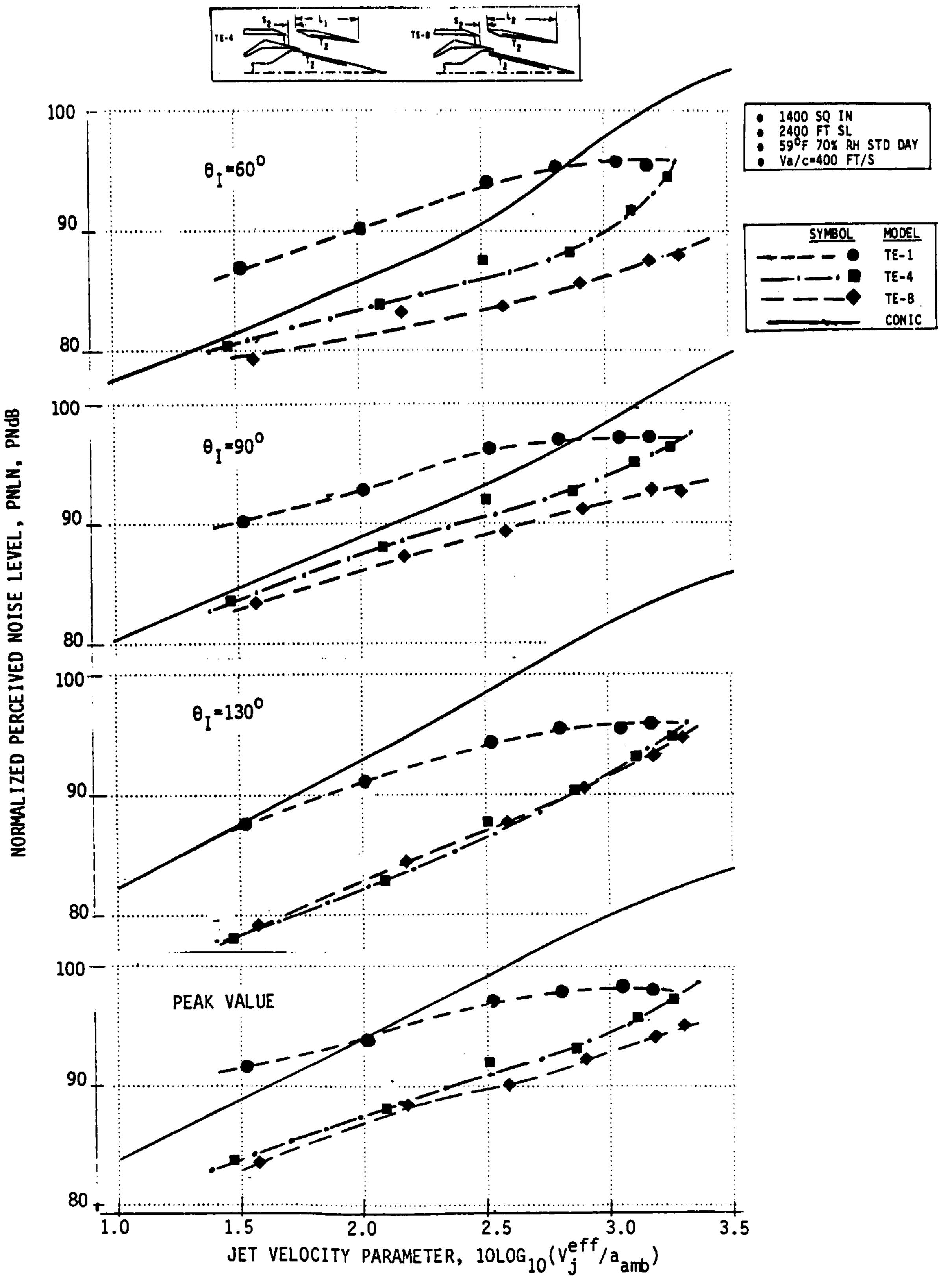

FIGURE 4-129. NORMALIZED PNL AS A FUNCTION OF JET VELOCITY PARAMETER FOR COMPARISON OF EJECTOR LENGTH VARIATION, TREATED EJECTOR/PLUG, TE-4 VERSUS TE-8, SIMULATED-FLIGHT, AT θ_I = 60°, 90°, 130° AND PEAK VALUE

4.5.3 Diagnostic Data Review

Representative comparisons of jet plume characteristics for nominal, L1, and extended length, L2, ejectors are available from laser velocimeter plume measurements at takeoff cycle for Configurations TE-4 and TE-8. Normalized mean velocity data are presented for static data points 4009 and 8009 as follows:

- Figure 4-130: Axial traverses at centerline, 1.54"R, 3.07"R and 4.22"R.

- Figure 4-131: Radial traverses at various locations aft of the ejector exit, starting at 1/8" aft and progressing to X/Deq = 10.0.

For the simulated-flight data points 4010 and 8010, similar comparisons to those of the static are presented in Figures 4-132 and 4-133.

In reviewing the plume measurements, the following are noted:

- Just aft of the ejector exit planes, at X/Deq = 1.6 for TE-4 and 1.96 for TE-8, the mean velocity is somewhat higher in the peak velocity zones for the shorter TE-4 ejector configuration. This is due to the closer proximity of the measurement plane to the exit plane and, therefore, the shorter decay distance for the TE-4 plume.

- From the plug tip and aft, the TE-8 mean velocity levels are always slightly higher. This is felt contributes to the increased low and mid-frequency noise levels observed in the three length comparison sets of Figures 4-112, 4-113 and 4-114. The longer region of turbulent mixing zone produces a higher content of mid-to-low frequency noise.

- Distributions of mean velocity at any radial cross section are fairly similar for the two ejector lengths, however, the longer ejector tends to wash out identity of the inner nozzle stream sooner than for the short ejector. This is expected attributable to the longer length of forced high speed jet flow toward the center of the jet causing faster outer/inner stream mixing.

As an indication of relative aerodynamic performance changes due to ejector length variation, thrust loss due to base drag for the length comparison model sets, i.e., TE-2 versus TE-10, TE-3 versus TE-7, and TE-4 versus TE-8 are presented in Figures 4-134, 4-135 and 4-136, respectively. Static and simulated-flight values are provided for each. Review suggests:

- Performance of the short and long ejector sets are compatible within themselves, i.e., TE-2 = TE-3 = TE-4 and TE-10 = TE-7 = TE-8. This would be expected as the thrust loss calculated is due to chute base drag and changes in treatment application are not anticipated to effect pumping/ventilating characteristics.

- In each comparison, the simulated-flight thrust loss is lower than the static by a slight amount, indicating forward motion with an ejector still allows enhanced pumping/ventilation capability and the chute base areas are better ventilated. This is exactly opposite to non-ejected systems where forward velocity prohibits easy turning of the externally flowing media and causes poorer ventilation/lower base pressure and subsequently higher base drag.

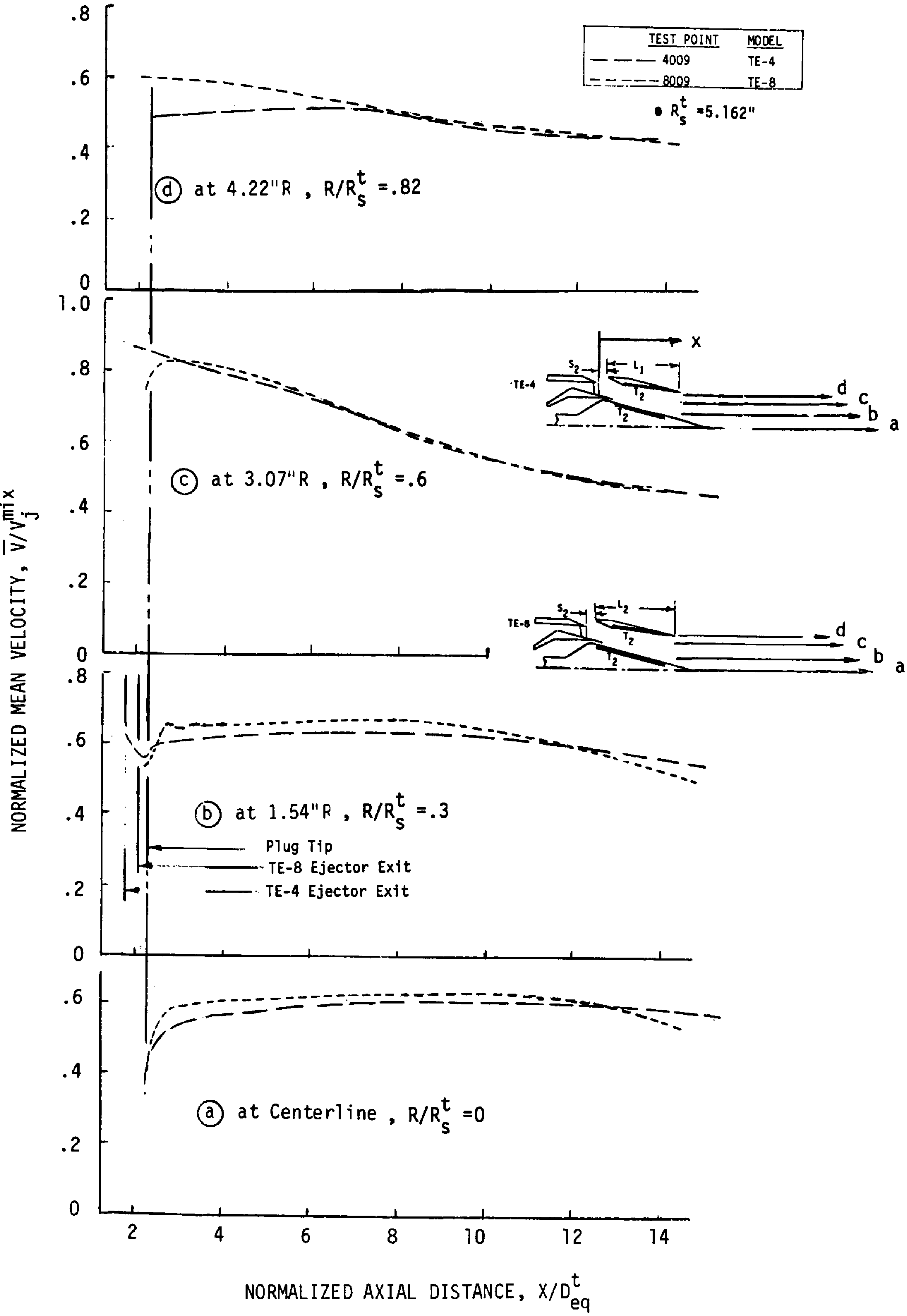

FIGURE 4-130. AXIAL VARIATION OF THE MEAN VELOCITY (AXIAL COMPONENT) IN THE PLUME OF CONFIGURATIONS TE-4 AND TE-8 AT TAKEOFF CONDITION, STATIC, TEST POINTS 4009 AND 8009

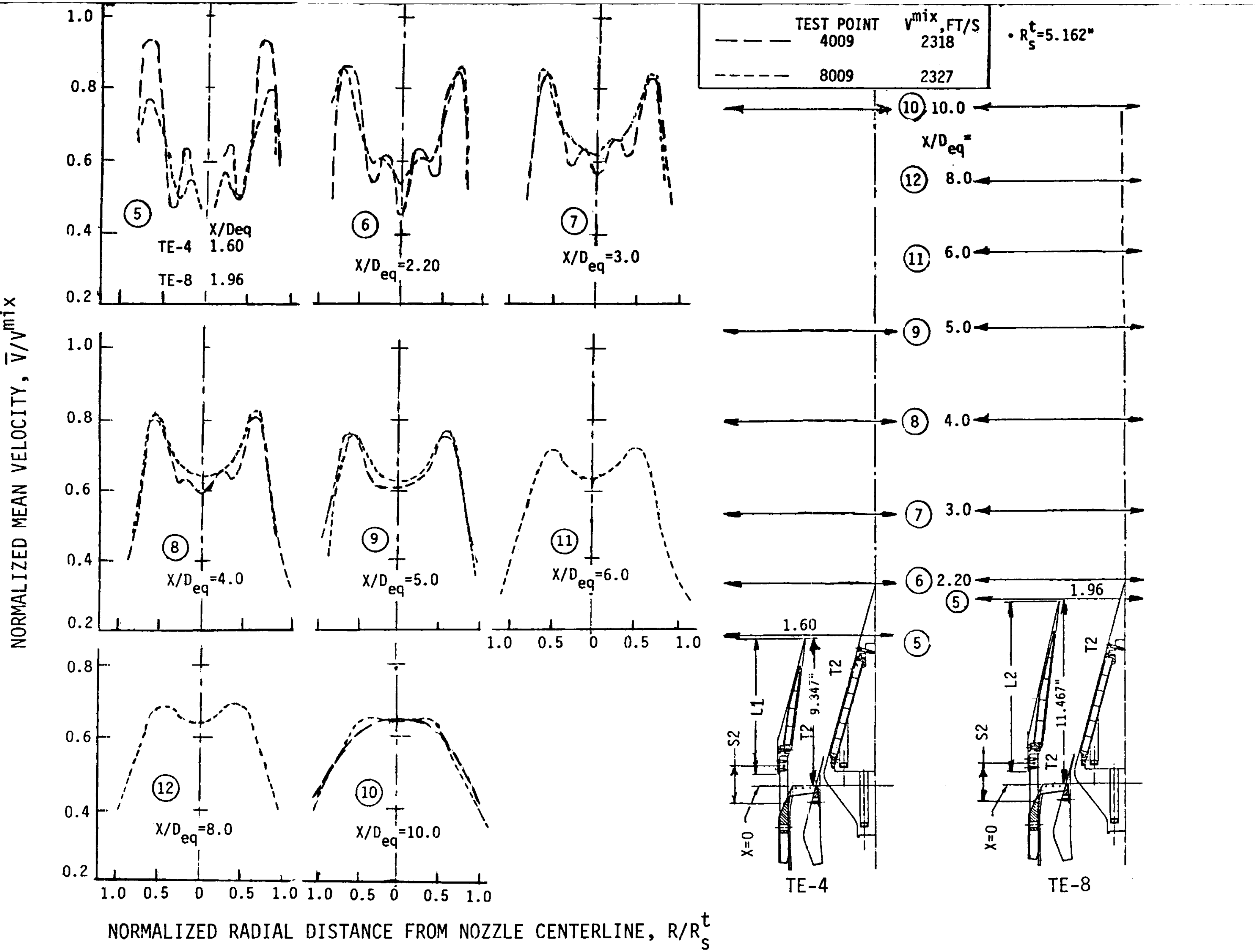

FIGURE 4-131. RADIAL VARIATION OF THE MEAN VELOCITY (AXIAL COMPONENT) IN THE PLUME OF CONFIGURATIONS TE-4 AND TE-8 AT TAKEOFF CONDITION, STATIC, TEST POINTS 4009 AND 8009

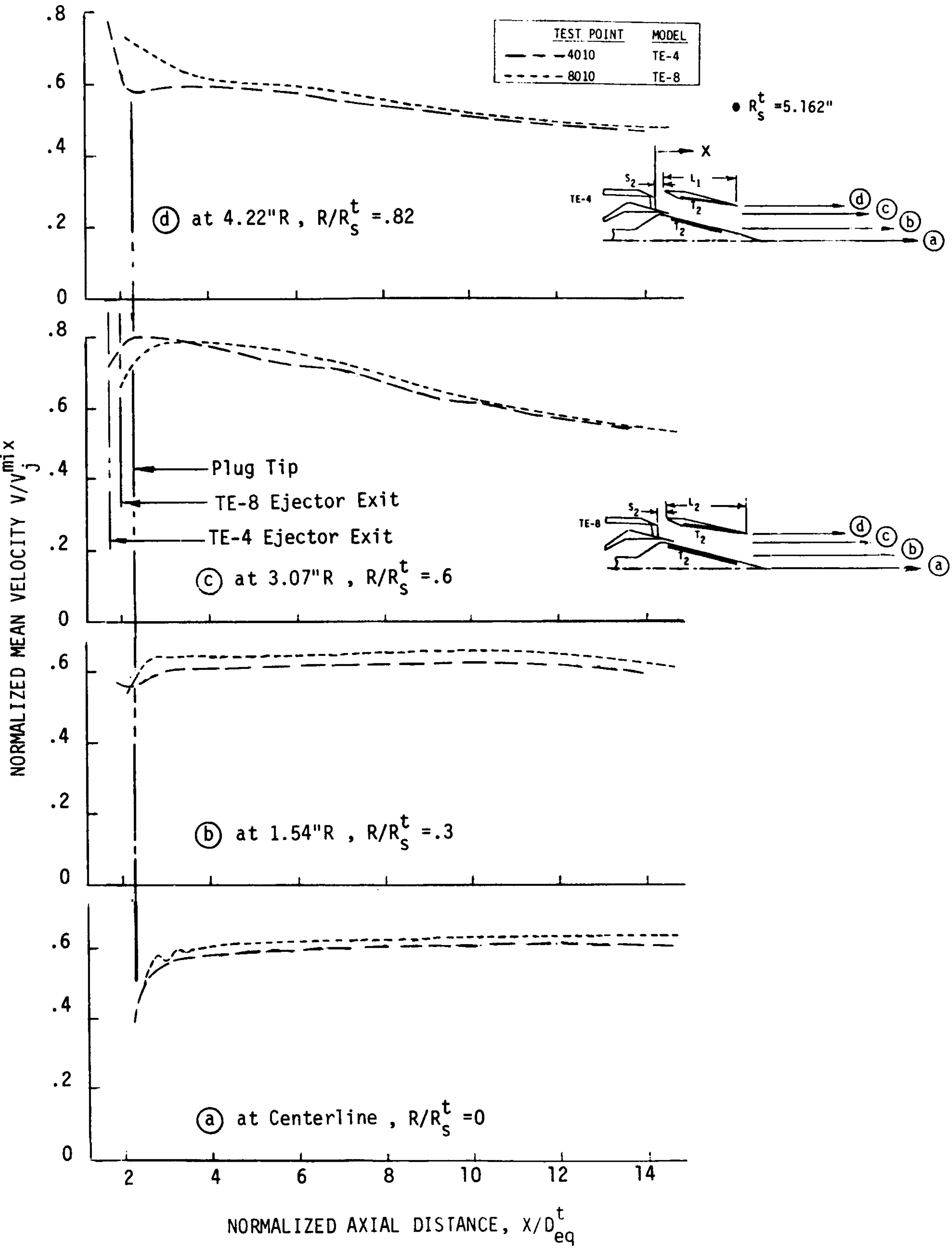

FIGURE 4-132. AXIAL VARIATION OF THE MEAN VELOCITY (AXIAL COMPONENT) IN THE PLUME OF CONFIGURATIONS TE-4 AND TE-8 AT TAKEOFF CONDITION, SIMULATED-FLIGHT, TEST POINTS 4010 AND 8010

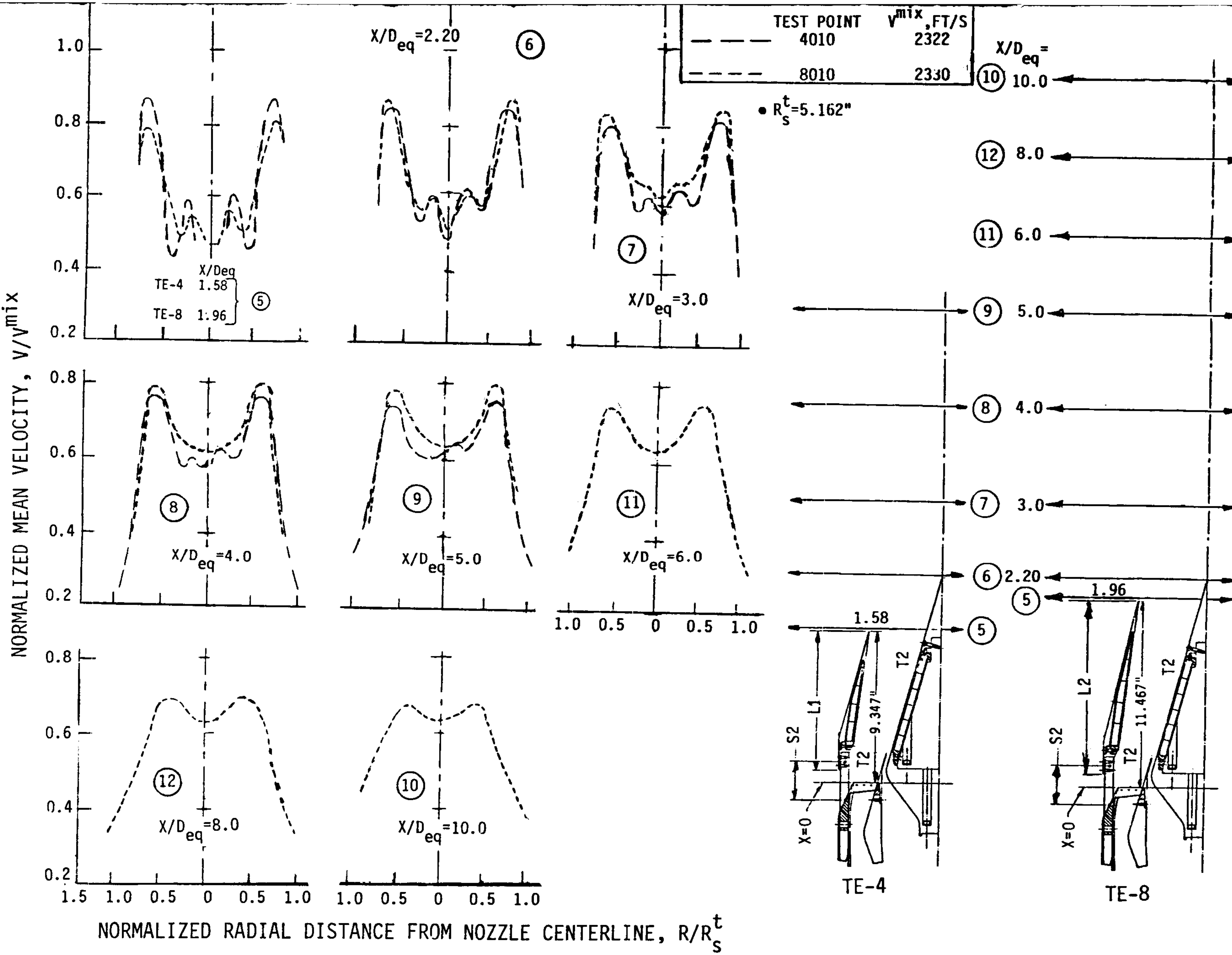

FIGURE 4-133. RADIAL VARIATION OF THE MEAN VELOCITY (AXIAL COMPONENT) IN THE PLUME OF CONFIGURATIONS TE-4 AND TE-8 AT TAKEOFF CONDITION, FLIGHT, TEST POINTS 4010 AND 8010

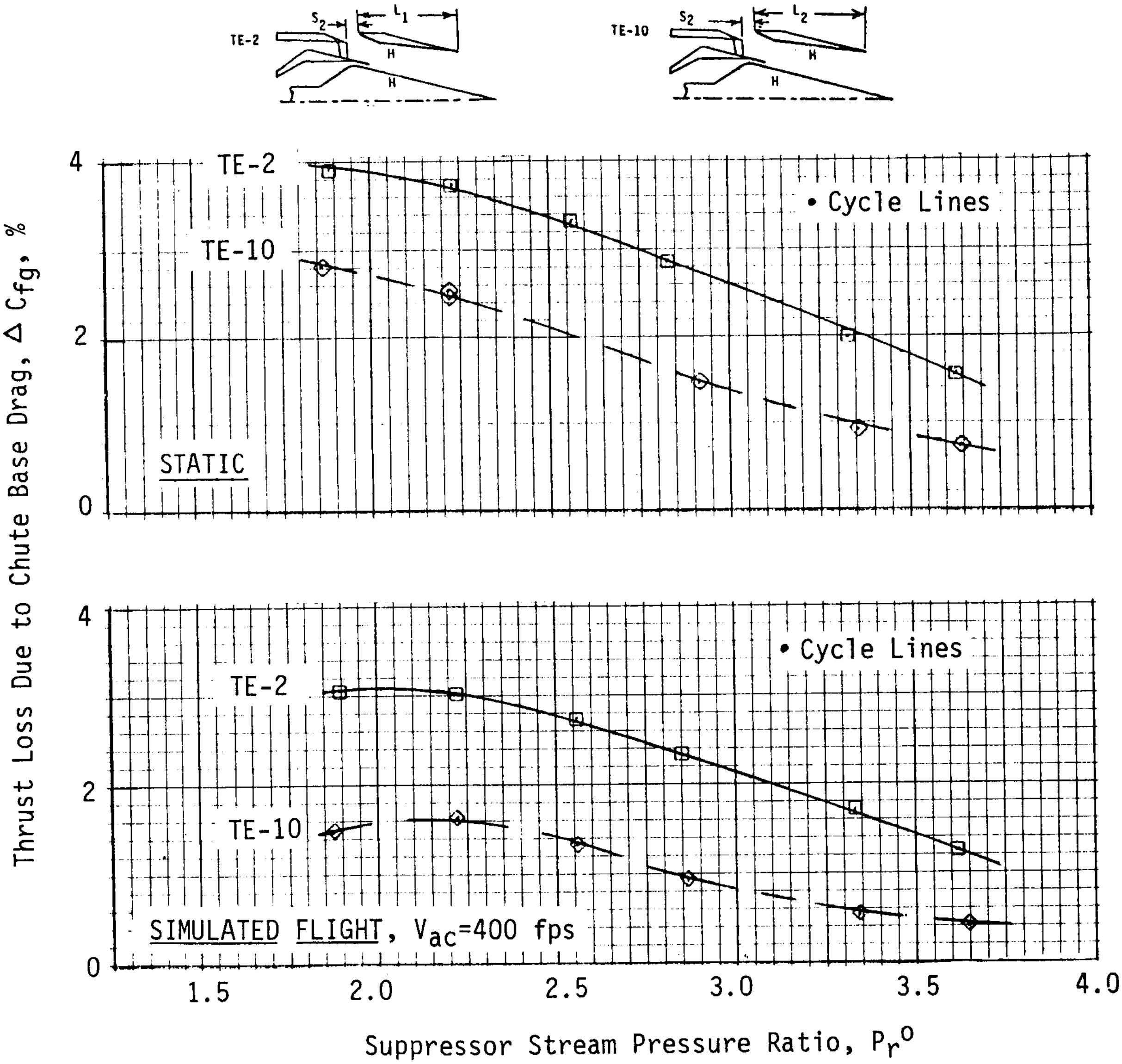

FIGURE 4-134. VARIANCE IN THRUST LOSS COEFFICIENT DUE TO CHUTE BASE DRAG AS A FUNCTION OF EJECTOR LENGTH: TE-2 (L1) VS TE-10 (L2); HARDWALL EJECTOR AND PLUG

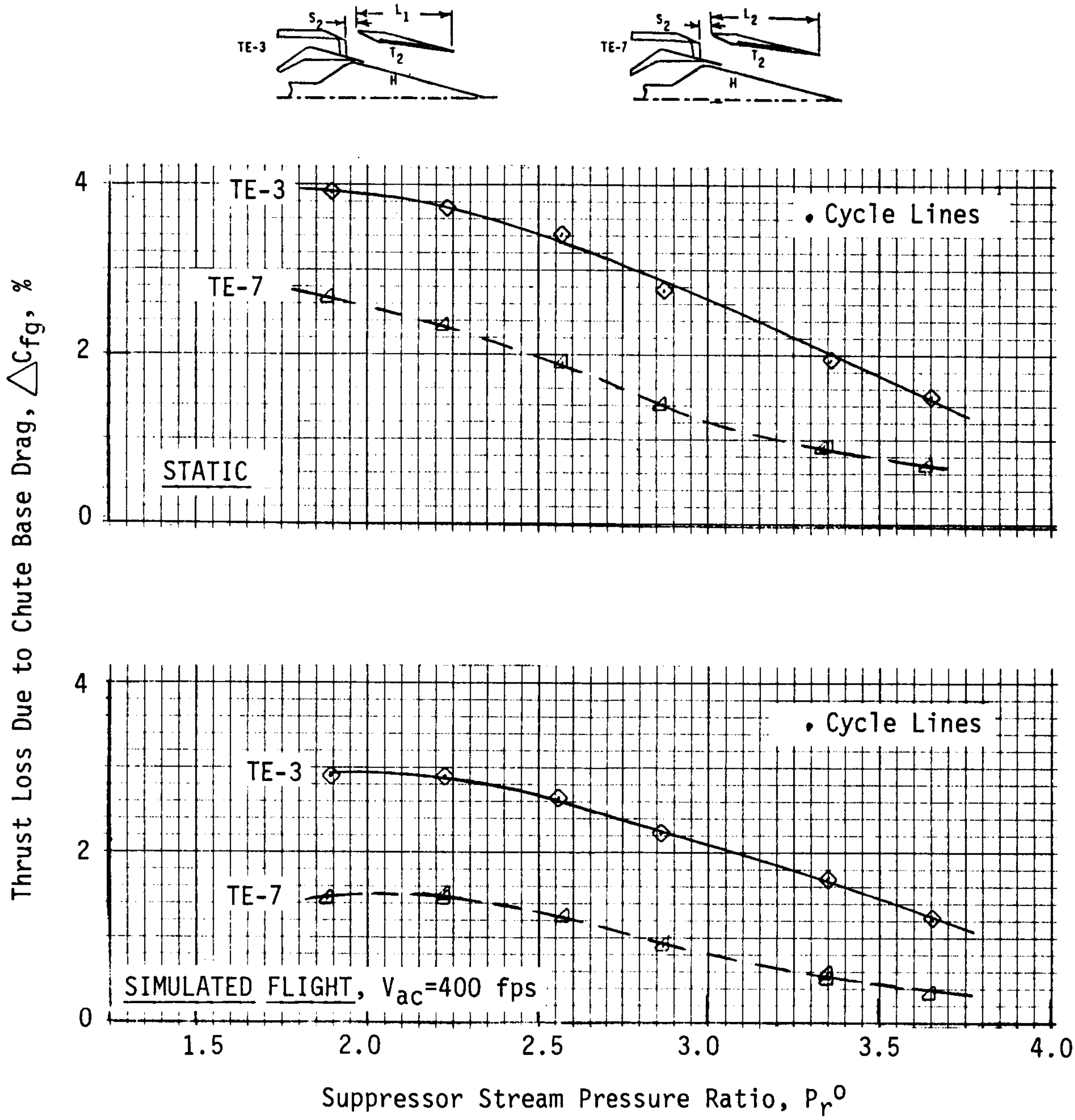

FIGURE 4-135. VARIANCE IN THRUST LOSS COEFFICIENT DUE TO CHUTE BASE DRAG AS A FUNCTION OF EJECTOR LENGTH: TE-3(L1) VS TE-7 (L2); TREATED EJECTOR-HARDWALL PLUG

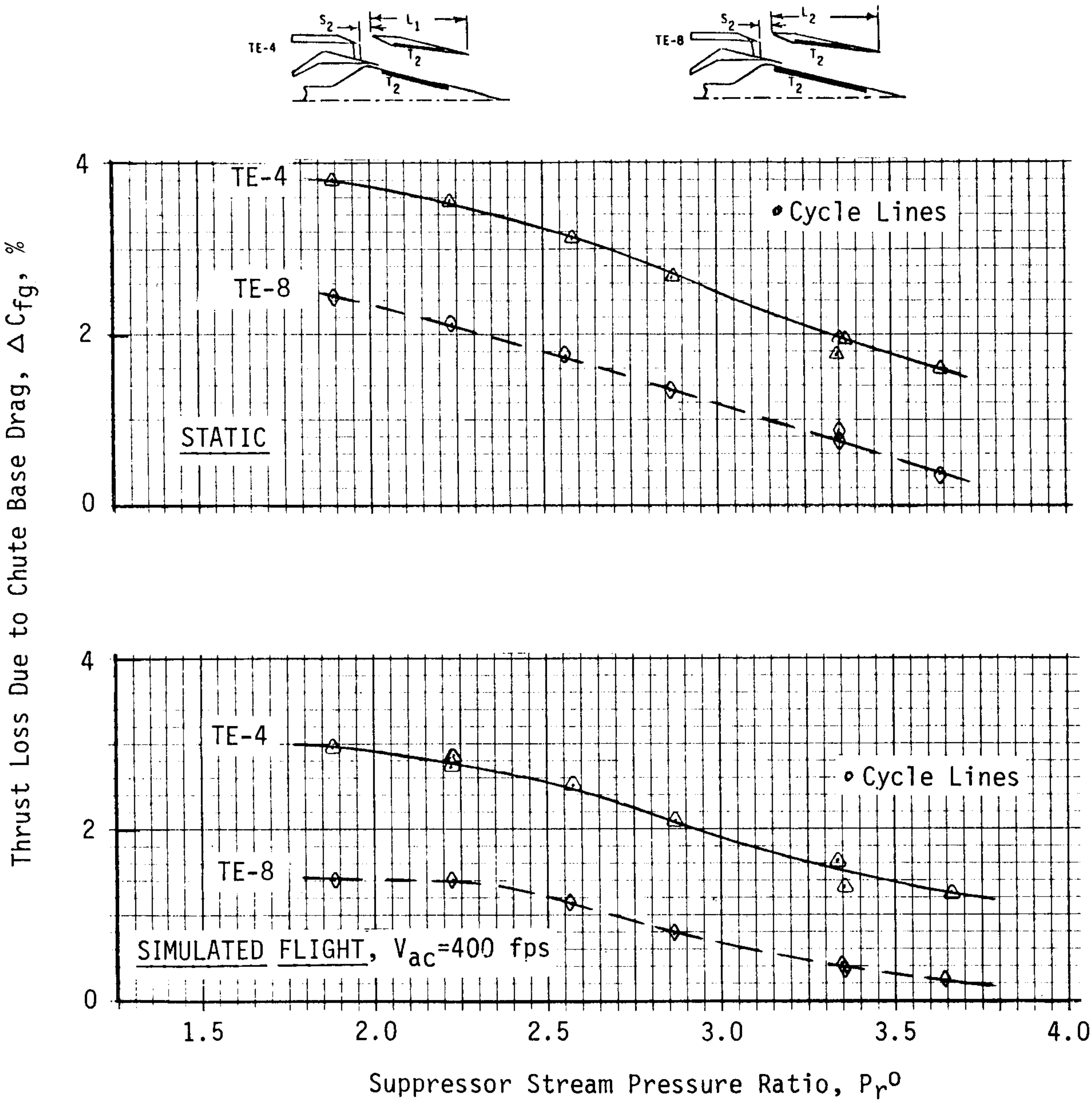

FIGURE 4-136. VARIANCE THRUST LOSS COEFFICIENT DUE TO CHUTE BASE DRAG AS A FUNCTION OF EJECTOR LENGTH: TE-4 (L1) VS TE-8 (L2); TREATED EJECTOR AND PLUG

- o In each figure, the extended length ejector's thrust loss is significantly below that of the nominal length ejector, indicating that it has better pumping/ventilating characteristics, which raise chute base pressure and lower base drag.

4.6 EFFECTIVENESS OF PLUG TREATMENT ON SHOCK NOISE ALLEVIATION

4.6.1 Background and Overview

Just prior to the time period during which this program's work scope was being formulated, NASA and industry became interested in furthering the work of Dr. Lucio Maestrello on shock noise reduction through the porous plug concept. Dr. Maestrello's earlier work on jet noise suppression, Reference 18 and 19, had shown that a plug nozzle with porous centerbody provided shock free flow over a wide range of pressure ratios. The elimination of "shock associated noise" and "screeching" was accomplished by equalization of pressure along the jet axis through use of the porous plug surface. The interior cavities of the centerbody were vented to the jet stream all along their lengths and acted as settling chambers whose pressures were nearly equal to ambient. The vented interior cavities tended to equalize the abrupt positive and negative pressure gradients of the jet stream.

NASA-Langley had issued a request for proposal and subsequent contract to further study this porous plug concept in a more detailed and parametric test phase. In the meantime, this contract's model system afforded an opportunity to explore a variation of the porous plug concept, i.e., use of a softwall plug surface, through acoustic treatment application, to attempt to accomplish the same purpose. Configuration TE-6 was thus developed to apply treatment to the centerbody of the inner flow plug nozzle. Figures 3-14 and 3-21 show the test model in sketch and photograph; treatment panels are constructed per Figure 3-31 and acoustically packed per Figure 3-32. In several respects, this model was significantly different than those of early work on the porous plug concept: a) it incorporated a dual flow coannular nozzle with outer stream mechanical suppressed, whereas, early porous plug studies evolved around single flow high radius ratio plug nozzles, and b) shock noise from this 20-chute suppressor was already substantially reduced below that of a reference conical nozzle without aid of additional porous or softwall plug techniques. The test objective for Configuration TE-6, in comparion to the similar hardwall plug test of Configuration TE-1 (per Figures 3-9 and 3-19), was to evaluate potential for still further reduction of shock-associated noise through further weakening of the shock structure.

Testing was performed along the same cycle line of engine operability as for other test configurations, per Table 3-1, however, interest was primarily in the higher pressure ratio points of takeoff and above. In summary, acoustic test results were not encouraging:

- o Forward quadrant shock noise is nominally similar to that of the hardwall plug case. Individual angle comparisons show that a) at many angles, noise levels for TE-6 are the same as TE-1 and correlate equivalently to the shock strength parameter β , b) for static operation, TE-6 levels are slightly higher at several angles, and c) in simulated-flight, TE-6 levels are slightly lower at several angles.

- o EPNL is unchanged at T/O cycle and above, where shock noise is normally quite influential.
- o Peak jet noise in the aft quadrant increased several ΔPNL for static and increased slightly for flight at high cycle conditions.

4.6.2 Detailed Acoustic Data Presentation

As softwall plug application was anticipated to impact only forward quadrant shock noise (assuming that aft quadrant shock noise is dominated by jet mixing noise, as it is for most nozzles) the first check, of necessity, would compare forward quadrant measured data as a function of shock strength parameter β. Harper-Bourne and Fisher, Reference 16, have developed theoretical and experimental guidelines for estimating the characteristics of broadband shock noise for jets operating above critical pressure ratio. They suggest that shock noise can be correlated on the basis of this shock strength parameter, β, defined as $\sqrt{M_j^2-1}$. This finding has been verified by numerous other studies; References 8, 9 and 20 through 24. Figures 4-137 and 4-138 compare the TE-6 and TE-1 data at θ_I = 50° through 100° as a function of the β parameter, i.e., on 10 Log β^{eff}, for static and simulated flight conditions, respectively. (β^{eff} is defined in Section 3.3.1.2 and is a mixed stream parameter.)

The data are only for those points operating at supercritical mixed pressure ratio, i.e., cutback cycle and above. Review of the two figures indicates:

- o For static, the softwall plug does not reduce forward quadrant noise any further than the hardwall plug, in fact, for angles of θ_I = 60°, 80° and 100°, the softwall levels are slightly above those of the hardwall. At 70° and 90°, levels for the two configurations are identical.
- o The simulated-flight correlated data show similar minimal changes between soft and hard plug surfaces; small changes do occur, but show mixed conclusions. Softwall levels are the same as hardwall at θ_I = 80°, 90° and 100°, slightly above the hardwall at 60° and slightly below at 50° and 70°.
- o The data correlate very uniformly against the shock strength parameter, showing β dependency in the range of 2 to 2.7 for all data. Conical nozzle shock noise dominated data, as reference, normally correlate with a β dependency near 4.0.

Further comparisons of the measured data are made in Figures 4-139 and 4-140 for jet noise dependency. Normalized PNL, static and flight, are correlated with the mixed jet velocity parameter, 10 Log (V_j^{eff}/a_{amb}). These comparisons are at θ_I = 60°, 90°, 130° and peak angle. Results at forward angles compare similarly to those of Figures 4-137 and 4-138 in that levels are nominally the same for the two configurations. In the aft quadrant, θ_I = 130° and peak value, static noise levels for the treated plug are substantially above the hardwall configuration, 2 to 2.5 dB for all cycle points. For simulated flight, however, the levels are similar at θ_I = 130° and peak angle except at highest cycle points of takeoff and above. Here, again, the softwall plug is slightly noisier than the hardwall plug, by .5 to 1.5 dB, indicating aft quadrant jet mixing noise is somehow slightly amplified by use of the non-smooth plug surface.

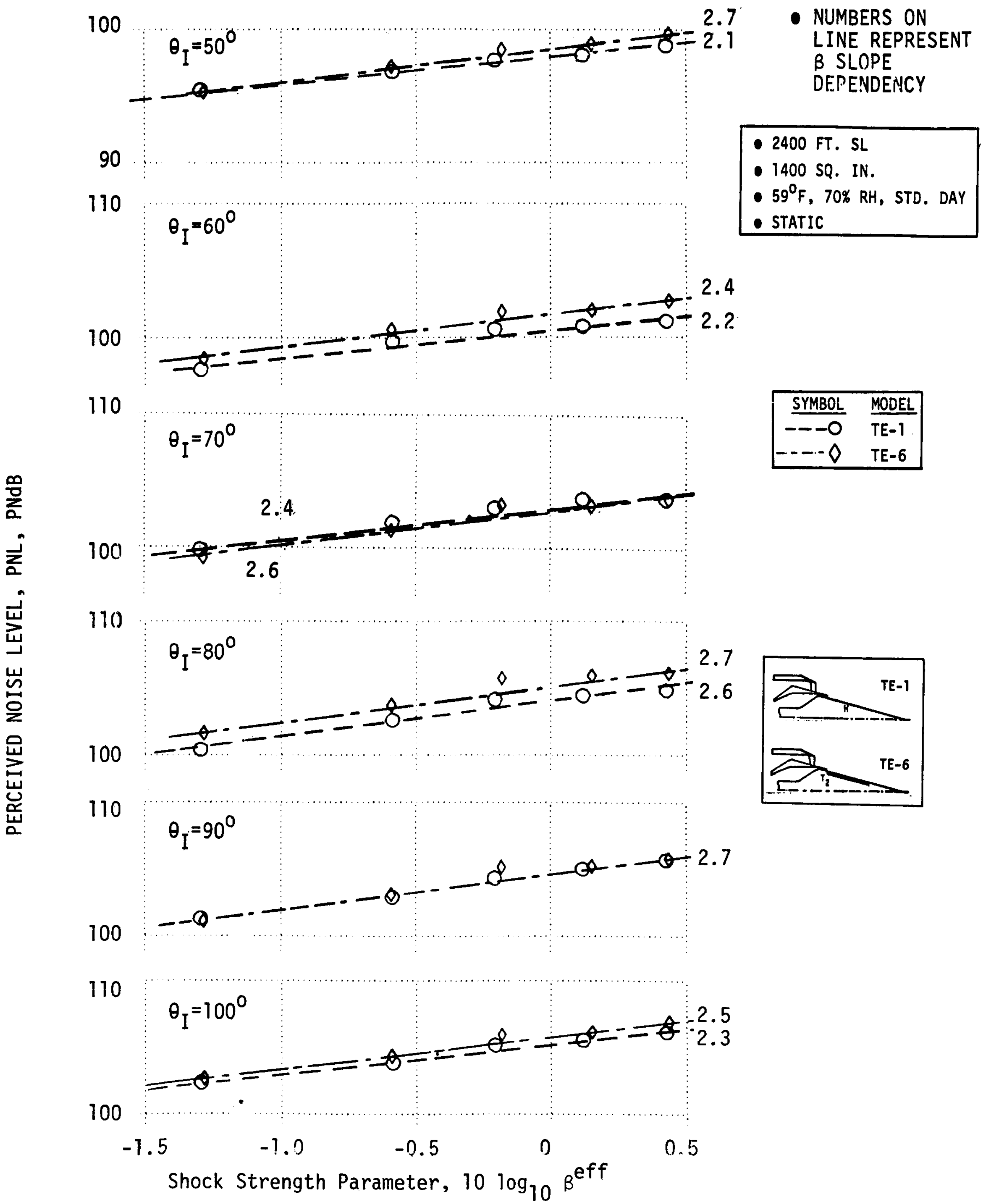

FIGURE 4-137. CORRELATION OF FORWARD QUADRANT PNL DEPENDENCY ON SHOCK STRENGTH PARAMETER FOR CONFIGURATIONS TE-1 AND TE-6, STATIC

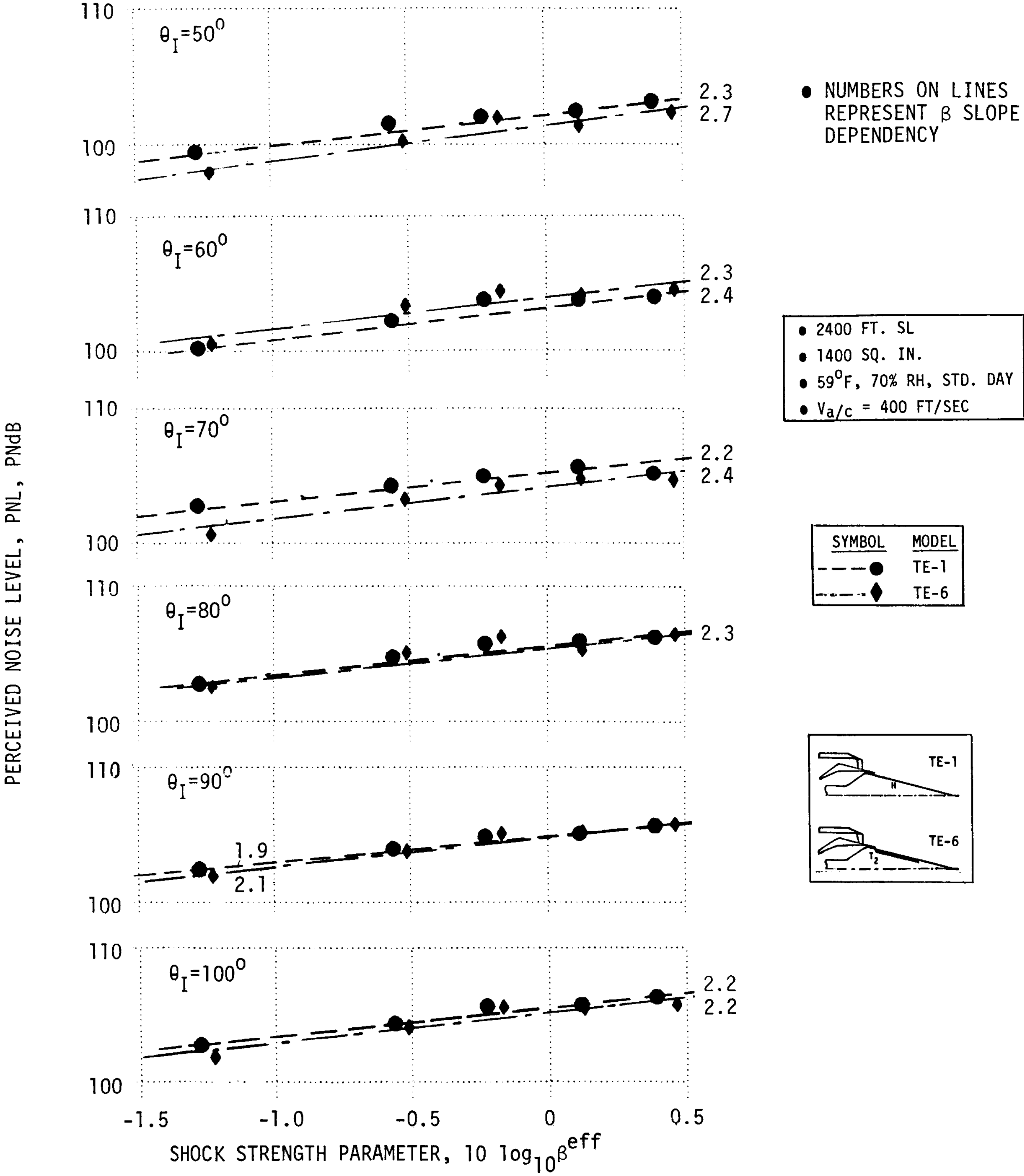

FIGURE 4-138. CORRELATION OF FORWARD QUADRANT PNL DEPENDENCY ON SHOCK STRENGTH PARAMETER FOR CONFIGURATIONS TE-1 AND TE-6, SIMULATED-FLIGHT

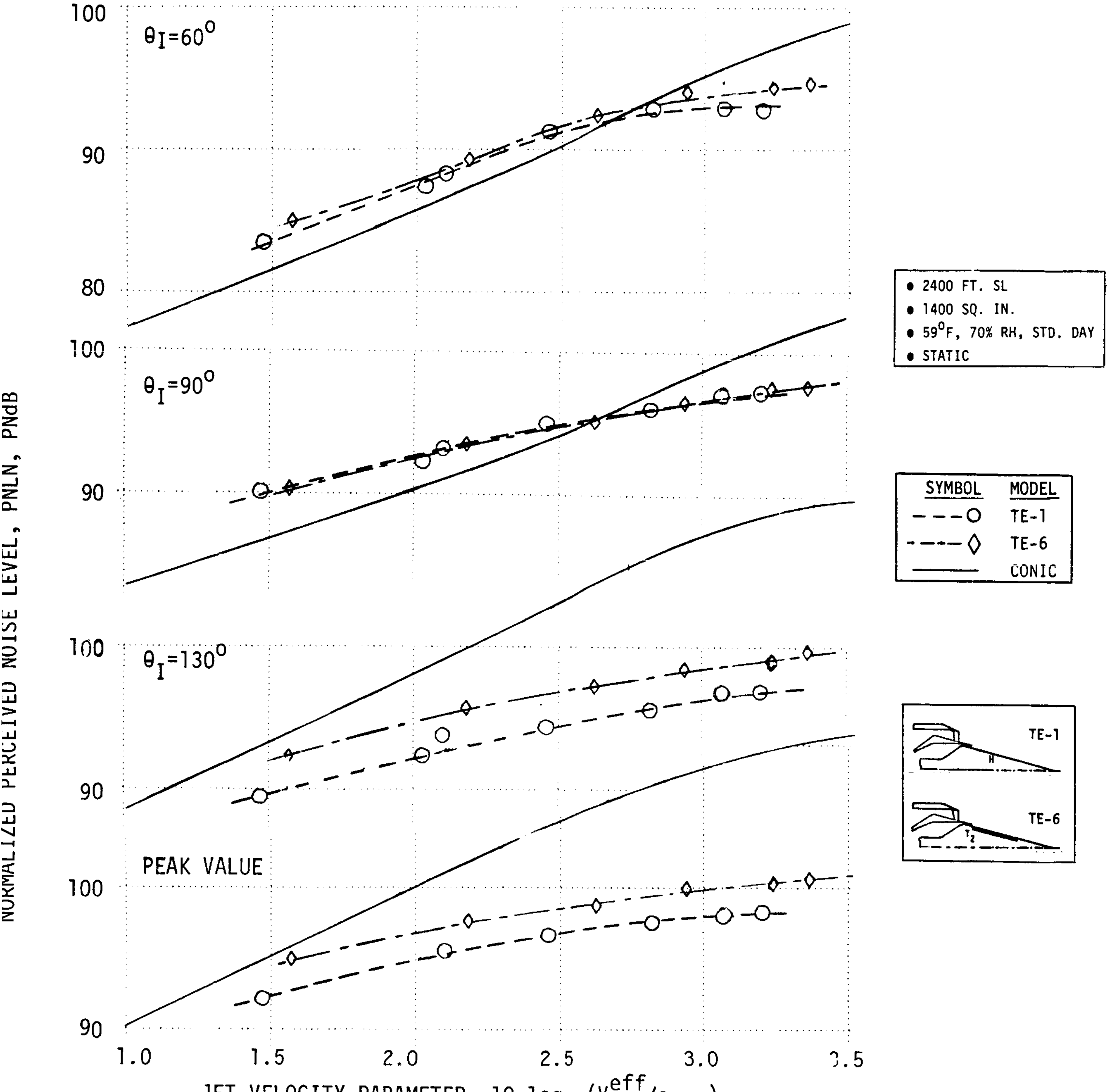

FIGURE 4-139. NORMALIZED PNL AS A FUNCTION OF JET VELOCITY PARAMETER FOR COMPARISONS OF CONFIGURATIONS TE-1 AND TE-6, STATIC, AT θ_I=60°, 90°, 130°, AND PEAK VALUE

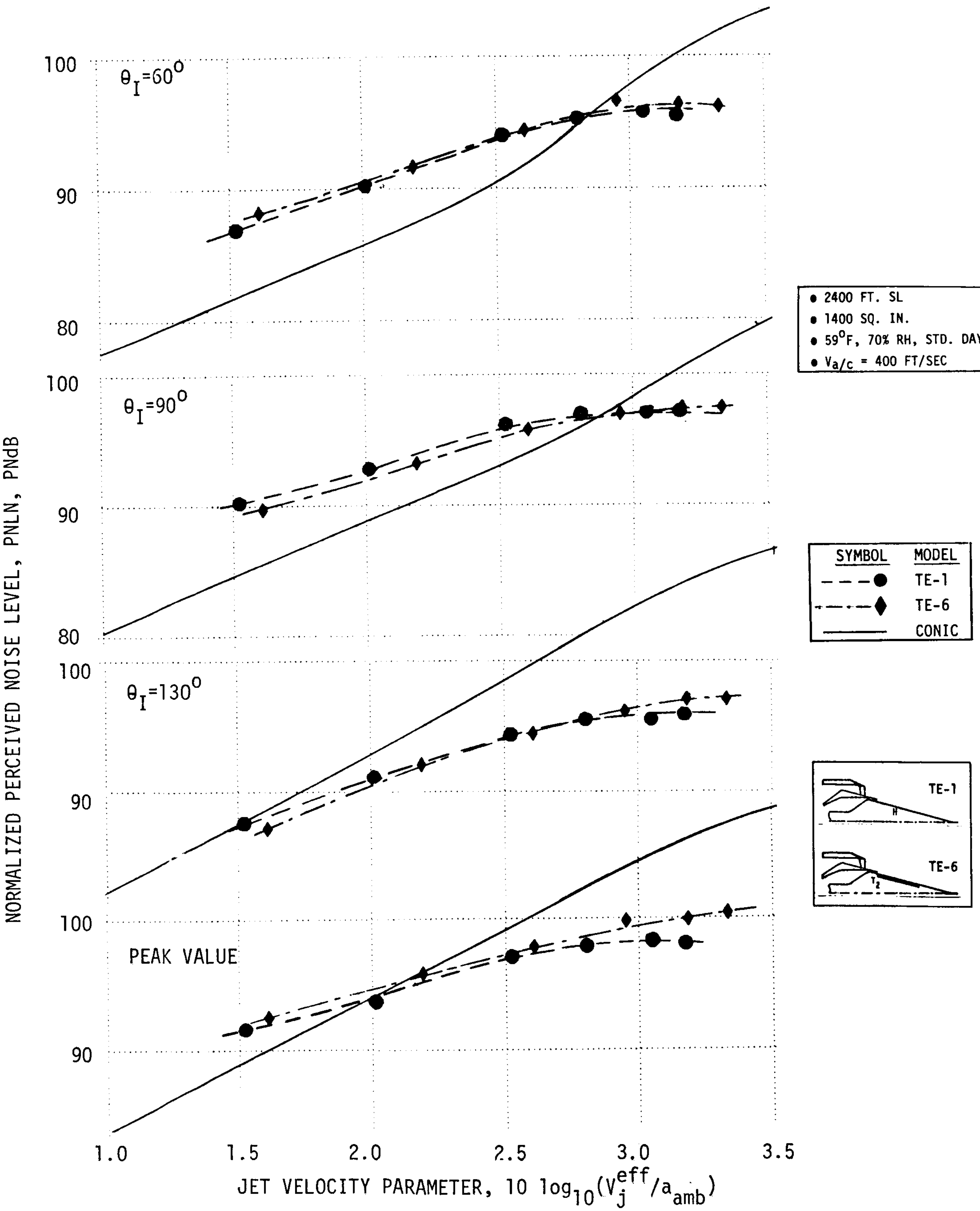

FIGURE 4-140. NORMALIZED PNL AS A FUNCTION OF JET VELOCITY PARAMETER FOR COMPARISON OF CONFIGURATIONS TE-1 AND TE-6, SIMULATED-FLIGHT, AT θ_I = 60°, 90°, 130°, AND PEAK VALUE

If gauged on the "overview parameter" of EPNL (based on 2400' sideline PNL directivity at 400 ft/sec simulated-flight speed) per Figure 4-141, the TE-6 soft plug is seen no more effective than the TE-1 hard plug at the higher cycle conditions where shock noise would be of prime consideration. At lower cycle conditions, the soft plug is seen to lower EPNL very slightly.

Further detailed data at the takeoff cycle are presented in Figure 4-142 as OASPL and PNL directivity, static and flight, and in Figures 4- 143 and 4-144 as 1/3-OBSPL spectra at $\theta_I = 60^o$, 90^o and 130^o for static and simulated-flight, respectively. Directivity comparisons show mixed effectiveness in the forward quadrant and slight amplification of most aft quadrant and peak noise levels. The aft quadrant, $\theta_I = 130^o$, spectra are seen to be amplified over the entire frequency range for both static and flight whereas $\theta_I = 60^o$ and 90^o spectra are mixed.

Several post-analysis thoughts are offered relative to the data review:

- o Early porous plug work of Dr. Maestrello indicated that a long plug was necessary to effect the porous plug concept's noise reduction; short plugs being ineffective.

- o The increase in aft quadrant noise levels is puzzling, no obvious explanation readily forthcoming, possible implication being the increased surface roughness of the plug treatment application. Concern is expressed as to whether this noise increase remains when the ejectors are applied, and if so, does it lend to less than full suppression potential being realized by the ejector/treatment systems. In another area of analysis, Section 4.4, addition of plug treatment to the already treated ejector/suppressor system was seen ineffective at high cycle operation; no further noise suppression was gained.

4.6.3 Diagnostic Data Review

Several laser velocimeter data comparisons are available for the TE-1 and TE-6 configurations at takeoff cycle conditions. For static test points 1009 and 6009, the normalized mean velocity data are presented in the following:

- o Figure 4-145 Axial traverses at centerline, 3.07"R and 4.22"R.

- o Figure 4-146 Slant traverses parallel to the 15° plug surface, initiated near the inner nozzle lip (3.19"R), at the center of the suppressor nozzle flow element (4.44"R), and near the tip of the suppressor nozzle (5.16"R).

- o Figure 4-147 Radial traverses just aft of the plug tip at $x/D_{eq} = 2.20$.

For flight test points 1010 and 6010, the following comparisons are available:

- o Figure 4-148 Axial traverses at centerline, 3.17"R and 4.22"/4.44"R.

- o Figure 4-149 Radial traverses just aft of the plug tip at $x/D_{eq} = 2.20$.

Review of the traces shows:

- 2400 FT. SL
- 1400 SQ. IN.
- $59^{0}F$, 70% RH, STD. DAY
- $V_{a/c}$ = 400 FT/SEC

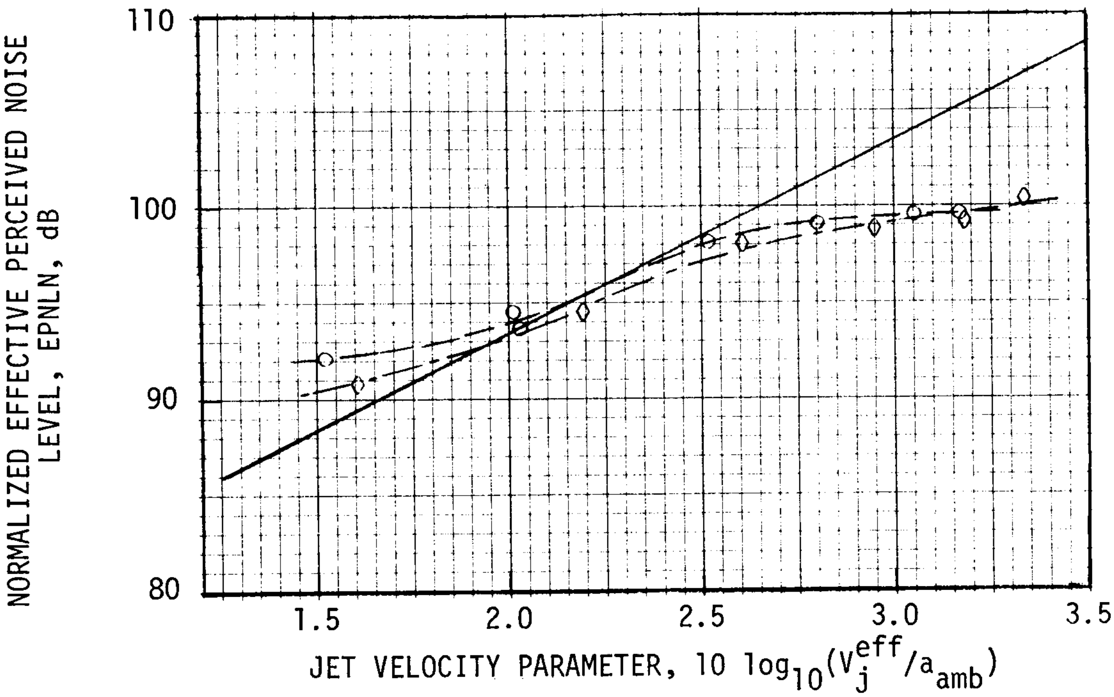

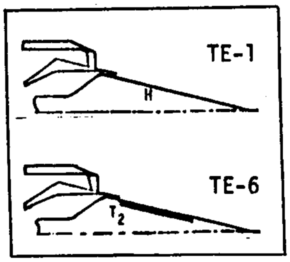

SYMBOL	MODEL
---O	TE-1
-·-·-◊	TE-6
———	CONIC

FIGURE 4-141. EPNL CORRELATION WITH JET VELOCITY PARAMETER FOR COMPARISON OF CONFIGURATIONS TE-1 AND TE-6, HARDWALL VS. TREATED PLUG

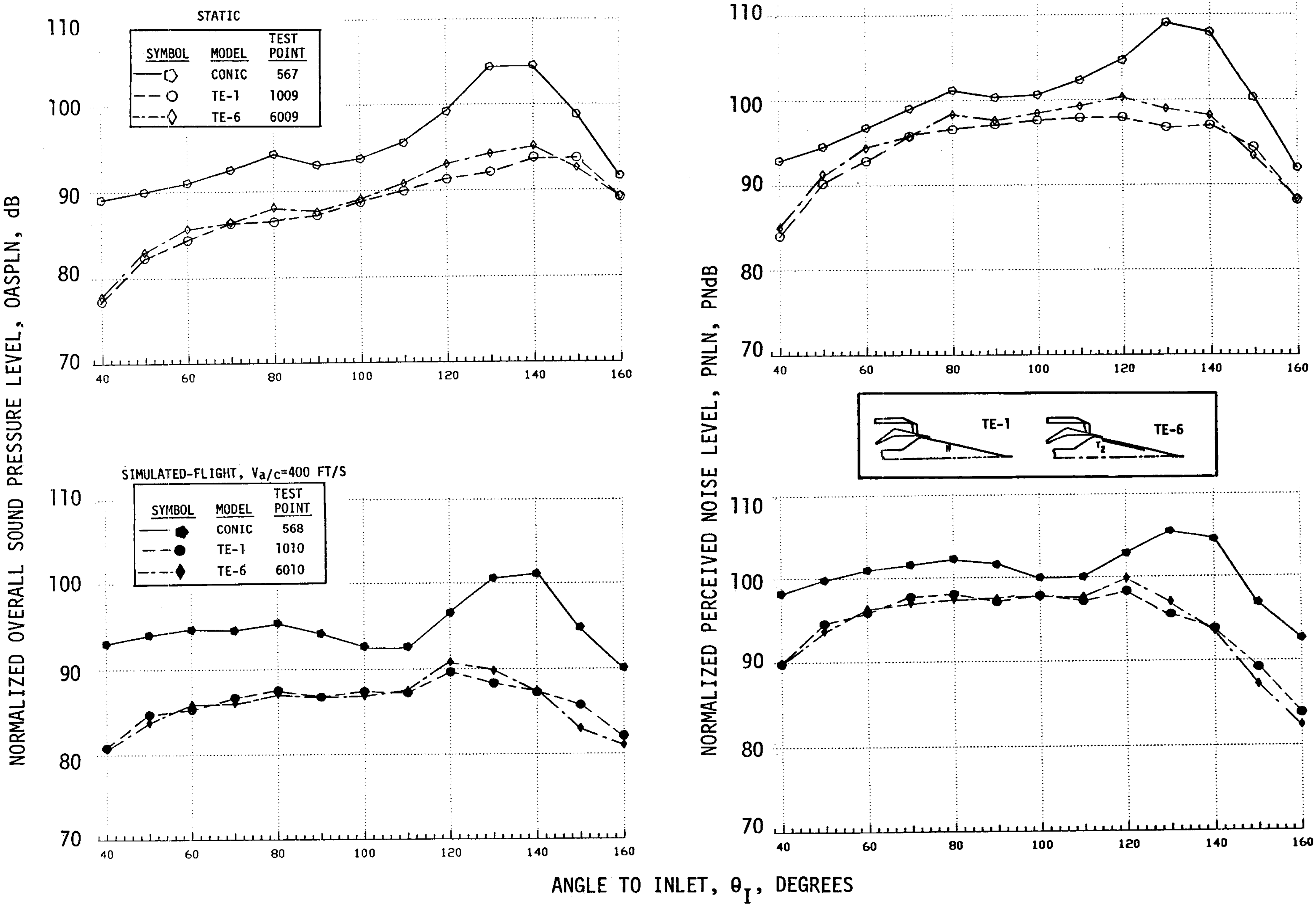

FIGURE 4-142. STATIC AND SIMULATED-FLIGHT DIRECTIVITY COMPARISONS OF OASPL AND PNL AT TAKEOFF FOR COMPARISON OF CONFIGURATIONS TE-1 AND TE-6, HARDWALL VS. TREATED PLUG

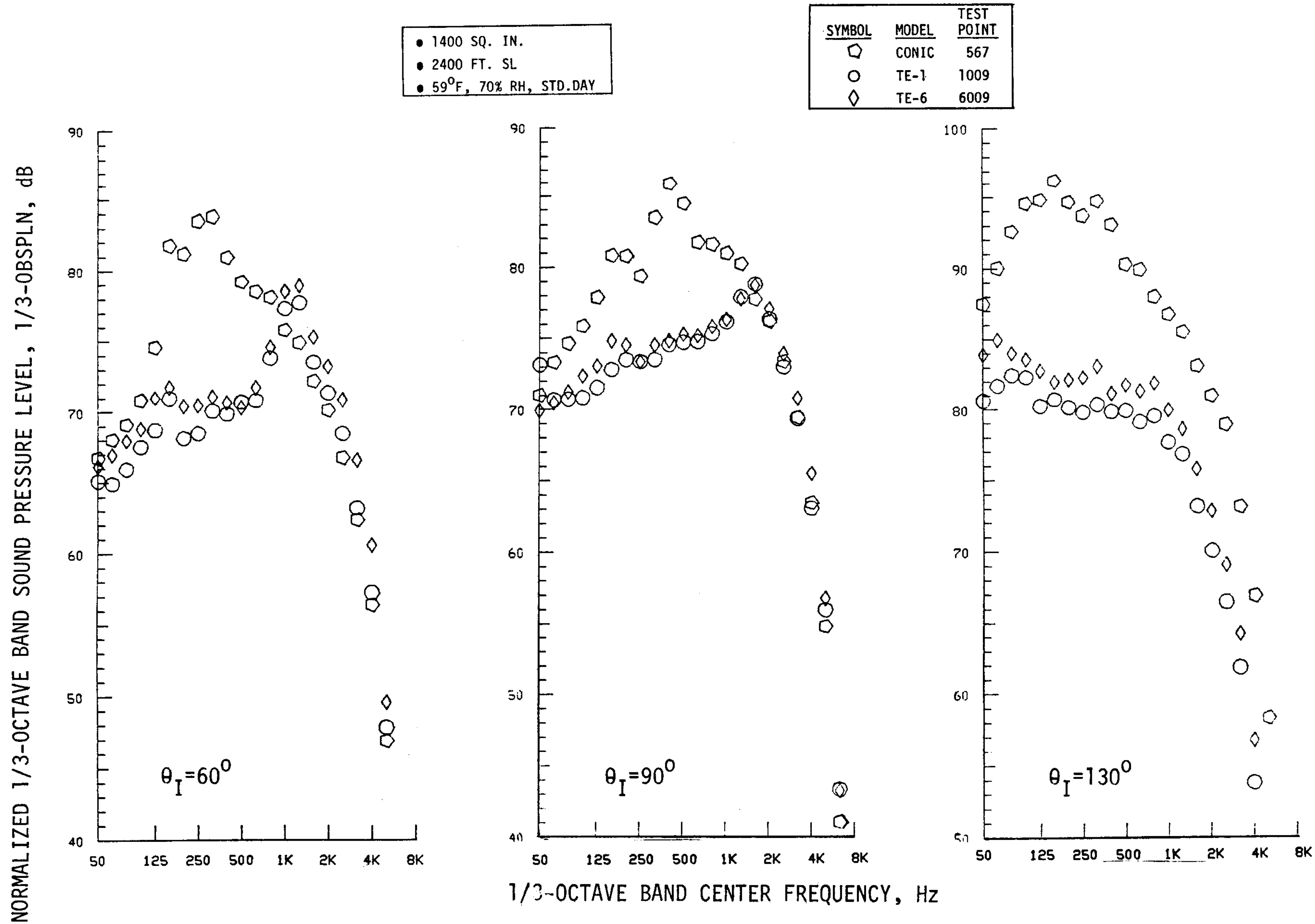

FIGURE 4-143. NORMALIZED SPECTRA AT θ_I=60°, 90°, AND 130° FOR COMPARISON OF CONFIGURATIONS TE-1 AND TE-6, HARDWALL VS. TREATED PLUG, STATIC, AT TAKEOFF

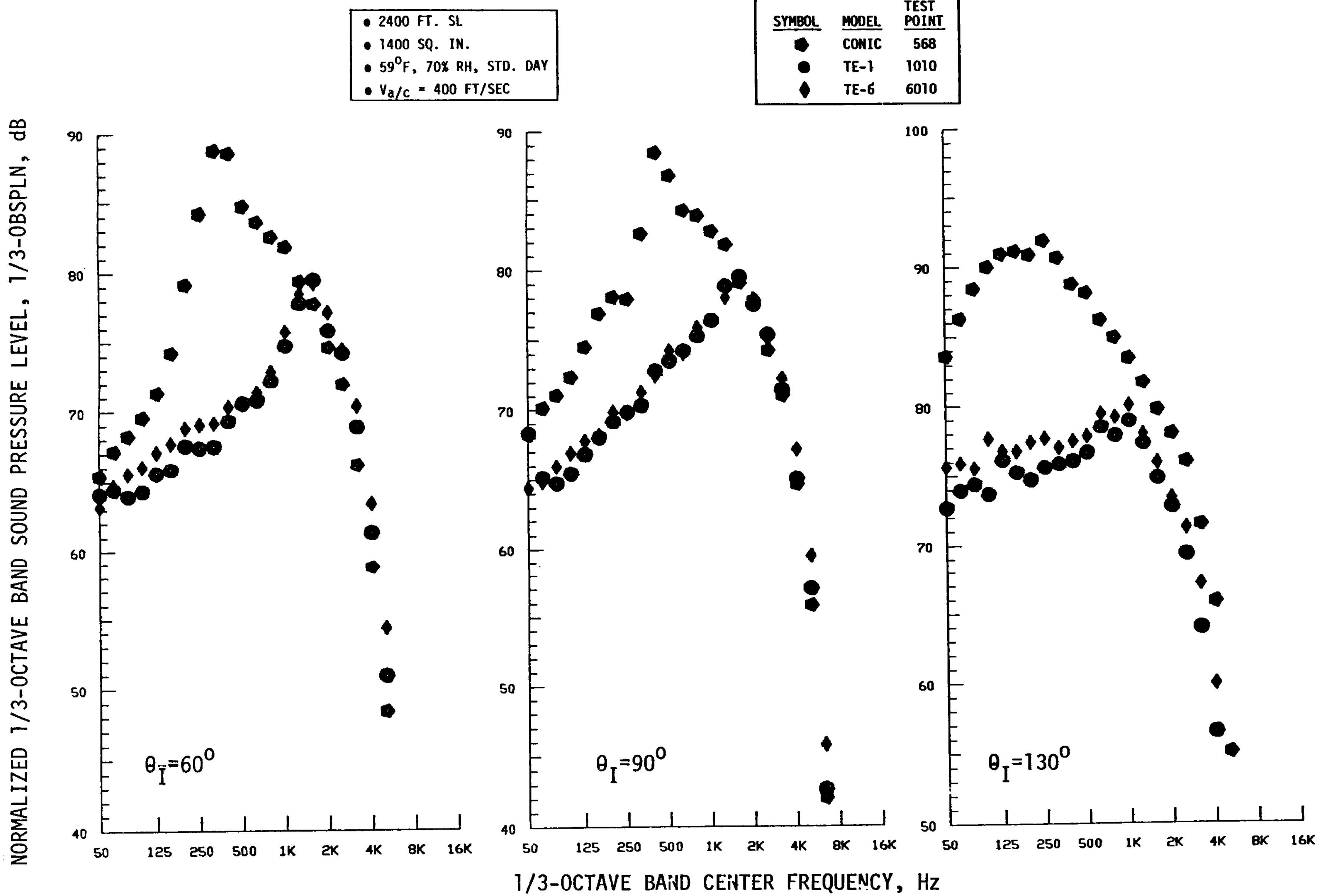

FIGURE 4-144. NORMALIZED SPECTRA AT θ_I=60°, 90°, AND 130° FOR COMPARISON OF CONFIGURATIONS TE-1 AND TE-6, HARDWALL VS. TREATED PLUG, SIMULATED-FLIGHT, AT TAKEOFF

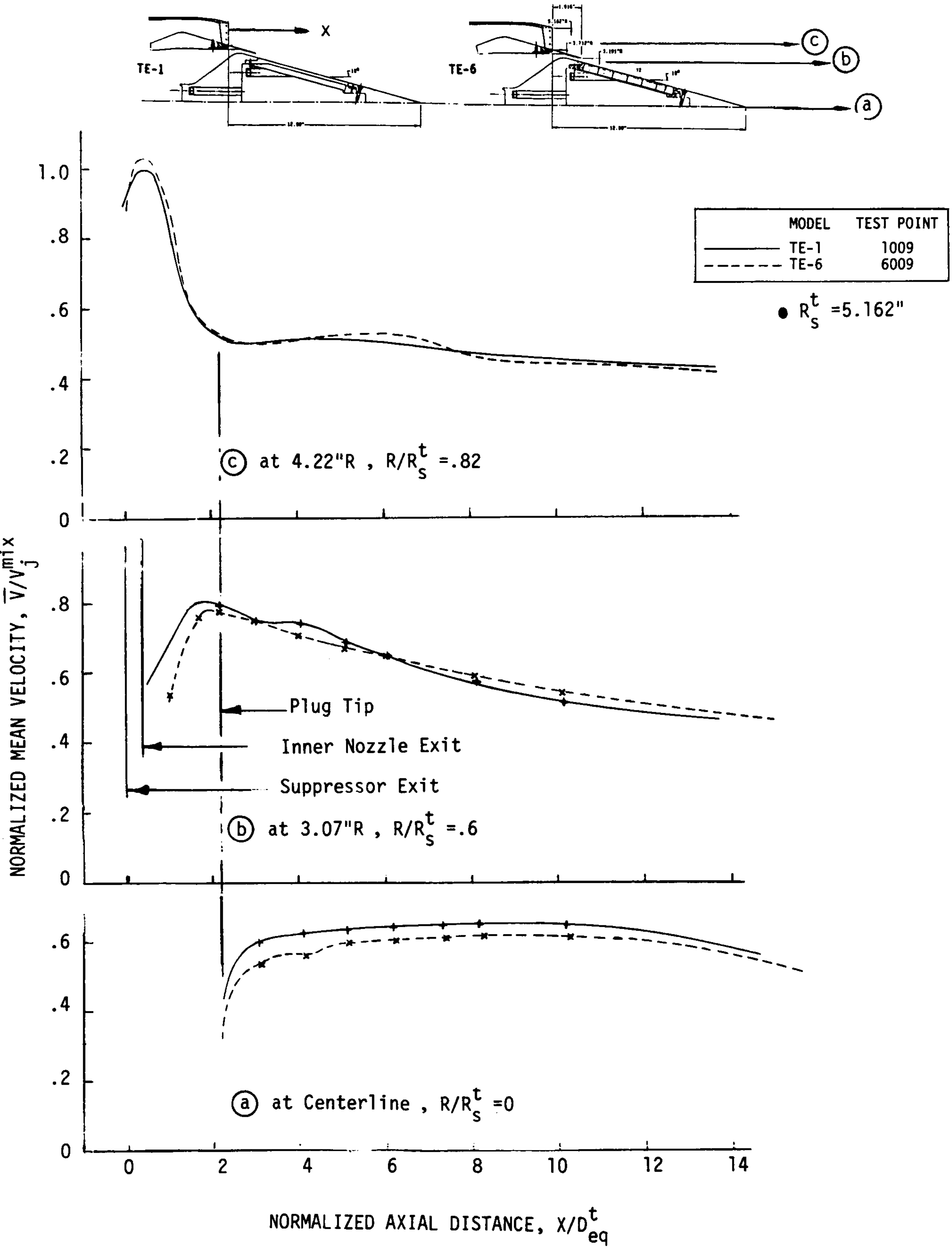

FIGURE 4-145. AXIAL VARIATION OF THE MEAN VELOCITY (AXIAL COMPONENT) IN THE PLUME OF CONFIGURATIONS TE-1 AND TE-6 AT TAKEOFF, STATIC, TEST POINTS 1009 AND 6009

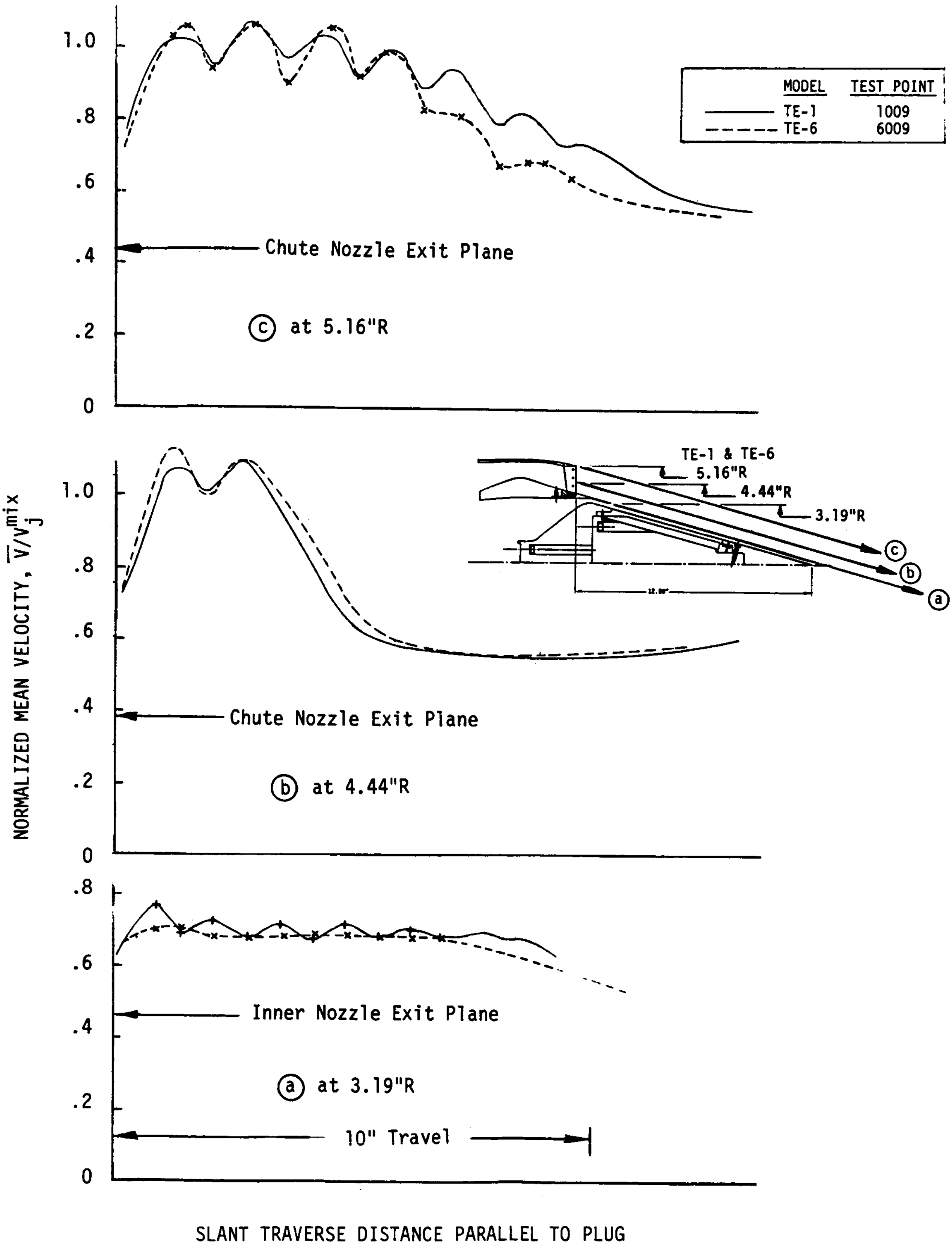

FIGURE 4-146. COMPARISON OF AXIAL VARIATION OF THE MEAN VELOCITY DISTRIBUTION PARALLEL TO THE PLUG SURFACE IN THE PLUME OF CONFIGURATIONS TE-1 AND TE-6 AT TAKEOFF, STATIC, TEST POINTS 1009 AND 6009

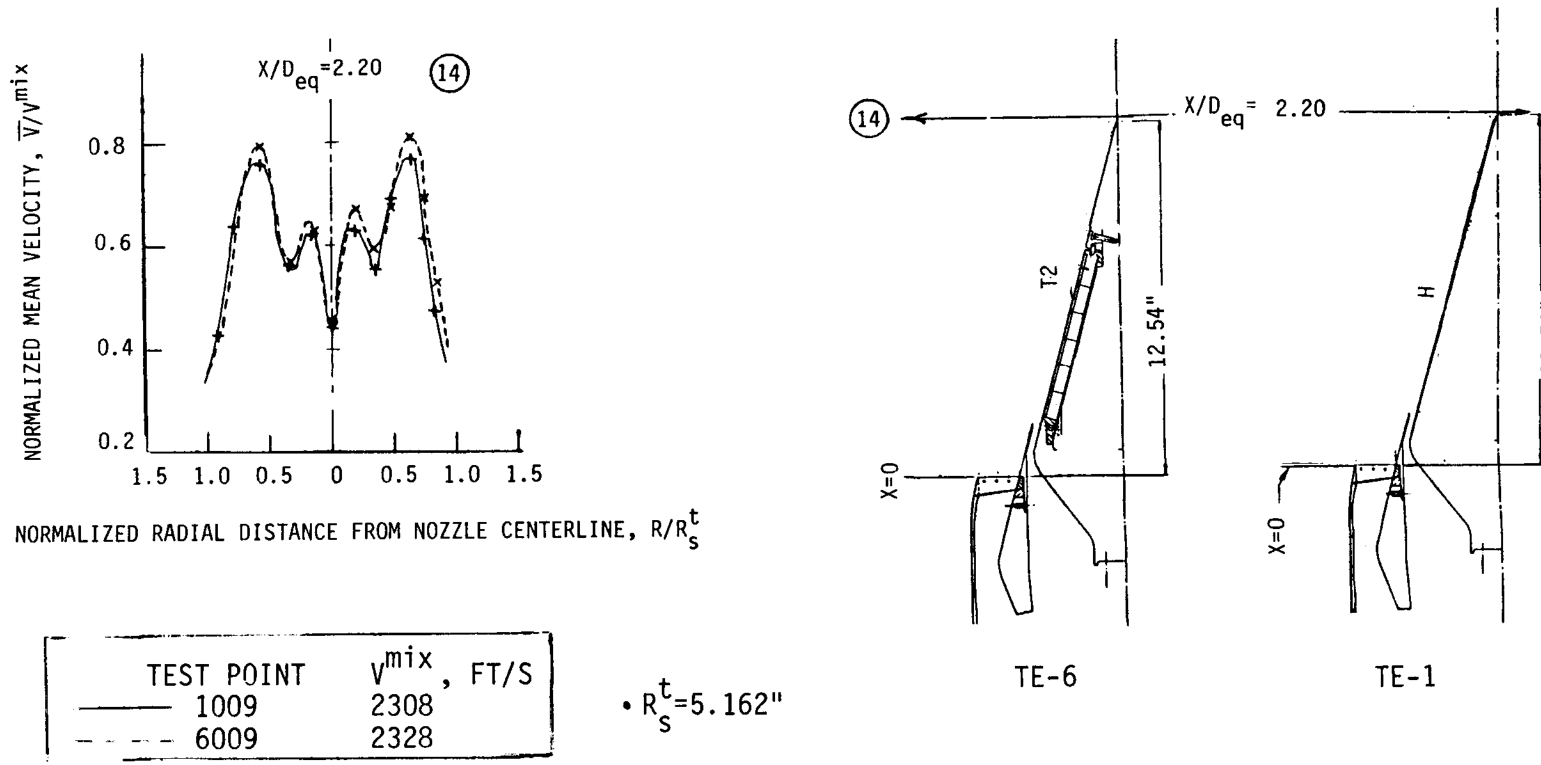

FIGURE 4-147. RADIAL VARIATION OF THE MEAN VELOCITY (AXIAL COMPONENT) IN THE PLUME OF CONFIGURATIONS TE-1 AND TE-6 AT TAKEOFF CONDITION, STATIC, TEST POINTS 1009 AND 6009

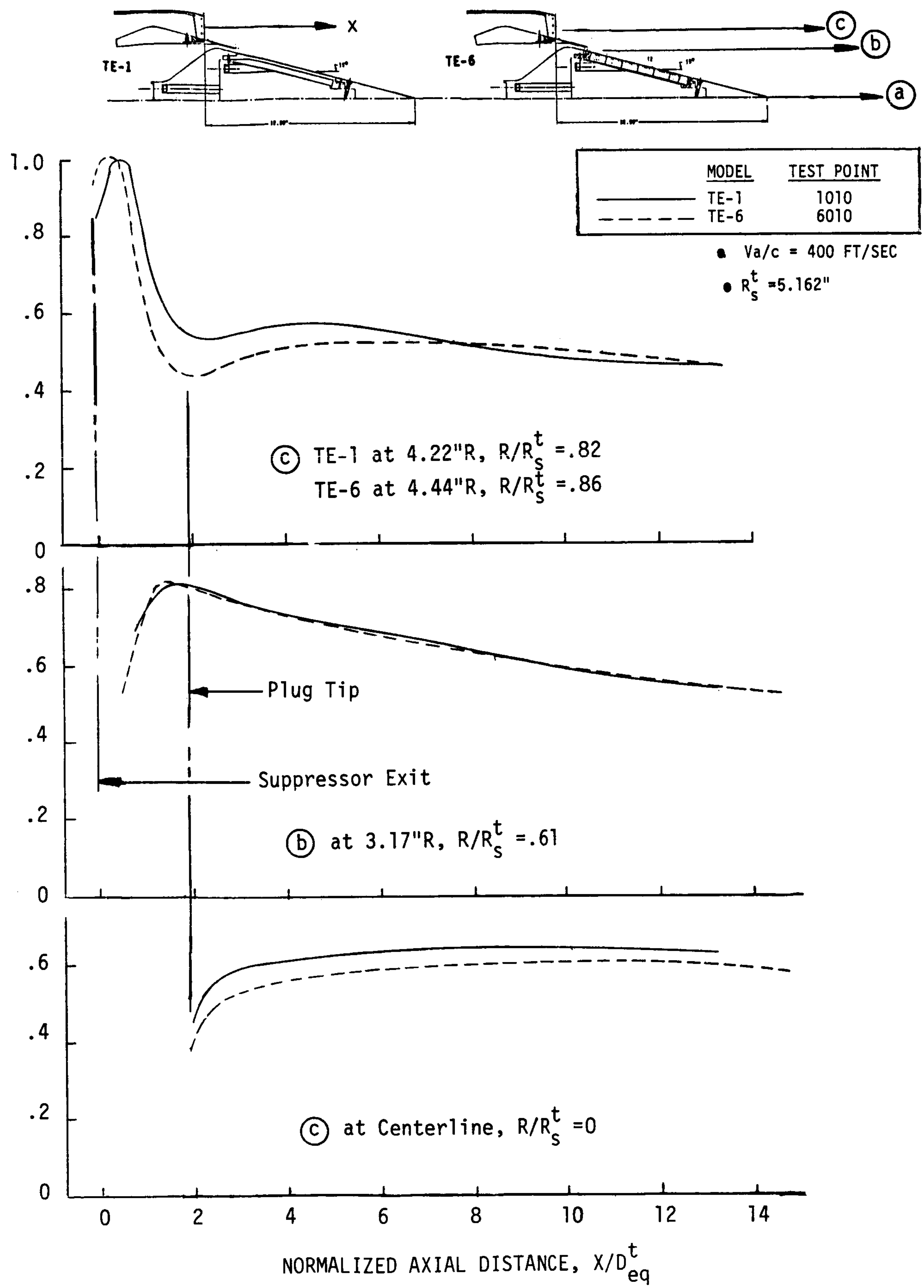

FIGURE 4-148. AXIAL VARIATION OF THE MEAN VELOCITY (AXIAL COMPONENT) IN THE PLUME OF CONFIGURATIONS TE-1 AND TE-6 AT TAKEOFF, SIMULATED-FLIGHT, TEST POINTS 1010 AND 6010

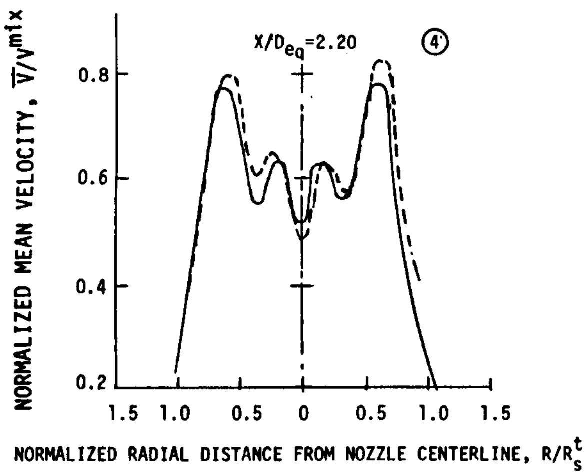

TEST POINT	V^{mix}, FT/S
——— 1010	2320
- - - - 6010	2321

• R_s^t=5.162"

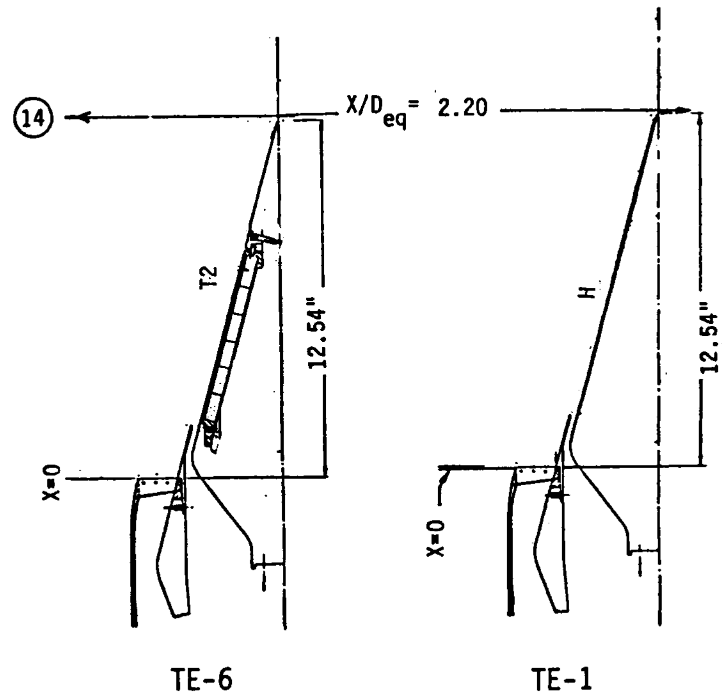

FIGURE 4-149. RADIAL VARIATION OF THE MEAN VELOCITY (AXIAL COMPONENT) IN THE PLUME OF CONFIGURATIONS TE-1 AND TE-6 TAKEOFF CONDITION, STATIC, TEST POINTS 1010 AND 6010

- o Per Figure 4-146, the shock structure near the treated plug (bottom of figure) is indeed mitigated, as indicated by the lower level of mean velocity without variations in level due to passage through shock cells. However, the shock structure in the outer and center section of the jet (top and center of figure) is relatively unaffected. This is a strong shock structure of high-velocity-gradient content and controls the generated shock related noise.

- o Figure 4-145 axial traces indicate similarly that the center of the jet (bottom of figure) is slightly lower in mean velocity with the treated plug due to shock structure weakening and maintains slightly lower velocity for a long distance aft of the plug tip. The main jet flow (top and center of figure) is relatively unaffected, however, of slightly higher peak velocity for the TE-6 configuration, possibly accounting for the slight increase in aft quadrant peak noise levels.

- o Simulated-flight, Figure 4-148 (bottom), again shows slight decrease in mean velocity aft of the plug tip for the center of the jet; the outer jet plumes (top and center of figure) are similar in structure except for a slight dip in the trace for TE-6/6010 at the outer radius (top of figure). This, however, is due to the trace being acquired at a slightly greater radius; 4.44" relative to 4.22" of trace TE-1/1010.

- o Radial traverses of Figures 4-147 and 4-149 near the plug tip each show slightly higher peak velocity for the soft plug configuration, again implicating the slightly higher aft quadrant jet noise.

Review of the shadowgraph data in CDR Volume II for test points 1009 and 6009 also show no discernable change in major shock structure in the axial region from suppressor exit to plug tip.

4.7 AERODYNAMIC PERFORMANCE EVALUATION FROM CHUTE BASE PRESSURE MEASUREMENTS

4.7.1 Thrust Loss Estimates Based on Chute Base Pressure Measurements

In order to assess the influence of ejector application to primary nozzle suppressor base pressure and hence the nozzle thrust coefficient, (8) static pressure taps were applied within the chute base regions. These are defined schematically and pictorially in Section 3.2.3's Figures 3-34 and 3-35, respectively. The measurements acquired from these instrumentation items during acoustic tests, summarized in CDR Volume I's Tables 6-1 through 6-10, were then used for estimation of a representative average pressure reading within the projected base area of the 20 chutes. From this, the change in the outer nozzle thrust coefficient, due to chute base drag, was calculated. In this section, the method employed to calculate the thrust loss is described and thrust loss data calculated for each test configuration are presented, both for the static and simulated-flight test conditions.

4.7.2 Thrust Loss Calculation Procedure

Locations of the (8) static pressure taps in the chute base region of the 20-chute suppressor nozzle are defined in Figure 4-150. The projected base area of each of the chutes is suitably divided into (8) elemental areas, A^i, each associated with a static pressure tap. The static pressure data, P_S^i, measured by each of the taps for a given nozzle flow condition, is assumed constant over its associated area. An area weighted chute average base pressure, PBAV, is calculated from the (8) static pressure measurements as follows:

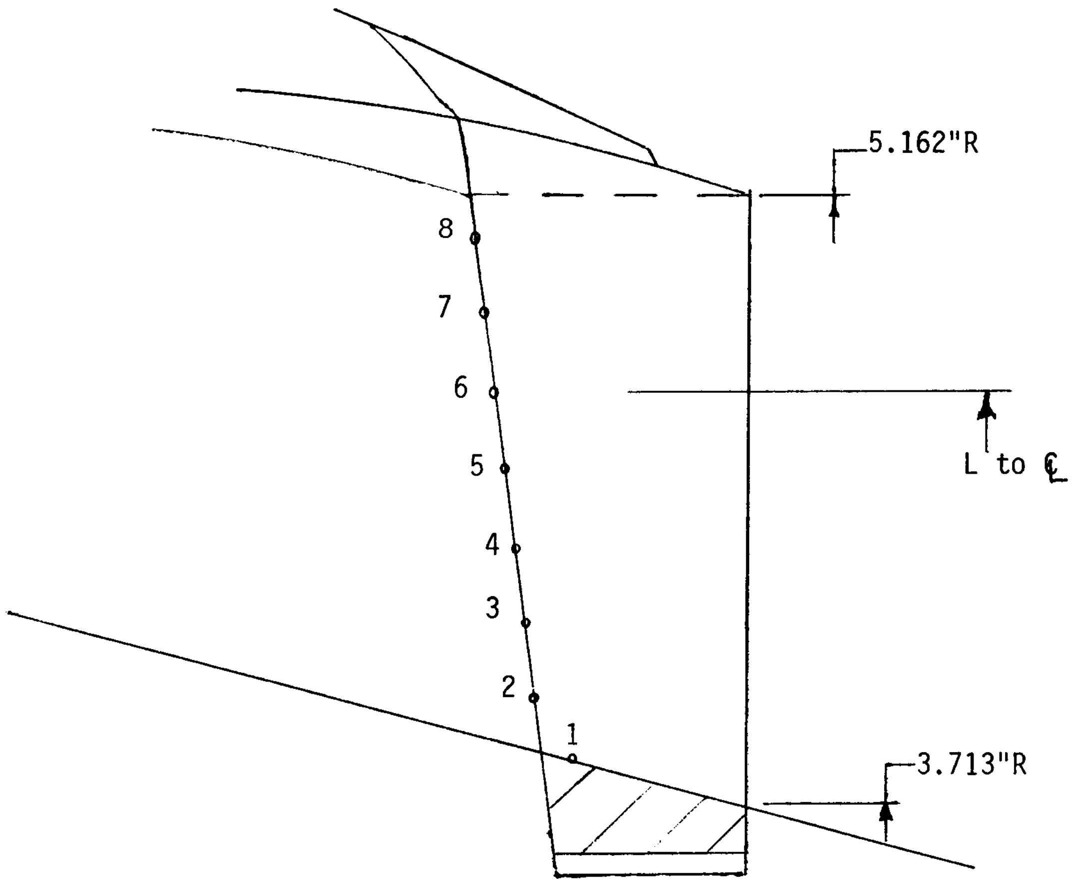

Ps ITEM NO.	CHUTE NO.	L, "to ℄	A^i, ASSIGNED CHUTE ELEMENTAL AREA, in^2	A^i/A^T,
PS08	8	5.080	.1128	.1279
PS07	7	4.918	.1109	.1257
PS06	6	4.751	.1107	.1256
PS05	5	4.578	.1108	.1257
PS04	4	4.398	.1109	.1258
PS03	3	4.210	.1111	.1260
PS02	2	4.013	.1108	.1257
PS01	1	3.807	.1037	.1176
			A^T=.8817 in^2 Per Chute	1.000

- Total Annulus Area=40.384 in^2
- Flow Area, $A_{flow}=A_8=22.75$ in^2
- Blocked Area=$A_{chute}=17.634$ in^2
- Blocked Area Per Chute=.8817 in^2
- Refer to Figure 2-30 of CDR Volume I

FIGURE 4-150. CHUTE BASE AREA DISTRIBUTION ASSOCIATED WITH BASE PRESSURE INSTRUMENTATION

$$PBAV = \Sigma P_S^i A^i / \Sigma A^i$$

or

PBAV = .1176 PS01+.1257 PS02+.1260 PS03+.1258 PS04+ .1257 PS05+.1256 PS06+.1257 PS07+.1279 PS08, psia

The base drag, FDCHUT, associated with each chute, is then calculated as follows:

$$FDCHUT = (AVPT20-PBAV)\Sigma A^i$$

FDCHUT = (AVPT20-PBAV) .8817 , Lb.

The total base drag, FD, associated with the base area of the 20 chutes is calculated by:

FD = 20 FDCHUT , Lb.

The ideal thrust, FSUPR, of the outer stream nozzle is calculated from:

$FSUPR = W^o V^o/g$, Lb.

where W^o is the weight flow rate through the suppressor, V^o is the fully expanded jet velocity, and g is gravitational constant. The change in thrust coefficient, DLCCFG or ΔC_{fg}, due to the chute base drag is finally computed as:

DLCCFG = (FD/FSUPR)X100 , %

4.7.3 Thrust Loss Calculation Data Presentation

The above calculated values: PBAV, FDCHUT, FD, FSUPR and DLCCFG are summarized in CDR Volume I's Tables 6-1 through 6-10 for the ten test Configurations TE-1 through TE-10, respectively. The thrust loss parameter, ΔC_{fg}, is presented graphically in Figures 4-151 through 4-160 for Configurations TE-1 through TE-10, respectively; plotted as a function of suppressor stream pressure ratio, P_r^o. Each figure has separate static (top), simulated-flight (center), and composite static/simulated-flight (bottom) data presentations. For static and simulated-flight plots, distinction is noted for a) cycle line of operation (see Section 3.3.1 for explanation), b) low T_T^o = 810 to 870°R, and c) $V_{a/c}$ = 200 and 400 ft/sec. For the composite plots of static and simulated-flight, only the data for cycle line of operation are overlain.

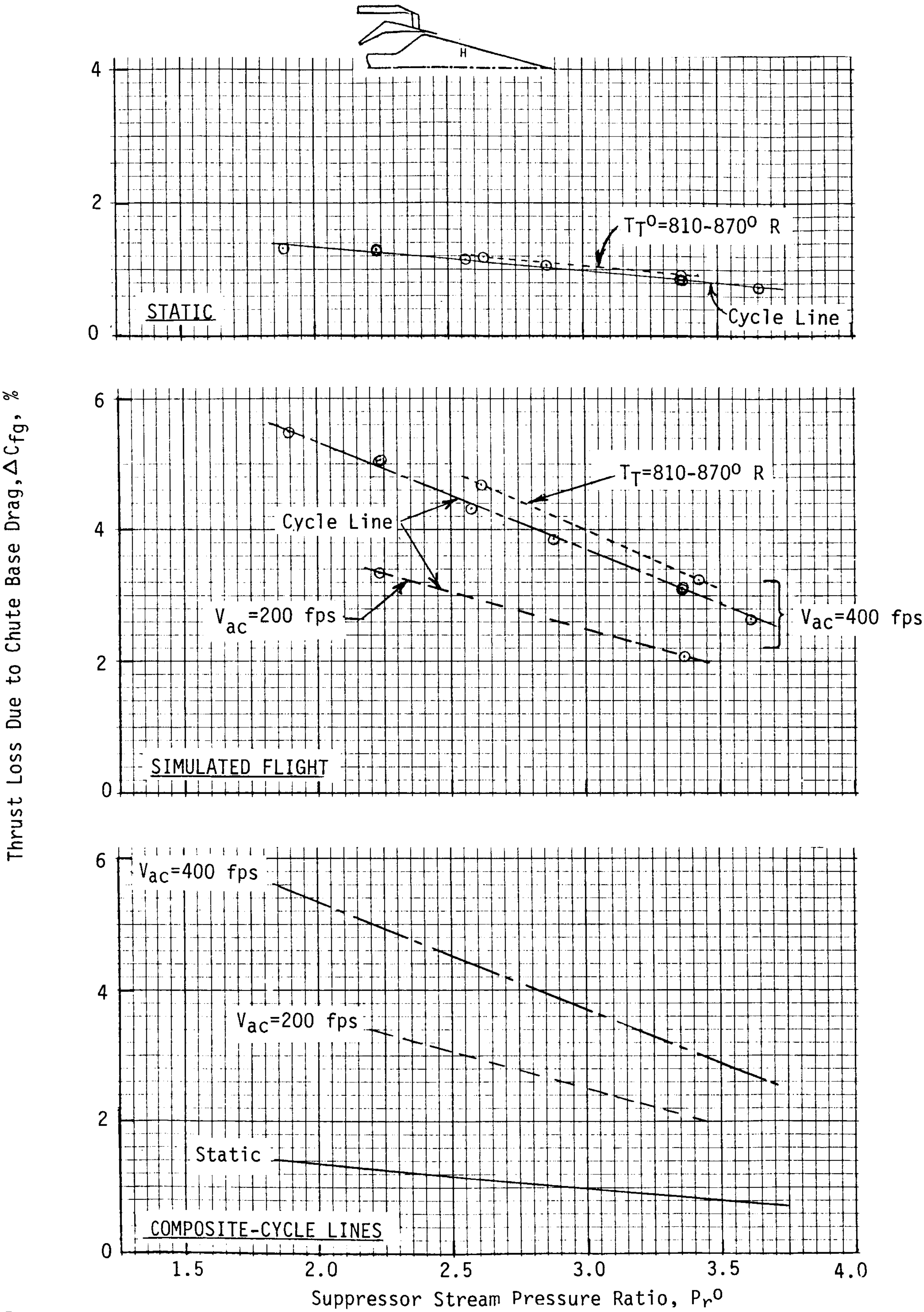

FIGURE 4-151. THRUST LOSS COEFFICIENT DUE TO CHUTE BASE DRAG OF CONFIGURATION TE-1

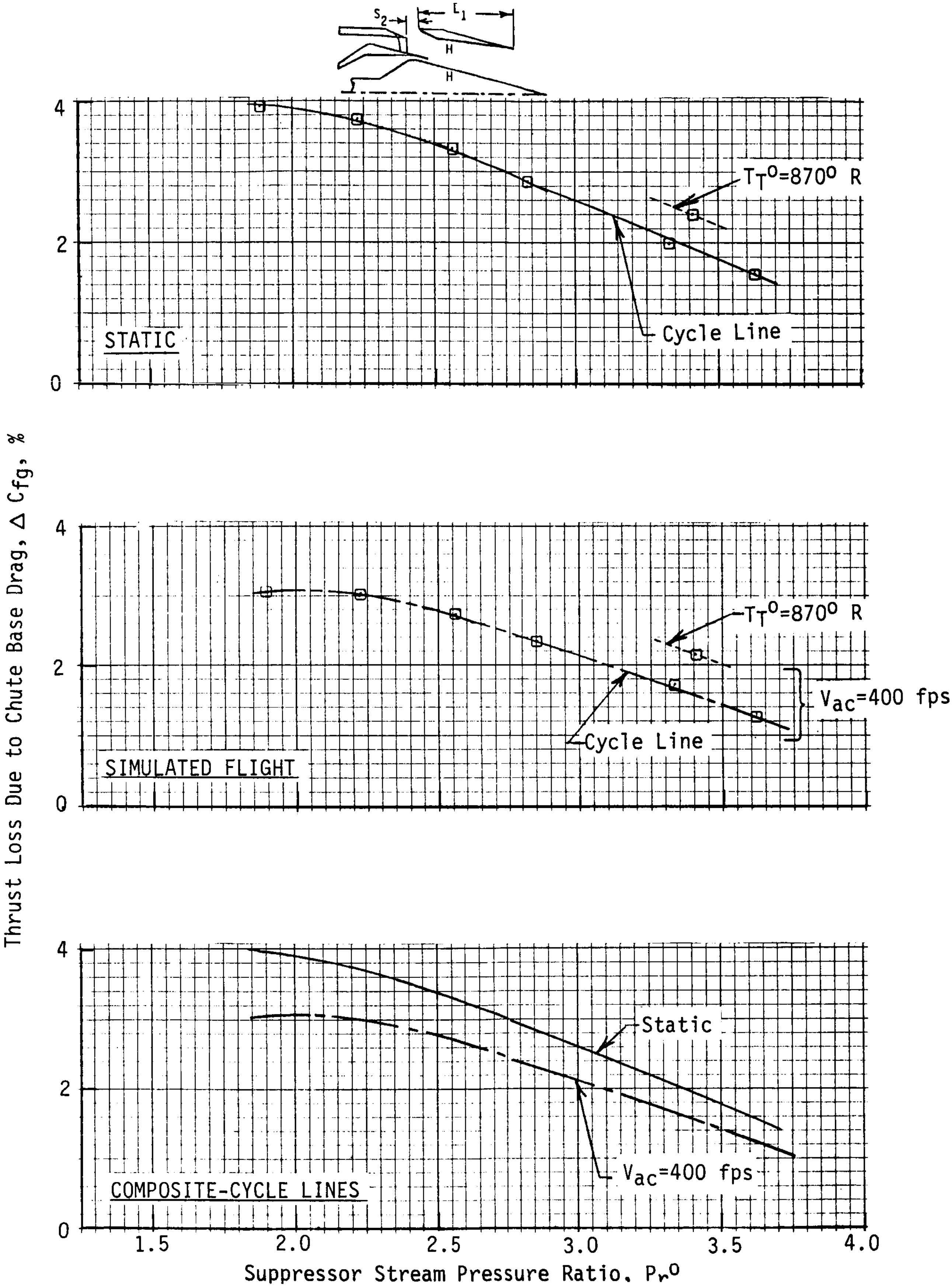

FIGURE 4-152. THRUST LOSS COEFFICIENT DUE TO CHUTE DRAG OF CONFIGURATION TE-2

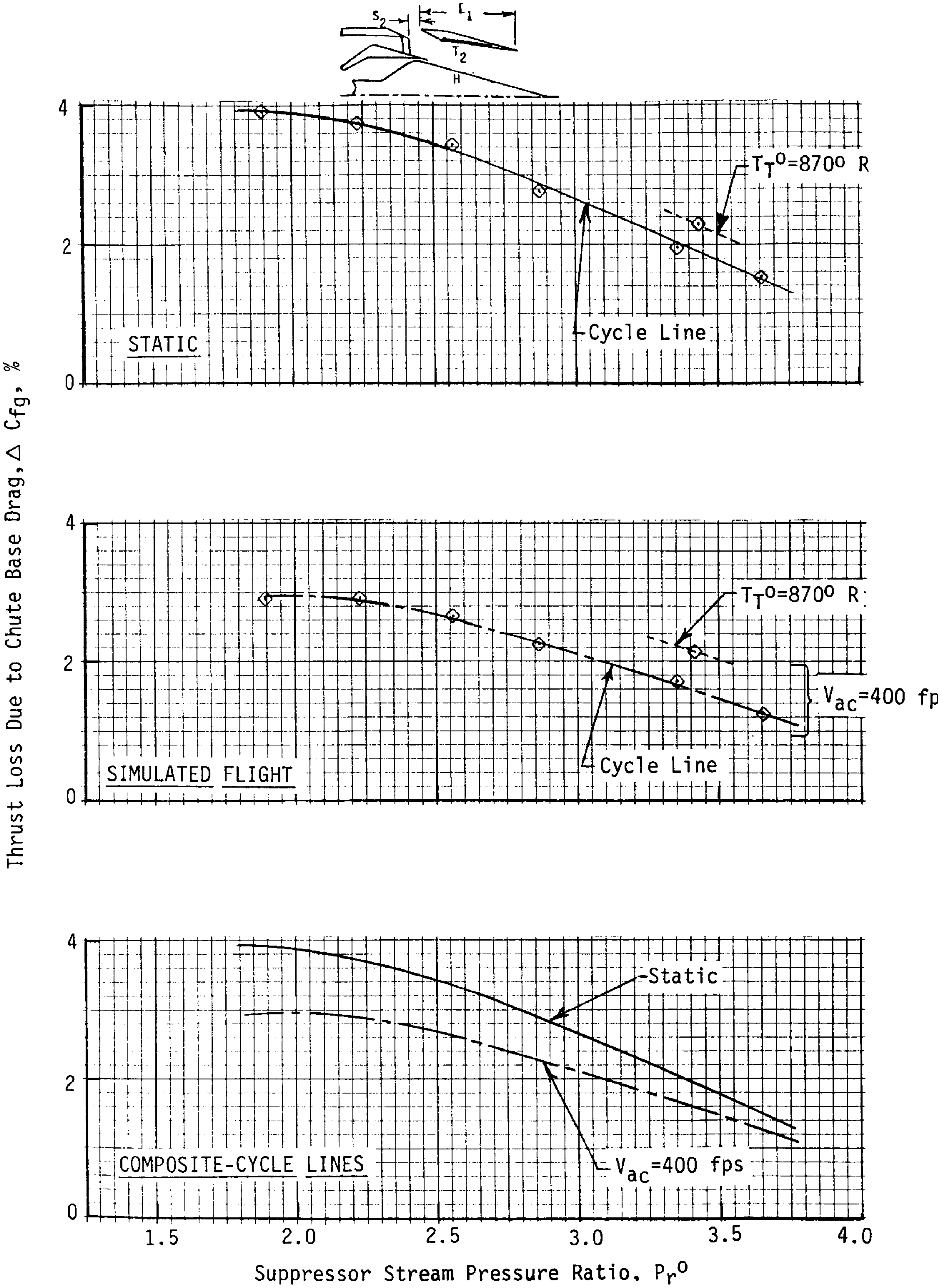

FIGURE 4-153. THRUST LOSS COEFFICIENT DUE TO CHUTE BASE DRAG OF CONFIGURATION TE-3

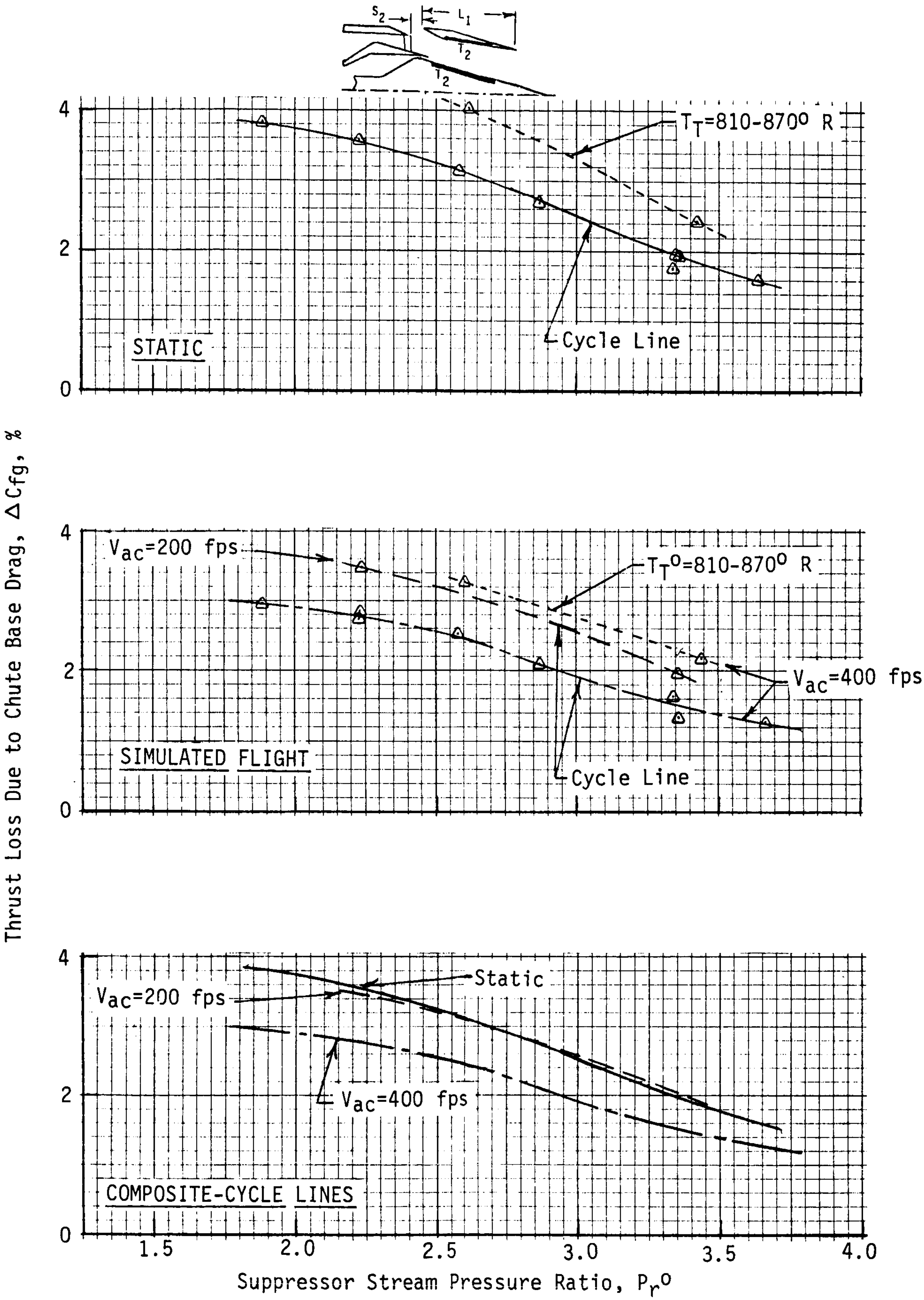

FIGURE 4-154. THRUST LOSS COEFFICIENT DUE TO CHUTE BASE DRAG OF CONFIGURATION TE-4

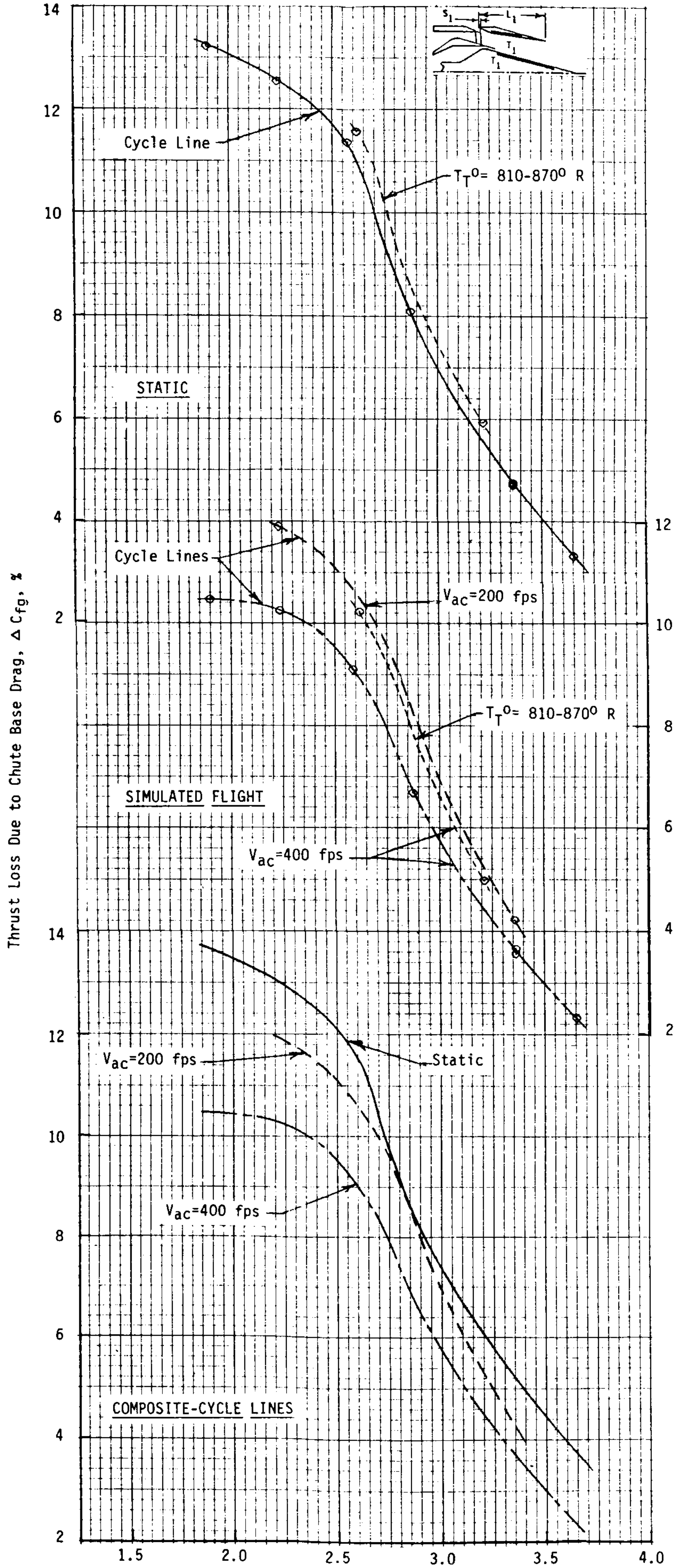

FIGURE 4-155. THRUST LOSS COEFFICIENT DUE TO CHUTE BASE DRAG OF CONFIGURATION TE-5

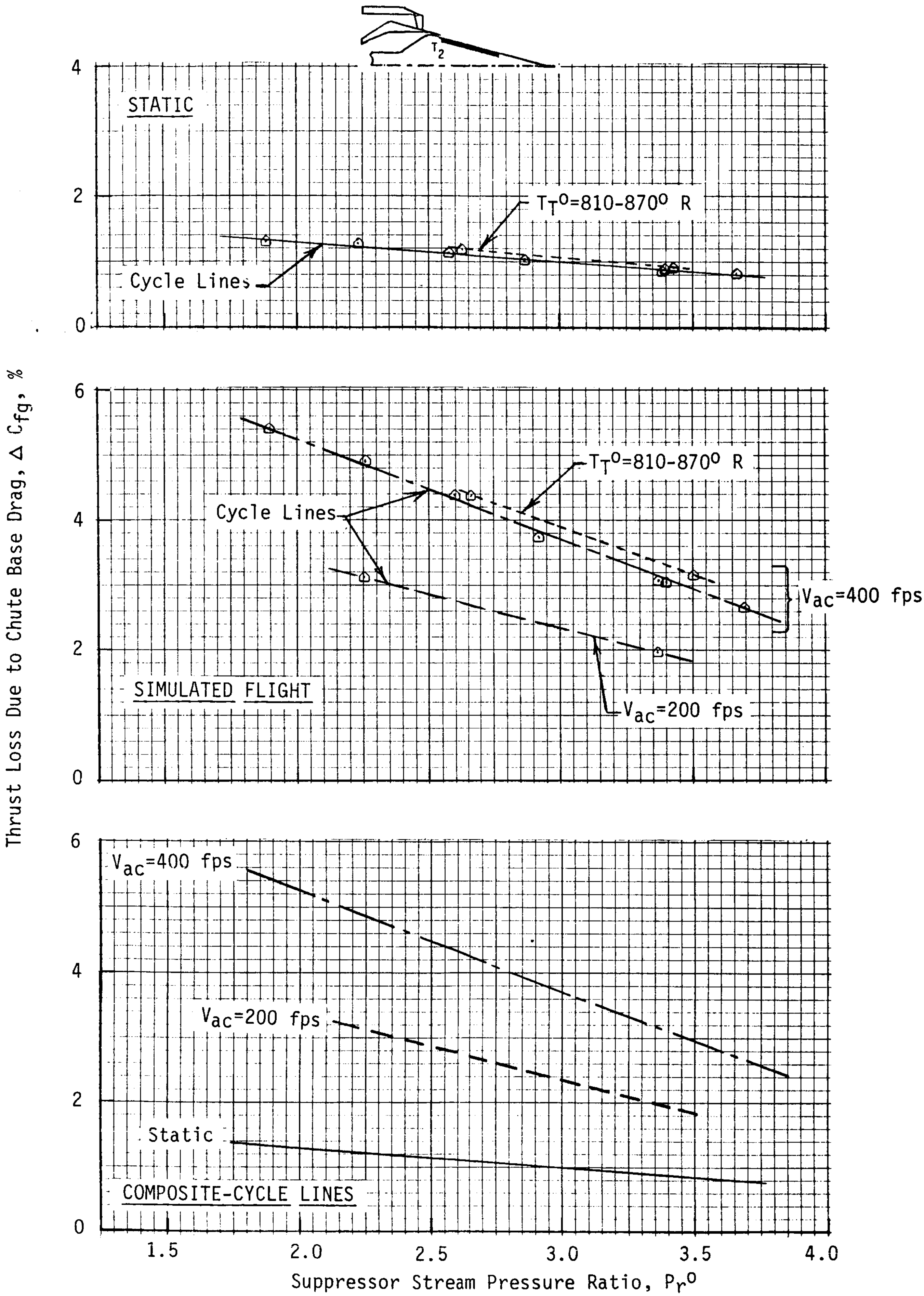

FIGURE 4-156. THRUST LOSS COEFFICIENT DUE TO CHUTE BASE DRAG OF CONFIGURATION TE-6

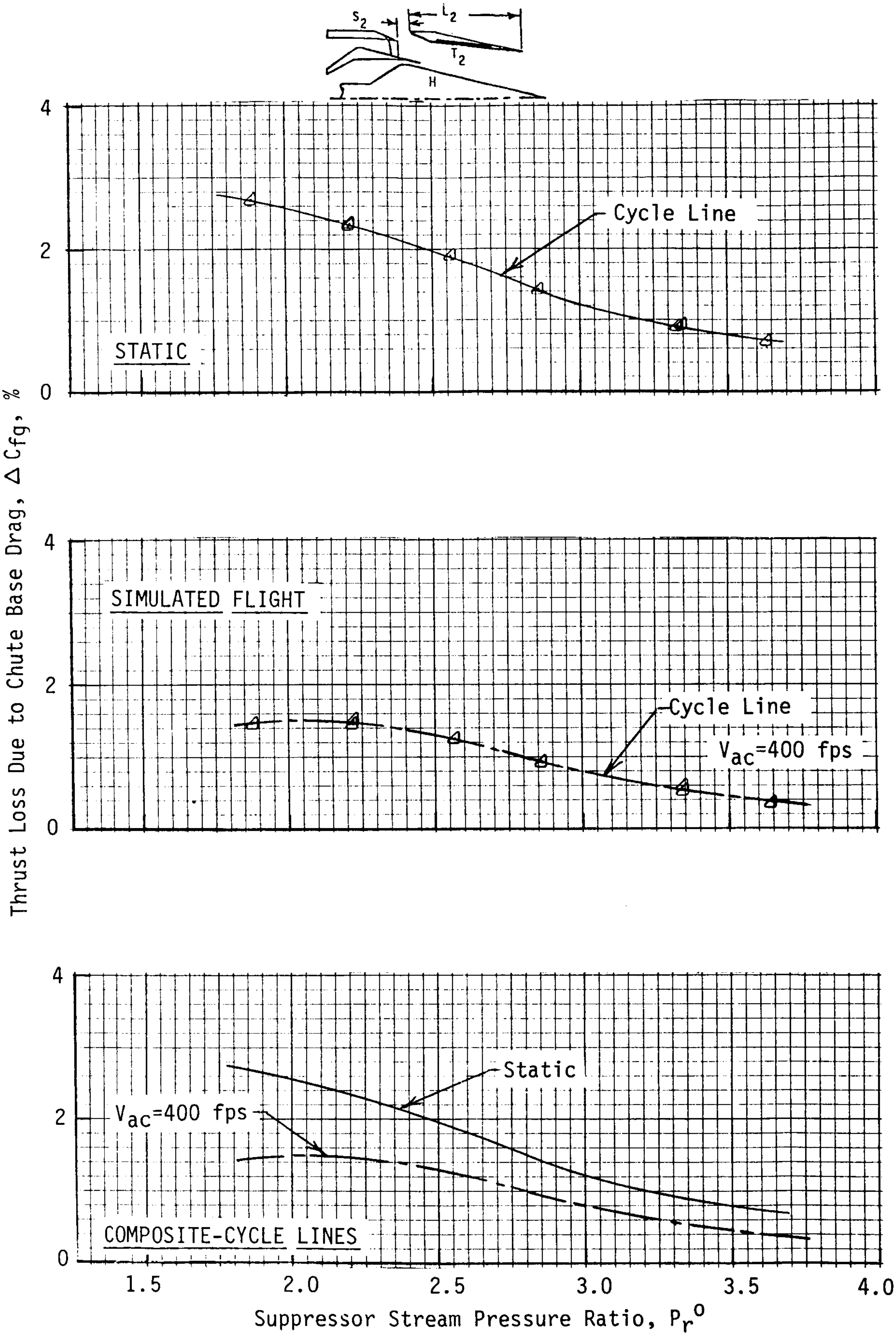

FIGURE 4-157. THRUST LOSS COEFFICIENT DUE TO CHUTE BASE DRAG OF CONFIGURATION TE-7

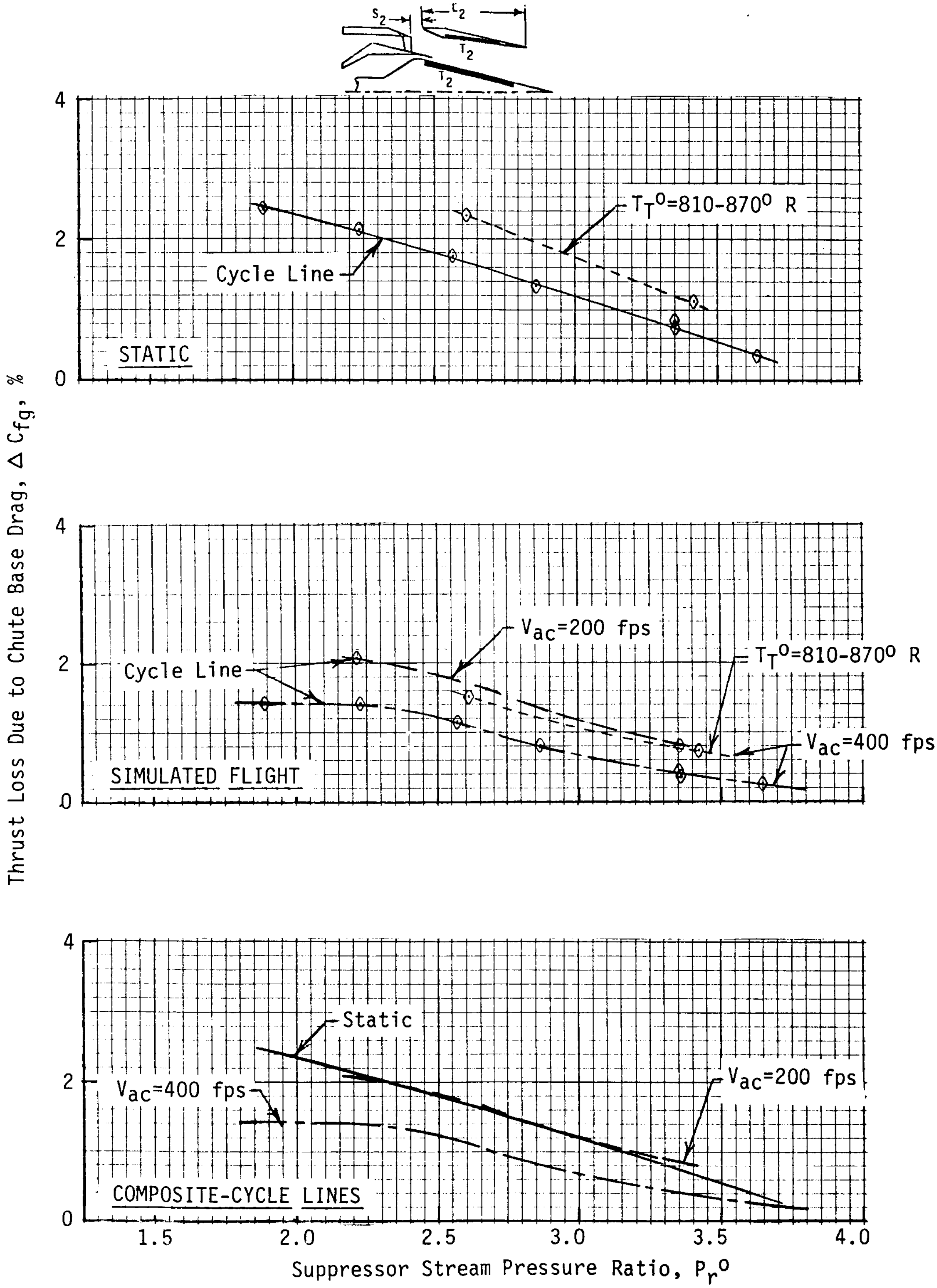

FIGURE 4-158. THRUST LOSS COEFFICIENT DUE TO CHUTE BASE DRAG OF CONFIGURATION TE-8

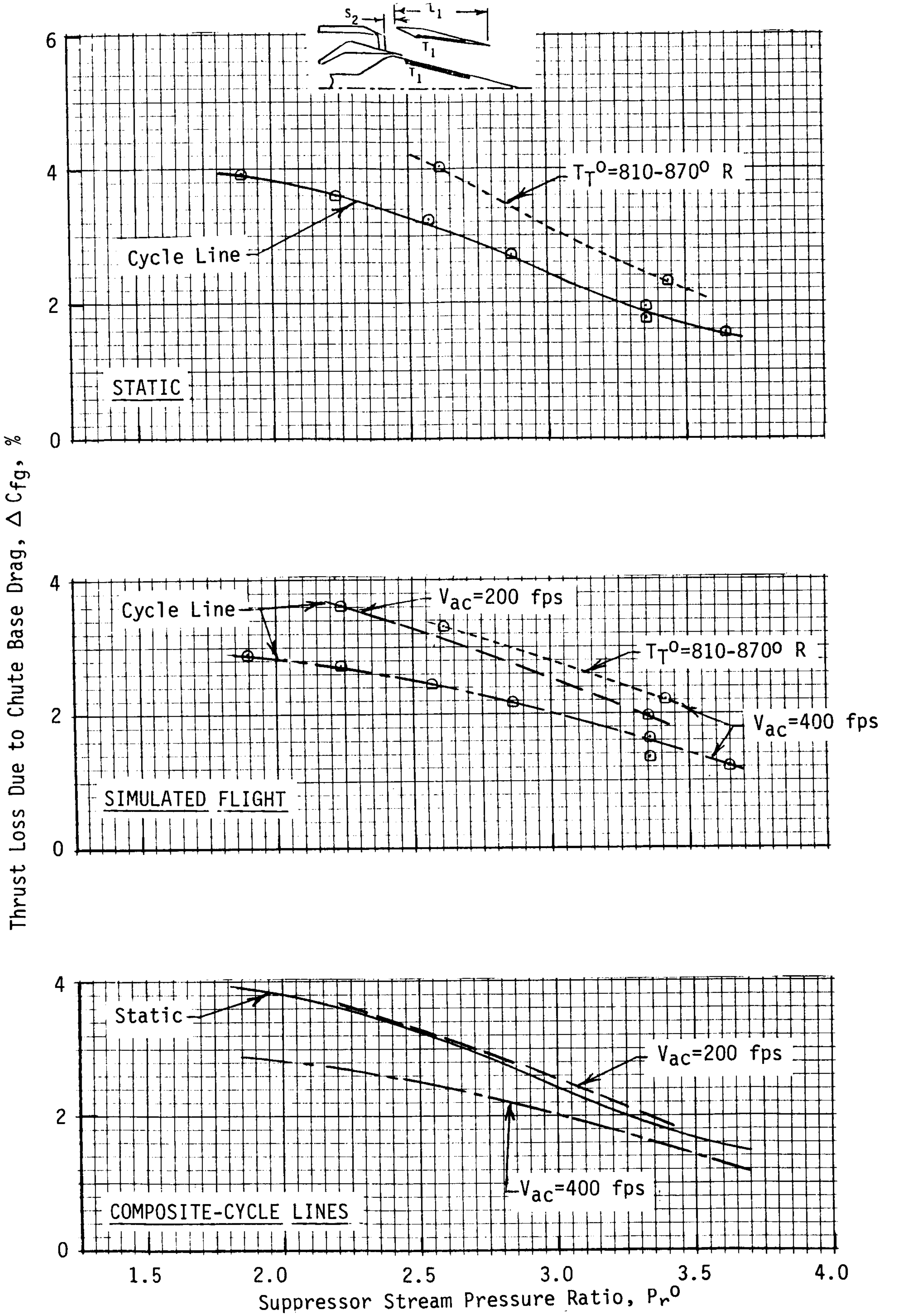

FIGURE 4-159. THRUST LOSS COEFFICIENT DUE TO CHUTE BASE DRAG OF CONFIGURATION TE-9

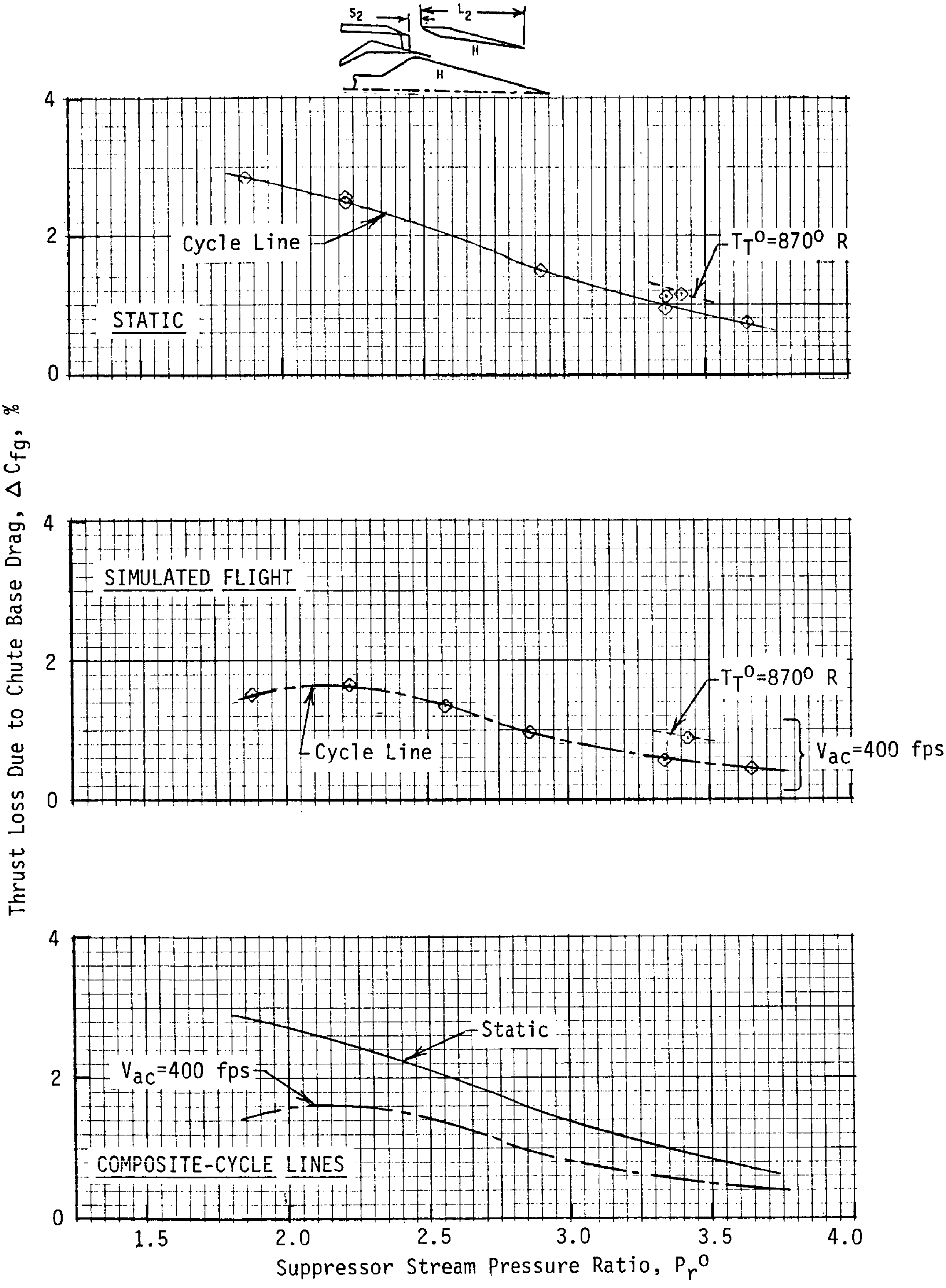

GURE 4-160. THRUST LOSS COEFFICIENT DUE TO CHUTE BASE DRAG OF CONFIGURATION TE-10

5.0 EJECTOR TREATMENT THEORY/EXPERIMENT CORRELATION

This section presents and discusses the theoretical modeling and correlation of predictions with measured data for the effect of the treated shroud upon farfield noise.

5.1 OBJECTIVE

The purpose of this study is to establish a method for predicting the suppression to be expected from a treated shroud when used in conjunction with the type of dual-flow, multi-element suppressor nozzle in this program. Basic parameters include treatment impedance, length, and placement (i.e., shroud-only versus shroud-and-plug surfaces); and, nozzle exit temperature, pressure, and velocity. Measured data from the experimental program are used to establish the validity of the method.

5.2 PREDICTION METHOD FOR THE EFFECT OF THE SHROUD, HARDWALL AND TREATED

The method includes prediction of source-location (to enable prediction of the effect of treatment on that portion of noise generated within the treated section of the shroud), duct-propagation effects (to estimate the treatment suppression in terms of the modal-energy-distribution within the shroud), and treatment impedance (under the conditions of temperature, pressure, and flow velocities within the shroud). The method is intended to be suitable for engineering selection of design values for the basic parameters of concern.

5.2.1 Effect of Shroud on Farfield Radiation

5.2.1.1 Original M*S Method

The number of variables and complexity of the problem impose a need to use a combination of both engineering-analysis and empirical correlation of data. That was done in developing the original M*S method, documented in Reference 25, which includes correlation of the effect of basic parameters on source-generation (level versus frequency) and source-location (level versus axial distance from the nozzle in each frequency band). The original method assumed a model for duct-propagation effects which provided a reasonable first approximation to measured suppression for single-layer resonator treatment and farfield radiation patterns. The correlation of this method with prior data, both hardwall and treated, is documented together with a detailed description of the method in Reference 25.

The following summarizes that portion of the original method concerned with determining the suppression by the treatment and the farfield directivity of that suppression. The data on the effect of adding treatment were correlated in terms of reduction of sound power level and one-third-octave band SPL spectra, and of farfield directivity. The suppression expected from the treatment was predicted analytically, using the source-location information developed in Reference 25, by means of ray acoustics, taking into account the absorption of energy for each interaction with the treatment. The analysis assumes that the ejector does not perturb the noise generation.

The acoustic ray model used in the analysis is illustrated in Figure 5-1. : consists of a line of 25 equally spaced sources, located axially from the ızzle exit station to 2.5 times the peak location downstream of the nozzle :it and located radially at the periphery of the outermost element. In a ıe-third-octave band, a range in relative levels from the peak to 8 dB below ıe peak is covered. Angles of incidence from 10° to 80° are used in 10° ıcrements, based on an omnidirectional source distribution, and the ːductions in PWL are determined for the upper and lower band limits and the idpoint frequency of all one-third-octave bands. To determine the total PWL ːduction, the number of reflections of the acoustic ray associated with an ıgle of incidence and source location are calculated based on the ejector ːngth and diameter. The power reduction for each reflection is determined and ıen summed over all reflections. This is repeated for each source location, ıd, taking into account the relative level of each source, the reduction is ımmed over all sources. The reduction is summed over each angle of incidence) determine the total power reduction for each frequency. By antilogarith-ically averaging the reduction at the lower limiting, midpoint, and upper imiting frequencies, the reduction over a one-third-octave band is estimated.

To determine the reduction due to each reflection within the ejector, the reatment resistance and reactance must be known at the lower limiting, idpoint, and upper limiting frequencies of a given one-third-octave band. ıe reduction in sound power level (PWL) is determined using the following two ıuations:

$$\alpha_a = \frac{4R \cos(\theta_i)}{(1+R\cos\theta_i)^2 + (X\cos\theta_i)^2} \qquad (1)$$

where: α_a = absorption coefficient

R = normalized specific resistance

X = normalized specific reactance

θ_i = incidence angle, as defined on Figure 5-1

ORIGINAL PAGE IS OF POOR QUALITY

$$\Delta PWL = -10 \log_{10} (1-\alpha_a), \text{ dB} \qquad (2)$$

n the case of SDOF treatment, a routine to determine the resistance and eactance is included in the original program. For other treatment materials, he resistance and reactance values can be input independently.

To convert this reduction in PWL to a reduction in SPL in the farfield, he directivity must be known. Figure 5-2 shows an example of the effect of a reated ejector. The change in SPL relative to the hardwall ejector is reatest and approximately constant where the hardwall ejector reduction in PL is smallest (70° to 120°), Reference 25. At other angles, the change in PL due to treatment is smaller but constant with angle. Data from references isted in Reference 25 have been used to develop the directivity correlation hown in Figure 5-2 and typical data are plotted on the figure to show epresentative correlation.

For angles of θ_c - 50° to θ_c (θ_c is the critical refraction angle per eference 25) $\Delta SPL = 1.2 \times \Delta PWL$. For all other angles, $\Delta SPL = 0.6 \times \Delta PWL$.

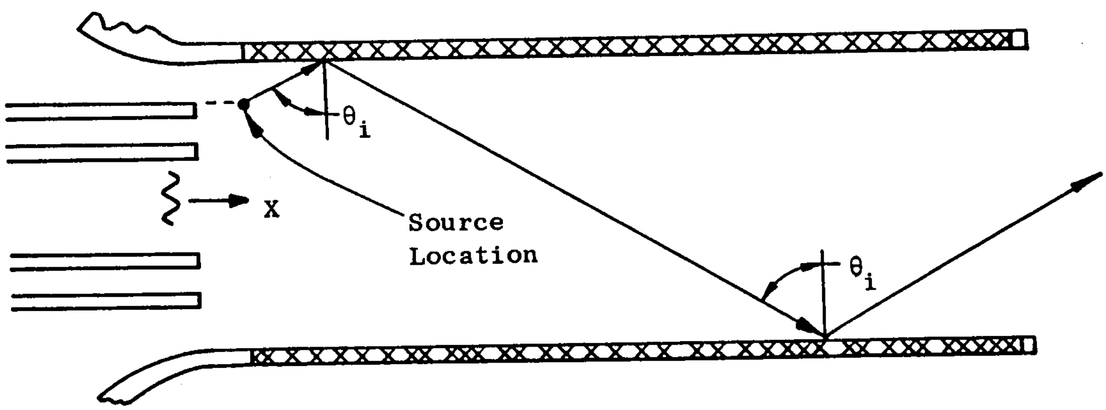

FIGURE 5-1 ACOUSTIC RAY ANALYSIS FOR TREATED EJECTOR

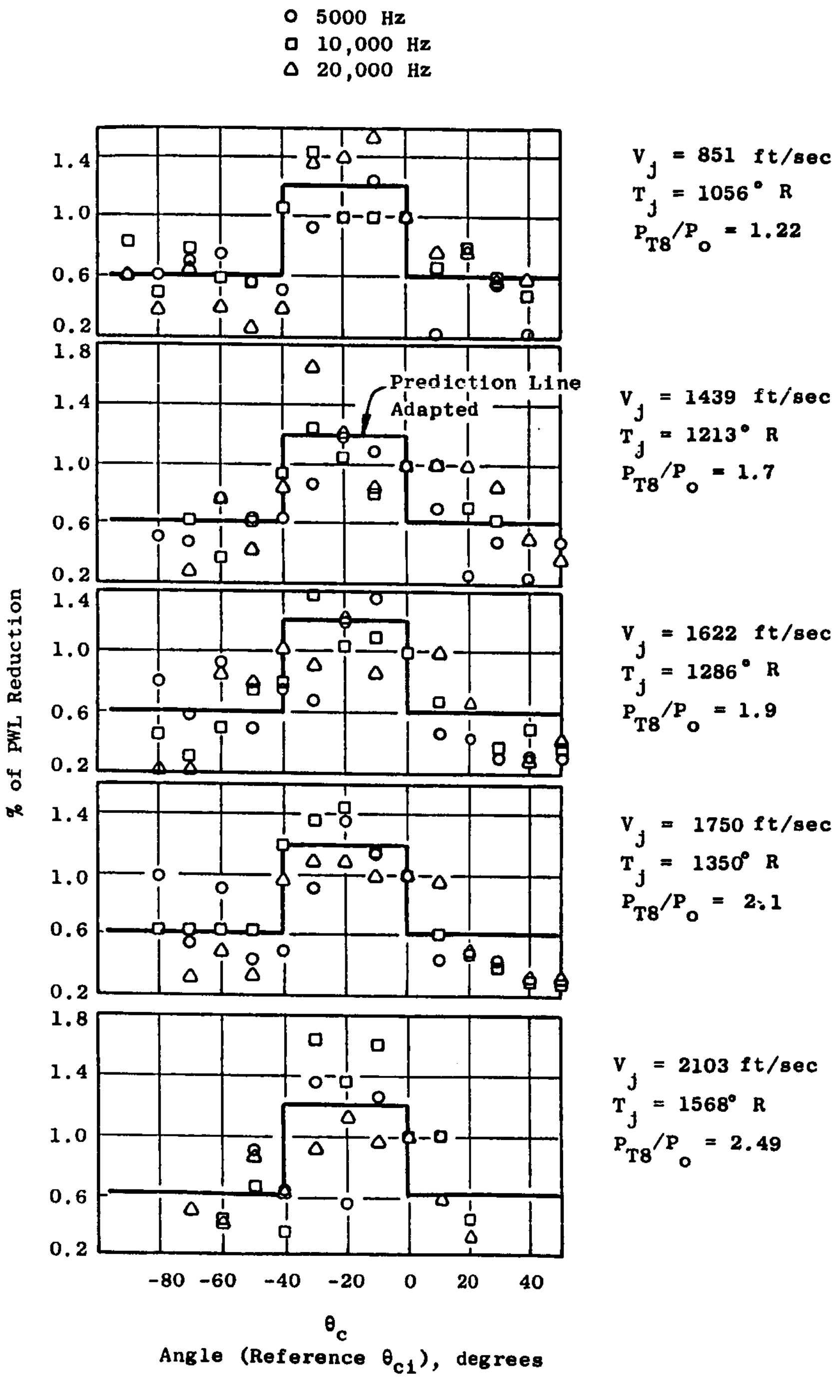

FIGURE 5-2 DIRECTIVITY CORRELATION FOR EJECTOR TREATMENT EFFECTS

5.2.1.2 Improvements Incorporated in this Program

The original M*S method had a simplified model for duct propagation and was limited to treatment of the shroud surface only, not including the plug.

Since the original formulation, an improved analytical model has been developed for this program, based on References 26, 27, and 28 to handle annular geometry and to estimate the modal weighting function of all modes that can propagate. This improved model enables a better estimate of the energy attenuation of the treatment, because of its improved estimate of modal energy density and the effect of airflow Mach number.

The model incorporates a rectangular duct approximation to annular geometry which provides a very close approximation to annular duct eigenvalues when the annular hub-to-tip ratio is in the range of approximately 0.5 to 1.0. These eigenvalues determine the mode indices which then enable estimation of the cut-on-ratio parameter developed by Rice and Sawdy, Reference 29. The development of the rectangular duct approximation is based upon the coordinant systems defined in Figure 5-3. In an annular duct of inner radius r_1 and the outer radius r_2, the sound propagating in the duct is represented by:

$$p(r,\theta,x,t) = \sum_m \sum_n \left\{ A_{mn} J_m(k_r^{mn} \cdot r) + B_{mn} Y_m(k_r^{mn} \cdot r) \right\} e^{i(\omega t - k_x^{mn} \cdot x)} \quad (3)$$

where $J_m($ $)$ and $Ym($ $)$ are Bessel functions of the first and second kinds of the integer order m respectively, and k_r^{mn} is the nth radial mode of the mth circumferential order (spinning mode of m diametral nodes). In a duct with uniform flow at Mach, M_0, the propagation wave number k_x^{mn} is related to the radial eigenvalue k_r^{mn} through the dispersion relationship:

$$k_x^{mn} = \frac{-M_0 k + \sqrt{k^2 - (1-M_0^2)\,(k_r^{mn})^2}}{(1-M_0^2)} \quad (4)$$

where $k = 2\pi f/c$, c = speed of sound, and f = frequency.

The cutoff ratio of the (mn) mode is defined as $k/\{R\ell(k_r^{mn})\sqrt{(1-M_0^2)}\}$ where $R\ell(k_r^{mn})$ represents the real part of k^{mn}. For the mode to propagate, the cut-off ratio must be greater than 1.

- Height, $H = (r_2 - r_1)$
- Hub-to-Tip Ratio, $HTR = (r_1/r_2)$

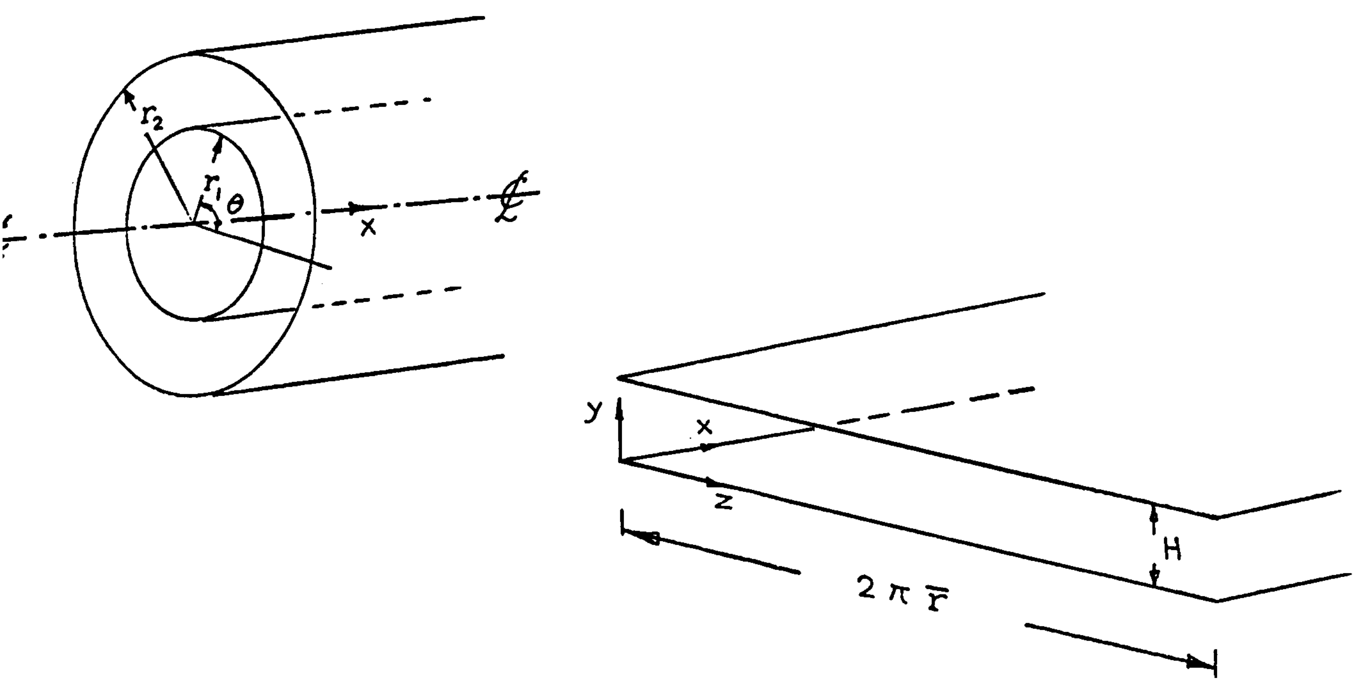

FIGURE 5-3 RECTANGULAR DUCT APPROXIMATION TO AN ANNULAR DUCT

Now, in a rectangular duct of height $H = (r_2 - r_1)$ and width $2\pi\bar{r}$, where $\bar{r} = \frac{(r_1+r_2)}{2}$, the pressure field can be represented by:

$$p(y,z,x,t) = \sum_{mn}\sum \{A_n \cos(k_y^n \cdot y) + B_n \mathrm{Sin}(k_y^n \cdot y) + C_m \mathrm{Cos}(k_z^m \cdot z) + D_m \mathrm{Sin}(k_z^m \cdot z)\} e^{i(\omega t - k_x^{mn} \cdot x)} \qquad (5)$$

the axial wave number, K_x^{mn}, is related to the transverse eigenvalues, K_y^n and K_z^m as follows:

$$k_x^{mn} = \frac{-M_o k + \sqrt{k^2 - (1-M_o^2)(K^{mn})^2}}{1-M_o^2} \qquad (6)$$

where: $(K^{nm})^2 = (k_y^n)^2 + (k_z^m)^2$

$k_y^n = \frac{\pi n}{H}$

$k_z^m = \frac{m}{\bar{r}}$

n = radial mode index = 0, 1, 2, ..., n

m = circumferential mode index = 0, 1, 2,..., m

Based on the geometry defined in Figure 5-3, these equations simplify to:

$$K^{mn}H = \sqrt{(\pi n)^2 + \left[2\left(\frac{1-HTR}{1+HTR}\right)m\right]^2} \qquad (7)$$

and the "Cut-off-Ratio" as defined in Reference 29 becomes, for the hardwall:

$$C.O.R. = \frac{k}{K^{mn}\sqrt{1-M_o^2}} = \frac{2\pi\eta_y}{K^{mn}H\sqrt{1-M_o^2}} = \left(\sqrt{\left[\left(\frac{n}{2\eta_y}\right)^2 + \left(\frac{m}{\eta_z}\right)^2\right]\left(1-M_o^2\right)}\right)^{-1} \qquad (8)$$

where: $\eta_y = Hf/c$ and $\eta_z = 2\pi\bar{r}f/c$

f = sound frequency, Hz

c = speed of sound

This specifies the cut-off-ratio in terms of geometry and the modal indices, m and n.

The degree of agreement for the rectangular versus exact solution is summarized in Table 5-1: for the hub-tip-ratio, HTR, equal to or greater than 0.5 the agreement is very good. Nevertheless, even at lower values of the ratio, this method is an improvement over the original.

In the modification to the M*S program, this approach was implemented to allow calculation of treatment either on the inner wall of the shroud, only, as in the original M*S, or on both the shroud and the plug. The geometry of the ray-acoustics model is given in Figure 5-4.

Equation (8) is used to determine the number of propagating modes. Propagation occurs only for C.O.R. $>$ 1. Then the maximum number of modes are determined (from Equation (8)) by:

$$\text{for } n = 0 \qquad m_{max} = \eta_z \sqrt{1-M_o^2} \qquad (9)$$

$$\text{for } m = 0 \qquad n_{max} = 2\eta_y / \sqrt{1-M_o^2} \qquad (10)$$

Also, the ray angle is closely approximated by (Reference 30):

$$\Theta = \sin^{-1}(1/\text{C.O.R.}) \qquad (11)$$

A modal-weighting-function was derived by counting the modes in each 10° increment from 0° through 90° and dividing by the number of modes that would have been in the increment if the distribution had been uniform (i.e., total number divided by nine). This function was used to modify the original assumption of an omnidirectional source; otherwise, the same approach was used as in the original analysis, with the geometric model of Figure 5-4 rather than 5-1, and with the flow effects added to the propagation model.

The algorithm incorporating these improvements is included in Appendix A.

5.2.2 Acoustic Treatment Impedance Prediction

A complete description of the experimental and theoretical work carried out to define the designs of the acoustic treatment used in the models tested in this program, is included in the CDR Volume II Appendix B: it is the GE Report TM 84-395, "Acoustic Treatment Design for the AST Shroud (NASA Contract Number NAS3-23275)" by A.A. Syed. This document includes chapters on: prediction methods for bulk absorber impedance; measured impedance data for the Astroquartz material used in the models; in-situ measurements of the propagation constant of the Astroquartz material in a duct with airflow; and, design of the AST shroud treatment.

Impedance prediction was done by the Delany and Bazley method (Reference 31). Extensive measurements were made, and documented in Reference 4, of the Astroquartz D.C. flow resistance and Normal Impedance and compared with predictions from two methods: a "multi-degree-of-freedom method", and the Delaney and Bazley method. Based on the overall agreement for a large range of test parameters, the Delaney and Bazley method was adopted for this program.

TABLE 5-1

COMPARISON OF THE PROPAGATING WAVE NUMBERS FOR ANNULAR SOLUTION AND RECTANGULAR DUCT APPROXIMATION

PROPAGATING WAVE NUMBERS

MODAL INDICES		HTR EXACT SOLUTION 0.25	0.5	0.75	APPROXIMATION 0.25	0.5	0.75
m	n	(k_r^{mn} · H)			(K^{mn} · H)		
0	1	3.337	3.195	3.15	3.142	3.142	3.142
	2	6.403	6.321	6.287	6.283	6.283	6.283
1	0	1.237	0.68	0.287	1.2	0.666	0.286
	1	3.758	3.285	3.167	3.36	3.211	3.154
	2	6.607	6.355	6.295	6.397	6.318	6.290
2	0	2.257	1.345	0.575	2.4	1.333	0.571
	1	4.77	3.535	3.205	3.95	3.413	3.193
	2	7.222	6.475	6.315	6.726	6.423	6.309
16	0	13.552	9.035	4.475	19.2	10.66	4.57
	1	17.45	11.63	5.7	19.45	11.12	5.54

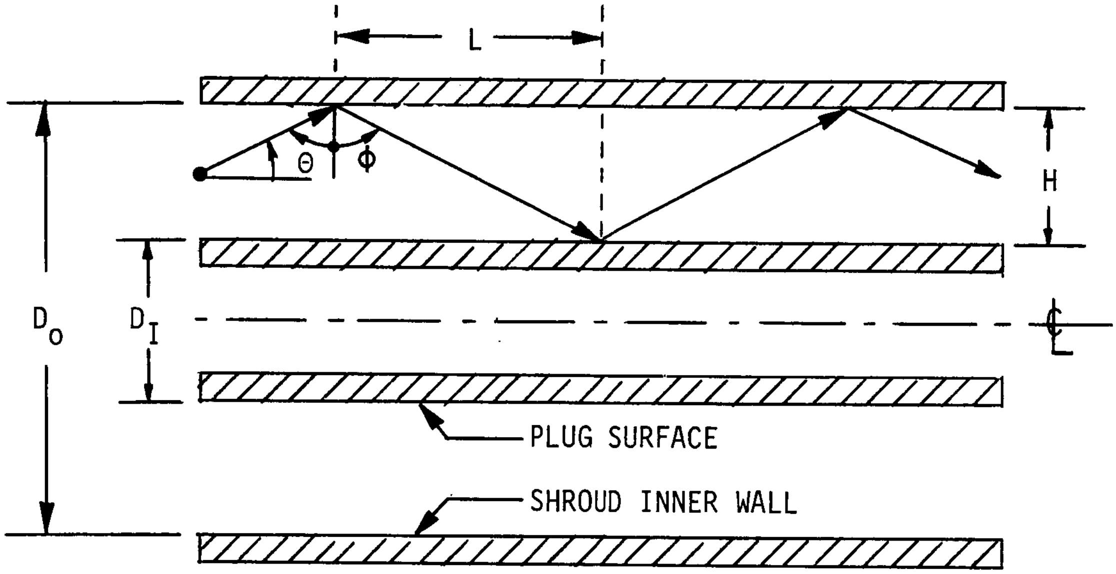

$$H = D_O \times \frac{(1\text{-}HTR)}{NST}$$

$$L = H \times \tan \Phi$$

HTR = Hub-Tip-Ratio = D_I/D_O

NST = Number of Sides Treated

= 1 for Outer Wall Treated

= 2 for Both Sides Treated

FIGURE 5-4 GEOMETRY OF THE IMPROVED RAY-ACOUSTICS MODEL

The in-situ measurements of the effect of grazing flow indicated there may be some influence but no significant impact on the acoustic properties in the first 1.27cm.

The design selection was made with the intent to achieve acoustic resistance of approximately 1 ρc and reactance as close to zero as possible over the frequency range of interest for the temperature and pressure of the test conditions. The analytical method described in Reference 4 was used to extrapolate from lab to model-test conditions; related experience with other treatment design applications at elevated temperature and pressure, using linear materials (resistance dependent upon air viscosity), has indirectly confirmed the validity of this analytical method.

Because the test conditions depended upon the simulated engine power settings, two designs were selected to achieve or bracket the intended values of acoustic impedance. In both cases, the thickness of the model treatment panel was 1.016 cm (0.4 inch); the first design was an Astroquartz density of 0.0160 gm/cc (1.00 lb/cu.ft.) and the second was 0.0401 gm/cc (2.50 lb/cu.ft.). The laboratory values of D.C. flow resistance for these two designs were 12.5 and 41.0 Rayls (cgs), respectively.

Evaluation of the measured temperatures and pressures during the model testing indicated that a range of conditions should be considered, including those listed in Table 5-2. The resulting impedance predictions for the two designs are in Tables 5-3 and 5-4. Design #1 (with a laboratory D.C. flow resistance of 41.0 Rayls (cgs) generally meets the design intent ($R/\rho c \cong 1.0$, $X/\rho c \cong 0.$) more uniformly than Design #2 (with a flow resistance of 12.5 Rayls). The effect of increasing temperature and pressure is seen to be relatively small, with Design #1 being less sensitive than Design #2.

5.3 SUMMARY OF MEASURED DATA AND COMPARISON WITH PREDICTION

Suppression data are included in Appendix C for all cases of interest, including hardwall shroud effects relative to the unshrouded exhaust system, and treatment effects relative to the hardwall shrouds (of both lengths). These data include power settings of "cutback", "intermediate", and "take-off".

For the theory-experiment comparison, data for 1/3-octave band PWL suppression are summarized in Tables 5-5 through 5-7 for "static" and 5-8 through 5-10 for "flight" conditions. Predicted suppression data are also shown in these tables, side-by-side with the measured data. The predictions were made with the revised M*S method, including the improved duct propagation analytical model. Predictions by the original version of the M*S where applicable, outer-wall treatment only, showed that there was essentially no difference between the original and revised model. The revised model is necessary, of course, to be able to predict the effect of treating the plug (both sides treated).

The measured data often shows positive or negative "suppression" at frequencies below 250 Hz, amounting to between 1/2 to 1 dB; this is probably an implicit indication of the data repeatability, and could be interpreted as a "tare" to be applied to the suppression in the frequency bands in which suppression is actually occurring.

TABLE 5-2

MODEL TEST CONDITIONS FOR IMPEDANCE PREDICTION

SHROUD LENGTH	POWER SETTING	TEST CONDITION TEMPERATURE (^{o}C)	PRESSURE (Atm)
Short	Cutback	340.	2.14
	Takeoff	427.	2.34
Long	Cutback	427.	2.34
	Takoeff	571.	3.0

TABLE 5-3

IMPEDANCE PREDICTIONS*, DESIGN #1 (41.0 RAYLS)

TEMPERATURE	340°C		427°C		571°C	
PRESSURE	2.14 ATM		2.34 ATM		3.00 ATM	
FREQUENCY (Hz)	$R/\rho c$	$X/\rho c$	$R/\rho c$	$X/\rho c$	$R/\rho c$	$X/\rho c$
50	0	-19.21	0	-20.75	0	-22.94
63	0	-14.85	0	-16.04	0	-17.74
80	0.11	-11.67	0.03	-12.61	0	-13.94
100	0.38	- 9.09	0.35	- 9.81	0.23	-10.85
125	0.57	- 7.01	0.57	-7.57	0.48	- 8.37
160	0.69	- 5.50	0.70	-5.94	0.64	- 6.57
200	0.77	- 4.30	0.79	-4.65	0.75	- 5.15
250	0.82	- 3.27	0.86	-3.53	0.83	- 3.92
315	0.86	- 2.53	0.89	-2.74	0.87	- 3.05
400	0.88	- 1.94	0.92	-2.11	0.90	- 2.36
500	0.90	- 1.45	0.94	-1.59	0.92	- 1.78
630	0.93	- 1.04	0.97	-1.15	0.95	- 1.31
800	0.97	- 0.73	1.01	-0.82	0.98	- 0.95
1000	1.03	- 0.46	1.07	-0.55	1.03	- 0.65
1250	1.14	- 0.25	1.16	-0.33	1.11	- 0.40
1600	1.29	- 0.15	1.30	-0.21	1.23	- 0.24
2000	1.44	- 0.20	1.44	-0.22	1.37	- 0.19
2500	1.40	- 0.40	1.43	-0.39	1.47	- 0.31
3150	1.16	- 0.41	1.23	-0.44	1.33	- 0.44
4000	1.06	- 0.22	1.08	-0.28	1.12	- 0.36
5000	1.17	- 0.20	1.15	-0.15	1.10	- 0.17
6300	1.10	- 0.21	1.15	-0.22	1.19	- 0.19
8000	1.10	- 0.14	1.08	-0.13	1.08	- 0.18
10000	1.06	- 0.13	1.09	-0.15	1.12	- 0.13

*For Full Scale Frequencies: Calculated for Scale Model Thickness

TABLE 5-4

IMPEDANCE PREDICTIONS*, DESIGN #2 (12.5 RAYLS)

TEMPERATURE	340°C		427°C		571°C	
PRESSURE	2.14 ATM		2.34 ATM		3.00 ATM	
FREQUENCY (Hz)	R/ρc	X/ρc	R/ρc	X/ρc	R/ρc	X/ρc
50	0	-17.67	0	-19.02	0	-21.00
63	0.21	-13.75	0.07	-14.79	0	-16.32
80	0.40	-10.89	0.30	-11.70	0.23	-12.90
100	0.51	- 8.56	0.45	- 9.18	0.41	-10.12
125	0.57	- 6.68	0.54	- 7.16	0.52	- 7.89
160	0.59	- 5.31	0.58	- 5.68	0.57	- 6.26
200	0.59	- 4.22	0.58	- 4.51	0.59	- 4.97
250	0.57	- 3.26	0.57	- 3.48	0.58	- 3.84
315	0.54	- 2.57	0.55	- 2.75	0.56	- 3.04
400	0.51	- 2.01	0.53	- 2.15	0.54	- 2.39
500	0.48	- 1.53	0.50	- 1.65	0.51	- 1.85
630	0.47	- 1.12	0.48	- 1.22	0.49	- 1.38
800	0.46	- 0.79	0.48	- 0.87	0.47	- 1.01
1000	0.47	- 0.48	0.48	- 0.56	0.47	- 0.68
1250	0.51	- 0.18	0.52	- 0.25	0.49	- 0.37
1600	0.61	0.11	0.60	0.02	0.55	- 0.09
2000	0.86	0.40	0.80	0.31	0.69	0.19
2500	1.55	0.43	1.35	0.46	1.07	0.47
3150	1.58	- 0.55	1.74	- 0.30	1.74	0.16
4000	0.80	- 0.41	0.94	- 0.52	1.26	- 0.62
5000	0.82	0.17	0.76	0.02	0.73	- 0.21
6300	1.38	- 0.24	1.39	0.05	1.08	0.26
8000	0.81	- 0.17	0.84	- 0.18	1.10	- 0.36
10000	1.11	- 0.26	1.27	- 0.05	1.00	0.17

*For Full Scale Frequencies: Calculated for Scale Model Thickness

TABLE 5-5 CUTBACK POWER, STATIC

ONE-THIRD OCTAVE BAND POWER LEVEL SUPPRESSION, dB

1/3 OB FREQ. (Hz)	SHORT SHROUD										LONG SHROUD					
			TREATMENT #1				TREATMENT #2						TREATMENT #2			
	HARDWALL		BOTH, S1+		BOTH, S2+		OUTER		BOTH		HARDWALL		OUTER		BOTH	
	M**	P**	M	P	M	P	M	P	M	P	M	P	M	P	M	P
63	1.4	0.2	0.2	0	0.4	0	-0.3	0	0.2	0	-0.8	0.2	0.8	0	0.8	0
80	1.3	0.5	0.1	0	0.3	0	-0.5	0	0	0	-1.0	0.5	0.7	0	0.6	0
100	1.5	0.9	0	0	0	0	-0.6	0	-0.1	0	-0.9	0.9	0.7	0	0.6	0
125	1.2	1.4	0.1	0	0	0	-0.5	0	0	0	-0.4	1.4	0.2	0	0.3	0
160	1.3	2.2	-0.2	0	-0.3	0	-0.6	0	-0.2	0	-0.6	2.2	0.5	0	0.4	0
200	1.5	3.1	-0.1	0.1	-0.5	0.1	-0.7	0.1	-0.2	0.1	-0.4	3.2	0.4	0	0.3	0
250	1.8	4.3	0	0.1	-0.4	0.1	-0.3	0	-0.1	0.1	0	4.3	0.8	0.1	0.5	0.2
315	2.7	4.7	-0.2	0.4	-0.7	0.2	-0.5	0.3	-0.2	0.3	1.3	4.8	0.6	0.4	0.3	0.5
400	4.2	5.1	-0.4	0.9	-0.8	1.0	-0.8	0.6	-0.3	0.7	3.0	5.2	0.7	0.8	0.5	1.1
500	6.1	5.9	-0.4	1.4	-0.6	1.4	-1.0	0.8	-0.5	1.0	4.9	6.0	1.0	1.2	0.8	1.5
630	7.3	6.1	-0.1	1.8	0.2	1.7	-0.7	1.2	-0.2	1.4	6.0	6.3	1.3	1.8	1.1	2.2
800	8.2	6.3	0.4	2.4	0.9	2.5	-0.3	1.7	0.6	1.9	7.4	7.5	1.8	2.5	1.5	3.0
1000	7.4	6.5	0.8	2.9	1.1	2.9	0.1	2.1	1.3	2.4	6.8	6.6	2.3	3.1	2.1	3.6
1250	6.6	6.5	1.2	3.5	1.2	3.5	0.4	2.7	1.5	2.9	6.2	6.7	2.4	3.7	2.4	4.1
1600	6.0	6.3	1.3	4.1	0.9	4.1	0.7	3.3	1.7	4.4	5.2	6.5	2.9	4.4	3.2	4.8
2000	6.1	5.9	1.5	4.2	0.4	4.2	1.0	3.7	1.9	3.9	4.6	6.0	2.7	5.4	3.6	5.8
2500	5.9	5.3	1.7	4.8	-0.2	4.7	1.1	4.7	1.8	4.8	4.5	5.4	2.1	6.2	3.9	6.4
3150	6.4	4.5	1.7	4.7	-1.1	4.7	0.5	4.7	1.4	4.8	4.4	4.7	0.8	6.8	3.8	6.9
4000	*	3.1	1.4	5.4	-1.4	5.4	-0.8	4.8	0.1	5.1	4.4	3.2	0.8	6.5	3.2	6.9
5000	*	1.0	1.3	5.8	*	5.7	*	5.2	-1.4	5.4	*	1.2	*	7.1	2.2	7.6
6300	*	-2.6	*	5.9	*	5.9	*	5.8	*	5.9	*	-2.5	*	8.5	0.5	8.8
8000	*	-3.3	*	6.6	*	6.6	*	6.2	*	6.4	*	-3.2	*	8.7	*	9.2
10000	*	-3.3	*	6.6	*	6.6	*	6.4	*	6.5	*	-3.2	*	8.8	*	9.3

*DATA NOT RELIABLE
**M = MEASURED, P = PREDICTED
+S1 = CLOSE SPACING; ALL OTHERS ARE AT S2 = WIDE SPACING

ONE-THIRD OCTAVE BAND POWER LEVEL SUPPRESSION, dB

1/3 OB FREQ. (Hz)	SHORT SHROUD										LONG SHROUD					
			TREATMENT #1				TREATMENT #2						TREATMENT #2			
	HARDWALL		BOTH, S1+		BOTH, S2+		OUTER		BOTH		HARDWALL		OUTER		BOTH	
	M**	P**	M	P	M	P	M	P	M	P	M	P	M	P	M	P
63	0.2	0.2	0.6	0	0.7	0	-0.2	0	0.6	0	-1.6	0.2	0.8	0	0.8	0
80	0.5	0.3	0.3	0	0.5	0	-0.3	0	0.5	0	-1.8	0.3	0.8	0	0.7	0
100	0.4	0.6	0.3	0	0.3	0	-0.2	0	0.4	0	-2.0	0.6	0.7	0	0.7	0
125	0.2	0.9	0.3	0	0.3	0	-0.3	0	0.2	0	-2.1	1.0	0.8	0	0.8	0
160	0.5	1.6	0.1	0	-0.3	0	-0.5	0	0.1	0	-1.7	1.6	0.9	0	0.9	0
200	0.2	2.4	0.1	0	-0.1	0	-0.1	0	0.3	0	-1.6	2.4	0.9	0.1	0.8	0.1
250	0.3	3.2	0.3	0.1	-0.2	0.1	0	0.1	0.4	0.1	-1.6	3.3	1.2	0.1	0.9	0.1
315	1.1	3.9	0.1	0.3	-0.4	0.3	-0.1	0.2	0.1	0.3	-0.8	4.0	1.1	0.2	0.8	0.3
400	2.3	4.9	-0.1	0.5	-0.5	0.5	-0.5	0.3	-0.2	0.4	0.7	5.0	1.2	0.5	0.8	0.6
500	3.9	5.4	-0.1	0.9	-0.7	0.9	-0.6	0.6	-0.2	0.7	2.0	5.6	1.7	0.8	1.2	1.0
630	5.1	5.8	-0.1	1.4	-0.5	1.4	-0.3	0.9	0	1.1	3.1	6.0	1.8	1.3	1.2	1.6
800	6.5	6.2	0.4	1.6	0	1.6	-0.2	1.1	0.5	1.3	5.0	6.4	2.2	1.9	1.6	2.1
1000	6.0	6.4	0.6	2.0	0.3	2.0	0.1	1.5	0.9	1.6	4.9	6.6	2.6	2.1	2.1	2.4
1250	5.6	6.2	1.0	2.1	0.3	2.1	0.5	1.7	1.4	1.8	4.4	6.4	3.3	2.7	2.8	2.9
1600	5.9	5.9	1.5	2.6	0.2	2.6	0.9	2.2	1.7	2.3	4.7	6.0	3.3	3.4	3.2	3.6
2000	5.7	5.6	1.8	2.6	-0.2	2.6	1.0	2.4	1.9	2.5	4.4	5.7	3.1	3.7	3.8	3.8
2500	5.3	5.2	1.5	3.0	-1.0	3.0	0.9	3.0	1.5	3.0	3.9	5.3	2.4	4.4	4.0	4.5
3150	5.2	4.4	1.3	3.0	-1.4	3.0	0.4	3.0	0.9	3.0	3.9	4.6	1.0	4.3	3.7	4.4
4000	5.8	3.4	0.7	3.1	-2.1	3.1	-0.8	2.9	-0.6	2.9	5.6	3.5	0.5	4.7	2.8	4.9
5000	*	1.8	1.1	3.8	*	3.8	*	3.5	*	3.6	*	1.9	*	4.9	1.1	5.2
6300	*	-1.1	*	4.1	*	4.0	*	4.0	*	4.0	*	-0.9	*	5.7	-0.7	5.9
8000	*	-3.5	*	4.1	*	3.9	*	4.0	*	4.0	*	-3.4	*	5.7	*	7.7
10000	*	-3.6	*	4.1	*	4.1	*	4.1	*	4.1	*	-3.4	*	6.4	*	6.6

*DATA NOT RELIABLE
**M = MEASURED, P = PREDICTED
+S1 = CLOSE SPACING; ALL OTHERS ARE AT S2 = WIDE SPACING

TABLE 5-7 TAKEOFF POWER, STATIC

ONE-THIRD OCTAVE BAND POWER LEVEL SUPPRESSION, dB

1/3 OB FREQ. (Hz)	SHORT SHROUD										LONG SHROUD					
			TREATMENT #1				TREATMENT #2						TREATMENT #2			
	HARDWALL		BOTH, S1+		BOTH, S2+		OUTER		BOTH		HARDWALL		OUTER		BOTH	
	M**	P**	M	P	M	P	M	P	M	P	M	P	M	P	M	P
63	-0.3	0.1	0.4	0	-0.8	0	-0.1	0	0.8	0	-1.4	0.1	0.4	0	0.6	0
80	-0.7	0.2	0.7	0	-0.6	0	0.1	0	1.1	0	-1.8	0.2	0.4	0	0.6	0
100	-0.7	0.2	0.9	0	-0.9	0	-0.2	0	1.2	0	-2.2	0.3	0.5	0	0.7	0
125	-1.7	0.5	1.5	0	-0.6	0	0.5	0	1.6	0	-2.7	0.6	0.7	0	0.6	0
160	-1.7	0.8	1.3	0	-1.1	0	0.3	0	1.5	0	-2.9	0.8	0.6	0	0.6	0
200	-1.6	1.3	1.1	0.1	-1.3	0	0.5	0	1.4	0.1	-2.9	1.4	0.6	0	0.5	0
250	-1.8	1.9	1.2	0.1	-0.9	0	0.7	0	1.5	0.1	-2.6	2.0	0.5	0	0.6	0
315	-1.5	2.6	1.2	0.2	-0.7	0.2	0.8	0.1	1.5	0.1	-2.3	2.7	0.6	0.2	0.5	0.2
400	-0.3	3.4	0.7	0.3	-1.0	0.3	0.3	0.2	1.2	0.2	-1.3	3.5	0.5	0.3	0.7	0.4
500	0.1	3.9	0.8	0.6	-0.9	0.6	0.4	0.4	1.2	0.5	-0.8	4.1	0.7	0.5	0.5	0.6
630	0.5	4.2	1.1	0.8	-0.2	0.8	0.7	0.5	1.6	0.6	-0.1	4.4	1.0	0.8	0.7	1.0
800	1.5	4.5	1.4	1.1	0.4	1.1	0.8	0.8	2.2	0.9	1.2	4.7	1.4	1.2	1.1	1.4
1000	2.4	4.4	1.3	1.3	0.6	1.3	0.8	1.0	2.5	1.1	2.3	4.6	1.5	1.4	1.3	1.6
1250	2.8	4.2	1.1	1.4	0.6	1.4	0.9	1.1	2.7	1.2	3.1	4.4	1.9	1.9	1.9	2.1
1600	2.5	4.2	0.9	1.7	0.3	1.7	1.1	1.4	2.4	1.5	3.3	4.4	2.1	2.0	2.3	2.2
2000	2.7	4.0	0.3	1.7	-0.8	1.7	0.8	1.5	1.8	1.6	2.8	4.2	1.9	2.2	2.6	2.3
2500	2.9	3.7	0.3	1.7	-0.9	1.7	0.9	1.6	1.3	1.7	2.4	3.9	1.4	2.7	2.9	2.8
3150	3.3	3.3	0.5	2.0	-1.0	2.0	0.5	2.0	0.9	2.0	2.5	3.5	0	2.8	2.6	2.8
4000	3.7	2.6	0.3	2.1	-1.4	2.1	-0.2	2.0	0.2	2.0	2.9	2.8	-0.8	2.9	1.4	3.4
5000	*	1.4	0.4	2.2	*	2.2	*	2.1	*	2.1	*	1.6	*	3.3	-0.4	3.4
6300	*	-0.7	*	2.3	*	2.3	*	2.3	*	2.3	*	-0.5	*	3.7	*	3.7
8000	*	-4.4	*	2.3	*	2.3	*	2.2	*	2.3	*	-4.2	*	4.8	*	3.9
10000	*	-5.1	*	2.4	*	2.4	*	2.3	*	2.4	*	-4.9	*	3.8	*	3.9

*DATA NOT RELIABLE
**M = MEASURED, P = PREDICTED
+S1 = CLOSE SPACING; ALL OTHERS ARE AT S2 = WIDE SPACING

ONE-THIRD OCTAVE BAND POWER LEVEL SUPPRESSION, dB

1/3 OB FREQ. (Hz)	SHORT SHROUD										LONG SHROUD					
			TREATMENT #1				TREATMENT #2						TREATMENT #2			
	HARDWALL		BOTH, S1+		BOTH, S2+		OUTER		BOTH		HARDWALL		OUTER		BOTH	
	M**	P**	M	P	M	P	M	P	M	P	M	P	M	P	M	P
63	2.0	1.2	0.9	0	0.4	0	-0.1	0	1.1	0	0.7	1.2	-0.1	0	-0.4	0
80	1.1	2.0	0.9	0	0	0	-0.2	0	0.4	0	-0.4	2.0	0	0	-1.4	0
100	0.1	2.8	0.5	0	0.1	0	0.0	0	0.2	0	-1.1	2.8	-0.2	0	-1.0	0
125	2.1	3.5	0.2	0	-0.8	0	-1.1	0	0.4	0	-0.2	3.5	0.7	0	-0.0	0.1
160	1.0	4.4	0.6	0	-0.3	0	-0.4	0	0.3	0	-0.5	4.4	0.1	0	0.7	0.1
200	0.5	4.7	0.6	0.1	-0.2	0	-0.1	0.1	0.3	0.1	-0.8	5.3	0.0	-0.1	0.6	0.1
250	0.6	6.0	0.6	0.2	0.4	0	0.1	0.2	0.4	0.2	-0.3	6.1	0.3	0.2	0.7	0.3
315	1.2	5.9	0.6	0.6	0.4	0.3	-0.1	0.4	0.5	0.5	1.1	6.1	-0.2	0.4	0.1	0.6
400	2.9	5.9	0.9	1.0	0.6	1.2	-0.5	0.7	0.1	0.8	2.4	6.1	-0.1	0.9	0.1	1.1
500	3.3	6.4	0.6	1.5	0.4	1.5	-0.3	0.9	0.1	1.1	2.9	6.5	0.5	1.3	0.6	1.7
630	4.5	6.5	0.9	1.8	0.3	1.8	-0.1	1.2	0.8	1.5	4.4	6.7	0.8	1.9	1.5	2.3
800	4.3	6.5	1.5	2.4	0.7	2.4	0.6	1.7	1.8	1.9	4.7	6.7	1.2	2.6	2.2	3.0
1000	3.7	6.8	2.2	2.9	1.1	2.8	1.4	2.1	2.3	2.3	4.6	7.0	1.9	3.0	3.1	3.5
1250	4.3	7.0	3.1	3.3	2.2	3.3	2.1	2.5	3.2	2.7	4.4	7.2	2.1	3.6	3.8	4.0
1600	5.1	6.7	3.1	4.0	1.8	4.0	2.4	3.2	3.1	3.4	4.4	6.9	2.4	4.4	4.4	4.8
2000	5.9	6.2	3.3	4.2	1.6	4.2	2.7	3.7	3.3	3.9	4.2	6.4	2.8	5.4	4.6	5.8
2500	6.6	5.5	3.5	4.8	1.1	4.7	2.9	4.7	3.5	4.7	4.7	5.7	2.3	6.2	4.1	6.4
3150	6.5	4.6	3.6	4.6	0.5	4.6	2.0	4.5	3.3	4.6	5.1	4.8	1.6	6,7	3.0	6.8
4000	6.0	3.3	4.2	5.0	0.6	4.9	0.7	4.4	2.5	4.7	4.8	3.4	0.4	6.0	2.0	6.4
5000	*	1.1	3.7	5.2	-0.4	5.2	-1.2	4.8	2.0	4.9	*	1.3	*	6.4	1.0	6.9
6300	*	-2.5	*	5.5	*	5.5	*	5.4	*	5.5	*	-2.3	*	7.8	*	8.1
8000	*	-3.1	*	6.1	*	6.1	*	5.7	*	5.9	*	-2.9	*	7.8	*	8.3
10000	*	-3.1	*	6.1	*	6.6	*	5.8	*	6.1	*	-2.9	*	7.9	*	8.4

*DATA NOT RELIABLE
**M = MEASURED, P = PREDICTED
+S1 = CLOSE SPACING; ALL OTHERS ARE AT S2 = WIDE SPACING

TABLE 5-9 INTERMEDIATE POWER, FLIGHT

ONE-THIRD OCTAVE BAND POWER LEVEL SUPPRESSION, dB

1/3 OB FREQ. (Hz)	SHORT SHROUD										LONG SHROUD					
			TREATMENT #1				TREATMENT #2						TREATMENT #2			
	HARDWALL		BOTH, S1+		BOTH, S2+		OUTER		BOTH		HARDWALL		OUTER		BOTH	
	M**	P**	M	P	M	P	M	P	M	P	M	P	M	P	M	P
63	*	0.8	0.1	0	0	0	-0.3	0	-0.2	0	-0.3	0.9	-0.1	0	0	0
80	0.9	1.4	0.2	0	-0.1	0	-0.5	0	-0.5	0	0.1	1.4	0.1	0	-0.1	0
100	1.5	1.9	0.1	0	-0.6	0	-0.6	0	-0.5	0	-1.2	2.0	0.2	0	0.1	0
125	0.7	2.6	0	0	-0.6	0	-0.8	0	-0.5	0	-0.7	2.6	0.3	0	0.4	0
160	1.4	3.6	0.2	0	0.2	0	-0.9	0	-0.8	0	-0.2	3.7	0.3	0	0.6	0
200	0.6	4.3	0	0.1	-0.2	0.1	-0.4	0	-0.3	0.1	0	4.4	0.3	0	0.4	0.1
250	1.1	4.8	-0.2	0.2	-0.2	0.1	-0.3	0.1	-0.7	0.2	0.3	4.9	0.1	0.2	0.3	0.2
315	1.4	5.1	-0.2	0.4	-0.2	0.4	-0.6	0.2	-0.7	0.3	1.1	5.2	0.2	0.3	0.2	0.5
400	2.1	5.7	-0.4	0.6	-0.2	0.6	-0.9	0.3	-0.8	0.5	2.0	5.9	0	0.5	0.3	0.7
500	3.0	6.0	-0.6	0.9	-0.4	0.9	-1.1	0.6	-0.7	0.7	2.8	6.1	0.5	1.0	0.5	1.2
630	3.7	6.2	-0.2	1.4	0	1.4	-1.2	0.9	-1.0	1.1	4.3	6.3	0.9	1.5	1.5	1.7
800	4.9	6.6	0	1.5	0.4	1.5	-1.2	1.1	-0.7	1.2	4.9	6.8	1.0	1.9	2.0	2.1
1000	5.2	6.9	-0.3	1.8	0.4	1.8	-0.2	1.3	-0.5	1.5	6.0	7.1	1.2	2.0	2.7	2.2
1250	6.2	6.6	1.3	2.0	1.6	2.0	-0.2	1.6	-0.8	1.7	5.8	6.8	1.5	2.6	3.4	2.8
1600	5.4	6.1	1.7	2.6	1.7	2.6	1.1	2.2	0.5	2.3	6.1	6.3	1.8	3.3	3.7	3.6
2000	5.7	5.7	1.1	2.6	1.1	2.6	1.7	2.3	0.6	2.4	6.8	5.9	1.6	3.6	4.0	3.7
2500	7.0	5.2	2.5	2.9	1.8	2.8	2.0	2.8	1.6	2.9	6.8	5.4	1.1	4.0	4.3	4.1
3150	7.9	4.3	2.9	2.6	1.1	2.6	1.8	2.6	1.8	2.6	6.1	4.4	0.8	3.8	3.5	4.8
4000	7.4	3.2	2.6	2.8	1.0	2.7	1.1	2.6	1.3	2.6	5.4	3.4	-0.3	4.0	2.8	4.2
5000	6.8	1.7	1.6	3.3	0.5	3.3	-0.9	3.0	1.0	3.2	5.3	1.8	*	4.3	1.7	4.5
6300	*	-1.1	*	3.6	*	3.6	*	3.6	*	3.6	*	-0.9	*	5.1	0.1	5.2
8000	*	-3.5	*	3.8	*	3.8	*	3.6	*	3.7	*	-3.3	*	5.2	*	5.3
10000	*	-3.4	*	3.7	*	3.7	*	3.6	*	3.7	*	-3.3	*	5.8	*	6.0

*DATA NOT RELIABLE
**M = MEASURED, P = PREDICTED
+S1 = CLOSE SPACING; ALL OTHERS ARE AT S2 = WIDE SPACING

TABLE 5-10 TAKEOFF POWER, FLIGHT

ONE-THIRD OCTAVE BAND POWER LEVEL SUPPRESSION, dB

1/3 OB FREQ. (Hz)	SHORT SHROUD										LONG SHROUD					
			TREATMENT #1				TREATMENT #2						TREATMENT #2			
	HARDWALL		BOTH, S1+		BOTH, S2+		OUTER		BOTH		HARDWALL		OUTER		BOTH	
	M**	P**	M	P	M	P	M	P	M	P	M	P	M	P	M	P
63	-0.2	0.4	1.1	0	-0.2	0	0	0	0.8	0	-0.5	0.4	0.2	0	-0.3	0
80	-0.2	0.7	1.2	0	-0.6	0	-0.4	0	0.4	0	-1.5	0.7	0.5	0	-0.3	0
100	-0.2	1.0	1.0	0	-1.0	0	-0.4	0	0.5	0	-1.5	1.1	0.3	0	-0.6	0
125	-0.4	1.5	0.8	0	-0.9	0	-0.3	0	0.4	0	-1.2	1.5	0	0	-0.6	0
160	0.2	1.8	1.1	0	-0.2	0	0.3	0	0.8	0	-1.2	1.9	0.2	0	-0.6	0
200	-1.0	2.4	0.9	0.1	-0.3	0.1	0.3	0	0.4	0	-1.5	2.5	0.3	0	-0.5	0.1
250	-1.3	2.9	0.5	0.2	-0.6	0.1	0	0.1	0.2	0.1	-1.0	3.1	0.3	0.1	-0.6	0.1
315	-1.0	3.4	0.6	0.2	-0.6	0.2	0.6	0.1	0.3	0.2	-0.8	3.5	0.5	0.3	-0.5	0.3
400	-0.7	3.8	0.7	0.4	-0.6	0.4	-0.3	0.3	0.3	0.3	0.1	4.0	0.2	0.4	-0.5	0.5
500	-0.1	4.1	0.9	0.7	-0.4	0.7	0	0.5	0.5	0.5	1.0	4.3	0.2	0.6	-0.3	0.7
630	0.4	4.5	1.1	0.8	-0.2	0.8	0	0.5	0.7	0.6	2.4	4.7	0.6	0.8	0	1.0
800	1.8	4.6	1.5	1.1	0.3	1.1	0.1	0.8	1.1	0.8	2.8	4.8	0.9	1.2	0.3	1.4
1000	2.1	4.4	2.4	1.2	1.2	1.2	1.1	0.9	2.1	1.0	3.9	4.6	1.8	1.4	1.5	1.6
1250	2.1	4.2	3.0	1.3	1.6	1.3	0.9	1.0	2.6	1.1	5.6	4.4	1.6	1.9	1.3	2.0
1600	2.8	4.0	2.9	1.7	1.0	1.7	0.7	1.4	2.2	1.4	6.6	4.2	1.7	2.0	1.9	2.1
2000	3.7	3.7	1.0	1.6	-1.1	1.6	-0.4	1.5	-0.1	1.5	6.0	3.9	1.7	2.1	2.5	2.2
2500	4.0	3.3	0.8	1.5	-0.3	1.8	0.2	1.5	-0.2	1.5	5.4	3.5	1.3	2.4	2.8	2.5
2150	4.1	2.9	0.4	1.8	-0.5	1.8	-0.5	1.8	-0.3	1.8	5.1	3.1	0.6	2.5	2.0	2.5
4000	4.3	2.2	0.3	1.9	0.4	1.9	-1.5	1.8	-0.7	1.8	4.4	2.3	-0.1	2.6	1.2	2.7
5000	3.7	1.0	1.4	2.0	-0.1	2.0	*	1.9	-0.4	1.9	4.5	1.2	*	2.9	0.1	3.1
6300	*	-1.0	*	2.1	*	2.1	*	2.1	*	2.1	*	-0.8	*	3.4	*	3.4
8000	*	-4.7	*	2.2	*	2.2	*	2.2	*	2.2	*	-4.5	*	3.6	*	3.7
10000	*	-5.3	*	2.2	*	2.2	*	2.1	*	2.2	*	-5.2	*	3.6	*	2.2

*DATA NOT RELIABLE
**M = MEASURED, P = PREDICTED
+S1 = CLOSE SPACING; ALL OTHERS ARE AT S2 = WIDE SPACING

5.4 DISCUSSION

The data in Tables 5-5 through 5-10 show remarkably good agreement between predicted and measured suppression for those frequency bands dominated by the mid-to-low frequency jet noise.

The largest suppression, both measured and predicted, occurs for the lowest power setting (cutback); it is less for the intermediate setting; and, least for takeoff. This trend is due to the shift of the source location further downstream as the nozzle exit Mach number increases so that there is less and less treatment length available between the local source location and the end of the shroud.

The hardwall shroud by itself suppresses the jet noise very effectively over the entire frequency range. This effect is predicted very well.

For the treated shroud, predicted and measured suppression is about the same for the two treatment designs. To a large extent, this is believed to be the result of relatively small differences in normalized impedances of the two designs under operating conditions and of axial variation of the temperature and pressure of the airflow within the shroud. The actual normalized impedances departed in localized areas significantly from these values tabulated in Tables 5-3 and 5-4 which are based upon the estimated average conditions listed in Table 5-2.

Relative benefits of the long versus short shroud and of treatment on the outer wall, only, versus on both walls, are predicted reasonably well.

At frequencies above 2000 Hz, the prediction of treatment suppression consistently is higher than the measured data. This discrepancy existed in the predictions by the original M*S method and is one of the main reasons that the improved analytical model, discussed in Section 5.2, was incorporated. The factor in the improved propagation model which was expected to improve this part of the correlation, was the effect of duct Mach number on the axial propagation constant, and the increase in modal cut-on-ratio associated with this factor. The discrepancies in the high frequency end of the spectrum did not show up in the original development of the M*S method because the correlation was made with treatment consisting of single-layer honeycomb with perforate facesheet, the so-called single-degree-of-freedom (SDOF) treatment, which had poor high frequency impedance properties. The Astroquartz bulk absorber used in this program, on the other hand, has near optimum impedance (particularly reactance) from 1000 Hz and above. That, in combination with the increasing number of higher-order modes with increasing frequency and with the source-location prediction that says the higher the frequency, the closer its source is to the nozzle exit plane, resulted in an increasing level of predicted suppression with increasing frequency.

This discrepancy in high frequency suppression, in fact, is probably a consequence of the gap between the nozzle exit plane and the beginning of the shroud. The highest frequencies are generated in close proximity to the nozzle and can very easily leak out that gap, which provides a flanking path that assumes more and more importance as the suppression of the shroud itself increases.

Overall, the suppression as predicted is the correct order of magnitude for the effects of the variations included in the comparisons of the Tables 5-5 through 5-10, and the algorithm in Appendix A is deemed a reasonably good method for engineering preliminary design studies.

6.0 CONCLUSIONS

This program, along with its companion aerodynamic performance investigation contract, NAS3-23038, was successful in establishing the chute-suppressor/ treated ejector system as a viable concept for AST/VCE application. A large acoustic and diagnostic measurements data base has been accumulated with pertinent results documented within this report. Detailed measurements are thoroughly documented within a two volume companion comprehensive data report (Reference 3) and stand ready for future developmental use, when required.

Within the design parameters investigated, the suppressor/ejector system has been found to allow substantially improved suppression levels, well beyond those attainable by the basic unejected coannular-chuted suppressor. The optimum-tested suppressor/treated ejector system allowed 2400 ft. sideline peak PNL suppression at takeoff of 11.4 ΔPNdB relative to a conic nozzle; a very significant 4.8 ΔPNL greater than the baseline 20-chute suppressor. Simulation flight EPNL for the same condition yielded 9.8 ΔEPNL for the suppressor/ejector system, an additinal 5.2 ΔEPNL above that of the unejected system.

Ejector performance at lower velocity, e.g., cutback cycle, is even more significant, 6.8 Δpeak PNL and 6.3 ΔEPNL additional suppression provided by the treated ejector/plug system. The retention of acoustic suppression effectiveness to very low operating cycles is uncharacteristic of most mechanical jet noise (unejected) systems previously investigated. Most follow the pattern where suppessor absolute noise levels approach those of the reference conical nozzle at low jet velocity. Retention of suppression at low cycles through ejector application offers a significant advantage for quiet part power, e.g., cutback, operation.

Other specific conclusions include the following:

- In comparing static to flight acoustic performance, the suppressor/ ejector system does not lose suppression nearly as rapidly as the unejected baseline suppressed nozzle.

- Application of the hardwall ejector, in itself, provides a major portion of the ejector system's suppression effectiveness, contributing significantly to both forward and aft quadrant suppression. Of major significance is that the forward radiated jet noise is still reduced substantially at all cycle conditions, even though aft quadrant suppression levels may diminish.

- Application of treatment to the ejector inner flowsurface is primarily effective within the longer ejector system, effectiveness being marginal within the shorter ejector length. The longer ejector with the single surface treatment is, however, seen primarily effective on suppression of forward quadrant radiated noise, peak noise angles being minimally effected.

- Addition of further treatment to the plug surface significantly improves suppression beyond that attained with just the ejector surface treatment.

- o Treatment design variation, within the limits evaluated with the bulk absorber Astroquartz material, was not critical to attained suppression levels.

- o Ejector length increase was primarily effective in further reduction of forward quadrant radiated noise; the aft quadrant peak noise levels showed mixed results relative to short versus long ejectors.

- o Axial location of the ejector system was very significant, the further aft location showing both aerodynamic base pressure (ΔC_{fg}) and acoustic suppression superiority. At takeoff cycle, nearly 2 dB increased suppression was noted for static and 1 dB for flight PNL using the further aft ejector location.

- o Use of a softwall plug surface as a pseudo-porous plug within an unejected/chute-suppressed nozzle showed no further reduction of forward quadrant shock associated noise, even though shock structure in the close vicinity of the plug surface was softened.

Of other major significance within the program was the updating of an existing computer coding to predict the suppression to be expected from a treated shroud used in conjunction with dual-flow multi-element suppressor nozzles. The original coding had a simplified model for duct propagation and was limited to treatment applied to the ejector surface only, not including the plug. The revised coding improved the analytical model to handle annular geometry and to estimate the modal weighting function of all modes that can propagate. This improved coding enables a better estimate of the energy attenuation of the treatment, because of its improved estimate of modal energy density and the effect of airflow Mach number. Comparisons of measured and predicted suppression levels, using the revised coding, showed very good agreement for many of the geometric and treatment design changes investigated.

Even though a significant acoustic data base was acquired and major advances were made in levels of suppression attainable, the suppressor/ejector system remains un-optimized in its maximum level of attainable suppression. The system was "optimized" only within the allowable range of parameters capable of investigation within the limited number of test configurations. Further investigation into certain aspects of ejector nozzle development will be beneficial in the future to enhance acoustic performance, particularly when a more exact aerodynamic cycle is selected for takeoff and cutback operation of a product AST/VCE. The revised predictive coding will also aid in pre-test optimization. Major technical goals yet to be achieved include development of high temperature acoustic treatments capable of sustained operation within the ejector environment.

7.0 NOMENCLATURE

a,c	Speed of Sound, m/s, f/s
A_{flow} = A8	Nozzle flow area, m^2, in^2
A_{chute}, $A_{blocked}$	Blocked area of chute, in^2
A^i	Chute elemental base area, in^2
A^T	Total chute base area, in^2
AST	Advanced Supersonic Technology
AVPT20	Test Cell Average Barometric Pressure, psia
C, ℄	Centerline
C/B	Cutback
CDR	Comprehensive Data Report
COR	Cut-off-Ratio
C_{fg}	Thrust Coefficient
Deq	Equivalent conical nozzle diameter based on total flow area, in.
D,d	Diameter, in
DLCCFG	Delta thrust coefficient, %
DMS	Data Management System
EPNL	Effective Perceived Noise Level, EPNdB
EPNLN	Normalized Effective Perceived Noise Level, EPNdB
f	frequency, Hertz
F	Thrust, Newtons, Lbs
FD	Total base drag of 20 chutes, Lb
FDCHUT	Base drag per chute, Lb
fps	feet per sec
F_{ref}	Reference thrust, 22820 Newtons, 5130 Lbs
FSUPR	Ideal thrust of outer stream (suppressor) nozzle, Lb
FTFSDR	Flight Transformed - Full Scale Data Reduction

H	Histogram or Hardwall surface of plug/ejector
hp	Horsepower
Hz	Hertz, Cycles per Sec
L	Radial distance of instrumentation item to nozzle centerline, in.
L1	Nominal length ejector
L2	Extended length ejector
LBM	Defined as 10 loα eff, where, $B^{eff} = \sqrt{(M_j^{eff})^2 - 1}$; $M_j^{eff} = \frac{2}{\gamma - 1}\left[(P_r^{eff})^{\frac{\gamma-1}{\gamma}} - 1\right]$: $P_r^{eff} = \frac{P_r^o A^o + P_r^i A^i}{A^o + A^i}$
LV	Laser Velocimeter
LVM	Defined as 10 log (Vj^{mix}/a_{amb})
M	Mach No.
NF	Normalization factor; defined as -10 log $\left(\frac{F}{F_{ref}}\right)\left(\frac{\rho}{\rho_{amb}}\right)^{\omega - 1}$, dB
Mc	Convection Mach No Relative to Nozzle
Mco	Convection Mach No Relative to Nozzle - Convection Mach No Relative to Observer
Mo	Convection Mach No Relative to Observer
M*S	Motsinger-Sieckman Prediction Method
OAPWL, PWL	Overall sound power level, dB re 10^{-12} watts
1/3 OBPWL	1/3 Octave band sound power level, dB re 10^{-12} watts
OASPL	Overall sound pressure level, dB re .0002 dynes/cm^2
OASPLN	Normalized overall sound pressure level, OASPL+NF, dB re .0002 dynes/cm^2
1/3 OBSPL	1/3 Octave band sound pressure level, dB re .0002 dynes/cm^2
P	Pressure, psia
P_{amb}	Ambient pressure, pascal, psia
PBAV	Chute average base pressure,psia
PNL	Perceived noise level, dB

PNLN	Normalized perceived noise level, PNL+NF, dB
P/R,Pr	Pressure ratio; defined as ratio of total to ambient
P_S, P_s^i,	Static pressure, psia
PRI,P_r^i	Inner nozzle pressure ratio
PRO,P_r^o	Outer nozzle pressure ratio
r_1	Inner duct radius, in
r_2	Outer duct radius, in
R	Radial distance to location of axial LV traverse, in, and normalized specific resistance
R_{hub}	Radius to hub of outer stream suppressor, in
R_{obs}	Distance from exhaust nozzle to microphone, ft
$R^t{}_s$	Radius of suppressor at the chute tip, in
R_{tip}	Radius to tip of outer stream suppressor, in
S1	Nominal position of ejector axial location
S2	Extended position of ejector axial location
Scfm	Standard cubic feet per minute
SDOF	Single degree of freedom
SPL	Sound pressure level, dB
SPLN	Normalized sound pressure level, SPL+NF, dB
T	Temperature, ^oK, ^oR, ^oF
T1	High density acoustic treatment design
T2	Low density acoustic treatment design
TE	Treated Ejector
T/O	Takeoff
T_S	Static Temperature, ^oF, ^oR
TTI, $T_T{}^i$	Total Temperature of inner flow, ^oR, ^oR
TTO, $T_T{}^o$	Total Temperature of outer flow, ^oR, ^oR
V	Velocity, n/s, f/s

V	Mean Velocity, m/s, f/s
V'	Turbulent Velocity, m/s, f/s
VABI	Variable Area Bypass Injector
VAC, $V_{a/c}$	Simulated flight velocity, m/s, f/s
VCE	Variable Cycle Engine
VJI, V_j^i	Inner stream velocity, m/s, f/s
VJO, V_j^o	Outer stream velocity, m/s, f/s
VJMIX, V_j^{mix}	Mixed stream velocity, m/s, f/s
W	Ideal calculated weight flow rate $K_{g/s}$, Lb/s
X	Normalized specific reactance
x	Axial distance of instrumentation item to ejector inlet surface, in, or, axial distance from exit plane of primary nozzle, in
x'	Axial distance from exit plane of ejector nozzle, in
α_a	Absorption coefficient
β	Shock strength parameter
γ	Ratio of specific heats
Δ	Delta
θ_c	Critical refraction angle, degrees
θ_i	Incidence angle, degrees
θ_I	Angle relative to inlet, degrees
ρ	Jet density
ρ_{amb}	Ambient air density
ω	Density exponent

SUPERSCRIPTS

i	Inner Jet (Nozzle) Conditions
mix,eff	Mass Averaged Conditions
o	Outer Jet (nozzle) Conditions

SUBSCRIPTS

ac,a/c	aircraft
amb	Ambient
fs	free-stream
j	jet
r	Ratio
ref	Reference
S	Static
T	Total (Stagnation)

8.0 REFERENCES

1. Wagenknecht, C.D. and Bediako, E.O., "Aerodynamic Performance Investigation of Advanced Mechanical Suppressor and Ejector Nozzle Concepts for Jet Noise Reduction", Contract NAS3-23038 - GE Final Tech. Report (R83AEB122-3), NASA CR-174860, Feb. 1985.

2. Wolf, J.P., "Preliminary Design of an AST Engine Exhaust System Incorporating an Ejector Shroud and a 20 Chute Noise Suppressor", NASA-GE Contract NAS3-23038, GE TM 82-219, April, 1982.

3. Brausch, J.F. and Hoerst, D.J., "Simulated Flight Acoustic Investigation of Treated Ejector Effectiveness on Advanced Mechanical Suppressors for High Velocity Jet Noise Reduction", Contract NAS3-23275 - GE Comprehensive Data Report R85AEB517, December, 1985.

4. Syed, A.A., "Acoustic Treatment Design for the AST Shroud (NASA Contract Number NAS3-23275)", GE TM No. 84-395, July, 1984.

5. Vogt, P.G., Bhutiani, P.K., and Knott, P.R., "Free-Jet Acoustic Investigation of High Radius Ratio Coannular Plug Nozzles", General Electric Company, Comprehensive Data Report, Volume I, R81AEG212, Contract NAS3-20619, January 1981.

6. Shields, F.D., and Bass, H.E., "Atmospheric Absorption of High Frequency Noise and Application to Fractional Octave Bands", University of Mississippi, NASA CR-2760, June 1977.

7. Knott, P.R., "Supersonic Jet Exhaust Noise Investigation", Volume I, Summary Report, AFAL-TR-76-68, July 1976.

8. Janardan, B.A., Majjigi, R.K., Brausch, J.F., and Knott, P.R., "Free-Jet Investigation of Mechanically Suppressed, High-Radius-Ratio Coannular Plug Model Nozzles", Final Technical Report for NASA-GE Contract NAS3-21608, GE TM No. R81AEG484, NASA CR-3596, May, 1985.

9. Yamamoto, K., Brausch, J.F., et. al., "Experimental Investigation of Shock-Cell Noise Reduction for Single Stream Nozzles in Simulated Flight", Final Technical Report for NASA-GE Contract NAS3-22514, NASA CR-3845, December, 1984.

10. Janardan, B.A., Yamamoto, K., et. al., "Experimental Investigation of Shock-Cell Noise Reduction for Dual-Stream Nozzles in Simulated Flight", Final Technical Report for NASA-GE Contract NAS3-23166, NASA CR-3846, November, 1984.

11. Hoch, R.E., Duponchel, J.P., Cocking, B.J., and Bryce, W.D., "Studies of the Influence of Density on Jet Noise", Journal of Sound and Vibration, Volume 28, Number 4, 1973, pp. 649-668.

12. Janardan, B.A., et. al., "Free-Jet Investigation of Mechanically Suppressed, High-Radius-Ratio Coannular Plug Model Nozzles", Comprehensive Data Report for NASA-GE Contract NAS3-21608, GE TM No. R81AEG484, May, 1981.

13. Blozy, J.T., et. al., "Acoustic and Aerodynamic Performance Investigation of Inverted Velocity Profile Coannular Plug Nozzles", Comprehensive Data Report for NASA-GE Contract NAS3-19777, GE TM No. R79AEG166, January, 1979.

14. Vdoviak, J.W., Knott, P.R., and Ebacker, J.J., "Aerodynamic/Acoustic Performance of YJ101/Double Bypass VCE with Coannular Plug Nozzle", Final Report for NASA-GE Contract NAS3-20582, GE TM No. R80AEG369, NASA CR-159869, January, 1981.

15. Gliebe, P.R., Motsinger, R.E., and Sieckman, A., "High Velocity Jet Noise Source Location and Reduction - Task 6 Supplement - Computer Programs: Engineering Correlation (M*S) Jet Noise Prediction Method and Unified Aeroacoustic Prediction Model (M*G*B) for Nozzles of Arbitrary Shape", GE TM No. R79AEG290, FAA Report No. FAA-RD-76-79, VIA, March, 1979.

16. Harper-Bourne, M., and Fisher, M., "The Noise From Shock Waves in Supersonic Jets", Proceedings of the AGARD Conference on Noise Mechanisms, Brussels, Belgium, AGARD CP131, 1973.

17. Brausch, J.F., Whittaker, R.W., Knott, P.R., "Acoustic and Aerodynamic Nozzle Performance Design Considerations for the NASA AST/VCE Core Drive (CDFS) Acoustic Nozzle Program", GE TM No. TM80-216, March, 1980.

18. NASA Technical Memo 78802, NASA-Langley, Initial Results of a Porous Plug Nozzle for Supersonic Jet Noise Suppression, Dr. Lucio Maestrello, November 1978.

19. AIAA 79-0653, An Experimental Study on Porous Plug Jet Noise Suppressor, L. Maestrello, NASA-Langley Research Center.

20. Stringas, E.J., "High Velocity Jet Noise Source Location and Reduction, Task 2 - Theoretical Developments and Basic Experiments", Report Number FAA-RD-76-79, II, October, 1977.

21. Tanna, H.K., "An Experimental Study of Jet Noise - Part II: Shock Associated Noise", Journal of Sound and Vibration, Volume 50, 1977, Pages 429-444.

22. Sardhia, V., "Some Flight Simulation Experiments on Jet Noise From Supersonic Under Expanded Flows, "AIAA Journal, Volume 16, 1978, Pages 710-716.

23. Knott, P.R., Janardan, B.A., et al, "Free-Jet Acoustic Investigation of High Radius-Ratio Coannular Plug Nozzles", NASA CR-3818, October, 1984.

24. Janardan, B.A., Majjigi, R.K., et al, "Experimental Investigation of Shock-Cell Noise Reduction for Dual-Stream Nozzles in Simulated Flight", NASA CR-3846, November, 1984.

25. Gliebe, P.R. Motsinger, R., and Sieckman, A., "High Velocity Jet Noise Source Location and Reduction, Task 3 - Experimental Investigation of Suppression Principles", Report Number FAA-RD-76-79, III-I (R78AEG627), December, 1978.

26. Syed, A.A., Private Communication, "3-D Rectangular Approximation to the Sound Propagation in an Annular Duct", February, 1981.

27. Mungur, P. and Plumblee, H.E., "Propagation and Attenuation of Sound in a Soft-Walled Annular Duct Containing Sheared Flow", Basic Aerodynamic Noise Research, NASA SP-207, Pages 305-372.

28. Yurkovich, R., Attenuation of Acoustic Modes in Circular and Annular Ducts in the Presence of Uniform Flow", AIAA Paper 74-552, June, 1974.

29. Rice, E.J. and Sawdy, D.T., "A Theoretical Approach to Sound Propagation and Radiation for Ducts with Suppressors", NASA TM 82612, May, 1981.

30. Rice, E.J., "Acoustic Liner Optimum Impedance for Spinning Modes with Mode Cut-Off Ratio as the Design Criterion", NASA TM X-73411, July, 1976.

31. Delaney, M.E. and Bazley, E.N., "Acoustical Properties of Fibrous Absorbent Materials", Applied Acoustics (3), 1970.

APPENDIX A

ALGORITHM FOR PREDICTING THE EJECTOR SUPPRESSION, HARDWALL AND TREATED

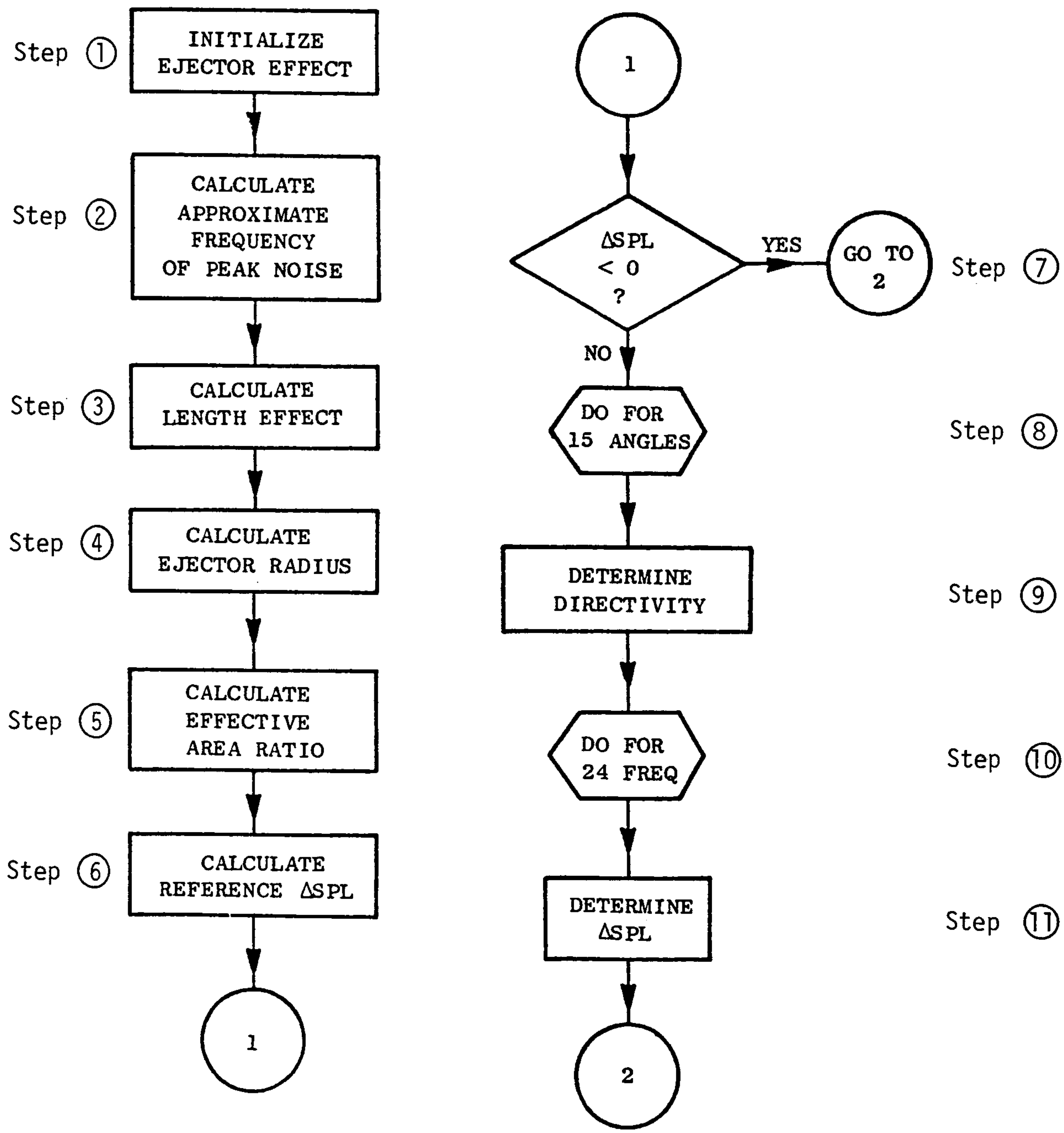

FIGURE A-1. ORIGINAL M*S ANALYSIS STEPS IN SUBROUTINE EJECTS

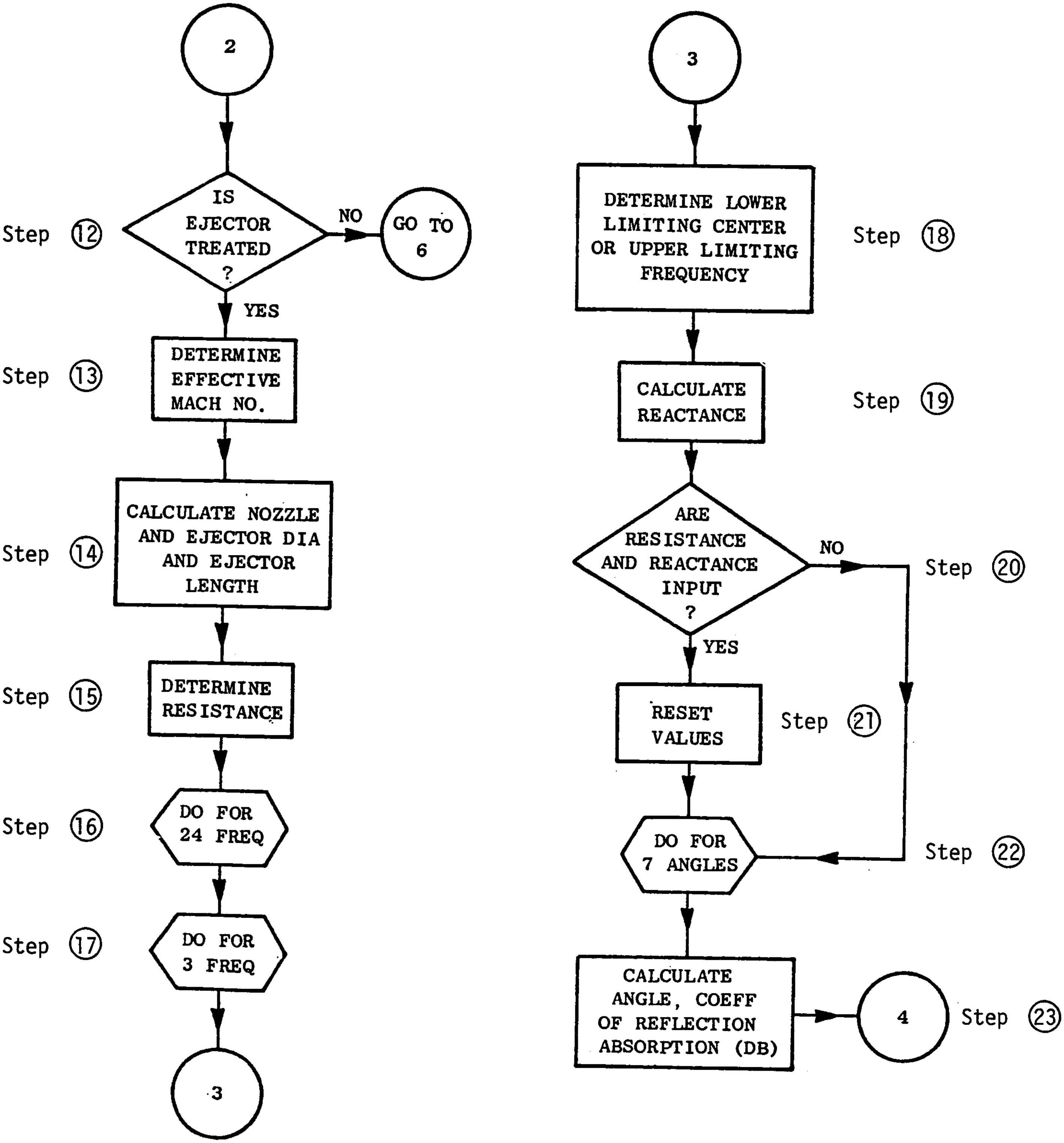

FIGURE A-1 (CONTINUED). ORIGINAL M*S ANALYSIS STEPS IN SUBROUTINE EJECTS

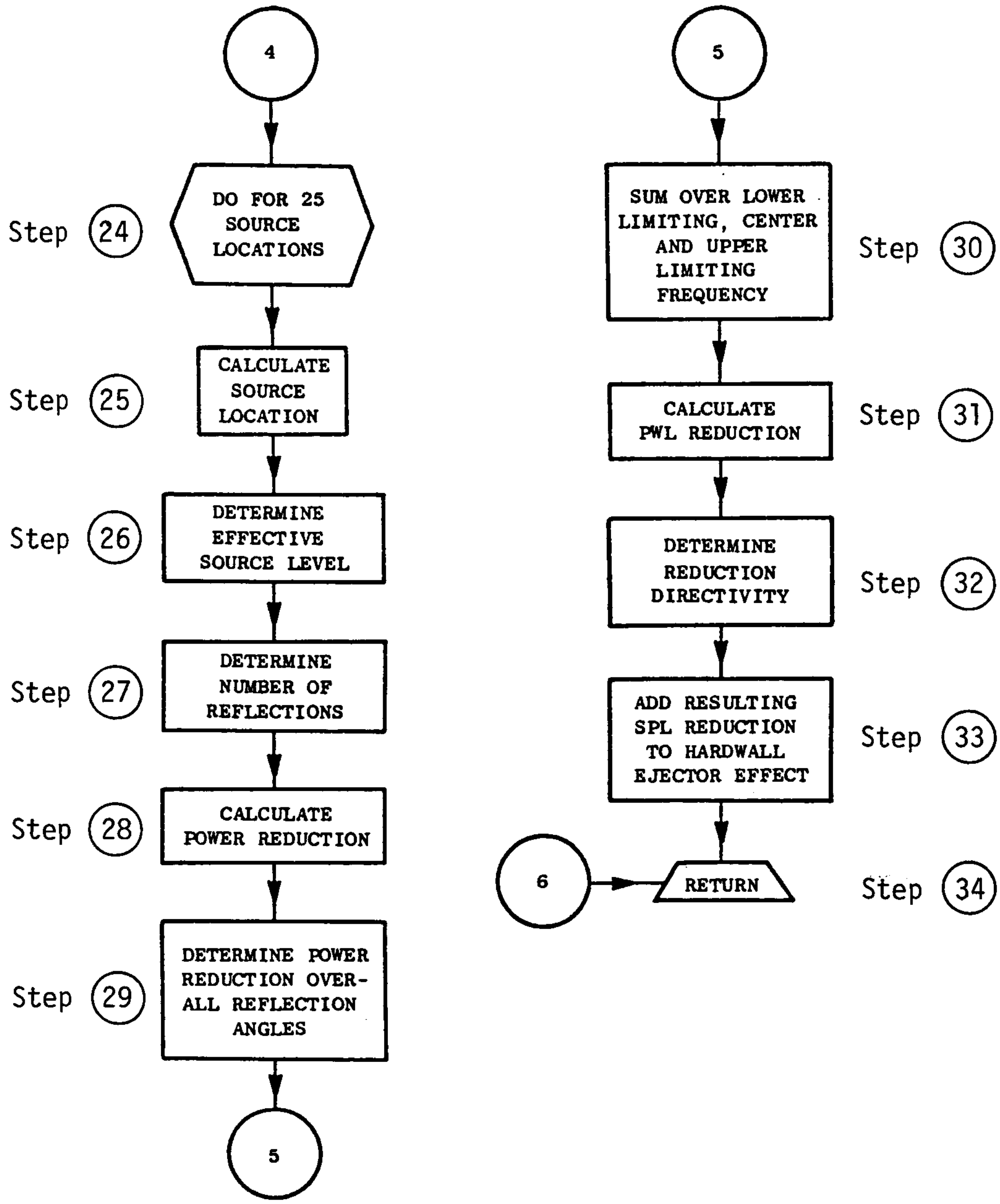

FIGURE A-1 (CONCLUDED). ORIGINAL M*S ANALYSIS STEPS IN SUBROUTINE EJECTS

```
            SUBROUTINE EJECTS
      C    EJECTS -- EJECTOR EFFECT SUBROUTINE
            COMMON /QM/ M,OJ
            COMMON/CM1/L(9,24),X(24),F(24),E(24),S(15,24),KK(24,5),C(15,5),
          1 O(20),RR(49),RX(49),P(20),R(15,24),Y1(24),Y(24),C1(15),RVE(20),
          1 S1(24),G(2,24),C2(15),T(20),D(20),W(5),A(4),V(3),E1(15,24)
            COMMON /CM2/ V8,A0,W8,K1,Y9,T8,T5,R7,P1,Z9,DJ,AJ,H,U,E9
          1 ,T0,V9,C9,D8,D1,V0,09,A8,Q,L9,A6,A7,S6,P9,P9,ALT,SL,AN1
            COMMON /CM3/ IIAS(2),IICASE(6),IDCASE(6),IDENT(6)
            REAL L,KK,K1
            REAL L8,L9,L2,K6,L3,M
      C         HARDWALL EJECTOR EFFECTS
            DO 110 I=1,15
            DO 110 J=1,24                                                 Step 1
      110      F1(I,J)=0.0
            FP=.3*V8/SQRT(4*A8/P1)                                        Step 2
            L8=5*ALOG10(L9/2)                                             Step 3
            D3=SQRT(A6*A7*A8*AN1/P1+S6**2-A7*A8*AN1/P1)                   Step 4
            AS=A6 $ IF(Y9.GT.3) GO TO 133 $ IF(R9.EQ.0) GO TO 140
      133      AS=A6/(10**(12.78*(D3/S6-1)**2+.046))                      Step 5
      140      D2=L8-23.59*AS-(110*(ALOG10(P9/1.9))**2)+.005*(T8-T0)+30   Step 6
            IF(D2.LT.0) GO TO 280                                         Step 7
      C         DIRECTIVITY EFFECTS                                       Step 8
            DO 270 I=1,15 $ AJ=(I+1)*10
           IF(AJ.GT.OJ-60) GO TO 165 $ DE=.64*D2 $ GO TO 220              Step 9
      165      IF(AJ.LT.OJ-30) GO TO 180
            IF(AJ.GT.OJ) GO TO 200 $ DE=.2*D2 $ GO TO 220
      180      DE=D2*(-4.888E-4*(AJ-OJ+60)**2+.64)
            IF(DE.GT.0) GO TO 220 $ DE=0 $ GO TO 270
      200  IF(AJ.GT.OJ+20) GO TO 210 $ DE=D2*SQRT((AJ-OJ)/20) $ GO TO 220
      210      DE=D2*(.00925*(AJ-OJ-20)+1)
      C         SPECTRAL EFFECTS                                          Step 10
      220      DO 260 J=1,24 $ IF(FP.GT.1.12*F(J)) GO TO 250              Step 11
            IF(F(J)/FP.GT.8) GO TO 240
            E1(I,J)=.2*(F(J)/FP-1)**2-DE $ GO TO 260
      240      F1(I,J)=9.5-DE $ GO TO 260
      250      E1(I,J)=-DE
      260      CONTINUE
      270      CONTINUE
      280      IF(A(1).EQ.0) GO TO 820                                    Step 12
      C         EJECTOR TREATMENT EFFECTS                                 Step 13
            XJ=M/5.0 $ IF(M.LT.1.13) GO TO 330 $ XJ=.226
      330      D4=SQRT(4*A8*AN1/P1) $ L3=L9*D4                            Step 14
            D3=D3*2.0
      C         SDOF RESISTANCE AND REACTANCE                             Step 15
            YJ=.8216-2.5094*XJ
            IF(XJ.LT..08929) GO TO 460
            YJ=.60504-3.48606*(XJ-.08929)
            IF(XJ.LT..22321) GO TO 460
            YJ=.13819-2.00751*(XJ-.22321)
            IF(XJ.LT..26786) GO TO 460
            YJ=.04855-.90634*(XJ-.26786)
            IF(XJ.LT..32143) GO TO 460
            YJ=0
      460      T1=(A(1)+.85*A(3)*YJ)/12
            RS=(.3*XJ)/A(2)
      500      DO 815 J=1,24 $ A4=0                                       Step 16
```

FIGURE A-2. ORIGINAL M*S

```
      C         FREQUENCY DETERMINATION                                          Ste
            DO 755 K8=1,3 $ IF(K8-2) 520,530,540                                 Step
      520         P3=F(J)*6.28318*.89 $ GO TO 550
      530         P3=F(J)*6.28318 $ GO TO 550                                    Step 18
      540         P3=F(J)*6.28318*1.12
      550         X4=(P3*T1)/(A0*A(2))-1/TAN((P3*A(4)/12)/A0)                   Step 19
            IF(A(1).NE.10) GO TO 590                                             Step 20
            IP=K8+2*J-2
            RS=RR(IP)                                                            Step 21
            X4=RX(IP)
      590         A3=0 $ DO 730 I=9,15 $ K6=0 $ AJR=((I+1)*10-90)*PI/180         Step 22
            A1=4*RS*COS(AJR)/((1+RS*COS(AJR))**2+(X4*COS(AJR))**2)
      C         ABSORPTION PER REFLECTION                                        Step 23
            A2=10*ALOG10(1-A1)
            DO 690 K=1,25 $ XJ=((2.5*X(J))/25)*K                                 Step 24
      C         SOURCE LOCATIONS                                                 Step 25
            ZJ=XJ/X(J)
            S2J=-11.19136+32.76957*ZJ-37.633732*ZJ**2+23.970385*ZJ**3
            S2J=S2J-10.115712*ZJ**4+2.4045214*ZJ**5-.23576959*ZJ**6              Step 26
            S2J=S2J-11.6
      C         EFFECT FOR ALL REFLECTIONS
            DO 675 JJ=1,11$IF(JJ.GT.1) GO TO 660$L2=(D3/2-S6)*TAN(AJR)+XJ
            GO TO 670
      660         L2=L2+D3*TAN(AJR)
      670         IF(L2.GT.L3) GO TO 680                                         Step 27
      675         CONTINUE
      680         K6=K6+10**(((JJ-1)*A2+S2J)/10)                                 Step 28
      690         CONTINUE
      C         POWER LEVEL REDUCTION                                            Step 29
            AJ=(I+1)*10 $ K6=10*ALOG10(K6)
            YJ=1.5*PI*(COS((AJ-5)*PI/180)-COS((AJ+5)*PI/180))
            A3=A3+(2.227525E-6*4E-8*YJ*10**(K6/10))
      730         CONTINUE                                                       Step 30
            A3=10*ALOG10(A3)+130-6.45175
            A4=A4+10**(A3/10)
      755   CONTINUE $ A4=10*ALOG10(A4/3)                                        Step 31
      C         DIRECTIVITY EFFECTS
            DO 815 I=1,15 $ AJ=(I+1)*10 $ A5=A4                                  Step 32
            IF(AJ.LT.OJ-50) GO TO 800 $ IF(AJ.LT.OJ) GO TO 810
      800         A5=A4/2
      810         E1(I,J)=E1(I,J)+(A5*1.2)                                       Step 33
      815         CONTINUE
      820         RETURN $ END                                                   Step 34
```

FIGURE A-2 (CONCLUDED). ORIGINAL M*S

```
SUBROUTINE EJECTS
C      EJECTS -- EJECTOR EFFECT SUBROUTINE
COMMON /QM/ M,OJ
COMMON/CM1/L(9,24),X(24),F(24),E(24),S(15,24),KK(24,5),C(15,5),O(2Ø),
& RR(49),RX(49),P(2Ø),R(15,24),Y1(24),Y(24),C1(15),RVE(2Ø),
& S1(24),G(2,24),C2(15,2),T(2Ø),D(2Ø),W(5),A(4),V(3),E1(15,24)
COMMON /CM2/ V8,AØ,W8,K1,Y9,T8,T5,R7,P1,Z9,DJ,AJ,H,U,E9,AA
& ,TØ,V9,C9,D8,D1,VØ,O9,A8,Q,L9,A6,A7,S6,P9,R9,ALT,SL,AN1,NFLT
&  ,HTR,NST,XMJMX,TJMX,VJMX
COMMON /CM3/AS,CASEID,E3,FNL(2Ø)
REAL L,KK,K1,IMH,IMH1
CHARACTER AS*2Ø,NAME*6Ø,ADDRES*6Ø,IDENT*6Ø,CASEID*6Ø
REAL L8,L9,L2,KG,L3,M
REAL MACH
DIMENSION IMH(1Ø),WTGFN(1Ø),IMH1(1Ø)
INTEGER TM
REAL LAMBDA
C                 HARDWALL EJECTOR EFFECTS
SONSPD=49.Ø1*SQRT(TJMX)
D3=SQRT(A6*A7*A8*AN1/P1+S6**2-A7*A8*AN1/P1)                       Step 4
AITCH=D3*(1-HTR)
RBAR=D3*(1+HTR)/2.
MACH=VJMX/SONSPD
IF(MACH.GT..95)MACH=.95
DO 11Ø I=1,15
DO 11Ø J=1,24                                                      Step 1
11Ø E1(I,J)=Ø.Ø
FP=.3*V8/SQRT(4*A8/P1)                                             Step 2
L8=5*ALOG1Ø(L9/2)                                                  Step 3
A5=A6 ; IF(Y9.GT.3) GO TO 133 ; IF(R9.EQ.Ø) GO TO 14Ø              Step 5
133 A5=A6/(1Ø**(12.78*(D3/S6-1)**2+.Ø46))
14Ø D2=L8-23.59*A5-(11Ø*(ALOG1Ø(P9/1.9))**2)+.ØØ5*(T8-TØ)+3Ø       Step 6
IF(D2.LT.Ø) GO TO 28Ø                                              Step 7
C                 DIRECTIVITY EFFECTS
DO 27Ø I=1,15 ; AJ=(I+1)*1Ø
IF(AJ.GT.OJ-6Ø) GO TO 165 ; DE=.64*D2 ; GO TO 22Ø
165 IF(AJ.LT.OJ-3Ø) GO TO 18Ø
IF(AJ.GT.OJ) GO TO 2ØØ ; DE=.2*D2 ; GO TO 22Ø
18Ø DE=D2*(-4.888E-4*(AJ-OJ+6Ø)**2+.64)                   Step 9
IF(DE.GT.Ø) GO TO 22Ø ; DE=Ø ; GO TO 27Ø
2ØØ IF(AJ.GT.OJ+2Ø) GO TO 21Ø ; DE=D2*SQRT((AJ-OJ)/2Ø) ; GO TO 22Ø
21Ø DE=D2*(.ØØ925*(AJ-OJ-2Ø)+1)
C                 SPECTRAL EFFECTS                                 Step 8
22Ø DO 26Ø J=1,24 ; IF(FP.GT.1.12*F(J)) GO TO 25Ø
IF(F(J)/FP.GT.8) GO TO 24Ø
E1(I,J)=.2*(F(J)/FP-1)**2-DE ; GO TO 26Ø
24Ø E1(I,J)=9.5-DE ; GO TO 26Ø          Step 11      Step 10
25Ø E1(I,J)=-DE
26Ø CONTINUE
27Ø CONTINUE
A(1)=1Ø.
28Ø IF(A(1).EQ.Ø) GO TO 82Ø                                        Step 12
C                 EJECTOR TREATMENT EFFECTS
XJ=M/5.Ø ; IF(M.LT.1.13) GO TO 33Ø ; XJ=.226                      Step 13
33Ø D4=SQRT(4*A8*AN1/P1) ; L3=L9*D4                                Step 14
D3=D3*2.Ø
5ØØ DO 815 J=1,24 ; A4=Ø
TM=Ø.ØØ                                      (Step 15 eliminated)
C                 FREQUENCY DETERMINATION
DO 755 K8=1,3 ; GO TO (52Ø,53Ø,54Ø),K8
52Ø P3=F(J)*6.28318*.89 ; GO TO 55Ø
53Ø P3=F(J)*6.28318 ; GO TO 55Ø                           Step 18
54Ø P3=F(J)*6.28318*1.12
55Ø CONTINUE                          Steps 19 and 20 eliminated
IP=K8+2*J-2                                                        Step 16
RS=RR(IP)                                                 Step 17
X4=RX(IP)                                         Step 21
LAMBDA=2.*P1*SONSPD/P3
ETAY=AITCH/LAMBDA
ETAZ=2.*P1*RBAR/LAMBDA
XMAX=(2*ETAY/SQRT(1-MACH**2))+1
NMAX=IFIX(XMAX)
YMAX=(ETAZ/SQRT(1-MACH**2))+1
```

FIGURE A-3. PROGRAM LISTING OF REVISED VERSION OF SUBROUTINE EJECTS

Step 17   Step

```
MMAX=IFIX(YMAX)
IF(NMAX.EQ.1.AND.MMAX.EQ.1)GOTO 815
DO 855 LZER=1,10;IMH(LZER)=1E-10;IMH1(LZER)=1E-10
855 WTGFN(LZER)=0.
TM=0
DO 880 NM=1,NMAX
DO 870 MM=1,MMAX
NIND=NM-1
MIND=MM-1
IF(NIND.EQ.0)GOTO 830
GOTO 840
830 IF(MIND.NE.0)GOTO 840
PHI=0
GOTO 850
840 CONTINUE
PARAM=SQRT(((P1*NIND)**2)+(2*MIND*(1-HTR)/(1+HTR))**2)
COR=2*P1*ETAY/(PARAM*SQRT(1-MACH**2))
IF(COR.LE.1.)GOTO 870
PHI=(ARSIN(1/COR))*180./P1
850 CONTINUE
DO 860 LDIF=1,9
BETA=LDIF*10.
IF(PHI.GT.BETA)GOTO 860
IMH(LDIF)=IMH(LDIF)+1
GOTO 865
860 CONTINUE
865 CONTINUE
TM=TM+1
 870 CONTINUE
880 CONTINUE
DO 890 LANG=1,9
LL=10-LANG
IMH1(LL)=IMH(LANG)
WTGFN(LL)=10*ALOG10(9*IMH1(LL)/TM)
890 CONTINUE
590 A3=0 ; DO 730 I=9,17 ; K6=0 ; AJR=((I+1)*10-90)*P1/180        Step 22
N=I-8
A1=4*RS*COS(AJR)/((1+RS*COS(AJR))**2+(X4*COS(AJR))**2)
C            ABSORPTION PER REFLECTION
XXX=1-A1                                                          Step 23
IF(XXX.LT.0.0000001)XXX=0.0000001
A2=10*ALOG10(XXX)
DO 690 K=1,25 ; XJ=((2.5*X(J))/25)*K                              Step 24
C            SOURCE LOCATIONS
ZJ=XJ/X(J) ; S2J=-11.19136+32.76997*ZJ-37.633732*ZJ**2+23.970385*ZJ**3
S2J=S2J-10.115712*ZJ**4+2.4045214*ZJ**5-.23576959*ZJ**6    Steps 25 & 26
S2J=S2J-11.6
C            EFFECT FOR ALL REFLECTIONS
DO 675 JJ=1,11;IF(JJ.GT.1) GO TO 660;L2=(D3/2-S6)*TAN(AJR)+XJ;GO TO 670
660 L2=L2+D3*TAN(AJR)*(1.0-HTR)/NST
C
C                                                                 Step 27
670 IF(L2.GT.L3) GO TO 680
675 CONTINUE
680 CONTINUE
FORK=((JJ-1)*A2+WTGFN(N)+S2J)/10                      Revised Step 28
K6=K6+10**FORK
690 CONTINUE
C            POWER LEVEL REDUCTION
AJ=(I+1)*10 ; K6=10*ALOG10(K6)                                    Step 29
YJ=1.5*P1*(COS((AJ-5)*P1/180)-COS((AJ+5)*P1/180))
A3=A3+(2.227525E-6*4E-8*YJ*10**(K6/10))
730 CONTINUE                                                      Step 30
A3=10*ALOG10(A3)+130-6.45175
A4=A4+10**(A3/10) ; 755 CONTINUE ; A4=10*ALOG10(A4/3)             Step 31
C            DIRECTIVITY EFFECTS FOR TREATMENT
DO 8615 I=1,15 ; AJ=(I+1)*10 ; A5=A4
IF(AJ.LT.OJ-50) GO TO 800 ; IF(AJ.LT.OJ) GO TO 810                Step 32
800 A5=A4/2
810 E1(I,J)=E1(I,J)+(A5*1.2)                                      Step 33
8615 CONTINUE
815 CONTINUE
820 RETURN ; END                                                  Step 34
```

FIGURE A-3(CONCLUDED). PROGRAM LISTING OF REVISED VERSION OF SUBROUTINE EJECTS

```
  1ØØØC       MS   -- ENGINEERING CORRELATION FOR TASK 3
  1Ø1Ø COMMON /QM/ M,OJ
  1Ø2Ø COMMON/CM1/L(9,24),X(24),F(24),E(24),S(15,24),KK(24,5),C(15,5),O(2Ø),
  1Ø3Ø& RR(49),RX(49),P(2Ø),R(15,24),Y1(24),Y(24),C1(15),RVE(2Ø),
  1Ø4Ø& S1(24),G(2,24),C2(15,2),T(2Ø),D(2Ø),W(5),A(4),V(3),E1(15,24)
  1Ø5Ø COMMON /CM2/ V8,AØ,W8,K1,Y9,T8,T5,R7,P1,Z9,DJ,AJ,H,U,E9,AA
  1Ø6Ø& ,TØ,V9,C9,D8,D1,VØ,O9,A8,O,L9,A6,A7,S6,P9,R9,ALT,SL,AN1,NFLT
* 1Ø65& ,HTR,NST,XMJMIX,TJMX,VJMX
  1Ø7Ø COMMON /CM3/AS,CASEID,E3,PNL(2Ø)
  1Ø72      COMMON /CM4/ CASE
  1Ø8Ø REAL L,KK,K1
  1Ø9Ø CHARACTER AS*2Ø,NAME*6Ø,ADDRES*6Ø,IDENT*6Ø
  1Ø91      CHARACTER CASEID *6Ø /" "/
  1Ø92      CHARACTER CASE   *6
  11ØØ DIMENSION HEAD(1Ø)
  111Ø NAMELIST/ID/NAME,ADDRES,IDENT
  112Ø NAMELIST/INPUT/ Y9,P9,TT3,A9,RP,K9,N,89,R4,R6,S1J,SS,A7,
  113Ø& N1,DT,Z5,DN,AA8,TT4,P4,TT5,ALT,SL,U,E9,AA,VØ,A6,L9,A,P5,RR,RX
  114Ø& ,CASEID,NFLT
  1142     & ,CASE,IFLSUM,NENG,REFLJ,SHLDJ,T1985
* 1143     &  ,HTR,NST
  115ØC
  116Ø REAL M,K2,KØ,L9
  1162      REAL NENG
  117ØC
  1172      DATA IFILE  /11/
  1174      DATA IFLSUM /"NO"/
  1176      DATA NO     /"NO"/
  118Ø DATA F/5Ø.,63.,8Ø.,1ØØ.,125.,16Ø.,2ØØ.,25Ø.,315.,4ØØ.,5ØØ.,63Ø.,
  119Ø& 8ØØ.,1ØØØ.,125Ø.,16ØØ.,2ØØØ.,25ØØ.,315Ø.,4ØØØ.,5ØØØ.,63ØØ.,8ØØØ.,
  12ØØ& 1ØØØØ./
  121Ø DATA C1/15*1./
  122Ø DATA HEAD(1)/6ØH ** MS NAMELIST INPUT **
  123Ø&                                        /
  124Ø DATA C2/Ø.7,1.Ø,1.35,1.8,2.35,2.7,3.4,4.2,5.Ø,
  125Ø& 5.5,5.2,4.9,4.5,3.8,2.8,Ø.Ø,Ø.Ø,Ø.Ø,Ø.Ø,
  1255& Ø.Ø,Ø.Ø,Ø.Ø,Ø.1,Ø.4,Ø.9,1.7,2.9,4.2,5.4,6.7/
  126Ø DATA (S1(J),G(1,J),G(2,J),J=1,24)
  127Ø& /-.699,131.8,.72,-.6Ø2,135.4,.72,-.5Ø2,139.2,.72,-.398,142.4,
  128Ø&  .72,-.3Ø1,145.,.7,-.2Ø1,147.5,.68,-.Ø97,148.6,.64,Ø.,148.7,.6,
  129Ø&  .Ø97,148.,.55,.2Ø4,147.2,.5,.3Ø1,146.5,.45,.398,146.7,.39,
  13ØØ&  .498,144.8,.33,.6Ø2,143.9,.27,.699,142.5,.2,.799,141.,.15,
  131Ø&  .9Ø3,139.5,.Ø9,1.,138.3,.Ø4,1.Ø97,137.,Ø.,1.2Ø4,135.5,Ø.,1.3Ø1,
  132Ø&  134.1,Ø.,1.398,132.6,Ø.,1.498,131.3,Ø.,1.6Ø2,13Ø.,Ø./
  1325 DATA NFLT/1/
  133Ø CALL NLISTP(HEAD)
  134Ø PRINT 1Ø1
  135Ø 1Ø1 FORMAT(1H1////////////////
  136Ø& 5ØX,"XX       XX     XXXXXX"/
  137Ø& 5ØX,"XXX     XXX     XXXXXX"/
  138Ø& 5ØX,"XXXX   XXXX     XX    "/
  139Ø& 5ØX,"XX XXXX XX     XX    "/
  14ØØ& 5ØX,"XX  XX  XX     XXXXXX"/
  141Ø& 5ØX,"XX       XX     XXXXXX"/
  142Ø& 5ØX,"XX       XX         XX"/
  143Ø& 5ØX,"XX       XX         XX"/
  144Ø& 5ØX,"XX       XX     XXXXXX"/
  145Ø& 5ØX,"XX       XX     XXXXXX"//////
  146Ø&/4ØX,41H XXXXX X    X  XXXXX XXXXXX XXXXXX X    X
  147Ø&/4ØX,41HX         X  X  X         X    X        XX  XX
  148Ø&/4ØX,41HXXX      XX    XXX       X    X        X XX X
  149Ø&/4ØX,41H   XXX     X        XXX   X    XXXX     X    X
  15ØØ&/4ØX,41H     X     X          X   X    X        X    X
  151Ø&/4ØX,41HXXXXX      X    XXXXX     X    XXXXXX X    X)
```

* INDICATES CHANGE TO ORIGINAL PROGRAM

HTR = HUB-TIP-RATIO
NST = NUMBER OF SIDES TREATED

FIGURE A-4. LISTING OF THE REVISED M*S PROGRAM

```
1520 PRINT 103
1530 103 FORMAT(///33X,48HHIGH VELOCITY JET NOISE PROGRAM (CONTRACT DOT-OS,
1540&7H-30034,/44X,33HTASK 3 -- ENGINEERING CORRELATION///)
1550 READ(5,ID)
1560 PRINT 13,NAME,ADDRES,IDENT
1570 13 FORMAT(3(30X,A60/))
1580 250 FORMAT(1H1///,"    HIGH VELOCITY JET NOISE PROGRAM - ENGINEERING",
1590& " CORRELATION"///)
1592      IFRST=0
1594C
1600 245 CONTINUE
1610C
1620 T0=519 ; P0=14.7 ; RJ=.076475 ; P1=3.14159
1630 K1=1
1640 R7=0 ; K2=0 ; K7=0
1650 A0=49.01(*SQRT(T0)
1660 READ(5,INPUT,END=9999)
1662C
1663      IF (IFRST.NE.0) GO TO 5
1664      IFRST=1
1665      IF (IFLSUM.EQ.NO) GO TO 5
1666      REWIND IFILE
1667C
1670 5 T3=TT3 ; R9=RP ; R1=DT ; R2=DN ; A8=AA8
1680 T4=TT4 ; T5=TT5 ; AN1=N
1690 PRINT 250
1700 PRINT 19,CASEID
1710 19 FORMAT(2X,A60///)
1712   18 FORMAT (2X,"CASE NUMBER ",A6)
1714      PRINT 18,CASE
1720 PRINT 2000
1730 2000 FORMAT(25X,"*** INPUT ***"//)
1740C
1750C
1760  GO TO(295,370,320,415,425,425),Y9
1770C        CONICAL NOISE ENTRY
1780 295 R1=SQRT(A9/P1) ; A7=0 ; R2=SQRT(A9/P1+R9**2) ; AN1=1 ; R9=0
1790 N=1
1800 GO TO 390
1810C          MULTI-CHUTE/SPOKE NOISE ENTRY
1820 320 R2=N*(R4+SS)/(2*P1)
1830 R1=SQRT(4*((R4+R6)/2)*(R2-R9*12)/P1)/24
1840 R2=R2/12
1850 S1J=SS/R4+1
1860 PRINT 2002,N,2*R1,A7
1870 2002 FORMAT(" NO OF CHUTES/SPOKES=",I4/" DIA OF CHUTE EQUIV AREA",
1880& " TUBE=",F10.3,5X,"ARD=",F10.3)
1890 GO TO 390
1900C          MULTI-TUBE NOISE ENTRY
1910 370 R1=R1/24;R2=SQRT(N*A7*R1**2+R9**2)
1920 PRINT 2004,N,2*R1,A7
1930 390 PRINT 2006,T0,P0,T3,P9
1940 395 PRINT 2016,A6,V0
1950 2016 FORMAT(" EJECTOR AREA RATIO PARAMETER=",F10.3,5X,"V0=",F10.1)
1960 PRINT 2008,R9*2,B9
1970 2004 FORMAT(" NO OF TUBES=",I4,5X,
1980&/" DIA OF TUBES=",F10.3,5X,"ARD=",F10.3)
1990 2006 FORMAT(" T0 =",F6.0,5X,"P0    =",F8.3/" TT8=",F6.0,5X,"PT8/P0=",
2000&F8.3)
2010 2008 FORMAT(" PLUG DIA=",F10.3,5X,"CANT=",F10.3///25X,"***OUTPUT ***")
2020 GO TO 525
2030C          COANNULAR NOISE ENTRY
2040 415 R1=SQRT(A9/P1);A7=1
2050 425 GO TO(485,435,460),Y9-3
```

FIGURE A-4 (CONTINUED). LISTING OF THE REVISED M*S PROGRAM

```
2060C            MULTI-TUBE  COANNULAR ENTRY
2070 435 CONTINUE
2080 R1=R1/24
2090 PRINT 2010,N,2*R1,A7
2100 2010 FORMAT(" NO OF TUBES=",I4,5X,
2110& /" DIA OF TUBES=",F10.3,5X,"ARD=",F10.3)
2120 GO TO 485
2130C            MULTI-CHUTE/SPOKE COANNULAR ENTRY
2140 460 CONTINUE
2150 R1=SQRT(4*A9/(PI*N))/2
2160 PRINT 2012,N,A7,2*R1
2170 2012 FORMAT(" NO OF CHUTES/SPOKES=",I4,5X,"ARD=",F10.3/
2180& " DIA OF CHUTE EQUIV AREA TUBE=",F10.3)
2190 S1J=SS/R4+1
2200 485 PRINT 2014,R2,A8,A9,T5,P5,T0,P0,T4,P4
2210 2014 FORMAT(" NOZZLE OUTER DIA=",F10.3/" A8=",F10.3,5X,"A28=",
2220& F10.3/" TT28=",F6.0,5X,"PT28/P0=",F10.3/" T0=",F6.0,5X,
2230& "P0=",F8.3/" TT8=",F6.0,5X,"PT8/P0=",F10.3)
2240 T3=T5;P9=P5
2250 R7=(R2-SQRT(R2**2-4*A9*A7/PI))/2
2260 GO TO 395
2270 525 CONTINUE
2280 H=SQRT(ALT**2+SL**2)
2290 A3=N*PI*R1**2
2300C           RADIUS RATIO CALCULATION
2310 R8=1-A7*A3/(PI*R2**2);IF( R8.LT.0 ) GO TO  550;R8=SQRT(R8);GO TO 555
2320 550 R8=0
2330 555 T8=T3;G8=1.35
2340C           ITERATION FOR GAMMA
2350 DO 600 J=1,50
2360 T3=T8/(P9**((G8-1)/G8))
2370 G9=1.4
2380 IF( T3.LT.788.302 ) GO TO  590
2390 G9=2.23700/T3**.070271
2400 590 IF( ABS(G8-G9).LT..001 ) GO TO  615
2410 G8=G9
2420 600 CONTINUE
2430 GO TO 810
2440C           CALCULATION OF FLOW PARAMETERS
2450 615 C3=G9*.06855/(G9-1)
2460 U3=223.79*SQRT(T8*C3*(1-1/((P9**((G9-1)/G9)))))
2470 R3=2.7*P0/T3
2480 D4=2*SQRT(A3/PI)
2490 IF( Y9.LT.4 ) GO TO  675
2500 IF( T8.EQ.T4 ) GO TO  660
2510C            PRINT AND RESET VARIABLES
2520 PRINT 2017
2530 PRINT 2018,U3,R3,R7
2540 2017 FORMAT(/" OUTER NOZZLE EXIT CONDITIONS")
2550 2018 FORMAT(" U28=",F10.1,5X,"RHO28=",F10.4,5X,"DUCT H=",F10.3)
2560 T3=T4;P9=P4;U5=U3;R5=R3;G2=G9;C4=C3
2570 GO TO 555
2580 660 PRINT 2130
2590 2130 FORMAT(/" INNER NOZZLE EXIT CONDITIONS")
2600 PRINT 2020,U3,R3
2610 2020 FORMAT(" U8=",F10.1,5X,"RHO8=",F10.4)
2620 S6=R2/2
2630 GO TO 1485
2640 675 PRINT 2022,2*R2,D4
2650 PRINT 2023
2660 PRINT 2124,U3,R3,A3/N,A3
2670 2022 FORMAT(/" DIA OF OUTER ROW=",F10.3,5X,"EQUIV AREA DIA=",F10.3/)
2680 2023 FORMAT(/" NOZZLE EXIT CONDITIONS")
2690 2124 FORMAT(" U8=",F10.1,5X,"RHO8=",F10.4,5X,"AT=",F10.3,5X,
```

FIGURE A-4 (CONTINUED). LISTING OF THE REVISED M*S PROGRAM

```
27ØØ& " A8=",F1Ø.3)
271Ø S6=R2;A9=A3
272Ø GO TO (1425,7Ø5,7ØØ),Y9
273ØC              MULTI-ELEMENT POST-MERGED NOISE CALCULATIONS
274Ø 7ØØ R2=R2-R2*SIN(B9*P1/18Ø)/COS(B9*P1/18Ø)
275Ø 7Ø5 IF( R8.LT..6 ) GO TO  72Ø
276Ø R2=R2*(-1.947*ALOG1Ø(R8/1.954))*(1-.2525*ALOG1Ø(T8/175Ø))
277Ø R2=R2*SQRT(R8/.716)
278Ø 72Ø A5=(N*P1*(R2-R1)**2)/((SQRT(N)-1)**2)
279Ø A1=A5/A3
28ØØ PJ=((P9-1)*PØ*4633.Ø6)/(U3**2*R3)+1
281Ø KØ=((C3*T3)+(U3**2/5ØØ82)-(TØ*.24))/PJ
282Ø K2=PØ/(1Ø.73*R3*PJ**2)
283Ø X3=K2*(C3-.24)*28.966*A1
284Ø X2=(A1*K2*PJ*6.95184+(U3**2/5ØØ82))/X3
285Ø X1=(-1*KØ)/X3
286Ø XØ=(-1*TØ*.24)/X3
287ØC              ITERATE FOR U MERGED/U8
288Ø VJ=.5
289Ø DO 8Ø5 I=1,5Ø
29ØØ F2=XØ+X1*VJ+X2*VJ**2+VJ**3
291Ø F1=X1+2*X2*VJ+3*VJ**2
292Ø V1=VJ-F2/F1
293Ø IF( ABS(V1-VJ).LT..Ø1*V1 ) GO TO  82Ø
294Ø VJ=V1
295Ø 8Ø5 CONTINUE
296Ø 81Ø PRINT ,"DID NOT CONVERGE"
297Ø GO TO  9999
298Ø 82Ø VJ=V1*U3
299Ø D5=SQRT(1.273237*A5)
3ØØØ R5=R3*PJ/((VJ/U3)**2*A1)
3ØØ5 VJMX=VJ
3ØØ6 TJMX=(PØ*TØ*.Ø76474)/(14.69597*R5)
3Ø1Ø PRINT 2125
3Ø2Ø 2125 FORMAT(/" MERGED FLOW CONDITIONS")
3Ø3Ø PRINT 2Ø24,VJ,R5,D5,A5
3Ø4Ø 2Ø24 FORMAT(" U5=",F1Ø.1,5X,"RHO5=",F1Ø.4,5X,"D5=",F1Ø.3,5X,
3Ø5Ø& "A5=",F1Ø.3)
3Ø6ØC              CHECK FOR OTHER POSSIBLE SOLUTIONS
3Ø7Ø X1=X1+V1*(X2+V1)
3Ø8Ø X2=X2+V1
3Ø9Ø Q1=X2**2-4*X1
31ØØ IF( Q1.LT.Ø ) GO TO  91Ø
311Ø Y1J=(-X2-SQRT(Q1))/2
312Ø Y2=(-X2+SQRT(Q1))/2
313Ø IF( Y1J.LT.Ø ) GO TO  89Ø
314Ø IF( Y1J.GT.1 ) GO TO  89Ø
315Ø PRINT 2Ø26,Y1J
316Ø 2Ø26 FORMAT(" ROOT#2=",F1Ø.4)
317Ø 89Ø IF( Y2.LT.Ø ) GO TO  91Ø
318Ø IF( Y2.GT.1 ) GO TO  91Ø
319Ø PRINT 2Ø28,Y2
32ØØ 2Ø28 FORMAT(" ROOT#3=",F1Ø.4)
321ØC              SET INPUT VARIABLES TO CONICAL ROUTINE
322Ø 91Ø V8=VJ;A8=A5;W8=R5*A5*V8
323Ø T5=(PØ*28.966*A1*V1**2)/(PJ*R3*1Ø.73)
324Ø G8=1.4
325Ø IF( T5.LT.788.3Ø2 ) GO TO  935
326Ø G8=2.237Ø8/T5**.Ø7Ø271
327Ø 935 M=VJ/SQRT(G8*T5*1716.49)
328Ø T9=T8
329Ø T8=T5*(1+((G8-1)/2)*M**2)
33ØØ IF( Y9.GT.4 ) GO TO  1515
331ØC              CALCULATE MERGED NOISE
```

FIGURE A-4 (CONTINUED). LISTING OF THE REVISED M*S PROGRAM

```
960 K1=1;CALL SUB1
IF( Y9.LT.4 ) GO TO  975;IF( U3.LT.VJ ) GO TO  975
Z9=10*ALOG10(A5/A3)+5.8
Z9=Z9*4*(VJ/U3-.5)**2-Z9;CALL SUB2
975 CALL SUB5;IF( K9.EQ.0 ) GO TO  990;CALL SUB3
AS="MERGED NOISE"
CALL PNTT8
990 CALL SUB4
IF( Y9.GT.3 ) GO TO  1595
C            MULTI-ELEMENT PRE-MERGED NOISE CALCULATIONS
C            SET INPUT TO CONICAL ROUTINE
V8=U3;A8=A3/AN1;G2=G9;W8=R3*A8*V8;T8=T9
1015 K1=2;CALL SUB1
C            CUTOFF/SHIELDING CALCULATION
K7=0;Z8=0
DJ=2*R1 ; B8=B9*P1/180.0
Z9=10*ALOG10(AN1)
IF( Y9.LT.3 ) GO TO  1060
IF( Y9.EQ.5 ) GO TO  1060
Z8=1+AN1/6;DJ=R4/12;B8=0
GO TO 1075
1060 DO 1070 J=1,(Z5+1)
Z8=Z8+(2*(Z5-J+1)+1)*(1-1/SIJ)**(J-1)
1070 CONTINUE
1075 Z8=5*ALOG10(Z8)
C            CALCULATION OF CRITICAL ANGLE
M=.6*V8/SQRT(2368.76*(T3+T0)/2);OJ=(A0/(V8*.6/M))/(1+M)
M=V8/SQRT(G2*T3*1716.49)
OJ=180-ATAN(SQRT(1-OJ**2)/OJ)*180/P1
GJ=IFIX(OJ/10)-1
C            XC CALCULATION
Z2=DJ*(4+1.15*M+.85*M**2)
AJR=ATAN(1/(2*Z2/DJ))
C            POINT OF MERGING FOR CUTOFF
XM=(SIJ-1)*DJ*SIN(1.5708-AJR+B8)*(COS(AJR)/SIN(2*AJR-B8))
IF (XM.LT.0.0) XM=100.0*DJ
Z2=0
IF( Y9.EQ.3 ) GO TO  1145;IF( Y9.EQ.6 ) GO TO  1145;DJ=2*R1
1145 IF( M.LT.1 ) GO TO  1170
DJ=2*R1
C            XP CALCULATION
Z2=DJ*6*(SQRT(M**2-1))**.778151
C            CRITICAL FREQUENCY CALCULATION FOR ABSORPTION
1170 F0=A0/(2*DJ)
1175 DO 1295 J=1,24
SX=.8/((F(J)*DJ/V8)**.82)
C            ABSORPTION EFFECT
ZZ=Z9
IF( F(J).LT.F0 ) GO TO  1220
ZZ=Z8
IF( F(J).GT.4*F0 ) GO TO  1220
ZZ=((Z9-Z8)/(-.60206))*ALOG10(F(J)/F0)+Z9
C            SOURCE LOCATIONS
1220 Z3=Z2+DJ*SX
SJ=XM/Z3
TC=0;X(J)=0;IF( K7.EQ.2 ) GO TO  1265;X(J)=Z3
C          CUTOFF EFFECT
IF( R8.GT..65 ) GO TO  1265;IF( SJ.GE.4 ) GO TO  1265
TC=22.652929-44.688299*SJ+43.858243*SJ**2-25.284491*SJ**3
TC=TC+8.4045899*SJ**4-1.4693844*SJ**5+.1039457*SJ**6
IF( R8.LT..6 ) GO TO  1265
TC=TC-TC*(R8-.6)/.05
1265 DO 1295 I=1,15
IF( K7.EQ.2 ) GO TO  1290
```


FIGURE A-4 (CONTINUED). LISTING OF THE REVISED M*S PROGRAM

```
IF( ((I+1)*1Ø).LT.OJ ) GO TO  129Ø
S(I,J)=S(GJ,J)+RVE(GJ)-RVE(I)
GO TO 1295
129Ø S(I,J)=S(I,J)-TC+ZZ
1295 CONTINUE
C          EJECTOR EFFECTS DETERMINED
CALL AEROCALC(TT4,P4,AA8,VJI,TJI,WI,PØ,TØ)
CALL AEROCALC(TT5,P5,A9,VJO,TJO,WO,PØ,TØ)
CALL AEROSUM(VJI,TT4,AA8,WI,VJO,TT5,A9,WO,PØ,TØ,XMJMIX)
IF( A6.EQ.Ø ) GO TO  131Ø;IF(K7.EQ.2)GO TO 13ØØ;CALL EJECTS
13ØØ DO 13Ø8 J=1,24; DO 13Ø8 I=1,15
S(I,J)=S(I,J)+E1(I,J)
13Ø8 CONTINUE
131Ø IF( K7.EQ.2 ) GO TO  1365;CALL SUB5
IF(K9.EQ.Ø) GO TO 1335
CALL SUB3
AS="PREMERGED NOISE"
CALL PNTT8
1335 IF( Y9.GT.3 ) GO TO  163Ø;CALL SUB6;CALL SUB4
C          CHECK FOR SHOCK CELL NOISE
IF (P9.LT.1.9) GO TO 1395;V9=U3;C9=41.43*SQRT(G9*T3);D8=2*R1
IF(Y9.LT.3) GO TO 1355;D8=(R4+R6)/12
1355 CALL SHKSUB;K7=2;GO TO 1175
C          CHUTE OR SPOKE CORRECTION
1365 Z9=-2*P9
137Ø CALL SUB2
CALL SUB5
IF( K9.EQ.Ø ) GO TO  139Ø;AS="SHOCK (M-E) NOISE"
CALL SUB3;CALL PNTT8
139Ø IF( Y9.GT.4 ) GO TO  1685;CALL SUB6
1395 IF( K9.EQ.Ø ) GO TO  14ØØ;K1=3
14ØØ CALL SUB3
AS="TOTAL NOISE"
CALL PNTT8
     IF (IFLSUM.EQ.NO) GO TO 245
     GO TO 21ØØ
C          CONICAL NOZZLE NOISE
1425 V8=U3;A8=A9;W8=R3*U3*A8;AS="CONICAL MIXING NOISE"
CALL SUB1;CALLSUB5;IF(K9.EQ.Ø)GO TO 1445;IF(P9.LT.1.9)GO TO 1475
CALL SUB3;CALL PNTT8
C          CHECK FOR SHOCK CELL NOISE
1445 IF(P9.LT.1.9) GO TO 1465;CALL SUB4;V9=V8
C9=41.43*SQRT(G9*2.7*PØ/R3);D8=SQRT(4*A8/P1);CALL SHKSUB;CALL SUB5
IF( K9.EQ.Ø ) GO TO  1461;CALL SUB3;AS="CONICAL SHOCK NOISE"
CALL PNTT8
1461 CALL SUB6
1465 AS="CONICAL TOTAL NOISE";IF( K9.EQ.Ø ) GO TO  1475;K1=3
1475 CALL SUB3;CALL PNTT8
     IF (IFLSUM.EQ.NO) GO TO 245
     GO TO 21ØØ
C          COANNULAR NOZZLE NOISE
1485 PRINT 2135
2135 FORMAT(//" COANNULAR NOZZLE FLOW PARAMETERS")
IF( Y9.EQ.4 ) GO TO  1545;A3=A9;V7=U3;T3=2.7*PØ/R5;V6=R3;T8=T5
R3=R5;C3=C4;P9=P5;A4=A8;U3=U5
R2=SQRT(((P1*R2**2/4)-(A8+R9**2*P1/4))/P1)
R2=R2-R2*SIN(B9*P1/18Ø)/COS(B9*P1/18Ø)
C          GO TO POST-MERGED VELOCITY CALCULATION
GO TO 72Ø
1515 A8=A4+A5
W4=V6*A4*V7;W5=W8
W8=W4+W5;V8=(V7*W4+VJ*W5)/W8
T5=T8;A9=A3;T8=(T4*W4+T5*W5)/W8
T5=T9;U5=U3;U3=V7;R5=R3;R3=V6
```

FIGURE A-4 (CONTINUED). LISTING OF THE REVISED M*S PROGRAM

```
A3=A4;IF( U3.LT.VJ ) GO TO  1580;V8=U3;T8=T4;W8=R3*V8*A8;GO TO 1580
1545 W4=R3*A8*U3;W5=R5*A9*U5
A3=A8;A8=A8+A9
W8=W4+W5;VJ=U5;A5=A9
IF( U3.LT.U5 ) GO TO  1570;V8=U3;T8=T4;W8=R3*V8*A8
GO TO 1580
1570 V8=(U3*W4+U5*W5)/W8
T8=(T4*W4+T5*W5)/W8
1580 PRINT 2131 ; PRINT 2030,V8,T8,W8,A8
2131 FORMAT(/" MIXED FLOW CONDITIONS")
2030 FORMAT(" U6=",F10.1,5X,"TT6=",F6.0,5X,"W6=",F10.3,5X,
& "A6=",F10.3)
C          DETERMINE POST-MERGED NOISE
GO TO 960
1595 V8=U5;T3=2.7*P0/R5;T8=T5
W5=U5*A9*R5;K1=2
C          PRE-MERGED NOISE DETERMINATION
IF( Y9.EQ.4 ) GO TO  1615;A8=A9/AN1;W8=W5/AN1;GO TO 1015
1615 A8=.075*A9;W8=.075*W5;CALL SUB1
GO TO 1310
C          CHECK FOR OUTER STREAM SHOCK
1630 IF (P5.LT.1.9) GO TO 1685;CALL SUB6;CALL SUB4
P9=P5
V9=U5;C9=41.43*SQRT(G2*2.7*P0/R5);D8=2.5*R7
 GO TO(1660,1655,1650),Y9-3
1650 D8=(R4+R6)/12;GO TO 1355
1655 D8=2*R1;GO TO 1355
1660 CALL SHKSUB;Z9=10*ALOG10(SQRT(4*A9/P1)/D8);CALL SUB2
CALL SUB5
IF( K9.EQ.0 ) GO TO  1685
CALL SUB3;AS="OUTER SHOCK NOISE";CALL PNTT8
C          CHECK FOR INNER STREAM SHOCK
1685 IF (P4.LT.1.9) GO TO 1725;C9=41.43*SQRT(G9*2.7*P0/R3);V9=U3
CALL SUB6;CALL SUB4
D8=SQRT(4*A3/P1);IF(Y9.EQ.4)GO TO 1700;D8=SQRT(D8**2+(2*R9)**2)-(2*R9)
1700 CALL SHKSUB
IF( R9.EQ.0 ) GO TO  1710;Z9=-3;CALL SUB2
1710 CALL SUB5
IF( K9.EQ.0 ) GO TO  1725;CALL SUB3;AS="INNER SHOCK NOISE"
CALL PNTT8
1725 CALL SUB6;IF( K9.EQ.0 ) GO TO  1730;K1=3
1730 CALL SUB3
AS="TOTAL NOISE";CALL PNTT8
C
      IF (IFLSUM.EQ.NO) GO TO 245
2100 ENGCOR=10.0*ALOG10(NENG)
      COR=ENGCOR+SHLDJ+REFLJ+T1985
      WRITE (IFILE) CASE,ALT,SL,E3,(PNL(I)+COR,I=2,15)
      GO TO 245
9999 IF (IFLSUM.NE.NO) ENDFILE IFILE
      STOP
END
CSUB1
SUBROUTINE SUB1
COMMON/CM1/L(9,24),X(24),F(24),E(24),S(15,24),KK(24,5),C(15,5),O(20),
& RR(49),RX(49),P(20),R(15,24),Y1(24),Y(24),C1(15),RVE(20),
& S1(24),G(2,24),C2(15,2),T(20),D(20),W(5),A(4),V(3),E1(15,24)
COMMON /CM2/ V8,A0,W8,K1,Y9,T8,T5,R7,P1,Z9,DJ,AJ,H,U,E9,AA
& ,T0,V9,C9,D8,D1,V0,O9,A8,Q,L9,A6,A7,S6,P9,R9,ALT,SL,AN1,NFLT
*& ,HTR,NST,XMJMIX,TJMX,VJMX
COMMON /CM3/AS,CASEID,E3,PNL(20)
REAL L,KK,K1
CHARACTER AS*20,NAME*60,ADDRES*60,IDENT*60,CASEID*60
C          SAE ARP 876 (1975 REV) CONICAL NOZZLE NOISE
```

FIGURE A-4 (CONTINUED). LISTING OF THE REVISED M*S PROGRAM

```
51ØØ XJ=ALOG1Ø(V8/AØ)
511Ø WE=2
512Ø IF( XJ.GT.Ø.22 ) GO TO  3Ø1Ø
513Ø WE=W(1)+W(2)*XJ+W(3)*XJ**2+W(4)*XJ**3+W(5)*XJ**4
514Ø 3Ø1Ø DEN=((W8/(A8*V8))/.Ø76475)**WE
515Ø Q2=1Ø*ALOG1Ø(DEN*(A8/(1**2)))
516Ø DO 3Ø24 I=1,15
517ØC             OASPL AND FLIGHT EFFECTS
518Ø O(I)=Q2+C(I,1)+C(I,2)*XJ+C(I,3)*XJ**2+C(I,4)*XJ**3+C(I,5)*XJ**4+C1(I)
519Ø IF (K1.EQ.1) GO TO 3Ø22
5191 RVE(I)=-6Ø*ALOG1Ø(1/(1-(VØ/AØ)*COS(((I+1)*1Ø-AA)*P1/18Ø)))
5192 GO TO 3Ø24
52ØØ 3Ø22 DUM=(1-(VØ/AØ)*COS(((I+1)*1Ø-AA)*P1/18Ø))
521Ø RVE(I)=1Ø*ALOG1Ø((V8/(V8-(VØ*COS(AA*P1/18Ø))))**C2(I,NFLT)*DUM)
522Ø 3Ø24 CONTINUE
523Ø IF( Y9.NE.4 )GO TO 3Ø28;IF( T8.NE.T5 )GO TO 3Ø28;A8=(R7/2)**2*P1
524Ø 3Ø28 DO 3Ø66 J=1,24
525Ø T(1)=54Ø;T(2)=1Ø8Ø;T(3)=162Ø
526Ø DO 3Ø66 I=1,15
527Ø Z1=SIN((I+1)*P1/18)
528Ø XJ=ALOG1Ø(F(J)*2*SQRT(A8/P1)/(V8*Z1+AØ*(1-Z1)))
529Ø DO 3Ø42 K=1,24
53ØØ E(K)=KK(K,1)+KK(K,2)*XJ+KK(K,3)*XJ**2+KK(K,4)*XJ**3+KK(K,5)*XJ**4
531Ø 3Ø42 CONTINUE
532Ø K6=I-7
533Ø IF( K6.GT.Ø ) GO TO  3Ø5Ø
534Ø K6=1
535Ø 3Ø5Ø IF( T8.GT.1Ø8Ø ) GO TO  3Ø58
536Ø N1=3*K6-2
537Ø RJ1=1
538Ø GO TO 3Ø62
539Ø 3Ø58 N1=3*K6-1
54ØØ RJ1=2
541Ø 3Ø62 S(I,J)=O(I)+(E(N1+1)-E(N1))*((T8-T(RJ1))/(T(RJ1+1)-T(RJ1)))+E(N1)
542Ø S(I,J)=S(I,J)-RVE(I)
543Ø 3Ø66 CONTINUE;RETURN
544ØCSUB3
545Ø ENTRY SUB3
546ØC             EXTRAPOLATION AND OASPL AND PNL CALCULATION
547Ø DO 311Ø K=1,15
548Ø DO 1Ø J=1,24;X(J)=S(K,J);1Ø CONTINUE
549Ø IF( K1.EQ.3 ) GO TO  31Ø8
55ØØ AJ=(K+1)*1Ø
551Ø D1=1
552Ø CALL EXTP
553Ø DO 2ØJ=1,24;S(K,J)=X(J);2Ø CONTINUE
554Ø 31Ø8 CALL PNLPT;T(K)=V(2);O(K)=V(1);P(K)=V(3)
555Ø 311Ø CONTINUE;RETURN
556ØCSUB5
557Ø ENTRY SUB5
558ØC             PWL CALCULATION
559Ø O9=Ø;DO 32Ø7 I=1,24;A2=Ø;DO 32Ø4 J=1,15;AJ=(J+1)*1Ø
56ØØ YJ=1.5*P1*(COS((AJ-5)*P1/18Ø)-COS((AJ+5)*P1/18Ø))
561Ø A2=A2+(2.227525E-6*4E-8*YJ*1Ø**(S(J,I)/1Ø))
562Ø 32Ø4 CONTINUE
563Ø Y(I)=1Ø*ALOG1Ø(A2)+13Ø+1.24939
564Ø O9=O9+1Ø**(Y(I)/1Ø)
565Ø 32Ø7 CONTINUE
566Ø O9=1Ø*ALOG1Ø(O9)
567Ø RETURN
568ØCSUB4
569Ø ENTRY SUB4
57ØØC             RESET VARIABLES
571Ø DO 34Ø2 J=1,24;DO 34Ø1 I=1,15;R(I,J)=S(I,J)
```

FIGURE A-4 (CONTINUED). LISTING OF THE REVISED M*S PROGRAM

```
 3401 CONTINUE;Y1(J)=Y(J);3402 CONTINUE;RETURN
CSUB2
 ENTRY SUB2
C           DELTA SPL CORRECTION
 DO 3406 J=1,24;DO 3406 I=1,15;S(I,J)=S(I,J)+Z9
 3406 CONTINUE;RETURN
CSUB6
 ENTRY SUB6
C           SPL AND PWL ADDITION
 O9=0
 DO 3506 J=1,24;DO 3503 I=1,15
 S(I,J)=10*ALOG10(10**(S(I,J)/10)+10**(R(I,J)/10))
 3503 CONTINUE
 Y(J)=10*ALOG10(10**(Y1(J)/10)+10**(Y(J)/10))
 O9=O9+10**(Y(J)/10)
 3506 CONTINUE
 O9=10*ALOG10(O9)
 RETURN;END
 SUBROUTINE EXTP
C         EXTP -- SPL EXTRAPOLATION SUBROUTINE
 COMMON/CM1/L(9,24),X(24),F(24),E(24),S(15,24),KK(24,5),C(15,5),O(20),
& RR(49),RX(49),P(20),R(15,24),Y1(24),Y(24),C1(15),RVE(20),
& S1(24),G(2,24),C2(15,2),T(20),D(20),W(5),A(4),V(3),E1(15,24)
 COMMON /CM2/ V8,A0,W8,K1,Y9,T8,T5,R7,P1,Z9,DJ,AJ,H,U,E9,AA
& ,T0,V9,C9,D8,D1,V0,O9,A8,O,L9,A6,A7,S6,P9,R9,ALT,SL,ANI,NFLT
*& ,HTR,NST,XMJMIX,TJMX,VJMX
 COMMON /CM3/AS,CASEID,E3,PNL(20)
 REAL L,KK,K1
 CHARACTER AS*20,NAME*60,ADDRES*60,IDENT*60,CASEID*60
 REAL L1
 G3=0
 DOP=1/(1-V0/A0*COS((AJ-AA)*P1/180))
 L1=H
 IF(U.EQ.2.)L1=H/SIN((AJ-AA)*P1/180)
 Q=20*(ALOG10(L1/D1))
 IF(E9.EQ.0.) GO TO 470
 DIS=L1
 IF(E9.LT.2.0) GO TO 400
 IF(ALT/DIS.LT..035) GO TO 400
 IF(ALT.LT.100.0) GO TO 400
 DIS=L1*100.0/ALT
C            EGA CURVE FIT
 400 C1J=(.20411435E-20*DIS)-.66703095E-16
 C1J=(C1J*DIS)+.72854603E-12
 C1J=(C1J*DIS)-.32650913E-08
 C1J=(C1J*DIS)+.49614255E-05
 C1J=(C1J*DIS)+.44663072E-02
 G1=(C1J*DIS)+.59387702
 C1J=(.16573369E-24*DIS)-.46152934E-20
 C1J=(C1J*DIS)+.32361609E-16
 C1J=(C1J*DIS)+.39118972E-13
 C1J=(C1J*DIS)-.10464995E-08
 C1J=(C1J*DIS)+.29126338E-05
 C1J=(C1J*DIS)-.54370996E-03
 G2=(C1J*DIS)+.59506112
 IF(DIS.LE.4000.) GO TO 470
 G2=5.010264
 G1=15.44041+.0001*(DIS-4000)
 470 DO 670 J=1,24
 IF(F(J).GT.4000.) GO TO 510
 P3=F(J)
 GO TO 520
 510 P3=.89*F(J)
C            AIR ATTENUATION CURVE FIT
```


FIGURE A-4 (CONTINUED). LISTING OF THE REVISED M*S PROGRAM

```
6340 520 B1=(-.19973809E-14*P3)+.36618630E-10
6350 B2=(B1*P3)+.32351924E-07
6360 B3=(B2*P3)+.13498887E-02
6370 PA=(B3*P3)+.17604677E-01
6380 IF(E9.EQ.0.) GO TO 660
6390 IF(P3.EQ.63) GO TO 610
6400 IF(P3.GE.2000.) GO TO 630
6410 ZJ=.2*ALOG(P3/62.5)/ALOG(2)
6420 GO TO 640
6430 610 ZJ=0
6440 GO TO 640
6450 630 ZJ=1.0
6460 640 G3=(ZJ*(G1-G2))+G2
6470 660 COR=Q+G3+PA*((L1-D1)/1000)
6472 IF (DOP.LT.0.89) GO TO 662
6473 IF (DOP.GT.1.12) GO TO 661
6474 E(J)=X(J)-COR ; GO TO 670
6475 661 IF (J.EQ.1) GO TO 663 ; E(J)=X(J-1)-COR ; GO TO 670
6476 662 IF (J.EQ.24) GO TO 663 ; E(J)=X(J+1)-COR ; GO TO 670
6477 663 E(J)=X(J)-3-COR
6480 670 CONTINUE
6481 DO 680 J=1,24
6482 680 X(J)=E(J)
6490 RETURN
6500 END
6510 SUBROUTINE SHKSUB
6520C        SHKSUB -- SAE SHOCK CELL NOISE PREDICTION SUBROUTINE
6530 COMMON/CM1/L(9,24),X(24),F(24),E(24),S(15,24),KK(24,5),C(15,5),O(20),
6540& RR(49),RX(49),P(20),R(15,24),Y1(24),V(24),C1(15),RVE(20),
6550& S1(24),G(2,24),C2(15,2),T(20),D(20),W(5),A(4),V(3),E1(15,24)
6560 COMMON /CM2/ V8,A0,W8,K1,Y9,T8,T5,R7,P1,Z9,DJ,AJ,H,U,E9,AA
6570& ,T0,V9,C9,D8,D1,V0,O9,A8,Q,L9,A6,A7,S6,P9,R9,ALT,SL,AN1,NFLT
*6571&  ,HTR,NST,XMJMIX,TJMX,VJMX
6580 COMMON /CM3/AS,CASEID,E3,PNL(20)
6590 REAL L,KK,K1
6600 CHARACTER AS*20,NAME*60,ADDRES*60,IDENT*60,CASEID*60
6610 A0=49.018*SQRT(T0)
6615 DEK=2.575*ALOG10((V0+100)/100)
6620 D1=1;B=SQRT((V9/C9)**2-1)
6630 D0=10*ALOG10(((B**2)*D8/D1)**2)
6640 DO 390 K8=1,15
6650 AJR=(K8+1)*P1*10/180
6651 DUM=1-(V0/A0)*COS(((K8+1)*10-AA)*P1/180)
6660 DO 380 J=1,24
6670 SJ=ALOG10(F(J)*1.1*D8*8/A0)
6680 DO 250 K=2,24
6690 IF(SJ.GT.S1(K)) GO TO 240
6700 210 C1J=G(2,K-1)+(SJ-S1(K-1))*(G(2,K)-G(2,K-1))/(S1(K)-S1(K-1))
6710 G1=G(1,K-1)+(SJ-S1(K-1))*(G(1,K)-G(1,K-1))/(S1(K)-S1(K-1))
6720 GO TO 260
6730 240 IF(K.EQ.24) GO TO 210
6740 250 CONTINUE
6750 260 H1=0
6760 F1=(2*P1*F(J)*1.31*B*D8/(.7*V9))*(1+(.7*V9/A0)*COS(AJR))
6770 DO 360 I=1,5
6780 F2=0
6790 KSTART=0;DO 330 K=KSTART,(8-(I+1))
6800 ZI=I ; ZK=K
6810 F3=F1*(ZI*(1.0-.06*((ZI+1.0)/2.0+ZK)))
6820 F2=F2+(COS(F3)*SIN(.115*F3)/(.115*F3))
6830 330 CONTINUE
6840 IF(C1J.LT..01) GO TO 360
6850 H1=H1+((C1J**(I**2))*F2)
6860 360 CONTINUE
```

FIGURE A-4 (CONTINUED). LISTING OF THE REVISED M*S PROGRAM

```
S(K8,J)=D0+G1+10*ALOG10(1+.25*H1)+DEK
IF(K8.GT.7) GO TO 380
S(K8,J)=S(K8,J)+40*ALOG10(1/DUM)
380 CONTINUE
390 CONTINUE
RETURN
END
SUBROUTINE PNLPT
C          PNLPT -- CALCULATES PNL, OASPL, AND PNLT
COMMON/CM1/L(9,24),X(24),F(24),E(24),S(15,24),KK(24,5),C(15,5),O(20),
& RR(49),RX(49),P(20),R(15,24),Y1(24),Y(24),C1(15),RVE(20),
& S1(24),G(2,24),C2(15,2),T(20),D(20),W(5),A(4),V(3),E1(15,24)
COMMON /CM2/ V8,A0,W8,K1,Y9,T8,T5,R7,P1,Z9,DJ,AJ,H,U,E9,AA
& ,T0,V9,C9,D8,D1,V0,O9,A8,Q,L9,A6,A7,S6,P9,R9,ALT,SL,AN1,NFLT
& ,HTR,NST,XMJMIX,TJMX,VJMX
COMMON /CM3/AS,CASEID,E3,PNL(20)
REAL L,KK,K1
CHARACTER AS*20,NAME*60,ADDRES*60,IDENT*60,CASEID*60
TJ=0
V(1)=0
V(2)=0
DO 370 J=1,24
IF(X(J).GT.0.) GO TO 200
X(J)=1
200 IF(X(J).GE.L(7,J)) GO TO 320
IF(X(J).GE.L(5,J)) GO TO 300
IF(X(J).GE.L(3,J)) GO TO 280
IF(X(J).GE.L(1,J)) GO TO 260
AN=0
GO TO 330
260 AN=0.1*(10**(L(2,J)*(X(J)-L(1,J))))
GO TO 330
280 AN=10**(L(4,J)*(X(J)-L(5,J)))
GO TO 330
300 AN=10**(L(6,J)*(X(J)-L(5,J)))
GO TO 330
320 AN=10**(L(8,J)*(X(J)-L(9,J)))
330 V(1)=V(1)+10**(X(J)/10)
V(2)=V(2)+AN
IF(TJ.GT.AN) GO TO 370
TJ=AN
370 CONTINUE
V(2)=33.22*ALOG10(V(2)*.15+TJ*.85)+40
V(1)=10*ALOG10(V(1))
CALL TPNLC(X,P2)
980 V(3)=V(2)+P2
RETURN
END
*TPNLC          THIS SECTION CALCULATES TONE CORRECTED PNL
C               SPECTRAL IRREGULARITY CORRECTION
C
C               THIS PROCEDURE DETERMINES A SPECTRAL IRREGULARITY
C               (E.G.,PURE TONE) CORRECTION FACTOR "C" VIA SECTION B36.3
C               OF THE FAA NOISE CERTIFICATION DOCUMENT (NOV 17,1969) AS
C               A FUNCTION OF THE UNCORRECTED 1/3 OCTAVE SPECTRUM,SPL.
C
      SUBROUTINE TPNLC(SPL,PTCOR)
      DIMENSION SPL(24),ISPLF(24),SC(24),SPLP(24),SPLPP(24),SP(25),
     & SBAR(24),F(24)
C
C     *INITIALIZE SPL FLAG*
      DO 1 I=1,24
    1 ISPLF(I) = 0
C
```

OF POOR QUALITY

FIGURE A-4 (CONTINUED) LISTING OF THE REVISED M*S PROGRAM

```
C    *STEP 1*
      DO 5 I=4,24
    5 SC(I)=SPL(I) - SPL(I-1)
C
C    *STEP 2 AND 3*
      DO 10 I=5,24
      IF(ABS(SC(I)-SC(I-1)).LE.5.0) GO TO 10
      IF(SC(I).GT.0.0.AND.SC(I).GT.SC(I-1)) ISPLF(I)=1
      IF(SC(I).LE.0.0.AND.SC(I-1).GT.0.0) ISPLF(I-1)=1
   10 CONTINUE
C
C    *STEP 4*
      DO 25 I=1,24
      IF(ISPLF(I).EQ.0) GO TO 20
      IF(I.EQ.24) GO TO 15
C          STEP 4B MODIFIED SUCH THAT PRECEDING AND FOLLOWING
C          NON-FLAGGED SOUND PRESSURE LEVELS EMPLOYED IN AVERAGE.
      II = I
      DO 11 J=1,20
      II = II-1
      IF(ISPLF(II).EQ.0) GO TO 12
   11 CONTINUE
   12 SPLL = SPL(II)
      IP1 = I+1
      DO 13 J=IP1,24
      IF(ISPLF(J).EQ.0) GO TO 14
   13 CONTINUE
      J = 24
   14 SPLU = SPL(J)
      SPLP(I) = (SPLL+SPLU)/2.
      GO TO 25
   15 SPLP(24) = SPL(23)+SC(23)
      GO TO 25
   20 SPLP(I) = SPL(I)
   25 CONTINUE
C
C    *STEP 5*
      DO 30 I=4,24
   30 SP(I) = SPLP(I)-SPLP(I-1)
      SP(3) = SP(4)
      SP(25) = SP(24)
C
C    *STEP 6*
      DO 35 I=3,23
   35 SBAR(I) = (SP(I)+SP(I+1)+SP(I+2))/3.
C
C    *STEP 7*
      SPLPP(1) = SPL(1)
      SPLPP(2) = SPL(2)
      SPLPP(3) = SPL(3)
      DO 40 I=4,24
   40 SPLPP(I) = SPLPP(I-1)+SBAR(I-1)
C
C    *STEP 8*
      DO 45 I=1,24
   45 F(I) = SPL(I)-SPLPP(I)
C
C    *STEP 9 AND 10*
      CMAX = 0.0
      DO 65 I=1,24
      IF(I.GE.11.AND.I.LE.21) GO TO 50
C     *FREQ<500HZ OR FREQ>5000HZ*
      TC2 = F(I)/6.
      TC3 = 3.333
```

FIGURE A-4 (CONTINUED). LISTING OF THE REVISED M*S PROGRAM

```
8130       GO TO 55
8140C      *500<=FREQ<=5000HZ*
8150    50 TC2 = F(I)/3.
8160       TC3 = 6.666
8170    55 IF(F(I).LT.3.0) GO TO 65
8180       IF(F(I).GE.20.0) GO TO 60
8190       CMAX = AMAX1(CMAX,TC2)
8200       GO TO 65
8210    60 CMAX = AMAX1(CMAX,TC3)
8220    65 CONTINUE
8230       PTCOR=CMAX
8240   500 RETURN
8250       END
8260 SUBROUTINE PNTT8
8270C PNTT8 -- PRINT AND EPNL CALC SUBROUTINE
8280C
8290 COMMON/CM1/L(9,24),X(24),F(24),E(24),S(15,24),KK(24,5),C(15,5),O(20),
8300& RR(49),RX(49),P(20),R(15,24),Y1(24),V(24),C1(15),RVE(20),
8310& S1(24),G(2,24),C2(15,2),T(20),D(20),W(5),A(4),V(3),E1(15,24)
8320 COMMON /CM2/ V8,A0,W8,K1,Y9,T8,T5,R7,P1,Z9,DJ,AJ,H,U,E9,AA
8330& ,T0,V9,C9,D8,D1,V0,O9,A8,Q,L9,A6,A7,S6,P9,R9,ALT,SL,AN1,NFLT
*8333&  ,HTR,NST,XMJMIX,TJMX,VJMX
8340 COMMON /CM3/AS,CASEID,E3,PNL(20)
8342      COMMON /CM4/ CASE
8350 REAL L,KK,K1
8360 CHARACTER AS*20,NAME*60,ADDRES*60,IDENT*60,CASEID*60
8362      CHARACTER CASE   *6
8370C
8380 REAL MP,KT
8390C
8400 1000 FORMAT(/////50X,"*  ",A20)
8410 1001 FORMAT(50X,"*",F7.1," FOOT ALTITUDE")
8420 1002 FORMAT(50X,"*",F7.1," FOOT SIDELINE")
8430 1004 FORMAT(50X,"*",F7.1," FOOT ARC")
8440 1006 FORMAT(50X,"*  NO EGA")
8450 1008 FORMAT(50X,"*  FULL EGA")
8460 1009 FORMAT(50X,"*  100 FOOT LAYER EGA")
8470 1010 FORMAT(50X,"*",F6.0,"DEGREE STANDARD DAY"//50X,"ACOUSTIC ANGLE",
8480& " FROM INLET"/"0 FREQ     20     30     40     50     60     70",
8490& "     80     90    100    110    120    130    140    150",
8500& "    160    PWL")
8510 1012 FORMAT(F7.0,16F7.1)
8520 1014 FORMAT(1X,A6,16F7.1)
8530 1016 FORMAT(" EPNL=",F6.1)
8540 1017 FORMAT(1H1///,35X,"HIGH VELOCITY JET NOISE PROGRAM -",
8550& " ENGINEERING CORRELATION"///)
8560 1018 FORMAT(33X,A60/)
8570C
8580 PRINT 1017 ; PRINT 1018,CASEID
8582 1019 FORMAT (33X,"CASE NUMBER ",A6)
8584      PRINT 1019,CASE
8590 PRINT 1000,AS
8600 IF(U.EQ.1.) GO TO 160
8610 IF (SL.NE.0.0) GO TO 159 ; IF (V0.NE.0.0) GO TO 159
8620 PRINT 1002,H ; GO TO 170
8630 159 PRINT 1001,ALT
8640 PRINT 1002,SL
8650 GO TO 170
8660 160 PRINT 1004,H
8670 170 GO TO (171,172,173),E9+1
8680 171 PRINT 1006 ; GO TO 200
8690 172 PRINT 1008 ; GO TO 200
8700 173 PRINT 1009
8710 200 PRINT 1010,T0
```

FIGURE A-4 (CONTINUED). LISTING OF THE REVISED M*S PROGRAM

```
8720 DO 320 J=1,24
8730 PRINT 1012,F(J),(S(I,J),I=1,15),Y(J)
8740 320 CONTINUE
8750 AS="OASPL"
8760 PRINT 1014,AS,(O(I),I=1,15),O9
8770 AS="PNL"
8780 PRINT 1014,AS,(T(I),I=1,15)
8782      DO 322 I=1,15
8783  322 PNL(I)=T(I)
8790 AS="PNLT"
8800 PRINT 1014,AS,(P(I),I=1,15)
8810 PRINT," "
8820 PRINT," "
8821 DO 1015 I=1,15
8822 1015 P(I)=T(I)
8823 XXX=V0 ; IF(V0.GT.0.) GO TO 8825
8824 V0=300.0
8825 8825 CONTINUE
8830 IF(V0.EQ.0.) GO TO 1080
8840 IF(U.EQ.1.) GO TO 1080
8850C          EPNL CALCULATION
8860 T1=0.
8870 MP=0.0
8880 Z1=0.
8890 Z3=0.
8900 SJ=0.
8910C          FLYOVER TIME CALCULATION
8920 DO 500 J1=1,15
8930 AJ=(J1+1)*10-AA
8940 T(J1)=(H/SIN(AJ*PI/180.))/A0
8950 7670 WJ=H/(SIN(AJ*PI/180.)/COS(AJ*PI/180.))
8960 ASK=(AJ-10)*PI/180.
8970 KT=(H/(SIN(ASK)/COS(ASK))-WJ)/V0
8980 7685 IF(J1.EQ.1) GO TO 490
8990 D(J1)=T(J1)+D(J1-1)+KT-T(J1-1)
9000 GO TO 500
9010 490 D(J1)=T(J1)+KT
9020 500 CONTINUE
9030 KT=D(8)
9040 DO 540 J=1,15
9050 T(J)=D(J)-KT
9060 540 CONTINUE
9070C          PNLT MAX SEARCH
9080 DO 610 J=1,15
9090 IF(P(J).GT.MP) GO TO 590
9100 GO TO 610
9110 590 MP=P(J)
9120 TJ=T(J)
9130 610 CONTINUE
9140 CJ=MP-10.
9150C          INITIAL AND FINAL TIME DETERMINATION
9160 DO 680 J=1,15
9170 IF(P(J).LT.CJ) GO TO 680
9180 IF((J-1).LT.1) GO TO 750
9190 D7=T(J)-(T(J)-T(J-1))*(P(J)-CJ)/(P(J)-P(J-1))
9200 GO TO 690
9210 680 CONTINUE
9220 690 DO 740 JJ=1,15
9230 J=16-JJ
9240 IF(P(J).LT.CJ) GO TO 740
9250 IF((J+1).GT.15) GO TO 780
9260 D9=T(J)+(T(J+1)-T(J))*(P(J)-CJ)/(P(J)-P(J+1))
9270 GO TO 820
9280 740 CONTINUE
```

FIGURE A-4 (CONTINUED). LISTING OF THE REVISED M*S PROGRAM

```
 750 Z1=P(2)-P(1)
 D7=T(1)-((P(1)-CJ)/Z1)*(T(2)-T(1))
 GO TO 690
 780 Z3=P(14)-P(15)
 D9=T(15)+((P(15)-CJ)/Z3)*(T(15)-T(14))
 T(16)=D9
 P(16)=CJ
C           INTEGRATION START
 820 IF(Z1.EQ.0.) GO TO 880
 T1=IFIX(2.*TJ-D7)
 I=0
 GO TO 900
 880 T1=IFIX(2.*(TJ-T(1)))
 I=1
 900 TJ=TJ-T1/2
 910 IF(TJ.GT.T(I+1)) GO TO 1020
 TT=T(I)
 IF(I.EQ.0) TT=D7
 IF(TT.EQ.T(I+1)) GO TO 950
 Q1=(TJ-TT)/(T(I+1)-TT)
 GO TO 960
 950 Q1=(TJ-T(I+1))/(T(I+2)-T(I+1))
 960 RJ=P(I)+Q1*(P(I+1)-P(I))
 IF(RJ.LT.CJ) GO TO 990
 SJ=SJ+10.**(RJ/10.)
 990 TJ=TJ+.5
 GO TO 910
 1020 I=I+1
 IF(Z3.EQ.0.) GO TO 1050
 IF(I.GT.15) GO TO 1060
 GO TO 910
 1050 IF(I.LE.(16)) GO TO 910
 1060 E3=(10.*ALOG10(SJ))-13.
 PRINT 1016, .1*IFIX(10.*E3+.5)
 1080 V0=XXX
 RETURN
 END
 BLOCK DATA
C TAKE PLACE OF ALFIL AND PNLFIL
 COMMON/CM1/L(9,24),X(24),F(24),E(24),S(15,24),KK(24,5),C(15,5),O(20),
& RR(49),RX(49),P(20),R(15,24),Y1(24),Y(24),C1(15),RVE(20),
& S1(24),G(2,24),C2(15,2),T(20),D(20),W(5),A(4),V(3),E1(15,24)
 COMMON /CM2/ V8,A0,W8,K1,Y9,T8,T5,R7,P1,Z9,DJ,AJ,H,U,E9,AA
& ,T0,V9,C9,D8,D1,V0,O9,AB,Q,L9,A6,A7,S6,P9,R9,ALT,SL,ANI,NFLT
&  ,HTR,NST,XMJMIX,TJMX,VJMX
 COMMON /CM3/AS,CASEID,E3,PNL(20)
 REAL L,KK,K1
 CHARACTER AS*20,NAME*60,ADDRES*60,IDENT*60,CASEID*60
C           SAE JET MIXING NOISE CURVE FIT COEFFICIENTS
 DATA W/
& .79847856,6.0060324,2.6130686,-17.028296,-31.584975/
 DATA ((C(I,N),N=1,5),I=1,15)/
& 134.0671,78.13129,13.57216,-35.85844,-86.82891,
& 134.5827,77.92338,14.75807,-33.24901,-101.6892,
& 135.0606,77.93685,16.55295,-33.08064,-109.8477,
& 135.5802,77.94105,18.44398,-31.98636,-124.1251,
& 136.3070,78.56058,20.13687,-32.57560,-131.9922,
& 137.0408,78.27523,22.26973,-35.10086,-143.0645,
& 137.9991,79.33667,22.17358,-29.12441,-136.9456,
& 139.2326,80.80132,23.77030,-31.64966,-146.2695,
& 140.7755,83.32237,21.13044,-34.51163,-119.4629,
& 142.7406,86.50671,22.49117,-33.24900,-111.0132,
& 144.8893,92.72220,28.02726,-47.22204,-120.3369,
& 147.1450,101.6591,50.97311,-80.30287,-254.0784,
```


FIGURE A-4 (CONTINUED). LISTING OF THE REVISED M*S PROGRAM

```
9910& 149.5492,105.6868,40.77499,-100.0806,-262.8197,
9920& 150.9042,107.0227,32.56691,-150.7574,-323.1343,
9930& 151.0189,98.95452,-15.66443,-131.8180,-88.57726/
9940 DATA ((KK(I,N),N=1,5),I=1,24)/
9950& -10.54902,1.771008,-8.731992,.101391,.8636305,
9960& -10.47272,-2.038344,-9.375026,1.117183,.9349618,
9970& -10.92039,-2.967566,-8.846933,1.269824,.7043903,
9980& -10.61639,4.452847,-8.556268,-.4737891,.7829865,
9990& -10.04622,-1.11499,-10.29365,1.407677,.9611449,
10000& -10.20316,-1.654881,-10.75808,1.045175,1.144233,
10010& -10.57207,3.833069,-8.472411,.0446222,.7277405,
10020& -10.23615,-1.286685,-11.13199,1.076169,1.066819,
10030& -10.64444,-3.383546,-11.9358,1.695872,1.549694,
10040& -10.5277;,2.105704,-8.993265,.4974295,.7802992,
10050& -11.03052,-3.665336,-10.5132,1.784495,.7993335,
10060& -11.68293,-6.134871,-10.17043,1.993965,.5740519,
10070& -11.20320,-1.423282,-8.568622,1.369792,.5003525,
10080& -12.46326,-7.189952,-9.689162,2.508981,.4032442,
10090& -13.19008,-9.252206,-7.828305,3.004999,-.2370745,
10100& -11.88213,-5.22407,-8.782326,1.981059,.3970906,
10110& -14.57344,-11.73308,-8.161604,3.560226,-.2413976,
10120& -16.53499,-15.38885,-5.695258,4.655082,-.9454673,
10130& -12.96843,-10.26358,-8.530573,3.485636,.195912,
10140& -17.11034,-17.86003,-6.628826,4.850326,-.8765574,
10150& -20.00749,-21.11827,-3.229256,5.837981,-1.727925,
10160& -14.20073,-14.80855,-7.363175,4.301735,-.494157,
10170& -19.20043,-22.94389,-5.903727,6.094622,-1.100933,
10180& -22.78446,-26.49346,-1.355867,6.749632,-2.499507/
10190C             PNL CALCULATION COEFFICIENTS
10200 DATA ((L(J,I),J=1,9),I=1,24)/
10210& 49.,.079520,55.,.058098,64.,.043478,91.01,.030103,52.,
10220& 44.,.068160,51.,.058098,60.,.040570,85.88,.030103,51.,
10230& 39.,.068160,46.,.052288,56.,.036831,87.32,.030103,49.,
10240& 34.,.059640,42.,.047534,53.,.036831,79.85,.030103,47.,
10250& 30.,.053013,39.,.043573,51.,.035336,79.76,.030103,46.,
10260& 27.,.053013,36.,.043573,48.,.033333,75.96,.030103,45.,
10270& 24.,.053013,33.,.040221,46.,.033333,73.96,.030103,43.,
10280& 21.,.053013,30.,.037349,44.,.032051,74.91,.030103,42.,
10290& 18.,.053013,27.,.034859,42.,.030675,94.63,.030103,41.,
10300& 16.,.053013,25.,.034859,40.,.030103,100.0,.030103,40.,
10310& 16.,.053013,25.,.034859,40.,.030103,100.0,.030103,40.,
10320& 16.,.053013,25.,.034859,40.,.030103,100.0,.030103,40.,
10330& 16.,.053013,25.,.034859,40.,.030103,100.0,.030103,40.,
10340& 16.,.053013,25.,.034859,40.,.030103,100.0,.030103,40.,
10350& 15.,.059640,23.,.034859,38.,.030103,100.0,.030103,38.,
10360& 12.,.053013,21.,.040221,34.,.029960,100.0,.029960,34.,
10370& 09.,.053013,18.,.037349,32.,.029960,100.0,.029960,32.,
10380& 05.,.047712,15.,.034859,30.,.029960,100.0,.029960,30.,
10390& 04.,.047712,14.,.034859,29.,.029960,100.0,.029960,29.,
10400& 05.,.053013,14.,.034859,29.,.029960,100.0,.029960,29.,
10410& 06.,.053013,15.,.034859,30.,.029960,100.0,.029960,30.,
10420& 10.,.068160,17.,.037349,31.,.029960,100.0,.029960,31.,
10430& 17.,.079520,23.,.037349,37.,.042285,44.29,.029960,34.,
10440& 21.,.059640,29.,.043573,41.,.042285,50.72,.029960,37./
10450 END
10460 SUBROUTINE EJECTS
10470C     EJECTS -- EJECTOR EFFECT SUBROUTINE
10480 COMMON /QM/ M,OJ
10490 COMMON/CM1/L(9,24),X(24),F(24),E(24),S(15,24),KK(24,5),C(15,5),O(20),
10500& RR(49),RX(49),P(20),R(15,24),Y1(24),Y(24),C1(15),RVE(20),
10510& S1(24),G(2,24),C2(15,2),T(20),D(20),W(5),A(4),V(3),E1(15,24)
10520 COMMON /CM2/ V8,A0,W8,K1,Y9,T8,T5,R7,P1,Z9,DJ,AJ,H,U,E9,AA
10530& ,T0,V9,C9,D8,D1,V0,O9,A8,Q,L9,A6,A7,S6,P9,R9,ALT,SL,AN1,NFLT
*10535&  ,HTR,NST,XMJMIX,TJMX,VJMX
```

FIGURE A-4 (CONTINUED). LISTING OF THE REVISED M*S PROGRAM

```
10540 COMMON /CM3/AS,CASEID,E3,PNL(20)
10550 REAL L,KK,K1,IMH,IMH1
10560 CHARACTER AS*20,NAME*60,ADDRES*60,IDENT*60,CASEID*60
10570 REAL L8,L9,L2,K6,L3,M
10580 REAL MACH
10590 DIMENSION IMH(10),WTGFN(10),IMH1(10)
10600 INTEGER IM
10605 REAL LAMBDA
10610C               HARDWALL EJECTOR EFFECTS
10630 SONSPD=49.01*SQRT(TJMX)
10640 D3=SQRT(A6*A7*A8*AN1/P1+S6**2-A7*A8*AN1/P1)
10650 AITCH=D3*(1-HTR)
10660 RBAR=D3*(1+HTR)/2.
10670 MACH=VJMX/SONSPD
10700 IF(MACH.GT..95)MACH=.95
11030 DO 110 I=1,15
11040 DO 110 J=1,24
11050 110 E1(I,J)=0.0
11060 FP=.3*V8/SQRT(4*A8/P1)
11070 L8=5*ALOG10(L9/2)
11090 A5=A6 ; IF(Y9.GT.3) GO TO 133 ; IF(R9.EQ.0) GO TO 140
11100 133 A5=A6/(10**(12.78*(D3/S6-1)**2+.046))
11110 140 D2=L8-23.59*A5-(110*(ALOG10(P9/1.9))**2)+.005*(T8-T0)+30
11120 IF(D2.LT.0) GO TO 280
11130C               DIRECTIVITY EFFECTS
11140 DO 270 I=1,15 ; AJ=(I+1)*10
11150 IF(AJ.GT.OJ-60) GO TO 165 ; DE=.64*D2 ; GO TO 220
11160 165 IF(AJ.LT.OJ-30) GO TO 180
11170 IF(AJ.GT.OJ) GO TO 200 ; DE=.2*D2 ; GO TO 220
11180 180 DE=D2*(-4.888E-4*(AJ-OJ+60)**2+.64)
11190 IF(DE.GT.0) GO TO 220 ; DE=0 ; GO TO 270
11200 200 IF(AJ.GT.OJ+20) GO TO 210 ; DE=D2*SQRT((AJ-OJ)/20) ; GO TO 220
11210 210 DE=D2*(.00925*(AJ-OJ-20)+1)
11220C               SPECTRAL EFFECTS
11230 220 DO 260 J=1,24 ; IF(FP.GT.1.12*F(J)) GO TO 250
11240 IF(F(J)/FP.GT.8) GO TO 240
11250 E1(I,J)=.2*(F(J)/FP-1)**2-DE ; GO TO 260
11260 240 E1(I,J)=9.5-DE ; GO TO 260
11270 250 E1(I,J)=-DE
11280 260 CONTINUE
11290 270 CONTINUE
11295 A(1)=10.
11300 280 IF(A(1).EQ.0) GO TO 820
11310C               EJECTOR TREATMENT EFFECTS
11320 XJ=M/5.0 ; IF(M.LT.1.13) GO TO 330 ; XJ=.226
11330 330 D4=SQRT(4*A8*AN1/P1) ; L3=L9*D4
11340 D3=D3*2.0
11470 500 DO 815 J=1,24 ; A4=0
11475 IM=0.00
11480C               FREQUENCY DETERMINATION
11490 DO 755 K8=1,3 ; GO TO (520,530,540),K8
11500 520 P3=F(J)*6.28318*.89 ; GO TO 550
11510 530 P3=F(J)*6.28318 ; GO TO 550
11520 540 P3=F(J)*6.28318*1.12
11530 550 CONTINUE
11550 IP=K8+2*J-2
11560 RS=RR(IP)
11570 X4=RX(IP)
11580 LAMBDA=2.*P1*SONSPD/P3
11590 ETAY=AITCH/LAMBDA
11600 ETAZ=2.*P1*RBAR/LAMBDA
11610 XMAX=(2*ETAY/SQRT(1-MACH**2))+1
11612 NMAX=IFIX(XMAX)
11620 YMAX=(ETAZ/SQRT(1-MACH**2))+1
```

ORIGINAL PAGE IS OF POOR QUALITY

FIGURE A-4 (CONTINUED). LISTING OF THE REVISED M*S PROGRAM

```
11621 MMAX=IFIX(YMAX)
11624 IF(NMAX.EQ.1.AND.MMAX.EQ.1)GOTO 815
11626 DO 855 LZER=1,1Ø;IMH(LZER)=1E-1Ø;IMH1(LZER)=1E-1Ø
11627 855 WTGFN(LZER)=Ø.
11629 TM=Ø
1163Ø DO 88Ø NM=1,NMAX
1164Ø DO 87Ø MM=1,MMAX
1165Ø NIND=NM-1
1166Ø MIND=MM-1
1167Ø IF(NIND.EQ.Ø)GOTO 83Ø
1168Ø GOTO 84Ø
1169Ø 83Ø IF(MIND.NE.Ø)GOTO 84Ø
117ØØ PHI=Ø
1171Ø GOTO 85Ø
11719 84Ø CONTINUE
1173Ø PARAM=SQRT(((P1*NIND)**2)+(2*MIND*(1-HTR)/(1+HTR))**2)
1174Ø COR=2*P1*ETAY/(PARAM*SQRT(1-MACH**2))
1175Ø IF(COR.LE.1.)GOTO 87Ø
1176Ø PHI=(ARSIN(1/COR))*18Ø./P1
1177Ø 85Ø CONTINUE
118ØØ DO 86Ø LDIF=1,9
1181Ø BETA=LDIF*1Ø.
1182Ø IF(PHI.GT.BETA)GOTO 86Ø
1183Ø IMH(LDIF)=IMH(LDIF)+1
11835 GOTO 865
1184Ø 86Ø CONTINUE
11845 865 CONTINUE
1185Ø TM=TM+1
1186Ø  87Ø CONTINUE
1187Ø 88Ø CONTINUE
1188Ø DO 89Ø LANG=1,9
1189Ø LL=1Ø-LANG
119ØØ IMH1(LL)=IMH(LANG)
1191Ø WTGFN(LL)=1Ø*ALOG1Ø(9*IMH1(LL)/TM)
1192Ø 89Ø CONTINUE
1193Ø 59Ø A3=Ø ; DO 73Ø I=9,17 ; K6=Ø ; AJR=((I+1)*1Ø-9Ø)*P1/18Ø
1194Ø N=I-8
1195Ø A1=4*RS*COS(AJR)/((1+RS*COS(AJR))**2+(X4*COS(AJR))**2)
1196ØC            ABSORPTION PER REFLECTION
11962 XXX=1-A1
11964 IF(XXX.LT.Ø.ØØØØØØ1)XXX=Ø.ØØØØØØ1
1197Ø A2=1Ø*ALOG1Ø(XXX)
1198Ø DO 69Ø K=1,25 ; XJ=((2.5*X(J))/25)*K
1199ØC            SOURCE LOCATIONS
12ØØØ ZJ=XJ/X(J) ; S2J=-11.19136+32.76997*ZJ-37.633732*ZJ**2+23.97Ø385*ZJ**3
12Ø1Ø S2J=S2J-1Ø.115712*ZJ**4+2.4Ø45214*ZJ**5-.23576959*ZJ**6
12Ø2Ø S2J=S2J-11.6
12Ø3ØC            EFFECT FOR ALL REFLECTIONS
12Ø4Ø DO 675 JJ=1,11;IF(JJ.GT.1) GO TO 66Ø;L2=(D3/2-S6)*TAN(AJR)+XJ;GO TO 67Ø
12Ø5Ø 66Ø L2=L2+D3*TAN(AJR)*(1.Ø-HTR)/NST
12Ø54C
12Ø56C
12Ø6Ø 67Ø IF(L2.GT.L3) GO TO 68Ø
12Ø7Ø 675 CONTINUE
12Ø77 68Ø CONTINUE
12Ø78 FORK=((JJ-1)*A2+WTGEN(N)+S2J)/1Ø
12Ø8Ø K6=K6+1Ø**FORK
12Ø9Ø 69Ø CONTINUE
121ØØC            POWER LEVEL REDUCTION
1211Ø AJ=(I+1)*1Ø ; K6=1Ø*ALOG1Ø(K6)
1212Ø YJ=1.5*P1*(COS((AJ-5)*P1/18Ø)-COS((AJ+5)*P1/18Ø))
1213Ø A3=A3+(2.227525E-6*4E-8*YJ*1Ø**(K6/1Ø))
1214Ø 73Ø CONTINUE
1215Ø A3=1Ø*ALOG1Ø(A3)+13Ø-6.45175
```

FIGURE A-4 (CONTINUED). LISTING OF THE REVISED M*S PROGRAM

```
A4=A4+10**(A3/10) ; 755 CONTINUE ; A4=10*ALOG10(A4/3)
C           DIRECTIVITY EFFECTS FOR TREATMENT
DO 8615 I=1,15 ; AJ=(I+1)*10 ; A5=A4
IF(AJ.LT.OJ-50) GO TO 800 ; IF(AJ.LT.OJ) GO TO 810
800 A5=A4/2
810 E1(I,J)=E1(I,J)+(A5*1.2)
8615 CONTINUE
815 CONTINUE
PRINT 8377,E1;8377 FORMAT(1X,15F7.2)
820 RETURN ; END
C
* SUBROUTINE AEROCALC(TT,PR,A,VJ,TJ,W,PAMB,TAMB)        THIS ENTIRE SUBROUTINE WAS ADDED
C
RHOISA=.076474
TISA=518.67
RISA=53.35045
GISA=32.174
PISA=14.695972
GAMREF=1.4
C
CSAMB=SQRT(GAMREF*GISA*RISA*TAMB)
REAL MJ
C
GAMMA=1.402
DO 10 J=1,50
C5=GAMMA/(GAMMA-1.0)
TJ=TT/(PR**(1./C5))
GAMOLD=GAMMA
GAMMA=GAM(TJ)
IF(ABS(GAMMA-GAMOLD).LT.1.0E-5) GOTO 20
10 CONTINUE
C
20 VJ=SQRT((TT-TJ)*(2.*GISA*RISA*C5))
IF(TT.EQ.TJ)VJ=0.001
C
RHOJET=(PAMB*TISA*RHOISA)/(PISA*TJ)
C
MJ=(((TT/TJ)-1.0)*(2.0/(GAMMA-1.0)))**0.5
IF(MJ-1.0)30,40,40
30 W=RHOJET*VJ*A
GOTO 60
40 C1=2.0/(GAMMA+1.0)
C2=(GAMMA-1.0)/2.0
C3=0.5/(C1*C2)
AM=MJ*MJ
A1=(A/MJ)*(C1*(1+C2*(MJ**2.)))**C3
W=RHOJET*VJ*A1
60 F=W*VJ/GISA
C
50 RETURN
END
C
* SUBROUTINE AEROSUM(VJINNER,TTINNER,AINNER,WINNER,VJOUTER,TTOUTER,   THIS ENTIRE SUBROUTINE WAS ADDED
* & AOUTER,WOUTER,PAMB,TAMB,XMJM)
C
COMMON /QM/ M,OJ
C
COMMON/CM1/L(9,24),X(24),F(24),E(24),S(15,24),KK(24,5),C(15,5),O(20),
& RR(49),RX(49),P(20),R(15,24),Y1(24),Y(24),C1(15),RVE(20),
& S1(24),G(2,24),C2(15,2),T(20),D(20),W(5),A(4),V(3),E1(15,24)
COMMON /CM2/ V8,A0,W8,K1,Y9,T8,T5,R7,P1,Z9,DJ,AJ,H,U,E9,AA
& ,T0,V9,C9,D8,D1,V0,O9,A8,Q,L9,A6,A7,S6,P9,R9,ALT,SL,AN1,NFLT
& ,HTR,NST,XMJMIX,TJMX,VJMX
C
```


FIGURE A-4 (CONTINUED). LISTING OF THE REVISED M*S PROGRAM

```
COMMON /CM3/AS,CASEID,E3,PNL(20)
C
      COMMON /CM4/ CASE
C
GISA=32.174
RISA=53.35
PISA=14.695972
TISA=518.67
RHOISA=0.076474
C
VJM=(VJINNER*WINNER+VJOUTER*WOUTER)/(WINNER+WOUTER)
TTM=(TTINNER*WINNER+TTOUTER*WOUTER)/(WINNER+WOUTER)
C
ATOTAL=AINNER+AOUTER
C
GAMMA=1.4
DO 10 J=1,50
C5=GAMMA/(GAMMA-1.0)
TJM=TTM-(VJM**2.0)/(2.0*GISA*RISA*C5)
GAMOLD=GAMMA
GAMMA=GAM(TJM)
IF(ABS(GAMMA-GAMOLD).LT.1.0E-5) GOTO 20
10 CONTINUE
20 CONTINUE
RHOJET=(PAMB*TISA*RHOISA)/(PISA*TJM)
XMJM=(((TTM/TJM)-1.0)*(2.0/(GAMMA-1.0)))**0.5
IF(XMJM-1.0)30,40,40
C
30 WT=RHOJET*VJM*ATOTAL
GOTO 60
40 C13=2.0/(GAMMA+1.0)
C23=(GAMMA-1.0)/2.0
C3=0.5/(C13*C23)
A1=(ATOTAL/XMJM)*(C13*(1+C23*(XMJM**2.)))**C3
WT=RHOJET*VJM*A1
60 FT=WT*VJM/GISA
50 RETURN
END
*GAM      GAMMA AS A FUNCTION OF STATIC TEMP
      FUNCTION GAM(T)
      IF (T.LE.788.303) GO TO 10
      IF (T.GE.3778.768) GO TO 20
      GAM=2.23708/T**.070271
      GO TO 30
   10 GAM=1.4
      GO TO 30
   20 GAM=1.254
   30 RETURN
END
```

FIGURE A-4 (CONCLUDED). LISTING OF THE REVISED M*S PROGRAM

APPENDIX B

GENERAL ELECTRIC LASER VELOCIMETER SYSTEM

General Arrangement

The laser velocimeter (LV) available for use during this program is a system developed under a USAF/DOT-sponsored program and reported in detail in Reference B-1. The basic optics system is a differential Doppler, backscatter, single-package arrangement that has the proven feature of ruggedness for the severe environments encountered in close proximity to high velocity, high temperature jets. Figure 3-5 of Section 3.1.4 shows a photograph of the LV system in the General Electric Anechoic Test Facility. The dimensions of the control volume are 0.636 cm (0.25 inch) for the major axis and 0.518 cm (0.020 inch) for the minor axis. The range of the LV control volume from the laser hardware is 2.16 m (85.0 inches). The three steering mirrors and the beam splitter are mounted on adjustable supports, all of the same aluminum alloy, which minimizes temperature-alignment problems.

LV Actuator and Seeding

A remotely actuated platform is used which has three axes: vertical, horizontal, and axial. Travel capabilities are 0.813 m (32 inches), 0.813 m (32 inches) and 5.79 m (228 inches), respectively. Resolution is $\pm$ .16 cm ($\pm$1/16 inch) for each axis except for the last 5.28 m (208 inches) of axial travel, which hs a resolution of $\pm$.32 cm ($\pm$1/8 inch).

Seeding is by injection of aluminum oxide (Al_2O_3) powder, nominal 1-micron diameter, into the supply air to the burner and into the region of the nozzle to seed the entrained air. The powder-feeder equipment used is described in Reference B-1, except that the fluidized bed column supply air is heated to about 394.1^{o}K (250^o F) to prevent powder aggregation by moisture absorption.

Signal Processing and Recording

The LV signal processor used is a direct-counter (time-domain) type similar to that reported in Reference B-1, but with improvements. These improvements result in a lowered rate of false validations and improved linearity and resolution. Turbulent-velocity probability distributions (histograms) are recorded by a 256-channel NS633 pulse-height analyzer. All the data acquired from the laser unit is transmitted to a minicomputer system which stores the data on diskettes and performs all the necessary data reduction functions.

The processing capabilities of the General Electric LV system are as follows:

- Velocity range - 10.7 to 1,524 mps (35 to 5,000 fps)
- Random error for single particle accuracy (error associated with system inaccuracies such as fringe spacing, linearity, stability, burst noise) - 0.75%

- Bias error for mean velocity - 0.5%
- False data rejection capability (possibility of accepting bad data) - $<$0.0002%.

The system uses a 16-fringe control volume where all of the eight center fringes are used in the data acceptance/rejection testing.

LV Data Reduction Procedures

The concept of using LV measurements for obtaining the mean and turbulent velocity profiles may be described as follows: Two beams of monochromatic light intersect at a point in space and set up a fringe pattern of known spacing (Figure B-1). The flow is seeded with small particles which pass through the measuring volume. The light scattered from the particles is collected, and the laser signal processor measures the time it takes for the particles to pass through each fringe. Knowing the distance and time for each validated particle enables the construction of the usual histogram (see insert on Figure B-1). Then by statistical techniques, the mean value (which corresponds to the mean velocity) and the standard deviation (which corresponds to the turbulent velocity) are constructed. The method of calculation used to obtain the mean and turbulent velocities from LV measurements is described below.

Histogram

A histogram is an estimate of the first-order probability density of the amplitude of a given sample. To obtain a velocity histogram, the time-dependent LV velocity, V(t), is accumulated and divided into classes bounded by values of velocity increments V_i. For each independent sample of velocity, a class interval is formed such that $V_i \leq V(t) \leq V_{i+1}$. During a measurement period, k_i number of velocity samples are accumulated in each sample class V_i. From the total sample of measured velocity points, the histogram is constructed as shown in Figure B-1. The mean velocity and turbulent velocity derived from the histogram are obtained as described below.

Mean Velocity

The mean velocity of the jet, V_j, obtained from the discrete velocity sample is calculated by:

$$\bar{V}_j = \sum_{\substack{\text{All Class} \\ \text{Intervals}}} \left(\frac{V_{i+1} + V_i}{2} \right) \frac{k_i}{N}$$

where

$\frac{V_{i+1} + V_i}{2}$ is the value of the sampled axial velocity component at the center of the class interval

k_i is the number of velocity samples in the class interval

N is the total number of velocity samples ($= \sum k_i$) in the histogram

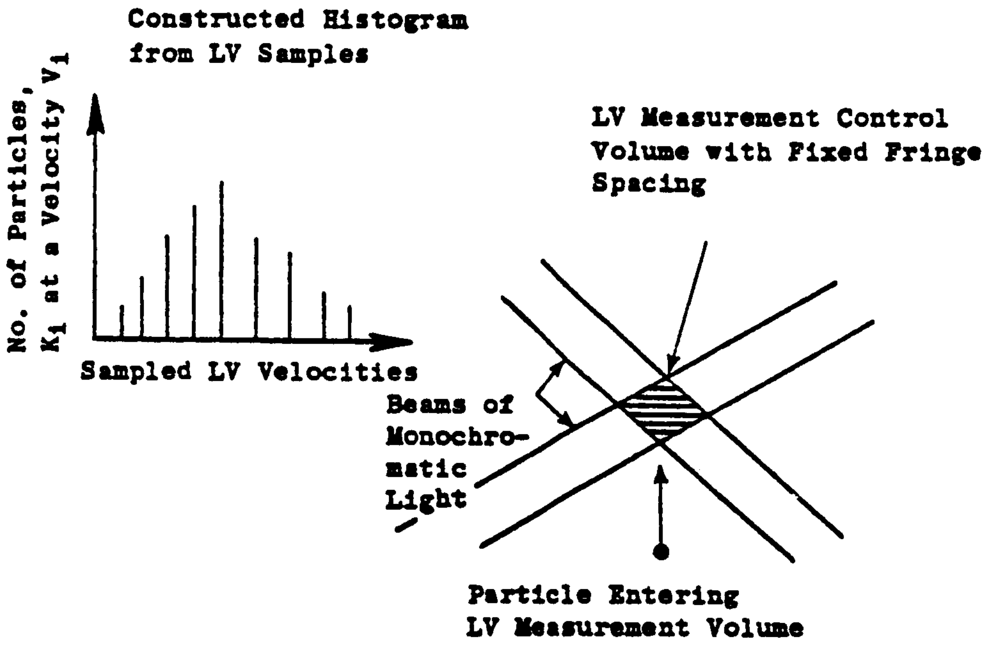

FIGURE B-1. SCHEMATIC OF LASER VELOCITY MEASUREMENTS

Turbulent Velocity

To obtain the turbulent velocity, v', from the sampled data contained in the histogram, the standard square root of the statistical variance is performed. This calculation is performed using the following equation:

$$v' = \left\{ \sum_{\substack{\text{All Class} \\ \text{Intervals}}} \left(\frac{\frac{V_{i+1} + V_i}{2} - \bar{V}_j}{N} \right)^2 k_i \right\}^{1/2}$$

Statistical Errors for LV Mean and Turbulent Velocity Measurements

With any large data sample, as obtained through the collection of velocity samples in an LV histogram, guidelines for estimating the accuracy of each measurement are required. Table B-1 provides estimates of the percent error obtained for a mean velocity or turbulent velocity LV measurement.

Table B-1 lists the percent error for a 95% confidence statement of mean velocity measurement as a function of the total number, N, of velocity samples contained in the histogram and the turbulence level, v'/V_j. Table B-1 also gives the percent error for a 95% confidence statement of the turbulent velocity estimate as a function of N, the total number of velocity samples. As can be seen from Table B-1, a fairly small sample of velocity measurements is required to obtain a good estimate of the mean velocity. For the turbulent velocity, the number of data samples required for a good estimate increases substantially. The usual number of samples obtained with the General Electric LV during a routine data-taking measurement performed during this program is approximately 1,000 samples. For a simple and quick diagnostic-type information, this amount of samples is sufficient.

LV Traverses for Mean Velocity Profiles

In addition to the above described stationary mode of LV operation for the determination of mean and turbulent velocities at discrete points, the LV can be operated also in a traversing mode to obtain continuous profiles of mean velocities. These traverses are possible along any of the three LV axes. During these traverses, the data describing the velocity levels and the location of the measurement volume are recorded continuously on an X-Y plotter. The traversing speeds are adjusted as well as traverses repeated for obtaining well-defined mean velocity profiles. While exact sampling rates during these traverses are not recorded in any way, it is felt that an estimated rate of approximately 250 samples per inch of traverse is needed for a well-defined smooth profile.

LV System for Minihistograms

The LV System has been modified to have the following additional features in a traversing mode:

- o A modified slant traverse mechanism that enables LV traverses to be made along an axis that is other than truly vertical (i.e., parallel to the plug surface) of an annular plug nozzle.

TABLE B-1. ESTIMATES OF ERROR IN MEAN AND TURBULENT VELOCITIES MEASURED BY LV

(a) **Estimated Percent Error in the LV Measurement of Mean Velocity with 95% Confidence.**

N	$v'/\bar{V}j$			
	0.2	0.1	0.05	0.025
10	14.1	7	3.5	1.76
20	9.3	4.7	2.3	1.20
30	7.4	3.7	1.9	0.93
40	6.3	3.2	1.6	0.80
60	5.0	2.6	1.3	0.65
120	3.6	1.8	0.9	0.45

(b) **Estimated Percent Error for LV Turbulent Velocity Measurements with 95% Confidence.**

N	Percent Error
20	31.5
40	21.8
60	17.8
120	12.6
240	9.12
480	6.45
960	4.56
5000	2.0
25000	0.89

- A fine traverse mechanism (10 revolutions on a potentiometer for 33 inches of total travel; usable fine traverse distance is 20 inches) that is available during both the slant and vertical movements. This drive system allows for more smoothly controlled vertical traverses required for obtaining minihistograms.

- Modified software that enables mean velocity data to be obtained during any of the traverses (that is, axial or vertical, radial and slant) from minihistograms in the form of plots of mean velocity data points plotted as a function of their traverse location. During the current program, the mean velocity data measured with the minihistograms have been obtained from the acceptable data samples set to 20. This number of acceptable samples yields an estimated 5% error in the LV mean velocity measurements with a statistical 95% confidence level within a given flow regime having a turbulent velocity ratio ($v'/\overline{V}_j$) of 10%.

References

B-1. Knott, P.R., "Supersonic Jet Exhaust Noise Investigation", Volume I, Summary Report, AFAPL-TR-76-68, July 1976.

APPENDIX C

MEASURED SUPPRESSIONS FROM THE EJECTOR

5JB86004

DELTA, SPL(1) - SPL(2)

IDENTIFICATION

INPUT (1) 83F-ZER-1ØØ3 X1ØØ35
(2) 83F-ZER-2ØØ3 X2ØØ35

OUTPUT CBS TE1-TE2 XØ1Ø21

ANGLES MEASURED FROM INLET,DEGREES

FREQ	4Ø.Ø	5Ø.Ø	6Ø.Ø	7Ø.Ø	8Ø.Ø	9Ø.Ø	1ØØ.Ø	11Ø.Ø	12Ø.Ø	13Ø.Ø	14Ø.Ø	15Ø.Ø	16Ø.Ø	AVG	S.D.	PWL
5Ø	1.Ø	2.8	1.8	2.2	1.3	5.8	1Ø.Ø	1.8	-Ø.2	1.3	2.8	1.9	Ø.3	2.5	2.7	2.Ø
63	1.Ø	1.8	Ø.8	1.3	1.5	Ø.Ø	1.3	Ø.Ø	1.3	Ø.3	1.8	1.9	1.5	1.1	Ø.7	1.4
8Ø	Ø.5	1.5	Ø.8	1.2	2.3	1.Ø	Ø.3	Ø.5	Ø.Ø	Ø.8	2.3	1.4	1.8	1.1	Ø.7	1.3
1ØØ	Ø.8	Ø.8	2.Ø	1.9	2.3	Ø.3	1.3	1.8	Ø.5	2.Ø	2.Ø	1.2	1.Ø	1.4	Ø.7	1.5
125	Ø.5	Ø.5	1.Ø	1.9	2.Ø	Ø.5	1.3	Ø.5	1.5	Ø.5	2.8	Ø.7	Ø.8	1.1	Ø.7	1.2
16Ø	1.5	2.5	1.8	1.1	2.Ø	1.Ø	1.Ø	1.5	1.3	1.3	2.3	Ø.2	Ø.Ø	1.3	Ø.7	1.3
2ØØ	1.Ø	4.8	1.8	2.3	2.5	1.5	1.5	1.Ø	1.5	1.3	1.8	Ø.9	-Ø.7	1.6	1.2	1.5
25Ø	1.5	3.3	1.8	2.2	2.8	2.Ø	2.3	2.Ø	1.8	1.3	2.5	Ø.2	-Ø.2	1.8	1.Ø	1.8
315	1.Ø	5.3	3.5	4.1	4.Ø	2.5	2.5	1.3	3.3	2.3	3.8	2.4	Ø.3	2.8	1.4	2.7
4ØØ	3.Ø	5.Ø	4.8	4.9	4.8	4.3	3.5	3.3	3.8	4.3	5.5	5.4	4.Ø	4.4	Ø.8	4.2
5ØØ	3.5	5.Ø	4.8	5.3	6.Ø	4.5	4.5	4.Ø	5.8	6.3	8.8	9.7	7.5	5.8	1.8	6.1
63Ø	4.3	4.5	5.Ø	5.9	6.Ø	3.8	5.Ø	4.5	6.3	8.3	11.5	12.2	1Ø.5	6.8	2.9	7.3
8ØØ	5.3	4.8	4.8	5.6	6.5	4.8	5.3	5.3	8.3	9.5	11.8	13.7	13.Ø	7.6	3.3	8.2
1ØØØ	4.3	5.8	6.Ø	5.7	6.3	4.3	3.8	3.5	7.5	9.6	12.Ø	14.7	13.3	7.5	3.8	7.4
125Ø	4.3	6.1	5.8	6.5	5.1	3.8	4.1	2.8	7.3	9.3	11.1	14.Ø	13.3	7.2	3.6	6.6
16ØØ	5.8	7.8	6.6	6.5	5.6	3.6	3.3	3.3	6.8	8.8	1Ø.8	14.Ø	13.1	7.4	3.5	6.Ø
2ØØØ	5.8	8.6	8.1	7.7	5.8	3.3	4.1	2.8	6.9	9.1	11.1	15.7	13.6	7.9	3.8	6.1
25ØØ	5.6	8.4	7.9	8.4	6.6	3.9	3.6	2.1	6.4	1Ø.2	13.1	16.Ø	13.6	8.1	4.2	5.9
315Ø	4.7	7.5	7.Ø	8.Ø	5.9	4.2	4.2	2.9	7.Ø	1Ø.Ø	13.Ø	17.3	14.9	8.2	4.4	5.9
4ØØØ	3.Ø	7.8	6.3	8.3	6.5	4.5	4.8	3.3	7.8	1Ø.1	14.8	2Ø.2	16.3	8.7	5.3	6.4
5ØØØ	3.2	8.Ø	7.2	9.3	6.2	4.4	4.4	3.7	9.2	11.6	16.2	22.1		8.8	5.6	7.Ø
63ØØ		8.3	7.5	9.2	6.2	4.2	4.4	3.5	9.3	13.1	17.7			8.3	4.4	7.4
8ØØØ				9.7	5.3	4.5	5.3	2.9	1Ø.9					6.4	3.2	8.5
1ØØØØ																9.Ø
125ØØ																
16ØØØ																
2ØØØØ																
25ØØØ																
315ØØ																
4ØØØØ																
5ØØØØ																
63ØØØ																
8ØØØØ																
OASPL	2.8	4.6	4.3	4.9	4.7	3.3	3.9	2.9	4.2	3.7	4.7	3.3	1.5			
PNL	4.4	6.7	6.2	6.5	5.7	3.5	3.8	2.9	5.6	6.5	8.3	8.7	6.5			
PNLT	5.5	6.7	6.2	6.5	5.7	3.5	3.8	2.9	5.6	7.Ø	8.3	8.7	6.5			
DBA	4.5	6.3	6.Ø	6.4	5.8	3.9	4.Ø	3.5	6.6	7.7	1Ø.Ø	11.1	8.8			

LOCATION	ACOUSTIC RANGE	AVG CORR SPEED	AVG CORR THRUST
C41 ANECH CH	24ØØ.Ø FT SL	-Ø.1E 31 RPM	-Ø.1E 31 LB

TEST CASE FOR TREATED EJECTOR TEØ1 VS TEØ2

DELTA, SPL(1) - SPL(2)

IDENTIFICATION

INPUT (1) 83F-ZER-1ØØ5 X1ØØ55
(2) 83F-ZER-2ØØ5 X2ØØ55

OUTPUT ITS TE1-TE2 XØ1Ø21

ANGLES MEASURED FROM INLET,DEGREES

FREQ	4Ø.Ø	5Ø.Ø	6Ø.Ø	7Ø.Ø	8Ø.Ø	9Ø.Ø	1ØØ.Ø	11Ø.Ø	12Ø.Ø	13Ø.Ø	14Ø.Ø	15Ø.Ø	16Ø.Ø	AVG	S.D.	PWL
5Ø	Ø.8	1.5	Ø.3	Ø.3	Ø.8	4.5	8.3	Ø.3	-Ø.2	Ø.Ø	1.3	Ø.4	-Ø.5	1.3	2.4	Ø.7
63	Ø.5	Ø.8	Ø.Ø	Ø.1	Ø.8	-Ø.2	1.Ø	Ø.Ø	Ø.3	Ø.Ø	1.3	-Ø.1	-Ø.5	Ø.3	Ø.5	Ø.2
8Ø	Ø.3	1.Ø	-Ø.5	Ø.6	1.5	Ø.3	-Ø.2	Ø.Ø	-Ø.2	1.Ø	1.5	Ø.2	Ø.Ø	Ø.4	Ø.7	Ø.5
1ØØ	-Ø.2	Ø.3	1.3	Ø.5	Ø.8	-Ø.2	Ø.5	Ø.8	Ø.8	Ø.5	Ø.8	Ø.4	-Ø.5	Ø.4	Ø.5	Ø.4
125	Ø.5	Ø.8	Ø.8	1.Ø	1.8	Ø.Ø	Ø.5	Ø.3	Ø.8	-Ø.2	Ø.8	-Ø.8	-Ø.2	Ø.4	Ø.7	Ø.2
16Ø	1.3	2.3	1.8	Ø.5	1.5	Ø.5	1.Ø	1.Ø	1.5	Ø.3	Ø.3	-Ø.6	-Ø.5	Ø.8	Ø.9	Ø.5
2ØØ	Ø.Ø	3.8	1.Ø	1.6	1.5	Ø.8	1.Ø	Ø.5	Ø.5	Ø.Ø	Ø.3	-Ø.6	-2.2	Ø.6	1.4	Ø.2
25Ø	Ø.8	1.5	1.5	1.9	1.8	1.3	1.5	1.Ø	Ø.8	Ø.5	Ø.3	-2.1	-3.Ø	Ø.6	1.5	Ø.3
315	-Ø.2	3.5	3.Ø	2.5	2.Ø	1.5	1.Ø	1.Ø	1.8	1.3	1.5	-1.1	-2.5	1.2	1.6	1.1
4ØØ	2.Ø	4.8	3.3	3.5	4.Ø	2.3	2.8	2.3	2.5	2.Ø	2.3	1.7	Ø.8	2.6	1.Ø	2.3
5ØØ	2.5	4.3	3.5	3.9	4.8	3.3	3.Ø	2.8	4.Ø	4.Ø	5.8	3.2	3.3	3.7	Ø.9	3.9
63Ø	4.Ø	4.8	4.3	4.7	4.5	3.5	4.3	3.8	4.8	5.Ø	7.8	5.2	5.5	4.8	1.1	5.1
8ØØ	5.3	5.5	4.5	4.6	5.Ø	3.8	4.8	5.Ø	6.5	7.Ø	8.3	8.2	8.3	5.9	1.6	6.5
1ØØØ	7.3	8.Ø	5.5	5.1	5.3	4.3	3.8	3.3	6.3	7.1	8.5	8.4	9.Ø	6.3	1.9	6.Ø
125Ø	8.5	1Ø.3	8.1	7.Ø	4.8	3.1	3.3	3.1	6.1	5.8	8.6	7.2	9.5	6.6	2.5	5.6
16ØØ	7.8	11.3	9.8	8.4	6.1	3.1	3.3	4.1	5.6	5.6	8.3	8.Ø	9.1	7.Ø	2.6	5.9
2ØØØ	5.1	8.1	8.4	8.2	6.3	3.6	3.8	3.3	5.4	5.4	8.3	9.2	1Ø.6	6.6	2.4	5.7
25ØØ	3.9	6.9	6.1	7.2	6.6	4.1	2.9	2.4	5.4	7.4	1Ø.1	1Ø.5	11.6	6.6	2.9	5.3
315Ø	4.2	7.7	6.5	6.3	5.4	3.7	3.7	2.4	6.7	7.5	1Ø.7	11.3	11.4	6.7	3.Ø	5.2
4ØØØ	3.5	8.3	6.6	7.8	5.8	3.5	4.3	3.Ø	7.3	7.6	12.1	13.4	12.8	7.4	3.5	5.8
5ØØØ	2.9	9.Ø	8.Ø	9.7	6.7	4.2	3.4	3.5	8.7	9.1	13.7	15.8		7.9	4.1	6.7
63ØØ	6.4	9.8	9.Ø	9.5	5.7	4.9	3.9	4.Ø	8.8	9.1	14.2			7.8	3.1	6.9
8ØØØ			11.2	9.9	5.1	5.3	4.8	3.9	1Ø.7					7.3	3.2	8.3
1ØØØØ																8.2
125ØØ																
16ØØØ																
2ØØØØ																
25ØØØ																
315ØØ																
4ØØØØ																
5ØØØØ																
63ØØØ																
8ØØØØ																
OASPL	3.3	5.5	4.7	4.6	4.Ø	2.6	3.1	2.4	2.9	2.Ø	2.4	Ø.6	-Ø.2			
PNL	4.8	7.5	6.4	6.3	5.2	3.3	3.3	2.9	4.5	4.Ø	5.1	3.6	1.4			
PNLT	3.4	7.5	6.4	6.3	5.2	3.3	3.3	2.9	4.5	4.Ø	6.3	3.6	1.4			
DBA	5.8	8.2	7.Ø	6.6	5.4	3.4	3.6	3.4	5.1	5.Ø	6.6	5.1	3.6			

LOCATION	ACOUSTIC RANGE	AVG CORR SPEED	AVG CORR THRUST
C41 ANECH CH	24ØØ.Ø FT SL	-Ø.1E 31 RPM	-Ø.1E 31 LB

TEST CASE FOR TREATED EJECTOR TEØ1 VS TEØ2

DELTA, SPL(1) - SPL(2)

IDENTIFICATION

INPUT (1) 83F-ZER-1ØØ9 X1ØØ95
(2) 83F-ZER-2ØØ9 X2ØØ95

OUTPUT TOS TE1-TE2 XØ1Ø21

ANGLES MEASURED FROM INLET,DEGREES

FREQ	4Ø.Ø	5Ø.Ø	6Ø.Ø	7Ø.Ø	8Ø.Ø	9Ø.Ø	1ØØ.Ø	11Ø.Ø	12Ø.Ø	13Ø.Ø	14Ø.Ø	15Ø.Ø	16Ø.Ø	AVG	S.D.	PWL
5Ø	Ø.Ø	1.Ø	Ø.5	Ø.2	-Ø.5	2.8	7.3	4.8	-Ø.5	-Ø.5	Ø.3	-Ø.3	-1.7	1.Ø	2.5	-Ø.2
63	-Ø.2	Ø.8	-Ø.2	-Ø.4	-Ø.2	-Ø.5	-Ø.2	Ø.2	-Ø.2	-Ø.7	-Ø.7	-Ø.1	-Ø.7	-Ø.3	Ø.4	-Ø.5
8Ø	-Ø.7	-Ø.2	-Ø.5	-1.3	Ø.Ø	-Ø.7	-1.Ø	-1.1	-1.Ø	-Ø.2	-Ø.5	-Ø.6	-1.5	-Ø.7	Ø.4	-Ø.8
1ØØ	-1.2	-1.2	-Ø.2	-Ø.8	Ø.Ø	-Ø.7	-Ø.5	-Ø.3	-Ø.7	Ø.Ø	-Ø.2	-Ø.3	-2.5	-Ø.7	Ø.7	-Ø.8
125	-3.2	-3.7	-2.7	-1.5	-Ø.5	-1.5	Ø.Ø	-Ø.3	-Ø.5	-1.7	-Ø.5	-2.1	-3.5	-1.7	1.3	-1.9
16Ø	-1.7	-1.7	-2.5	-2.Ø	-1.7	-2.2	-1.Ø	-Ø.2	-Ø.2	-Ø.7	-1.7	-2.6	-3.7	-1.7	1.Ø	-2.2
2ØØ	-2.Ø	Ø.3	-1.5	-1.Ø	-Ø.7	-1.7	-1.2	-Ø.3	-1.2	-1.5	-2.7	-2.8	-4.Ø	-1.6	1.1	-2.5
25Ø	-3.2	-3.2	-1.7	-1.Ø	Ø.Ø	Ø.Ø	-1.2	-Ø.1	-1.5	-1.5	-2.2	-3.6	-3.5	-1.8	1.3	-2.4
315	-2.Ø	Ø.3	-1.Ø	-Ø.5	-Ø.5	-1.Ø	-Ø.7	-1.4	-2.Ø	-1.2	-2.5	-2.6	-4.5	-1.5	1.2	-2.2
4ØØ	-Ø.2	Ø.8	Ø.3	Ø.7	1.Ø	Ø.5	Ø.8	-Ø.2	-Ø.7	-1.Ø	-1.7	-2.1	-1.7	-Ø.3	1.1	-1.1
5ØØ	-2.2	Ø.8	1.3	1.3	1.8	1.Ø	Ø.8	-Ø.4	-Ø.2	-Ø.5	Ø.5	-1.1	-2.Ø	Ø.1	1.3	-Ø.1
63Ø	-1.2	-Ø.2	Ø.5	1.7	2.3	1.Ø	1.5	1.2	Ø.8	Ø.5	Ø.8	-1.1	-1.2	Ø.5	1.1	Ø.6
8ØØ	2.5	2.Ø	Ø.8	1.5	2.Ø	1.3	2.3	1.6	2.3	1.5	1.5	-Ø.6	Ø.5	1.5	Ø.8	1.5
1ØØØ	3.Ø	5.5	4.5	4.3	3.3	2.3	1.8	Ø.5	2.3	1.6	2.Ø	-Ø.8	Ø.5	2.4	1.8	2.2
125Ø	Ø.5	4.3	5.1	6.8	4.3	2.6	2.8	1.4	2.1	2.1	1.8	Ø.7	1.5	2.8	1.8	2.9
16ØØ	Ø.3	2.3	2.3	5.1	5.6	3.3	3.3	2.2	2.1	1.1	2.6	-Ø.5	2.3	2.5	1.7	2.8
2ØØØ	Ø.1	2.6	2.6	3.4	3.6	3.3	3.3	2.6	3.4	2.1	2.8	2.5	3.3	2.7	Ø.9	3.Ø
25ØØ	Ø.6	3.6	3.6	4.8	3.4	2.4	2.1	1.4	3.4	2.7	3.6	3.3	3.4	2.9	1.1	2.9
315Ø	-Ø.1	4.2	3.2	4.8	4.2	2.7	3.4	2.5	4.2	3.5	4.Ø	2.8	3.4	3.3	1.2	3.5
4ØØØ	-1.Ø	4.1	3.6	6.Ø	4.3	3.Ø	4.Ø	2.1	5.3	3.4	5.6	3.4	4.3	3.7	1.8	3.9
5ØØØ	-1.6	5.3	4.8	7.5	4.4	3.9	4.4	3.Ø	6.Ø	4.6	6.7	3.6		4.4	2.3	4.8
63ØØ	Ø.4	5.Ø	4.5	8.Ø	4.9	3.9	4.4	3.3	5.5	4.6	7.Ø			4.7	2.Ø	5.Ø
8ØØØ			5.5	7.2	4.1	4.8	5.1	3.8	7.Ø	5.1				5.3	1.2	5.6
1ØØØØ						3.7								3.7	.1E 19	5.4
125ØØ																
16ØØØ																
2ØØØØ																
25ØØØ																
315ØØ																
4ØØØØ																
5ØØØØ																
63ØØØ																
8ØØØØ																
OASPL	-Ø.7	1.2	1.5	2.5	2.1	1.1	1.4	Ø.5	-Ø.1	-Ø.5	-Ø.7	-1.2	-2.3			
PNL	-Ø.2	1.9	2.Ø	3.6	3.4	2.1	2.3	1.4	1.Ø	Ø.Ø	-Ø.3	-1.6	-2.5			
PNLT	-1.5	1.8	1.5	3.6	3.4	2.6	2.3	1.4	1.Ø	Ø.Ø	-Ø.2	-Ø.5	-2.5			
DBA	Ø.6	2.9	3.1	4.4	3.7	2.3	2.2	1.1	1.2	Ø.5	Ø.2	-1.7	-2.8			

LOCATION	ACOUSTIC RANGE	AVG CORR SPEED	AVG CORR THRUST
C41 ANECH CH	24ØØ.Ø FT SL	-Ø.1E 31 RPM	-Ø.1E 31'LB

TEST CASE FOR TREATED EJECTOR TEØ1 VS TEØ2

DELTA, SPL(1) - SPL(2)

IDENTIFICATION

INPUT (1) 83F-4ØØ-1ØØ4 X1ØØ45
(2) 83F-4ØØ-2ØØ4 X2ØØ45

OUTPUT CBF TE1-TE2 XØ1Ø21

ANGLES MEASURED FROM INLET,DEGREES

FREQ	4Ø.Ø	5Ø.Ø	6Ø.Ø	7Ø.Ø	8Ø.Ø	9Ø.Ø	1ØØ.Ø	11Ø.Ø	12Ø.Ø	13Ø.Ø	14Ø.Ø	15Ø.Ø	16Ø.Ø	AVG	S.D.	PWL
5Ø	5.Ø	14.1	1.8	11.9	Ø.2	5.8	6.9	Ø.7	-1.Ø	-Ø.1	Ø.5	Ø.1	-Ø.4	3.5	4.9	3.5
63	1.6	8.6	-Ø.2	8.Ø	Ø.1	-Ø.3	2.3	-Ø.1	Ø.6	2.8	1.7	1.1	-Ø.9	2.Ø	3.Ø	2.Ø
8Ø	2.1	4.4	-Ø.6	3.6	1.Ø	-Ø.9	Ø.3	Ø.1	Ø.8	2.1	1.Ø	Ø.8	-Ø.4	1.1	1.6	1.1
1ØØ	1.5	1.1	-1.2	Ø.4	Ø.3	-1.1	1.6	1.Ø	Ø.4	Ø.4	Ø.5	Ø.1	-1.1	Ø.3	Ø.9	Ø.1
125	-Ø.Ø	Ø.9	-Ø.2	-Ø.Ø	1.7	-Ø.8	Ø.5	Ø.1	2.6	4.7	3.2	1.7	Ø.9	1.2	1.6	2.1
16Ø	1.7	1.3	-1.1	1.3	1.Ø	-Ø.2	1.1	1.5	Ø.5	1.8	1.4	Ø.8	Ø.4	Ø.9	Ø.8	1.Ø
2ØØ	1.7	1.8	Ø.1	Ø.2	1.Ø	-Ø.5	Ø.3	-1.3	Ø.2	2.4	Ø.5	-Ø.1	-Ø.9	Ø.4	1.1	Ø.5
25Ø	2.7	3.1	Ø.3	1.1	1.8	1.2	1.1	Ø.5	Ø.Ø	1.9	Ø.1	-1.7	-3.5	Ø.7	1.8	Ø.6
315	4.5	1.9	1.7	1.5	3.4	1.6	-Ø.4	-Ø.9	Ø.7	3.5	1.3	-Ø.9	-2.6	1.2	2.Ø	1.2
4ØØ	4.5	4.Ø	3.Ø	2.8	3.9	3.2	1.4	Ø.1	2.6	5.3	4.9	2.5	-Ø.5	2.9	1.8	2.9
5ØØ	5.7	5.Ø	2.7	3.2	3.9	2.4	2.1	1.2	2.4	6.Ø	6.1	4.4	1.3	3.6	1.7	3.3
63Ø	5.7	4.7	2.7	3.4	4.2	2.7	2.6	2.Ø	3.6	8.3	8.3	7.Ø	5.1	4.6	2.1	4.5
8ØØ	5.Ø	4.Ø	3.Ø	3.8	3.7	2.7	2.7	2.Ø	3.4	8.3	8.7	8.Ø	5.5	4.7	2.3	4.3
1ØØØ	5.5	3.8	2.8	3.Ø	3.2	2.2	2.2	1.7	4.2	8.3	9.Ø	9.Ø	6.7	4.7	2.7	4.3
125Ø	2.7	2.3	1.3	1.7	2.4	2.Ø	2.7	2.1	4.4	7.9	9.9	9.Ø	6.8	4.2	3.1	3.7
16ØØ	2.7	3.3	1.8	3.1	4.5	3.Ø	3.7	2.9	5.3	8.2	8.7	1Ø.8	8.1	5.1	2.9	4.3
2ØØØ	4.7	4.8	3.8	4.5	4.2	2.8	4.6	4.6	5.8	9.6	1Ø.8	1Ø.7	8.2	6.1	2.7	5.1
25ØØ	5.1	6.2	5.5	5.Ø	5.5	3.8	4.2	4.6	8.8	1Ø.7	11.7	11.3	1Ø.6	7.2	3.Ø	5.9
315Ø	5.Ø	6.8	6.1	6.9	7.1	4.9	5.1	5.3	8.4	1Ø.1	11.4	11.4	1Ø.Ø	7.6	2.4	6.6
4ØØØ	3.3	5.9	5.4	7.5	6.6	4.2	5.9	5.5	7.7	9.4	11.2	11.1	8.6	7.1	2.5	6.5
5ØØØ	1.1	6.2	5.Ø	6.9	6.Ø	5.5	5.9	5.7	6.6	7.8	8.7	11.Ø		6.4	2.3	6.Ø
63ØØ	3.5	6.3	6.3	8.6	5.7	3.7	5.2	3.9	4.6	6.6	6.1			5.5	1.5	5.5
8ØØØ			5.5	7.6	4.Ø	2.9	3.8	1.2	1.Ø					3.8	2.2	3.1
1ØØØØ																1.9
125ØØ																
16ØØØ																
2ØØØØ																
25ØØØ																
315ØØ																
4ØØØØ																
5ØØØØ																
63ØØØ																
8ØØØØ																
OASPL	4.Ø	4.4	2.5	3.5	3.6	2.5	2.8	2.Ø	3.2	5.7	4.9	3.7	Ø.8			
PNL	4.1	4.8	3.6	4.3	4.3	3.Ø	3.7	3.1	4.5	7.1	7.3	7.5	3.6			
PNLT	3.Ø	4.8	3.7	4.4	4.3	3.Ø	3.7	3.1	4.5	7.1	7.3	7.5	3.6			
DBA	4.2	3.9	2.9	3.6	3.9	2.8	3.2	2.6	4.3	7.7	8.3	7.9	4.6			

LOCATION	ACOUSTIC RANGE	AVG CORR SPEED	AVG CORR THRUST
C41 ANECH CH	24ØØ.Ø FT SL	-Ø.1E 31 RPM	-Ø.1E 31 LB

TEST CASE FOR TREATED EJECTOR TEØ1 VS TEØ2

DELTA, SPL(1) - SPL(2)

IDENTIFICATION

INPUT (1) 83F-400-1006 X10065
(2) 83F-400-2006 X20065

OUTPUT ITF TE1-TE2 X01021

ANGLES MEASURED FROM INLET,DEGREES

FREQ	40.0	50.0	60.0	70.0	80.0	90.0	100.0	110.0	120.0	130.0	140.0	150.0	160.0	AVG	S.D.	PWL
50	5.1	11.0	2.9	8.9	1.9	4.5	7.0	1.8	0.5	0.8	1.3	0.4	-0.5	3.5	3.6	1.8
63	3.8	7.0	2.9	6.5	1.2	1.5	2.3	0.5	0.3	1.3	1.0	-0.1	-1.0	2.1	2.4	0.9
80	2.2	3.0	0.6	1.9	1.5	0.5	0.5	0.3	1.4	2.9	2.1	1.5	-0.2	1.4	1.0	1.5
100	2.8	2.0	0.8	0.8	1.0	0.8	1.4	2.1	1.5	0.5	1.0	-0.6	0.0	1.1	0.9	0.7
125	2.1	1.3	1.1	0.6	1.4	0.5	1.0	0.5	1.4	2.0	1.6	1.5	1.2	1.2	0.5	1.4
160	2.2	0.9	0.5	1.0	1.9	1.0	1.9	0.8	0.9	0.5	0.6	-0.4	-0.7	0.9	0.8	0.6
200	2.2	1.7	0.9	0.7	1.8	1.0	0.4	0.5	1.4	1.6	0.8	0.2	0.7	1.1	0.6	1.1
250	3.8	3.8	1.8	2.1	2.3	1.5	2.2	1.7	1.4	1.3	1.4	-0.6	-1.0	1.7	1.3	1.4
315	4.8	1.5	2.3	2.7	3.5	1.8	0.5	0.9	3.0	2.4	1.4	0.8	0.4	2.0	1.3	2.1
400	3.5	3.5	3.5	3.4	4.3	2.8	3.0	1.9	3.4	2.9	3.8	1.7	-1.2	2.8	1.4	3.0
500	5.5	4.5	3.8	4.4	4.8	3.3	2.8	2.0	3.6	4.6	5.0	3.0	1.8	3.8	1.1	3.7
630	5.0	4.0	3.0	4.7	3.7	3.3	2.6	3.2	5.0	6.9	8.1	7.9	6.1	4.9	1.9	4.9
800	3.0	1.7	1.3	3.4	4.3	3.5	3.5	2.9	6.5	7.5	8.8	9.0	6.8	4.8	2.6	5.2
1000	6.3	4.3	3.8	5.2	4.0	3.3	4.2	3.2	6.6	8.9	10.3	11.0	9.9	6.2	2.9	6.2
1250	5.7	4.0	3.1	4.1	3.1	2.5	4.7	3.8	5.8	7.9	9.8	9.8	8.9	5.6	2.6	5.4
1600	6.5	6.2	3.7	5.1	5.5	4.3	3.4	4.4	6.3	8.6	9.3	10.1	8.8	6.3	2.2	5.7
2000	7.1	8.1	6.8	7.5	6.6	4.6	4.4	5.0	8.3	11.5	13.4	13.4	11.2	8.3	3.1	7.0
2500	8.3	9.5	8.6	9.2	6.9	5.4	5.5	6.4	8.9	10.2	11.6	12.1	10.4	8.7	2.2	7.9
3150	6.4	7.9	6.6	8.8	6.1	5.7	5.8	5.4	9.9	10.4	12.2	13.4	11.2	8.4	2.7	7.4
4000	2.1	5.9	4.5	6.9	6.3	5.0	6.6	6.7	9.5	9.5	11.6	11.9	9.3	7.4	2.8	6.8
5000	4.5	8.6	6.6	8.8	6.6	5.4	6.1	5.3	8.9	8.6	8.3	10.7		7.4	1.9	7.1
6300	3.9	9.0	5.7	9.0	5.8	4.8	6.0	4.9	7.3	7.5	6.9			6.4	1.7	6.5
8000			6.6	10.0	5.3	3.8	4.4	3.4	6.4	9.4				6.2	2.5	6.2
10000																5.0
12500																
16000																
20000																
25000																
31500																
40000																
50000																
63000																
80000																
OASPL	5.1	5.2	4.0	5.3	4.5	3.5	3.6	3.2	4.6	4.7	4.6	2.9	1.0			
PNL	6.0	6.5	5.5	6.8	5.5	4.3	4.1	4.1	6.0	6.8	7.5	7.3	4.6			
PNLT	4.9	7.3	5.4	6.7	5.5	4.3	4.1	4.1	5.9	6.3	7.5	7.3	4.6			
DBA	6.0	5.9	4.8	6.0	5.0	3.9	4.1	3.9	6.1	7.4	8.5	8.6	6.2			

LOCATION	ACOUSTIC RANGE	AVG CORR SPEED	AVG CORR THRUST
C41 ANECH CH	2400.0 FT SL	-0.1E 31 RPM	-0.1E 31' LB

TEST CASE FOR TREATED EJECTOR TE01 VS TE02

DELTA, SPL(1) - SPL(2)

IDENTIFICATION

INPUT (1) 83F-4ØØ-1Ø1Ø X1Ø1Ø5
(2) 83F-4ØØ-2Ø1Ø X2Ø1Ø5

OUTPUT TOF TE1-TE2 XØ1Ø21

ANGLES MEASURED FROM INLET,DEGREES

FREQ	4Ø.Ø	5Ø.Ø	6Ø.Ø	7Ø.Ø	8Ø.Ø	9Ø.Ø	1ØØ.Ø	11Ø.Ø	12Ø.Ø	13Ø.Ø	14Ø.Ø	15Ø.Ø	16Ø.Ø	AVG	S.D.	PWL
5Ø	1.3	7.3	1.Ø	5.Ø	-Ø.2	2.9	6.2	4.2	-Ø.8	-1.3	Ø.2	Ø.4	-Ø.8	2.Ø	2.9	Ø.3
63	-Ø.4	2.4	-Ø.1	1.8	-Ø.1	-1.1	Ø.5	Ø.5	-1.3	-1.Ø	-Ø.Ø	Ø.2	-Ø.5	Ø.1	1.1	-Ø.2
8Ø	-1.Ø	1.4	-Ø.9	Ø.4	Ø.9	-Ø.8	-1.1	-Ø.4	-1.Ø	-Ø.Ø	Ø.3	Ø.4	-1.3	-Ø.2	Ø.8	-Ø.2
1ØØ	-Ø.Ø	Ø.2	-1.6	-Ø.2	-Ø.1	-1.1	-Ø.8	Ø.3	-Ø.Ø	-1.7	1.Ø	-Ø.3	-1.Ø	-Ø.4	Ø.8	-Ø.4
125	-Ø.7	-Ø.2	-Ø.4	-Ø.5	-Ø.Ø	-1.1	-Ø.3	-Ø.1	Ø.2	Ø.1	Ø.6	Ø.6	-Ø.2	-Ø.2	Ø.5	Ø.2
16Ø	-Ø.7	-Ø.4	-1.2	-Ø.6	-Ø.3	-Ø.6	-1.1	-Ø.2	-1.Ø	-1.7	-Ø.3	-Ø.7	-2.Ø	-Ø.8	Ø.5	-1.Ø
2ØØ	-Ø.1	Ø.Ø	-Ø.9	-Ø.7	-Ø.1	-Ø.6	-Ø.5	-Ø.8	-1.2	-2.Ø	-Ø.8	-1.8	-2.6	-Ø.9	Ø.8	-1.3
25Ø	-Ø.Ø	1.2	-Ø.5	-Ø.1	Ø.5	Ø.2	-Ø.Ø	-Ø.5	-1.Ø	-1.6	-Ø.8	-2.Ø	-3.3	-Ø.6	1.2	-1.Ø
315	-Ø.Ø	-Ø.8	-Ø.Ø	Ø.3	Ø.9	-Ø.5	-Ø.6	-1.9	-Ø.1	-1.Ø	-1.Ø	-1.4	-1.5	-Ø.6	Ø.8	-Ø.7
4ØØ	1.Ø	1.Ø	Ø.9	Ø.9	1.2	1.5	1.2	-Ø.4	-Ø.4	-Ø.7	Ø.4	-1.5	-2.1	Ø.2	1.2	-Ø.1
5ØØ	1.7	1.7	1.7	1.1	2.5	1.2	Ø.8	-Ø.9	Ø.8	-Ø.Ø	Ø.7	-1.5	-1.1	Ø.7	1.2	Ø.4
63Ø	1.9	1.6	1.6	2.1	2.7	1.Ø	1.3	Ø.1	1.8	2.1	2.3	2.7	2.Ø	1.8	Ø.7	1.8
8ØØ	1.3	2.Ø	1.9	2.7	2.3	1.3	1.9	Ø.9	2.1	2.3	3.3	3.Ø	1.5	2.Ø	Ø.7	2.1
1ØØØ	2.7	Ø.9	Ø.6	1.3	2.8	1.3	1.8	Ø.Ø	2.3	2.9	3.6	3.8	1.8	2.Ø	1.1	2.1
125Ø	2.2	3.Ø	2.4	3.Ø	3.6	2.Ø	2.6	1.6	2.9	2.4	4.Ø	5.1	2.9	2.9	Ø.9	2.8
16ØØ	1.6	3.6	3.5	5.5	5.1	3.3	3.Ø	1.8	3.7	3.1	4.5	5.9	3.5	3.7	1.3	3.7
2ØØØ	Ø.9	3.3	2.4	4.1	4.1	3.2	4.Ø	2.6	6.1	6.8	8.7	8.9	6.8	4.8	2.5	4.Ø
25ØØ	1.1	3.5	3.1	3.9	4.Ø	3.Ø	4.4	3.8	6.4	6.2	7.8	8.8	6.5	4.8	2.2	4.1
315Ø	Ø.7	3.7	3.Ø	4.Ø	4.5	2.5	5.Ø	3.5	6.4	6.7	8.9	9.3	7.2	5.Ø	2.5	4.3
4ØØØ	Ø.5	4.2	2.9	4.8	3.9	2.4	5.1	3.1	6.4	5.7	7.5	7.2	5.5	4.6	2.Ø	4.3
5ØØØ	-Ø.3	4.4	2.7	4.5	4.7	2.4	3.9	3.2	4.3	4.1	4.7	6.8		3.8	1.7	3.7
63ØØ	Ø.7	6.4	5.4	7.1	3.2	1.Ø	3.5	2.Ø	4.7	4.3	5.9			4.Ø	2.2	4.1
8ØØØ		3.5	2.Ø	4.3	1.4	Ø.7	2.4	1.9	3.3	5.2				2.7	1.5	2.9
1ØØØØ						Ø.6								Ø.6	.1E 19	1.2
125ØØ																
16ØØØ																
2ØØØØ																
25ØØØ																
315ØØ																
4ØØØØ																
5ØØØØ																
63ØØØ																
8ØØØØ																
OASPL	1.3	2.3	2.Ø	3.2	3.1	1.8	2.1	Ø.7	1.3	Ø.4	1.Ø	Ø.4	-Ø.8			
PNL	1.1	2.7	2.5	3.8	3.8	2.2	3.Ø	1.7	2.8	2.1	3.2	2.8	Ø.3			
PNLT	1.1	3.5	3.2	5.Ø	3.8	2.2	3.Ø	1.7	3.4	2.1	2.1	2.8	1.4			
DBA	1.7	2.7	2.5	3.8	3.8	2.3	2.8	1.3	2.6	2.1	3.Ø	2.9	Ø.8			

LOCATION	ACOUSTIC RANGE	AVG CORR SPEED	AVG CORR THRUST
C41 ANECH CH	24ØØ.Ø FT SL	-Ø.1E 31 RPM	-Ø.1E 31 LB

TEST CASE FOR TREATED EJECTOR TEØ1 VS TEØ2

DELTA, SPL(1) - SPL(2)

IDENTIFICATION

INPUT (1) 83F-ZER-1ØØ3 X1ØØ35
(2) 83F-ZER-ØØØ3 XØØØ35

OUTPUT CBS TE1-T1Ø XØ11Ø1

ANGLES MEASURED FROM INLET,DEGREES

FREQ	4Ø.Ø	5Ø.Ø	6Ø.Ø	7Ø.Ø	8Ø.Ø	9Ø.Ø	1ØØ.Ø	11Ø.Ø	12Ø.Ø	13Ø.Ø	14Ø.Ø	15Ø.Ø	16Ø.Ø	AVG	S.D.	PWL
5Ø	-1.5	Ø.3	Ø.8	Ø.3	Ø.Ø	3.3	8.3	-Ø.2	-1.7	-1.7	-Ø.5	Ø.4	-1.Ø	Ø.5	2.7	Ø.1
63	-2.2	-Ø.7	-Ø.2	-Ø.5	-Ø.5	-2.7	-Ø.7	-1.5	-Ø.5	-Ø.7	-Ø.2	-Ø.8	-1.2	-1.Ø	Ø.8	-Ø.8
8Ø	-1.5	-1.2	-Ø.2	-Ø.2	Ø.Ø	-1.Ø	-1.5	-1.5	-1.7	-1.2	-Ø.2	-Ø.8	-2.Ø	-1.Ø	Ø.7	-1.Ø
1ØØ	-2.Ø	-1.2	Ø.3	Ø.Ø	Ø.3	-2.2	-1.Ø	-1.2	-1.7	-Ø.5	-Ø.2	-1.1	-1.7	-Ø.9	Ø.9	-Ø.9
125	-1.5	-2.Ø	Ø.3	Ø.8	1.3	-1.Ø	-Ø.2	-1.7	Ø.3	-Ø.7	Ø.Ø	-Ø.3	-1.5	-Ø.5	1.Ø	-Ø.4
16Ø	-Ø.5	Ø.3	Ø.8	-Ø.6	Ø.5	-Ø.2	-Ø.5	-Ø.7	-Ø.7	-Ø.7	-Ø.4	-1.3	-1.7	-Ø.4	Ø.7	-Ø.6
2ØØ	-1.7	2.6	Ø.6	1.4	1.1	-Ø.4	-Ø.2	-1.2	Ø.1	-Ø.2	-Ø.7	-1.3	-1.7	-Ø.1	1.3	-Ø.4
25Ø	-Ø.2	Ø.6	Ø.8	1.4	Ø.8	Ø.8	1.3	-Ø.2	Ø.1	-1.2	Ø.3	-Ø.3	-2.Ø	Ø.2	1.Ø	-Ø.Ø
315	-Ø.5	2.8	2.5	3.4	3.Ø	Ø.8	1.3	Ø.3	2.3	Ø.8	Ø.8	Ø.9	-Ø.2	1.4	1.3	1.3
4ØØ	1.8	2.5	3.3	3.4	3.5	3.Ø	2.8	1.8	3.3	2.8	3.8	4.2	3.8	3.1	Ø.7	3.Ø
5ØØ	2.7	3.Ø	3.7	3.5	4.7	3.2	3.2	3.Ø	5.Ø	6.Ø	6.2	7.4	7.Ø	4.5	1.6	4.9
63Ø	3.9	2.4	3.6	4.4	5.1	2.9	4.4	2.4	5.9	6.9	9.4	11.Ø	1Ø.4	5.6	3.Ø	6.Ø
8ØØ	5.Ø	3.7	5.Ø	5.6	6.Ø	3.8	5.Ø	3.5	7.7	9.Ø	11.3	13.9	13.5	7.2	3.7	7.4
1ØØØ	4.6	5.3	6.1	6.4	6.4	3.6	3.1	2.1	7.6	9.2	11.3	14.5	14.4	7.3	4.Ø	6.8
125Ø	5.4	4.8	6.1	6.8	5.4	3.4	3.6	2.1	6.3	9.5	11.1	13.3	15.2	7.1	4.Ø	6.2
16ØØ	7.7	6.5	6.8	7.4	4.6	2.6	2.6	1.8	6.Ø	8.9	1Ø.8	13.Ø	13.7	7.1	3.8	5.2
2ØØØ	8.4	7.7	8.7	7.3	5.3	1.3	2.1	1.Ø	5.7	8.7	1Ø.2	12.8	15.7	7.3	4.3	4.6
25ØØ	8.2	7.Ø	7.2	7.9	6.4	2.4	1.9	Ø.3	5.5	8.Ø	11.3	13.8	15.Ø	7.3	4.3	4.5
315Ø	7.3	5.1	7.4	8.6	6.3	2.Ø	2.3	1.2	4.9	7.9	11.6	14.5	13.9	7.1	4.2	4.4
4ØØØ	6.2	5.1	6.4	8.2	5.7	2.2	2.2	1.4	4.4	7.8	12.1	15.8	15.2	7.1	4.7	4.4
5ØØØ	6.5	4.7	6.2	8.3	5.5	2.Ø	3.3	2.3	6.9	9.8	13.6	18.2		7.3	4.7	5.4
63ØØ		5.9	6.4	9.3	6.2	1.9	5.2	4.1	8.2	13.2	15.3			7.6	4.1	6.9
8ØØØ				11.4	8.Ø	4.4	7.8	6.2	12.6					8.4	3.1	1Ø.3
1ØØØØ																16.Ø
125ØØ																
16ØØØ																
2ØØØØ																
25ØØØ																
315ØØ																
4ØØØØ																
5ØØØØ																
63ØØØ																
8ØØØØ																
OASPL	1.4	2.6	3.6	4.Ø	3.7	1.9	2.8	1.3	3.Ø	2.Ø	2.2	1.3	-Ø.6			
PNL	4.9	5.1	6.Ø	6.Ø	5.Ø	1.8	2.3	1.1	4.4	5.1	6.2	6.8	4.5			
PNLT	6.Ø	5.1	6.Ø	6.Ø	5.Ø	1.8	2.3	1.1	3.9	5.6	6.1	6.8	4.5			
DBA	4.6	4.8	5.8	6.2	5.3	2.8	3.1	2.Ø	5.8	6.8	8.4	9.9	8.1			

LOCATION	ACOUSTIC RANGE	AVG CORR SPEED	AVG CORR THRUST
C41 ANECH CH	24ØØ.Ø FT SL	-Ø.1E 31 RPM	-Ø.1E 31 LB

TEST CASE FOR TREATED EJECTOR TEØ1 VS TE1Ø

DELTA, SPL(1) - SPL(2)

IDENTIFICATION

INPUT (1) 83F-ZER-1ØØ5 X1ØØ55
(2) 83F-ZER-ØØØ5 XØØØ55

OUTPUT ITS TE1-T1Ø XØ11Ø1

ANGLES MEASURED FROM INLET,DEGREES

FREQ	4Ø.Ø	5Ø.Ø	6Ø.Ø	7Ø.Ø	8Ø.Ø	9Ø.Ø	1ØØ.Ø	11Ø.Ø	12Ø.Ø	13Ø.Ø	14Ø.Ø	15Ø.Ø	16Ø.Ø	AVG	S.D.	PWL
5Ø	-2.2	-1.2	Ø.Ø	-1.Ø	-Ø.5	2.5	7.Ø	-1.2	-2.Ø	-3.2	-1.5	-Ø.6	-2.Ø	-Ø.5	2.6	-1.1
63	-2.5	-Ø.7	-Ø.5	-1.7	-1.2	-3.Ø	-Ø.7	-1.5	-Ø.5	-1.5	-1.Ø	-1.6	-2.2	-1.4	Ø.8	-1.6
8Ø	-2.2	-2.2	-1.Ø	-Ø.7	-1.2	-2.Ø	-1.5	-2.Ø	-2.Ø	-1.5	-Ø.7	-2.3	-2.2	-1.7	Ø.6	-1.8
1ØØ	-3.2	-2.Ø	-Ø.2	-Ø.7	-1.Ø	-2.5	-Ø.5	-1.2	-1.2	-1.7	-1.2	-2.3	-3.5	-1.6	1.Ø	-2.Ø
125	-3.2	-3.2	-Ø.7	-Ø.5	Ø.3	-2.Ø	-1.Ø	-2.Ø	-1.Ø	-2.2	-1.5	-2.6	-4.2	-1.8	1.3	-2.1
16Ø	-1.5	-Ø.9	Ø.1	-1.9	-Ø.2	-1.2	-Ø.5	-1.Ø	-Ø.9	-1.4	-1.4	-3.3	-4.2	-1.4	1.2	-1.7
2ØØ	-2.5	1.1	Ø.1	Ø.2	-Ø.2	-1.4	-Ø.4	-1.7	-Ø.4	-1.9	-1.4	-3.Ø	-4.7	-1.3	1.5	-1.6
25Ø	-1.5	-1.7	-Ø.2	Ø.7	-Ø.2	-Ø.4	Ø.6	-1.2	-Ø.9	-2.7	-1.2	-2.8	-5.7	-1.3	1.7	-1.6
315	-2.2	1.8	1.5	1.2	Ø.5	-Ø.5	Ø.3	-Ø.7	Ø.Ø	-1.2	-Ø.7	-2.6	-5.2	-Ø.6	1.9	-Ø.8
4ØØ	Ø.3	1.8	1.8	1.9	1.8	Ø.8	1.5	Ø.5	1.5	-Ø.2	1.5	-Ø.1	-1.7	Ø.9	1.1	Ø.7
5ØØ	Ø.5	1.5	2.5	2.2	2.5	1.Ø	2.Ø	1.2	2.7	2.2	3.2	1.1	-Ø.Ø	1.7	Ø.9	2.Ø
63Ø	2.6	2.4	2.9	2.9	2.6	1.9	3.1	1.6	3.6	2.6	4.9	3.5	2.9	2.9	Ø.8	3.1
8ØØ	4.8	4.2	5.Ø	4.4	4.Ø	2.3	4.5	2.3	5.Ø	6.Ø	7.5	5.9	5.3	4.7	1.4	5.Ø
1ØØØ	7.6	7.3	6.1	5.4	4.6	2.6	2.9	2.1	6.1	5.5	7.6	6.Ø	5.9	5.4	1.8	4.9
125Ø	9.9	1Ø.3	8.6	7.3	4.1	2.1	2.9	1.6	4.8	4.7	6.6	4.6	6.4	5.7	2.8	4.4
16ØØ	11.4	11.8	11.8	9.6	5.1	1.9	2.6	2.1	4.3	4.4	6.3	4.8	6.7	6.4	3.6	4.7
2ØØØ	1Ø.1	9.7	1Ø.7	1Ø.1	6.8	1.6	2.3	1.8	3.7	3.5	6.2	5.5	8.4	6.2	3.4	4.4
25ØØ	9.7	8.5	8.Ø	8.6	6.7	2.7	1.2	Ø.3	4.Ø	4.5	7.3	7.9	8.3	6.Ø	3.1	3.9
315Ø	9.3	7.4	7.6	8.1	6.Ø	1.8	2.3	1.Ø	3.9	4.2	7.9	7.7	8.9	5.9	2.9	3.9
4ØØØ	8.7	7.6	8.4	8.7	5.2	1.5	1.7	Ø.9	4.1	4.3	8.7	9.1	1Ø.2	6.1	3.3	3.9
5ØØØ	8.8	8.2	9.2	1Ø.3	6.6	2.1	3.3	2.6	6.5	6.6	11.4	12.2		7.3	3.4	5.6
63ØØ		1Ø.2	1Ø.5	11.7	7.2	3.4	5.5	5.2	8.5	8.5	12.8			8.4	3.Ø	7.2
8ØØØ				14.5	1Ø.4	6.5	9.1	8.8	13.5					1Ø.4	3.Ø	11.6
1ØØØØ																16.9
125ØØ																
16ØØØ																
2ØØØØ																
25ØØØ																
315ØØ																
4ØØØØ																
5ØØØØ																
63ØØØ																
8ØØØØ																
OASPL	1.4	3.3	4.1	3.7	2.6	Ø.8	2.1	Ø.6	1.5	-Ø.2	Ø.3	-1.2	-2.4			
PNL	5.8	7.Ø	7.2	6.8	4.6	1.5	2.Ø	1.Ø	2.9	1.7	3.3	1.3	-1.6			
PNLT	5.8	7.Ø	7.2	6.8	4.6	1.5	2.Ø	Ø.5	2.9	1.7	4.4	1.3	-1.6			
DBA	6.1	7.2	7.5	6.7	4.6	1.9	2.6	1.6	3.9	3.2	4.9	3.Ø	Ø.8			

LOCATION	ACOUSTIC RANGE	AVG CORR SPEED	AVG CORR THRUST
C41 ANECH CH	24ØØ.Ø FT SL	-Ø.1E 31 RPM	-Ø.1E 31 LB

TEST CASE FOR TREATED EJECTOR TEØ1 VS TE1Ø

C8

DELTA, SPL(1) - SPL(2)

IDENTIFICATION

INPUT (1) 83F-ZER-1ØØ9 X1ØØ95
(2) 83F-ZER-ØØØ9 XØØØ95

OUTPUT TOS TE1-T1Ø XØ11Ø1

ANGLES MEASURED FROM INLET, DEGREES

FREQ	4Ø.Ø	5Ø.Ø	6Ø.Ø	7Ø.Ø	8Ø.Ø	9Ø.Ø	1ØØ.Ø	11Ø.Ø	12Ø.Ø	13Ø.Ø	14Ø.Ø	15Ø.Ø	16Ø.Ø	AVG	S.D.	PWL
5Ø	-1.7	-Ø.7	Ø.3	-Ø.7	-1.Ø	2.Ø	7.8	4.3	-1.5	-2.7	-2.Ø	-1.1	-1.7	Ø.1	3.Ø	-1.3
63	-2.5	-Ø.7	-Ø.7	-1.Ø	-Ø.7	-2.5	-Ø.7	-Ø.3	-1.Ø	-1.5	-2.5	-Ø.8	-Ø.7	-1.2	Ø.8	-1.4
8Ø	-2.Ø	-2.2	-1.2	-1.Ø	-Ø.2	-1.2	-1.2	-1.1	-1.5	-1.5	-2.Ø	-1.8	-1.7	-1.4	Ø.5	-1.8
1ØØ	-3.2	-2.7	-1.2	-1.2	-1.Ø	-2.5	-Ø.7	-1.1	-1.2	-1.Ø	-2.5	-2.3	-2.7	-1.8	Ø.9	-2.2
125	-3.7	-5.Ø	-3.Ø	-1.2	-Ø.7	-2.2	-1.2	-1.3	-1.Ø	-2.5	-2.5	-3.1	-3.2	-2.3	1.2	-2.7
16Ø	-2.Ø	-3.2	-2.2	-3.1	-2.5	-3.Ø	-1.7	-Ø.4	-1.2	-1.7	-2.9	-3.8	-3.5	-2.4	1.Ø	-2.9
2ØØ	-3.4	-1.2	-1.9	-1.3	-Ø.7	-2.7	-Ø.9	-1.5	-Ø.7	-1.7	-3.4	-3.8	-3.2	-2.Ø	1.1	-2.9
25Ø	-2.5	-3.7	-1.9	-1.1	-Ø.9	-1.4	-Ø.9	-1.1	-1.2	-2.7	-2.9	-3.3	-3.Ø	-2.1	1.Ø	-2.6
315	-1.5	Ø.Ø	-1.Ø	Ø.2	-Ø.5	-2.2	-1.Ø	-1.9	-1.2	-1.4	-2.7	-3.3	-3.5	-1.5	1.2	-2.3
4ØØ	-Ø.2	-Ø.2	Ø.3	Ø.1	Ø.3	-Ø.2	Ø.3	-1.Ø	Ø.5	-1.Ø	-2.Ø	-2.6	-2.2	-Ø.6	1.1	-1.3
5ØØ	Ø.2	Ø.5	2.2	1.7	1.2	-Ø.3	Ø.2	-Ø.8	-Ø.Ø	Ø.2	-1.Ø	-2.9	-2.3	-Ø.1	1.4	-Ø.8
63Ø	3.1	2.6	2.9	2.4	1.9	Ø.1	1.4	-Ø.2	1.1	Ø.1	-Ø.6	-2.2	-2.6	Ø.8	1.9	-Ø.1
8ØØ	7.Ø	6.7	6.2	5.1	3.Ø	Ø.8	1.8	Ø.9	1.7	1.7	Ø.3	-1.3	-1.7	2.5	3.Ø	1.2
1ØØØ	8.4	1Ø.3	1Ø.3	9.4	5.6	1.9	1.4	Ø.Ø	2.3	2.Ø	Ø.6	-1.5	-1.4	3.8	4.4	2.3
125Ø	7.7	9.8	11.6	11.5	7.9	3.6	2.6	Ø.4	1.8	2.2	Ø.1	-Ø.2	-Ø.8	4.5	4.6	3.1
16ØØ	8.2	8.8	8.8	1Ø.6	8.9	5.1	3.9	Ø.9	1.8	Ø.9	Ø.Ø	-1.7	1.4	4.4	4.2	3.3
2ØØØ	8.4	7.7	8.4	8.1	7.1	3.8	3.3	1.3	1.7	1.Ø	Ø.5	-1.Ø	Ø.4	3.9	3.5	2.8
25ØØ	8.2	8.2	8.Ø	8.1	5.7	2.7	1.7	-Ø.4	1.2	1.3	Ø.5	Ø.3	Ø.2	3.5	3.5	2.4
315Ø	6.8	6.9	6.8	8.1	5.8	1.Ø	2.3	1.1	1.8	1.9	Ø.9	Ø.2	-Ø.4	3.3	3.Ø	2.5
4ØØØ	6.7	7.1	7.6	8.7	5.4	1.4	2.4	1.3	2.9	1.5	1.6	Ø.8	-Ø.5	3.6	3.1	2.9
5ØØØ	7.5	8.2	9.2	1Ø.5	6.5	2.8	4.5	2.6	4.4	4.1	4.6	3.2		5.7	2.6	4.7
63ØØ	8.5	1Ø.9	11.4	13.8	7.9	4.1	6.7	5.1	6.4	6.5	5.8			7.9	3.Ø	6.5
8ØØØ			15.3	16.4	12.Ø	7.9	9.8	9.8	11.8	12.Ø				11.9	2.8	1Ø.8
1ØØØØ																16.9
125ØØ																
16ØØØ																
2ØØØØ																
25ØØØ																
315ØØ																
4ØØØØ																
5ØØØØ																
63ØØØ																
8ØØØØ																
OASPL	Ø.2	1.6	3.2	3.7	2.5	Ø.5	1.2	-Ø.3	-Ø.1	-1.2	-2.2	-2.3	-2.3			
PNL	3.Ø	4.6	5.8	6.5	5.1	2.1	2.Ø	Ø.4	Ø.9	-Ø.4	-1.4	-2.7	-2.4			
PNLT	1.9	4.5	5.3	5.9	5.1	2.6	2.Ø	Ø.4	Ø.4	-1.Ø	-Ø.3	-1.5	-2.4			
DBA	4.5	6.2	7.4	7.7	5.6	2.4	2.Ø	Ø.2	1.2	Ø.5	-1.Ø	-2.6	-2.7			

LOCATION	ACOUSTIC RANGE	AVG CORR SPEED	AVG CORR THRUST
C41 ANECH CH	24ØØ.Ø FT SL	-Ø.1E 31 RPM	-Ø.1E 31 LB

TEST CASE FOR TREATED EJECTOR TEØ1 VS TE1Ø

C9

DELTA, SPL(1) - SPL(2)

IDENTIFICATION

INPUT (1) 83F-4ØØ-1ØØ4 X1ØØ45
(2) 83F-4ØØ-ØØØ4 XØØØ45

OUTPUT CBF TE1-T1Ø XØ11Ø1

ANGLES MEASURED FROM INLET, DEGREES

FREQ	4Ø.Ø	5Ø.Ø	6Ø.Ø	7Ø.Ø	8Ø.Ø	9Ø.Ø	1ØØ.Ø	11Ø.Ø	12Ø.Ø	13Ø.Ø	14Ø.Ø	15Ø.Ø	16Ø.Ø	AVG	S.D.	PWL
5Ø	2.8	11.5	Ø.4	1Ø.2	-Ø.6	5.5	9.2	-Ø.3	-1.8	-1.1	-1.Ø	-1.4	-2.2	2.4	5.Ø	2.2
63	-Ø.5	6.4	-Ø.4	6.6	-1.2	-1.3	2.Ø	-1.6	-Ø.3	Ø.9	Ø.5	-Ø.6	-1.6	Ø.7	2.8	Ø.7
8Ø	-Ø.8	3.4	-Ø.6	2.4	-Ø.5	-3.4	-1.2	-1.7	-Ø.7	Ø.4	Ø.Ø	-1.4	-1.4	-Ø.4	1.8	-Ø.4
1ØØ	-2.3	-1.2	-1.9	-Ø.8	-Ø.6	-3.8	Ø.9	-1.Ø	-Ø.8	-1.3	-Ø.8	-1.4	-1.3	-1.3	1.1	-1.1
125	-3.3	-Ø.7	-1.7	-Ø.9	1.Ø	-3.Ø	-Ø.7	-1.1	-Ø.8	1.Ø	Ø.6	-1.2	Ø.1	-Ø.8	1.3	-Ø.2
16Ø	-1.6	-Ø.4	-1.4	Ø.5	Ø.2	-1.1	-1.4	-1.4	-Ø.1	Ø.4	-Ø.4	-2.3	-Ø.8	-Ø.7	Ø.9	-Ø.5
2ØØ	-1.6	Ø.3	-Ø.4	-1.1	Ø.3	-3.Ø	-Ø.9	-2.4	Ø.2	-Ø.4	-Ø.4	-1.7	-1.9	-1.Ø	1.1	-Ø.8
25Ø	-Ø.6	1.7	-Ø.4	Ø.5	1.Ø	-Ø.3	1.Ø	-Ø.3	-Ø.4	Ø.3	-1.Ø	-2.4	-4.5	-Ø.4	1.6	-Ø.3
315	1.2	-Ø.3	Ø.9	1.3	4.2	Ø.6	-Ø.4	-1.2	1.9	2.6	Ø.7	-1.Ø	-2.1	Ø.7	1.7	1.1
4ØØ	1.5	3.Ø	2.5	2.1	4.4	2.9	1.4	-Ø.Ø	2.3	4.7	3.2	1.Ø	-1.5	2.1	1.7	2.4
5ØØ	3.7	2.7	2.7	3.Ø	4.1	1.9	1.4	Ø.9	2.8	5.1	5.Ø	4.3	1.Ø	3.Ø	1.4	2.9
63Ø	2.9	3.4	3.4	3.2	4.8	2.1	3.Ø	1.1	4.1	9.Ø	8.8	7.6	5.9	4.6	2.5	4.4
8ØØ	2.4	2.6	2.8	3.8	4.7	2.5	3.5	2.7	5.Ø	8.1	9.Ø	8.6	5.8	4.7	2.4	4.7
1ØØØ	1.2	1.4	3.Ø	3.2	4.8	2.3	3.Ø	1.9	5.Ø	9.Ø	9.6	1Ø.4	7.6	4.8	3.3	4.6
125Ø	Ø.6	2.5	3.1	3.5	3.8	2.4	3.Ø	2.7	5.5	8.7	1Ø.1	1Ø.Ø	7.7	4.9	3.2	4.4
16ØØ	1.1	3.3	3.6	4.1	4.Ø	2.4	3.7	2.8	5.9	8.6	9.4	1Ø.4	8.4	5.2	3.Ø	4.4
2ØØØ	2.4	3.2	4.5	4.7	5.Ø	2.1	3.2	3.Ø	4.7	7.9	9.5	11.Ø	7.4	5.3	2.8	4.2
25ØØ	3.2	5.Ø	6.6	5.6	5.6	2.9	2.2	3.Ø	5.3	7.2	8.6	9.4	7.3	5.5	2.3	4.7
315Ø	3.7	5.9	6.5	7.Ø	7.Ø	3.Ø	3.5	3.1	4.5	6.4	7.8	9.3	6.9	5.7	2.Ø	5.1
4ØØØ	2.8	2.8	5.9	7.5	6.1	1.9	3.6	3.2	5.4	6.5	8.6	9.5	6.3	5.4	2.4	4.8
5ØØØ	Ø.9	3.1	4.9	6.3	6.3	2.5	5.Ø	3.8	5.3	6.5	7.3	9.9		5.1	2.4	4.7
63ØØ	3.Ø	4.4	6.1	8.3	5.3	1.Ø	5.2	4.1	6.8	7.4	7.2			5.4	2.2	5.2
8ØØØ			4.3	7.2	6.5	2.4	6.4	5.1	8.9					5.9	2.1	6.Ø
1ØØØØ																7.8
125ØØ																
16ØØØ																
2ØØØØ																
25ØØØ																
315ØØ																
4ØØØØ																
5ØØØØ																
63ØØØ																
8ØØØØ																
OASPL	1.3	3.2	2.9	3.7	4.1	2.Ø	2.7	1.7	3.3	4.5	3.8	2.3	Ø.1			
PNL	1.8	3.3	4.3	4.5	4.7	2.1	2.8	2.2	4.2	6.1	6.7	6.8	2.9			
PNLT	Ø.8	3.3	4.5	4.7	4.2	2.1	2.8	1.7	4.2	6.1	6.7	6.8	2.9			
DBA	1.8	3.Ø	3.9	4.2	4.6	2.3	3.Ø	2.4	4.7	7.5	8.1	8.1	4.7			

LOCATION	ACOUSTIC RANGE	AVG CORR SPEED	AVG CORR THRUST
C41 ANECH CH	24ØØ.Ø FT SL	-Ø.1E 31 RPM	-Ø.1E 31 LB

TEST CASE FOR TREATED EJECTOR TEØ1 VS TE1Ø

C1

DELTA, SPL(1) - SPL(2)

IDENTIFICATION

INPUT (1) 83F-4ØØ-1ØØ6 X1ØØ65
(2) 83F-4ØØ-ØØØ6 XØØØ65

OUTPUT ITF TE1-T1Ø XØ11Ø1

ANGLES MEASURED FROM INLET,DEGREES

FREQ	4Ø.Ø	5Ø.Ø	6Ø.Ø	7Ø.Ø	8Ø.Ø	9Ø.Ø	1ØØ.Ø	11Ø.Ø	12Ø.Ø	13Ø.Ø	14Ø.Ø	15Ø.Ø	16Ø.Ø	AVG	S.D.	PWL
5Ø	2.6	9.3	1.2	6.6	1.Ø	4.5	9.Ø	Ø.8	-Ø.2	-Ø.2	-Ø.7	-1.1	-1.2	2.4	3.7	Ø.7
63	1.Ø	5.4	2.3	4.8	Ø.1	-Ø.2	2.3	-1.Ø	-1.5	-Ø.2	-Ø.5	-1.3	-1.7	Ø.7	2.3	-Ø.3
8Ø	-1.8	1.3	Ø.2	Ø.9	Ø.3	-1.7	-Ø.5	-1.5	-Ø.1	Ø.9	Ø.6	-Ø.Ø	-Ø.4	-Ø.1	1.Ø	Ø.1
1ØØ	-Ø.7	Ø.Ø	Ø.Ø	-Ø.2	-Ø.5	-2.Ø	Ø.1	-Ø.4	-Ø.8	-2.Ø	-1.6	-1.8	-Ø.9	-Ø.8	Ø.8	-1.2
125	-1.6	-Ø.5	-Ø.1	-Ø.3	1.Ø	-2.Ø	-1.5	-3.1	Ø.1	-Ø.4	-Ø.6	-1.5	-Ø.4	-Ø.8	1.1	-Ø.7
16Ø	-Ø.7	-Ø.8	-Ø.2	Ø.4	Ø.2	-Ø.7	Ø.3	-Ø.4	Ø.9	-Ø.2	-Ø.7	-1.4	-Ø.7	-Ø.3	Ø.6	-Ø.2
2ØØ	-Ø.7	Ø.Ø	-Ø.Ø	-1.1	1.Ø	-2.Ø	-Ø.9	-Ø.8	Ø.9	-Ø.3	Ø.5	Ø.6	Ø.4	-Ø.2	Ø.9	-Ø.Ø
25Ø	Ø.3	2.Ø	Ø.3	1.1	Ø.5	-Ø.5	1.4	-Ø.3	1.3	-Ø.1	Ø.3	-1.1	-1.Ø	Ø.3	Ø.9	Ø.3
315	1.5	-Ø.5	1.Ø	2.1	3.Ø	-Ø.2	Ø.7	Ø.3	2.2	Ø.9	Ø.9	-Ø.7	-Ø.4	Ø.9	1.1	1.1
4ØØ	1.Ø	2.Ø	2.Ø	2.9	3.5	1.5	2.Ø	Ø.1	2.5	2.9	2.7	Ø.5	-Ø.1	1.8	1.1	2.Ø
5ØØ	3.5	3.Ø	2.2	3.6	3.6	1.5	2.5	1.6	3.6	3.1	3.9	2.2	1.2	2.7	Ø.9	2.8
63Ø	Ø.9	1.2	1.2	3.3	4.1	1.9	2.8	1.6	5.1	7.5	7.8	7.7	7.Ø	4.Ø	2.7	4.3
8ØØ	Ø.8	1.1	1.6	3.5	4.5	2.3	3.8	2.2	6.6	7.5	8.6	8.7	6.9	4.5	2.9	4.9
1ØØØ	2.2	2.5	3.3	5.2	4.8	2.3	5.Ø	3.Ø	6.7	9.4	1Ø.5	1Ø.8	9.8	5.8	3.3	6.Ø
125Ø	3.3	4.3	4.1	6.5	4.7	2.9	4.7	3.5	6.2	8.5	1Ø.3	1Ø.9	9.7	6.1	2.8	5.8
16ØØ	5.8	7.2	6.7	7.4	6.3	3.4	4.8	4.Ø	5.8	8.4	9.7	9.9	8.6	6.8	2.Ø	6.1
2ØØØ	7.Ø	9.5	9.2	1Ø.Ø	7.7	3.1	4.5	4.4	6.Ø	8.3	1Ø.Ø	11.Ø	8.Ø	7.6	2.5	6.8
25ØØ	7.5	9.6	9.7	1Ø.7	7.6	3.9	4.3	3.6	6.2	6.7	8.6	9.1	7.8	7.3	2.3	6.8
315Ø	5.4	6.9	7.5	1Ø.5	7.Ø	3.5	4.2	4.Ø	5.8	6.5	8.7	9.6	7.7	6.7	2.1	6.1
4ØØØ	3.3	5.3	6.1	9.5	5.6	2.2	4.2	4.3	6.3	6.Ø	7.8	9.1	6.1	5.8	2.1	5.4
5ØØØ	3.2	4.8	5.4	9.Ø	6.5	1.7	5.Ø	3.4	7.Ø	6.8	6.9	9.8		5.8	2.4	5.3
63ØØ	4.7	6.4	6.2	1Ø.Ø	7.1	1.8	6.6	4.6	8.8	9.4	8.4			6.7	2.4	6.5
8ØØØ			6.3	11.3	9.6	4.4	7.9	6.1	12.4					8.3	2.9	9.Ø
1ØØØØ																11.1
125ØØ																
16ØØØ																
2ØØØØ																
25ØØØ																
315ØØ																
4ØØØØ																
5ØØØØ																
63ØØØ																
8ØØØØ																
OASPL	2.6	4.3	4.2	5.7	4.7	2.2	3.6	2.3	4.1	3.6	3.3	1.6	Ø.5			
PNL	4.5	6.4	6.5	7.9	5.9	2.8	3.8	3.Ø	5.Ø	5.8	6.7	6.4	4.2			
PNLT	4.5	7.3	6.5	7.9	5.9	2.8	3.8	2.5	4.9	5.8	5.7	6.4	4.2			
DBA	4.1	5.6	5.8	7.3	5.8	2.9	4.3	3.2	5.6	7.Ø	8.1	8.2	6.1			

LOCATION	ACOUSTIC RANGE	AVG CORR SPEED	AVG CORR THRUST
C41 ANECH CH	24ØØ.Ø FT SL	-Ø.1E 31 RPM	-Ø.1E 31'LB

TEST CASE FOR TREATED EJECTOR TEØ1 VS TE1Ø

DELTA, SPL(1) - SPL(2)

IDENTIFICATION

INPUT (1) 83F-4ØØ-1Ø1Ø X1Ø1Ø5
(2) 83F-4ØØ-ØØ1Ø XØØ1Ø5

OUTPUT TOF TE1-T1Ø XØ11Ø1

ANGLES MEASURED FROM INLET,DEGREES

FREQ	4Ø.Ø	5Ø.Ø	6Ø.Ø	7Ø.Ø	8Ø.Ø	9Ø.Ø	1ØØ.Ø	11Ø.Ø	12Ø.Ø	13Ø.Ø	14Ø.Ø	15Ø.Ø	16Ø.Ø	AVG	S.D.	PWL
5Ø	1.1	6.3	Ø.7	4.2	-1.1	2.7	8.Ø	3.7	-1.8	-1.5	-1.5	-Ø.8	-1.2	1.4	3.3	-Ø.6
63	-1.Ø	1.6	Ø.1	1.8	-1.1	-1.3	Ø.5	Ø.3	-2.Ø	-1.7	-1.Ø	-1.3	-1.5	-Ø.5	1.2	-1.3
8Ø	-2.3	-Ø.1	-1.1	-Ø.3	-Ø.6	-3.3	-1.5	-1.4	-1.7	-1.5	-1.7	-1.3	-2.Ø	-1.5	Ø.9	-1.6
1ØØ	-1.5	-1.1	-1.1	-Ø.6	-1.1	-3.1	-Ø.8	-1.5	-1.2	-2.7	-1.Ø	-1.8	-1.7	-1.5	Ø.7	-1.6
125	-1.5	-1.2	-1.1	-Ø.9	Ø.1	-2.Ø	-Ø.5	-1.3	-Ø.9	-1.3	-1.5	-1.8	-1.5	-1.2	Ø.6	-1.4
16Ø	-Ø.8	-1.6	-1.Ø	-Ø.1	-1.1	-1.8	-1.2	-Ø.3	-Ø.5	-2.2	-1.7	-2.3	-1.5	-1.2	Ø.7	-1.5
2ØØ	-Ø.5	-1.2	-Ø.9	-1.7	-Ø.8	-2.8	-1.Ø	-1.2	-1.1	-3.3	-1.3	-1.2	-1.9	-1.5	Ø.8	-1.7
25Ø	-1.Ø	Ø.3	-Ø.7	-Ø.4	-Ø.8	-1.Ø	Ø.3	-1.3	-1.Ø	-2.2	-1.7	-1.6	-1.8	-1.Ø	Ø.8	-1.4
315	-Ø.5	-1.5	-Ø.5	-Ø.4	Ø.7	-2.3	-Ø.5	-1.5	Ø.3	-1.7	-1.Ø	-1.Ø	-Ø.9	-Ø.8	Ø.8	-Ø.9
4ØØ	1.Ø	Ø.5	Ø.7	Ø.5	Ø.2	Ø.2	Ø.3	-1.Ø	Ø.1	-Ø.6	-Ø.Ø	-Ø.8	Ø.6	Ø.1	Ø.6	-Ø.1
5ØØ	3.1	1.4	1.7	Ø.8	1.6	-Ø.1	Ø.3	-Ø.7	1.7	Ø.2	1.1	Ø.3	2.Ø	1.Ø	1.Ø	Ø.9
63Ø	4.6	3.1	1.6	1.7	1.5	Ø.1	1.Ø	Ø.4	2.7	2.8	3.2	3.6	4.4	2.4	1.4	2.4
8ØØ	3.3	2.3	1.5	1.9	3.1	Ø.7	2.8	1.7	3.8	3.Ø	4.1	4.2	4.2	2.8	1.1	3.Ø
1ØØØ	5.6	4.6	4.Ø	3.9	4.5	2.1	1.5	1.8	4.1	4.7	4.8	4.7	4.7	3.9	1.3	3.9
125Ø	5.5	7.5	7.3	7.3	7.8	3.9	4.5	2.5	4.7	4.9	5.5	6.1	5.5	5.6	1.6	5.3
16ØØ	7.6	8.7	9.8	1Ø.3	8.5	5.6	5.1	3.5	4.5	4.5	5.7	5.9	5.7	6.6	2.2	6.6
2ØØØ	7.6	8.7	7.7	8.9	6.9	4.Ø	5.Ø	3.8	4.7	4.5	5.8	6.1	4.9	6.Ø	1.8	5.8
25ØØ	7.Ø	7.8	7.8	7.6	5.7	3.5	3.6	2.3	4.3	4.1	5.4	6.Ø	5.Ø	5.4	1.8	5.1
315Ø	5.8	6.8	6.1	6.6	5.7	1.6	3.8	2.9	3.4	4.1	6.1	7.5	5.8	5.1	1.7	4.6
4ØØØ	4.3	5.1	5.6	7.Ø	4.Ø	1.4	3.4	2.6	4.3	4.Ø	5.7	5.8	4.1	4.4	1.5	4.1
5ØØØ	3.6	4.7	4.8	6.2	5.3	1.Ø	4.Ø	3.2	5.1	4.7	4.7	6.4		4.5	1.4	4.2
63ØØ	5.5	6.6	6.9	8.8	6.Ø	1.2	5.5	3.8	9.Ø	9.3	8.5			6.5	2.5	6.3
8ØØØ			7.1	9.1	8.9	4.1	8.1	7.6	13.3					8.3	2.8	9.5
1ØØØØ																11.6
125ØØ																
16ØØØ																
2ØØØØ																
25ØØØ																
315ØØ																
4ØØØØ																
5ØØØØ																
63ØØØ																
8ØØØØ																
OASPL	3.2	4.1	4.4	5.Ø	4.3	1.8	2.5	1.1	1.8	Ø.1	Ø.1	-Ø.8	-1.1			
PNL	5.Ø	5.8	6.1	6.6	5.1	2.3	3.3	2.Ø	3.Ø	2.1	2.9	2.1	1.Ø			
PNLT	4.Ø	6.6	6.2	7.1	4.6	2.3	3.3	1.5	3.Ø	2.1	1.8	2.1	2.Ø			
DBA	5.3	6.1	6.4	6.9	5.9	3.Ø	3.4	2.1	3.5	2.8	3.4	3.4	2.8			

LOCATION	ACOUSTIC RANGE	AVG CORR SPEED	AVG CORR THRUST
C41 ANECH CH	24ØØ.Ø FT SL	-Ø.1E 31 RPM	-Ø.1E 31' LB

TEST CASE FOR TREATED EJECTOR TEØ1 VS TE1Ø

C12

DELTA, SPL(1) - SPL(2)

IDENTIFICATION

INPUT (1) 83F-ZER-2ØØ3 X2ØØ35
(2) 83F-ZER-3ØØ3 X3ØØ35

OUTPUT CBS TE2-TE3 XØ2Ø31

ANGLES MEASURED FROM INLET,DEGREES

FREQ	4Ø.Ø	5Ø.Ø	6Ø.Ø	7Ø.Ø	8Ø.Ø	9Ø.Ø	1ØØ.Ø	11Ø.Ø	12Ø.Ø	13Ø.Ø	14Ø.Ø	15Ø.Ø	16Ø.Ø	AVG	S.D.	PWL
5Ø	-1.Ø	-Ø.8	-Ø.8	-Ø.5	Ø.2	-Ø.3	-1.5	-Ø.5	Ø.2	Ø.2	-1.5	-Ø.Ø	Ø.2	-Ø.4	Ø.6	-Ø.2
63	-1.Ø	-Ø.5	Ø.2	-1.3	-Ø.3	-Ø.Ø	-Ø.5	Ø.2	-Ø.8	Ø.5	-Ø.8	-Ø.Ø	-Ø.3	-Ø.3	Ø.5	-Ø.2
8Ø	-Ø.8	-1.3	-Ø.Ø	-1.2	-1.Ø	-Ø.Ø	-Ø.3	-Ø.3	Ø.5	Ø.5	-1.8	-Ø.Ø	-Ø.5	-Ø.5	Ø.7	-Ø.4
1ØØ	-Ø.2	Ø.Ø	-1.Ø	-1.1	-Ø.7	-Ø.5	-1.Ø	-1.Ø	Ø.3	-Ø.7	-1.5	-Ø.2	Ø.Ø	-Ø.6	Ø.5	-Ø.7
125	-Ø.2	-1.Ø	Ø.3	-Ø.6	-Ø.5	Ø.5	-1.Ø	-Ø.2	-Ø.7	Ø.3	-2.5	-Ø.2	-Ø.7	-Ø.5	Ø.8	-Ø.7
16Ø	-Ø.7	-1.Ø	Ø.Ø	-Ø.8	-Ø.5	Ø.3	-Ø.7	-Ø.7	-1.2	Ø.Ø	-1.7	-Ø.7	Ø.Ø	-Ø.6	Ø.6	-Ø.7
2ØØ	-1.Ø	-Ø.7	Ø.3	-1.1	Ø.Ø	-Ø.5	-1.2	-Ø.5	-1.Ø	Ø.5	-1.5	-1.2	-Ø.7	-Ø.7	Ø.6	-Ø.7
25Ø	-Ø.2	-1.Ø	Ø.Ø	-Ø.2	Ø.Ø	-Ø.2	-Ø.7	Ø.Ø	Ø.Ø	Ø.3	-1.2	-1.Ø	-Ø.2	-Ø.3	Ø.5	-Ø.3
315	Ø.Ø	-Ø.5	-Ø.5	-Ø.8	-Ø.2	-Ø.5	-1.Ø	-Ø.5	-Ø.2	Ø.3	-1.5	-1.7	Ø.3	-Ø.5	Ø.6	-Ø.5
4ØØ	-Ø.7	-1.7	-1.2	-1.6	-Ø.2	-1.2	-1.Ø	-Ø.5	Ø.5	Ø.3	-Ø.7	-1.7	-Ø.2	-Ø.8	Ø.7	-Ø.4
5ØØ	Ø.Ø	-Ø.7	-Ø.5	-1.8	-1.5	-Ø.7	-1.7	-1.2	Ø.3	Ø.3	-1.5	-2.7	-Ø.7	-1.Ø	Ø.9	-Ø.9
63Ø	-Ø.5	-Ø.Ø	Ø.2	-1.7	-Ø.3	Ø.2	-1.5	-1.3	Ø.2	Ø.2	-1.8	-1.8	-Ø.8	-Ø.7	Ø.8	-Ø.7
8ØØ	-Ø.5	1.Ø	Ø.5	-Ø.3	-Ø.5	Ø.5	-Ø.5	-Ø.3	-Ø.3	-Ø.Ø	-Ø.8	-1.8	-Ø.8	-Ø.3	Ø.7	-Ø.3
1ØØØ	Ø.2	Ø.2	Ø.4	Ø.Ø	Ø.4	1.2	Ø.7	1.4	Ø.4	-Ø.1	-1.1	-2.3	-Ø.6	Ø.1	1.Ø	Ø.5
125Ø	Ø.6	Ø.3	1.6	-Ø.4	1.1	1.6	Ø.9	1.1	Ø.3	Ø.3	-Ø.2	-2.6	Ø.1	Ø.4	1.1	Ø.7
16ØØ	1.Ø	1.Ø	1.7	Ø.3	1.3	1.8	1.Ø	1.5	1.Ø	1.4	-Ø.8	-2.5	Ø.3	Ø.7	1.2	1.1
2ØØØ	1.9	1.8	1.8	Ø.7	1.8	2.4	Ø.8	2.3	1.3	1.7	-Ø.4	-2.6	-Ø.1	1.Ø	1.4	1.5
25ØØ	1.2	1.8	1.8	Ø.3	1.9	2.1	1.4	2.4	2.1	1.2	-1.7	-1.6	1.4	1.1	1.3	1.7
315Ø	Ø.2	Ø.7	1.7	-Ø.5	1.6	1.6	Ø.4	1.8	1.2	1.4	-Ø.2	-2.6	-Ø.6	Ø.5	1.3	1.1
4ØØØ	-Ø.9	-Ø.6	Ø.9	-2.3	Ø.Ø	Ø.8	-1.5	Ø.2	Ø.1	Ø.9	-2.3	-4.4	-1.1	-Ø.8	1.6	-Ø.3
5ØØØ	-2.2	-2.2	-1.7	-4.7	-1.Ø	-Ø.5	-1.8	-1.1	-1.7	-Ø.5	-4.2	-5.7		-2.3	1.7	-1.6
63ØØ		-4.1	-3.8	-5.7	-2.1	-2.1	-3.4	-2.2	-2.1	-1.8	-4.8			-3.2	1.4	-2.7
8ØØØ				-7.1	-1.7	-2.7	-4.4	-2.7	-4.1					-3.8	1.9	-3.6
1ØØØØ																-2.7
125ØØ																
16ØØØ																
2ØØØØ																
25ØØØ																
315ØØ																
4ØØØØ																
5ØØØØ																
63ØØØ																
8ØØØØ																
OASPL	-Ø.3	-Ø.4	Ø.2	-Ø.7	Ø.Ø	Ø.4	-Ø.4	Ø.1	-Ø.1	Ø.2	-1.4	-Ø.3	-Ø.1			
PNL	Ø.6	Ø.5	Ø.9	-Ø.3	Ø.8	1.1	Ø.1	Ø.9	Ø.4	Ø.4	-1.4	-1.4	-Ø.3			
PNLT	-Ø.7	Ø.5	Ø.9	-Ø.3	Ø.8	1.1	Ø.1	Ø.9	Ø.4	Ø.4	-1.5	-1.4	-Ø.3			
DBA	Ø.2	Ø.3	Ø.8	-Ø.4	Ø.6	1.1	Ø.2	Ø.7	Ø.3	Ø.3	-1.1	-1.8	-Ø.4			

LOCATION	ACOUSTIC RANGE	AVG CORR SPEED	AVG CORR THRUST
C41 ANECH CH	24ØØ.Ø FT SL	-Ø.1E 31 RPM	-Ø.1E 31 LB

TEST CASE FOR TREATED EJECTOR TEØ2 VS TE2Ø

DELTA, SPL(1) - SPL(2)

IDENTIFICATION

INPUT (1) 83F-ZER-2ØØ5 X2ØØ55
(2) 83F-ZER-3ØØ5 X3ØØ55

OUTPUT ITS TE2-TE3 XØ2Ø31

ANGLES MEASURED FROM INLET,DEGREES

FREQ	4Ø.Ø	5Ø.Ø	6Ø.Ø	7Ø.Ø	8Ø.Ø	9Ø.Ø	1ØØ.Ø	11Ø.Ø	12Ø.Ø	13Ø.Ø	14Ø.Ø	15Ø.Ø	16Ø.Ø	AVG	S.D.	PWL
5Ø	-1.Ø	-Ø.3	-Ø.Ø	-Ø.1	Ø.7	-Ø.Ø	-Ø.8	-Ø.Ø	-Ø.Ø	-Ø.Ø	-Ø.5	-Ø.Ø	-Ø.Ø	-Ø.1	Ø.4	-Ø.1
63	-Ø.8	-Ø.5	Ø.2	-1.1	-Ø.Ø	-Ø.5	-Ø.5	Ø.2	-Ø.5	Ø.5	-Ø.3	Ø.5	-Ø.5	-Ø.2	Ø.5	Ø.Ø
8Ø	-Ø.5	-1.3	Ø.7	-1.1	-1.Ø	-Ø.3	-Ø.Ø	-Ø.3	-Ø.Ø	-Ø.5	-Ø.8	Ø.7	-Ø.Ø	-Ø.3	Ø.6	-Ø.Ø
1ØØ	-Ø.2	-Ø.2	-Ø.2	-Ø.5	Ø.Ø	Ø.3	-Ø.7	-Ø.5	-Ø.7	-Ø.5	-Ø.5	Ø.5	Ø.3	-Ø.2	Ø.4	-Ø.2
125	-Ø.5	-1.Ø	Ø.5	-Ø.7	-Ø.2	Ø.Ø	-Ø.7	-Ø.2	-1.Ø	Ø.3	-Ø.2	Ø.5	-Ø.2	-Ø.3	Ø.5	-Ø.1
16Ø	-1.Ø	-Ø.7	-Ø.2	-Ø.9	Ø.Ø	-Ø.2	-Ø.7	-Ø.7	-Ø.7	Ø.3	Ø.3	-Ø.5	-Ø.7	-Ø.5	Ø.4	-Ø.3
2ØØ	-Ø.7	-Ø.2	Ø.5	-1.1	Ø.Ø	-Ø.5	-1.Ø	-Ø.2	-Ø.2	Ø.5	Ø.5	Ø.5	Ø.Ø	-Ø.1	Ø.6	Ø.1
25Ø	-Ø.5	-1.Ø	-Ø.2	-Ø.8	Ø.5	-Ø.2	-Ø.7	-Ø.2	Ø.Ø	Ø.Ø	Ø.5	1.8	Ø.3	-Ø.Ø	Ø.7	Ø.2
315	Ø.3	-Ø.2	-Ø.7	-Ø.5	Ø.5	Ø.3	-Ø.7	Ø.Ø	-Ø.2	Ø.3	-Ø.2	Ø.3	-Ø.2	-Ø.1	Ø.4	-Ø.1
4ØØ	-Ø.7	-2.Ø	Ø.Ø	-1.2	Ø.Ø	-1.Ø	-1.2	-Ø.5	Ø.5	-Ø.5	Ø.8	Ø.5	-Ø.7	-Ø.5	Ø.8	-Ø.1
5ØØ	-Ø.7	-Ø.7	-Ø.5	-1.4	-1.Ø	-Ø.7	-1.2	-Ø.2	-Ø.2	-Ø.2	-Ø.7	Ø.3	-Ø.5	-Ø.6	Ø.5	-Ø.5
63Ø	-Ø.5	-1.Ø	-Ø.Ø	-Ø.9	-Ø.Ø	-Ø.Ø	-1.5	-Ø.5	Ø.5	Ø.5	-1.Ø	Ø.7	-Ø.5	-Ø.3	Ø.7	-Ø.2
8ØØ	-Ø.3	Ø.2	Ø.2	-Ø.6	-Ø.Ø	Ø.2	-1.Ø	-1.Ø	-Ø.5	-Ø.5	Ø.5	Ø.7	-Ø.3	-Ø.2	Ø.5	-Ø.4
1ØØØ	-Ø.1	Ø.2	Ø.9	-Ø.4	Ø.2	-Ø.3	Ø.2	Ø.7	-Ø.1	-Ø.1	Ø.4	Ø.4	-Ø.3	Ø.1	Ø.4	Ø.2
125Ø	Ø.9	Ø.6	1.3	-Ø.4	1.1	1.4	Ø.6	Ø.8	Ø.1	Ø.1	-Ø.2	1.1	-Ø.9	Ø.5	Ø.7	Ø.5
16ØØ	1.Ø	1.2	2.2	Ø.9	1.8	1.Ø	1.Ø	Ø.5	1.Ø	Ø.9	-Ø.3	Ø.8	-Ø.2	Ø.9	Ø.7	Ø.8
2ØØØ	1.4	2.3	1.8	Ø.4	1.6	1.6	Ø.8	Ø.8	Ø.5	1.2	Ø.6	Ø.4	-Ø.1	1.Ø	Ø.7	1.Ø
25ØØ	1.4	1.6	1.8	-Ø.9	1.1	1.4	1.6	1.6	1.6	Ø.5	-Ø.4	Ø.9	-Ø.8	Ø.9	1.Ø	1.2
315Ø	Ø.2	1.2	1.Ø	-1.3	Ø.6	Ø.4	Ø.4	1.1	Ø.5	Ø.4	-Ø.5	Ø.9	Ø.7	Ø.4	Ø.7	Ø.4
4ØØØ	-Ø.7	-Ø.6	Ø.4	-2.5	-Ø.5	-Ø.5	-1.2	-Ø.Ø	-Ø.9	-Ø.3	-2.1	-Ø.7	-Ø.4	-Ø.8	Ø.8	-Ø.7
5ØØØ	-1.7	-2.2	-2.Ø	-4.8	-1.5	-1.5	-1.5	-1.4	-2.2	-1.2	-3.4	-2.5		-2.2	1.Ø	-1.9
63ØØ	-3.Ø	-4.3	-3.3	-6.2	-2.4	-2.3	-2.4	-2.2	-2.8	-2.6	-4.Ø			-3.2	1.2	-2.8
8ØØØ			-5.9	-6.3	-1.2	-3.2	-3.7	-2.5	-3.6					-3.8	1.8	-3.4
1ØØØØ																-2.4
125ØØ																
16ØØØ																
2ØØØØ																
25ØØØ																
315ØØ																
4ØØØØ																
5ØØØØ																
63ØØØ																
8ØØØØ																
OASPL	-Ø.3	-Ø.4	Ø.4	-Ø.7	Ø.3	Ø.1	-Ø.4	-Ø.1	-Ø.2	Ø.Ø	-Ø.2	Ø.4	-Ø.2			
PNL	Ø.4	Ø.7	1.Ø	-Ø.7	Ø.7	Ø.6	Ø.1	Ø.3	Ø.2	-Ø.Ø	Ø.1	Ø.5	-Ø.2			
PNLT	Ø.5	Ø.7	1.Ø	-Ø.7	Ø.7	Ø.6	Ø.1	Ø.3	Ø.2	-Ø.6	-1.Ø	Ø.5	-Ø.2			
DBA	Ø.2	Ø.3	Ø.9	-Ø.4	Ø.7	Ø.6	Ø.Ø	Ø.3	Ø.1	Ø.Ø	-Ø.Ø	Ø.6	-Ø.3			

LOCATION	ACOUSTIC RANGE	AVG CORR SPEED	AVG CORR THRUST
C41 ANECH CH	24ØØ.Ø FT SL	-Ø.1E 31 RPM	-Ø.1E 31'LB

TEST CASE FOR TREATED EJECTOR TEØ2 VS TE2Ø

DELTA, SPL(1) - SPL(2)

IDENTIFICATION

INPUT (1) 83F-ZER-2ØØ9 X2ØØ95
(2) 83F-ZER-3ØØ9 X3ØØ95

OUTPUT TOS TE2-TE3 XØ2Ø31

ANGLES MEASURED FROM INLET,DEGREES

FREQ	4Ø.Ø	5Ø.Ø	6Ø.Ø	7Ø.Ø	8Ø.Ø	9Ø.Ø	1ØØ.Ø	11Ø.Ø	12Ø.Ø	13Ø.Ø	14Ø.Ø	15Ø.Ø	16Ø.Ø	AVG	S.D.	PWL
5Ø	-Ø.3	-Ø.5	-Ø.5	Ø.3	1.Ø	Ø.5	-1.Ø	-Ø.3	-Ø.5	-Ø.Ø	-Ø.5	-Ø.5	Ø.5	-Ø.1	Ø.6	-Ø.2
63	-Ø.3	-1.Ø	-Ø.Ø	-Ø.6	Ø.2	-Ø.3	Ø.2	1.Ø	-Ø.5	Ø.5	Ø.2	-Ø.5	-Ø.Ø	-Ø.1	Ø.5	-Ø.1
8Ø	-Ø.5	-Ø.Ø	Ø.5	-Ø.5	Ø.5	Ø.5	Ø.5	Ø.7	Ø.5	-Ø.5	-Ø.3	-Ø.3	-Ø.Ø	Ø.1	Ø.5	-Ø.2
1ØØ	-Ø.2	Ø.3	Ø.5	-Ø.2	-1.2	Ø.Ø	-Ø.5	-Ø.2	Ø.3	Ø.3	-Ø.5	-Ø.7	Ø.5	-Ø.2	Ø.5	-Ø.2
125	1.3	1.3	1.8	Ø.3	Ø.3	Ø.8	-Ø.5	Ø.3	-Ø.5	1.Ø	-Ø.2	Ø.5	Ø.5	Ø.5	Ø.7	Ø.4
16Ø	Ø.8	-Ø.7	1.5	Ø.3	1.3	1.Ø	Ø.3	-Ø.2	-Ø.5	Ø.Ø	Ø.3	-Ø.5	Ø.8	Ø.3	Ø.7	Ø.1
2ØØ	Ø.3	-Ø.7	1.Ø	-Ø.4	1.3	1.Ø	Ø.3	Ø.5	Ø.5	1.3	Ø.8	Ø.Ø	Ø.5	Ø.5	Ø.6	Ø.5
25Ø	1.5	1.Ø	1.Ø	Ø.Ø	1.Ø	-Ø.2	Ø.3	Ø.Ø	1.Ø	1.3	Ø.5	1.Ø	Ø.8	Ø.7	Ø.5	Ø.8
315	1.3	Ø.3	Ø.5	Ø.3	Ø.8	Ø.8	Ø.8	1.Ø	1.3	Ø.8	Ø.5	-Ø.2	1.8	Ø.8	Ø.5	Ø.6
4ØØ	Ø.3	-Ø.5	Ø.Ø	-Ø.2	Ø.3	Ø.Ø	-Ø.5	Ø.8	1.Ø	1.Ø	Ø.8	Ø.Ø	1.Ø	Ø.3	Ø.6	Ø.6
5ØØ	2.Ø	Ø.3	Ø.3	-Ø.5	-Ø.2	-Ø.2	Ø.Ø	Ø.8	1.Ø	1.3	-Ø.5	Ø.Ø	1.Ø	Ø.4	Ø.8	Ø.4
63Ø	2.Ø	1.7	1.7	-Ø.4	-Ø.3	Ø.7	-Ø.Ø	Ø.5	Ø.2	1.Ø	Ø.2	1.Ø	Ø.7	Ø.7	Ø.8	Ø.6
8ØØ	1.Ø	2.Ø	2.5	Ø.8	1.Ø	Ø.7	-1.Ø	Ø.2	Ø.7	Ø.7	Ø.5	1.2	Ø.7	Ø.8	Ø.8	Ø.6
1ØØØ	1.7	1.2	1.4	-Ø.1	Ø.4	Ø.4	Ø.4	Ø.9	-Ø.1	Ø.9	Ø.2	1.9	Ø.9	Ø.8	Ø.6	Ø.6
125Ø	1.6	1.1	1.3	-Ø.6	1.4	1.4	-Ø.1	Ø.8	Ø.3	Ø.8	Ø.8	1.9	1.4	Ø.9	Ø.7	Ø.8
16ØØ	1.5	2.Ø	1.7	-Ø.1	Ø.8	1.Ø	-Ø.2	-Ø.Ø	Ø.7	1.7	Ø.5	3.3	1.8	1.1	1.Ø	Ø.8
2ØØØ	1.9	1.5	1.Ø	-Ø.4	1.1	1.1	-Ø.2	-Ø.2	-Ø.7	1.5	Ø.6	1.1	1.9	Ø.8	Ø.9	Ø.4
25ØØ	1.2	1.8	1.6	-1.1	Ø.9	1.1	Ø.6	1.1	Ø.1	1.2	Ø.3	Ø.9	1.9	Ø.9	Ø.8	Ø.7
315Ø	Ø.2	1.Ø	1.2	-1.6	Ø.4	Ø.1	-Ø.1	Ø.3	-Ø.Ø	Ø.6	Ø.5	Ø.9	2.4	Ø.5	Ø.9	Ø.1
4ØØØ	-Ø.2	Ø.1	Ø.9	-2.3	Ø.Ø	Ø.Ø	-1.5	-Ø.5	-Ø.6	Ø.2	-Ø.3	1.3	Ø.9	-Ø.2	1.Ø	-Ø.5
5ØØØ	-Ø.7	-1.5	-Ø.8	-4.4	-Ø.5	-1.8	-2.Ø	-1.9	-2.8	-Ø.7	-1.4	1.Ø		-1.5	1.3	-1.8
63ØØ	-Ø.5	-1.6	-1.1	-4.5	-2.1	-1.8	-3.1	-3.Ø	-2.1	-1.3	-2.Ø			-2.1	1.1	-2.3
8ØØØ			-3.1	-4.6	-Ø.2	-2.7	-3.5	-2.5	-2.5	-1.Ø				-2.6	1.4	-2.4
1ØØØØ						-1.4								-1.4	.1E 19	-Ø.3
125ØØ																
16ØØØ																
2ØØØØ																
25ØØØ																
315ØØ																
4ØØØØ																
5ØØØØ																
63ØØØ																
8ØØØØ																
OASPL	1.1	Ø.7	1.2	-Ø.1	Ø.6	Ø.6	-Ø.1	Ø.4	Ø.4	Ø.6	Ø.1	-Ø.2	Ø.4			
PNL	1.2	1.2	1.3	-Ø.5	Ø.7	Ø.7	-Ø.2	Ø.2	Ø.5	Ø.9	Ø.4	Ø.2	Ø.7			
PNLT	1.2	1.8	1.8	-Ø.5	Ø.7	Ø.2	-Ø.2	Ø.2	Ø.5	Ø.9	Ø.3	Ø.2	Ø.7			
DBA	1.5	1.3	1.4	-Ø.3	Ø.8	Ø.8	-Ø.1	Ø.5	Ø.5	1.Ø	Ø.3	Ø.4	Ø.8			

LOCATION	ACOUSTIC RANGE	AVG CORR SPEED	AVG CORR THRUST
C41 ANECH CH	24ØØ.Ø FT SL	-Ø.1E 31 RPM	-Ø.1E 31 LB

TEST CASE FOR TREATED EJECTOR TEØ2 VS TE2Ø

DELTA, SPL(1) - SPL(2)

IDENTIFICATION

INPUT (1) 83F-4ØØ-2ØØ4 X2ØØ45
(2) 83F-4ØØ-3ØØ4 X3ØØ45

OUTPUT CBF TE2-TE3 XØ2Ø31

ANGLES MEASURED FROM INLET,DEGREES

FREQ	4Ø.Ø	5Ø.Ø	6Ø.Ø	7Ø.Ø	8Ø.Ø	9Ø.Ø	1ØØ.Ø	11Ø.Ø	12Ø.Ø	13Ø.Ø	14Ø.Ø	15Ø.Ø	16Ø.Ø	AVG	S.D.	PWL
5Ø	-1.5	-Ø.9	-Ø.7	-1.4	Ø.8	-Ø.3	-Ø.Ø	-1.9	Ø.2	Ø.5	Ø.2	Ø.7	-Ø.3	-Ø.3	Ø.9	Ø.Ø
63	-1.4	-Ø.7	-Ø.7	Ø.Ø	Ø.7	-Ø.8	-Ø.3	-Ø.8	-Ø.3	-Ø.8	-Ø.3	-Ø.3	1.Ø	-Ø.3	Ø.7	-Ø.1
8Ø	-1.2	-Ø.5	Ø.3	-Ø.5	-Ø.2	Ø.2	-Ø.5	-Ø.3	-Ø.5	-1.Ø	-Ø.3	-Ø.3	Ø.7	-Ø.3	Ø.5	-Ø.2
1ØØ	-2.Ø	-Ø.5	Ø.3	-1.2	Ø.5	-Ø.5	-Ø.8	-Ø.7	-Ø.8	-Ø.1	-Ø.Ø	-Ø.Ø	1.7	-Ø.3	Ø.9	Ø.Ø
125	-1.1	-Ø.2	-Ø.4	-Ø.2	-Ø.7	Ø.3	-Ø.5	-Ø.6	-2.2	-2.5	-1.6	-1.5	Ø.4	-Ø.8	Ø.9	-1.1
16Ø	-1.6	-Ø.6	1.Ø	Ø.2	Ø.6	Ø.3	-1.2	-1.5	Ø.Ø	-Ø.4	-1.1	-1.2	-Ø.1	-Ø.4	Ø.8	-Ø.4
2ØØ	-1.5	-Ø.7	Ø.5	-Ø.2	Ø.5	-Ø.7	-Ø.7	Ø.2	-Ø.2	-Ø.2	Ø.4	-Ø.4	Ø.7	-Ø.2	Ø.6	-Ø.1
25Ø	-1.7	-1.Ø	Ø.3	-1.2	Ø.5	-Ø.5	-Ø.9	-Ø.3	Ø.8	Ø.1	Ø.3	Ø.3	1.3	-Ø.2	Ø.9	Ø.1
315	-1.7	-1.Ø	Ø.Ø	-Ø.6	Ø.3	-Ø.7	-Ø.7	1.1	Ø.4	-Ø.6	-Ø.4	Ø.3	Ø.Ø	-Ø.3	Ø.7	-Ø.1
4ØØ	-1.5	-1.2	-Ø.2	-Ø.6	-Ø.5	-1.Ø	-1.8	Ø.5	-Ø.5	Ø.Ø	-1.Ø	-Ø.2	Ø.1	-Ø.6	Ø.7	-Ø.5
5ØØ	-2.Ø	-2.5	-Ø.2	-1.5	-1.Ø	-1.3	-1.2	Ø.9	Ø.5	-Ø.1	-Ø.3	Ø.2	Ø.8	-Ø.6	1.1	-Ø.3
63Ø	-1.8	-2.3	-Ø.Ø	-1.7	-Ø.5	-Ø.3	-Ø.2	1.1	Ø.4	-Ø.5	-Ø.1	Ø.7	Ø.6	-Ø.3	1.Ø	-Ø.1
8ØØ	-1.8	-1.3	-Ø.Ø	-1.8	Ø.5	Ø.5	Ø.2	2.Ø	1.1	Ø.3	Ø.9	1.2	1.3	Ø.2	1.2	Ø.6
1ØØØ	-1.Ø	-Ø.1	1.4	Ø.2	2.Ø	1.7	1.6	3.2	1.4	Ø.3	Ø.2	Ø.5	1.4	1.Ø	1.1	1.4
125Ø	1.7	2.7	3.1	1.8	2.4	2.1	1.5	3.6	1.6	1.2	Ø.1	Ø.9	1.4	1.9	Ø.9	2.1
16ØØ	2.4	2.4	3.5	Ø.7	2.1	3.Ø	1.3	3.6	2.7	2.3	1.7	1.Ø	2.Ø	2.2	Ø.9	2.4
2ØØØ	2.3	2.7	3.4	1.6	3.4	2.9	1.3	3.8	3.3	3.2	1.Ø	2.9	3.7	2.7	Ø.9	2.7
25ØØ	3.2	3.3	3.8	2.3	3.2	2.4	1.8	5.Ø	1.7	1.5	1.Ø	2.8	1.8	2.6	1.1	2.9
315Ø	2.5	3.3	4.3	1.6	1.7	1.9	1.4	4.2	Ø.Ø	Ø.1	-1.5	Ø.3	Ø.1	1.5	1.7	2.Ø
4ØØØ	1.5	2.5	3.5	Ø.4	1.8	1.6	Ø.2	3.4	-1.9	-1.8	-3.6	-1.9	-1.3	Ø.3	2.3	Ø.7
5ØØØ	Ø.4	1.2	2.8	-Ø.7	-Ø.3	-1.3	-1.7	Ø.3	-3.3	-3.6	-5.Ø	-3.4		-1.2	2.3	-1.2
63ØØ	-4.Ø	-1.2	-Ø.5	-4.4	-2.2	-2.1	-3.Ø	-Ø.3	-2.3	-4.4	-4.8			-2.7	1.6	-2.5
8ØØØ			-3.4	-5.9	-2.1	-3.1	-3.3	Ø.2	-Ø.3					-2.5	2.1	-2.2
1ØØØØ																-2.1
125ØØ																
16ØØØ																
2ØØØØ																
25ØØØ																
315ØØ																
4ØØØØ																
5ØØØØ																
63ØØØ																
8ØØØØ																
OASPL	-Ø.4	Ø.2	1.5	Ø.1	1.1	1.Ø	Ø.4	1.9	Ø.6	-Ø.2	-Ø.2	Ø.Ø	Ø.7			
PNL	Ø.9	1.3	2.5	Ø.4	1.9	1.6	Ø.7	2.7	1.3	Ø.5	Ø.4	Ø.6	Ø.8			
PNLT	2.1	1.3	2.4	Ø.3	1.9	1.6	Ø.7	2.7	1.2	Ø.5	Ø.4	Ø.6	Ø.8			
DBA	Ø.6	1.1	2.3	Ø.6	1.7	1.6	Ø.9	2.8	1.2	Ø.5	Ø.2	Ø.7	1.Ø			

LOCATION	ACOUSTIC RANGE	AVG CORR SPEED	AVG CORR THRUST
C41 ANECH CH	24ØØ.Ø FT SL	-Ø.1E 31 RPM	-Ø.1E 31 LB

TEST CASE FOR TREATED EJECTOR TEØ2 VS TE2Ø

DELTA, SPL(1) - SPL(2)

IDENTIFICATION

INPUT (1) 83F-4ØØ-2ØØ6 X2ØØ65
(2) 83F-4ØØ-3ØØ6 X3ØØ65

OUTPUT ITF TE2-TE3 XØ2Ø31

ANGLES MEASURED FROM INLET,DEGREES

FREQ	4Ø.Ø	5Ø.Ø	6Ø.Ø	7Ø.Ø	8Ø.Ø	9Ø.Ø	1ØØ.Ø	11Ø.Ø	12Ø.Ø	13Ø.Ø	14Ø.Ø	15Ø.Ø	16Ø.Ø	AVG	S.D.	PWL
5Ø	-1.7	-Ø.8	-Ø.8	-Ø.4	Ø.6	-Ø.Ø	-Ø.8	-Ø.5	-Ø.Ø	Ø.2	-1.5	Ø.2	1.2	-Ø.3	Ø.8	Ø.1
63	-2.2	-Ø.4	-Ø.5	-Ø.1	Ø.2	-1.5	-1.Ø	-Ø.Ø	-Ø.Ø	-Ø.3	-1.5	-Ø.Ø	Ø.7	-Ø.5	Ø.8	-Ø.3
8Ø	-2.8	-Ø.8	Ø.5	-Ø.7	-Ø.Ø	-Ø.5	-Ø.3	-Ø.Ø	-Ø.5	-1.Ø	-1.Ø	-Ø.5	Ø.Ø	-Ø.6	Ø.8	-Ø.5
1ØØ	-2.5	-1.3	-Ø.Ø	-Ø.8	Ø.Ø	-1.Ø	-1.2	-Ø.7	-1.5	-Ø.2	-1.8	Ø.3	Ø.4	-Ø.8	Ø.9	-Ø.6
125	-2.Ø	Ø.3	-Ø.2	-Ø.5	Ø.Ø	-Ø.2	-1.7	-1.1	-1.Ø	-Ø.5	-1.6	-2.Ø	-Ø.4	-Ø.9	Ø.8	-1.Ø
16Ø	-1.2	-Ø.5	Ø.1	-Ø.5	Ø.1	-1.Ø	-1.3	Ø.3	-Ø.8	Ø.9	-1.4	-Ø.2	-Ø.3	-Ø.4	Ø.7	-Ø.4
2ØØ	-1.6	-1.Ø	Ø.2	-Ø.6	Ø.3	-1.2	-1.Ø	-Ø.2	-Ø.2	Ø.6	-Ø.2	Ø.3	Ø.3	-Ø.3	Ø.7	-Ø.2
25Ø	-2.2	-1.2	Ø.Ø	-1.3	Ø.5	-1.Ø	-2.4	-Ø.9	Ø.2	Ø.7	-1.Ø	-Ø.1	Ø.8	-Ø.6	1.1	-Ø.3
315	-1.7	-1.2	-Ø.2	-1.Ø	-Ø.2	-1.Ø	-1.Ø	-Ø.6	-1.1	Ø.5	-1.3	-1.1	-1.4	-Ø.9	Ø.6	-Ø.8
4ØØ	-1.5	-1.Ø	-1.2	-1.1	-Ø.5	-2.Ø	-2.1	-Ø.7	-Ø.8	Ø.6	-2.Ø	-1.8	-Ø.5	-1.1	Ø.8	-1.Ø
5ØØ	-2.2	-1.5	-1.5	-1.6	-1.2	-1.7	-2.1	-Ø.7	-Ø.5	Ø.5	-1.3	-1.6	-Ø.3	-1.2	Ø.8	-1.Ø
63Ø	-2.Ø	-1.7	-Ø.2	-1.9	Ø.3	-Ø.5	-1.3	-Ø.6	-Ø.3	-Ø.3	-2.Ø	-2.6	-1.7	-1.2	Ø.9	-Ø.9
8ØØ	Ø.5	1.Ø	1.4	-Ø.1	-Ø.Ø	-Ø.3	-1.8	-1.Ø	-1.2	Ø.7	-Ø.8	-1.2	-Ø.4	-Ø.2	1.Ø	-Ø.6
1ØØØ	-1.3	Ø.2	Ø.2	-Ø.5	Ø.7	Ø.4	-Ø.4	Ø.8	-Ø.6	Ø.3	-1.2	-Ø.7	-Ø.9	-Ø.2	Ø.7	-Ø.1
125Ø	1.Ø	2.4	2.1	1.1	2.4	1.8	-Ø.8	1.4	Ø.9	1.5	-Ø.3	Ø.1	Ø.5	1.1	1.Ø	1.1
16ØØ	2.6	2.6	3.Ø	1.4	2.6	1.2	1.Ø	1.2	1.4	2.4	1.2	Ø.3	1.4	1.7	Ø.8	1.6
2ØØØ	2.8	3.5	3.2	1.8	2.6	2.3	1.1	1.6	2.3	2.4	Ø.1	1.1	1.7	2.Ø	Ø.9	2.1
25ØØ	Ø.6	1.5	1.5	1.2	2.4	1.1	1.Ø	1.9	1.6	3.4	2.2	1.7	3.7	1.8	Ø.9	1.5
315Ø	-Ø.4	1.Ø	2.Ø	Ø.4	1.6	-Ø.2	-Ø.2	2.1	-Ø.2	2.8	1.Ø	1.2	2.4	1.1	1.1	Ø.7
4ØØØ	Ø.9	2.2	2.4	Ø.3	-Ø.3	-1.Ø	-2.3	-Ø.Ø	-2.6	-1.7	-4.3	-3.4	-1.9	-Ø.9	2.1	-Ø.6
5ØØØ	-3.Ø	-1.7	-Ø.2	-2.6	-2.1	-2.9	-2.7	-1.9	-4.3	-3.2	-4.1	-4.1		-2.7	1.2	-2.7
63ØØ	-4.3	-3.6	-Ø.4	-5.Ø	-1.8	-3.7	-4.1	-4.Ø	-4.1	-3.3	-5.1			-3.6	1.4	-3.7
8ØØØ			-3.8	-5.5	-1.2	-3.9	-4.4	-4.3	-2.8	-4.4				-3.8	1.3	-3.9
1ØØØØ																-3.9
125ØØ																
16ØØØ																
2ØØØØ																
25ØØØ																
315ØØ																
4ØØØØ																
5ØØØØ																
63ØØØ																
8ØØØØ																
OASPL	-Ø.7	Ø.4	1.Ø	Ø.Ø	Ø.9	Ø.1	-Ø.8	Ø.1	-Ø.4	Ø.4	-1.2	-Ø.4	Ø.3			
PNL	Ø.7	1.6	1.7	Ø.6	1.4	Ø.3	-Ø.1	Ø.6	Ø.2	Ø.9	-Ø.5	-Ø.3	Ø.1			
PNLT	1.8	Ø.8	1.9	Ø.5	1.4	Ø.3	-Ø.1	Ø.1	Ø.2	1.4	-1.5	-1.6	Ø.1			
DBA	Ø.5	1.3	1.7	Ø.6	1.5	Ø.7	-Ø.4	Ø.6	-Ø.1	Ø.8	-Ø.9	-Ø.9	-Ø.4			

LOCATION	ACOUSTIC RANGE	AVG CORR SPEED	AVG CORR THRUST
C41 ANECH CH	24ØØ.Ø FT SL	-Ø.1E 31 RPM	-Ø.1E 31'LB

TEST CASE FOR TREATED EJECTOR TEØ2 VS TE2Ø

DELTA, SPL(1) - SPL(2)

IDENTIFICATION

INPUT (1) 83F-4ØØ-2Ø1Ø X2Ø1Ø5
(2) 83F-4ØØ-3Ø1Ø X3Ø1Ø5

OUTPUT TOF TE2-TE3 XØ2Ø31

ANGLES MEASURED FROM INLET,DEGREES

FREQ	4Ø.Ø	5Ø.Ø	6Ø.Ø	7Ø.Ø	8Ø.Ø	9Ø.Ø	1ØØ.Ø	11Ø.Ø	12Ø.Ø	13Ø.Ø	14Ø.Ø	15Ø.Ø	16Ø.Ø	AVG	S.D.	PWL
5Ø	-Ø.Ø	-Ø.8	Ø.5	Ø.2	Ø.3	Ø.7	-Ø.5	-Ø.Ø	-Ø.3	Ø.5	-1.5	-Ø.5	-1.Ø	-Ø.2	Ø.7	-Ø.7
63	Ø.6	Ø.1	Ø.2	Ø.4	Ø.2	Ø.7	Ø.2	1.Ø	Ø.5	Ø.2	-1.5	-1.Ø	-1.3	Ø.Ø	Ø.8	-Ø.9
8Ø	Ø.5	-Ø.3	Ø.5	-1.5	-Ø.5	-Ø.Ø	-Ø.Ø	Ø.5	Ø.Ø	-Ø.7	-1.7	-1.5	-1.Ø	-Ø.4	Ø.8	-1.2
1ØØ	-Ø.3	-Ø.Ø	Ø.7	-1.1	-Ø.2	Ø.5	Ø.Ø	-Ø.5	-1.Ø	1.Ø	-1.7	-1.2	-Ø.7	-Ø.4	Ø.8	-Ø.8
125	Ø.3	Ø.Ø	Ø.Ø	-Ø.1	Ø.3	1.Ø	-Ø.2	Ø.3	-Ø.9	-Ø.7	-1.8	-1.5	-Ø.6	-Ø.3	Ø.8	-1.Ø
16Ø	Ø.3	Ø.9	1.8	Ø.3	Ø.3	Ø.5	Ø.3	Ø.1	Ø.1	Ø.6	-Ø.9	-Ø.2	-Ø.2	Ø.3	Ø.6	-Ø.1
2ØØ	-Ø.1	-Ø.3	Ø.9	-Ø.3	Ø.8	Ø.3	-Ø.6	Ø.4	Ø.6	1.1	-Ø.9	Ø.8	1.Ø	Ø.3	Ø.7	Ø.3
25Ø	-1.Ø	Ø.Ø	Ø.5	-Ø.9	Ø.5	Ø.3	-Ø.5	Ø.5	Ø.4	Ø.7	-1.1	Ø.2	Ø.2	-Ø.Ø	Ø.6	Ø.1
315	-Ø.4	-Ø.2	Ø.1	-Ø.5	Ø.3	-Ø.2	Ø.Ø	Ø.7	-1.Ø	-Ø.8	-1.4	-1.1	-3.4	-Ø.6	1.Ø	-1.Ø
4ØØ	-1.Ø	-Ø.7	-Ø.7	-Ø.3	Ø.3	-Ø.5	-1.3	-Ø.8	Ø.6	Ø.6	-1.1	Ø.2	1.1	-Ø.3	Ø.8	-Ø.1
5ØØ	-Ø.4	-Ø.9	-Ø.7	-Ø.8	-Ø.4	-Ø.7	-Ø.3	Ø.Ø	Ø.6	1.2	-Ø.6	Ø.8	1.8	-Ø.Ø	Ø.9	Ø.3
63Ø	Ø.8	Ø.4	-Ø.4	-1.1	-Ø.2	-Ø.Ø	-Ø.9	Ø.7	Ø.3	Ø.3	-Ø.4	-Ø.5	Ø.5	-Ø.Ø	Ø.6	Ø.Ø
8ØØ	Ø.2	Ø.2	Ø.Ø	-1.Ø	Ø.9	Ø.2	-1.3	Ø.Ø	Ø.4	Ø.9	-Ø.3	Ø.4	Ø.8	Ø.1	Ø.7	Ø.1
1ØØØ	1.2	3.Ø	2.3	1.1	1.2	Ø.9	-Ø.8	1.1	Ø.5	1.3	Ø.1	Ø.5	1.3	1.1	Ø.9	1.Ø
125Ø	Ø.5	1.2	2.1	1.1	2.3	1.6	-Ø.6	Ø.5	-Ø.4	2.1	-Ø.1	Ø.2	Ø.6	Ø.9	1.Ø	Ø.8
16ØØ	1.4	Ø.6	Ø.8	-Ø.Ø	Ø.4	-Ø.Ø	-Ø.3	Ø.5	Ø.6	2.2	Ø.6	Ø.3	1.4	Ø.7	Ø.7	Ø.5
2ØØØ	1.3	Ø.9	-Ø.5	-1.6	Ø.5	Ø.3	-Ø.3	Ø.7	-Ø.4	-1.Ø	-2.9	-1.6	-Ø.8	-Ø.4	1.2	-Ø.1
25ØØ	1.Ø	1.7	1.4	-Ø.6	Ø.9	Ø.4	-Ø.8	-Ø.6	-Ø.7	Ø.5	-Ø.8	Ø.1	-Ø.1	Ø.2	Ø.9	Ø.3
315Ø	Ø.6	1.3	1.Ø	-Ø.5	Ø.1	Ø.1	-1.6	Ø.4	-1.3	-Ø.8	-2.9	-1.Ø	-1.3	-Ø.5	1.2	-Ø.2
4ØØØ	-Ø.6	Ø.7	Ø.4	-1.6	-Ø.5	-Ø.5	-2.6	-Ø.7	-3.1	-2.4	-4.1	-2.Ø	-1.8	-1.5	1.4	-1.3
5ØØØ	-2.Ø	-Ø.7	-Ø.5	-2.7	-2.2	-2.9	-3.1	-2.8	-3.3	-3.2	-4.7	-3.5		-2.6	1.2	-2.6
63ØØ	-2.8	-2.6	-2.9	-5.5	-2.5	-2.5	-4.6	-3.9	-3.9	-3.5	-7.Ø			-3.8	1.4	-3.7
8ØØØ		-2.Ø	-2.3	-4.8	-1.7	-3.1	-4.4	-3.9	-1.8	-2.8				-3.Ø	1.2	-2.8
1ØØØØ						-3.4								-3.4.1E 19		-3.Ø
125ØØ																
16ØØØ																
2ØØØØ																
25ØØØ																
315ØØ																
4ØØØØ																
5ØØØØ																
63ØØØ																
8ØØØØ																
OASPL	Ø.4	Ø.7	Ø.8	-Ø.3	Ø.7	Ø.4	-Ø.6	Ø.3	Ø.1	Ø.5	-1.2	-Ø.8	-Ø.7			
PNL	Ø.7	Ø.7	Ø.4	-1.Ø	Ø.4	Ø.1	-Ø.7	Ø.3	-Ø.Ø	Ø.6	-Ø.8	-Ø.6	-Ø.6			
PNLT	-Ø.3	Ø.1	-Ø.1	-1.6	Ø.4	-Ø.4	-Ø.7	Ø.3	-Ø.7	Ø.1	Ø.2	-Ø.6	-1.2			
DBA	Ø.8	1.1	Ø.9	-Ø.3	Ø.9	Ø.5	-Ø.7	Ø.4	Ø.2	1.Ø	-Ø.5	Ø.1	Ø.4			

LOCATION	ACOUSTIC RANGE	AVG CORR SPEED	AVG CORR THRUST
C41 ANECH CH	24ØØ.Ø FT SL	-Ø.1E 31 RPM	-Ø.1E 31' LB

TEST CASE FOR TREATED EJECTOR TEØ2 VS TE2Ø

C1

DELTA, SPL(1) - SPL(2)

IDENTIFICATION

INPUT (1) 83F-ZER-2ØØ3 X2ØØ35
(2) 83F-ZER-4ØØ3 X4ØØ35

OUTPUT CBS TE2-TE4 XØ2Ø41

ANGLES MEASURED FROM INLET,DEGREES

FREQ	4Ø.Ø	5Ø.Ø	6Ø.Ø	7Ø.Ø	8Ø.Ø	9Ø.Ø	1ØØ.Ø	11Ø.Ø	12Ø.Ø	13Ø.Ø	14Ø.Ø	15Ø.Ø	16Ø.Ø	AVG	S.D.	PWL
5Ø	-Ø.5	-1.Ø	-Ø.3	-Ø.7	Ø.5	-Ø.8	-Ø.3	Ø.5	1.Ø	Ø.2	-Ø.8	2.Ø	1.2	Ø.1	Ø.9	Ø.8
63	-1.5	-Ø.8	Ø.2	-Ø.1	Ø.5	-Ø.3	Ø.5	Ø.7	-Ø.Ø	1.Ø	-Ø.3	1.7	Ø.7	Ø.2	Ø.8	Ø.7
8Ø	-Ø.Ø	-1.8	-Ø.Ø	Ø.3	Ø.5	-Ø.Ø	Ø.5	-Ø.3	-Ø.Ø	Ø.2	-Ø.3	1.Ø	Ø.2	Ø.Ø	Ø.6	Ø.2
1ØØ	-Ø.3	-Ø.8	-Ø.5	-Ø.3	Ø.5	-Ø.5	-Ø.Ø	-Ø.8	Ø.2	-Ø.5	-Ø.5	Ø.7	Ø.7	-Ø.1	Ø.5	-Ø.1
125	-Ø.2	-Ø.5	Ø.Ø	1.2	1.3	Ø.Ø	Ø.3	-Ø.2	-Ø.7	-Ø.2	-1.7	Ø.8	Ø.5	Ø.Ø	Ø.8	-Ø.3
16Ø	-Ø.5	-1.2	Ø.8	-Ø.8	1.Ø	Ø.8	Ø.Ø	-Ø.2	-Ø.5	-Ø.5	-1.2	Ø.Ø	Ø.5	-Ø.2	Ø.7	-Ø.4
2ØØ	Ø.3	-1.5	Ø.3	-Ø.3	1.Ø	-Ø.5	-Ø.5	Ø.Ø	-Ø.2	Ø.5	-1.2	-Ø.5	Ø.5	-Ø.2	Ø.7	-Ø.3
25Ø	-Ø.5	-1.5	Ø.Ø	Ø.5	Ø.3	Ø.Ø	Ø.5	-Ø.5	-Ø.5	Ø.5	-Ø.7	Ø.8	-Ø.5	-Ø.1	Ø.6	-Ø.1
315	-Ø.3	-Ø.8	-Ø.3	Ø.4	Ø.2	-Ø.5	-Ø.3	-Ø.Ø	-Ø.3	Ø.5	-1.5	-Ø.3	Ø.2	-Ø.2	Ø.5	-Ø.2
4ØØ	-Ø.3	-1.3	-Ø.5	-Ø.6	Ø.2	-Ø.8	-Ø.Ø	-Ø.Ø	Ø.2	Ø.2	-Ø.5	-Ø.8	Ø.2	-Ø.3	Ø.5	-Ø.1
5ØØ	Ø.2	-Ø.8	-Ø.8	-Ø.6	-Ø.3	-1.1	-Ø.8	-Ø.3	-Ø.3	Ø.2	-1.3	-1.1	Ø.2	-Ø.5	Ø.5	-Ø.5
63Ø	Ø.6	-Ø.4	-Ø.4	-Ø.Ø	Ø.4	-Ø.1	Ø.6	-Ø.1	-Ø.2	Ø.1	-1.7	-Ø.6	-Ø.1	-Ø.2	Ø.6	-Ø.2
8ØØ	Ø.8	Ø.5	1.2	1.Ø	2.Ø	Ø.8	1.3	1.Ø	-Ø.8	Ø.4	-Ø.8	Ø.Ø	Ø.Ø	Ø.6	Ø.8	Ø.4
1ØØØ	1.4	1.5	2.Ø	2.4	2.8	2.1	2.1	2.1	1.Ø	Ø.2	-Ø.7	-Ø.2	Ø.4	1.3	1.1	1.4
125Ø	2.1	1.3	2.5	2.6	3.6	2.4	3.1	2.6	Ø.3	Ø.7	-Ø.2	-Ø.1	-Ø.1	1.5	1.5	1.8
16ØØ	2.3	1.1	2.4	2.2	3.2	3.Ø	4.2	2.7	Ø.9	1.2	-Ø.4	-1.2	-Ø.2	1.7	1.6	2.3
2ØØØ	3.5	2.5	3.5	2.5	3.9	3.Ø	3.2	3.9	1.2	Ø.5	-Ø.7	-2.Ø	-Ø.5	1.9	2.Ø	2.6
25ØØ	2.4	2.2	3.2	1.6	3.8	3.3	3.Ø	3.9	2.Ø	Ø.2	-1.4	-Ø.9	-Ø.3	1.8	1.8	2.8
315Ø	1.4	Ø.9	2.6	2.1	4.3	1.8	2.3	3.4	1.9	Ø.5	-1.Ø	-2.1	Ø.2	1.4	1.7	2.4
4ØØØ	-Ø.2	-Ø.4	2.1	Ø.2	2.1	Ø.2	1.1	2.7	Ø.3	-Ø.2	-3.3	-2.8	-Ø.9	Ø.1	1.8	1.1
5ØØØ	-2.Ø	-2.2	-1.Ø	-2.Ø	Ø.5	-2.2	Ø.3	1.3	-Ø.5	-1.3	-3.6	-4.4		-1.4	1.7	-Ø.4
63ØØ		-3.4	-2.2	-2.9	-Ø.7	-2.9	Ø.3	Ø.9	-1.2	-1.9	-4.8			-1.9	1.7	-1.Ø
8ØØØ				-2.6	Ø.8	-2.4	Ø.8	2.Ø	-Ø.4					-Ø.3	1.9	-Ø.3
1ØØØØ																3.8
125ØØ																
16ØØØ																
2ØØØØ																
25ØØØ																
315ØØ																
4ØØØØ																
5ØØØØ																
63ØØØ																
8ØØØØ																
OASPL	Ø.1	-Ø.5	Ø.5	Ø.6	1.4	Ø.6	1.Ø	Ø.8	-Ø.1	Ø.2	-Ø.8	1.1	Ø.8			
PNL	1.5	Ø.6	1.8	1.3	2.5	1.6	2.1	2.Ø	Ø.4	Ø.3	-1.Ø	-Ø.1	Ø.3			
PNLT	Ø.Ø	Ø.6	1.8	1.3	2.5	1.6	2.1	1.5	-Ø.1	Ø.3	Ø.Ø	-Ø.1	Ø.3			
DBA	1.1	Ø.5	1.5	1.5	2.4	1.7	2.1	1.9	Ø.2	Ø.4	-Ø.9	-Ø.4	Ø.2			

LOCATION	ACOUSTIC RANGE	AVG CORR SPEED	AVG CORR THRUST
C41 ANECH CH	24ØØ.Ø FT SL	-Ø.1E 31 RPM	-Ø.1E 31 LB

TEST CASE FOR TREATED EJECTOR TEØ2 VS TEØ4

DELTA, SPL(1) - SPL(2)

IDENTIFICATION

INPUT (1) 83F-ZER-2ØØ5 X2ØØ55
(2) 83F-ZER-4ØØ5 X4ØØ55

OUTPUT ITS TE2-TE4 XØ2Ø41

ANGLES MEASURED FROM INLET,DEGREES

FREQ	4Ø.Ø	5Ø.Ø	6Ø.Ø	7Ø.Ø	8Ø.Ø	9Ø.Ø	1ØØ.Ø	11Ø.Ø	12Ø.Ø	13Ø.Ø	14Ø.Ø	15Ø.Ø	16Ø.Ø	AVG	S.D.	PWL
5Ø	-Ø.8	-Ø.8	Ø.7	Ø.1	1.2	Ø.2	-Ø.5	1.Ø	-Ø.Ø	-Ø.Ø	1.Ø	2.Ø	Ø.2	Ø.3	Ø.8	Ø.9
63	-1.Ø	-Ø.8	Ø.5	Ø.4	Ø.7	Ø.2	Ø.7	Ø.7	Ø.7	Ø.5	1.Ø	3.Ø	1.Ø	Ø.6	Ø.9	1.5
8Ø	-Ø.5	-1.3	Ø.7	Ø.4	Ø.5	-Ø.3	Ø.7	Ø.7	Ø.5	-Ø.5	1.Ø	2.7	1.5	Ø.5	1.Ø	1.2
1ØØ	Ø.2	-Ø.5	-Ø.3	Ø.3	1.2	-Ø.5	Ø.2	-Ø.3	-Ø.8	Ø.2	1.5	2.5	1.5	Ø.4	1.Ø	1.Ø
125	-Ø.5	-1.2	Ø.Ø	Ø.8	1.Ø	-Ø.7	Ø.Ø	Ø.Ø	-Ø.7	-Ø.5	Ø.8	2.8	1.Ø	Ø.2	1.1	Ø.5
16Ø	-Ø.5	-1.2	Ø.3	-Ø.4	1.3	Ø.Ø	Ø.Ø	Ø.5	-1.Ø	-Ø.2	1.Ø	1.3	Ø.8	Ø.1	Ø.8	Ø.2
2ØØ	Ø.5	-1.2	Ø.3	Ø.2	1.Ø	-Ø.7	Ø.Ø	Ø.3	Ø.Ø	1.3	Ø.5	Ø.5	1.5	Ø.3	Ø.7	Ø.5
25Ø	-Ø.2	-1.2	-Ø.2	Ø.7	1.Ø	Ø.Ø	1.Ø	Ø.3	-Ø.2	Ø.Ø	Ø.8	2.5	Ø.8	Ø.4	Ø.9	Ø.5
315	-Ø.3	-Ø.3	-1.Ø	Ø.3	1.2	-Ø.3	Ø.2	-Ø.Ø	-Ø.3	Ø.2	-Ø.5	1.2	1.Ø	Ø.1	Ø.7	Ø.1
4ØØ	-Ø.Ø	-1.8	-Ø.5	-Ø.5	Ø.2	-Ø.3	-Ø.3	Ø.2	-Ø.Ø	-Ø.5	Ø.2	Ø.7	Ø.2	-Ø.2	Ø.6	-Ø.Ø
5ØØ	-Ø.1	-1.1	-Ø.1	-Ø.5	-Ø.1	-Ø.8	-Ø.3	Ø.4	-Ø.3	-Ø.3	-1.1	Ø.9	Ø.9	-Ø.2	Ø.6	-Ø.2
63Ø	-Ø.1	-1.4	-Ø.2	-Ø.Ø	Ø.6	-Ø.4	Ø.1	-Ø.1	Ø.1	Ø.3	-1.2	1.1	Ø.6	-Ø.Ø	Ø.7	-Ø.Ø
8ØØ	Ø.8	-Ø.Ø	1.2	1.2	2.Ø	Ø.Ø	1.Ø	-Ø.3	-Ø.8	-Ø.1	-Ø.Ø	Ø.5	Ø.5	Ø.5	Ø.8	Ø.1
1ØØØ	1.1	Ø.8	1.5	2.Ø	2.3	Ø.3	1.1	1.6	Ø.3	-Ø.Ø	-Ø.5	1.1	-Ø.1	Ø.9	Ø.9	Ø.7
125Ø	2.4	1.8	2.5	2.1	3.1	2.1	2.3	1.6	-Ø.5	Ø.2	-1.5	2.1	-Ø.1	1.4	1.4	1.Ø
16ØØ	3.5	1.9	3.4	2.6	3.2	2.5	3.2	Ø.9	Ø.4	-Ø.Ø	-1.1	1.5	-Ø.2	1.7	1.6	1.4
2ØØØ	4.3	3.2	3.7	2.5	5.2	2.Ø	2.4	1.9	Ø.2	-Ø.5	-1.2	1.2	Ø.Ø	1.9	1.9	1.7
25ØØ	3.4	2.7	2.7	1.1	3.8	2.3	3.Ø	2.2	Ø.7	-1.8	-1.7	1.4	-Ø.3	1.5	1.8	1.8
315Ø	1.7	Ø.4	2.1	Ø.8	3.1	Ø.3	2.1	2.4	Ø.4	-1.5	-2.2	1.4	1.2	Ø.9	1.5	1.2
4ØØØ	-Ø.5	-Ø.9	1.3	-1.3	Ø.6	-1.3	Ø.3	Ø.9	-1.4	-2.2	-3.Ø	-Ø.5	-Ø.4	-Ø.6	1.2	-Ø.4
5ØØØ	-1.5	-2.5	-Ø.8	-2.6	-Ø.2	-2.9	Ø.Ø	Ø.1	-1.5	-2.6	-3.4	-1.1		-1.6	1.2	-1.3
63ØØ	-1.3	-3.4	-1.9	-2.6	-Ø.4	-3.4	Ø.3	Ø.1	-2.4	-3.2	-4.Ø			-2.Ø	1.5	-1.6
8ØØØ			-1.6	-1.6	1.3	-2.6	1.1	1.5	-1.4					-Ø.5	1.7	-Ø.6
1ØØØØ																3.5
125ØØ																
16ØØØ																
2ØØØØ																
25ØØØ																
315ØØ																
4ØØØØ																
5ØØØØ																
63ØØØ																
8ØØØØ																
OASPL	Ø.2	-Ø.5	Ø.6	Ø.7	1.6	Ø.3	Ø.8	Ø.5	-Ø.2	Ø.Ø	Ø.7	2.3	Ø.9			
PNL	2.Ø	1.Ø	2.Ø	1.Ø	2.7	Ø.9	1.6	1.Ø	-Ø.Ø	-Ø.3	-Ø.1	1.6	1.2			
PNLT	1.9	1.Ø	1.4	1.Ø	2.7	Ø.9	1.6	1.Ø	-Ø.5	-Ø.3	-Ø.1	1.6	1.2			
DBA	1.4	Ø.5	1.7	1.4	2.5	1.Ø	1.6	Ø.9	-Ø.1	-Ø.1	-Ø.5	1.2	Ø.7			

LOCATION	ACOUSTIC RANGE	AVG CORR SPEED	AVG CORR THRUST
C41 ANECH CH	24ØØ.Ø FT SL	-Ø.1E 31 RPM	-Ø.1E 31·LB

TEST CASE FOR TREATED EJECTOR TEØ2 VS TEØ4

DELTA, SPL(1) - SPL(2)

IDENTIFICATION

INPUT (1) 83F-ZER-2ØØ9 X2ØØ95
(2) 83F-ZER-4ØØ9 X4ØØ95

OUTPUT TOS TE2-TE4 XØ2Ø41

ANGLES MEASURED FROM INLET,DEGREES

FREQ	4Ø.Ø	5Ø.Ø	6Ø.Ø	7Ø.Ø	8Ø.Ø	9Ø.Ø	1ØØ.Ø	11Ø.Ø	12Ø.Ø	13Ø.Ø	14Ø.Ø	15Ø.Ø	16Ø.Ø	AVG	S.D.	PWL
5Ø	-Ø.Ø	-Ø.5	Ø.2	Ø.Ø	1.2	Ø.7	-Ø.Ø	1.7	Ø.2	Ø.5	Ø.2	1.Ø	1.Ø	Ø.5	Ø.6	Ø.7
63	-Ø.5	-Ø.5	1.Ø	Ø.6	1.5	Ø.2	1.5	1.5	Ø.5	1.2	1.7	1.5	Ø.2	Ø.8	Ø.8	1.2
8Ø	Ø.5	-Ø.Ø	1.Ø	1.3	1.7	Ø.5	1.2	2.2	1.Ø	Ø.7	2.2	Ø.7	Ø.5	1.1	Ø.7	1.Ø
1ØØ	1.Ø	1.Ø	1.2	1.Ø	1.Ø	-Ø.Ø	1.7	2.Ø	Ø.7	Ø.7	2.Ø	1.2	1.5	1.2	Ø.6	1.4
125	2.5	2.5	2.5	2.5	2.3	Ø.8	Ø.5	1.5	Ø.5	Ø.5	1.Ø	2.Ø	1.3	1.6	Ø.9	1.4
16Ø	1.Ø	Ø.8	2.Ø	1.1	2.5	1.5	2.3	2.Ø	Ø.3	Ø.5	2.3	1.3	1.8	1.5	Ø.7	1.4
2ØØ	1.5	-Ø.2	1.3	1.1	2.5	Ø.5	1.8	1.5	1.5	1.8	2.Ø	1.5	1.8	1.4	Ø.7	1.7
25Ø	2.3	1.5	1.3	1.3	1.8	Ø.8	2.3	1.Ø	1.3	1.5	1.8	2.Ø	1.5	1.5	Ø.5	1.7
315	2.2	Ø.5	1.2	1.8	1.7	Ø.2	1.7	2.2	2.Ø	1.Ø	1.7	1.5	1.7	1.5	Ø.6	1.6
4ØØ	1.7	Ø.7	1.5	Ø.8	1.2	Ø.5	Ø.5	1.2	2.Ø	Ø.7	2.2	1.2	1.Ø	1.2	Ø.6	1.4
5ØØ	3.4	1.2	1.4	1.1	1.7	Ø.4	Ø.7	1.4	1.4	1.2	Ø.2	Ø.9	1.2	1.2	Ø.8	Ø.9
63Ø	4.9	4.1	2.8	1.2	1.4	Ø.4	Ø.6	Ø.9	1.1	Ø.6	1.3	1.4	Ø.6	1.6	1.4	1.1
8ØØ	5.Ø	5.2	4.7	3.3	2.5	Ø.8	Ø.8	1.Ø	Ø.7	1.2	1.7	2.3	-Ø.2	2.2	1.8	1.5
1ØØØ	4.9	4.5	5.5	4.5	4.1	1.1	1.1	2.1	Ø.8	1.Ø	Ø.8	2.8	-Ø.1	2.5	1.9	1.8
125Ø	5.6	4.Ø	5.Ø	4.1	5.1	2.4	1.6	2.3	1.Ø	Ø.4	1.3	1.9	-Ø.1	2.7	1.9	2.Ø
16ØØ	5.3	4.6	3.6	2.1	4.Ø	3.3	2.5	Ø.7	Ø.4	1.2	Ø.1	3.8	Ø.1	2.4	1.8	1.9
2ØØØ	4.8	3.7	3.Ø	Ø.6	3.4	1.7	2.2	1.4	Ø.2	Ø.2	Ø.3	1.2	Ø.8	1.8	1.5	1.5
25ØØ	3.7	3.2	2.5	Ø.3	2.3	1.8	2.3	1.2	-Ø.3	-Ø.3	-Ø.4	Ø.9	-Ø.6	1.3	1.5	1.2
315Ø	2.9	1.7	1.9	Ø.Ø	2.3	-Ø.2	Ø.8	1.2	-Ø.1	-Ø.8	-Ø.2	1.1	1.Ø	Ø.9	1.1	Ø.6
4ØØØ	1.Ø	1.6	1.6	-1.3	Ø.8	-1.8	-Ø.9	Ø.7	-1.7	-1.9	-1.5	Ø.5	Ø.1	-Ø.2	1.3	-Ø.6
5ØØØ	1.Ø	-Ø.5	-Ø.3	-2.7	-Ø.7	-3.7	-Ø.7	-Ø.7	-3.Ø	-2.9	-1.1	1.4		-1.2	1.6	-1.7
63ØØ	2.5	Ø.8	Ø.6	-2.2	-1.5	-3.7	-Ø.7	-Ø.9	-2.4	-2.9	-2.3			-1.1	1.8	-2.Ø
8ØØØ			1.6	-Ø.1	1.3	-2.9	-Ø.4	1.2	-Ø.2	Ø.3				Ø.1	1.4	-Ø.2
1ØØØØ																4.4
125ØØ																
16ØØØ																
2ØØØØ																
25ØØØ																
315ØØ																
4ØØØØ																
5ØØØØ																
63ØØØ																
8ØØØØ																
OASPL	2.6	2.1	2.6	1.8	2.5	1.Ø	1.3	1.5	1.1	Ø.9	1.6	1.3	1.1			
PNL	3.8	3.1	2.9	1.1	2.6	1.2	1.6	1.2	Ø.9	Ø.7	1.5	1.5	1.3			
PNLT	3.6	2.7	2.9	Ø.6	2.6	1.2	1.6	1.2	Ø.4	Ø.1	2.5	1.5	1.3			
DBA	4.2	3.6	3.7	2.2	3.2	1.5	1.4	1.4	1.Ø	Ø.9	1.3	1.6	1.3			

LOCATION	ACOUSTIC RANGE	AVG CORR SPEED	AVG CORR THRUST
C41 ANECH CH	24ØØ.Ø FT SL	-Ø.1E 31 RPM	-Ø.1E 31 LB

TEST CASE FOR TREATED EJECTOR TEØ2 VS TEØ4

DELTA, SPL(1) - SPL(2)

IDENTIFICATION

INPUT (1) 83F-4ØØ-2ØØ4 X2ØØ45
(2) 83F-4ØØ-4ØØ4 X4ØØ45

OUTPUT CBF TE2-TE4 XØ2Ø41

ANGLES MEASURED FROM INLET,DEGREES

FREQ	4Ø.Ø	5Ø.Ø	6Ø.Ø	7Ø.Ø	8Ø.Ø	9Ø.Ø	1ØØ.Ø	11Ø.Ø	12Ø.Ø	13Ø.Ø	14Ø.Ø	15Ø.Ø	16Ø.Ø	AVG	S.D.	PWL
5Ø	Ø.7	Ø.4	1.Ø	1.1	3.1	Ø.1	3.7	2.Ø	Ø.7	1.6	1.Ø	2.Ø	1.2	1.4	1.Ø	1.5
63	-Ø.5	-Ø.2	1.1	1.2	2.1	-Ø.2	1.5	Ø.6	Ø.2	Ø.4	1.8	1.3	1.6	Ø.8	Ø.9	1.1
8Ø	-1.Ø	Ø.6	1.3	Ø.9	2.Ø	Ø.1	Ø.7	Ø.5	-Ø.4	Ø.1	1.1	1.1	-Ø.2	Ø.5	Ø.8	Ø.4
1ØØ	-Ø.9	Ø.1	1.5	1.Ø	1.7	-Ø.7	Ø.7	Ø.5	-Ø.4	Ø.6	Ø.3	1.3	-Ø.8	Ø.4	Ø.9	Ø.2
125	-Ø.6	Ø.1	Ø.3	Ø.9	1.7	-Ø.3	Ø.8	Ø.4	-Ø.4	-Ø.4	1.1	1.4	Ø.8	Ø.5	Ø.8	Ø.4
16Ø	-Ø.9	-Ø.1	1.1	1.5	1.8	1.Ø	Ø.9	1.2	Ø.1	Ø.7	-Ø.6	-1.1	Ø.5	Ø.5	Ø.9	Ø.3
2ØØ	-Ø.8	Ø.1	Ø.6	Ø.1	2.1	-Ø.6	Ø.6	Ø.8	-Ø.5	Ø.5	Ø.7	Ø.5	Ø.4	Ø.3	Ø.7	Ø.3
25Ø	-1.6	-1.Ø	Ø.5	Ø.9	1.6	-Ø.Ø	Ø.4	-Ø.1	-Ø.1	1.1	Ø.7	1.2	1.2	Ø.4	Ø.9	Ø.4
315	-1.7	-1.1	-Ø.2	1.Ø	1.5	-Ø.8	Ø.9	1.Ø	Ø.7	Ø.2	Ø.9	1.2	1.Ø	Ø.4	1.Ø	Ø.5
4ØØ	-1.2	-Ø.9	-Ø.1	Ø.8	Ø.5	-Ø.9	Ø.1	Ø.4	-Ø.2	Ø.4	Ø.Ø	1.3	Ø.9	Ø.1	Ø.7	Ø.1
5ØØ	-1.4	-2.4	-Ø.7	-Ø.6	Ø.9	-Ø.7	-Ø.3	1.2	Ø.2	Ø.6	Ø.3	1.1	Ø.5	-Ø.1	1.1	Ø.1
63Ø	-2.Ø	-1.7	Ø.3	Ø.1	1.1	-Ø.4	Ø.9	Ø.7	1.7	1.Ø	1.7	2.1	2.6	Ø.6	1.4	Ø.8
8ØØ	-1.3	-1.Ø	-Ø.Ø	-Ø.3	3.3	1.5	2.6	2.5	2.4	1.3	1.Ø	2.1	2.2	1.3	1.5	1.8
1ØØØ	-Ø.1	Ø.7	1.9	2.1	4.5	2.6	3.6	2.9	1.8	1.5	Ø.4	2.1	1.6	2.Ø	1.3	2.3
125Ø	2.4	3.8	4.3	3.9	5.1	2.8	3.9	3.9	1.8	2.Ø	Ø.1	1.4	1.8	2.9	1.4	3.2
16ØØ	3.Ø	3.2	4.6	3.6	4.Ø	3.6	4.Ø	3.Ø	2.2	1.5	1.3	-Ø.1	1.1	2.7	1.4	3.1
2ØØØ	2.6	2.7	3.7	3.6	6.1	3.Ø	3.1	3.2	2.9	1.9	1.4	3.Ø	2.3	3.Ø	1.1	3.3
25ØØ	3.3	3.4	4.1	3.7	5.7	3.4	3.6	4.Ø	1.6	1.7	Ø.Ø	2.2	1.3	2.9	1.5	3.5
315Ø	2.4	3.7	4.1	3.5	4.7	2.2	3.7	3.9	2.3	2.6	1.6	4.2	2.8	3.2	Ø.9	3.3
4ØØØ	-1.1	Ø.4	3.4	2.5	4.4	2.Ø	2.7	4.4	4.1	3.6	2.8	4.9	4.7	3.Ø	1.7	2.5
5ØØØ	-1.8	-Ø.1	2.6	1.Ø	4.4	Ø.7	4.4	3.3	4.Ø	3.6	2.7	4.6		2.5	2.1	2.Ø
63ØØ	-2.Ø	1.6	2.3	1.2	3.8	Ø.9	4.9	5.2	5.7	4.9	3.4			2.9	2.4	2.7
8ØØØ			2.2	1.1	6.1	2.5	5.7	7.9	8.6					4.9	2.9	5.7
1ØØØØ																8.3
125ØØ																
16ØØØ																
2ØØØØ																
25ØØØ																
315ØØ																
4ØØØØ																
5ØØØØ																
63ØØØ																
8ØØØØ																
OASPL	Ø.Ø	Ø.6	1.9	1.9	3.2	1.4	2.2	2.1	Ø.9	Ø.8	Ø.7	1.2	Ø.7			
PNL	1.3	1.6	3.Ø	2.6	4.Ø	2.Ø	2.7	2.6	1.6	1.3	1.Ø	1.Ø	1.Ø			
PNLT	1.3	1.6	3.Ø	2.6	4.Ø	2.Ø	2.7	2.6	1.5	1.3	1.Ø	1.Ø	1.Ø			
DBA	1.Ø	1.6	2.8	2.6	4.Ø	2.2	2.9	2.7	1.6	1.3	Ø.7	1.5	1.4			

LOCATION	ACOUSTIC RANGE	AVG CORR SPEED	AVG CORR THRUST
C41 ANECH CH	24ØØ.Ø FT SL	-Ø.1E 31 RPM	-Ø.1E 31 LB

TEST CASE FOR TREATED EJECTOR TEØ2 VS TEØ4

C2

DELTA, SPL(1) - SPL(2)

IDENTIFICATION

INPUT (1) 83F-4ØØ-2ØØ6 X2ØØ65
(2) 83F-4ØØ-4ØØ6 X4ØØ65

OUTPUT ITF TE2-TE4 XØ2Ø41

ANGLES MEASURED FROM INLET,DEGREES

FREQ	4Ø.Ø	5Ø.Ø	6Ø.Ø	7Ø.Ø	8Ø.Ø	9Ø.Ø	1ØØ.Ø	11Ø.Ø	12Ø.Ø	13Ø.Ø	14Ø.Ø	15Ø.Ø	16Ø.Ø	AVG	S.D.	PWL
5Ø	-1.9	-Ø.4	-1.8	-1.1	Ø.Ø	Ø.2	Ø.7	Ø.5	-Ø.3	Ø.2	-Ø.5	2.2	1.5	-Ø.Ø	1.2	Ø.9
63	-2.4	-Ø.5	-Ø.6	-1.1	Ø.Ø	-1.Ø	-Ø.Ø	Ø.5	-1.2	Ø.Ø	Ø.3	2.Ø	1.Ø	-Ø.2	1.1	Ø.5
8Ø	-3.2	-Ø.6	-Ø.4	-Ø.9	Ø.Ø	-1.Ø	Ø.3	Ø.5	-1.Ø	-1.Ø	-Ø.2	Ø.5	1.Ø	-Ø.5	1.Ø	-Ø.1
1ØØ	-2.2	-Ø.5	-1.Ø	-Ø.1	-Ø.5	-1.5	Ø.Ø	-Ø.7	-1.2	-Ø.7	Ø.Ø	1.3	Ø.5	-Ø.5	Ø.9	-Ø.2
125	-2.7	Ø.Ø	-Ø.7	-Ø.5	1.1	-1.2	-Ø.2	-Ø.5	-1.4	-1.4	-Ø.7	-1.1	-Ø.7	-Ø.8	Ø.9	-1.Ø
16Ø	-1.3	-Ø.4	-1.1	Ø.5	Ø.Ø	-1.Ø	-Ø.4	Ø.2	-Ø.7	Ø.4	-Ø.7	Ø.2	Ø.1	-Ø.3	Ø.6	-Ø.3
2ØØ	-1.9	-Ø.5	-Ø.9	-1.1	Ø.Ø	-2.2	-Ø.2	-Ø.7	-1.5	-Ø.2	-Ø.2	1.Ø	-Ø.7	-Ø.7	Ø.9	-Ø.7
25Ø	-2.2	-Ø.7	-1.2	-Ø.8	-Ø.2	-1.5	-Ø.4	-1.5	-1.1	Ø.1	-Ø.1	Ø.6	Ø.2	-Ø.7	Ø.8	-Ø.6
315	-2.7	-Ø.7	-1.2	-Ø.7	Ø.3	-1.5	Ø.3	-Ø.7	-1.1	-Ø.6	-Ø.2	-Ø.2	-1.2	-Ø.8	Ø.8	-Ø.7
4ØØ	-2.2	-Ø.7	-1.5	-Ø.8	-Ø.2	-1.5	-1.1	-Ø.7	-1.Ø	Ø.1	-Ø.5	Ø.3	1.Ø	-Ø.7	Ø.9	-Ø.7
5ØØ	-2.Ø	-Ø.7	-2.Ø	-1.6	-1.Ø	-1.5	-Ø.Ø	-Ø.4	-Ø.9	-Ø.4	-1.4	-Ø.6	-Ø.6	-1.Ø	Ø.6	-Ø.8
63Ø	-2.5	-Ø.7	-Ø.7	-1.4	Ø.Ø	-1.7	-Ø.2	-Ø.9	-Ø.6	Ø.2	-Ø.4	Ø.1	Ø.2	-Ø.7	Ø.8	-Ø.6
8ØØ	-2.7	-Ø.7	-1.Ø	-1.Ø	Ø.7	-1.Ø	1.1	-Ø.1	-Ø.9	-Ø.Ø	-Ø.2	Ø.1	-Ø.1	-Ø.5	Ø.9	-Ø.4
1ØØØ	-4.Ø	-1.8	-1.5	-Ø.8	1.7	-Ø.3	1.Ø	Ø.9	-Ø.8	-1.Ø	-1.2	-1.Ø	-1.5	-Ø.8	1.5	-Ø.4
125Ø	-1.8	Ø.7	Ø.7	1.6	3.Ø	1.5	1.3	1.3	-Ø.7	Ø.1	-Ø.7	Ø.1	-Ø.5	Ø.5	1.3	Ø.7
16ØØ	-Ø.3	1.2	1.7	1.4	2.8	1.2	3.6	1.5	-Ø.8	-Ø.9	-1.3	-1.3	-1.4	Ø.6	1.7	1.Ø
2ØØØ	2.5	4.Ø	3.9	2.5	3.4	Ø.4	2.6	1.4	-1.5	-2.5	-4.2	-2.1	-3.1	Ø.6	2.9	1.4
25ØØ	-Ø.Ø	1.4	1.7	1.6	3.2	1.4	1.6	Ø.4	1.6	2.5	1.2	2.1	2.5	1.6	Ø.8	1.5
315Ø	-1.1	1.9	1.7	Ø.7	2.9	-Ø.9	2.6	3.9	Ø.9	3.Ø	1.8	3.Ø	2.9	1.8	1.5	1.4
4ØØØ	-2.1	-Ø.6	Ø.6	Ø.2	Ø.6	-1.4	1.1	2.4	1.4	4.1	2.4	5.Ø	3.8	1.3	2.2	Ø.2
5ØØØ	-2.7	-Ø.7	Ø.5	-1.2	1.3	-2.Ø	1.8	2.8	1.8	3.2	3.1	4.5		1.Ø	2.3	Ø.4
63ØØ	-2.5	-Ø.3	1.5	-Ø.6	2.7	-1.8	3.9	3.6	3.6	5.5	4.4			1.8	2.7	1.3
8ØØØ			1.2	Ø.1	5.Ø	1.Ø	4.5	5.4	6.2					3.4	2.5	3.4
1ØØØØ																5.3
125ØØ																
16ØØØ																
2ØØØØ																
25ØØØ																
315ØØ																
4ØØØØ																
5ØØØØ																
63ØØØ																
8ØØØØ																
OASPL	-1.9	-Ø.Ø	-Ø.Ø	Ø.1	1.3	-Ø.3	Ø.9	Ø.2	-Ø.9	-Ø.3	-Ø.5	Ø.8	Ø.4			
PNL	-1.Ø	Ø.9	Ø.9	Ø.8	2.1	-Ø.1	1.7	Ø.9	-Ø.7	-Ø.3	-Ø.8	-Ø.2	-Ø.1			
PNLT	-1.1	-Ø.2	1.Ø	Ø.8	2.1	-Ø.1	1.7	Ø.9	-Ø.7	Ø.3	-1.8	-Ø.2	-Ø.1			
DBA	-1.4	Ø.5	Ø.7	Ø.7	2.Ø	Ø.2	1.5	Ø.7	-Ø.8	-Ø.3	-Ø.8	-Ø.3	-Ø.5			

LOCATION	ACOUSTIC RANGE	AVG CORR SPEED	AVG CORR THRUST
C41 ANECH CH	24ØØ.Ø FT SL	-Ø.1E 31 RPM	-Ø.1E 31 LB

TEST CASE FOR TREATED EJECTOR TEØ2 VS TEØ4

DELTA, SPL(1) - SPL(2)

IDENTIFICATION

INPUT (1) 83F-4ØØ-2Ø1Ø X2Ø1Ø5
(2) 83F-4ØØ-4Ø1Ø X4Ø1Ø5

OUTPUT TOF TE2-TE4 XØ2Ø41

ANGLES MEASURED FROM INLET,DEGREES

FREQ	4Ø.Ø	5Ø.Ø	6Ø.Ø	7Ø.Ø	8Ø.Ø	9Ø.Ø	1ØØ.Ø	11Ø.Ø	12Ø.Ø	13Ø.Ø	14Ø.Ø	15Ø.Ø	16Ø.Ø	AVG	S.D.	PWL
5Ø	Ø.4	-1.4	-Ø.1	-Ø.7	Ø.8	Ø.9	2.1	1.1	Ø.5	1.5	1.2	1.5	-Ø.2	Ø.6	1.Ø	Ø.7
63	Ø.6	Ø.3	1.1	Ø.2	Ø.6	Ø.3	1.3	1.Ø	Ø.5	1.Ø	2.Ø	1.7	-Ø.2	Ø.8	Ø.6	1.Ø
8Ø	-Ø.4	-Ø.4	Ø.3	-Ø.1	Ø.6	-Ø.4	1.1	Ø.5	Ø.5	Ø.3	1.5	1.8	Ø.Ø	Ø.4	Ø.7	Ø.8
1ØØ	-Ø.5	-Ø.4	1.3	Ø.5	Ø.1	-Ø.4	1.6	Ø.8	-Ø.2	Ø.8	Ø.8	1.3	Ø.8	Ø.5	Ø.7	Ø.8
125	Ø.Ø	-Ø.1	Ø.1	Ø.8	1.9	-Ø.4	Ø.8	Ø.8	-Ø.3	Ø.2	1.Ø	Ø.5	Ø.5	Ø.4	Ø.6	Ø.4
16Ø	Ø.5	Ø.4	Ø.8	1.6	1.1	Ø.3	1.Ø	1.2	Ø.8	1.Ø	Ø.4	Ø.1	Ø.9	Ø.8	Ø.4	Ø.7
2ØØ	-Ø.1	Ø.1	1.2	-Ø.Ø	1.1	-1.1	Ø.4	Ø.8	Ø.4	Ø.9	Ø.4	1.2	Ø.5	Ø.4	Ø.7	Ø.6
25Ø	Ø.3	-Ø.4	Ø.1	-Ø.1	Ø.3	-Ø.4	Ø.9	Ø.4	Ø.5	Ø.8	Ø.Ø	Ø.3	Ø.6	Ø.2	Ø.4	Ø.4
315	-Ø.2	-Ø.2	-Ø.5	-Ø.Ø	Ø.8	-1.2	Ø.Ø	1.3	Ø.9	Ø.4	Ø.7	Ø.5	1.2	Ø.3	Ø.7	Ø.5
4ØØ	Ø.Ø	Ø.8	-Ø.5	-Ø.1	Ø.8	-Ø.7	-Ø.2	Ø.9	1.3	Ø.8	-Ø.4	Ø.1	1.6	Ø.3	Ø.7	Ø.6
5ØØ	1.5	Ø.3	-Ø.2	-Ø.3	Ø.4	-Ø.7	-Ø.9	1.2	Ø.5	1.3	Ø.3	1.4	1.9	Ø.5	Ø.9	Ø.7
63Ø	2.5	Ø.9	-Ø.7	-Ø.6	Ø.3	-Ø.3	-Ø.2	Ø.8	1.Ø	1.2	1.Ø	1.Ø	1.7	Ø.7	Ø.9	Ø.8
8ØØ	2.9	1.9	Ø.5	-Ø.5	2.1	-Ø.1	Ø.4	1.2	Ø.7	1.Ø	Ø.8	1.2	1.8	1.1	Ø.9	1.Ø
1ØØØ	3.6	4.7	3.3	2.3	3.8	Ø.8	-Ø.1	2.1	1.Ø	1.6	1.2	1.1	2.1	2.1	1.4	1.8
125Ø	3.5	4.2	4.4	4.1	5.1	2.7	1.8	1.3	Ø.4	2.2	1.3	Ø.8	1.9	2.6	1.5	2.3
16ØØ	4.3	3.7	4.4	3.4	3.4	2.Ø	2.8	1.5	-Ø.2	Ø.8	Ø.9	-Ø.1	1.1	2.2	1.6	2.2
2ØØØ	3.8	2.6	1.7	1.4	1.8	Ø.2	1.5	1.1	-2.8	-3.4	-3.2	-2.8	-2.8	-Ø.1	2.6	Ø.7
25ØØ	2.9	2.Ø	1.4	-Ø.5	1.3	Ø.1	-Ø.7	-Ø.9	-2.Ø	-1.8	-1.6	-2.Ø	-Ø.8	-Ø.2	1.6	Ø.2
315Ø	2.8	1.9	Ø.9	-1.1	Ø.5	-1.7	-Ø.4	Ø.8	-1.2	-2.1	-1.8	-Ø.9	-1.2	-Ø.3	1.5	-Ø.2
4ØØØ	-1.2	-1.4	Ø.1	-1.1	-Ø.Ø	-1.4	-1.3	Ø.5	-Ø.9	-1.6	-Ø.7	Ø.3	-Ø.7	-Ø.7	Ø.7	-Ø.8
5ØØØ	-2.1	-1.Ø	Ø.Ø	-2.8	Ø.4	-1.7	-Ø.Ø	Ø.8	Ø.1	-Ø.5	1.1	Ø.7		-Ø.4	1.2	-Ø.7
63ØØ	-1.7	-1.4	-Ø.8	-2.3	2.Ø	-1.Ø	2.Ø	1.9	2.Ø	2.9	2.4			Ø.5	2.Ø	Ø.4
8ØØØ		2.7	2.9	Ø.3	5.2	1.2	3.7	4.9	7.2	7.4				3.9	2.5	4.3
1ØØØØ																7.3
125ØØ																
16ØØØ																
2ØØØØ																
25ØØØ																
315ØØ																
4ØØØØ																
5ØØØØ																
63ØØØ																
8ØØØØ																
OASPL	2.Ø	2.Ø	1.9	1.1	2.1	Ø.4	Ø.6	1.1	Ø.5	Ø.9	Ø.8	1.2	Ø.3			
PNL	2.6	2.Ø	1.7	Ø.4	1.6	-Ø.Ø	Ø.6	1.Ø	-Ø.1	Ø.4	Ø.5	Ø.6	Ø.9			
PNLT	1.5	1.2	1.1	-Ø.2	1.6	-Ø.Ø	Ø.6	Ø.5	-Ø.8	-Ø.1	1.5	Ø.6	Ø.9			
DBA	3.2	3.Ø	2.6	1.6	2.6	Ø.7	Ø.8	1.2	Ø.3	1.Ø	Ø.6	Ø.7	1.5			

LOCATION	ACOUSTIC RANGE	AVG CORR SPEED	AVG CORR THRUST
C41 ANECH CH	24ØØ.Ø FT SL	-Ø.1E 31 RPM	-Ø.1E 31•LB

TEST CASE FOR TREATED EJECTOR TEØ2 VS TEØ4

C-4

C2

DELTA, SPL(1) - SPL(2)

IDENTIFICATION

INPUT (1) 83F-ZER-7ØØ3 X7ØØ35
(2) 83F-ZER-ØØØ3 XØØØ35

OUTPUT CBS TE7-T1Ø XØ71Ø1

ANGLES MEASURED FROM INLET,DEGREES

FREQ	4Ø.Ø	5Ø.Ø	6Ø.Ø	7Ø.Ø	8Ø.Ø	9Ø.Ø	1ØØ.Ø	11Ø.Ø	12Ø.Ø	13Ø.Ø	14Ø.Ø	15Ø.Ø	16Ø.Ø	AVG	S.D.	PWL
5Ø	-1.Ø	-Ø.5	-Ø.2	-Ø.5	Ø.6	-2.2	Ø.3	-2.Ø	-Ø.7	-Ø.7	-Ø.2	Ø.3	Ø.Ø	-Ø.5	Ø.8	-Ø.1
63	-Ø.7	-1.Ø	-Ø.5	-1.2	-Ø.5	-3.Ø	-Ø.5	-2.Ø	-Ø.7	-Ø.2	Ø.3	-Ø.5	Ø.3	-Ø.8	Ø.9	-Ø.2
8Ø	-1.Ø	-Ø.5	-1.Ø	-Ø.5	-Ø.6	-1.Ø	-1.Ø	-2.Ø	-1.Ø	-Ø.5	Ø.Ø	Ø.Ø	-Ø.2	-Ø.7	Ø.5	-Ø.3
1ØØ	-Ø.7	-Ø.7	-Ø.5	-1.2	-Ø.2	-Ø.7	-1.2	-2.2	-1.5	-Ø.5	Ø.5	Ø.Ø	Ø.Ø	-Ø.7	Ø.7	-Ø.4
125	-Ø.7	-Ø.5	-Ø.7	-Ø.5	Ø.9	-Ø.2	-Ø.2	-1.7	Ø.Ø	Ø.Ø	Ø.8	Ø.5	-Ø.2	-Ø.2	Ø.7	Ø.Ø
16Ø	-1.Ø	-Ø.2	-1.2	-Ø.5	Ø.1	-Ø.5	-Ø.5	-1.7	-Ø.5	-Ø.5	Ø.Ø	Ø.3	Ø.3	-Ø.5	Ø.6	-Ø.4
2ØØ	-1.Ø	Ø.Ø	-2.Ø	-Ø.5	Ø.1	-Ø.2	Ø.Ø	-1.7	-Ø.7	-Ø.5	Ø.Ø	Ø.3	Ø.5	-Ø.4	Ø.8	-Ø.4
25Ø	-1.Ø	-Ø.8	-2.Ø	-1.Ø	-Ø.8	-Ø.5	-Ø.8	-1.5	-Ø.8	-Ø.8	-Ø.3	-Ø.Ø	-Ø.Ø	-Ø.8	Ø.6	-Ø.7
315	-Ø.3	-1.Ø	-2.5	-Ø.5	Ø.5	-Ø.8	-Ø.8	-1.5	-Ø.8	-Ø.8	-Ø.3	Ø.2	Ø.7	-Ø.6	Ø.9	-Ø.6
4ØØ	-Ø.3	-Ø.8	-2.8	-1.Ø	-Ø.1	-Ø.5	-Ø.5	-1.3	-Ø.8	-Ø.5	-Ø.5	Ø.2	Ø.2	-Ø.7	Ø.8	-Ø.7
5ØØ	-Ø.3	-1.3	-3.6	-1.3	-Ø.2	-1.3	-1.1	-1.3	-1.1	-Ø.6	-Ø.8	-Ø.1	-Ø.1	-1.Ø	Ø.9	-1.Ø
63Ø	-Ø.9	-1.4	-4.6	-1.6	-Ø.3	-1.4	-2.1	-2.9	-1.4	-Ø.7	-Ø.6	Ø.1	Ø.9	-1.3	1.4	-1.5
8ØØ	-1.7	-2.2	-5.2	-2.2	-1.1	-2.2	-2.7	-3.4	-1.2	-1.5	-Ø.5	Ø.3	Ø.6	-1.8	1.5	-2.Ø
1ØØØ	-1.8	-2.3	-6.3	-3.1	-2.Ø	-3.Ø	-3.3	-4.1	-1.8	-1.6	-Ø.8	-Ø.Ø	Ø.5	-2.3	1.8	-2.7
125Ø	-1.4	-2.7	-6.7	-3.4	-1.9	-3.4	-3.2	-3.9	-2.2	-2.Ø	-1.Ø	-Ø.2	Ø.4	-2.4	1.8	-2.9
16ØØ	-2.3	-2.6	-6.6	-3.1	-3.3	-3.8	-4.3	-4.6	-2.4	-1.9	-1.1	-Ø.3	-1.Ø	-2.9	1.7	-3.5
2ØØØ	-2.3	-2.4	-5.9	-3.6	-2.3	-4.3	-4.1	-4.9	-2.2	-1.5	-Ø.9	-Ø.8	Ø.2	-2.7	1.8	-3.7
25ØØ	-1.7	-1.8	-5.8	-3.Ø	-1.9	-3.5	-3.Ø	-3.8	-1.6	-1.4	Ø.4	-Ø.2	Ø.5	-2.1	1.8	-2.9
315Ø	-Ø.6	-1.1	-4.4	-1.9	-Ø.5	-2.6	-1.9	-1.6	-Ø.9	Ø.3	1.4	2.4	Ø.4	-Ø.8	1.8	-1.5
4ØØØ	Ø.7	1.1	-3.4	Ø.5	1.2	-1.3	-Ø.3	-2.5	-1.9	-Ø.8	1.1	-Ø.6	-Ø.6	-Ø.5	1.5	-1.1
5ØØØ	3.3	3.2	-Ø.8	2.3	3.8	1.4	1.9	-1.5	Ø.7	1.5	1.9	1.6		1.6	1.6	1.Ø
63ØØ		6.2	2.Ø	5.6	7.1	3.9	4.2	1.1	2.Ø	4.1	3.6			4.Ø	1.9	3.6
8ØØØ				7.8	9.9	6.2	6.8	3.1	4.4					6.4	2.4	5.9
1ØØØØ																8.3
125ØØ																
16ØØØ																
2ØØØØ																
25ØØØ																
315ØØ																
4ØØØØ																
5ØØØØ																
63ØØØ																
8ØØØØ																
OASPL	-Ø.9	-1.Ø	-2.6	-1.4	-Ø.6	-1.8	-1.6	-2.6	-1.Ø	-Ø.6	Ø.Ø	Ø.Ø	Ø.1			
PNL	-Ø.8	-1.6	-4.4	-2.2	-1.2	-2.7	-2.4	-3.3	-1.5	-Ø.7	-Ø.1	Ø.1	Ø.2			
PNLT	Ø.2	-1.6	-3.9	-2.2	-1.2	-2.7	-2.4	-3.3	-2.1	-Ø.7	-1.2	Ø.1	Ø.2			
DBA	-1.1	-1.9	-5.Ø	-2.4	-1.5	-2.8	-2.9	-3.5	-1.5	-1.Ø	-Ø.5	Ø.1	Ø.3			

LOCATION	ACOUSTIC RANGE	AVG CORR SPEED	AVG CORR THRUST
C41 ANECH CH	24ØØ.Ø FT SL	-Ø.1E 31 RPM	-Ø.1E 31 LB

TEST CASE FOR TREATED EJECTOR TEØ7 VS TE1Ø

DELTA, SPL(1) - SPL(2)

IDENTIFICATION

INPUT (1) 83F-ZER-7ØØ5 X7ØØ55
(2) 83F-ZER-ØØØ5 XØØØ55

OUTPUT ITS TE7-T1Ø XØ71Ø1

ANGLES MEASURED FROM INLET,DEGREES

FREQ	4Ø.Ø	5Ø.Ø	6Ø.Ø	7Ø.Ø	8Ø.Ø	9Ø.Ø	1ØØ.Ø	11Ø.Ø	12Ø.Ø	13Ø.Ø	14Ø.Ø	15Ø.Ø	16Ø.Ø	AVG	S.D.	PWL
5Ø	-1.2	-1.2	-Ø.2	-Ø.5	-1.Ø	-2.7	Ø.3	-1.5	-1.Ø	-Ø.7	-Ø.7	-Ø.2	-Ø.7	-Ø.9	Ø.7	-Ø.6
63	-Ø.7	-Ø.2	-Ø.5	-1.Ø	-1.2	-2.7	-Ø.2	-1.Ø	-Ø.5	-Ø.5	-Ø.7	-Ø.2	-Ø.7	-Ø.8	Ø.7	-Ø.6
8Ø	-Ø.7	-Ø.7	-1.5	-1.Ø	-1.2	-1.Ø	-Ø.7	-1.7	-Ø.5	-Ø.7	-1.Ø	-Ø.2	Ø.3	-Ø.8	Ø.5	-Ø.4
1ØØ	-1.Ø	-1.Ø	-1.5	Ø.Ø	-Ø.7	-1.2	-Ø.5	-1.Ø	-Ø.2	-Ø.7	-Ø.5	-Ø.2	-Ø.5	-Ø.7	Ø.4	-Ø.5
125	-1.5	-1.2	-2.Ø	-1.2	-Ø.2	-1.Ø	-Ø.2	-Ø.7	-Ø.2	-Ø.2	-Ø.7	Ø.Ø	-Ø.7	-Ø.8	Ø.6	-Ø.5
16Ø	-1.5	-1.5	-2.5	-Ø.5	-1.2	-Ø.7	Ø.Ø	-1.5	-1.Ø	-Ø.5	-Ø.5	Ø.Ø	-Ø.5	-Ø.9	Ø.7	-Ø.6
2ØØ	-1.Ø	-Ø.7	-2.2	-1.Ø	-1.2	-Ø.7	-Ø.5	-1.2	-Ø.2	-1.5	-Ø.5	-Ø.2	-Ø.2	-Ø.9	Ø.6	-Ø.7
25Ø	-1.Ø	-1.5	-4.Ø	-1.3	-1.Ø	-1.Ø	-Ø.5	-1.3	-Ø.8	-1.Ø	-1.Ø	-Ø.5	-Ø.8	-1.2	Ø.9	-Ø.9
315	-1.Ø	-1.3	-4.Ø	-1.Ø	-1.3	-1.Ø	-Ø.Ø	-1.8	-Ø.5	-Ø.5	-Ø.8	-Ø.3	-1.Ø	-1.1	1.Ø	-Ø.8
4ØØ	-1.Ø	-1.3	-4.5	-Ø.8	-1.3	-1.Ø	-Ø.3	-1.5	-Ø.5	-Ø.8	-1.3	-Ø.8	-Ø.5	-1.2	1.1	-Ø.9
5ØØ	-1.3	-1.8	-5.1	-1.3	-1.6	-2.3	-Ø.3	-1.8	-Ø.8	-1.1	-1.6	-1.6	-2.1	-1.7	1.1	-1.4
63Ø	-1.1	-1.6	-5.4	-1.9	-1.9	-1.4	-1.1	-2.1	-1.4	-Ø.9	-1.6	-Ø.9	-1.6	-1.8	1.2	-1.5
8ØØ	-1.4	-2.2	-5.7	-2.5	-2.4	-2.4	-1.4	-3.Ø	-1.2	-Ø.5	-1.7	-1.9	-1.9	-2.2	1.2	-1.8
1ØØØ	-1.5	-2.3	-6.3	-3.1	-3.3	-2.5	-2.5	-2.8	-1.3	-1.6	-2.1	-2.5	-2.Ø	-2.6	1.3	-2.3
125Ø	-2.4	-2.7	-7.2	-3.4	-3.7	-3.7	-3.4	-3.2	-1.7	-2.3	-2.7	-3.7	-2.4	-3.3	1.3	-3.Ø
16ØØ	-2.3	-2.6	-6.6	-3.8	-4.Ø	-4.5	-3.3	-3.1	-2.4	-2.4	-2.3	-4.Ø	-2.Ø	-3.3	1.3	-3.2
2ØØØ	-2.3	-2.2	-6.7	-3.4	-3.9	-4.6	-3.1	-2.6	-1.9	-1.5	-2.7	-2.6	-2.3	-3.1	1.4	-2.9
25ØØ	-1.5	-1.8	-6.1	-2.5	-3.Ø	-4.Ø	-3.Ø	-2.5	-Ø.8	-Ø.7	-1.3	-2.Ø	-1.7	-2.4	1.5	-2.5
315Ø	Ø.1	-Ø.9	-5.6	-1.4	-1.9	-2.1	-Ø.9	-Ø.6	-Ø.6	Ø.4	-Ø.1	Ø.4	-Ø.1	-1.Ø	1.6	-1.Ø
4ØØØ	1.5	1.1	-3.1	Ø.8	Ø.Ø	-Ø.2	Ø.5	-1.8	-Ø.3	-Ø.Ø	-Ø.6	-3.1	-1.5	-Ø.5	1.5	-Ø.4
5ØØØ	3.6	4.3	Ø.Ø	3.1	2.7	2.2	3.Ø	Ø.3	1.5	1.3	1.4	Ø.2		2.Ø	1.4	1.8
63ØØ		7.6	2.8	6.2	5.5	4.2	5.Ø	1.7	3.5	4.7	2.9			4.4	1.8	4.Ø
8ØØØ				8.7	7.1	7.Ø	8.1	4.4	5.7					6.8	1.6	6.6
1ØØØØ																8.8
125ØØ																
16ØØØ																
2ØØØØ																
25ØØØ																
315ØØ																
4ØØØØ																
5ØØØØ																
63ØØØ																
8ØØØØ																
OASPL	-1.2	-1.4	-3.4	-1.4	-1.7	-2.Ø	-1.1	-1.9	-Ø.8	-Ø.8	-Ø.8	-Ø.3	-Ø.5			
PNL	-1.2	-1.7	-5.1	-1.9	-2.2	-2.8	-1.8	-2.1	-1.1	-Ø.8	-1.Ø	-Ø.8	-Ø.8			
PNLT	-Ø.2	-1.7	-4.5	-1.9	-1.7	-2.8	-1.8	-2.6	-1.1	-Ø.1	-Ø.Ø	Ø.4	-Ø.8			
DBA	-1.4	-2.Ø	-5.6	-2.4	-2.7	-3.Ø	-2.1	-2.5	-1.2	-1.1	-1.5	-1.3	-1.1			

LOCATION	ACOUSTIC RANGE	AVG CORR SPEED	AVG CORR THRUST
C41 ANECH CH	24ØØ.Ø FT SL	-Ø.1E 31 RPM	-Ø.1E 31 'LB

TEST CASE FOR TREATED EJECTOR TEØ7 VS TE1Ø

C2

DELTA, SPL(1) - SPL(2)

IDENTIFICATION

INPUT (1) 83F-ZER-7ØØ9 X7ØØ95
(2) 83F-ZER-ØØØ9 XØØØ95

OUTPUT TOS TE7-T1Ø XØ71Ø1

ANGLES MEASURED FROM INLET,DEGREES

FREQ	4Ø.Ø	5Ø.Ø	6Ø.Ø	7Ø.Ø	8Ø.Ø	9Ø.Ø	1ØØ.Ø	11Ø.Ø	12Ø.Ø	13Ø.Ø	14Ø.Ø	15Ø.Ø	16Ø.Ø	AVG	S.D.	PWL
5Ø	-Ø.5	-Ø.7	-Ø.2	-Ø.2	-Ø.5	-1.2	1.8	-1.2	-Ø.2	-Ø.2	-Ø.7	-Ø.2	-Ø.2	-Ø.4	Ø.7	-Ø.4
63	-Ø.7	-Ø.2	Ø.5	Ø.Ø	Ø.Ø	-2.2	Ø.Ø	-1.Ø	-Ø.5	Ø.Ø	-Ø.7	-Ø.5	Ø.3	-Ø.4	Ø.7	-Ø.4
8Ø	-Ø.2	-1.Ø	-Ø.2	-Ø.2	-Ø.2	Ø.Ø	-Ø.5	-Ø.5	-Ø.2	Ø.Ø	-Ø.7	-Ø.7	-Ø.5	-Ø.4	Ø.3	-Ø.6
1ØØ	-Ø.2	-Ø.7	-1.Ø	-Ø.2	-Ø.5	-Ø.5	-Ø.5	-Ø.7	Ø.3	Ø.3	-Ø.5	-Ø.5	-1.Ø	-Ø.5	Ø.4	-Ø.5
125	-Ø.7	-2.Ø	-1.2	-1.Ø	-1.Ø	-Ø.5	-Ø.5	-Ø.5	-Ø.2	Ø.Ø	Ø.3	-Ø.5	-Ø.7	-Ø.7	Ø.6	-Ø.4
16Ø	Ø.3	-Ø.2	-Ø.5	-1.Ø	-1.7	-1.7	-Ø.7	-Ø.2	Ø.Ø	-Ø.2	Ø.Ø	-Ø.2	-1.Ø	-Ø.6	Ø.6	-Ø.4
2ØØ	-1.Ø	-1.Ø	-Ø.2	-1.Ø	Ø.Ø	-Ø.7	Ø.Ø	-1.2	-Ø.5	-Ø.5	-Ø.2	-Ø.2	-1.2	-Ø.6	Ø.5	-Ø.5
25Ø	-Ø.3	-1.5	-Ø.3	-1.Ø	-Ø.5	-1.Ø	-Ø.3	-Ø.5	-Ø.Ø	-Ø.3	-Ø.Ø	-Ø.3	-1.Ø	-Ø.5	Ø.5	-Ø.3
315	-Ø.3	-Ø.8	-Ø.3	-Ø.3	-Ø.5	-1.3	-1.Ø	-1.Ø	-Ø.3	-Ø.3	Ø.5	-1.3	-1.3	-Ø.6	Ø.5	-Ø.5
4ØØ	-1.Ø	-Ø.3	-Ø.Ø	-Ø.5	-Ø.8	-Ø.5	-Ø.5	-Ø.8	Ø.2	-Ø.3	-Ø.5	-Ø.5	-Ø.8	-Ø.5	Ø.3	-Ø.5
5ØØ	-1.1	-1.1	-Ø.3	-Ø.6	-Ø.6	-Ø.8	-Ø.1	-Ø.8	-Ø.3	-Ø.6	-Ø.6	-Ø.8	-1.1	-Ø.7	Ø.3	-Ø.6
63Ø	-1.4	-1.9	-Ø.9	-1.1	-1.1	-1.6	-Ø.9	-1.4	-Ø.4	-Ø.4	Ø.1	-Ø.6	-1.9	-1.Ø	Ø.6	-Ø.6
8ØØ	-1.7	-2.5	-1.2	-1.2	-1.7	-1.7	-Ø.9	-1.4	-1.Ø	-1.Ø	-Ø.7	-Ø.9	-1.9	-1.4	Ø.5	-1.1
1ØØØ	-1.3	-2.8	-1.1	-1.6	-1.8	-1.8	-1.3	-2.1	-1.6	-1.1	-Ø.3	-1.Ø	-1.5	-1.5	Ø.6	-1.3
125Ø	-2.4	-2.5	-1.5	-2.2	-2.2	-2.7	-1.9	-2.4	-1.5	-1.5	-1.2	-Ø.9	-1.9	-1.9	Ø.5	-1.7
16ØØ	-2.5	-3.4	-1.9	-2.1	-2.8	-3.Ø	-2.3	-2.3	-1.6	-1.9	-1.3	-1.3	-Ø.5	-2.1	Ø.8	-1.9
2ØØØ	-1.3	-2.4	-1.7	-2.1	-2.4	-2.8	-1.9	-2.1	-1.4	-1.8	-1.2	-1.1	-2.6	-1.9	Ø.6	-1.8
25ØØ	-1.5	-1.8	-Ø.8	-1.8	-2.Ø	-2.Ø	-1.5	-1.5	-Ø.8	-Ø.9	-1.1	-Ø.5	-2.Ø	-1.4	Ø.5	-1.3
315Ø	-Ø.4	-Ø.4	-Ø.1	-Ø.4	-Ø.9	-1.1	-Ø.4	Ø.1	Ø.6	Ø.8	1.6	Ø.9	-Ø.9	-Ø.Ø	Ø.8	Ø.1
4ØØØ	1.2	1.8	1.8	Ø.8	Ø.5	Ø.7	1.2	-Ø.5	1.1	Ø.9	Ø.4	2.5	-2.1	Ø.8	1.1	Ø.7
5ØØØ	3.8	4.Ø	5.2	3.5	3.2	3.6	3.2	1.Ø	2.8	2.5	3.1	3.4		3.3	1.Ø	2.9
63ØØ	6.Ø	7.2	7.7	6.9	5.7	5.1	6.2	4.1	4.8	4.9	5.3			5.8	1.1	5.2
8ØØØ			1Ø.6	9.Ø	8.3	7.9	8.8	5.Ø	7.6	7.7				8.1	1.6	7.5
1ØØØØ																9.9
125ØØ																
16ØØØ																
2ØØØØ																
25ØØØ																
315ØØ																
4ØØØØ																
5ØØØØ																
63ØØØ																
8ØØØØ																
OASPL	-Ø.6	-1.2	-Ø.6	-Ø.9	-1.Ø	-1.3	-Ø.6	-1.1	-Ø.3	-Ø.2	-Ø.4	-Ø.5	-Ø.6			
PNL	-Ø.8	-1.Ø	-Ø.7	-1.1	-1.3	-1.5	-Ø.9	-1.3	-Ø.4	-Ø.4	-Ø.2	-Ø.5	-1.Ø			
PNLT	-Ø.8	-1.6	-Ø.7	-1.1	-1.3	-Ø.9	-Ø.9	-Ø.7	-1.Ø	-Ø.4	Ø.8	Ø.5	Ø.1			
DBA	-1.1	-1.7	-Ø.9	-1.3	-1.6	-1.9	-1.2	-1.6	-Ø.8	-Ø.7	-Ø.4	-Ø.7	-1.1			

LOCATION	ACOUSTIC RANGE	AVG CORR SPEED	AVG CORR THRUST
C41 ANECH CH	24ØØ.Ø FT SL	-Ø.1E 31 RPM	-Ø.1E 31 LB

TEST CASE FOR TREATED EJECTOR TEØ7 VS TE1Ø

DELTA, SPL(1) - SPL(2)

IDENTIFICATION

INPUT (1) 83F-4ØØ-7ØØ4 X7ØØ45
(2) 83F-4ØØ-ØØØ4 XØØØ45

OUTPUT CBF TE7-T1Ø XØ71Ø1

ANGLES MEASURED FROM INLET, DEGREES

FREQ	4Ø.Ø	5Ø.Ø	6Ø.Ø	7Ø.Ø	8Ø.Ø	9Ø.Ø	1ØØ.Ø	11Ø.Ø	12Ø.Ø	13Ø.Ø	14Ø.Ø	15Ø.Ø	16Ø.Ø	AVG	S.D.	PWL
5Ø	-Ø.3	-Ø.5	Ø.4	Ø.2	Ø.Ø	-Ø.2	4.Ø	-Ø.5	-Ø.2	Ø.Ø	Ø.Ø	-Ø.2	Ø.Ø	Ø.2	1.2	Ø.1
63	Ø.2	-Ø.8	-Ø.3	-Ø.8	-Ø.2	Ø.3	3.3	-1.Ø	Ø.3	Ø.3	Ø.Ø	-Ø.2	Ø.3	Ø.1	1.Ø	Ø.1
8Ø	-Ø.5	Ø.4	Ø.5	-Ø.1	Ø.Ø	-Ø.7	Ø.Ø	-Ø.5	Ø.3	Ø.3	Ø.8	-Ø.2	-Ø.5	-Ø.Ø	Ø.4	Ø.Ø
1ØØ	-Ø.8	-Ø.Ø	Ø.5	-Ø.2	Ø.Ø	-Ø.2	Ø.8	-Ø.7	Ø.Ø	Ø.3	Ø.5	-Ø.2	Ø.8	Ø.Ø	Ø.5	Ø.2
125	-Ø.3	Ø.1	-Ø.2	-Ø.2	-Ø.Ø	-Ø.5	-Ø.2	-Ø.5	-1.2	-1.5	-Ø.8	-1.4	Ø.4	-Ø.5	Ø.6	-Ø.7
16Ø	-Ø.6	-Ø.2	Ø.4	-Ø.6	-Ø.2	Ø.Ø	-1.5	-2.1	Ø.5	Ø.3	Ø.Ø	-1.3	Ø.2	-Ø.4	Ø.8	-Ø.1
2ØØ	-Ø.3	-Ø.1	Ø.8	Ø.1	Ø.3	-Ø.5	-Ø.2	-Ø.2	Ø.6	-Ø.4	Ø.1	Ø.1	-Ø.3	-Ø.Ø	Ø.4	-Ø.Ø
25Ø	-Ø.2	1.Ø	Ø.3	-Ø.2	Ø.Ø	-Ø.5	Ø.2	-Ø.1	-Ø.2	-Ø.7	-Ø.2	-Ø.1	-1.1	-Ø.1	Ø.5	-Ø.3
315	-Ø.2	-Ø.5	-Ø.2	Ø.Ø	Ø.5	-Ø.3	Ø.2	-Ø.5	Ø.9	Ø.4	-Ø.1	-Ø.3	Ø.7	Ø.Ø	Ø.4	Ø.2
4ØØ	-Ø.8	Ø.5	Ø.5	-1.Ø	Ø.5	Ø.5	Ø.5	Ø.3	-Ø.2	Ø.3	Ø.3	-Ø.5	Ø.Ø	Ø.1	Ø.5	Ø.1
5ØØ	-Ø.3	-Ø.Ø	Ø.7	Ø.2	-Ø.3	-Ø.5	-Ø.8	-Ø.6	-Ø.5	-Ø.7	-Ø.3	-Ø.8	-1.1	-Ø.4	Ø.5	-Ø.5
63Ø	-Ø.5	Ø.2	-Ø.Ø	-Ø.8	-Ø.3	-1.Ø	-1.9	-1.3	-Ø.8	-Ø.4	-Ø.4	-Ø.5	-Ø.6	-Ø.6	Ø.5	-Ø.8
8ØØ	-Ø.3	-Ø.5	-Ø.Ø	-Ø.5	-2.1	-1.8	-2.5	-1.6	-Ø.5	-Ø.7	-Ø.3	-Ø.6	-Ø.5	-Ø.9	Ø.8	-1.2
1ØØØ	-3.3	-2.8	-2.Ø	-2.7	-2.9	-2.3	-2.4	-1.9	-1.3	-Ø.7	-Ø.8	Ø.2	-Ø.8	-1.8	1.1	-1.9
125Ø	-2.9	-2.6	-2.6	-3.2	-3.7	-2.9	-3.5	-2.4	-Ø.1	-Ø.4	-Ø.1	-Ø.Ø	Ø.2	-1.9	1.5	-2.1
16ØØ	-3.4	-2.6	-3.6	-4.Ø	-3.7	-3.8	-3.1	-1.7	-Ø.6	-Ø.1	-Ø.8	Ø.2	-Ø.1	-2.1	1.6	-2.4
2ØØØ	-3.4	-3.1	-2.3	-3.7	-3.8	-3.3	-3.6	-3.2	-1.4	-Ø.2	-Ø.3	Ø.2	-Ø.1	-2.2	1.6	-2.8
25ØØ	-4.Ø	-3.3	-2.2	-4.1	-3.4	-2.8	-2.8	-2.1	-Ø.6	Ø.1	-Ø.Ø	Ø.5	-Ø.8	-2.Ø	1.6	-2.3
315Ø	-3.6	-2.8	-2.5	-3.9	-1.6	-1.6	-2.2	-1.3	-Ø.2	Ø.2	Ø.3	Ø.3	-Ø.3	-1.5	1.5	-1.6
4ØØØ	-Ø.2	-Ø.8	-Ø.6	-1.6	-1.2	-1.Ø	-Ø.9	-1.Ø	1.3	1.1	1.6	1.2	Ø.3	-Ø.1	1.1	-Ø.4
5ØØØ	Ø.2	Ø.9	Ø.2	-Ø.7	Ø.6	Ø.1	Ø.3	-Ø.3	1.7	1.5	1.7	Ø.6		Ø.6	Ø.8	Ø.4
63ØØ	1.7	1.9	1.4	Ø.7	1.9	Ø.6	Ø.7	Ø.7	2.4	2.Ø	1.8			1.4	Ø.6	1.3
8ØØØ			1.1	1.8	2.5	1.4	2.Ø	Ø.9	3.4					1.9	Ø.9	2.Ø
1ØØØØ																2.9
125ØØ																
16ØØØ																
2ØØØØ																
25ØØØ																
315ØØ																
4ØØØØ																
5ØØØØ																
63ØØØ																
8ØØØØ																
OASPL	-1.5	-1.1	-Ø.9	-1.7	-1.6	-1.8	-1.7	-1.4	-Ø.3	-Ø.3	-Ø.Ø	-Ø.4	-Ø.Ø			
PNL	-2.4	-2.Ø	-1.5	-2.6	-2.3	-2.1	-2.2	-1.9	-Ø.3	-Ø.2	-Ø.2	-Ø.1	-Ø.4			
PNLT	-3.4	-2.Ø	-1.4	-2.6	-2.3	-2.1	-2.2	-1.8	-Ø.4	-Ø.2	-Ø.2	-Ø.1	-Ø.4			
DBA	-2.4	-2.1	-1.8	-2.7	-2.6	-2.4	-2.6	-1.8	-Ø.6	-Ø.4	-Ø.3	-Ø.2	-Ø.4			

LOCATION	ACOUSTIC RANGE	AVG CORR SPEED	AVG CORR THRUST
C41 ANECH CH	24ØØ.Ø FT SL	-Ø.1E 31 RPM	-Ø.1E 31 LB

TEST CASE FOR TREATED EJECTOR TEØ7 VS TE1Ø

DELTA, SPL(1) - SPL(2)

IDENTIFICATION

INPUT (1) 83F-4ØØ-7ØØ6 X7ØØ65
(2) 83F-4ØØ-ØØØ6 XØØØ65

OUTPUT ITF TE7-T1Ø XØ71Ø1

ANGLES MEASURED FROM INLET, DEGREES

FREQ	4Ø.Ø	5Ø.Ø	6Ø.Ø	7Ø.Ø	8Ø.Ø	9Ø.Ø	1ØØ.Ø	11Ø.Ø	12Ø.Ø	13Ø.Ø	14Ø.Ø	15Ø.Ø	16Ø.Ø	AVG	S.D.	PWL
5Ø	-Ø.1	-Ø.1	Ø.2	-Ø.8	-Ø.2	-Ø.2	3.5	-Ø.7	-Ø.2	-Ø.2	-Ø.2	-Ø.2	-Ø.2	Ø.Ø	1.1	-Ø.2
63	-Ø.4	-Ø.2	-Ø.2	-Ø.5	-Ø.2	-Ø.5	2.5	-Ø.5	Ø.3	Ø.Ø	-Ø.2	Ø.5	Ø.3	Ø.1	Ø.8	Ø.2
8Ø	-Ø.6	-Ø.2	Ø.3	Ø.Ø	-Ø.5	-1.Ø	-Ø.5	-1.Ø	Ø.Ø	Ø.5	Ø.Ø	Ø.8	Ø.3	-Ø.1	Ø.5	Ø.2
1ØØ	-Ø.5	Ø.Ø	Ø.Ø	Ø.Ø	-Ø.2	-Ø.5	Ø.Ø	-Ø.5	-Ø.Ø	-Ø.2	-Ø.2	-Ø.2	-Ø.2	-Ø.2	Ø.2	-Ø.2
125	-Ø.7	Ø.Ø	Ø.Ø	-Ø.2	-Ø.3	-Ø.7	-Ø.3	-1.Ø	Ø.3	-Ø.5	Ø.Ø	-Ø.2	-Ø.2	-Ø.3	Ø.4	-Ø.2
16Ø	-Ø.9	-Ø.2	-Ø.4	-Ø.6	-Ø.5	-Ø.2	-Ø.3	-Ø.5	Ø.3	-Ø.7	Ø.1	Ø.4	-Ø.4	-Ø.3	Ø.4	-Ø.2
2ØØ	-Ø.8	-Ø.Ø	-Ø.3	-Ø.8	Ø.8	-Ø.7	-Ø.3	-Ø.7	Ø.1	-Ø.4	-Ø.2	-Ø.2	-Ø.6	-Ø.3	Ø.4	-Ø.3
25Ø	-Ø.5	Ø.Ø	-Ø.2	Ø.Ø	-Ø.2	Ø.Ø	-Ø.1	-Ø.6	Ø.5	-1.Ø	Ø.3	Ø.3	Ø.2	-Ø.1	Ø.4	-Ø.1
315	-Ø.7	-Ø.5	Ø.3	Ø.Ø	-Ø.Ø	-Ø.8	Ø.3	-Ø.3	Ø.1	-Ø.4	Ø.1	-Ø.1	-Ø.1	-Ø.2	Ø.4	-Ø.2
4ØØ	-Ø.8	-Ø.Ø	-Ø.Ø	Ø.5	Ø.2	Ø.5	Ø.5	-Ø.7	-Ø.1	-Ø.3	Ø.2	Ø.1	Ø.4	Ø.Ø	Ø.4	-Ø.1
5ØØ	-1.Ø	-Ø.Ø	-Ø.3	Ø.2	-Ø.3	-1.Ø	Ø.1	Ø.1	Ø.1	-1.3	-Ø.9	-1.2	-1.5	-Ø.5	Ø.6	-Ø.4
63Ø	-2.8	-2.3	-2.3	-1.7	-Ø.1	-Ø.8	-Ø.9	-1.8	-Ø.6	-Ø.3	Ø.1	Ø.5	Ø.6	-Ø.9	1.1	-1.Ø
8ØØ	-Ø.6	-Ø.6	-Ø.1	-Ø.8	-1.1	-1.6	-1.4	-1.6	-Ø.8	-1.2	-1.Ø	-1.5	-1.4	-1.Ø	Ø.5	-1.1
1ØØØ	-1.3	-1.6	-1.1	-1.6	-1.6	-2.4	-Ø.9	-1.6	-Ø.8	-Ø.9	Ø.Ø	-1.Ø	-Ø.6	-1.2	Ø.6	-1.3
125Ø	-1.6	-1.4	-1.9	-1.4	-1.9	-2.7	-1.8	-2.6	-Ø.9	-1.6	-Ø.9	-Ø.4	-Ø.8	-1.5	Ø.7	-1.8
16ØØ	-1.9	-2.2	-1.2	-1.9	-2.7	-3.7	-1.8	-1.8	-1.5	-1.5	-1.2	-Ø.6	-1.8	-1.8	Ø.8	-2.Ø
2ØØØ	-2.2	-1.9	-1.9	-2.4	-2.1	-3.8	-1.8	-1.9	-Ø.9	-Ø.9	-Ø.2	Ø.1	-Ø.6	-1.6	1.1	-1.9
25ØØ	-1.3	-1.1	-2.1	-2.6	-2.1	-2.4	-1.7	-2.Ø	Ø.5	-Ø.6	Ø.1	1.1	-Ø.2	-1.1	1.2	-1.3
315Ø	-Ø.9	-1.9	-1.4	-1.9	-1.2	-1.7	-Ø.9	-Ø.3	Ø.8	-Ø.2	Ø.3	-Ø.1	-Ø.8	-Ø.8	Ø.8	-Ø.8
4ØØØ	-1.Ø	-1.1	-Ø.6	-Ø.9	-Ø.5	-Ø.2	Ø.4	Ø.5	2.3	Ø.9	1.9	2.Ø	Ø.7	Ø.3	1.2	Ø.4
5ØØØ	-Ø.Ø	1.Ø	-Ø.3	Ø.4	1.3	Ø.5	1.8	-Ø.2	2.6	1.7	1.3	1.5		1.Ø	Ø.9	1.Ø
63ØØ	Ø.9	2.1	1.6	2.2	2.6	1.5	2.2	1.9	3.5	2.8	2.3			2.2	Ø.7	2.1
8ØØØ			3.3	2.8	3.9	3.3	3.3	2.8	4.5					3.4	Ø.6	3.3
1ØØØØ																3.7
125ØØ																
16ØØØ																
2ØØØØ																
25ØØØ																
315ØØ																
4ØØØØ																
5ØØØØ																
63ØØØ																
8ØØØØ																
OASPL	-1.1	-Ø.9	-Ø.8	-1.Ø	-1.Ø	-1.7	-Ø.8	-1.3	-Ø.2	-Ø.6	-Ø.1	Ø.1	-Ø.1			
PNL	-1.5	-1.2	-1.3	-1.6	-1.3	-1.8	-1.Ø	-1.4	Ø.1	-Ø.6	-Ø.3	-Ø.2	-Ø.2			
PNLT	-1.5	-Ø.4	-1.2	-1.5	-1.3	-1.8	-1.Ø	-1.3	Ø.1	-Ø.6	-1.3	1.Ø	-Ø.2			
DBA	-1.5	-1.4	-1.3	-1.5	-1.5	-2.3	-1.3	-1.7	-Ø.5	-Ø.9	-Ø.4	-Ø.4	-Ø.5			

LOCATION	ACOUSTIC RANGE	AVG CORR SPEED	AVG CORR THRUST
C41 ANECH CH	24ØØ.Ø FT SL	-Ø.1E 31 RPM	-Ø.1E 31'LB

TEST CASE FOR TREATED EJECTOR TEØ7 VS TE1Ø

DELTA, SPL(1) - SPL(2)

IDENTIFICATION

INPUT (1) 83F-4ØØ-7Ø1Ø X7Ø1Ø5
(2) 83F-4ØØ-ØØ1Ø XØØ1Ø5

OUTPUT TOF TE7-T1Ø XØ71Ø1

ANGLES MEASURED FROM INLET,DEGREES

FREQ	4Ø.Ø	5Ø.Ø	6Ø.Ø	7Ø.Ø	8Ø.Ø	9Ø.Ø	1ØØ.Ø	11Ø.Ø	12Ø.Ø	13Ø.Ø	14Ø.Ø	15Ø.Ø	16Ø.Ø	AVG	S.D.	PWL
5Ø	Ø.3	Ø.3	Ø.3	-Ø.2	-Ø.6	-1.Ø	3.5	-Ø.5	-Ø.7	Ø.Ø	-Ø.5	-Ø.5	-Ø.5	-Ø.Ø	1.1	-Ø.4
63	-Ø.8	-Ø.4	-Ø.3	Ø.3	-Ø.9	-1.Ø	1.Ø	-Ø.2	-Ø.2	Ø.Ø	Ø.Ø	-Ø.2	-Ø.2	-Ø.2	Ø.5	-Ø.2
8Ø	-1.Ø	-Ø.7	-Ø.2	-Ø.5	-Ø.2	-1.2	-Ø.7	-Ø.7	Ø.Ø	-Ø.2	-Ø.5	Ø.Ø	Ø.Ø	-Ø.5	Ø.4	-Ø.2
1ØØ	-Ø.2	Ø.Ø	Ø.8	-Ø.2	-Ø.5	-Ø.5	-Ø.2	-1.Ø	-Ø.5	-Ø.2	-Ø.5	Ø.Ø	-Ø.2	-Ø.3	Ø.4	-Ø.2
125	Ø.4	Ø.4	-Ø.Ø	-Ø.Ø	-Ø.3	Ø.Ø	Ø.Ø	-Ø.2	Ø.1	Ø.2	-Ø.5	Ø.Ø	-Ø.4	-Ø.Ø	Ø.3	-Ø.1
16Ø	Ø.1	-Ø.4	Ø.9	Ø.2	-Ø.Ø	-1.2	Ø.3	-Ø.2	-Ø.6	-Ø.1	-Ø.3	-Ø.3	-Ø.5	-Ø.2	Ø.5	-Ø.3
2ØØ	Ø.4	-Ø.6	Ø.2	-Ø.5	-Ø.2	-Ø.5	-Ø.Ø	-Ø.6	-Ø.2	-Ø.4	-Ø.7	-Ø.4	-Ø.2	-Ø.3	Ø.3	-Ø.4
25Ø	-Ø.2	Ø.Ø	Ø.5	Ø.Ø	-Ø.3	-Ø.3	Ø.3	-1.2	-Ø.7	-Ø.4	-1.1	-Ø.2	Ø.3	-Ø.3	Ø.5	-Ø.5
315	-Ø.Ø	-Ø.3	Ø.2	-Ø.5	-Ø.5	-Ø.8	Ø.3	-Ø.5	-Ø.6	-Ø.6	-Ø.9	-Ø.7	-1.2	-Ø.5	Ø.4	-Ø.6
4ØØ	Ø.7	-Ø.Ø	Ø.2	-Ø.5	-Ø.5	-Ø.Ø	-Ø.3	-Ø.8	-Ø.4	-Ø.6	-Ø.3	-Ø.2	Ø.4	-Ø.2	Ø.4	-Ø.4
5ØØ	Ø.2	Ø.2	1.Ø	Ø.2	-Ø.1	-Ø.3	Ø.Ø	-Ø.7	-Ø.6	-Ø.6	-Ø.6	-1.Ø	-Ø.3	-Ø.2	Ø.5	-Ø.4
63Ø	-Ø.8	Ø.2	-Ø.1	-Ø.6	-Ø.6	-Ø.4	-Ø.6	-1.1	-1.5	-1.2	-Ø.6	-Ø.6	-Ø.4	-Ø.6	Ø.4	-Ø.9
8ØØ	-Ø.4	-Ø.9	-Ø.4	-Ø.9	-1.7	-1.7	-Ø.1	-Ø.8	-1.1	-1.8	-Ø.7	-Ø.7	-Ø.6	-Ø.9	Ø.5	-1.Ø
1ØØØ	-3.7	-3.7	-2.4	-1.8	-2.Ø	-1.3	-1.2	-Ø.9	-Ø.9	-2.1	-1.3	-1.3	-Ø.9	-1.8	1.Ø	-1.5
125Ø	-1.8	-1.8	-1.1	-1.6	-2.2	-2.9	-Ø.9	-2.1	-Ø.6	-1.9	-1.5	-1.1	-Ø.7	-1.6	Ø.7	-1.6
16ØØ	-1.4	-2.5	-1.5	-1.9	-2.8	-2.3	-1.5	-Ø.9	-1.2	-1.3	-2.2	-1.2	-1.1	-1.7	Ø.6	-1.6
2ØØØ	-2.3	-2.4	-1.9	-2.3	-2.6	-2.3	-1.9	-1.6	-Ø.1	-1.5	-1.1	-1.2	-Ø.9	-1.7	Ø.7	-1.6
25ØØ	-2.1	-1.9	-1.9	-2.9	-2.3	-2.5	-1.1	-1.9	Ø.7	-Ø.3	-Ø.2	Ø.3	-Ø.2	-1.3	1.2	-1.2
315Ø	-1.7	-1.8	-1.3	-2.3	-1.4	-Ø.6	-Ø.3	Ø.4	-Ø.8	-Ø.2	1.Ø	1.4	Ø.3	-Ø.6	1.1	-Ø.6
4ØØØ	-Ø.4	-Ø.4	-Ø.1	-Ø.6	Ø.5	1.2	1.1	-Ø.4	-Ø.3	Ø.4	Ø.8	Ø.7	-Ø.6	Ø.1	Ø.7	Ø.3
5ØØØ	1.2	1.3	1.6	1.Ø	2.2	2.9	2.5	Ø.3	3.Ø	3.9	4.2	4.5		2.4	1.4	2.3
63ØØ	3.3	4.Ø	4.Ø	3.Ø	4.5	4.9	4.8	2.2	5.5	7.1	7.4			4.6	1.6	4.7
8ØØØ			6.8	5.9	7.6	7.5	7.8	4.6	8.4					6.9	1.3	7.2
1ØØØØ																8.6
125ØØ																
16ØØØ																
2ØØØØ																
25ØØØ																
315ØØ																
4ØØØØ																
5ØØØØ																
63ØØØ																
8ØØØØ																
OASPL	-Ø.5	-Ø.8	-Ø.4	-Ø.9	-1.1	-1.2	-Ø.5	-Ø.9	-Ø.6	-Ø.5	-Ø.5	-Ø.2	-Ø.3			
PNL	-1.Ø	-1.4	-1.Ø	-1.6	-1.5	-1.1	-Ø.6	-1.2	-Ø.2	-Ø.7	-Ø.5	-Ø.3	-Ø.4			
PNLT	-1.1	-Ø.6	-1.Ø	-1.6	-2.Ø	-Ø.5	-Ø.6	-1.2	-Ø.2	Ø.Ø	-Ø.5	-Ø.3	-Ø.4			
DBA	-1.3	-1.6	-1.Ø	-1.5	-1.8	-1.6	-Ø.9	-1.2	-Ø.7	-1.2	-Ø.9	-Ø.7	-Ø.5			

LOCATION	ACOUSTIC RANGE	AVG CORR SPEED	AVG CORR THRUST
C41 ANECH CH	24ØØ.Ø FT SL	-Ø.1E 31 RPM	-Ø.1E 31·LB

TEST CASE FOR TREATED EJECTOR TEØ7 VS TE1Ø

DELTA, SPL(1) - SPL(2)

IDENTIFICATION

INPUT (1) 83F-ZER-8ØØ3 X8ØØ35
(2) 83F-ZER-ØØØ3 XØØØ35

OUTPUT CBS TE8-T1Ø XØ81Ø1

ANGLES MEASURED FROM INLET,DEGREES

FREQ	4Ø.Ø	5Ø.Ø	6Ø.Ø	7Ø.Ø	8Ø.Ø	9Ø.Ø	1ØØ.Ø	11Ø.Ø	12Ø.Ø	13Ø.Ø	14Ø.Ø	15Ø.Ø	16Ø.Ø	AVG	S.D.	PWL
5Ø	-Ø.5	Ø.Ø	Ø.Ø	Ø.Ø	Ø.3	-1.2	-Ø.2	-1.5	-Ø.7	-Ø.5	-Ø.7	-1.2	-Ø.7	-Ø.6	Ø.6	-Ø.9
63	-Ø.7	-Ø.2	-Ø.7	-Ø.7	-Ø.7	-2.5	-Ø.5	-1.7	-1.Ø	Ø.5	Ø.Ø	-1.2	-Ø.7	-Ø.8	Ø.8	-Ø.6
8Ø	-Ø.5	Ø.Ø	-Ø.5	-Ø.5	-Ø.2	-Ø.7	-1.2	-1.7	-1.Ø	Ø.3	-Ø.5	-Ø.7	-Ø.7	-Ø.6	Ø.5	-Ø.5
1ØØ	-Ø.5	-Ø.2	-Ø.2	-Ø.7	-Ø.2	-1.Ø	-1.Ø	-1.5	-Ø.7	Ø.Ø	Ø.Ø	-Ø.7	-1.Ø	-Ø.6	Ø.5	-Ø.5
125	-Ø.7	Ø.Ø	-Ø.2	-Ø.2	Ø.Ø	-1.Ø	-Ø.5	-1.2	Ø.Ø	Ø.8	Ø.3	-Ø.2	-Ø.2	-Ø.3	Ø.5	-Ø.Ø
16Ø	-Ø.5	Ø.3	-Ø.5	Ø.Ø	-Ø.2	-1.2	-Ø.5	-1.7	-Ø.2	Ø.Ø	Ø.3	-Ø.5	-Ø.2	-Ø.4	Ø.6	-Ø.3
2ØØ	-Ø.7	Ø.8	-Ø.5	Ø.Ø	-Ø.2	-Ø.7	-Ø.5	-1.5	-Ø.5	Ø.Ø	Ø.3	-Ø.2	Ø.Ø	-Ø.3	Ø.6	-Ø.3
25Ø	-Ø.3	Ø.2	-Ø.8	-Ø.3	-Ø.8	-Ø.5	-1.3	-1.3	-Ø.5	-Ø.3	-Ø.Ø	-Ø.5	-Ø.5	-Ø.5	Ø.4	-Ø.5
315	-Ø.3	-Ø.5	-1.Ø	Ø.2	-Ø.Ø	-Ø.3	-Ø.8	-Ø.8	-Ø.Ø	-Ø.Ø	-Ø.3	-Ø.5	-Ø.3	-Ø.3	Ø.4	-Ø.3
4ØØ	-Ø.5	-Ø.3	-1.8	-Ø.Ø	-Ø.3	-Ø.5	-Ø.5	-Ø.8	-Ø.3	-Ø.Ø	-Ø.8	-Ø.3	-Ø.8	-Ø.5	Ø.5	-Ø.5
5ØØ	-Ø.3	-Ø.3	-2.1	-1.1	-Ø.6	-1.1	-Ø.8	-1.3	-Ø.6	Ø.2	-Ø.8	-Ø.3	-Ø.8	-Ø.8	Ø.6	-Ø.7
63Ø	Ø.1	-Ø.6	-2.6	-1.4	-1.1	-2.1	-1.6	-2.6	-Ø.4	Ø.1	-Ø.9	-Ø.1	-Ø.4	-1.1	1.Ø	-1.2
8ØØ	-Ø.9	-1.2	-3.5	-1.7	-1.9	-2.9	-2.7	-4.Ø	-Ø.7	Ø.Ø	Ø.Ø	Ø.8	-1.2	-1.5	1.4	-1.8
1ØØØ	-1.3	-1.8	-4.6	-2.6	-2.3	-3.5	-3.8	-4.3	-1.3	-Ø.4	-1.1	Ø.2	-Ø.Ø	-2.1	1.6	-2.6
125Ø	-1.6	-1.7	-5.5	-3.2	-3.2	-4.2	-4.4	-3.9	-2.2	-Ø.3	-1.Ø	Ø.3	-Ø.4	-2.4	1.8	-3.Ø
16ØØ	-2.Ø	-2.1	-6.1	-3.3	-4.8	-5.5	-5.5	-5.3	-2.6	-Ø.9	-1.1	-Ø.5	-2.Ø	-3.2	2.Ø	-4.2
2ØØØ	-3.1	-2.5	-6.2	-4.2	-4.6	-6.4	-5.6	-6.4	-3.2	-1.3	-1.9	-1.1	-Ø.6	-3.6	2.1	-5.Ø
25ØØ	-3.3	-3.1	-7.6	-4.3	-4.5	-6.3	-5.5	-5.8	-3.1	-2.2	-1.3	-2.Ø	-1.3	-3.9	2.Ø	-4.9
315Ø	-3.4	-3.2	-7.2	-3.9	-4.4	-5.9	-5.4	-5.2	-3.9	-2.7	-1.9	-Ø.4	-1.9	-3.8	1.9	-4.8
4ØØØ	-2.6	-2.Ø	-6.7	-3.3	-4.1	-5.1	-5.1	-4.6	-3.5	-2.4	-Ø.8	-1.1	-Ø.6	-3.2	1.9	-4.3
5ØØØ	-1.3	-1.2	-5.9	-1.8	-2.9	-3.7	-2.9	-3.6	-2.4	-1.4	Ø.Ø	Ø.2		-2.2	1.7	-3.Ø
63ØØ		1.3	-3.7	Ø.7	-Ø.7	-2.Ø	-1.2	-1.1	-Ø.7	1.6	1.1			-Ø.5	1.7	-1.Ø
8ØØØ				2.Ø	Ø.8	-Ø.6	-Ø.2	Ø.Ø	1.5					Ø.6	1.Ø	Ø.4
1ØØØØ																2.5
125ØØ																
16ØØØ																
2ØØØØ																
25ØØØ																
315ØØ																
4ØØØØ																
5ØØØØ																
63ØØØ																
8ØØØØ																
OASPL	-Ø.6	-Ø.4	-1.7	-1.Ø	-1.2	-2.2	-2.Ø	-2.5	-Ø.7	Ø.1	-Ø.2	-Ø.9	-Ø.7			
PNL	-1.Ø	-1.5	-4.3	-2.6	-2.9	-4.2	-3.8	-4.2	-1.6	-Ø.3	-Ø.3	-Ø.6	-Ø.8			
PNLT	-1.Ø	-1.5	-4.3	-2.6	-2.9	-4.2	-3.8	-3.7	-1.6	-Ø.3	-Ø.4	-Ø.6	-Ø.8			
DBA	-Ø.9	-1.3	-3.9	-2.3	-2.6	-3.8	-3.7	-3.9	-1.2	-Ø.2	-Ø.6	-Ø.2	-Ø.6			

LOCATION	ACOUSTIC RANGE	AVG CORR SPEED	AVG CORR THRUST
C41 ANECH CH	24ØØ.Ø FT SL	-Ø.1E 31 RPM	-Ø.1E 31 LB

TEST CASE FOR TREATED EJECTOR TEØ8 VS TE1Ø

DELTA, SPL(1) - SPL(2)

IDENTIFICATION

INPUT (1) 83F-ZER-8ØØ5 X8ØØ55
(2) 83F-ZER-ØØØ5 XØØØ55

OUTPUT ITS TE8-T1Ø XØ81Ø1

ANGLES MEASURED FROM INLET,DEGREES

FREQ	4Ø.Ø	5Ø.Ø	6Ø.Ø	7Ø.Ø	8Ø.Ø	9Ø.Ø	1ØØ.Ø	11Ø.Ø	12Ø.Ø	13Ø.Ø	14Ø.Ø	15Ø.Ø	16Ø.Ø	AVG	S.D.	PWL
5Ø	-Ø.5	-Ø.5	Ø.Ø	Ø.Ø	-Ø.7	-2.Ø	-Ø.2	-1.5	-1.Ø	-Ø.7	-1.Ø	-1.Ø	-Ø.7	-Ø.8	Ø.6	-Ø.9
63	-Ø.7	Ø.3	-Ø.2	-Ø.5	-Ø.7	-2.7	-Ø.5	-1.5	-1.Ø	Ø.Ø	-1.Ø	-1.2	-Ø.5	-Ø.8	Ø.8	-Ø.9
8Ø	-Ø.5	-Ø.2	-Ø.2	-Ø.2	-1.2	-Ø.7	-Ø.5	-2.Ø	-Ø.5	Ø.Ø	-1.Ø	-1.5	-Ø.7	-Ø.7	Ø.6	-Ø.9
1ØØ	-Ø.7	-Ø.7	-Ø.7	-Ø.5	-Ø.7	-1.Ø	Ø.Ø	-1.5	-Ø.2	-Ø.2	-Ø.5	-1.2	-Ø.5	-Ø.7	Ø.4	-Ø.7
125	-1.5	-Ø.5	-1.Ø	-Ø.7	-Ø.7	-Ø.7	-Ø.7	-1.2	-Ø.7	Ø.3	-1.2	-Ø.7	-Ø.7	-Ø.8	Ø.4	-Ø.7
16Ø	-1.2	-1.Ø	-Ø.5	-Ø.7	-1.2	-Ø.5	-Ø.2	-2.Ø	-1.2	-Ø.2	-Ø.7	-1.Ø	-Ø.5	-Ø.9	Ø.5	-Ø.8
2ØØ	-1.Ø	-Ø.7	-Ø.2	-Ø.7	-1.2	-Ø.5	Ø.Ø	-1.5	-1.Ø	-Ø.7	-Ø.7	-1.2	-Ø.7	-Ø.8	Ø.4	-Ø.9
25Ø	-1.Ø	-Ø.8	-1.Ø	-Ø.5	-Ø.8	-Ø.8	-Ø.5	-1.5	-Ø.8	-Ø.8	-1.Ø	-Ø.8	-1.3	-Ø.9	Ø.3	-Ø.9
315	-Ø.8	-Ø.3	-Ø.8	-Ø.8	-1.Ø	-1.Ø	-Ø.3	-1.5	-Ø.5	-Ø.5	-Ø.8	-Ø.5	-1.3	-Ø.8	Ø.4	-Ø.8
4ØØ	-Ø.8	-Ø.3	-1.Ø	-Ø.3	-1.Ø	-Ø.5	-Ø.Ø	-1.3	-Ø.8	-Ø.3	-1.Ø	-1.Ø	-1.3	-Ø.8	Ø.4	-Ø.8
5ØØ	-1.3	-Ø.8	-1.3	-Ø.6	-1.6	-1.8	-Ø.6	-2.1	-Ø.8	-Ø.8	-1.3	-Ø.8	-2.1	-1.2	Ø.5	-1.2
63Ø	-1.1	-Ø.6	-1.9	-Ø.9	-1.6	-1.9	-Ø.9	-1.9	-1.1	-Ø.7	-1.1	-Ø.9	-1.4	-1.2	Ø.5	-1.2
8ØØ	-1.2	-1.2	-1.7	-1.7	-2.2	-2.2	-1.7	-2.7	-1.2	-Ø.3	-Ø.7	-1.7	-1.9	-1.6	Ø.7	-1.5
1ØØØ	-1.5	-1.8	-2.8	-2.3	-2.8	-2.8	-3.Ø	-3.1	-1.1	-1.1	-1.6	-1.3	-2.3	-2.1	Ø.7	-2.1
125Ø	-2.6	-1.7	-4.5	-2.7	-3.9	-3.7	-3.4	-3.4	-1.7	-1.3	-2.Ø	-2.7	-2.1	-2.8	1.Ø	-2.7
16ØØ	-3.Ø	-2.1	-5.4	-3.1	-4.5	-4.5	-3.8	-4.1	-2.4	-2.2	-2.6	-2.Ø	-2.5	-3.2	1.1	-3.4
2ØØØ	-3.8	-3.Ø	-6.5	-4.2	-5.1	-5.6	-4.1	-4.4	-3.Ø	-2.Ø	-2.2	-2.9	-2.8	-3.8	1.3	-3.9
25ØØ	-3.5	-3.4	-7.1	-4.1	-5.3	-5.8	-4.8	-5.1	-2.9	-1.9	-2.1	-2.3	-3.5	-4.Ø	1.6	-4.3
315Ø	-3.6	-3.4	-7.4	-4.2	-4.7	-4.6	-3.7	-3.9	-3.2	-2.9	-1.7	-2.6	-2.1	-3.7	1.4	-3.8
4ØØØ	-2.8	-2.2	-6.5	-2.8	-3.8	-3.6	-2.8	-3.3	-2.Ø	-1.9	-1.Ø	-1.8	-1.4	-2.8	1.4	-2.9
5ØØØ	-1.3	Ø.4	-4.1	-1.3	-1.9	-2.2	-1.2	-1.6	-Ø.9	-Ø.3	1.1	-Ø.2		-1.1	1.3	-1.3
63ØØ		2.1	-3.1	1.5	Ø.3	-Ø.7	Ø.3	Ø.3	2.4	1.9	2.5			Ø.7	1.7	Ø.6
8ØØØ				3.4	2.1	1.2	2.8	2.9	3.9					2.7	Ø.9	2.8
1ØØØØ																4.7
125ØØ																
16ØØØ																
2ØØØØ																
25ØØØ																
315ØØ																
4ØØØØ																
5ØØØØ																
63ØØØ																
8ØØØØ																
OASPL	-1.1	-Ø.8	-1.3	-1.Ø	-1.8	-2.Ø	-1.3	-2.2	-Ø.9	-Ø.4	-1.Ø	-1.2	-Ø.7			
PNL	-1.4	-1.5	-3.4	-2.5	-3.4	-3.7	-2.7	-3.2	-1.6	-Ø.7	-1.1	-1.4	-1.Ø			
PNLT	-1.4	-Ø.4	-3.4	-2.5	-3.4	-3.7	-2.7	-3.8	-1.Ø	-Ø.7	-Ø.1	-1.4	-1.Ø			
DBA	-1.5	-1.3	-2.9	-2.Ø	-3.Ø	-3.3	-2.6	-3.Ø	-1.4	-Ø.8	-1.2	-1.2	-1.3			

LOCATION	ACOUSTIC RANGE	AVG CORR SPEED	AVG CORR THRUST
C41 ANECH CH	24ØØ.Ø FT SL	-Ø.1E 31 RPM	-Ø.1E 31 LB

TEST CASE FOR TREATED EJECTOR TEØ8 VS TE1Ø

DELTA, SPL(1) - SPL(2)

IDENTIFICATION

INPUT (1) 83F-ZER-8ØØ9 X8ØØ95
(2) 83F-ZER-ØØØ9 XØØØ95

OUTPUT TOS TE8-T1Ø XØ81Ø1

ANGLES MEASURED FROM INLET, DEGREES

FREQ	4Ø.Ø	5Ø.Ø	6Ø.Ø	7Ø.Ø	8Ø.Ø	9Ø.Ø	1ØØ.Ø	11Ø.Ø	12Ø.Ø	13Ø.Ø	14Ø.Ø	15Ø.Ø	16Ø.Ø	AVG	S.D.	PWL
5Ø	-Ø.5	Ø.3	-Ø.2	-Ø.2	-Ø.2	-1.2	1.8	-1.5	-Ø.5	-Ø.5	-1.Ø	-1.5	-1.2	-Ø.5	Ø.9	-1.1
63	-Ø.5	Ø.5	-Ø.2	-Ø.2	Ø.Ø	-2.7	Ø.5	-1.5	-Ø.7	-Ø.5	-1.Ø	-1.2	-Ø.2	-Ø.6	Ø.9	-Ø.9
8Ø	-Ø.7	-Ø.7	-Ø.7	Ø.3	Ø.3	Ø.Ø	-Ø.5	-1.2	Ø.Ø	Ø.Ø	-1.5	-1.2	-1.2	-Ø.6	Ø.6	-1.1
1ØØ	-1.Ø	-Ø.5	-1.Ø	Ø.Ø	Ø.Ø	-Ø.5	-Ø.7	-2.Ø	Ø.Ø	Ø.3	-1.2	-1.Ø	-1.5	-Ø.7	Ø.7	-1.Ø
125	-Ø.5	-Ø.2	-Ø.7	-Ø.7	-Ø.2	-Ø.5	-Ø.2	-1.Ø	-Ø.5	Ø.3	-Ø.7	-Ø.7	-1.7	-Ø.6	Ø.5	-Ø.8
16Ø	-Ø.2	-Ø.5	-Ø.5	-Ø.2	-1.2	-Ø.7	-Ø.5	-1.2	-Ø.5	Ø.5	-Ø.7	-1.Ø	-1.5	-Ø.6	Ø.5	-Ø.8
2ØØ	-Ø.7	Ø.5	-Ø.5	-Ø.5	Ø.Ø	-1.Ø	-Ø.2	-1.5	-Ø.5	-Ø.2	-Ø.7	-Ø.5	-1.Ø	-Ø.5	Ø.5	-Ø.6
25Ø	-Ø.Ø	-Ø.5	-Ø.8	-Ø.8	-Ø.Ø	-Ø.8	-Ø.5	-1.Ø	-Ø.3	-Ø.Ø	-1.Ø	-1.Ø	-Ø.8	-Ø.6	Ø.4	-Ø.7
315	-Ø.8	-Ø.Ø	-1.Ø	-Ø.3	-Ø.3	-Ø.5	-Ø.8	-1.3	-Ø.5	Ø.5	-Ø.5	-1.Ø	-Ø.5	-Ø.5	Ø.5	-Ø.5
4ØØ	-1.Ø	-Ø.3	-Ø.3	-Ø.8	-Ø.5	-Ø.8	-Ø.3	-1.3	-Ø.3	Ø.5	-1.5	-1.Ø	-1.5	-Ø.7	Ø.6	-Ø.8
5ØØ	-Ø.8	-Ø.3	-Ø.6	-Ø.1	-Ø.3	-Ø.8	-Ø.1	-1.3	-Ø.1	Ø.2	-Ø.6	-1.1	-1.1	-Ø.5	Ø.5	-Ø.6
63Ø	-Ø.6	-Ø.9	-Ø.9	-Ø.6	-Ø.1	-Ø.6	-Ø.6	-1.1	-Ø.4	Ø.3	-1.1	-Ø.4	-1.9	-Ø.7	Ø.5	-Ø.6
8ØØ	-1.2	-1.Ø	-2.Ø	-Ø.5	-Ø.7	-1.2	-Ø.7	-1.7	-1.2	-Ø.2	-1.2	-Ø.7	-1.7	-1.1	Ø.5	-1.Ø
1ØØØ	-1.8	-1.3	-2.1	-1.1	-1.3	-1.8	-1.3	-2.1	-1.1	Ø.4	-Ø.8	-1.3	-1.5	-1.3	Ø.6	-1.1
125Ø	-1.9	-1.5	-3.2	-1.9	-1.9	-2.4	-2.4	-2.9	-1.5	-Ø.Ø	-1.5	-1.7	-1.6	-1.9	Ø.8	-1.7
16ØØ	-2.8	-1.9	-4.9	-2.3	-2.3	-3.5	-2.5	-2.6	-1.4	-Ø.7	-2.1	-1.5	-1.Ø	-2.3	1.1	-2.Ø
2ØØØ	-2.3	-3.Ø	-5.2	-2.9	-2.1	-4.1	-2.9	-2.7	-1.7	-1.Ø	-1.9	-1.6	-2.6	-2.6	1.1	-2.3
25ØØ	-3.Ø	-2.6	-5.9	-3.6	-3.Ø	-3.8	-3.3	-3.3	-2.1	-Ø.9	-2.6	-1.3	-2.Ø	-2.9	1.2	-2.7
315Ø	-3.2	-1.9	-6.7	-2.4	-3.2	-3.9	-2.9	-2.7	-1.4	-1.Ø	-1.7	Ø.3	-3.2	-2.6	1.7	-2.3
4ØØØ	-1.6	-Ø.5	-5.5	-1.3	-1.8	-2.1	-1.1	-1.6	Ø.Ø	-Ø.1	-Ø.5	Ø.6	-2.4	-1.4	1.5	-1.Ø
5ØØØ	Ø.2	Ø.6	-4.2	Ø.1	Ø.1	Ø.Ø	Ø.3	Ø.1	1.8	1.9	1.3	2.5		Ø.4	1.7	Ø.8
63ØØ	1.8	3.5	-1.5	2.9	2.Ø	1.5	2.5	2.4	3.8	4.8	4.1			2.5	1.7	3.Ø
8ØØØ			1.5	4.5	4.Ø	3.9	4.5	4.8	6.8	7.4				4.7	1.8	5.5
1ØØØØ																7.7
125ØØ																
16ØØØ																
2ØØØØ																
25ØØØ																
315ØØ																
4ØØØØ																
5ØØØØ																
63ØØØ																
8ØØØØ																
OASPL	-Ø.6	-Ø.4	-1.Ø	-Ø.6	-Ø.6	-1.2	-Ø.7	-1.6	-Ø.5	Ø.1	-1.Ø	-1.Ø	-1.2			
PNL	-Ø.9	-Ø.7	-2.Ø	-1.7	-1.5	-2.5	-1.7	-2.Ø	-Ø.7	Ø.1	-1.Ø	-Ø.8	-1.2			
PNLT	-Ø.9	-Ø.7	-2.Ø	-1.6	-1.5	-2.5	-1.7	-2.Ø	-1.2	Ø.1	-1.Ø	-Ø.8	-1.2			
DBA	-1.Ø	-Ø.9	-2.Ø	-1.2	-1.2	-2.Ø	-1.5	-2.Ø	-Ø.9	Ø.1	-1.1	-Ø.9	-1.2			

LOCATION	ACOUSTIC RANGE	AVG CORR SPEED	AVG CORR THRUST
C41 ANECH CH	24ØØ.Ø FT SL	-Ø.1E 31 RPM	-Ø.1E 31 LB

TEST CASE FOR TREATED EJECTOR TEØ8 VS TE1Ø

DELTA, SPL(1) - SPL(2)

IDENTIFICATION

INPUT (1) 83F-4ØØ-8ØØ4 X8ØØ45
(2) 83F-4ØØ-ØØØ4 XØØØ45

OUTPUT CBF TE8-T1Ø XØ81Ø1

ANGLES MEASURED FROM INLET,DEGREES

FREQ	4Ø.Ø	5Ø.Ø	6Ø.Ø	7Ø.Ø	8Ø.Ø	9Ø.Ø	1ØØ.Ø	11Ø.Ø	12Ø.Ø	13Ø.Ø	14Ø.Ø	15Ø.Ø	16Ø.Ø	AVG	S.D.	PWL
5Ø	-1.2	-Ø.5	-Ø.6	-Ø.5	-Ø.6	-1.Ø	4.5	-2.Ø	-Ø.2	Ø.4	Ø.5	-Ø.3	-1.4	-Ø.2	1.6	-Ø.2
63	-1.Ø	-Ø.5	-Ø.9	-1.1	-Ø.5	-Ø.5	2.8	-Ø.8	Ø.6	Ø.9	Ø.5	1.4	-Ø.8	Ø.Ø	1.2	Ø.4
8Ø	-Ø.7	-Ø.5	-Ø.4	-1.Ø	Ø.1	-1.2	Ø.2	-1.Ø	2.1	2.2	3.Ø	3.Ø	-Ø.8	Ø.4	1.6	1.4
1ØØ	-1.Ø	-Ø.1	-Ø.4	-Ø.4	-Ø.6	-Ø.9	Ø.7	-Ø.2	1.Ø	1.6	2.3	3.1	-Ø.5	Ø.4	1.3	1.Ø
125	-1.Ø	-Ø.5	-1.Ø	-Ø.8	-Ø.2	-1.1	Ø.1	Ø.3	-1.Ø	Ø.Ø	Ø.9	2.9	-1.5	-Ø.2	1.1	Ø.Ø
16Ø	-1.2	Ø.2	-1.Ø	-Ø.3	-Ø.3	-Ø.1	-1.2	-2.4	-Ø.9	-Ø.9	-Ø.2	1.6	-3.Ø	-Ø.7	1.1	-Ø.7
2ØØ	-Ø.8	Ø.3	-Ø.2	-Ø.2	Ø.1	-Ø.7	-Ø.9	-1.9	-Ø.2	-1.3	-Ø.5	2.6	-2.7	-Ø.5	1.2	-Ø.6
25Ø	-Ø.1	Ø.6	-Ø.7	Ø.3	Ø.2	-Ø.9	-Ø.5	-1.3	-1.2	-Ø.8	-Ø.6	2.8	-3.3	-Ø.4	1.4	-Ø.7
315	-Ø.6	Ø.1	-Ø.1	-Ø.2	Ø.5	-Ø.4	-Ø.4	-1.6	Ø.Ø	Ø.2	-Ø.8	4.1	-1.4	-Ø.Ø	1.4	-Ø.1
4ØØ	-Ø.6	Ø.9	-Ø.1	-1.1	-Ø.Ø	-Ø.2	Ø.Ø	-1.1	-Ø.3	-Ø.2	Ø.5	4.Ø	-1.5	Ø.Ø	1.4	-Ø.1
5ØØ	-Ø.3	-Ø.1	-Ø.6	-Ø.4	-Ø.2	-Ø.9	-Ø.1	-Ø.7	-1.5	-Ø.5	-1.4	3.6	-2.4	-Ø.4	1.4	-Ø.6
63Ø	-1.1	Ø.2	-1.4	-Ø.6	-1.8	-2.8	-2.3	-3.3	-1.6	-Ø.3	-Ø.8	4.7	-1.8	-1.Ø	2.Ø	-1.5
8ØØ	-1.1	-Ø.6	-1.6	-1.4	-3.9	-4.1	-3.1	-3.7	-1.8	-1.5	-1.7	3.6	-2.2	-1.8	2.Ø	-2.2
1ØØØ	-3.4	-2.9	-3.6	-4.1	-4.5	-4.1	-3.6	-4.6	-3.Ø	-1.7	-1.9	3.8	-2.2	-2.8	2.2	-3.1
125Ø	-3.1	-3.4	-4.Ø	-4.3	-5.7	-5.4	-4.5	-5.4	-2.3	-2.3	-1.7	2.5	-2.5	-3.2	2.2	-3.8
16ØØ	-4.4	-3.8	-5.5	-6.Ø	-5.7	-6.1	-4.7	-5.3	-2.9	-1.7	-1.9	2.7	-2.6	-3.7	2.5	-4.4
2ØØØ	-4.9	-3.8	-4.4	-5.1	-5.5	-5.3	-4.7	-6.1	-3.6	-2.8	-3.5	1.5	-3.Ø	-3.9	1.9	-4.6
25ØØ	-5.1	-3.6	-4.2	-5.3	-4.9	-5.6	-4.6	-5.4	-2.4	-2.1	-1.8	2.2	-2.1	-3.5	2.2	-4.1
315Ø	-3.8	-3.3	-3.8	-5.2	-4.2	-4.1	-3.1	-4.1	-1.2	-1.Ø	-Ø.8	2.7	-Ø.9	-2.5	2.2	-3.Ø
4ØØØ	-3.2	-2.6	-3.Ø	-4.3	-2.9	-3.4	-2.Ø	-3.Ø	-Ø.4	Ø.6	Ø.9	2.7	-Ø.3	-1.6	2.1	-2.Ø
5ØØØ	-2.4	-1.7	-2.4	-2.9	-1.3	-1.7	-Ø.8	-1.2	Ø.7	1.2	1.6	1.7		-Ø.8	1.6	-1.Ø
63ØØ	-2.1	-Ø.1	-Ø.3	-1.Ø	1.Ø	-Ø.2	-Ø.3	-Ø.4	1.8	2.Ø	1.4			Ø.2	1.3	Ø.1
8ØØØ			2.3	1.7	2.1	Ø.3	1.2	Ø.5	3.4					1.6	1.1	1.9
1ØØØØ																3.1
125ØØ																
16ØØØ																
2ØØØØ																
25ØØØ																
315ØØ																
4ØØØØ																
5ØØØØ																
63ØØØ																
8ØØØØ																
OASPL	-1.9	-1.3	-2.1	-2.3	-2.6	-3.2	-2.3	-3.2	-1.2	-Ø.3	Ø.3	2.5	-1.6			
PNL	-3.2	-2.4	-3.2	-3.7	-3.6	-4.Ø	-3.3	-4.3	-1.7	-1.Ø	-Ø.5	3.2	-2.3			
PNLT	-3.2	-2.4	-3.2	-3.7	-3.6	-3.4	-3.3	-4.3	-1.7	-1.Ø	-Ø.5	3.2	-2.3			
DBA	-3.Ø	-2.4	-3.4	-3.7	-4.2	-4.4	-3.5	-4.3	-2.1	-1.2	-1.2	3.4	-2.2			

LOCATION	ACOUSTIC RANGE	AVG CORR SPEED	AVG CORR THRUST
C41 ANECH CH	24ØØ.Ø FT SL	-Ø.1E 31 RPM	-Ø.1E 81 LB

TEST CASE FOR TREATED EJECTOR TEØ8 VS TE1Ø

DELTA, SPL(1) - SPL(2)

IDENTIFICATION

INPUT (1) 83F-400-8006 X80065
(2) 83F-400-0006 X00065

OUTPUT ITF TE8-T10 X08101

ANGLES MEASURED FROM INLET, DEGREES

FREQ	40.0	50.0	60.0	70.0	80.0	90.0	100.0	110.0	120.0	130.0	140.0	150.0	160.0	AVG	S.D.	PWL
50	0.0	0.0	0.0	0.0	0.2	0.0	4.0	-1.0	-0.5	0.0	-0.7	-0.2	-0.7	0.1	1.2	-0.3
63	-0.1	0.4	-0.0	0.2	-0.3	-0.7	2.8	-1.5	-0.2	0.3	-0.5	0.0	-0.7	-0.0	1.0	-0.2
80	-0.7	-0.2	-0.1	0.2	-0.3	-1.0	-0.2	-1.2	0.4	1.5	1.0	1.7	-0.1	0.1	0.9	0.7
100	-0.3	0.6	-0.4	0.2	-0.5	-0.5	0.2	-0.5	-0.7	0.1	-0.0	1.0	-0.4	-0.1	0.5	-0.0
125	-0.7	0.3	-0.5	0.0	-0.4	-1.0	-0.2	-1.3	-0.3	-0.2	-0.2	0.5	-0.8	-0.4	0.5	-0.3
160	-1.1	-0.1	-0.6	-0.5	-0.6	-0.7	-0.4	-1.4	-0.9	-0.6	-0.1	0.7	-1.4	-0.6	0.6	-0.5
200	-1.1	-0.1	-0.2	-0.4	0.0	-0.7	-1.0	-1.3	-0.2	-0.2	-0.2	0.8	-0.5	-0.4	0.6	-0.4
250	-0.2	0.8	-0.5	-0.2	-0.5	-0.8	-0.4	-1.2	0.0	-0.5	-0.3	0.4	-1.0	-0.3	0.5	-0.4
315	-0.3	0.2	-0.3	-0.0	-0.3	-0.8	0.1	-0.7	-1.4	-0.4	0.2	1.1	-0.5	-0.2	0.6	-0.4
400	-0.5	0.2	-0.5	-0.0	-0.0	-0.3	-0.1	-1.4	-1.1	0.1	-0.1	0.7	-0.5	-0.3	0.6	-0.4
500	-0.5	0.2	-0.3	-0.3	-0.9	-1.6	0.2	-0.6	-0.6	-0.7	-0.5	0.5	-1.1	-0.5	0.6	-0.6
630	-2.9	-1.9	-3.3	-1.5	-1.7	-2.1	-0.9	-2.0	-1.7	-0.3	-0.5	0.5	-1.2	-1.5	1.0	-1.5
800	-2.9	-2.4	-2.6	-2.0	-2.8	-2.9	-2.7	-2.3	-1.6	-0.8	-1.3	-0.3	-1.3	-2.0	0.9	-2.0
1000	-4.0	-3.5	-3.9	-3.6	-4.1	-4.1	-2.0	-3.4	-2.3	-1.3	-1.1	-0.3	-1.7	-2.7	1.3	-2.7
1250	-4.6	-3.6	-5.1	-3.5	-4.5	-4.9	-3.5	-4.1	-3.0	-2.4	-2.0	-0.6	-1.9	-3.4	1.3	-3.6
1600	-4.7	-4.3	-4.5	-4.3	-5.1	-5.8	-4.1	-4.1	-3.7	-2.0	-1.9	-0.8	-2.7	-3.7	1.4	-4.0
2000	-5.3	-3.9	-6.4	-5.0	-4.9	-5.9	-4.2	-3.9	-3.6	-2.5	-2.0	-1.5	-2.6	-4.0	1.5	-4.3
2500	-2.9	-2.5	-5.8	-5.0	-5.1	-6.3	-4.5	-4.7	-3.8	-4.8	-3.6	-3.4	-3.3	-4.3	1.1	-4.5
3150	-2.6	-2.9	-6.2	-3.9	-5.0	-4.7	-4.3	-4.0	-2.5	-2.6	-2.3	-2.7	-1.9	-3.5	1.3	-3.7
4000	-2.7	-2.3	-6.0	-4.0	-3.9	-3.9	-3.2	-2.8	-0.9	-1.6	-1.4	-2.5	-0.9	-2.8	1.5	-2.8
5000	-1.2	-1.1	-6.0	-2.4	-1.9	-2.7	-1.5	-1.8	0.3	0.1	-0.0	-2.6		-1.7	1.7	-1.6
6300	-0.5	0.1	-4.9	-1.3	0.4	-1.4	-0.6	-0.2	2.3	2.7	2.1			-0.1	2.1	-0.1
8000			-2.3	1.1	2.5	1.7	1.5	1.4	4.7					1.5	2.1	2.1
10000																3.3
12500																
16000																
20000																
25000																
31500																
40000																
50000																
63000																
80000																
OASPL	-1.9	-1.3	-2.2	-1.7	-2.2	-2.9	-1.7	-2.3	-1.3	-0.3	-0.3	0.5	-0.7			
PNL	-3.2	-2.2	-3.9	-3.2	-3.5	-4.2	-2.9	-3.2	-2.3	-1.0	-0.9	-0.1	-1.2			
PNLT	-2.1	-2.2	-4.0	-3.3	-3.5	-4.2	-2.9	-3.2	-2.3	-1.0	-2.0	-0.1	-1.2			
DBA	-3.4	-2.7	-3.8	-3.0	-3.7	-4.2	-2.8	-3.1	-2.2	-1.1	-1.0	0.0	-1.2			

LOCATION	ACOUSTIC RANGE	AVG CORR SPEED	AVG CORR THRUST
C41 ANECH CH	2400.0 FT SL	-0.1E 31 RPM	-0.1E 31 LB

TEST CASE FOR TREATED EJECTOR TE08 VS TE10

DELTA, SPL(1) - SPL(2)

IDENTIFICATION

INPUT (1) 83F-4ØØ-8Ø1Ø X8Ø1Ø5
(2) 83F-4ØØ-ØØ1Ø XØØ1Ø5

OUTPUT TOF TE8-T1Ø XØ81Ø1

ANGLES MEASURED FROM INLET,DEGREES

FREQ	4Ø.Ø	5Ø.Ø	6Ø.Ø	7Ø.Ø	8Ø.Ø	9Ø.Ø	1ØØ.Ø	11Ø.Ø	12Ø.Ø	13Ø.Ø	14Ø.Ø	15Ø.Ø	16Ø.Ø	AVG	S.D.	PWL
5Ø	-Ø.1	1.2	Ø.6	Ø.7	Ø.Ø	-Ø.9	3.7	-1.1	-Ø.5	Ø.Ø	-Ø.2	4.Ø	-Ø.7	Ø.5	1.6	1.8
63	-Ø.7	Ø.3	-Ø.Ø	Ø.8	Ø.3	-Ø.6	1.5	-Ø.5	-Ø.3	Ø.Ø	-Ø.5	4.3	-Ø.7	Ø.3	1.4	2.Ø
8Ø	-Ø.3	Ø.2	Ø.1	Ø.5	Ø.4	-Ø.8	-Ø.5	-Ø.8	Ø.Ø	1.2	-Ø.3	4.9	-Ø.8	Ø.3	1.5	2.5
1ØØ	-Ø.Ø	1.2	Ø.4	Ø.2	Ø.9	-Ø.Ø	Ø.7	-Ø.5	-Ø.1	Ø.1	Ø.1	5.3	-Ø.5	Ø.6	1.5	2.2
125	Ø.7	1.7	Ø.2	Ø.7	-Ø.Ø	Ø.5	1.2	Ø.1	-Ø.5	Ø.Ø	-Ø.5	4.8	-Ø.7	Ø.6	1.4	1.4
16Ø	Ø.Ø	Ø.8	1.Ø	1.5	Ø.5	-Ø.3	Ø.2	-Ø.2	-Ø.2	-Ø.2	Ø.3	4.7	-Ø.4	Ø.6	1.4	1.2
2ØØ	1.Ø	Ø.5	Ø.2	Ø.5	Ø.7	-Ø.8	Ø.4	-1.Ø	-Ø.4	-Ø.1	Ø.Ø	5.2	Ø.1	Ø.5	1.5	Ø.6
25Ø	-Ø.Ø	1.2	Ø.2	Ø.7	Ø.5	-Ø.1	Ø.8	-Ø.8	-Ø.4	-Ø.Ø	-Ø.1	6.Ø	Ø.4	Ø.6	1.7	Ø.7
315	Ø.2	1.Ø	Ø.7	Ø.2	1.Ø	Ø.2	Ø.1	-Ø.Ø	-Ø.4	-Ø.6	Ø.Ø	5.3	-Ø.8	Ø.5	1.5	Ø.4
4ØØ	Ø.2	Ø.2	1.Ø	1.Ø	-Ø.1	-Ø.1	-Ø.7	-Ø.5	-Ø.5	-Ø.4	Ø.8	5.4	Ø.3	Ø.5	1.6	Ø.5
5ØØ	-Ø.Ø	Ø.7	Ø.4	Ø.9	Ø.1	Ø.2	-Ø.1	-1.4	-1.2	Ø.2	-Ø.2	4.5	-Ø.7	Ø.3	1.4	Ø.1
63Ø	-Ø.6	Ø.7	-Ø.3	Ø.7	-Ø.2	-Ø.2	-1.3	-1.5	-1.3	-1.Ø	Ø.1	5.1	-Ø.7	-Ø.Ø	1.7	-Ø.2
8ØØ	-Ø.1	Ø.4	-Ø.7	Ø.1	-Ø.5	-1.5	-Ø.7	-1.7	-1.5	-Ø.5	-Ø.7	4.5	-Ø.8	-Ø.3	1.6	-Ø.4
1ØØØ	-3.7	-2.5	-3.7	-1.1	-2.1	-1.3	-1.5	-1.3	-1.9	-1.7	-Ø.9	3.8	-1.4	-1.5	1.8	-1.2
125Ø	-Ø.8	-Ø.1	-2.4	-1.1	-1.7	-3.Ø	-1.6	-2.7	-1.6	-1.7	-1.9	3.5	-2.Ø	-1.3	1.6	-1.4
16ØØ	-1.2	-1.Ø	-3.Ø	-1.5	-2.4	-2.6	-2.9	-2.7	-2.5	-2.Ø	-2.5	2.3	-2.5	-1.9	1.4	-2.Ø
2ØØØ	-2.1	-1.7	-4.2	-2.4	-3.2	-3.7	-3.3	-3.3	-2.3	-2.2	-2.8	Ø.9	-2.4	-2.5	1.2	-2.6
25ØØ	-2.4	-2.8	-5.5	-3.2	-3.9	-3.8	-4.Ø	-4.1	-2.Ø	-2.2	-1.9	1.6	-2.5	-2.8	1.7	-3.Ø
315Ø	-2.1	-2.7	-5.9	-3.4	-3.2	-3.2	-3.2	-2.6	-1.2	-Ø.7	-Ø.5	3.1	-Ø.3	-2.Ø	2.2	-2.2
4ØØØ	-2.Ø	-2.3	-5.8	-2.7	-1.9	-1.9	-1.6	-1.5	-Ø.4	1.1	Ø.9	2.1	Ø.2	-1.2	2.Ø	-1.2
5ØØØ	-1.4	-Ø.8	-5.1	-1.1	-Ø.2	Ø.3	-Ø.6	Ø.6	1.8	2.2	1.1	2.3		-Ø.1	2.Ø	Ø.2
63ØØ	Ø.7	1.3	-3.9	1.2	1.9	1.3	1.1	1.4	3.9	4.7	4.5			1.6	2.3	1.9
8ØØØ			-1.6	2.8	3.8	3.7	3.5	3.2	7.Ø					3.2	2.5	4.2
1ØØØØ																5.2
125ØØ																
16ØØØ																
2ØØØØ																
25ØØØ																
315ØØ																
4ØØØØ																
5ØØØØ																
63ØØØ																
8ØØØØ																
OASPL	-Ø.4	Ø.1	-Ø.8	-Ø.1	-Ø.7	-1.2	-Ø.9	-1.4	-Ø.9	-Ø.2	-Ø.2	4.7	-Ø.6			
PNL	-Ø.9	-Ø.7	-2.5	-1.2	-2.Ø	-2.3	-2.1	-2.4	-1.4	-Ø.5	-Ø.2	4.6	-Ø.7			
PNLT	-2.Ø	Ø.1	-2.5	-1.2	-2.Ø	-2.3	-2.1	-2.9	-1.5	Ø.1	-1.3	4.6	-Ø.7			
DBA	-1.1	-Ø.6	-2.1	-Ø.9	-1.6	-2.Ø	-1.8	-2.1	-1.5	-Ø.9	-Ø.6	4.4	-Ø.7			

LOCATION	ACOUSTIC RANGE	AVG CORR SPEED	AVG CORR THRUST
C41 ANECH CH	24ØØ.Ø FT SL	-Ø.1E 31 RPM	-Ø.1E 31 LB

TEST CASE FOR TREATED EJECTOR TEØ8 VS TE1Ø

DELTA, SPL(1) - SPL(2)

IDENTIFICATION

INPUT (1) 83F-ZER-2ØØ3 X2ØØ35
(2) 83F-ZER-5ØØ3 X5ØØ35

OUTPUT CBS TE2-TE5 XØ2Ø51

ANGLES MEASURED FROM INLET,DEGREES

FREQ	4Ø.Ø	5Ø.Ø	6Ø.Ø	7Ø.Ø	8Ø.Ø	9Ø.Ø	1ØØ.Ø	11Ø.Ø	12Ø.Ø	13Ø.Ø	14Ø.Ø	15Ø.Ø	16Ø.Ø	AVG	S.D.	PWL
5Ø	-Ø.5	-1.Ø	-Ø.3	-Ø.5	-Ø.Ø	-1.Ø	-1.Ø	Ø.6	Ø.2	-Ø.5	Ø.2	3.2	2.7	Ø.2	1.4	1.6
63	-1.8	-1.Ø	-Ø.3	-Ø.3	-Ø.3	Ø.2	Ø.2	Ø.8	-Ø.3	1.Ø	Ø.7	3.2	2.7	Ø.4	1.4	1.6
8Ø	-Ø.Ø	-1.8	-Ø.Ø	Ø.3	-Ø.8	-Ø.Ø	Ø.2	Ø.6	Ø.2	Ø.2	Ø.2	2.2	1.7	Ø.3	1.Ø	Ø.8
1ØØ	-Ø.3	-Ø.3	-Ø.5	-Ø.1	-1.Ø	-Ø.8	-Ø.Ø	-Ø.4	-Ø.Ø	-Ø.5	Ø.2	1.5	2.2	Ø.Ø	Ø.9	Ø.3
125	Ø.5	-Ø.8	-Ø.Ø	Ø.4	-Ø.Ø	-Ø.8	-Ø.3	Ø.1	-1.Ø	-Ø.3	-1.3	1.5	1.2	-Ø.Ø	Ø.8	-Ø.2
16Ø	-Ø.7	-1.7	Ø.3	-Ø.6	Ø.3	Ø.3	-Ø.2	Ø.1	-1.2	-Ø.7	-Ø.5	Ø.8	Ø.5	-Ø.3	Ø.7	-Ø.4
2ØØ	Ø.Ø	-1.2	-Ø.2	-Ø.1	-Ø.5	-1.Ø	-Ø.5	-Ø.1	-Ø.2	Ø.3	-Ø.7	-2.Ø	Ø.Ø	-Ø.5	Ø.6	-Ø.5
25Ø	-Ø.2	-Ø.7	-Ø.2	Ø.5	-Ø.7	-Ø.2	Ø.Ø	Ø.4	-1.Ø	Ø.Ø	-Ø.7	-Ø.5	-1.2	-Ø.4	Ø.5	-Ø.4
315	-Ø.2	-1.Ø	-Ø.7	-Ø.1	-Ø.5	-1.2	Ø.3	Ø.4	-Ø.2	Ø.Ø	-2.2	-2.2	-1.Ø	-Ø.7	Ø.8	-Ø.6
4ØØ	-Ø.2	-1.5	-1.Ø	-Ø.6	-Ø.5	-Ø.7	-Ø.2	Ø.1	Ø.3	-Ø.7	-1.2	-2.Ø	-Ø.7	-Ø.7	Ø.6	-Ø.5
5ØØ	-Ø.Ø	-Ø.3	-Ø.3	-Ø.5	-Ø.8	-Ø.5	-Ø.5	Ø.3	-Ø.8	-Ø.5	-2.3	-3.5	-Ø.5	-Ø.8	1.Ø	-Ø.8
63Ø	Ø.2	-Ø.Ø	-Ø.Ø	-Ø.4	-Ø.Ø	-Ø.Ø	Ø.2	-Ø.2	-Ø.8	-Ø.8	-2.3	-2.8	-Ø.8	-Ø.6	Ø.9	-Ø.7
8ØØ	Ø.7	1.Ø	2.Ø	1.4	1.Ø	Ø.7	1.2	Ø.8	-Ø.8	-Ø.5	-1.8	-2.3	-Ø.3	Ø.2	1.3	Ø.Ø
1ØØØ	1.7	2.4	1.9	2.5	1.7	1.9	1.9	2.3	Ø.2	-Ø.8	-1.8	-2.8	-Ø.1	Ø.9	1.8	Ø.9
125Ø	2.7	2.4	2.9	3.4	2.4	2.7	3.2	2.8	-Ø.1	-1.6	-1.4	-3.8	-Ø.8	1.1	2.4	1.3
16ØØ	2.9	3.1	2.8	2.9	2.3	2.8	4.1	3.2	Ø.1	-1.Ø	-1.9	-4.2	-1.9	1.2	2.6	1.8
2ØØØ	3.5	3.2	3.Ø	2.6	2.7	2.2	3.Ø	3.3	-Ø.Ø	-1.6	-2.3	-6.Ø	-1.7	Ø.9	3.Ø	1.7
25ØØ	1.9	2.5	1.8	1.3	2.6	1.9	2.4	3.7	Ø.3	-2.3	-3.4	-4.9	-2.9	Ø.4	2.8	1.7
315Ø	Ø.7	1.3	2.3	1.9	1.9	Ø.4	Ø.9	2.Ø	-Ø.2	-1.8	-3.4	-5.6	-3.1	-Ø.2	2.5	Ø.8
4ØØØ	Ø.4	Ø.8	1.8	-Ø.6	Ø.4	-1.1	-Ø.1	1.5	-1.2	-1.6	-4.9	-6.1	-3.8	-1.1	2.4	-Ø.1
5ØØØ	-Ø.3	-Ø.1	-Ø.1	-1.Ø	-Ø.1	-2.1	Ø.1	Ø.9	-1.3	-1.5	-5.Ø	-6.6		-1.4	2.2	-Ø.6
63ØØ		Ø.7	-Ø.1	-1.Ø	-Ø.4	-2.1	1.1	1.2	-1.1	-1.Ø	-5.3			-Ø.8	1.9	-Ø.4
8ØØØ				Ø.5	1.6	-Ø.9	1.9	2.9	-Ø.3					1.Ø	1.4	Ø.8
1ØØØØ																3.6
125ØØ																
16ØØØ																
2ØØØØ																
25ØØØ																
315ØØ																
4ØØØØ																
5ØØØØ																
63ØØØ																
8ØØØØ																
OASPL	Ø.2	-Ø.3	Ø.5	Ø.6	Ø.4	Ø.4	Ø.9	1.Ø	-Ø.4	-Ø.2	-Ø.4	1.6	2.1			
PNL	1.6	1.4	1.6	1.2	1.4	1.1	1.7	2.1	-Ø.2	-Ø.7	-1.4	-1.4	Ø.Ø			
PNLT	1.6	1.4	1.6	1.2	1.4	1.1	1.7	2.1	-Ø.2	-Ø.7	-1.4	-1.4	Ø.Ø			
DBA	1.2	1.2	1.6	1.7	1.5	1.4	2.Ø	2.Ø	-Ø.3	-Ø.7	-1.7	-2.4	-Ø.3			

LOCATION	ACOUSTIC RANGE	AVG CORR SPEED	AVG CORR THRUST
C41 ANECH CH	24ØØ.Ø FT SL	-Ø.1E 31 RPM	-Ø.1E 31' LB

TEST CASE FOR TREATED EJECTOR TEØ2 VS TEØ5

DELTA, SPL(1) - SPL(2)

IDENTIFICATION

INPUT (1) 83F-ZER-2ØØ5 X2ØØ55
(2) 83F-ZER-5ØØ5 X5ØØ55

OUTPUT ITS TE2-TE5 XØ2Ø51

ANGLES MEASURED FROM INLET,DEGREES

FREQ	4Ø.Ø	5Ø.Ø	6Ø.Ø	7Ø.Ø	8Ø.Ø	9Ø.Ø	1ØØ.Ø	11Ø.Ø	12Ø.Ø	13Ø.Ø	14Ø.Ø	15Ø.Ø	16Ø.Ø	AVG	S.D.	PWL
5Ø	-Ø.5	-1.3	Ø.2	Ø.2	-Ø.Ø	-Ø.5	-Ø.3	1.3	Ø.5	-Ø.Ø	1.2	2.7	1.5	Ø.4	1.1	1.6
63	-1.Ø	-1.Ø	Ø.5	Ø.2	-Ø.5	-Ø.5	Ø.5	1.1	Ø.5	1.2	1.2	4.Ø	2.2	Ø.7	1.4	2.2
8Ø	-Ø.Ø	-1.5	Ø.5	Ø.4	-Ø.8	-Ø.5	Ø.7	Ø.6	-Ø.Ø	-Ø.3	1.Ø	3.2	3.Ø	Ø.5	1.3	1.6
1ØØ	-Ø.5	-Ø.5	-Ø.5	Ø.Ø	-Ø.5	-Ø.5	Ø.2	-Ø.2	-Ø.8	-Ø.3	1.5	2.7	3.Ø	Ø.3	1.3	1.1
125	-Ø.5	-1.3	-Ø.Ø	Ø.Ø	-Ø.5	-Ø.8	-Ø.3	-Ø.2	-Ø.5	-Ø.8	Ø.5	2.7	1.7	Ø.Ø	1.1	Ø.4
16Ø	-Ø.2	-1.5	-Ø.7	-1.2	-Ø.2	-Ø.5	-Ø.5	-Ø.1	-1.2	-Ø.5	1.Ø	1.Ø	Ø.8	-Ø.3	Ø.8	-Ø.1
2ØØ	Ø.3	-1.5	-Ø.2	-Ø.1	-Ø.7	-1.Ø	-Ø.2	Ø.1	-Ø.2	-Ø.2	Ø.5	Ø.5	1.Ø	-Ø.1	Ø.7	Ø.Ø
25Ø	-Ø.7	-1.7	-Ø.7	-Ø.3	-Ø.7	-Ø.7	Ø.5	-Ø.4	-Ø.5	-Ø.2	Ø.3	1.8	Ø.5	-Ø.2	Ø.9	Ø.Ø
315	-Ø.5	-Ø.5	-1.Ø	-Ø.2	-Ø.2	-1.Ø	Ø.5	Ø.4	-1.Ø	-1.2	-Ø.2	Ø.5	-Ø.2	-Ø.4	Ø.6	-Ø.4
4ØØ	-Ø.2	-2.Ø	-1.Ø	-1.Ø	-Ø.7	-Ø.5	Ø.Ø	Ø.4	-1.Ø	-1.Ø	Ø.8	Ø.5	-Ø.7	-Ø.5	Ø.8	-Ø.3
5ØØ	-Ø.8	-1.Ø	-Ø.5	-Ø.9	-1.Ø	-1.Ø	-Ø.5	Ø.6	-1.3	-1.3	-Ø.8	Ø.2	-Ø.5	-Ø.7	Ø.5	-Ø.6
63Ø	-Ø.3	-1.3	-Ø.5	-Ø.9	-Ø.5	-1.Ø	-Ø.Ø	-Ø.4	-1.Ø	-Ø.8	-Ø.8	Ø.7	-Ø.Ø	-Ø.5	Ø.5	-Ø.5
8ØØ	Ø.5	-Ø.3	1.Ø	Ø.7	Ø.2	-Ø.5	Ø.5	-Ø.2	-1.3	-1.Ø	Ø.2	Ø.2	Ø.2	Ø.Ø	Ø.7	-Ø.3
1ØØØ	Ø.2	Ø.4	1.2	1.2	Ø.7	-Ø.3	Ø.9	1.5	-Ø.6	-1.1	Ø.7	-Ø.1	-Ø.6	Ø.3	Ø.8	Ø.3
125Ø	Ø.7	Ø.4	Ø.9	Ø.4	1.2	Ø.9	1.9	1.Ø	-1.1	-Ø.9	-Ø.1	Ø.7	-1.8	Ø.3	1.Ø	Ø.4
16ØØ	Ø.1	-Ø.7	Ø.3	-Ø.5	Ø.6	1.3	2.3	Ø.7	Ø.1	-Ø.7	-Ø.9	Ø.1	-Ø.1	Ø.2	Ø.9	Ø.5
2ØØØ	-Ø.7	-Ø.8	-Ø.8	-1.4	Ø.5	-Ø.Ø	1.7	1.1	Ø.5	-Ø.8	-Ø.5	-Ø.8	-Ø.2	-Ø.2	Ø.9	Ø.3
25ØØ	-1.4	-2.2	-2.5	-3.7	-1.7	-1.1	Ø.8	1.7	Ø.5	-2.Ø	-Ø.9	Ø.6	-Ø.6	-1.Ø	1.5	-Ø.5
315Ø	-2.8	-3.4	-2.4	-3.8	-1.8	-2.8	-Ø.6	Ø.7	Ø.1	-Ø.8	-1.2	-Ø.3	Ø.4	-1.4	1.5	-1.4
4ØØØ	-3.8	-3.7	-1.7	-4.1	-2.9	-3.8	-2.1	-Ø.3	-1.5	-1.8	-1.4	-Ø.6	Ø.7	-2.1	1.5	-2.3
5ØØØ	-4.1	-4.6	-3.8	-5.2	-3.7	-4.1	-1.2	-1.1	-1.8	-2.Ø	-1.8	-1.1		-2.9	1.5	-2.6
63ØØ	-3.3	-4.3	-3.8	-5.Ø	-3.4	-4.9	-Ø.9	-1.1	-2.1	-2.Ø	-2.5			-3.Ø	1.4	-2.7
8ØØØ			-3.6	-4.8	-2.1	-4.4	-Ø.4	Ø.6	-1.1					-2.2	2.1	-2.Ø
1ØØØØ																Ø.3
125ØØ																
16ØØØ																
2ØØØØ																
25ØØØ																
315ØØ																
4ØØØØ																
5ØØØØ																
63ØØØ																
8ØØØØ																
OASPL	-Ø.3	-1.1	-Ø.3	-Ø.5	-Ø.3	-Ø.5	Ø.5	Ø.4	-Ø.6	-Ø.4	Ø.8	2.6	1.9			
PNL	-Ø.7	-1.2	-1.Ø	-1.9	-Ø.9	-1.Ø	Ø.6	Ø.7	-Ø.5	-Ø.8	Ø.4	1.3	1.3			
PNLT	-Ø.8	-1.2	-1.Ø	-1.9	-Ø.9	-1.Ø	Ø.6	Ø.2	-Ø.5	-Ø.8	Ø.4	1.3	1.3			
DBA	-Ø.2	-Ø.8	-Ø.2	-Ø.9	-Ø.1	-Ø.3	1.Ø	Ø.7	-Ø.8	-Ø.9	Ø.Ø	Ø.6	Ø.2			

LOCATION	ACOUSTIC RANGE	AVG CORR SPEED	AVG CORR THRUST
C41 ANECH CH	24ØØ.Ø FT SL	-Ø.1E 31 RPM	-Ø.1E 31'LB

TEST CASE FOR TREATED EJECTOR TEØ2 VS TEØ5

DELTA, SPL(1) - SPL(2)

IDENTIFICATION

INPUT (1) 83F-ZER-2ØØ9 X2ØØ95
(2) 83F-ZER-5ØØ9 X5ØØ95

OUTPUT TOS TE2-TE5 XØ2Ø51

ANGLES MEASURED FROM INLET,DEGREES

FREQ	4Ø.Ø	5Ø.Ø	6Ø.Ø	7Ø.Ø	8Ø.Ø	9Ø.Ø	1ØØ.Ø	11Ø.Ø	12Ø.Ø	13Ø.Ø	14Ø.Ø	15Ø.Ø	16Ø.Ø	AVG	S.D.	PWL
5Ø	-1.3	-2.3	-1.Ø	-1.Ø	-1.3	-1.3	-2.Ø	-3.3	-1.8	-1.3	-1.3	Ø.2	Ø.5	-1.3	1.Ø	-Ø.3
63	-1.8	-2.3	-1.Ø	-Ø.6	-1.3	-1.5	-Ø.3	-1.3	-1.5	-Ø.3	Ø.2	Ø.7	-Ø.3	-Ø.8	Ø.9	Ø.1
8Ø	-1.Ø	-1.8	-Ø.8	-Ø.2	-1.Ø	-1.Ø	-Ø.3	-Ø.5	-1.Ø	-1.3	Ø.2	Ø.2	-Ø.Ø	-Ø.6	Ø.6	-Ø.Ø
1ØØ	-Ø.8	-1.Ø	-Ø.5	-Ø.7	-1.5	-2.5	-Ø.8	-1.4	-1.5	-1.5	Ø.5	-Ø.5	Ø.2	-Ø.9	Ø.8	-Ø.3
125	1.Ø	-Ø.Ø	Ø.2	Ø.8	-Ø.8	-1.5	-1.8	-1.4	-1.3	-1.8	-1.3	-Ø.3	Ø.2	-Ø.6	1.Ø	-Ø.5
16Ø	-1.2	-2.Ø	-Ø.5	-Ø.7	-Ø.5	-Ø.5	-Ø.7	-1.8	-2.Ø	-1.7	-Ø.7	-Ø.7	-Ø.5	-1.1	Ø.6	-Ø.9
2ØØ	-Ø.7	-3.Ø	-1.7	-Ø.7	-1.2	-1.7	-1.Ø	-2.Ø	-1.Ø	-Ø.2	-1.5	-1.2	-Ø.5	-1.3	Ø.7	-1.1
25Ø	Ø.Ø	-Ø.7	-Ø.7	-Ø.5	-1.7	-2.2	-Ø.5	-2.Ø	-1.Ø	Ø.Ø	-1.Ø	-Ø.2	-Ø.7	-Ø.9	Ø.7	-Ø.7
315	-Ø.2	-1.2	-Ø.7	-Ø.5	-1.Ø	-2.Ø	-Ø.5	-Ø.3	-Ø.2	-Ø.2	-1.2	-Ø.7	-Ø.2	-Ø.7	Ø.5	-Ø.7
4ØØ	-Ø.5	-2.Ø	-Ø.7	-1.2	-1.7	-1.7	-1.5	-Ø.6	-Ø.2	-1.Ø	-Ø.7	-Ø.5	-1.Ø	-1.Ø	Ø.6	-Ø.8
5ØØ	1.5	-1.Ø	-1.Ø	-Ø.5	-1.Ø	-2.3	-1.3	-Ø.4	-1.Ø	-Ø.3	-1.8	-1.3	-1.Ø	-Ø.9	Ø.9	-1.1
63Ø	3.Ø	1.Ø	Ø.7	-Ø.2	-1.3	-1.3	-Ø.8	-Ø.8	-Ø.8	-Ø.3	-Ø.8	-Ø.5	-1.3	-Ø.2	1.2	-Ø.6
8ØØ	2.Ø	2.2	3.Ø	1.6	Ø.5	-1.Ø	-Ø.3	Ø.1	-Ø.8	-Ø.3	-1.Ø	Ø.2	-1.5	Ø.4	1.4	-Ø.2
1ØØØ	2.2	1.7	2.9	2.4	Ø.7	-Ø.6	-Ø.3	1.2	-Ø.6	Ø.4	-1.1	Ø.2	-1.6	Ø.6	1.4	Ø.2
125Ø	1.7	Ø.6	1.6	1.7	2.4	Ø.9	Ø.4	1.2	-Ø.1	Ø.1	-Ø.6	Ø.2	-1.8	Ø.6	1.1	Ø.5
16ØØ	Ø.6	Ø.3	Ø.6	Ø.Ø	Ø.8	1.3	Ø.8	Ø.9	-Ø.2	Ø.Ø	-1.2	Ø.8	-1.1	Ø.3	Ø.8	Ø.3
2ØØØ	Ø.5	-Ø.5	-Ø.Ø	-1.3	-Ø.5	-Ø.5	-Ø.Ø	-Ø.2	-1.8	-1.3	-1.8	-1.3	-2.Ø	-Ø.8	Ø.8	-Ø.8
25ØØ	-Ø.4	-Ø.2	-1.Ø	-1.8	-Ø.9	-1.1	-Ø.4	Ø.4	-1.5	-1.5	-1.2	-1.1	-1.6	-Ø.9	Ø.7	-Ø.9
315Ø	-1.1	-1.9	Ø.1	-1.3	-Ø.3	-2.1	-Ø.6	Ø.3	-1.4	-1.Ø	-2.7	Ø.2	-1.1	-1.Ø	Ø.9	-1.Ø
4ØØØ	-1.6	-1.5	Ø.Ø	-2.4	-Ø.6	-2.1	-1.4	Ø.7	-2.2	-1.6	-3.7	-Ø.1	-2.3	-1.4	1.2	-1.4
5ØØØ	-1.1	-2.3	-Ø.8	-2.5	-1.4	-3.1	-1.2	Ø.4	-2.6	-1.5	-4.Ø	Ø.6		-1.6	1.4	-1.8
63ØØ	Ø.4	-Ø.8	-Ø.6	-2.2	-2.1	-3.4	-Ø.9	Ø.4	-1.8	-2.3	-5.3			-1.7	1.7	-2.Ø
8ØØØ			-Ø.1	-1.5	-Ø.6	-3.6	-Ø.9	Ø.8	-1.8	-1.Ø				-1.1	1.3	-1.7
1ØØØØ						-1.2								-1.2.1E 19		Ø.5
125ØØ																
16ØØØ																
2ØØØØ																
25ØØØ																
315ØØ																
4ØØØØ																
5ØØØØ																
63ØØØ																
8ØØØØ																
OASPL	Ø.4	-Ø.5	Ø.2	-Ø.1	-Ø.5	-1.1	-Ø.7	-Ø.8	-1.Ø	-Ø.8	-Ø.6	-Ø.2	-Ø.1			
PNL	Ø.4	-Ø.3	Ø.2	-Ø.7	-Ø.5	-Ø.9	-Ø.4	-Ø.2	-Ø.8	-Ø.8	-1.Ø	-Ø.6	-Ø.5			
PNLT	Ø.3	Ø.4	Ø.2	-1.2	-Ø.5	-1.4	-Ø.4	-Ø.2	-Ø.8	-1.3	Ø.Ø	-Ø.6	-Ø.5			
DBA	1.2	Ø.4	1.Ø	Ø.3	Ø.2	-Ø.5	-Ø.2	Ø.2	-Ø.7	-Ø.3	-1.1	-Ø.5	-Ø.6			

LOCATION	ACOUSTIC RANGE	AVG CORR SPEED	AVG CORR THRUST
C41 ANECH CH	24ØØ.Ø FT SL	-Ø.1E 31 RPM	-Ø.1E 31' LB

TEST CASE FOR TREATED EJECTOR TEØ2 VS TEØ5

DELTA, SPL(1) - SPL(2)

IDENTIFICATION

INPUT (1) 83F-4ØØ-2ØØ4 X2ØØ45
(2) 83F-4ØØ-5ØØ4 X5ØØ45

OUTPUT CBF TE2-TE5 XØ2Ø51

ANGLES MEASURED FROM INLET,DEGREES

FREQ	4Ø.Ø	5Ø.Ø	6Ø.Ø	7Ø.Ø	8Ø.Ø	9Ø.Ø	1ØØ.Ø	11Ø.Ø	12Ø.Ø	13Ø.Ø	14Ø.Ø	15Ø.Ø	16Ø.Ø	AVG	S.D.	PWL
5Ø	-Ø.1	-Ø.Ø	Ø.8	Ø.3	1.3	-Ø.2	-Ø.1	1.5	1.Ø	Ø.3	Ø.5	2.5	2.Ø	Ø.8	Ø.9	1.2
63	-Ø.7	-Ø.9	1.Ø	1.2	Ø.2	-Ø.8	Ø.7	Ø.7	Ø.2	-Ø.9	1.1	2.Ø	Ø.8	Ø.4	Ø.9	Ø.5
8Ø	-1.3	-Ø.3	Ø.8	Ø.7	-Ø.2	-Ø.5	1.Ø	Ø.6	-1.2	-1.9	Ø.4	1.5	1.1	Ø.Ø	1.Ø	-Ø.Ø
1ØØ	-1.1	-Ø.3	1.Ø	Ø.6	Ø.2	-1.Ø	Ø.2	-Ø.1	-Ø.7	-1.2	Ø.3	2.3	1.4	Ø.1	1.Ø	Ø.2
125	-1.2	-Ø.2	Ø.3	Ø.6	Ø.5	-Ø.4	Ø.3	Ø.5	-3.2	-4.5	-2.3	Ø.1	-Ø.6	-Ø.8	1.6	-1.7
16Ø	-1.4	Ø.1	Ø.1	1.4	Ø.2	Ø.2	-Ø.6	-1.2	-Ø.2	-Ø.7	-Ø.9	-Ø.8	Ø.3	-Ø.3	Ø.7	-Ø.4
2ØØ	-1.6	-Ø.6	Ø.Ø	-Ø.2	Ø.6	-1.5	Ø.4	Ø.5	-Ø.2	-Ø.9	-Ø.1	Ø.8	Ø.6	-Ø.2	Ø.8	-Ø.1
25Ø	-1.3	-Ø.8	Ø.2	Ø.3	Ø.4	Ø.2	Ø.9	Ø.6	Ø.6	-Ø.7	Ø.6	2.Ø	1.7	Ø.4	Ø.9	Ø.4
315	-1.1	-Ø.3	Ø.7	1.4	1.5	-Ø.8	Ø.5	1.1	Ø.8	-Ø.8	-Ø.Ø	1.1	Ø.8	Ø.4	Ø.9	Ø.4
4ØØ	-Ø.9	Ø.1	Ø.1	1.3	1.3	-Ø.1	Ø.2	1.2	Ø.4	-Ø.3	-Ø.7	1.7	2.9	Ø.6	1.1	Ø.5
5ØØ	Ø.1	-Ø.7	Ø.6	Ø.7	Ø.4	-Ø.1	Ø.4	1.8	Ø.7	-Ø.2	-Ø.8	Ø.9	1.7	Ø.4	Ø.8	Ø.5
63Ø	-2.7	-1.5	-Ø.2	Ø.Ø	Ø.6	Ø.1	1.3	1.5	1.5	-Ø.4	Ø.4	1.4	2.4	Ø.3	1.4	Ø.7
8ØØ	-2.Ø	-1.Ø	-Ø.7	-Ø.4	2.8	1.6	2.2	3.1	2.Ø	-Ø.3	-Ø.4	Ø.7	1.3	Ø.7	1.6	1.3
1ØØØ	-Ø.8	Ø.2	1.2	2.3	3.8	2.5	2.6	2.6	1.3	-1.Ø	-1.2	Ø.1	Ø.3	1.1	1.6	1.5
125Ø	2.9	4.4	3.6	4.1	4.2	2.9	2.9	3.6	1.Ø	-Ø.4	-2.Ø	Ø.3	Ø.7	2.2	2.Ø	2.5
16ØØ	3.3	3.5	5.Ø	3.9	3.1	3.3	3.4	3.Ø	1.1	-1.1	-1.8	-2.5	-Ø.7	1.8	2.5	2.5
2ØØØ	3.5	3.7	3.7	3.7	4.3	2.6	1.7	2.6	Ø.6	-1.8	-2.7	-Ø.7	-Ø.8	1.6	2.4	2.2
25ØØ	3.3	3.2	3.2	3.1	3.Ø	2.Ø	1.8	2.1	-Ø.6	-1.8	-2.9	-Ø.7	-1.7	1.1	2.3	1.9
315Ø	2.Ø	2.6	2.6	1.8	1.7	-Ø.1	1.5	1.5	-Ø.8	-1.5	-2.7	-Ø.6	-1.2	Ø.5	1.8	1.Ø
4ØØØ	Ø.7	Ø.7	2.2	1.1	1.Ø	-Ø.3	-Ø.2	1.5	Ø.6	-Ø.4	-1.2	1.1	Ø.7	Ø.6	Ø.9	Ø.6
5ØØØ	-Ø.5	Ø.5	1.5	-Ø.7	Ø.4	-2.6	Ø.6	Ø.6	-Ø.7	-Ø.8	-2.Ø	-1.Ø		-Ø.4	1.2	-Ø.4
63ØØ	-1.2	1.6	Ø.9	-1.Ø	-Ø.2	-2.2	Ø.7	1.1	Ø.9	-Ø.8	Ø.1			-Ø.Ø	1.2	-Ø.1
8ØØØ			1.Ø	-Ø.7	1.7	-1.3	1.9	3.2	4.8					1.5	2.1	2.1
1ØØØØ																3.8
125ØØ																
16ØØØ																
2ØØØØ																
25ØØØ																
315ØØ																
4ØØØØ																
5ØØØØ																
63ØØØ																
8ØØØØ																
OASPL	-Ø.Ø	Ø.9	1.7	1.9	2.3	1.3	1.7	2.1	Ø.7	-1.Ø	-Ø.4	1.2	1.Ø			
PNL	1.5	2.1	2.7	2.4	2.7	1.4	1.6	2.3	Ø.7	-1.1	-1.2	-Ø.4	1.Ø			
PNLT	1.5	2.1	2.7	2.4	2.7	1.4	1.6	1.8	Ø.5	-1.1	-2.3	-Ø.4	1.Ø			
DBA	1.1	1.9	2.5	2.6	3.Ø	2.Ø	2.2	2.6	1.1	-Ø.7	-1.Ø	Ø.3	1.1			

LOCATION	ACOUSTIC RANGE	AVG CORR SPEED	AVG CORR THRUST
C41 ANECH CH	24ØØ.Ø FT SL	-Ø.1E 31 RPM	-Ø.1E 31' LB

TEST CASE FOR TREATED EJECTOR TEØ2 VS TEØ5

DELTA, SPL(1) - SPL(2)

IDENTIFICATION

INPUT (1) 83F-4ØØ-2ØØ6 X2ØØ65
(2) 83F-4ØØ-5ØØ6 X5ØØ65

OUTPUT ITF TE2-TE5 XØ2Ø51

ANGLES MEASURED FROM INLET,DEGREES

FREQ	4Ø.Ø	5Ø.Ø	6Ø.Ø	7Ø.Ø	8Ø.Ø	9Ø.Ø	1ØØ.Ø	11Ø.Ø	12Ø.Ø	13Ø.Ø	14Ø.Ø	15Ø.Ø	16Ø.Ø	AVG	S.D.	PWL
5Ø	-Ø.9	-Ø.9	-Ø.7	-Ø.7	-Ø.3	-Ø.8	-Ø.3	Ø.3	Ø.2	Ø.7	Ø.5	3.2	2.2	Ø.2	1.3	1.5
63	-1.8	-1.3	-Ø.3	-Ø.5	-Ø.3	-1.8	-Ø.3	Ø.3	-Ø.5	-Ø.3	1.Ø	3.Ø	2.2	-Ø.Ø	1.4	1.1
8Ø	-2.5	-1.3	-Ø.Ø	Ø.5	-Ø.5	-Ø.8	Ø.5	Ø.6	-Ø.7	-1.4	Ø.7	2.Ø	1.8	-Ø.1	1.3	Ø.4
1ØØ	-1.5	-1.3	-Ø.3	Ø.7	-Ø.3	-1.5	-Ø.3	-1.3	-1.7	-2.3	-Ø.8	1.8	Ø.6	-Ø.6	1.2	-Ø.6
125	-1.8	-Ø.5	-Ø.8	Ø.Ø	1.1	-Ø.8	-Ø.7	-1.3	-Ø.5	-2.1	-Ø.3	Ø.2	-Ø.1	-Ø.6	Ø.8	-Ø.7
16Ø	-1.Ø	-Ø.2	-Ø.2	1.1	-Ø.2	-Ø.5	-Ø.2	1.7	Ø.2	Ø.6	-Ø.4	1.1	1.1	Ø.2	Ø.8	Ø.3
2ØØ	-1.3	-Ø.7	-Ø.6	-Ø.8	-Ø.Ø	-1.3	Ø.8	Ø.4	-Ø.8	-Ø.1	-Ø.1	1.7	-Ø.3	-Ø.2	Ø.8	-Ø.2
25Ø	-1.3	-1.Ø	-Ø.8	Ø.2	-Ø.3	-Ø.5	Ø.2	-Ø.5	-Ø.2	-Ø.1	-Ø.5	1.2	Ø.8	-Ø.2	Ø.7	-Ø.1
315	-2.Ø	-Ø.8	-Ø.8	Ø.5	Ø.2	-Ø.5	1.2	Ø.8	Ø.1	-Ø.6	Ø.1	-Ø.4	-Ø.1	-Ø.2	Ø.8	-Ø.Ø
4ØØ	-1.Ø	-Ø.8	-1.3	Ø.1	-Ø.3	-Ø.5	Ø.Ø	Ø.4	-Ø.1	-Ø.2	-1.2	-Ø.2	1.7	-Ø.2	Ø.8	-Ø.2
5ØØ	-Ø.8	-1.Ø	-1.Ø	-Ø.9	-Ø.3	-Ø.8	Ø.5	1.1	Ø.4	-Ø.7	-1.7	-Ø.3	-Ø.1	-Ø.4	Ø.8	-Ø.2
63Ø	-Ø.5	Ø.2	-Ø.Ø	Ø.3	Ø.7	-Ø.Ø	1.Ø	Ø.3	-Ø.3	-Ø.2	-1.4	-Ø.6	-Ø.1	-Ø.Ø	Ø.6	Ø.Ø
8ØØ	-Ø.5	Ø.5	Ø.7	Ø.7	1.4	Ø.2	1.5	1.5	-Ø.1	-Ø.1	-1.Ø	-Ø.2	-Ø.Ø	Ø.4	Ø.8	Ø.5
1ØØØ	-1.3	-Ø.Ø	-Ø.5	1.2	3.2	1.7	2.2	2.Ø	-Ø.1	-Ø.7	-1.1	-Ø.6	-1.1	Ø.4	1.5	Ø.7
125Ø	1.5	2.5	2.2	3.6	3.7	3.5	2.6	2.3	Ø.5	-Ø.1	-Ø.6	-Ø.2	-Ø.2	1.6	1.6	1.8
16ØØ	2.2	2.7	3.5	3.9	4.Ø	3.Ø	4.1	2.2	Ø.4	-Ø.8	-Ø.9	-1.4	-Ø.7	1.7	2.1	2.1
2ØØØ	4.Ø	3.8	3.7	4.Ø	2.7	1.7	3.1	2.1	-Ø.4	-2.5	-3.6	-2.5	-2.5	1.1	2.9	2.Ø
25ØØ	Ø.5	1.2	Ø.5	1.6	2.Ø	1.7	2.2	1.1	2.8	2.6	1.4	2.6	3.4	1.8	Ø.9	1.6
315Ø	-Ø.3	Ø.7	-Ø.5	-Ø.4	1.2	-Ø.8	2.Ø	3.4	1.2	2.1	1.8	1.9	2.4	1.1	1.3	Ø.7
4ØØØ	-Ø.3	-Ø.Ø	Ø.2	Ø.3	-Ø.1	-Ø.3	Ø.9	2.Ø	1.5	2.5	1.3	2.6	2.6	1.Ø	1.1	Ø.5
5ØØØ	-3.1	-1.6	-Ø.3	-Ø.9	Ø.9	-Ø.6	2.1	2.1	1.1	2.4	1.8	1.8		Ø.5	1.7	Ø.4
63ØØ	Ø.2	1.2	2.2	Ø.9	2.1	-Ø.4	4.Ø	3.4	3.2	3.7	3.2			2.1	1.5	2.Ø
8ØØØ			2.1	1.7	3.2	Ø.8	4.8	4.5	4.Ø					3.1	1.6	3.1
1ØØØØ																4.8
125ØØ																
16ØØØ																
2ØØØØ																
25ØØØ																
315ØØ																
4ØØØØ																
5ØØØØ																
63ØØØ																
8ØØØØ																
OASPL	-Ø.3	Ø.5	Ø.7	1.4	1.7	Ø.9	1.7	1.3	-Ø.1	-Ø.6	-Ø.4	1.6	1.1			
PNL	Ø.8	1.5	1.1	1.6	1.7	Ø.9	2.2	1.6	Ø.3	-Ø.4	-Ø.7	-Ø.Ø	Ø.5			
PNLT	Ø.8	1.5	1.2	1.6	1.7	Ø.9	2.2	1.6	Ø.3	Ø.1	-1.7	-Ø.Ø	Ø.5			
DBA	Ø.7	1.5	1.5	2.1	2.4	1.6	2.3	1.7	Ø.2	-Ø.4	-1.Ø	-Ø.3	-Ø.Ø			

LOCATION	ACOUSTIC RANGE	AVG CORR SPEED	AVG CORR THRUST
C41 ANECH CH	24ØØ.Ø FT SL	-Ø.1E 31 RPM	-Ø.1E 31' LB

TEST CASE FOR TREATED EJECTOR TEØ2 VS TEØ5

DELTA, SPL(1) - SPL(2)

IDENTIFICATION

INPUT (1) 83F-4ØØ-2Ø1Ø X2Ø1Ø5
(2) 83F-4ØØ-5Ø1Ø X5Ø1Ø5

OUTPUT TOF TE2-TE5 XØ2Ø51

ANGLES MEASURED FROM INLET,DEGREES

FREQ	4Ø.Ø	5Ø.Ø	6Ø.Ø	7Ø.Ø	8Ø.Ø	9Ø.Ø	1ØØ.Ø	11Ø.Ø	12Ø.Ø	13Ø.Ø	14Ø.Ø	15Ø.Ø	16Ø.Ø	AVG	S.D.	PWL
5Ø	Ø.6	-1.4	-Ø.4	-Ø.2	-Ø.6	-1.2	-Ø.2	-2.Ø	-Ø.7	Ø.3	-Ø.2	1.8	1.Ø	-Ø.3	1.Ø	Ø.8
63	-Ø.2	-1.9	Ø.1	-Ø.Ø	-Ø.9	-1.2	Ø.1	-1.Ø	-1.Ø	-Ø.5	Ø.5	1.7	1.3	-Ø.2	1.Ø	Ø.8
8Ø	-Ø.7	-1.4	-Ø.7	-Ø.6	-1.7	-1.9	Ø.Ø	-1.3	-Ø.7	-1.7	-Ø.5	1.7	1.5	-Ø.6	1.2	Ø.4
1ØØ	-1.Ø	-1.4	-Ø.4	-Ø.3	-1.2	-1.9	Ø.5	-1.3	-2.8	-2.4	-2.2	1.3	Ø.5	-1.Ø	1.3	-Ø.9
125	-1.Ø	-1.4	-1.2	-Ø.5	Ø.Ø	-1.5	-1.Ø	-2.Ø	-1.5	-1.8	-1.Ø	Ø.8	Ø.7	-Ø.9	Ø.9	-Ø.8
16Ø	-Ø.7	-1.1	-Ø.8	-Ø.1	-Ø.9	-Ø.7	Ø.1	-Ø.9	Ø.1	Ø.1	-Ø.6	1.2	1.7	-Ø.2	Ø.8	Ø.1
2ØØ	-1.1	-1.5	-Ø.8	-1.3	-Ø.9	-1.9	Ø.1	Ø.2	-Ø.7	Ø.4	Ø.Ø	2.5	1.6	-Ø.3	1.3	Ø.Ø
25Ø	-1.Ø	-2.Ø	-1.2	-Ø.4	-1.5	-1.2	Ø.1	-Ø.4	-1.Ø	-Ø.2	-Ø.5	Ø.8	1.3	-Ø.6	Ø.9	-Ø.4
315	-1.5	-1.2	-1.2	-Ø.6	-Ø.5	-1.7	Ø.1	Ø.7	-Ø.9	-Ø.8	-Ø.5	-Ø.1	Ø.7	-Ø.6	Ø.8	-Ø.5
4ØØ	-Ø.7	-1.Ø	-1.7	-Ø.6	-Ø.7	-1.2	-Ø.4	Ø.2	-Ø.2	-Ø.9	-1.7	-Ø.3	1.2	-Ø.6	Ø.8	-Ø.6
5ØØ	Ø.5	-1.5	-Ø.7	-Ø.6	-1.4	-1.5	Ø.4	1.2	-Ø.8	Ø.1	-1.9	-Ø.Ø	Ø.7	-Ø.4	1.Ø	-Ø.4
63Ø	Ø.5	-Ø.9	-1.2	-Ø.5	-Ø.7	-Ø.7	Ø.7	1.Ø	Ø.Ø	Ø.Ø	-Ø.9	-Ø.1	Ø.3	-Ø.2	Ø.7	-Ø.1
8ØØ	Ø.2	-Ø.8	-Ø.7	-1.Ø	1.3	Ø.Ø	1.5	1.7	Ø.1	Ø.9	-Ø.8	Ø.4	Ø.5	Ø.3	Ø.9	Ø.3
1ØØØ	2.2	2.3	2.Ø	1.3	1.8	1.5	Ø.9	2.4	Ø.4	1.5	-Ø.7	Ø.3	Ø.4	1.2	Ø.9	1.1
125Ø	1.5	2.8	2.3	2.6	3.2	2.Ø	2.3	2.2	-Ø.1	1.3	-Ø.4	Ø.4	Ø.4	1.6	1.2	1.6
16ØØ	2.4	1.8	2.8	2.8	1.Ø	1.Ø	2.3	2.3	-Ø.8	Ø.Ø	-Ø.7	-1.5	-Ø.Ø	1.Ø	1.5	1.2
2ØØØ	1.3	Ø.6	Ø.4	Ø.2	-Ø.4	-1.3	Ø.3	Ø.9	-3.2	-2.8	-4.Ø	-2.9	-3.Ø	-1.1	1.9	-Ø.4
25ØØ	Ø.1	-Ø.1	Ø.1	-Ø.4	Ø.5	-Ø.8	-1.1	-Ø.6	-Ø.8	Ø.4	-1.Ø	-Ø.5	-Ø.Ø	-Ø.3	Ø.5	-Ø.3
315Ø	-Ø.Ø	-Ø.Ø	-Ø.3	-1.1	-Ø.Ø	-2.Ø	Ø.4	2.2	-1.2	-Ø.9	-1.7	-Ø.8	-Ø.7	-Ø.5	1.1	-Ø.5
4ØØØ	-Ø.3	-Ø.5	Ø.7	-Ø.4	Ø.5	-1.3	-Ø.1	2.1	Ø.3	1.4	-Ø.2	2.Ø	1.4	Ø.4	1.Ø	Ø.1
5ØØØ	-Ø.5	-Ø.Ø	Ø.7	-1.6	-Ø.4	-1.6	1.6	3.Ø	Ø.Ø	1.1	Ø.7	1.4		Ø.4	1.3	Ø.1
63ØØ	-2.6	-2.1	-1.5	-2.5	Ø.6	-1.1	1.7	2.9	Ø.4	2.3	1.2			-Ø.1	2.Ø	-Ø.2
8ØØØ		1.6	1.6	Ø.6	1.8	-Ø.5	2.2	3.Ø	1.9	3.Ø				1.7	1.1	1.7
1ØØØØ						Ø.5								Ø.5	.1E 19	3.3
125ØØ																
16ØØØ																
2ØØØØ																
25ØØØ																
315ØØ																
4ØØØØ																
5ØØØØ																
63ØØØ																
8ØØØØ																
OASPL	Ø.5	Ø.2	Ø.6	Ø.5	Ø.4	-Ø.3	Ø.7	Ø.9	-Ø.6	-Ø.4	-Ø.8	1.3	1.1			
PNL	Ø.7	Ø.2	Ø.5	Ø.1	-Ø.Ø	-Ø.9	Ø.4	Ø.9	-Ø.8	-Ø.2	-Ø.9	Ø.2	Ø.7			
PNLT	Ø.7	-Ø.6	-Ø.2	-Ø.5	-Ø.Ø	-1.4	Ø.4	Ø.9	-1.3	-Ø.2	Ø.1	Ø.2	Ø.7			
DBA	1.2	1.Ø	1.2	Ø.9	Ø.9	Ø.1	1.1	1.6	-Ø.4	Ø.3	-1.Ø	Ø.1	Ø.6			

LOCATION	ACOUSTIC RANGE	AVG CORR SPEED	AVG CORR THRUST
C41 ANECH CH	24ØØ.Ø FT SL	-Ø.1E 31 RPM	-Ø.1E 31 LB

TEST CASE FOR TREATED EJECTOR TEØ2 VS TEØ5

DELTA, SPL(1) - SPL(2)

IDENTIFICATION

INPUT (1) 83F-ZER-2ØØ3 X2ØØ35
(2) 83F-ZER-9ØØ3 X9ØØ35

OUTPUT CBS TE2-TE9 XØ2Ø91

ANGLES MEASURED FROM INLET,DEGREES

FREQ	4Ø.Ø	5Ø.Ø	6Ø.Ø	7Ø.Ø	8Ø.Ø	9Ø.Ø	1ØØ.Ø	11Ø.Ø	12Ø.Ø	13Ø.Ø	14Ø.Ø	15Ø.Ø	16Ø.Ø	AVG	S.D.	PWL
5Ø	-Ø.5	-1.Ø	-Ø.5	-Ø.7	Ø.5	Ø.Ø	Ø.3	1.Ø	Ø.3	Ø.Ø	-Ø.5	1.Ø	1.5	Ø.1	Ø.8	Ø.7
63	-1.7	-Ø.7	Ø.3	Ø.2	Ø.5	Ø.8	Ø.3	Ø.8	-Ø.2	1.Ø	Ø.3	Ø.8	Ø.8	Ø.2	Ø.8	Ø.6
8Ø	-Ø.2	-1.5	Ø.Ø	Ø.5	Ø.5	Ø.Ø	Ø.5	Ø.3	Ø.Ø	Ø.3	Ø.Ø	Ø.8	Ø.5	Ø.1	Ø.6	Ø.3
1ØØ	-Ø.3	-Ø.3	-Ø.5	-Ø.1	Ø.2	-Ø.8	Ø.5	-Ø.3	-Ø.Ø	-Ø.Ø	-Ø.Ø	-Ø.Ø	1.Ø	-Ø.Ø	Ø.4	Ø.1
125	Ø.2	-Ø.5	Ø.2	Ø.4	1.5	-Ø.3	Ø.5	Ø.5	-Ø.5	-Ø.Ø	-1.Ø	Ø.2	Ø.2	Ø.1	Ø.6	-Ø.1
16Ø	-Ø.5	-1.Ø	Ø.2	-Ø.3	Ø.7	Ø.5	-Ø.Ø	Ø.2	-Ø.8	-Ø.5	-Ø.8	-Ø.3	Ø.2	-Ø.2	Ø.5	-Ø.3
2ØØ	-Ø.Ø	-1.3	Ø.2	Ø.2	1.Ø	-Ø.5	-Ø.Ø	Ø.2	-Ø.3	Ø.5	-Ø.8	-1.3	Ø.5	-Ø.1	Ø.7	-Ø.2
25Ø	-Ø.5	-1.Ø	Ø.5	Ø.8	Ø.5	-Ø.Ø	Ø.7	-Ø.3	-Ø.3	Ø.5	-Ø.3	Ø.2	-Ø.5	Ø.Ø	Ø.6	Ø.Ø
315	-Ø.3	-Ø.8	-Ø.3	Ø.4	Ø.7	-Ø.8	Ø.2	-Ø.Ø	-Ø.3	Ø.7	-1.Ø	-1.3	-Ø.3	-Ø.2	Ø.6	-Ø.2
4ØØ	-Ø.8	-1.5	-Ø.5	-Ø.6	Ø.5	-Ø.3	Ø.2	-Ø.3	Ø.2	-Ø.8	-Ø.5	-1.Ø	Ø.7	-Ø.4	Ø.6	-Ø.3
5ØØ	-Ø.3	-1.Ø	-Ø.5	-Ø.6	-Ø.Ø	-Ø.3	-Ø.Ø	Ø.5	-Ø.Ø	-Ø.5	-1.5	-1.8	Ø.2	-Ø.4	Ø.7	-Ø.3
63Ø	-Ø.Ø	-Ø.8	-Ø.3	Ø.3	1.Ø	Ø.5	Ø.7	Ø.2	-Ø.3	-Ø.Ø	-1.8	-1.3	-Ø.Ø	-Ø.1	Ø.8	-Ø.1
8ØØ	Ø.2	Ø.2	1.Ø	1.4	1.5	1.2	1.7	Ø.7	-Ø.8	-Ø.Ø	-1.Ø	-1.3	Ø.7	Ø.4	1.Ø	Ø.3
1ØØØ	Ø.8	1.Ø	1.5	2.3	2.Ø	1.8	2.3	1.8	Ø.3	-Ø.2	-1.2	-2.2	Ø.3	Ø.8	1.4	Ø.9
125Ø	1.3	Ø.8	2.3	3.Ø	3.5	2.5	3.3	2.5	-Ø.2	-Ø.2	-Ø.7	-2.2	Ø.Ø	1.2	1.8	1.5
16ØØ	1.1	Ø.8	2.3	2.6	3.3	3.1	4.6	2.8	Ø.8	Ø.3	-1.7	-3.2	-Ø.2	1.3	2.2	2.1
2ØØØ	2.3	1.6	2.9	2.5	3.9	2.9	3.4	4.1	1.1	Ø.1	-1.4	-3.6	Ø.1	1.5	2.2	2.5
25ØØ	1.9	1.7	2.7	1.9	4.7	3.4	3.2	4.7	1.7	-Ø.3	-2.3	-2.3	Ø.7	1.7	2.3	2.9
315Ø	Ø.8	Ø.6	3.6	3.Ø	4.3	2.5	3.3	5.Ø	2.3	Ø.9	-Ø.7	-2.5	-Ø.5	1.7	2.2	3.1
4ØØØ	Ø.4	1.Ø	3.2	1.7	3.4	1.9	2.9	4.4	1.7	1.3	-1.Ø	-3.1	Ø.1	1.4	2.Ø	2.7
5ØØØ	Ø.1	Ø.4	2.2	Ø.8	3.3	1.1	3.6	4.4	1.7	2.3	-Ø.6	-2.9		1.3	2.Ø	2.5
63ØØ		1.3	2.6	2.Ø	3.5	1.5	5.Ø	5.5	3.1	2.9	-1.Ø			2.6	1.9	3.4
8ØØØ				3.7	6.2	3.Ø	5.7	7.5	4.Ø					5.1	1.7	5.Ø
1ØØØØ																7.8
125ØØ																
16ØØØ																
2ØØØØ																
25ØØØ																
315ØØ																
4ØØØØ																
5ØØØØ																
63ØØØ																
8ØØØØ																
OASPL	-Ø.1	-Ø.5	Ø.5	Ø.8	1.4	Ø.8	1.3	1.Ø	-Ø.1	Ø.1	-Ø.4	Ø.4	1.Ø			
PNL	Ø.8	Ø.4	1.7	1.6	2.7	1.8	2.5	2.3	Ø.4	-Ø.1	-Ø.9	-Ø.9	Ø.3			
PNLT	Ø.8	Ø.4	1.7	1.6	2.7	1.8	2.5	2.3	Ø.4	-Ø.1	Ø.2	-Ø.9	Ø.3			
DBA	Ø.5	Ø.2	1.4	1.7	2.4	1.9	2.5	1.9	Ø.Ø	-Ø.1	-1.1	-1.3	Ø.3			

LOCATION	ACOUSTIC RANGE	AVG CORR SPEED	AVG CORR THRUST
C41 ANECH CH	24ØØ.Ø FT SL	-Ø.1E 31 RPM	-Ø.1E 31' LB

TEST CASE FOR TREATED EJECTOR TEØ2 VS TEØ9

DELTA, SPL(1) - SPL(2)

IDENTIFICATION

INPUT (1) 83F-ZER-2ØØ5 X2ØØ55
(2) 83F-ZER-9ØØ5 X9ØØ55

OUTPUT ITS TE2-TE9 XØ2Ø91

ANGLES MEASURED FROM INLET,DEGREES

FREQ	4Ø.Ø	5Ø.Ø	6Ø.Ø	7Ø.Ø	8Ø.Ø	9Ø.Ø	1ØØ.Ø	11Ø.Ø	12Ø.Ø	13Ø.Ø	14Ø.Ø	15Ø.Ø	16Ø.Ø	AVG	S.D.	PWL
5Ø	-1.Ø	-1.2	Ø.8	-Ø.1	1.Ø	-Ø.2	Ø.Ø	1.3	-Ø.2	-Ø.2	Ø.5	Ø.8	Ø.8	Ø.1	Ø.8	Ø.6
63	-1.2	-Ø.2	Ø.5	-Ø.1	1.Ø	Ø.5	Ø.5	1.3	Ø.5	1.Ø	1.3	1.8	1.Ø	Ø.6	Ø.8	1.3
8Ø	-Ø.2	-1.5	1.Ø	Ø.4	Ø.Ø	-Ø.7	Ø.8	Ø.8	Ø.5	-Ø.5	1.Ø	1.3	1.Ø	Ø.3	Ø.8	Ø.8
1ØØ	-Ø.3	-Ø.5	-Ø.Ø	Ø.3	Ø.7	-Ø.3	Ø.5	-Ø.Ø	-Ø.3	Ø.2	1.Ø	1.Ø	1.7	Ø.3	Ø.6	Ø.8
125	-Ø.3	-Ø.8	Ø.5	Ø.3	1.2	-Ø.3	Ø.2	Ø.5	-Ø.3	-Ø.5	Ø.7	1.Ø	1.Ø	Ø.3	Ø.6	Ø.3
16Ø	-Ø.5	-1.Ø	-Ø.Ø	-Ø.7	1.Ø	Ø.5	-Ø.Ø	Ø.7	-1.Ø	-Ø.3	1.5	Ø.2	Ø.5	Ø.1	Ø.8	Ø.2
2ØØ	-Ø.Ø	-1.3	-Ø.3	-Ø.1	1.2	-Ø.8	Ø.2	Ø.2	Ø.5	Ø.2	Ø.7	-Ø.3	1.Ø	Ø.1	Ø.7	Ø.3
25Ø	-Ø.5	-1.Ø	-Ø.Ø	Ø.6	Ø.5	-Ø.Ø	1.2	-Ø.3	-Ø.5	Ø.2	Ø.7	1.5	1.Ø	Ø.3	Ø.7	Ø.4
315	-Ø.Ø	-Ø.3	-Ø.5	Ø.3	Ø.7	-Ø.8	Ø.5	Ø.5	-Ø.5	-Ø.3	Ø.2	Ø.2	1.2	Ø.1	Ø.6	Ø.1
4ØØ	-Ø.3	-2.Ø	-Ø.3	-Ø.5	Ø.2	-Ø.Ø	-Ø.3	Ø.2	-Ø.Ø	-Ø.5	1.2	Ø.5	Ø.2	-Ø.1	Ø.7	Ø.1
5ØØ	-Ø.5	-1.Ø	-Ø.5	-Ø.2	-Ø.Ø	-Ø.5	Ø.7	Ø.7	-Ø.5	-Ø.3	-Ø.8	Ø.2	1.Ø	-Ø.1	Ø.6	-Ø.1
63Ø	-Ø.3	-1.3	-Ø.8	-Ø.7	1.Ø	-Ø.3	Ø.2	-Ø.Ø	-Ø.3	Ø.2	-1.3	Ø.5	1.Ø	-Ø.1	Ø.7	-Ø.1
8ØØ	Ø.2	-Ø.3	1.Ø	Ø.9	1.5	-Ø.Ø	1.Ø	Ø.2	-Ø.5	-Ø.3	-Ø.Ø	Ø.2	1.Ø	Ø.4	Ø.6	Ø.2
1ØØØ	Ø.5	Ø.3	1.5	1.7	1.8	Ø.3	1.3	1.5	Ø.3	Ø.Ø	-Ø.7	-Ø.2	Ø.Ø	Ø.6	Ø.8	Ø.6
125Ø	1.5	1.3	2.Ø	2.Ø	2.3	1.8	2.8	1.3	-Ø.5	Ø.Ø	-1.5	Ø.5	Ø.Ø	1.Ø	1.2	Ø.8
16ØØ	2.8	1.8	3.1	2.5	3.1	2.6	3.1	1.1	Ø.3	Ø.6	-1.4	Ø.3	Ø.Ø	1.5	1.5	1.3
2ØØØ	3.3	2.6	3.6	3.Ø	4.4	2.4	2.9	2.4	Ø.6	-Ø.1	-1.1	-1.1	Ø.3	1.8	1.8	1.8
25ØØ	2.9	2.2	2.5	1.4	3.7	2.4	3.4	2.9	1.Ø	-1.Ø	-1.8	-Ø.3	-Ø.1	1.5	1.8	2.Ø
315Ø	1.3	Ø.8	2.6	1.1	3.3	Ø.8	3.Ø	3.5	1.3	Ø.4	-1.7	-Ø.2	Ø.5	1.3	1.5	1.9
4ØØØ	Ø.6	Ø.7	3.Ø	Ø.5	2.2	-Ø.1	1.2	3.2	Ø.5	Ø.Ø	-2.3	-Ø.8	Ø.6	Ø.7	1.5	1.1
5ØØØ	1.6	Ø.7	2.4	Ø.4	1.8	-Ø.2	2.8	3.6	1.2	Ø.5	-1.1	-Ø.7		1.1	1.4	1.6
63ØØ	2.4	1.6	2.6	1.7	3.2	Ø.2	3.5	4.5	1.6	Ø.7	-1.5			1.9	1.7	2.1
8ØØØ				3.2	5.2	1.2	4.7	5.8	2.6					3.8	1.7	3.3
1ØØØØ																5.4
125ØØ																
16ØØØ																
2ØØØØ																
25ØØØ																
315ØØ																
4ØØØØ																
5ØØØØ																
63ØØØ																
8ØØØØ																
OASPL	Ø.Ø	-Ø.5	Ø.6	Ø.5	1.3	Ø.3	1.Ø	Ø.7	-Ø.2	-Ø.1	Ø.7	1.Ø	1.Ø			
PNL	1.6	Ø.9	1.9	1.2	2.6	1.2	2.Ø	1.4	Ø.1	-Ø.2	Ø.3	Ø.6	1.3			
PNLT	1.6	Ø.9	1.9	1.2	2.6	1.2	2.Ø	1.4	Ø.1	-Ø.2	Ø.3	Ø.6	1.3			
DBA	Ø.9	Ø.3	1.5	1.3	2.2	1.1	1.8	1.1	-Ø.1	-Ø.1	-Ø.4	Ø.4	Ø.8			

LOCATION	ACOUSTIC RANGE	AVG CORR SPEED	AVG CORR THRUST
C41 ANECH CH	24ØØ.Ø FT SL	-Ø.1E 31 RPM	-Ø.1E 31 LB

TEST CASE FOR TREATED EJECTOR TEØ2 VS TEØ9

DELTA, SPL(1) - SPL(2)

IDENTIFICATION

INPUT (1) 83F-ZER-2ØØ9 X2ØØ95
(2) 83F-ZER-9ØØ9 X9ØØ95

OUTPUT TOS TE2-TE9 XØ2Ø91

ANGLES MEASURED FROM INLET,DEGREES

FREQ	4Ø.Ø	5Ø.Ø	6Ø.Ø	7Ø.Ø	8Ø.Ø	9Ø.Ø	1ØØ.Ø	11Ø.Ø	12Ø.Ø	13Ø.Ø	14Ø.Ø	15Ø.Ø	16Ø.Ø	AVG	S.D.	PWL
5Ø	-Ø.5	-Ø.5	Ø.Ø	Ø.Ø	1.Ø	Ø.3	Ø.Ø	1.3	Ø.3	Ø.3	Ø.3	-Ø.5	Ø.5	Ø.2	Ø.5	Ø.Ø
63	-1.2	-Ø.7	Ø.3	Ø.2	1.Ø	Ø.5	1.3	1.3	Ø.Ø	1.Ø	1.3	Ø.5	Ø.Ø	Ø.4	Ø.8	Ø.6
8Ø	Ø.3	-Ø.2	Ø.3	Ø.8	1.3	Ø.5	1.3	1.5	Ø.3	Ø.3	2.Ø	Ø.Ø	Ø.5	Ø.7	Ø.7	Ø.6
1ØØ	Ø.2	Ø.5	1.Ø	1.5	1.Ø	-Ø.3	1.5	1.2	Ø.5	-Ø.Ø	2.2	Ø.2	1.7	Ø.9	Ø.7	1.Ø
125	3.Ø	3.Ø	2.2	2.3	2.Ø	Ø.2	Ø.7	1.2	Ø.2	Ø.2	1.5	1.Ø	1.5	1.5	1.Ø	1.1
16Ø	1.7	1.Ø	2.7	1.Ø	2.2	1.Ø	1.5	1.7	-Ø.5	-Ø.Ø	2.5	Ø.2	1.7	1.3	1.Ø	1.Ø
2ØØ	1.Ø	-Ø.3	1.2	1.Ø	2.Ø	Ø.5	1.5	1.Ø	1.2	1.5	2.2	-Ø.Ø	1.7	1.1	Ø.7	1.1
25Ø	2.2	1.7	1.Ø	1.3	1.2	Ø.2	2.Ø	Ø.7	1.Ø	1.5	1.5	Ø.7	1.Ø	1.2	Ø.5	1.1
315	1.5	Ø.5	Ø.7	1.Ø	1.5	Ø.5	1.7	1.5	1.7	1.Ø	2.Ø	-Ø.Ø	1.7	1.2	Ø.6	1.1
4ØØ	1.Ø	Ø.7	Ø.7	Ø.5	1.Ø	Ø.2	Ø.7	Ø.7	1.2	Ø.2	1.7	-Ø.Ø	Ø.5	Ø.7	Ø.5	Ø.7
5ØØ	3.Ø	Ø.5	1.Ø	Ø.9	1.2	-Ø.3	Ø.5	1.2	Ø.5	Ø.7	Ø.5	-Ø.5	Ø.7	Ø.8	Ø.8	Ø.5
63Ø	4.Ø	3.2	2.2	Ø.8	1.2	Ø.2	Ø.7	Ø.5	Ø.5	-Ø.Ø	1.Ø	-Ø.Ø	Ø.2	1.1	1.3	Ø.6
8ØØ	2.7	2.7	3.7	2.8	2.2	Ø.2	Ø.7	Ø.5	Ø.2	Ø.2	1.Ø	Ø.5	-Ø.Ø	1.4	1.3	Ø.8
1ØØØ	2.Ø	2.Ø	2.8	3.2	3.Ø	Ø.Ø	Ø.8	1.3	Ø.3	Ø.5	Ø.8	Ø.8	Ø.3	1.3	1.1	1.Ø
125Ø	2.5	Ø.8	Ø.8	1.5	3.3	1.5	1.3	1.Ø	Ø.3	-Ø.2	1.Ø	Ø.3	Ø.3	1.1	1.Ø	Ø.9
16ØØ	2.8	1.3	Ø.1	-Ø.8	2.1	2.1	2.1	Ø.3	-Ø.2	Ø.3	Ø.3	1.3	Ø.5	Ø.9	1.1	Ø.7
2ØØØ	2.3	1.1	Ø.9	-1.4	1.1	Ø.1	1.4	Ø.1	-Ø.9	-Ø.4	Ø.4	-Ø.9	Ø.1	Ø.3	1.1	Ø.1
25ØØ	1.2	1.4	Ø.4	-Ø.5	Ø.9	Ø.2	1.4	1.2	-Ø.6	-Ø.5	Ø.4	-1.6	-Ø.1	Ø.3	Ø.9	Ø.4
315Ø	Ø.5	-Ø.2	Ø.8	-Ø.6	1.5	-1.2	Ø.5	1.3	-Ø.4	-Ø.4	2.1	Ø.8	1.3	Ø.5	1.Ø	Ø.2
4ØØØ	Ø.9	1.Ø	1.5	-1.3	Ø.9	-Ø.8	-Ø.1	1.2	-1.Ø	-Ø.2	1.2	Ø.4	Ø.4	Ø.3	Ø.9	Ø.1
5ØØØ	1.1	Ø.9	Ø.9	-1.2	1.3	-1.7	Ø.8	Ø.9	-1.1	-Ø.5	1.6	1.3		Ø.4	1.1	Ø.Ø
63ØØ	3.9	3.3	2.1	-Ø.3	Ø.7	-1.3	1.7	1.7	-Ø.4	-Ø.8	1.Ø			1.1	1.7	Ø.3
8ØØØ			2.8	1.2	3.Ø	-Ø.8	1.7	3.3	Ø.1	-Ø.1				1.4	1.5	1.1
1ØØØØ																2.3
125ØØ																
16ØØØ																
2ØØØØ																
25ØØØ																
315ØØ																
4ØØØØ																
5ØØØØ																
63ØØØ																
8ØØØØ																
OASPL	2.Ø	1.4	1.5	1.Ø	1.8	Ø.5	1.2	1.Ø	Ø.6	Ø.5	1.5	Ø.2	1.Ø			
PNL	2.2	1.3	Ø.9	-Ø.1	1.5	Ø.4	1.2	Ø.8	Ø.4	Ø.3	1.5	Ø.1	1.2			
PNLT	1.9	1.9	1.4	-Ø.6	1.5	Ø.4	1.2	Ø.8	Ø.4	Ø.3	2.5	Ø.1	1.2			
DBA	2.5	1.6	1.4	Ø.7	2.Ø	Ø.6	1.1	Ø.8	Ø.4	Ø.4	1.2	Ø.2	1.2			

LOCATION	ACOUSTIC RANGE	AVG CORR SPEED	AVG CORR THRUST
C41 ANECH CH	24ØØ.Ø FT SL	-Ø.1E 31 RPM	-Ø.1E 31' LB

TEST CASE FOR TREATED EJECTOR TEØ2 VS TEØ9

DELTA, SPL(1) - SPL(2)

IDENTIFICATION

INPUT (1) 83F-4ØØ-2ØØ4 X2ØØ45
(2) 83F-4ØØ-9ØØ4 X9ØØ45

OUTPUT CBF TE2-TE9 XØ2Ø91

ANGLES MEASURED FROM INLET,DEGREES

FREQ	4Ø.Ø	5Ø.Ø	6Ø.Ø	7Ø.Ø	8Ø.Ø	9Ø.Ø	1ØØ.Ø	11Ø.Ø	12Ø.Ø	13Ø.Ø	14Ø.Ø	15Ø.Ø	16Ø.Ø	AVG	S.D.	PWL
5Ø	Ø.8	-Ø.2	Ø.8	Ø.8	2.3	-1.1	2.2	2.Ø	1.Ø	2.1	Ø.3	2.8	-Ø.1	1.1	1.2	1.Ø
63	-Ø.7	-Ø.6	1.Ø	1.2	1.8	-Ø.5	2.1	1.2	Ø.4	1.4	Ø.3	2.Ø	1.6	Ø.9	1.Ø	1.1
8Ø	-1.5	Ø.8	1.5	1.4	2.6	-Ø.2	1.3	1.3	Ø.1	Ø.9	Ø.3	1.3	1.7	Ø.9	1.Ø	Ø.9
1ØØ	-Ø.5	-Ø.2	1.7	1.7	2.3	-Ø.7	1.Ø	Ø.5	-1.1	-Ø.3	-Ø.8	1.4	2.1	Ø.5	1.2	Ø.4
125	-Ø.4	Ø.3	Ø.7	1.9	2.3	Ø.2	Ø.1	-Ø.6	-2.3	-Ø.7	-Ø.7	1.1	1.2	Ø.2	1.2	-Ø.2
16Ø	-Ø.Ø	Ø.2	1.4	2.4	2.6	Ø.7	-Ø.1	Ø.Ø	Ø.3	1.6	-1.Ø	-Ø.6	Ø.8	Ø.6	1.1	Ø.4
2ØØ	-Ø.4	Ø.Ø	1.Ø	Ø.6	2.Ø	-Ø.4	Ø.6	1.4	-Ø.3	1.2	Ø.1	1.5	Ø.5	Ø.6	Ø.8	Ø.5
25Ø	-Ø.8	-Ø.8	Ø.7	1.1	1.8	Ø.2	Ø.9	-Ø.1	Ø.4	Ø.9	Ø.4	2.4	Ø.6	Ø.6	Ø.9	Ø.6
315	-1.6	-Ø.6	Ø.4	1.4	1.8	-Ø.1	Ø.8	Ø.5	Ø.7	Ø.8	Ø.4	2.8	Ø.8	Ø.6	1.1	Ø.6
4ØØ	-1.2	-Ø.7	-Ø.2	1.Ø	1.8	-Ø.4	-Ø.2	Ø.5	Ø.3	1.6	1.2	4.2	3.9	Ø.9	1.7	Ø.6
5ØØ	-1.5	-1.7	Ø.Ø	Ø.1	Ø.7	-Ø.1	Ø.1	1.8	Ø.8	1.9	Ø.7	3.2	2.2	Ø.6	1.4	Ø.7
63Ø	-1.5	-1.Ø	Ø.5	Ø.6	1.7	Ø.4	1.3	1.Ø	1.5	1.9	Ø.4	3.Ø	1.7	Ø.9	1.2	1.Ø
8ØØ	-Ø.7	-Ø.7	Ø.5	Ø.5	3.4	1.9	2.1	2.6	1.5	2.2	1.Ø	3.7	1.7	1.5	1.4	1.8
1ØØØ	Ø.2	1.2	2.5	2.5	4.4	2.6	3.Ø	2.8	1.9	2.2	Ø.6	3.5	1.7	2.2	1.1	2.4
125Ø	2.8	4.Ø	4.9	4.6	5.7	3.8	3.7	3.3	1.4	2.3	Ø.2	2.8	1.3	3.1	1.6	3.2
16ØØ	3.Ø	3.7	5.2	4.4	5.Ø	3.5	3.9	3.2	2.6	1.8	Ø.8	2.1	1.Ø	3.1	1.4	3.5
2ØØØ	2.8	3.2	4.4	3.8	6.1	3.5	3.2	3.Ø	2.8	2.7	Ø.9	4.2	2.1	3.3	1.2	3.5
25ØØ	3.2	3.7	5.2	4.5	6.1	4.2	3.1	3.3	1.9	3.2	1.Ø	5.1	1.6	3.5	1.5	3.8
315Ø	2.7	3.9	5.1	3.9	4.7	2.7	3.7	3.9	2.2	3.6	1.7	5.6	2.5	3.6	1.2	3.6
4ØØØ	-Ø.6	Ø.4	3.9	3.4	4.4	2.6	3.4	4.4	5.2	6.6	4.8	9.1	6.4	4.2	2.5	3.1
5ØØØ	-Ø.9	Ø.8	3.1	2.2	4.3	1.3	4.2	5.Ø	4.7	7.Ø	3.7	8.6		3.7	2.6	2.8
63ØØ	-1.5	2.Ø	3.2	1.9	4.5	1.6	5.2	6.Ø	5.7	5.7	3.7			3.4	2.3	3.2
8ØØØ				2.2	6.8	3.Ø	6.6	8.3	7.Ø					5.8	2.6	5.6
1ØØØØ																7.9
125ØØ																
16ØØØ																
2ØØØØ																
25ØØØ																
315ØØ																
4ØØØØ																
5ØØØØ																
63ØØØ																
8ØØØØ																
OASPL	Ø.3	1.Ø	2.4	2.4	3.5	1.8	2.1	2.Ø	Ø.9	1.4	Ø.1	2.1	1.2			
PNL	1.5	2.Ø	3.6	3.2	4.6	2.5	2.6	2.6	1.8	1.9	Ø.6	2.8	1.3			
PNLT	1.5	2.Ø	4.2	3.2	4.6	2.5	2.6	2.6	1.7	1.9	Ø.6	2.8	1.3			
DBA	1.3	2.1	3.4	3.2	4.4	2.7	2.8	2.7	1.6	2.Ø	Ø.6	3.1	1.6			

LOCATION	ACOUSTIC RANGE	AVG CORR SPEED	AVG CORR THRUST
C41 ANECH CH	24ØØ.Ø FT SL	-Ø.1E 31 RPM	-Ø.1E 31' LB

TEST CASE FOR TREATED EJECTOR TEØ2 VS TEØ9

DELTA, SPL(1) - SPL(2)

IDENTIFICATION

INPUT (1) 83F-4ØØ-2ØØ6 X2ØØ65
(2) 83F-4ØØ-9ØØ6 X9ØØ65

OUTPUT ITF TE2-TE9 XØ2Ø91

ANGLES MEASURED FROM INLET,DEGREES

FREQ	4Ø.Ø	5Ø.Ø	6Ø.Ø	7Ø.Ø	8Ø.Ø	9Ø.Ø	1ØØ.Ø	11Ø.Ø	12Ø.Ø	13Ø.Ø	14Ø.Ø	15Ø.Ø	16Ø.Ø	AVG	S.D.	PWL
5Ø	-1.5	-Ø.8	-Ø.9	-1.2	1.3	-Ø.5	1.5	Ø.7	Ø.2	1.7	Ø.2	Ø.5	1.Ø	Ø.2	1.1	Ø.6
63	-2.1	-Ø.9	-Ø.4	Ø.3	1.6	-Ø.8	Ø.5	Ø.7	-Ø.3	1.2	Ø.2	Ø.2	Ø.2	Ø.1	1.Ø	Ø.3
8Ø	-2.2	-Ø.1	Ø.2	Ø.9	1.5	-Ø.3	Ø.7	Ø.7	-Ø.3	Ø.7	Ø.2	-Ø.8	Ø.7	Ø.2	Ø.9	Ø.2
1ØØ	-1.3	-Ø.9	Ø.3	Ø.9	1.Ø	-1.3	1.Ø	-Ø.5	-Ø.3	1.Ø	-Ø.Ø	-Ø.Ø	Ø.7	Ø.1	Ø.9	Ø.2
125	-1.5	-Ø.3	-Ø.Ø	1.Ø	1.9	-Ø.5	Ø.5	Ø.5	-Ø.4	Ø.5	-Ø.1	-1.4	Ø.1	Ø.Ø	Ø.9	-Ø.1
16Ø	-Ø.3	-Ø.1	Ø.4	1.6	Ø.8	-Ø.3	Ø.Ø	1.1	Ø.Ø	1.5	-Ø.5	-1.5	Ø.5	Ø.2	Ø.9	Ø.2
2ØØ	-Ø.9	-Ø.3	Ø.8	-Ø.Ø	1.Ø	-1.8	Ø.5	Ø.Ø	-Ø.6	1.3	Ø.1	-Ø.1	-Ø.Ø	Ø.Ø	Ø.8	Ø.Ø
25Ø	-1.8	-1.Ø	-Ø.Ø	-Ø.1	Ø.7	-Ø.5	Ø.1	-Ø.3	-Ø.6	1.6	-Ø.1	-Ø.8	Ø.3	-Ø.2	Ø.8	Ø.Ø
315	-2.Ø	-Ø.5	-Ø.Ø	Ø.3	1.Ø	-Ø.5	Ø.7	-Ø.2	-Ø.3	Ø.6	Ø.5	-1.7	-Ø.5	-Ø.2	Ø.9	-Ø.1
4ØØ	-Ø.8	-Ø.5	-Ø.Ø	Ø.4	Ø.5	-1.Ø	-Ø.1	-Ø.4	-Ø.8	Ø.9	-Ø.7	-2.Ø	-Ø.2	-Ø.4	Ø.7	-Ø.3
5ØØ	-1.5	-1.3	-Ø.8	-Ø.6	-Ø.Ø	-Ø.8	-Ø.1	Ø.Ø	-Ø.9	1.1	-Ø.7	-1.5	-Ø.5	-Ø.6	Ø.7	-Ø.4
63Ø	-1.5	-Ø.5	Ø.2	-Ø.2	1.Ø	-Ø.8	Ø.6	-Ø.5	-Ø.4	1.5	-Ø.4	-1.3	-Ø.5	-Ø.2	Ø.8	-Ø.1
8ØØ	-1.5	-Ø.8	Ø.2	Ø.2	1.4	-Ø.Ø	1.3	Ø.2	-Ø.7	1.5	-Ø.Ø	-1.5	Ø.1	Ø.Ø	1.Ø	Ø.2
1ØØØ	-2.8	-1.1	-Ø.5	-Ø.1	2.7	Ø.2	1.6	Ø.3	-Ø.6	Ø.6	-Ø.7	-1.9	-1.2	-Ø.3	1.4	Ø.1
125Ø	-Ø.8	1.7	2.5	2.8	4.Ø	2.Ø	1.7	1.3	Ø.1	2.Ø	-Ø.1	-Ø.5	Ø.3	1.3	1.4	1.4
16ØØ	1.Ø	2.2	3.7	3.1	3.7	1.9	3.5	1.Ø	Ø.5	1.6	Ø.2	-1.1	Ø.5	1.7	1.5	1.9
2ØØØ	1.4	2.4	3.7	2.9	4.1	1.7	2.9	1.7	-Ø.5	Ø.Ø	-2.4	-2.4	-1.4	1.1	2.2	1.9
25ØØ	-Ø.6	Ø.6	1.7	2.1	4.6	2.6	2.9	1.1	2.9	4.6	2.7	2.9	3.5	2.5	1.5	2.2
315Ø	Ø.4	2.6	3.6	2.2	3.6	Ø.8	3.3	3.7	1.5	4.9	3.4	3.2	3.9	2.9	1.3	2.5
4ØØØ	-Ø.4	Ø.6	2.6	1.7	1.9	Ø.Ø	1.7	3.1	2.4	5.7	3.8	5.4	4.9	2.6	2.Ø	1.6
5ØØØ	-4.Ø	-2.3	1.2	-1.1	2.4	-Ø.6	2.7	3.1	2.9	6.Ø	4.4	4.7		1.6	3.Ø	Ø.9
63ØØ	-Ø.6	Ø.3	3.1	1.Ø	4.4	-Ø.1	5.Ø	4.4	3.6	6.3	3.2			2.8	2.3	2.4
8ØØØ			3.3	2.7	6.6	2.6	5.7	5.6	5.2					4.5	1.6	4.5
1ØØØØ																6.6
125ØØ																
16ØØØ																
2ØØØØ																
25ØØØ																
315ØØ																
4ØØØØ																
5ØØØØ																
63ØØØ																
8ØØØØ																
OASPL	-1.Ø	Ø.1	1.1	1.2	2.2	Ø.4	1.4	Ø.4	-Ø.4	1.2	-Ø.1	-Ø.5	Ø.4			
PNL	-Ø.1	1.1	2.Ø	1.8	3.1	Ø.9	2.1	1.Ø	Ø.2	1.7	Ø.1	-Ø.9	Ø.2			
PNLT	-Ø.2	1.1	2.1	1.9	3.1	Ø.9	2.1	1.Ø	Ø.2	2.2	Ø.1	-Ø.9	Ø.2			
DBA	-Ø.6	Ø.7	1.8	1.7	3.Ø	1.Ø	2.Ø	Ø.7	-Ø.3	1.3	-Ø.3	-1.3	-Ø.2			

LOCATION	ACOUSTIC RANGE	AVG CORR SPEED	AVG CORR THRUST
C41 ANECH CH	24ØØ.Ø FT SL	-Ø.1E 31 RPM	-Ø.1E 31 LB

TEST CASE FOR TREATED EJECTOR TEØ2 VS TEØ9

DELTA, SPL(1) - SPL(2)

IDENTIFICATION

INPUT (1) 83F-4ØØ-2Ø1Ø X2Ø1Ø5
(2) 83F-4ØØ-9Ø1Ø X9Ø1Ø5

OUTPUT TOF TE2-TE9 XØ2Ø91

ANGLES MEASURED FROM INLET,DEGREES

FREQ	4Ø.Ø	5Ø.Ø	6Ø.Ø	7Ø.Ø	8Ø.Ø	9Ø.Ø	1ØØ.Ø	11Ø.Ø	12Ø.Ø	13Ø.Ø	14Ø.Ø	15Ø.Ø	16Ø.Ø	AVG	S.D.	PWL
5Ø	Ø.9	1.3	1.2	Ø.3	2.Ø	Ø.4	1.4	-Ø.8	Ø.8	2.Ø	1.2	3.8	Ø.8	1.2	1.1	1.8
63	Ø.6	Ø.6	Ø.9	-Ø.Ø	1.4	Ø.6	1.3	Ø.4	Ø.8	1.3	2.2	4.4	Ø.Ø	1.1	1.2	1.8
8Ø	Ø.3	1.4	1.1	Ø.9	1.1	-Ø.4	2.1	Ø.6	Ø.8	Ø.8	1.2	4.6	Ø.5	1.2	1.2	1.8
1ØØ	Ø.Ø	Ø.7	1.3	1.3	1.7	Ø.3	2.1	Ø.2	Ø.Ø	Ø.7	Ø.2	3.8	Ø.8	1.Ø	1.Ø	1.2
125	Ø.9	Ø.4	Ø.8	1.4	2.9	Ø.1	1.3	Ø.6	-Ø.5	-Ø.2	1.2	2.6	Ø.5	Ø.9	1.Ø	Ø.7
16Ø	1.2	1.Ø	Ø.8	2.Ø	2.1	Ø.8	Ø.9	-Ø.2	1.2	1.1	Ø.2	1.4	1.4	1.1	Ø.6	Ø.9
2ØØ	Ø.Ø	1.6	1.1	Ø.7	1.9	-Ø.4	1.2	1.2	-Ø.Ø	1.3	Ø.8	Ø.9	1.4	Ø.9	Ø.7	Ø.8
25Ø	Ø.5	-Ø.Ø	Ø.3	Ø.6	1.1	-Ø.2	1.4	Ø.6	Ø.2	1.2	-Ø.1	-Ø.5	Ø.9	Ø.5	Ø.6	Ø.5
315	Ø.3	Ø.8	-Ø.5	Ø.7	1.5	-Ø.5	Ø.7	1.6	Ø.6	Ø.6	Ø.9	Ø.3	1.2	Ø.6	Ø.6	Ø.7
4ØØ	Ø.7	Ø.5	-Ø.3	Ø.4	1.3	-Ø.2	Ø.3	1.3	Ø.4	1.Ø	Ø.2	1.2	2.4	Ø.7	Ø.7	Ø.8
5ØØ	1.7	1.Ø	Ø.2	Ø.4	Ø.9	-Ø.5	Ø.2	1.4	Ø.7	1.8	Ø.5	1.3	2.6	Ø.9	Ø.8	1.Ø
63Ø	2.3	2.2	Ø.3	Ø.4	1.Ø	-Ø.5	Ø.7	1.7	Ø.3	1.9	1.4	1.Ø	2.Ø	1.1	Ø.9	1.1
8ØØ	3.4	3.1	Ø.7	Ø.3	2.2	Ø.2	Ø.8	1.5	Ø.8	1.9	1.2	1.5	2.5	1.5	1.Ø	1.4
1ØØØ	3.5	5.Ø	3.4	2.6	4.Ø	1.7	Ø.6	2.6	1.Ø	2.1	1.4	1.5	2.2	2.4	1.3	2.1
125Ø	3.7	5.2	4.8	4.7	5.2	3.Ø	2.1	2.4	Ø.4	2.8	1.9	1.2	2.2	3.Ø	1.6	2.8
16ØØ	4.9	4.5	4.5	4.7	4.7	2.7	3.Ø	2.9	Ø.1	1.8	1.5	1.1	1.8	2.9	1.6	3.Ø
2ØØØ	4.5	4.1	3.Ø	2.6	3.1	Ø.7	2.2	2.4	-1.8	-2.Ø	-2.4	-1.9	-1.6	1.Ø	2.6	1.7
25ØØ	3.6	2.7	1.6	Ø.6	2.1	Ø.6	Ø.7	Ø.9	-1.1	-Ø.4	-Ø.7	-Ø.3	-Ø.3	Ø.8	1.4	1.1
315Ø	3.4	2.3	1.6	Ø.1	1.5	-Ø.4	Ø.4	2.1	-1.6	-1.2	-1.2	-Ø.6	-Ø.7	Ø.4	1.6	Ø.7
4ØØØ	-Ø.4	-Ø.6	Ø.3	-Ø.2	1.8	-Ø.5	-Ø.Ø	1.9	-Ø.1	Ø.5	Ø.1	Ø.7	Ø.8	Ø.3	Ø.8	Ø.2
5ØØØ	2.Ø	Ø.7	2.5	Ø.1	1.6	-Ø.6	1.8	2.9	1.Ø	1.9	1.9	Ø.7		1.4	1.Ø	1.2
63ØØ	-Ø.2	-1.5	Ø.8	-Ø.4	2.2	Ø.9	2.9	3.9	2.8	2.5	3.4			1.6	1.7	1.6
8ØØØ			4.3	2.3	1.1	1.9	4.6	5.4	4.1	3.2				3.4	1.5	3.4
1ØØØØ																3.7
125ØØ																
16ØØØ																
2ØØØØ																
25ØØØ																
315ØØ																
4ØØØØ																
5ØØØØ																
63ØØØ																
8ØØØØ																
OASPL	2.4	2.9	2.3	2.Ø	2.8	Ø.8	1.2	1.6	Ø.4	1.2	Ø.9	3.Ø	Ø.8			
PNL	3.2	3.1	2.2	1.4	2.4	Ø.6	1.5	1.9	Ø.1	1.2	Ø.9	1.6	1.5			
PNLT	2.1	3.1	1.5	Ø.7	2.4	Ø.6	1.5	1.9	Ø.1	1.2	1.9	1.6	1.5			
DBA	3.5	3.9	3.1	2.5	3.4	1.3	1.5	2.1	Ø.4	1.6	1.Ø	1.1	1.9			

LOCATION	ACOUSTIC RANGE	AVG CORR SPEED	AVG CORR THRUST
C41 ANECH CH	24ØØ.Ø FT SL	-Ø.1E 31 RPM	-Ø.1E 31' LB

TEST CASE FOR TREATED EJECTOR TEØ2 VS TEØ9

1. Report No.	2. Government Accession No.	3. Recipient's Catalog No.
NASA CR-4019		

4. Title and Subtitle	5. Report Date
Simulated Flight Acoustic Investigation of Treated Ejector Effectiveness on Advanced Mechanical Suppressors for High Velocity Jet Noise Reduction	November 1986
	6. Performing Organization Code
7. Author(s)	8. Performing Organization Report No.
J.F. Brausch, R.E. Motsinger, and D.J. Hoerst	R85AEB518 (E-3134)
	10. Work Unit No.
	505-62-3A
9. Performing Organization Name and Address	11. Contract or Grant No.
General Electric Company Aircraft Engine Business Group Cincinnati, Ohio 45215-6301	NAS3-23275
	13. Type of Report and Period Covered
12. Sponsoring Agency Name and Address	Contractor Report Final
National Aeronautics and Space Administration Lewis Research Center Cleveland, Ohio 44135	14. Sponsoring Agency Code

15. Supplementary Notes

Project Manager, Jack H. Goodykoontz, Propulsion Systems Division, NASA Lewis Research Center.

16. Abstract

Ten scale-model nozzles were tested in an anechoic free-jet facility to evaluate the acoustic characteristics of a mechanically suppressed inverted-velocity-profile coannular nozzle with an acoustically treated ejector system. The nozzle system used was developed from aerodynamic flow lines evolved in a previous (NAS3-23038) contract, defined to incorporate the restraints imposed by the aerodynamic performance requirements of an Advanced Supersonic Technology/Variable Cycle Engine system through all its mission phases. Acoustic data of 188 test points were obtained, 87 under static and 101 under simulated flight conditions. The tests investigated variables of (a) hardwall ejector application to a coannular nozzle with 20-chute outer annular suppressor, (b) ejector axial positioning, (c) treatment application to ejector and plug surfaces, and (d) treatment design. Laser velocimeter, shadowgraph photograph and aerodynamic static pressure and temperature measurements were acquired on select models to yield diagnostic information regarding the flow field and aerodynamic performance characteristics of the nozzles. Salient results from analysis of the measured data include: (a) application of hardwall ejectors is significantly beneficial in reduction of both forward and aft quadrant noise, (b) application of treatment to plug and ejector surfaces is additionally effective, primarily at forward and broadside acoustic angles and in the cutback to intermediate cycle range, (c) the optimum treated ejector system added 5.5 ΔEPNL suppression to the baseline mechanically-suppressed nozzle at takeoff cycle, (d) all ejector systems yielded high forward quadrant suppression, not previously experienced with non-ejector systems, (e) axial location of the ejector is very significant, further aft location being both aerodynamically and acoustically superior, (f) treatment design variation, within limits evaluated, was not critical to suppression, and (g) treatment application to the plug surface of a non-ejector system was not effective in further reduction of shock noise. An existing computations methodology to predict ejector/treatment suppression was refined to handle treatment on both the shroud and plug surfaces and to improve the modal propagation model, including effects of flow on mode cut-on-ratio. Checks of the improved model with the measured suppression showed very good correlation. At the upper end of the frequency range, a discrepancy occurred that is thought to stem from noise leakage out of the gap between nozzle exit and ejector inlet, a flanking path.

17. Key Words (Suggested by Author(s))	18. Distribution Statement
Supersonic jet noise reduction; Mechanically suppressed ejector nozzle noise; Shock cell noise; Variable cycle engine; Treated ejector; Treatment effectiveness	Unclassified - unlimited STAR Category 71

19. Security Classif. (of this report)	20. Security Classif. (of this page)	21. No. of pages	22. Price*
Unclassified	Unclassified	413	A18

*For sale by the National Technical Information Service, Springfield, Virginia 22161